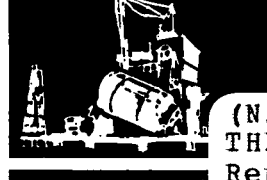
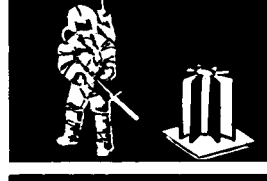
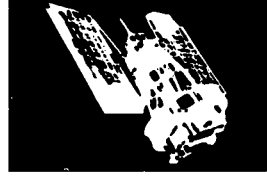
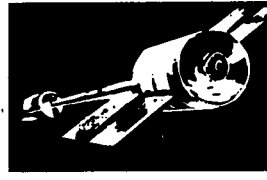
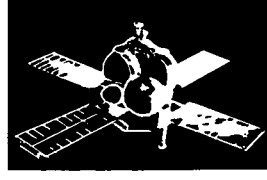
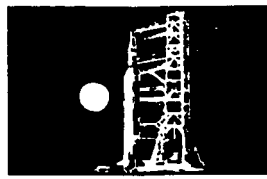
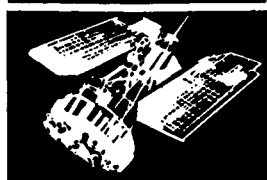


2(mix)

NTIS HC \$21.50

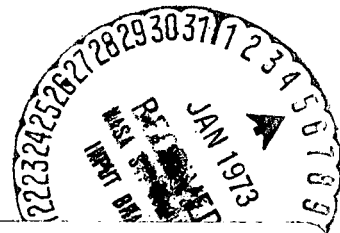
SPACE DIVISION



SD DOCUMENT NO. 72SD4243

LONG LIFE HIGH RELIABILITY THERMAL CONTROL SYSTEMS STUDY FINAL REPORT

AUGUST, 1972



(NASA-CR-123956) LONG LIFE RELIABILITY
THERMAL CONTROL SYSTEMS STUDY Final
Report, 1 Jul. 1970 - 31 Aug. T.R.
Scollon, Jr., et al (General Electric
Co.) Aug. 1972 386 p CACL 20M

N73-13950
Unclas
G3/33 16565

GENERAL  ELECTRIC

LONG LIFE HIGH RELIABILITY
THERMAL CONTROL SYSTEMS STUDY
FINAL REPORT
AUGUST, 1972


PREPARED UNDER CONTRACT NAS 8-26252 BY

SPACE SYSTEMS ORGANIZATION
GENERAL ELECTRIC COMPANY
VALLEY FORGE SPACE TECHNOLOGY CENTER
POST OFFICE BOX 8555

FOR

GEORGE C. MARSHALL SPACE FLIGHT CENTER
NATIONAL AERONAUTICS AND SPACE ADMINISTRATION
MARSHALL SPACE FLIGHT CENTER, ALABAMA 35812

Prepared by: T. R. Scollon, Jr.
R. E. Killen

Approved by: 
L. E. Blomstrom
Program Manager

Distribution

A&TS-PR-M 1 copy
A&TS-MS-IL 1 copy
A&TS-MS-IP 2 copies
A&TS-TU 1 copy
S&E-ASTN-PTC 125 copies + Reproducible copy; ATTN: Mr. J. D. Loose

FOREWORD

This report was prepared by the General Electric Space Systems Organization for the Marshall Space Flight Center of the National Aeronautics and Space Administration. The work was performed under Contract NAS 8-26252 and was administered by the Thermal Engineering Branch of the Propulsion and Thermodynamics Division, with Mr. J. D. Loose and Mr. G. A. Robinson as Project Technical Monitors. The work described herein was performed from July 1, 1970 to August 31, 1972. A Data Handbook, compiled during the course of the project, is issued under a separate cover.

The work of the following major contributors to the project is acknowledged: M. J. Carpitella, Thermal Analysis; H. Straub, Design; A. D. Maurer, Test Technician; and J. St. Leger, Reliability.

Preceding page blank

ABSTRACT

This report presents the results of a program undertaken to conceptually design and evaluate a passive, high reliability, long life thermal control system for Space Station application. The program consists of four steps: 1) investigate and select potential thermal system elements; 2) conceive, evaluate and select a thermal control system using these elements; 3) conduct a verification test of a prototype segment of the selected system; and 4) evaluate the utilization of waste heat from the power supply. The result of this project is a conceptual thermal control system design which employs heat pipes as primary components, both for heat transport and temperature control. The system, its evaluation, and the test results are described in this report.

TABLE OF CONTENTS

<u>Section</u>		<u>Page</u>
1	SUMMARY	1-1
	1.1 Scope	1-1
	1.2 Thermal Control Elements	1-1
	1.3 Thermal Control Systems Evaluation and Selection	1-3
	1.4 Verification Test	1-4
	1.5 Waste Heat Utilization.	1-6
2	PHASE I	2-1
	2.1 Scope	2-1
	2.2 Element Selection	2-1
	2.2.1 Judgment Criteria	2-1
	2.2.2 Rating	2-3
	2.3 Heat Pipes	2-13
	2.3.1 Theoretical Considerations	2-13
	2.3.2 Test Program	2-22
	2.3.3 Theoretical - Empirical Correlation	2-29
	2.4 Summary and Conclusions	2-32
3	PHASE II	3-1
	3.1 Scope	3-1
	3.2 Concept Formation and Selection	3-1
	3.2.1 Requirements and Constraints	3-2
	3.2.2 Thermal Environment	3-7
	3.2.3 Parametric Radiator Study.	3-10
	3.2.4 Alternative Concepts	3-19
	3.2.5 Preliminary Selection	3-31
	3.3 Definition of Preferred Systems	3-25
	3.3.1 Overview	3-35
	3.3.2 Updated Requirements	3-36
	3.3.3 Element Definition	3-38
	3.3.4 System Characteristics.	3-68
4	PHASE III.	4-1
	4.1 Objective	4-1
	4.2 Scope	4-1
	4.3 Description of Test Article	4-2
	4.3.1 Heat Pipes	4-4

TABLE OF CONTENTS (Cont'd)

<u>Section</u>	<u>Page</u>
4.3.2 Control Volumes	4-5
4.3.3 Interfaces	4-8
4.3.4 Radiators	4-13
4.3.5 Insulation	4-14
4.3.6 Article Mounting	4-14
4.4 Instrumentation	4-15
4.5 Integrated Article Configuration	4-17
4.6 Heat Pipe Charging.	4-17
4.7 Test Sequence/Anticipated Results	4-26
4.8 Test Description and Results.	4-29
4.9 Test Data Evaluation	4-34
4.10 Subsequent Testing.	4-39
4.11 Modification of Interface Cell System.	4-45
4.12 Re-Test	4-49
4.13 Interface Cell System-Discussion and Conclusions	4-52
4.14 Saddle System	4-60
4.14.1 System Design.	4-60
4.14.2 System Fabrication	4-63
4.14.3 Test Plan	4-65
4.14.4 Integrated Saddle System	4-68
4.14.5 Test	4-68
4.14.6 Conclusions.	4-73
5 PHASE IV	5-1
5.1 Scope	5-1
5.2 Requirements	5-2
5.2.1 General	5-2
5.2.2 Potential Users of Waste Heat	5-2
5.2.3 Description of Waste Heat Users	5-3
5.3 Evaluation of Power System Waste Heat Sources	5-8
5.3.1 Power System Definition	5-8
5.4 Heat Transmission Analysis.	5-19
5.4.1 Waste Heat Removal.	5-19
5.4.2 Energy Transport	5-30
5.4.3 Power Distribution	5-43
5.4.4 Heat Removal, Transport, and Distribution Summary	5-46
5.5 Maintenance Requirements	5-47
5.6 Nuclear Hazards	5-50

TABLE OF CONTENTS (Cont'd)

<u>Section</u>		<u>Page</u>
	5.7 Alternate Approaches to Waste Heat Utilization	5-53
	5.7.1 Primary Power System Concept	5-54
	5.7.2 Radioisotope Heaters	5-56
	5.7.3 Miscellaneous Energy Supply Approaches	5-63
6	CONCLUSIONS	6-1
7	RECOMMENDATIONS	7-1
8	NOMENCLATURE	8-1
9	REFERENCES	9-1
APPENDIX A	SINK TEMPERATURE PLOTS	A-1
APPENDIX B	HEAT PIPE CAPACITY COMPUTER PROGRAM	B-1
APPENDIX C	PHASE I TEST DATA	C-1

LIST OF ILLUSTRATIONS

<u>Figure</u>		<u>Page</u>
2-1	Simulated Channel Wick	2-24
2-2	Free-Standing Artery Wick	2-24
2-3	Test Set-up	2-27
3-1	Nominal Space Station Configuration	3-3
3-2	Variation of Fin Effectiveness with Length	3-12
3-3	Heat Dissipation vs Radiator Temperature and $\eta'\epsilon$ Product - 3000 ft ² Area and 200 ^o R Sink.	3-13
3-4	Heat Dissipation vs Radiator Temperature and $\eta'\epsilon$ Product - 3000 ft ² Area and 350 ^o R Sink.	3-13
3-5	Heat Dissipation vs Radiator Temperature and $\eta'\epsilon$ Product - 3000 ft ² Area and 400 ^o R Sink.	3-13
3-6	Heat Dissipation vs Radiator Temperature and $\eta'\epsilon$ Product - 3000 ft ² Area and 425 ^o R Sink.	3-13
3-7	Radiator Area vs Sink Temperature and $\eta'\epsilon$ Product - 136, 538 Btu/hr and 20 ^o F Radiator.	3-14
3-8	Radiator Area vs Sink Temperature and $\eta'\epsilon$ Product - 136, 538 Btu/hr and 40 ^o F Radiator.	3-14
3-9	Radiator Area vs Sink Temperature and $\eta'\epsilon$ Product - 136, 538 Btu/hr and 60 ^o F Radiator.	3-14
3-10	Radiator Area vs Sink Temperature and $\eta'\epsilon$ Product - 95, 577 Btu/hr and 40 ^o F Radiator	3-14
3-11	Radiator Area vs Sink Temperature and $\eta'\epsilon$ Product - 163, 846 Btu/hr and 40 ^o F Radiator.	3-15
3-12	Heat Dissipation vs Sink and Radiator Temperature - 3000 ft ² and $\eta'\epsilon$ of 0.50	3-15
3-13	Heat Dissipation vs Sink and Radiator Temperature - 3000 ft ² and $\eta'\epsilon$ of 0.67	3-15
3-14	Heat Dissipation vs Sink and Radiator Temperature - 3000 ft ² and $\eta'\epsilon$ of 0.80	3-15
3-15	Heat Dissipation vs Sink and Radiator Temperature - 3000 ft ² and $\eta'\epsilon$ of 0.90	3-16
3-16	Fin Effectiveness vs Heat Source Spacing and Radiating Temperature	3-18
3-17	Heat Transfer Techniques	3-21
3-18	System Concepts - Candidates 1 through 4	3-26
3-19	System Concepts - Candidates 5 through 7	3-27
3-20	Space Station Radiator Distribution	3-41
3-21	Required Effectiveness vs ΔT	3-43
3-22	Required FINHP Spacing vs ΔT	3-43
3-23	System Weight vs ΔT	3-44

LIST OF ILLUSTRATIONS (Cont'd)

<u>Figure</u>		<u>Page</u>
3-24	Required CIRHP Heat Flow vs Circumferential Position	3-50
3-25	Heat Pipe Interface Segment.	3-52
3-26	Interface Module	3-54
3-27	Interface - Component Heat Pipe to Longitudinal Heat Pipe	3-56
3-28	Interface - Penetration Element	3-57
3-29	Interface - Circumferential Heat Pipe to Fin Heat Pipe.	3-58
3-30	Interface - Component to Component Heat Pipe	3-59
3-31	Interface - Fin Heat Pipe to Radiator.	3-61
3-32	Modular Heat Pipe	3-62
3-33	Concept A - Gas Reservoir Configuration	3-65
3-34	Concept B - Gas Reservoir Configuration	3-67
3-35	Nodal Breakdown - Segment of Detailed Model	3-72
3-36	Nodal Breakdown - Simplified Model	3-74
3-37	Concept A - Controllable Heat Pipe Characteristics	3-75
3-38	Concept A - Control Midpoint Sensitivity	3-76
3-39	Concept A - Nominal Temperature Profile	3-82
3-40	Concept A - Orbital Temperature-Time History	3-83
3-41	Concept A - α/ϵ Sensitivity	3-83
3-42	Concept A - Blockage Sensitivity	3-84
3-43	Concept A - Internal Dissipation Sensitivity	3-85
3-44	Concept A - Maximum Dissipation Response	3-86
3-45	Concept B - Controllable Heat Pipe Characteristics	3-88
3-46	Concept B - Control Midpoint Sensitivity	3-91
3-47	Concept B - Nominal Temperature Profile	3-92
3-48	Concept B - Orbital Temperature-Time History	3-92
3-49	Concept B - α/ϵ Sensitivity	3-93
3-50	Concept B - Internal Dissipation Sensitivity	3-93
3-51	Selected Configuration	3-102
4-1	Heat Pipe System Segment Test Article	4-3
4-2	Wick Configurations	4-6
4-3	Mechanical Interface	4-9
4-4	Heat Pipe #5 Design	4-11
4-5	Interface Cell Cross-Section	4-12
4-6	Chamber Penetration	4-15
4-7	Thermocouple Locations	4-16
4-8	Photograph - Overall Test Article	4-18
4-9	Photograph - Bottom of Radiator Assembly (Side View).	4-19
4-10	Photograph - Bottom of Radiator Assembly (End View).	4-20
4-11	Photograph - Room Ambient Assembly	4-21
4-12	Photograph - Interface and Feed Through Detail	4-22
4-13	Fill Procedure - Fixed Conductance Heat Pipes	4-24

LIST OF ILLUSTRATIONS (Cont'd)

<u>Figure</u>		<u>Page</u>
4-14	Fill Procedure - Variable Conductance Heat Pipes	4-25
4-15	Test Data Profile - Case #1	4-29
4-16	Test Data Profile - Case #2	4-31
4-17	Test Data Profile - Case #3	4-32
4-18	Test Data Profile - Case #4	4-32
4-19	Test Data Profile - Case #5	4-33
4-20	Test Data Profile - Case #6	4-33
4-21	Test Data Profile - Case #7	4-34
4-22	"Advanced" Interface Conductance Detail	4-37
4-23	Case P1 Configuration.	4-40
4-24	Case P1 Results.	4-41
4-25	Case P2 and P3 Configuration	4-42
4-26	Case P2 Results.	4-42
4-27	Case P3 Results.	4-43
4-28	Schematic of Burnout Theory	4-45
4-29	Ammonia Fill Set-Up	4-48
4-30	Heater Details	4-50
4-31	Case R1 Results.	4-51
4-32	Case R2 Results.	4-52
4-33	Case R3 Results.	4-53
4-34	Case R4 Results.	4-53
4-35	Case R5 Results.	4-54
4-36	Methanol Interface Cell Data	4-57
4-37	Thermal Resistance of Interface Cell.	4-58
4-38	Saddle System #1	4-61
4-39	Saddle System #2	4-61
4-40	Saddle System Heat Pipe Cross-Sections	4-62
4-41	Saddle System Interface	4-64
4-42	Saddle System Insulation	4-67
4-43	Saddle System Thermocouple Locations	4-67
4-44	Photograph - Overall Saddle System	4-68
4-45	Photograph - Saddle System Detail (1)	4-69
4-46	Photograph - Saddle System Detail (2)	4-69
4-47	Case S1 Profile	4-70
4-48	Case S2 Profile	4-71
4-49	Case S3 Profile	4-71
4-50	Heat Pipe 1B Profile	4-72
4-51	Case S4 Profile	4-73
4-52	Case S5 Profile	4-74

LIST OF ILLUSTRATION (Cont'd)

<u>Figure</u>		<u>Page</u>
5-1	Simplified Isotope/Brayton Cycle	5-9
5-2	Simplified Reactor/Brayton Cycle	5-10
5-3	Simplified Reactor/Thermoelectric Cycle	5-11
5-4	Simplified Reactor/Organic Rankine Cycle	5-12
5-5	Isotope/Brayton System Configuration	5-13
5-6	SNAP-8 Reactor Assembly	5-15
5-7	Energy Removal Alternatives - Isotope/Brayton Cycle	5-21
5-8	Required Radiator Area vs Waste Heat Utilized - Isotope/Brayton Cycle.	5-22
5-9	Radiator Outlet Temperature vs Waste Heat Utilized - Isotope/Brayton Cycle	5-24
5-10	Kinematic Viscosity vs Temperature - Fluorocarbons (FC-75)	5-26
5-11	Shield Waste Heat Removal Concept and Heat Transfer Area Requirements	5-27
5-12	Required Radiator Area vs Waste Heat Utilized - Reactor/Brayton Cycle	5-29
5-13	Radiator Outlet Temperature vs Waste Heat Utilized - Reactor/Brayton Cycle	5-30
5-14	Required Radiator Area vs Waste Heat Utilized - Reactor/Organic Rankine Cycle	5-31
5-15	Radiator Outlet Temperature vs Waste Heat Utilized - Reactor/Organic Rankine Cycle	5-31
5-16	Energy Transport System Weight as a Function of Flow Path Length and Tube Diameter - H ₂ O	5-32
5-17	Energy Transport System Weight as a Function of Flow Path Length and Tube Diameter - DC 200	5-32
5-18	Energy Transport System Weight as a Function of Flow Path Length and Tube Diameter - NaK	5-33
5-19	Vapor Flow Parameter vs Temperature for Various Fluids	5-35
5-20	Capillary Flow Parameter vs Temperature for Various Fluids	5-36
5-21	Schematic of Heat Pipe Concepts	5-37
5-22	Required Vapor Space Diameters vs Heat Pipe Temperature at Various Power Levels.	5-38
5-23	Individual Heat Pipe Weight as a Function of Length and Heat Load	5-41
5-24	Variation of Heat Pipe Weight with Multiple, Parallel Paths - Isotope/Brayton Cycle	5-42
5-25	Required Heat Transfer Area Between Heat Pipes in Series as a Function of Heat Load.	5-43
5-26	Layout of Series Power Distribution Concept	5-44

LIST OF ILLUSTRATIONS (Cont)

5-27	Layout of Parallel Power Distribution Concept	5-46
5-28	Isotope/Brayton Waste Heat Utilization System	5-48
5-29	Layout of Series Power Distribution Concept Showing Quick Disconnect Coupling Locations	5-51
5-30	Radiation Damage Effects in DC-200	5-52
5-31	Isotope Heater Concept	5-59
5-32	Fraction of Isotope Power Remaining as a Function of Time . . .	5-60
5-33	Weight of Fuel and Shield vs Dose Rate and Thermal Power . . .	5-64
5-34	Cost of Fuel and Launch vs Dose Rate and Thermal Power . . .	5-64

LIST OF TABLES

<u>Table</u>		<u>Page</u>
2-1	Low α_s/ϵ Coating Trade-off	2-5
2-2	Mid α_s/ϵ Coating Trade-off	2-6
2-3	High α_s/ϵ Coating Trade-off	2-8
2-4	Insulation Trade-off	2-9
2-5	Louver System Trade-off.	2-11
2-6	Design of Tested Heat Pipes.	2-25
2-7	Test Sequence	2-28
2-8	Summary of Burn-Out Conditions from Test	2-28
2-9	Comparison of Theoretical and Actual Results.	2-30
3-1	Nominal Case Internal Dissipation.	3-6
3-2	Orbit/Orientation Sets to be Considered.	3-8
3-3	Environment Summary	3-10
3-4	Concept Heat Pipe Definition	3-29
3-5	Concept Weights.	3-30
3-6	Concept Characteristics	3-31
3-7	Concept Trade-off Matrix	3-34
3-8	Internal Dissipations	3-39
3-9	Heat Pipe Requirements	3-45
3-10	COMP Distribution	3-47
3-11	Heat Pipe Design Parameters	3-51
3-12	Concept A - Controllable FINHP Requirements	3-66
3-13	Concept B - Controllable COMHP Requirements	3-67
3-14	Weight Summary (Pounds)	3-69
3-15	Internode Conductances	3-73
3-16	Component Weight	3-75
3-17	Space Station Heat Pipe Concept A Analytical Results	3-77
3-18	Concept A - Temperature Variation with Orbit	3-87
3-19	Space Station Heat Pipe - Concept B	3-89
3-20	Concept B - Temperature Variation with Orbit	3-94
3-21	Failure Mode, Effects and Safety Analysis Summary	3-97
4-1	Containment Vessel Dimensions	4-4
4-2	Theoretical Interface Performance	4-13
4-3	Heat Pipe Methanol Charges.	4-23
4-4	Planned Test Sequence	4-27
4-5	Analytically, Predicted Test Results.	4-28
4-6	Test Sequence	4-31
4-7	Interface Temperature Drops	4-35
4-8	Maximum Heat Pipe Temperature Drops	4-35

LIST OF TABLES (Cont'd)

<u>Table</u>		<u>Page</u>
4-9	Summary of Methanol Interface Cell Data	4-55
4-10	Summary of Ammonia Interface Cell Data	4-59
4-11	Saddle System Heat Pipes	4-62
4-12	Saddle System Heat Pipe Charges	4-65
4-13	Summary of Saddle System Data	4-75
5-1	Summary of Waste Heat User Requirements	5-5
5-2	Candidate Power System Characteristics	5-18
5-3	Return Liquid Flow Annulus Width as a Function of Heat Length and Power Load.	5-39
5-4	Power Distribution System Characteristics for Series Configuration	5-45
5-5	Power Distribution System Characteristics for Parallel Configuration	5-45
5-6	Isotope/Brayton Weight Summary	5-55
5-7	Reactor/Brayton Weight Summary.	5-56
5-8	Thermoelectric System Weight Summary	5-57
5-9	Reactor Organic Rankine System Weight	5-58
5-10	Radioisotope Fuel Characteristics.	5-60
5-11	Required Radioisotope Fuel Inventories	5-61
5-12	Radioisotope Shield Weight	5-61
5-13	Radioisotope Fuel and Launch Costs	5-63
5-14	Miscellaneous Power Source Weights.	5-65
5-15	Weight Summary for the WHU Concept	5-66
5-16	Comparison of Candidate Concepts	5-66

SECTION 1

SUMMARY

1.1 SCOPE

Spacecraft energy management systems provide thermal control by removing or redistributing excess heat from within the vehicle interior while maintaining all specified component temperature levels and gradients. Current thermal control components in these systems include pumps, valves, sensors, controllers and other continually operating mechanical components. Long duration missions, such as required by the Space Station, will require a higher reliability than presently attainable with these active mechanical system elements.

The objective of the project was to develop a conceptual design of a passive advanced integrated heat transport, heat sink and temperature control system, which would perform with high reliability over a long operational lifetime, for application to the Space Station; to determine its performance and feasibility characteristics; and to demonstrate its adaptability to future spacecraft of similar geometric and thermal constraints. The objective was accomplished by a project with four separate phases; namely,

Phase I - Summary and Evaluation of Relevant Technology

Phase II - Design and Analysis of System Alternatives

Phase III - Verification Test of Central Heat Pipe Segment

Phase IV - Space Station Utilization of Waste Heat

This study was accomplished under an established set of constraints and requirements which included the use of a 33-foot diameter Space Station as defined in MSFC/ McDonnell Douglas Astronautics Company (MDAC) Phase "B" studies.

1.2 THERMAL CONTROL ELEMENTS

During Phase I, passive thermal control elements to be investigated for potential use on the Space Station thermal control system were defined and selected. Elements chosen included

thermal control coatings, insulation, space radiators, louvers, phase change materials, transport and controllable heat pipes, boilers, and sublimators. A review of data on these elements was performed with the data being cataloged into a Data Handbook. Element rating criteria was established and a trade-off matrix presented. As a result, the following specific elements were assessed as potentially applicable to a long life Space Station Application.

Coatings

For a low α/ϵ , series emittance tapes (teflon on aluminum) were selected. For a mid-range α/ϵ , C6A black paint (with an $\epsilon = 0.96$) and aluminum leaf paint (with an $\epsilon = 0.3$) were selected. For a high α/ϵ , metallic films with oxide overcoats were selected.

Insulation

Multilayered metallized plastic film structure, aluminum on mylar or gold on Kapton, was selected.

Louvers

Bimetallically activated louvers with polished blades were selected.

Heat of Fusion

Tetradecane and hexadecane were selected for this application.

Space Radiators, Boilers, Sublimators

No selection was made for specific types of these components because they were judged to be dependent on the specific application.

Heat Pipes

Theoretical and empirical data were evaluated for both transport and control heat pipes using various fluids, shapes, length, diameter, and wick configurations. A computer program was established to aid in this trade-off and the evaluation of empirical data obtained. It was found that the maximum heat transfer and temperature drops could be accurately predicted considering effects such as tube shape, fluid, length, and diameter. In addition, the

maximum heat capacity for heat pipes with conventional wicks could be accurately predicted. Correlation of theory and test for other wick configurations was not as successful.

With the potential thermal control elements for use in an advanced passive space station thermal control system thus established, it was possible to evolve and evaluate candidate total thermal control systems.

1.3 THERMAL CONTROL SYSTEMS EVALUATION AND SELECTION

During Phase II, candidate thermal control subsystems were configured. Constraints and requirements for the study were established, and later updated prior to performance calculations. Then a thermal environments study for all possible orbits and vehicle orientations yielded a possible sink temperature range from 329°R to 451°R. Using these inputs a radiator parametric study resulted in a requirement for the product of the surface emissivity and fin effectiveness to be between 0.7 and 0.8. This resulted in a fin heat pipe spacing range around the vehicle circumference from 3.5 to 10.3 inches and a 6-inch spacing was established. Separate studies indicated that (1) all concepts must use circumferential heat pipes to distribute external heat loads; (2) pure radiation or pure conduction from the pressure wall to the radiator was not feasible; (3) pure conduction from internal components to the pressure wall was not feasible; and (4) that louvers or controllable heat pipes were the only practical temperature control techniques.

Therefore, a total heat pipe transmission system with circumferential heat pipes and temperature control via louvers or controllable heat pipes was concluded as required. Seven concepts were established which used various combinations of component heat pipes (connecting components and longitudinal pipes), longitudinal heat pipes (used to axially tie space station modules together thermally), penetration heat pipes (used to penetrate the pressure wall connecting the longitudinal and circumferential heat pipes), circumferential heat pipes (used to distribute heat around the vehicle circumference), and fin heat pipes (used to tie the circumferential heat pipes to the 20-mil aluminum radiating outer skin of the space station) to distribute heat throughout the system. Louvers on the external skin and controllable heat pipes for either the fin or component heat pipes were evaluated for temperature control

using both one and separate radiator temperature zones. Louvers and a single temperature radiator were eliminated.

The two concepts selected for further study had component heat pipes which interface directly with the dissipators and transfer heat to longitudinal heat pipes (which couple the two common modules). Heat is transferred from the longitudinal heat pipes into penetration heat pipes which penetrate the pressure wall. Circumferential heat pipes interface with the external end of the penetration heat pipes and function as thermal headers for a large number of fin heat pipes. The fin and circumferential heat pipes distribute energy to the radiator. Three radiator networks were used compatible with 45°F, 65°F, and 90°F component source temperatures, respectively. In the first concept, the fin heat pipes are variable for temperature control, while the second concept has variable component heat pipes. The detail design of the radiator (including coating, area apportionment, fin heat pipe spacing, and number of circumferential heat pipes), distribution heat pipes (including the component, longitudinal, penetration, circumferential and fin pipes), interfaces (between all elements from source to sink), and control heat pipes was established for both concepts. The performance of both concepts was predicted using a detailed analytical thermal model. The concept using variable fin heat pipes required 5/1 temperature control in the variable heat pipe, and had a system weight of 7350 pounds. The concept using variable component heat pipes required 30/1 temperature control in the variable heat pipe, and had a system weight of 7387 pounds. A comparison evaluation showed that the MDAC pumped loop system weighed 8350 pounds and was less reliable. The concept with variable fin heat pipes was selected for further study and a test planned to evaluate a segment of such a system.

1.4 VERIFICATION TEST

During Phase III, a verification test of a segment of the thermal control system selected during Phase II was performed. Eventually, two hardware systems were fabricated and tested because the first, using a prototype design of the advanced interface technique recommended in Phase II work, could not be made to demonstrate satisfactory system performance. This performance was consequently attained with the second hardware system.

The first segment used "interface cells" for thermal transfer between heat pipes and was tested in a realistic environment. The segment was designed to transport and reject to thermal vacuum chamber cryowalls 30 watts dissipation from each of two simulated dissipators with a nominal 25^oF overall temperature drop. The chamber wall represented the pressure wall of the Space Station so that one-half of the system segment was in a room ambient (the Station cabin) and the remainder was in the T/V chamber (simulating space). A total of nine heat pipes (five different types) were interconnected through various interface cells. Isotropic wicking was used throughout and methanol was the working fluid. Two separate 2.5 ft² radiating panels, radiating from one side, had two controllable heat pipes with a 14 in³ reservoir volume containing nitrogen gas. The entire article, except the radiator surfaces was insulated. The segment was instrumented and tested, during which thermal equilibrium was established at each of seven combinations of component heat dissipation (10 to 60 watts total) and effective sink temperature (330^oR to 450^oR). Test results indicated that the heat pipes performed well as isothermal units, that a vapor/gas interface was established in the controllable heat pipes (axial conduction was observed), and that the interface temperature drops were significantly larger than expected, with the most probable cause due to the presence of non-condensables. Subsequent small-scale tests on this segment verified the presence of non-condensable gas in the interface cells. Careful refilling of some of the pipes with methanol and ammonia did improve the thermal performance of the pipes, but not significantly enough to warrant additional system testing.

The second system used conventional "saddle" thermal interface techniques and was entirely tested in an ambient (room) environment. Again, a total of nine heat pipes were employed. These were interconnected through axially oriented copper saddles. The saddle system had many points in common with the interface cell system including: 1) isotropic heat pipe wicking; 2) methanol working fluid; 3) two 2.5 ft² radiators; 4) four controllable heat pipes using nitrogen as the control gas; and 5) insulation from surrounding environment, with the exception of the radiating surfaces. Satisfactory system performance was demonstrated with this unit.

1.5 WASTE HEAT UTILIZATION

During Phase IV, the use of waste heat from the power supply was studied. This was a separate task conducted in parallel with the basic three phase project. Potential users of waste heat were identified with their temperature and power requirements. Waste heat sources defined included the Isotope/Brayton, Reactor/Brayton, Reactor/Thermoelectric, and Reactor/Organic Rankine Power Systems. Locations within these systems where energy could be tapped-off for waste heat use were identified along with the potential supply power and temperature available. Techniques for removing the waste heat from the power source at these locations were described. All four power cycles studied were determined to be compatible with a waste heat utilization concept. Active fluid loops and heat pipe energy transport schemes were compared and it was concluded that heat pipe transport schemes do not offer a significant enough weight advantage to warrant their development solely for this application. Series and parallel power distribution techniques were compared with the series configuration having the advantage of lower flow rates at higher power levels. Maintenance and nuclear hazards considerations involved with the utilization of nuclear waste heat were discussed. Alternate approaches to waste heat utilization including electrical heater, radioisotope heaters, and miscellaneous sources (fuel cells, batteries, hydrogen combustion, and solar cells) were compared on a weight, reliability, and cost basis. A waste heat utilization system using an active coolant energy transport loop (DC200 fluid) was judged best for this application.

SECTION 2

PHASE I

2.1 SCOPE

Phase I Summary and Evaluation of Relevant Technology, consisted of three tasks: 1) definition and selection of thermal control elements to be investigated, 2) review of data on these elements and selection of the most reliable member of each class, and 3) study of the differences between heat pipe theoretical and actual performance.

It should be noted that Phase I was not oriented to specific Space Station configurations. Instead, it was meant to select and provide properties for desirable building blocks for a long life thermal control system. Phase II will fit these blocks to space station requirements to determine the configuration of a high reliability system for this vehicle.

Items chosen for investigation were thermal control coatings, insulation, space radiators, louvers, phase change materials, boilers and sublimators. Information on these elements has been compiled into a data handbook, which is available under separate cover.

Element rating criteria and completed tradeoff matrices are presented for all selected elements. Heat pipe theory is reviewed, empirical testing performance defined, and conclusions drawn concerning heat pipe performance.

2.2 ELEMENT SELECTION

Elements within each thermal control class are evaluated in this section. Selection criteria and weighting factors for space station application are given, and completed tradeoff matrices are presented to indicate the apparent components of a long life, high reliability thermal control system.

2.2.1 JUDGMENT CRITERIA

Criteria for element evaluation were divided into three major categories: 1) technical aspects, 2) inherent reliability, and 3) safety. Individual considerations within each of

these groups were assigned weighting factors such that the relative weights of the three major categories were, 2-technical, 1-reliability, and 1-safety. This breakdown assured that components of high reliability and safety would not be neglected because of somewhat poorer technical performance (heavier weight, higher cost, etc.). This was in keeping with the central objective of the program. On the other hand, reliability was not allowed to dominate the evaluation and lead to unrealistic conclusions in Phase I and concepts in Phase II.

As always in a rating procedure such as this, assignment of weighting factors and evaluation of elements is subjective and open to critique. It is felt, however, that as long as the rating is done in a consistent manner, the process is valid and the high ranking elements will be the most desirable.

The maximum possible score for any element is 100. The division of these points is shown below. The questions which were answered to quantify relative merit for each criteria are also listed.

Technical (50)

1. Application (15) - How well does the element perform its function compared to others of the same type? Such things as beginning of life and degraded characteristics properties make up this sub-category.
2. Credibility (10) - Is the element flight-proven, laboratory tested, or conceptual?
3. Weight (4) - Is it heavier or lighter than the others ?
4. Volume (4) - Does the element occupy significantly more volume than others in its class ?
5. Cost/availability (4) - Is the component readily available and, if so, is it expensive?
6. Power Requirements (4) - Does the component require power for operation? How much?

7. Maintenance on Ground (5) - Is special handling necessary before launch? Is the element susceptible to mechanical or environmental damage?
8. Source of Contamination (4) - Can the element be a source of contamination to surrounding objects or environment?

Reliability (25)

1. Expected Life (10) - Does the element being considered have a longer or shorter expected life than other members of its class?
2. Maintenance in Space (10) - Will maintenance be required after launch? If so, how difficult will it be?
3. Complexity (5) - Is the element more or less complex than the others?

Safety (25)

1. Mechanical (10) - Can the element explode or fracture and be dangerous to crew?
2. Chemical (15) - Are chemicals present in the element which could be unsafe?

It should be noted that the elements within each class were rated on a relative (not absolute) basis. For example, the element judged most safe mechanically within a particular class received the full 10 points, even if it was not perfectly safe in an absolute sense.

2.2.2 RATING

Completed tradeoff matrices are presented and discussed in this section. The data required to evaluate all elements was obtained from the data handbook prepared as part of this project.

It was not the intent of this task to compare elements of different classes to each other (e.g., louvers to phase change materials as temperature control devices). It was, instead to pick out the most desirable element in each class. Therefore, each class is discussed separately below.

2.2.2.1 Thermal Control Coatings

Three classes of thermal control coatings have been established based on α_s/ϵ ratios.

1. Low α_s/ϵ ($< .4$). The data handbook lists properties for 24 low α_s/ϵ coatings. Seventeen of these are paints, five are second surface reflectors (series emittance coatings), and two are sprays. Degradation data was found for all but two of these coatings (Lockpaint and Schjeldahl Tape G-107300). Since degradation is a prime consideration for low α_s/ϵ coatings, these two could not be considered further.

Before completing the tradeoff chart, a preliminary study was performed to determine the technical application rank of each coating. Considerations were changes in α_s , quantity of degradation data available, the initial value of α_s , development or manufacturing problems, and ease of installation. Conclusions from this study were:

- a) The six best coatings in the application area are (in order) OSR, Teflon on aluminum series emittance tape, Teflon on silver series emittance tape, Z-93 paint, S-13G paint and S-13 paint.
- b) Because other white paints are rated lower in this area than the three listed above and offer no significant advantages in other areas, they may be omitted from the tradeoff matrix.
- c) Flame and plasma spray coatings should not be considered because of high initial α_s/ϵ values and manufacturing and installation problems.

Table 2-1 shows the complete rating. The first number in each block is the relative rank of the particular coating in the area under consideration and the second number is the points assessed. When the rating is judged equal for two coatings, both get the same rank and points.

As can be seen, the series emittance tapes were judged most suitable for space station application. These were followed by Z-93, S-13G, OSR and S-13.

2. Mid α_s/ϵ ($0.4 \approx 1.1$). Twenty-six of the coatings in the handbook have α_s/ϵ ratios in this range. Thirteen are black or gray paints, three are chemical surface finishes, and the remaining ten are metallized films. Degradation data for these coatings is not as readily available as for the low α_s/ϵ coatings because of the smaller frequency of use on space vehicles.

The two sub-classes within this category that are of prime interest are coatings with α_s/ϵ ratios of about 1 and ϵ 's of about .3 and near 1.0 respectively. The former group contains aluminum leaf paints and second surface reflectors, while the latter is made up of black paints. These are rated in Table 2-2. C6A black

Table 2-1 Low α_s/ϵ Coating Trade-Off

ELEMENT	TECHNICAL										RELIABILITY			SAFETY		TOTAL POINTS
	APPLICATION	CREDIBILITY	WEIGHT	VOLUME	COST/AVAIL.	POWER REQ'D.	MAINT. ON GROUND	SOURCE OF CONTAM.	EXPECTED LIFE	MAINT. IN SPACE	COMPLEXITY	MECHANICAL	CHEMICAL			
	15	10	4	4	4	4	5	4	10	5	10	15	100			
	4	1	1	1	1	1	3	2	2	1	1	1	84			
Z93	9	10	4	4	4	4	3	3	6	7	5	10	15			
	5	1	2	1	2	1	3	2	3	2	1	1	78			
S-13	7	10	3	4	3	4	3	3	4	7	5	10	15			
	4	1	2	1	2	1	3	2	2	2	1	1	82			
S-13G	9	10	3	4	3	4	3	3	6	7	5	10	15			
	1	1	4	1	4	1	4	1	1	3	3	1	79			
OSR	15	10	1	4	0	4	1	4	10	3	2	10	15			
	2	2	3	1	3	1	1	1	1	1	2	1	90			
TEFLON/ALU. TAPE	13	7	2	4	2	4	5	4	10	10	4	10	15			
	3	2	3	1	3	1	2	1	1	1	2	1	87			
TEFLON/SILVER TAPE	11	7	2	4	2	4	4	4	10	4	10	15				

Table 2-2. Mid α_s/ϵ Coating Trade-Off

ELEMENT	TECHNICAL										RELIABILITY			SAFETY		TOTAL POINTS
	APPLICATION	CREDIBILITY	WEIGHT	VOLUME	COST/AVAIL.	POWER REQ'D.	MAINT. ON GROUND	SOURCE OF CONTAM.	EXPECTED LIFE	MAINT. IN SPACE	COMPLEXITY	MECHANICAL	CHEMICAL			
$\epsilon \sim 1.0$	15	10	4	4	4	4	5	4	10	5	10	15	100			
3M VELVET BLACK	3	1	1	1	1	1	1	1	1	1	1	1	1			
	11	10	4	4	4	4	5	4	10	5	10	15	96			
C6A BLACK	1	1	1	1	1	1	1	1	1	1	1	1	1			
	15	10	4	4	4	4	5	4	10	5	10	15	100			
CAT-A-LAC BLACK	2	1	1	1	1	1	1	1	1	1	1	1	1			
	13	10	4	4	4	4	5	4	10	5	10	15	98			
EPOXY FLAT BLACK	4	1	1	1	1	1	1	1	1	1	1	1	1			
	10	10	4	4	4	4	5	4	10	5	10	15	95			
$\epsilon \sim .3$																
ALUM. LEAF PAINT	1	1	1	1	1	1	2	2	2	1	1	1	1			
	15	10	4	4	4	4	4	3	7	5	10	15	92			
SECOND SURF. REFL.	2	2	2	1	2	1	1	1	1	2	1	1	1			
	12	7	3	4	2	4	5	4	10	3	10	15	89			

paint by M. A. Bruder was rated the best of the four black paints for which degradation and/or flight data was available. Aluminum leaf paints were rated over the second surface reflectors primarily because of reported low degradation, credibility, and cost.

3. High α_s/ϵ (> 1.1). Three methods are available to obtain high α_s/ϵ coatings. These are plain metallic surfaces, metallic surfaces with oxide overcoats, or alodine finishes. It is somewhat meaningless to rate these coatings against one another since the particular application may make one method the obvious choice. For example, if merely exposing an area of aluminum structure to its environment produces the desired thermal balance, it is impractical to consider other finishes for these areas. Likewise, if a specific α_s/ϵ can be attained by only one of the methods, it must be used.

For rating purposes, therefore, it was assumed that a separate coating was necessary and that it could be obtained by all three methods. Table 2-3 shows the ratings for this case. Metallic surfaces with oxide overcoats come out best due to their stability and maintainability.

2.2.2.2 Insulation

The data handbook lists 69 specific insulation systems for which test information was available. These can be divided into four classes: 1) multilayer metallized films, 2) multilayer metallized films with flexible spacers, 3) rigidized multilayer structures, and 4) rigidized foams.

The best sample of each of these classes was selected on the basis of lowest effective emissivity. These four are rated against each other in Table 2-4. Ratings are made assuming an equal volume (or thickness) of insulation for all systems. In this case, the technical application rating becomes solely a function of effective emissivity. Because no accurate cost data was available, ratings in this category were made qualitatively to reflect ease of fabrication.

Multilayer metallized films were judged best due to their relative performance, weight and credibility. Flexible blankets of 24 to 35 layers of either aluminized mylar or goldized kapton are recommended for space station use.

Table 2-3. High α_s/ϵ Coating Trade-Off

ELEMENT	TECHNICAL										RELIABILITY				SAFETY		TOTAL POINTS
	APPLICATION	CREDIBILITY	WEIGHT	VOLUME	COST/AVAIL.	POWER REQ'D.	MAINT. ON GROUND	SOURCE OF CONTAM.	EXPECTED LIFE	MAINT. IN SPACE	COMPLEXITY	MECHANICAL	CHEMICAL				
WEIGHT	15	10	4	4	4	4	5	4	10	10	5	10	15	100			
METALLIC	2	1	1	1	1	1	3	1	1	1	1	1	1	94			
	13	10	4	4	4	4	1	4	10	5	10	15					
METALLIC WITH OXIDE OVERCOAT	1	1	2	1	2	1	1	1	1	2	1	1	1	96			
	15	10	3	4	3	4	5	4	10	3	10	15					
ALODINE	3	1	1	1	1	1	2	1	1	2	1	1	1	90			
	11	10	4	4	4	4	3	4	10	3	10	15					

Table 2-4. Insulation Trade-Off

ELEMENT	TECHNICAL										RELIABILITY			SAFETY		TOTAL POINTS
	APPLICATION	CREDIBILITY	WEIGHT	VOLUME	COST/AVAIL.	POWER REQ'D.	MAINT. ON GROUND	SOURCE OF CONTAM.	EXPECTED LIFE	MAINT. IN SPACE	COMPLEXITY	MECHANICAL	CHEMICAL			
WEIGHT	15	10	4	4	4	4	5	4	10	10	5	10	15	100		
MULTILAYER	1	1	1	1	2	1	2	1	2	2	2	1	1	91		
	15	10	4	4	3	4	3	4	8	7	4	10	15			
MULTILAYER WITH SPACERS	1	1	2	1	2	1	2	2	2	2	3	1	1	88		
	15	10	3	4	3	4	3	3	8	7	3	10	15			
RIGIDIZED	2	2	3	1	3	1	1	1	1	1	4	1	1	85		
	10	7	2	4	2	4	5	4	10	10	2	10	15			
RIGID FOAM	3	2	4	1	1	1	1	3	1	1	1	1	1	84		
	7	7	1	4	4	4	5	2	10	10	5	10	15			

2.2.2.3 Space Radiators

No formal rating was done for space radiators, since it is obvious that passive radiators should be used in preference to active (i. e. , liquid flow or heat pipe) elements where a choice exists.

Further space radiator trade-off studies are dependent upon specific application and will be evaluated during Phase II of this project.

2.2.2.4 Louvers

The data handbook lists five distinct louver systems which have been flown on spacecraft to date. Four of these were bimetallically actuated, and the fifth used fluid expansion bellows actuation. Three of the systems used polished aluminum sheets for blades, the fourth multi-layer insulation, and the fifth a rectangular cross-section of aluminum foil. The system sizes ranged from 0.8 square foot for Nimbus to about four square feet for the annular configuration used on Pioneer. It is obvious that there is tremendous latitude in louver design, and that the systems flown have been developed for specific missions. It is difficult to rate overall louver systems for this reason.

A more valid comparison is to rate the two actuators against each other and the three blade types between themselves. This has been done in Table 2-5.

It was assumed in this analysis that, for a particular application, any combination of actuator and blades could be employed. It was also assumed that the bellows system used a mechanical linkage to connect all blades (ganged actuation) while the bimetallic elements controlled each blade (or pair of blades) independently.

The advantage of simplified thermal analysis and evaluation of flight data (if position indicators are used) of the ganged system was not factored into the trade-off but will be considered in specific conceptual designs.

Table 2-5. Louver System Trade-Off

ELEMENT	TECHNICAL										RELIABILITY			SAFETY		TOTAL POINTS
	APPLICATION	CREDIBILITY	WEIGHT	VOLUME	COST/AVAIL.	POWER REQ'D	MAINT. ON GROUND	SOURCE OF CONTAM.	EXPECTED LIFE	MAINT. IN SPACE	COMPLEXITY	MECHANICAL	CHEMICAL			
ACTUATOR	15	10	4	4	4	4	5	4	10	5	10	15	100			
	1	1	1	1	1	1	2	1	1	1	1	1	1			
BIMETALLIC	15	10	4	4	4	4	3	4	10	5	10	15	98			
	1	1	2	2	1	1	1	1	2	1	2	2	2			
BELLOWS	15	10	2	3	4	4	5	4	8	5	8	14	92			
	1	1	2	3	4	4	5	4	8	5	8	14	92			
BLADE																
POLISHED ALUMINUM	3	1	1	1	1	1	1	1	1	1	1	1	97			
	12	10	4	4	4	4	5	4	10	5	10	15	97			
MULTILAYER INSULATION	1	1	3	3	2	1	2	1	1	3	1	1	90			
	15	10	2	2	3	4	4	4	10	3	10	15	90			
ALUMINUM FOIL STRUCTURE	2	1	2	2	2	1	2	1	1	2	1	1	92			
	14	10	3	3	3	4	4	4	10	4	10	15	92			

As can be seen, the bimetallic actuator was selected over the bellows/fluid type. This was primarily due to its greater reliability (failure of one element does not fail the system), smaller weight and smaller volume.

The polished aluminum blade was chosen because of its simplicity. The multilayer insulation blade offers less heat leak when the louvers are in the closed position. However, analysis indicates that the transverse heat leak through the louver blades is only a small portion of the total closed system heat leak. Thus the disadvantage of the aluminum blades is small and is overcome by the increase in effective emissivity in the open position due to the thinner blade structure.

Hence, a system such as flown on OAO, Pegasus, and Mariner is recommended.

2.2.2.5 Phase Change Materials

Thermal control by use of heat of fusion or phase change material (PCM) has often been considered but no such device has been space-qualified as yet. Hence, it is impossible to determine an optimum element for use in the space station.

The data handbook presents information on several candidate PCMS (not total systems). The most desirable materials for conceptual systems would seem to be the normal paraffins ($C_{2N+2}H_{4N+6}$) on the basis of their stability, melting temperatures, and amount of data available. Consequently, tetradecane ($C_{14}H_{30}$) and hexadecane ($C_{16}H_{34}$) are recommended for the conceptual studies of Phase II of this project. These materials should be contained between the heat source and sink so that all dissipated heat must pass through the PCM. The thickness of the PCM should be small to minimize the temperature differential through it.

2.2.2.6 Boilers/Sublimators

It is doubtful boilers and sublimators can be considered for continuous use in the space station system. Heat rejection capability is limited by the weight of the on-board expendable coolant and this fact indicates the units are applicable to short-term use only. Units have been flown on missions of less than 30 days and time of actual use in space is significantly less than this.

The porous plate sublimator and wick lined boiler offer the advantage of capillary pumping of the fluid to the heated surface. These units will be considered for cooling during short pulses of high thermal dissipation on the space station. It is noted, however, that overall reliability is lower than that of other elements discussed in this section because of the required control circuits and devices.

2.3 HEAT PIPES

The disparity between theoretical and actual performance of heat pipes has often been noted. The inability of analytical techniques to predict accurately the critical operating characteristics of heat pipes points up the fact that these elements, although basically simple units, involve several complex interrelated phenomenon. Consequently, heat pipe design to date has employed previous experience and trial and error methods, and has used theory mainly to assess relative merits of various pipe-wick-fluid combinations.

In order to evolve realistic concepts for the incorporation of heat pipes in the space station thermal control system, a knowledge of attainable heat pipe performance is required. To this end, heat pipe theory was reviewed and a test program established. It was intended that correlation between theory and practice would result in a series of operational derating factors, and allow more accurate heat pipe sizing later in the project.

2.3.1 THEORETICAL CONSIDERATIONS

Heat pipe theory is primarily concerned with the calculation of two quantities: 1) the maximum heat transport capacity, and 2) the temperature differential associated with this transport. Secondary areas under investigation are transient behavior and the characteristics of two fluid (i. e., controllable) heat pipes. Thermal control system studies, using heat pipes in a variety of applications, comprise the remainder of the analytical effort on these elements.

Only the maximum heat capacity ($Q_{max.}$) and temperature differential (ΔT) have been studied in Phase I of this project. It was felt that a working knowledge of these two parameters would be essential for realistic sizing of potential space station heat pipes.

2.3.1.1 Maximum Heat Capacity

The approach generally followed in determining the maximum heat capacity is to define all possible limiting phenomenon, determine Q_{max} for each limit, and select the lowest value. Four such limits have been identified for heat pipe operation, based on the following mechanisms: 1) liquid entrainment, 2) vapor sonic velocity, 3) boiling, and 4) capillary wicking.

2.3.1.1.1 Entrainment

Entrainment occurs when drops of refluxing liquid are sheared from the liquid-vapor interface by high velocity vapor flow. The drops are carried toward the condenser section of the pipe without absorbing heat in the evaporator. The result is a reduction of pipe capacity.

Parameters affecting the entrainment limit are surface tension, vapor velocity, and characteristics of the liquid vapor interface. Several investigators have recommended that the Weber number be used to determine the possibility of entrainment for a potential heat pipe design. The Weber number is defined by:

$$W_e = \frac{\rho_v V_v^2 d}{g_c \sigma} = \frac{Q^2 d}{g_c \rho_v \sigma \lambda^2 A_v^2}$$

This number is actually the ratio of vapor flow force to surface tension force on the liquid. A Weber number of unity theoretically represents a dynamic equilibrium between these components. In practice, local disturbances can upset this equilibrium ($W_e = 1$) and entrainment can occur. Thus, the Weber number should be kept well below unity to avoid this problem.

Methods of reducing the Weber number (or conversely, increasing this particular Q_{max}) are evident from the defining equation. The vapor flow passage should be made as large as possible, and the wick interlayer spacing as small as possible. Candidate fluids should have a high product of density, surface tension, and latent heat squared.

Entrainment is not a serious problem in heat pipes with uniform wick cross-sections along their length operating at steady state. There is simply no liquid-vapor interface normal to the bulk vapor flow. Because the pipes under investigation in this study were of this type, no entrainment was expected and Weber numbers were not calculated for most test conditions. As a reference, however, the number was determined for one pipe with Freon-11 working fluid (theoretically the poorest test fluid because of its low latent heat). At the wicking limit (discussed later) of this pipe, the Weber number was 0.48. Thus, a factor of safety of greater than two on the entrainment limit was designed into the pipe at its (wick) limiting Q_{max} .

2.3.1.1.2 Sonic Velocity

Choked vapor flow is an obvious heat pipe limit. Maximum heat capacity is determined as the amount of heat that can be transferred by vapor at sonic velocity. Therefore, Levy (Reference 9-1) gives the following equation:

$$Q_{max} = \frac{\rho_v V_a \lambda A_v}{2(\gamma + 1)}$$

This equation assumes a perfect gas model, constant heat input, single phase flow, and negligible radial velocities. Levy also constructed a two phase model of the choking condition and compared the results of both analyses with test results of Kemme (Reference 9-2). Fluid properties for use in the equations were taken at both the upstream and downstream ends of the evaporator. Test data fell within the bounds of these two predictions based on the two phase model, when the working fluid (sodium) was below about 600°C. Very good agreement was found between predictions of the perfect gas and two phase models when the upstream temperature was employed to evaluate fluid properties. From this, Levy concluded that the perfect gas model equation (as given above) was sufficiently accurate for calculations and will yield slightly conservative values of Q_{max} when fluid properties are taken at the temperature of the upstream end of the evaporator.

The sonic limit occurs near the melting point of the working fluid. Since water is the only fluid under consideration that could operate near its melting point, a calculation of Q_{max} based on the sonic limit was made for one of the test pipes using water operating at 60^oF. The limit in this case was 71.4 watts compared to a wick limit of about 46 watts. Therefore, it was not anticipated that any of the test pipes would reach the sonic limit.

2.3.1.1.3 Boiling

In normal operation, a heat pipe operates by evaporation at the liquid-vapor interface in the heated end of the pipe and condensation in the cooled section. At higher input flux, violent boiling can occur within the wick structure of the evaporator and can disrupt and limit performance. The problem, then, is to predict the maximum flux for normal operation.

It is obvious that at fluxes less than that required for the onset of nucleate boiling, the heat pipe will perform satisfactorily. Heat will be conducted through the liquid/wick matrix and vaporize the fluid at the wick boundary. Once nucleate boiling begins, vapor bubbles will form within the wick structure. Unless these bubbles have access to the vapor passage of the pipe, they will eventually block refluxing liquid flow and cause heat pipe burn-out.

Nucleate pool boiling in the fluids of interest typically occurs at less than 20 watts/sq. in. (~ 10,000 Btu/hr-sq. ft) of heat input. Heat pipes designed to this limit are thus either low heat capacity pipes or require large source/pipe interface areas. The heat pipes flown in space to date have been of this type. However, as these elements develop, the area requirement will become excessive for efficient thermal system design. Consequently, the boiling of fluids in wicks has been studied by several organizations.

Costello and Frea (Reference 9-3) studied the pool boiling of distilled and tap water in a fiberglass wick and, under certain conditions, obtained higher critical heat fluxes with wicking than on a plain metallic surface. They theorized that wicking increased wettability, number of nucleation sites, and liquid flow to the heater surface. Allingham and McEntire (Reference 9-4) investigated boiling in a water-saturated fiberglass wick that completely enclosed the heated surface. They calculated boiling film coefficients in the range of

300-1000 Btu/hr-sq ft °F. It should be noted, however, that their experimental apparatus offered more resistance to bubble removal from the wick structure than is normally found in heat pipes. Moss (Reference 9-5) examined the formation of vapor bubbles in a mesh wick using the neutron radiographic method and concluded that the presence of vapor in the wick does not necessarily lead to vapor-lock and burn-out. Kunz, et.al. (Reference 9-6), studied the boiling of water and freon-113 in various wick materials and decided that wick thickness was very important in determining dry-out conditions.

All of the above investigators agreed that vapor bubble escape from the wick structure of a heat pipe is critical to attaining heat fluxes higher than those associated with the onset of nucleate boiling. It has been suggested that, in a 1-g environment, bouyance is the mechanism that removes the bubbles and permits high heat capacities in laboratory-tested heat pipes. If this is true, operation in a 0-g environment must be limited to fluxes below nucleate boiling.

Conway (Reference 9-7) poses another possible mechanism for bubble removal. He suggests that if the wick over the heated surface is kept thin (e. g. , two or three layers of mesh), normal bubble growth will exceed surface tension effects at the wick/liquid/vapor interface and the bubble will escape to the vapor passage. In fact, he and Kelley (Reference 9-8) report attainment of steady state fluxes of 147,000 Btu/hr-sq. ft. (300 watts/sq. in.) in a water-stainless heat pipe with such a wick when all heat was input to the top of the pipe.

Analytical prediction of the boiling limits for heat pipes would be very involved. Such variables as fluid, wick material and configuration, manufacturing irregularities, cleanliness, wettability, and operating temperature should be considered. Some investigators (for example, Reference 9-4) attack the problem on a macroscopic basis, and obtain data correlation in terms of system properties and empirical constants. These equations, however, are for specific wicking configurations and are not generally applicable to heat pipe performance.

At present, the best approach seems to be empirical testing of the proposed pipes. However, if a design limit is required, it is suggested that some fraction, perhaps 1/3, of the critical heat flux (onset of film boiling) be employed. Rohsenow and Griffith (Reference 9-9) give the following correlation for this condition:

$$\frac{Q_{\max}}{A_h} = 143 \lambda \rho_v \left(\frac{\rho_l - \rho_v}{\rho_v} \right)^{0.6}$$

Again Freon-11 was chosen as the sample test fluid to determine the approximate magnitude of the boiling limit. Calculations showed a critical heat flux of about 10,200 Btu/hr-sq. ft. (20.7 watts/sq. in.) or a capacity of 32.5 watts (based on the 1/3 factor) for one particular test pipe. This value is over ten times that of the wicking limit. It was thus concluded that none of the test pipes would reach their boiling limits.

2.3.1.1.4 Wicking

Heat pipe capacity is most often limited by wick restrictions. Consequently, the majority of heat pipe analysis has been done on this subject.

Cotter (Reference 9-10) provided the initial analysis of a wick-limited heat pipe. His basic approach was to equate available capillary head to all accountable pressure losses within the closed fluid cycle. He derived expressions for these pressure terms, and went on to optimize wick configuration for maximum heat transport. Since this time, many investigators have considered a variety of wicking schemes, and all use Cotter's basic approach in theoretical calculations.

Pumping pressure in a heat pipe is provided by the difference in the radii of curvature of the liquid/vapor interfaces in the evaporator and condenser. The usual practice is to assume a spherical meniscus in the evaporator and an infinite curvature in the condenser in which case,

$$\Delta P_{\text{available}} = \frac{2\sigma \cos \theta}{r_c}$$

For heat pipes employing open channel wicks, this pumping head should be divided by two.

The capillary pumping pressure is opposed by pressure drops due to: 1) gravity, 2) viscous and inertial effects in the vapor passage, and 3) viscous and inertial effects in the liquid passage.

The gravitational head is given by:

$$\Delta P_{\text{gravity}} = \left(\frac{g}{g_c}\right) \rho_l \ell \sin \phi$$

Two expressions are given by Cotter for vapor flow pressure drop. The first applies where the radial Reynolds number is significantly less than unity, assumes viscous forces dominate inertial forces, and is determined by:

$$\Delta P_v = \frac{4 \eta_v \ell Q}{\pi g_c \rho_v r_v^4 \lambda}$$

The second equation assumes inertial forces dominate, applies for values of the radial Reynolds number much greater than unity, and is

$$\Delta P_v = \frac{(1 - 4/\pi^2) Q^2}{8 g_c \rho_v r_v^4 \lambda^2}$$

In the region of radial Reynolds numbers of unity, the common procedure is to calculate both and use the larger pressure drop for conservative values of Q_{max} .

The liquid pressure drop is due to viscous effects. All calculations are based on laminar flow and are generally modifications of Darcy's equation to fit the particular wicking arrangements. The following three wicks were analyzed and tested.

1. Conventional. A conventional wick is defined for this program as a multilayer metallic screen structure. Cotter presents the equation below for the pressure drop through this wick.

$$\Delta P_l = \frac{b \eta_l \ell Q}{\pi (r_w^2 - r_v^2) g_c \rho_l \epsilon' r_c^2 \lambda}$$

2. Channel. For heat pipes with grooved channel wicks, the following expression was derived,

$$\Delta P_l = \frac{8 \eta_l \ell Q}{\pi g_c \rho_l N (K_{ch} r_{hw})^4 \lambda}$$

3. Free-Standing Artery. The liquid pressure drop for this type of artery was actually the sum of two drops: 1) that in the artery itself and, 2) that from the tube circumferential wicking into and out of the artery. Thus,

$$\Delta P_l = \frac{Q}{g_c \lambda} \left[\frac{8 \pi \eta_l \ell}{(A_{ar})^2} + \frac{2b \eta_l \pi (r_v + r_{ar})}{4 \rho_l \epsilon' r_c^2} \left(\frac{1}{\ell_e} + \frac{1}{\ell_c} \right) \right]$$

All of the above equations were programmed for a digital computer to determine the wick-limited heat capacity of the tested heat pipes. Predicted values are presented with actual test results in a later section of this report. Appendix B describes the computer program and presents a listing of the code.

2.3.1.2 Temperature Differentials

Calculation of the total temperature differential in a heat pipe is considerably simpler than predicting its maximum heat capacity. The total drop is the sum of the drops through the tube walls, wicks, and vapor flow. Analytical models for these individual differentials can be constructed in a fairly straight forward manner.

Radial conduction through the tube wall at the evaporator produces the temperature drop,

$$\Delta T = \frac{Q}{K}; K = \frac{2 \pi \ell_e k_p}{\ln(r_p/r_w)}$$

The corresponding drop in the condenser wall is given by the similar equation,

$$\Delta T = \frac{Q}{K}; K = \frac{2\pi \ell c_n k_p}{\ell \ln(r_p/r_w)}$$

The differential across the evaporator wick depends on the operating regime. When the input heat flux is below that which causes nucleate boiling, the heat must be conducted radially through the wick/liquid matrix, and the following equation is recommended:

$$\Delta T = \frac{Q}{K}; K = \frac{2\pi \ell_e [\epsilon' k_l + (1 - \epsilon') k_w]}{\ell \ln(r_w/r_v)}$$

The evaporation process from the inner surface of the saturated liquid is, of course, isothermal. At higher heat fluxes, nucleation occurs within the wick structure and the temperature drop calculation is more complex. At present, no purely analytical model has been proposed that satisfactorily predicts the interaction of fluid flow and heat transfer within a porous material. Allingham and McEntire (Reference 9-4) report a data correlation from which a wick boiling film coefficient may be determined. Their equation is

$$\left[\frac{h}{C_l G'} \right] \left[\frac{C_l \eta_l}{k_l} \right]^{0.6} \left[\frac{\rho_l \sigma}{p} \right]^{0.21} = 0.072 \left[\frac{D_e G'}{\eta_l} \right]^{-0.77}$$

where

$$G' = \frac{Q}{A_h \epsilon' \lambda} \frac{\rho_l}{\rho_v}$$

The associated temperature drop is determined from

$$\Delta T = \frac{Q}{hA}$$

The vapor temperature differential from the evaporator to the condenser sections of the pipe is very small in comparison to other drops in the system. Evaluation of this differential can be made using the calculated vapor pressure drop (Section 2.3.1.1.4) and the Clausius-Clapeyron equation,

$$\Delta T = \frac{RT_o^2 \Delta P_v}{M \lambda P}$$

Finally, the heat must be conducted through the wick/liquid matrix at the condenser. The temperature drop is,

$$\Delta T = \frac{Q}{K}; K = \frac{2\pi l_{cn} [\epsilon' k_l + (1 - \epsilon') k_w]}{\ln r_w / r_v}$$

Differentials have been calculated for the various test pipes and conditions. Results are compared to actual test data in a later section of this report.

2.3.2 TEST PROGRAM

A test program was undertaken to provide heat pipe performance data which could be compared to theoretical predictions as discussed in Section 2.3.1. The set of heat pipes constructed for this purpose was chosen to permit the evaluation of several heat pipe variables on performance. The tested pipes, test set-up, and results are presented in this section.

2.3.2.1 Test Heat Pipes

Six heat pipes were fabricated and tested to determine the effect of differences in fluids, wicks, tube shape, length and radius. Selection criteria for the fluids and configurations considered are discussed below.

Two of the heat pipes were tested with four working fluids; water, ammonia, methanol and Freon-11. Each of these fluids has been or will be (in the near future) used in a spaceborne heat pipe. In addition, all are applicable to the space station temperature range.

Three wick configurations were employed. The conventional or multilayer metallic mesh wick was used as a baseline design. Two so-called composite wicks, the free-standing artery and the channel concept, were chosen because of potential for improved performance. Again, all three of these designs either have been or will be used in spaceborne heat pipes. The expense of the regular channel-type wick (approximately \$300 plus \$100 per foot of pipe length from the French Tube Company) prevented its consideration in this Phase I testing. Instead, a simulated channel wick was built up of screen and spacer wires as shown in Figure 2-1. It was hoped that this wick would perform the same as the regular type of channel design and would be much less expensive. The design detail of the artery wick is similar to that employed in the ATS-E heat pipes as reported in Reference 9-11. Figure 2-2 shows this design. All three wicks were uniform along the entire pipe length.

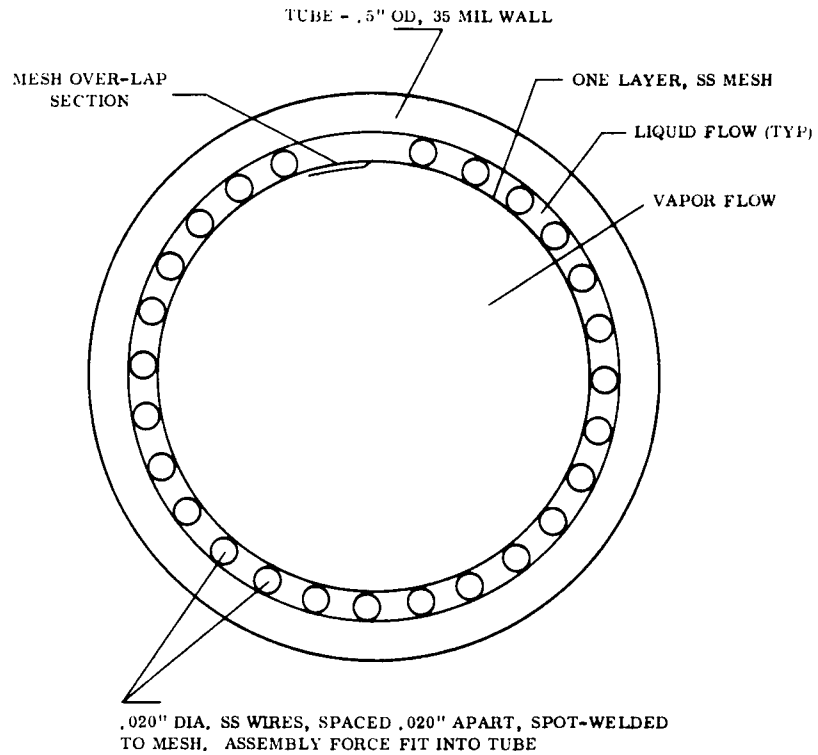
Circular and square cross-section heat pipes were assembled. From stress, weight, and manufacturing viewpoints, the circular cross-section is optimum, while interfacing with sources and sinks is easier with square cross-sections.

Table 2-6 gives the design detail of the six selected configurations. The philosophy was to designate one pipe (Pipe A) as a baseline and, by comparing its performance to that of each of the others in turn, to determine the effect of one variable at a time.

It should be noted that no attempt was made to optimize any of the heat pipes designed for this task. Dimensions and fabrication techniques were chosen on the basis of availability and ease of manufacture.

2.3.2.2 Test Procedure

All heat pipes were ultrasonically cleaned and chemically passivated prior to final assembly. End-caps and fill tubes were welded to each pipe. A valve/pressure gauge unit was attached to the heat pipe to be tested and the entire assembly was pressure-checked to 200 psig.



NOTE: LIQUID FLOW CHANNEL FORMED BY TWO ADJACENT SPACER WIRES, TUBE WALL, AND SINGLE LAYER OF MESH.

Figure 2-1. Simulated Channel Wick

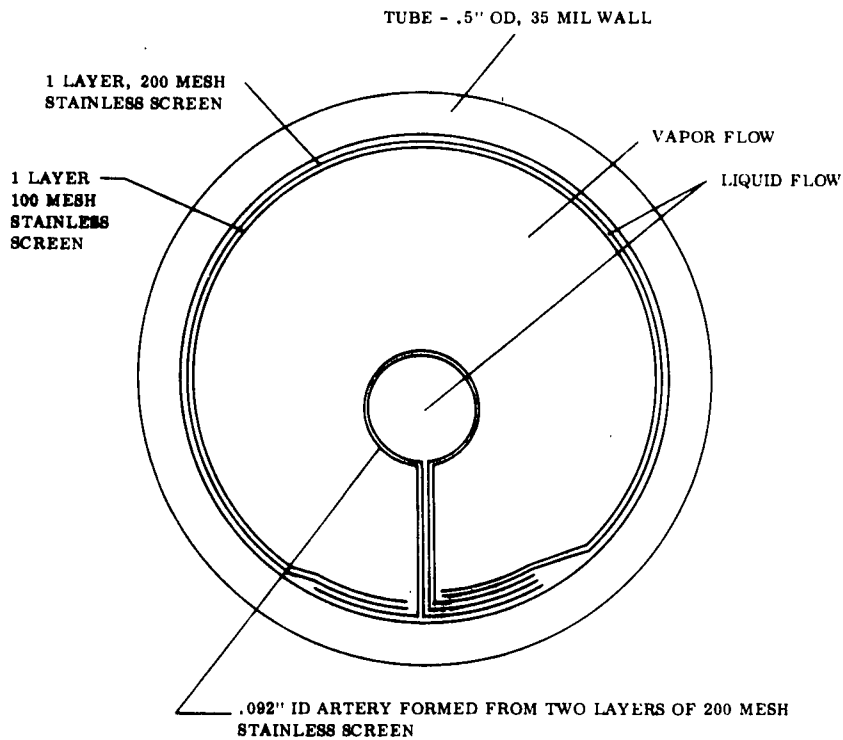


Figure 2-2. Free-Standing Artery Wick

Table 2-6. Design of Tested Heat Pipes

Pipe	Length, ft.	Tube		Wick		Fill, ml
		OD, in	ID, in	Type	Description*	
A	4	.500	.430	Conv.	4 layers of 100 mesh stainless	19.2
B	4	.500	.430	Art.	.092" artery of 200 mesh stainless + 2 layers against tube ID	11.2
C	4	.500	.430	Chan.	26 stainless spacer wires covered by 1 layer 100 mesh stainless	13.9
D	2	.500	.430	Conv.	4 layers of 100 mesh stainless	9.6
E	4	1.000	.902	Conv.	8 layers of 100 mesh stainless	108.6
F	4	Square (1 X 1)		Conv.	100 mesh stainless spot-welded to pipe wall (Aw = .174 sq.in.)	90.3

* "Stainless" infers stainless steel

Note: All tubing 304 stainless steel

A diffusion pump was employed to evacuate the heat pipe and fill system before charging. Water, methanol and freon were transferred to the pipes in the liquid phase from a graduated burette. Ammonia was condensed into the pipes from a metered vapor tank. In all cases, the charge included a small excess of liquid ($\sim 10\%$) over the calculated volumes shown in Table 2-6. Fill tubes were not pinched off because some of the pipes were recharged with different fluids for sequential tests. Between these refillings, the pipes were baked out in an oven above 350°F overnight and re-evacuated to remove all of the previous fluid.

The test arrangement is shown in Figure 2-3. An aluminum collar was machined to be clamped on the one-half inch OD pipes and two cartridge heaters were embedded in this collar to provide a heat source with a source/pipe interface area of 4.71 sq. in. An existing copper collar of similar design was used with the one inch OD pipe and provided an interface area of 6.28 sq. in. The capability of both of these sources was in excess of one kilowatt. The heat sink was an aluminum trough with a cooling (LN_2) coil and a penetration for the heat pipes. The trough was filled with distilled water at the beginning of each test and the LN_2 valve opened. A stir provided circulation within the trough. Ice was allowed to form on the LN_2 coil and testing was begun. As the ice was melted, more LN_2 was admitted so that an ice/water solution was always present, guaranteeing a 32°F constant sink temperature. Time did not permit testing at lower sink temperatures.

Ten copper-constantan thermocouples were used to monitor system temperature. Three of these were spot-welded on the evaporator section, three on the condenser section, two on the adiabatic section, and the remaining two were placed in the heat sink. Thermocouple output was read on a multipoint recorder.

The heater coil and heat pipe adiabatic section were insulated from the ambient environment with a foam-type material and regular closed-cell pipe insulation. Operation of the heat pipe near ambient temperature further minimized heat leaks. Approximate values of these leaks were determined based on observed system temperatures and are presented in the next section of this report. Thermal input to the heat pipe was calculated as power to the heaters minus the heat leaks.

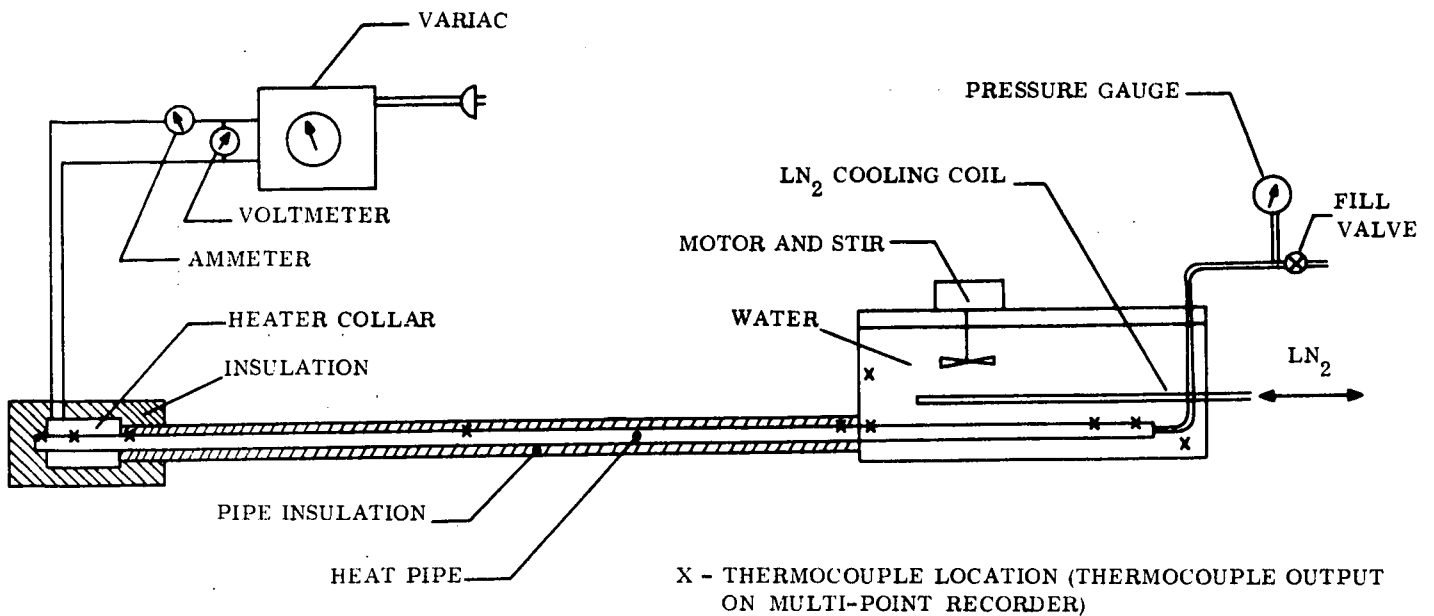


Figure 2-3. Test Set-up

Twelve tests were run with the pipe/fluid combinations shown in Table 2-7. Each test was run until a burn-out occurred (i. e., maximum heat capacity was exceeded). Burn-out was detected by a rapid temperature increase at that point in the evaporator furthest removed from liquid resupply. An attempt was made to burn out each pipe twice, once with the pipe level and a second time with the evaporator end elevated. The Q_{max} condition was approached incrementally from below and temperature data was recorded at each equilibrium point.

2.3.2.3 Test Results

Test data is shown in Appendix C of this report. Burn-out information and temperature differentials are summarized in Table 2-8. Differentials are reported for the last equilibrium point before the instability of burn-out occurred.

Table 2-7. Test Sequence

Test No.	Pipe	Fluid
1	A	Water
2	A	Ammonia
3	A	Methanol
4	A	Freon-11
5	B	Water
6	B	Ammonia
7	B	Methanol
8	B	Freon-11
9	C	Water
10	F	Water
11	D	Water
12	E	Water

Table 2-8. Summary of Burn-Out Conditions From Test

Test No.	Pipe	Fluid	Evaporator Elevation, in.	Input, w	Heat Leak, w*	Q max, w	$\Delta T, ^\circ F^{**}$
1	A	Water	0	53	3	50	9
			1	42	-2	44	6
2	A	Ammonia	0	15	-1	16	8
			1.5	10	-2	12	8
3	A	Methanol	0	15	6	9	5
			1	12	7	5	14
4	A	Freon-11	0	< 5	~	<5	~
5	B	Water	0	37	1	36	7
6	B	Ammonia	0	10	-10	20	19
7	B	Methanol	0	10	-2	12	9
8	B	Freon-11	0	< 5	~	<5	~
9	C	Water	0	35	-12	47	3
10	F	Water	2	250	58	192	24
			2.5	125	2	123	17
11	D	Water	0	97	7	90	8
			1.5	67	-1	68	13
12	E	Water	4.2	150	27	123	25
			5	100	19	81	13

* All values rounded to the nearest watt. Positive value is heat loss, negative value is heat gain.

** ΔT is measured from outer pipe surface at evaporator to outer pipe surface at condenser.

Values of vapor pressure were not recorded during testing. The insensitivity of the available pressure gauges in the temperature range of interest prevented the use of the measurements in an analytical manner. The gauges were used qualitatively to determine leaks and as an indication of relative changes in vapor temperature.

A simple test was performed after each burn-out to partially assess the failure mode. The heat pipe was tilted with the evaporator below the condenser while the input power was left unchanged from its burn-out value. Temperature response of the evaporator section was noted. If the heat pipe recovered (i. e., temperatures returned to the pre-burn-out values) it was concluded that the pipe had been wick or boiling limited. Failure due to entrainment or sonic vapor velocity is not a function of orientation in a 1-g field and consequently recovery from these failures by tilting is not possible.

In all of the heat pipes tested, normal operation could be restored by this tilting test. Therefore, all burn-outs were caused by wicking or boiling failures. Differentiation between these failures will be discussed in the next section.

2.3.3 THEORETICAL - EMPIRICAL CORRELATION

A comparison of theoretically and empirically determined Q_{max} and ΔT for the twelve test points is shown in Table 2-9. Test data has been extrapolated where necessary to burn-out conditions at zero evaporator elevation. Thus, all values in Table 2-9 correspond to 0-g heat pipe performance.

Various conclusions can be drawn from these results concerning the effects of fluid, tube shape, and wick configuration on heat pipe operation. These will be discussed below.

1. The four test fluids affected performance about as expected. In both pipe A and pipe B, water was the best fluid, followed by ammonia, methanol and Freon-11. The actual burn-out points for both Freon-11 pipes were below five watts. No attempt was made to test at lower than five watts because heat leaks were of this same magnitude.

Table 2-9. Comparison of Theoretical and Actual Results

Test	Pipe	Fluid	Theoretical		Actual	
			Q max, w	$\Delta T, ^\circ F^*$	Q max, w	$\Delta T, ^\circ F$
1	A	H ₂ O	37	7	50	9
2	A	NH ₃	29	5	16	8
3	A	CH ₃ OH	8	2	9	5
4	A	R-11	3	1	< 5	~
5	B	H ₂ O	735	70	36	7
6	B	NH ₃	1080	103	20	19
7	B	CH ₃ OH	380	37	12	9
8	B	R-11	93	10	<5	~
9	C	H ₂ O	347	54	47	3
10	F	H ₂ O	291	20	364	24
11	D	H ₂ O	90	12	90	8
12	E	H ₂ O	210	16	212	13

Note: ΔT based on theoretical burn-out heat flux

2. Tube shape has little effect on heat pipe operation. Calculations for Test 10 (square pipe F) were made by scaling appropriate pressure losses (as determined for circular pipes) to account for the different cross-section. As can be seen, the ratio of theoretical to actual Q max. for tests 1 and 10 are about equal, indicating that no unexpected difficulties in square heat pipe operation were encountered.
3. For calculation of Q max. with conventional wicks, the value of "b" in the liquid viscous pressure drop equation was chosen as 15. Tests 1 and 10 indicate that a value of 12 will match data more closely. However, in tests 11 and 12 the original value was shown to be very close. This discrepancy is apparently a result of differences in wick fabrication and installation procedures. It is thus concluded that the value of "b" cannot be closely controlled. A value of 12 is recommended to yield slightly conservative burn-out levels.
4. Comparison of calculated and actual Q max. for the free-standing artery wick indicate that the artery was never completely full. This condition negates the purpose of the artery and the performance attained is solely due to wicking within the mesh forming the structure. Results show that this situation occurred during testing (comparing calculated and actual Q max).

The artery would not fill under any of the following conditions: a) the artery improperly made, b) non-condensable gas entrapped in the artery, c) insufficient charge of fluid. At the conclusion of test 5, the charge of water in the pipe was increased to 205% of the calculated fill, and the test was repeated with no significant change in burn-out level. This would indicate that the artery was not fabricated correctly or that a non-condensable was present. Further testing is necessary to determine which of these two alternatives apply.

5. The theoretical value of Q max. listed in Table 2-9 for Test 9 (simulated channel wick) is based on a wick-limited heat pipe. Test 9 results indicate a much lower burn-out point and some time was spent trying to explain this reduction.

The covered channel wick depends on the single screen layer for its pumping pressure and uses the spaces between the 0.020 inch wires as liquid flow passages. If the liquid loses contact with the screen in the evaporator, pumping will be severely reduced. This is thought to be the situation in Test 9. The liquid will separate from the screen if vapor bubbles form within the liquid channels and create a back-pressure on the liquid flow. Failure due to vapor bubble formation and growth will occur when the local superheat at the heated surface exceeds that which can be supported by the surface tension within liquid in the channel. In other words, the pressure within the vapor bubble breaks the liquid film in the channel.

Calculations based on wick construction, observed Q_{max} , and the Classius-Clapeyron equation show that this condition existed in Test 9. The critical temperature differential across the liquid within the flow passages was determined as 9.5°F . Based on pure conduction through the liquid at the burn-out point, the differential could have been as high as 19°F , enough to cause failure by vapor bubble formation. The fact that the heat pipe supported the flux that it did indicates that conduction through the stainless wire spacers aided in lessening the temperature stratification across the liquid.

It should be noted that regular channel wick heat pipes (grooves milled into the tube ID) experience much less temperature gradient across the liquid channels because of the integral heat conduction "fins" provided. These pipes can thus attain higher Q_{max} values than the tested unit with stainless steel space wires.

6. Results from Tests 1, 11 and 12 indicate that, for heat pipes operating in the normal housekeeping temperature range and under moderate heat loads, Q_{max} is an inverse function of effective length and a direct function of wick cross-sectional area (conventional wicks).
7. Calculated temperature differentials through the heat pipes agreed favorably with those observed during testing. It should be remembered that the theoretical ΔT values in Table 2-9 are based on the theoretical Q_{max} . Differentials can be scaled directly to obtain actual values.

2.4 SUMMARY AND CONCLUSIONS

The objective of Phase I of this project was to review the technology of thermal control elements and to evaluate the applicability of each to a long life, high reliability thermal control system for the Space Station. In addition, an analytical and empirical study of heat pipes was to be performed to permit accurate sizing of these elements in conceptual system designs. This report summarizes the results of this effort.

Data compiled on all elements investigated during Phase I was assembled into a data handbook. Section 2.2 discusses the selection of two most desirable elements in each of several classes. The major conclusions of this task are listed below.

1. A series emittance tape (second surface reflector) of Teflon on aluminum was judged the best of the low α_s/ϵ coatings available. Z-93 white paint was the best of the "conventional" coatings.

2. C6A black paint and aluminum leaf paint were selected in the mid α_s/ϵ coating range, with emissivities of about 0.9 and 0.3 respectively.
3. Of the high α_s/ϵ coatings, a metallic film with an oxide overcoat was found most desirable.
4. Multilayer metallized plastic film structures were chosen as the optimum insulations systems. Specifically, aluminum on mylar or gold on kapton were recommended.
5. Louver systems with bimetallic actuation and polished aluminum blades were selected over those with fluid actuation and more complex blade designs.
6. Tetradecane and hexadecane, two of the normal paraffins, are recommended as phase change materials for heat of fusion devices.
7. No rating was performed for space radiators, boilers and sublimators because selection of these components depends on specific application parameters.

It should be noted that the various space station thermal control concepts developed in Phase II may necessitate the use of elements other than those recommended above. These choices are made for a general, long life thermal control systems and do not include localized requirements and constraints.

Comparison of theoretical and empirical heat pipe performance yielded the following conclusions:

1. Effects of tube shape, fluid, length and diameter can be adequately predicted using the theoretical model.
2. Analytically determined temperature drops from heat source to heat sink approximated those observed during testing.
3. The maximum heat capacity for heat pipes with conventional (multilayer metallic mesh) wick can be predicted with a good degree of confidence.
4. The simulated channel wick made up of mesh and stainless wire should not be employed in the evaporator section of the heat pipe. Vapor bubble formation within the liquid flow channels significantly degrades performance.

5. Extreme care must be exercised in the fabrication and charging of heat pipes using free-standing artery wicks. Results indicated that the artery of such a pipe tested did not fill completely with liquid.

In total, Phase I has provided, a) data on various thermal control elements, b) a list of the most desirable elements for a high reliability system, and c) a better understanding of heat pipe operation. These items will be used extensively during concept generation and evaluation in Phase II.

SECTION 3

PHASE II

3.1 SCOPE

The objective of Phase II was to conceptually design and analyze a passive long life, high reliability thermal control system for a specific Space Station configuration. A further objective was to demonstrate the adaptability of the selected system to other spacecraft of similar thermal constraints.

Section 3.2 describes the vehicle requirements and constraints assumed, the preliminary analyses performed, the concepts investigated, and the selection of two systems for more detailed study. These two systems are discussed in depth in Section 3.3. It should be emphasized that the requirements and constraints established in Section 3.2 for preliminary concept evaluation and selection were updated in Section 3.3 prior to final concept evaluation to provide a more accurate comparison with the baseline pumped loop system.

3.2 CONCEPT FORMATION AND SELECTION

The following tasks were designated to define and select two potential long life, high reliability thermal control systems for further study.

1. Definition of Requirements and Constraints of Specific Space Station Configuration
2. Definition and Analysis of Credible External Environments of this Vehicle
3. Generation of Parametric Heat Rejection Data
4. Generation and Preliminary Analysis of Several Proposed System Concepts
5. Selection of Two "Best" Concepts

Each of these tasks will be discussed in the following subsections.

3.2.1 REQUIREMENTS AND CONSTRAINTS

The NASA/MSFC-McDonnell Douglas Astronautics Company version of the 33 foot diameter Space Station was considered baseline for heat pipe system incorporation. Specific Space Station design requirements and constraints employed in Phase II work were obtained from two sources: (a) the statement of work in the original RFP, and (b) McDonnell Douglas Space Station documents provided by the NASA/MSFC technical monitor (References 9-12 to 9-16).

In most cases, the MDAC reports clarified or expanded the provisions of the statement of work. The few points of conflict were resolved in favor of the statement of work pending customer approval. Phase II tasks up to and including concept generation, evaluation and selection were based on the integrated list of requirements and constraints shown below. The assumed parameters which were modified per customer direction at the start of the detailed analysis task in Section 3.3 are not incorporated below. They will be discussed in Section 3.3.

3.2.1.1 Configuration Definition (See Figure 3-1)

1. Station consists of two stacked "common modules", interconnecting 10' diameter tunnel, and equipment/power bay in conic nose section.
2. Each common module contains two stacked decks. Decks are consecutively numbered from 1 to 4, with Deck 1 being furthest from the power module.
3. Reference Space Station for all Phase II analyses will utilize an Isotope/Brayton EPS.
4. Outer cylindrical wall surrounding the two common modules will be employed as a space radiator. Radiation area available is 3,000 sq. ft.
5. Effect of docked modules on thermal performance will be evaluated as a percent blockage on the radiator.
6. The ends of the manned portion of the station will be assumed unavailable for EC/LS radiator.

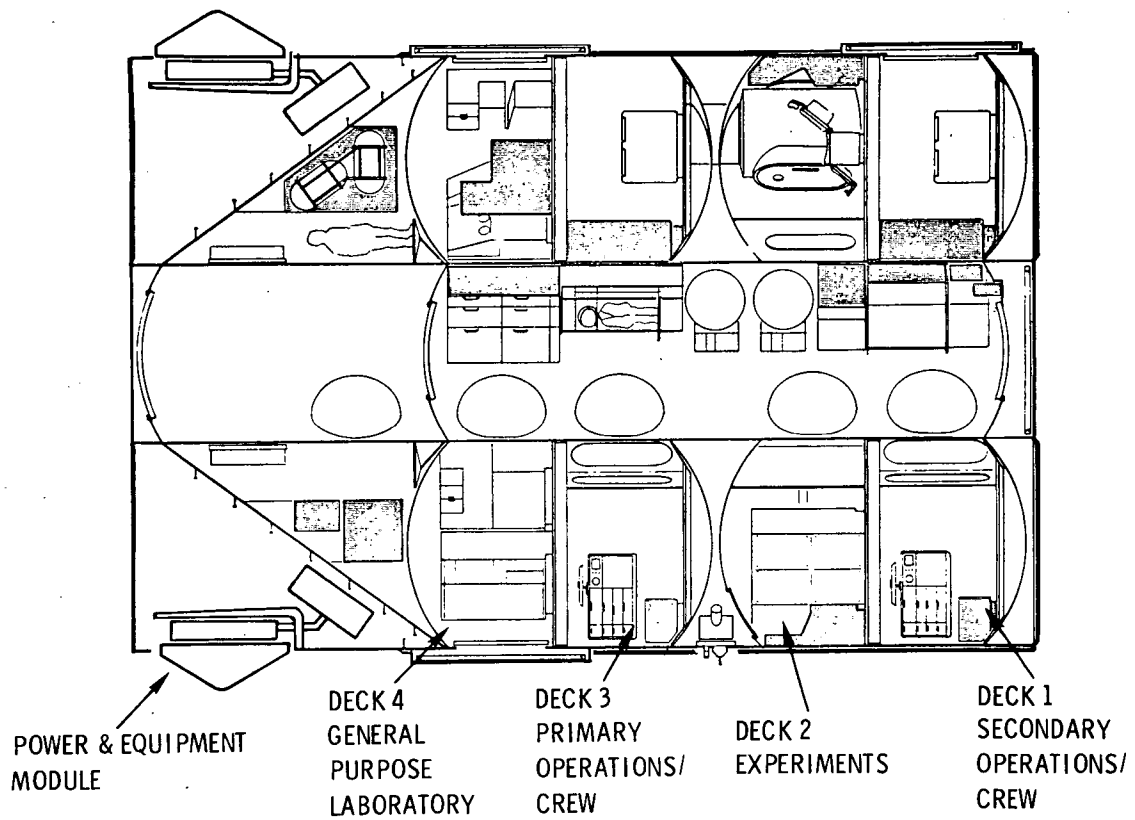


Figure 3-1. Nominal Space Station Configuration

3.2.1.2 Orbital Heating Parameters

1. Nominal values of orbital heating constants will be as follows:

$$\begin{aligned} \text{Solar Flux}^*(S) &= 429 \text{ Btu/hr-ft}^2 \text{ (1-sigma tolerance = } \pm 2.12 \text{ Btu/hr-ft}^2\text{)} \\ \text{Albedo Factor (a)} &= .30 \text{ (1-sigma tolerance = } \pm .06\text{)} \\ \text{Earth Flux (E)} &= 75.3 \text{ Btu/hr-ft}^2 \text{ (1-sigma tolerance = } \pm 6.65 \text{ Btu/hr-ft}^2\text{)} \end{aligned}$$

*Seasonal variation: +3.43%, - 3.26%

2. Seasonal variations and 2-sigma limits (stacked) on the above constants are combined to yield the following extreme heating conditions:

$$\begin{aligned} \text{Minimum: } S &= 411 \text{ Btu/hr-ft}^2, a = .18, E = 62.0 \text{ Btu/hr-ft}^2 \\ \text{Maximum: } S &= 448 \text{ Btu/hr-ft}^2, a = .42, E = 88.6 \text{ Btu/hr-ft}^2 \end{aligned}$$

3. Surface α/ϵ ratios will be considered as shown below:

<u>α/ϵ</u>	<u>α</u>	<u>ϵ</u>	<u>Description</u>
.194	.13	.67	Beginning of life (BOL) for 2 mil Teflon on Aluminum series emittance tape
.299	.20	.67	Anticipated end of life (EOL) (After one year) for above tape
.189	.17	.90	Beginning of life for Z - 93 white paint
.400	.36	.90	MDAC anticipated EOL values for Z-93 white paint (for comparative purposes)
.205	.17	.83	Beginning of life for 5 mil Teflon on Aluminum series emittance tape
.301	.25	.83	Anticipated EOL values (after 1 year) for 5 mil Teflon on Aluminum series emittance tape

4. Thermal coatings will be replaced when the design end of life properties have been reached. The internal dissipation will be reduced if required to either: allow adequate replacement time; or continue operation with further coating degradation.

3.2.1.3 Internal Thermal Loads

1. Table 3-1 defines the EC/LS system components which must be cooled, and the steady state heat dissipation and temperature requirements of each. These values will be used in nominal case calculations.
2. Maximum and minimum internal dissipation levels will be determined by applying +20% and -30% factors, respectively, to the nominal case values as given in Table 3-1.

3.2.1.4 General Constraints

1. Life - Minimum life is ten years with refurbishment possible on a two to three years cycle. Resupply cycle for expendables is nominally 90 days with 180 days maximum.
2. Artificial G - During the first two years of operation, artificial gravity will be imposed on the Station by rotating it at a low spin rate (2 to 4 rpm) for a time sufficient to permit thermal equilibrium to occur. G levels of from .3 to .7 are expected. Docking of separate modules will not be permitted during artificial "g" operations, to that effective blockage will be zero.
3. Penetrations - Present penetrations through the station pressure shell include RCS thruster lines, seven docking ports, view ports, air locks, fluid lines and electrical harness. The requirement for additional penetrations will not eliminate candidate conceptual thermal system designs, but will be considered a negative factor in the evaluation of such systems.
4. Commonality - Commonality and modular designs will be stressed in conceptual systems.
5. Shielding - Micrometeoroid shielding will be provided in all designs to protect the pressurized portion of spacecraft. It will be assumed (per MDAC studies) that a .020 inch thick aluminum shield backed up by a .010" aluminum shield is sufficient (see Figure 3-31).
6. Condensate - No condensation of atmospheric water vapor will be allowed within the pressurized portion of the Station.
7. Redundancy - All conceptual systems will be designed so that either common module plus the interconnecting tunnel will support twelve men for an indefinite time.

Table 3-1. Nominal Case Internal Dissipations

	Dissipation per Common Module, Btu/hr	Temperature Required °F
<u>COMPONENT</u>		
IVA Support	2,000	45
H ₂ O Chiller	500	45
CO ₂ Conversion	572	45
H ₂ O Electrolysis	1,410	45
Temperature and Humidity Control	12,300	45
Battery	2,000	65
Urine Recovery	8,100	65
CO ₂ Removal	12,176	65
Shower/Dishwasher/ Clothes Washer	--	65
Cold plates	29,211	65

Total dissipation = 68,269 Btu/hr per Common Module

= 136,538 Btu/hr for entire Station

(33,564 Btu/hr at 45° F,

102,974 Btu/hr at 65° F)

3.2.2 THERMAL ENVIRONMENT

The most important parameters effecting the thermal environment of a space vehicle are the beta angle (the angle between the orbital plane and the sun vector), orbit altitude, and orientation with respect to the earth and sun. Of lesser importance are the yearly solar intensity variations, statistical variations of solar flux (caused by measurement uncertainties) and variations in albedo factor and earthshine (caused by local earth temperature, cloud cover and terrain).

It is necessary to define the above parameters to evaluate the boundary conditions on a particular vehicle. Because the Space Station is to be operated in a wide variety of orbits and orientations, it was impossible to define and analyze all possible conditions. Instead, a number of apparent "worst-case" orbit/orientation sets were generated within the following guidelines:

1. 55 degree inclination, 200 to 300 nautical mile altitude orbit
2. Sun synchronous, 270 nautical mile altitude orbit
3. Polar, 270 nautical mile altitude orbit

The six "worst-case" conditions selected for evaluation are shown in Table 3-2. These sets were chosen to establish bounds on possible thermal environments in terms of absolute level and rate of change.

The parameter chosen to represent total thermal environment was effective sink temperature. In the absence of molecular heating (as is the case for all orbits under consideration), sink temperature is defined by:

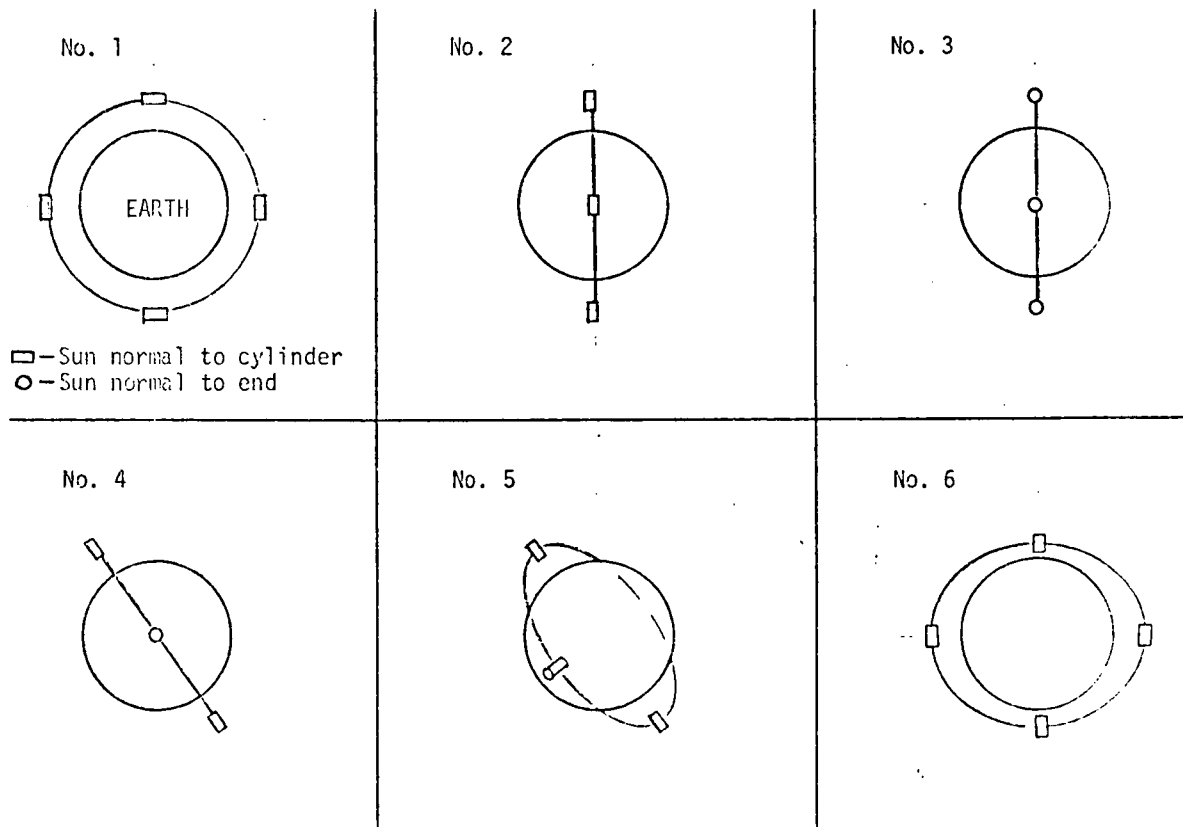
$$T_{sK} = \left(\frac{\alpha/\epsilon (S+A) + E}{\sigma'} \right)^{1/4}$$

Table 3-2. Orbit/Orientation Sets to be Considered

No.	Description	Day	Alt, nm	Incl. deg	Beta, deg	Flux Level*	Stabilization
1	Hottest Average	80	270	90	90	Max	Earth
2	Hottest Instantaneous	356	270	90	0	Max	Sun
3	Coldest Average	173	270	90	0	Min	Sun
4	Large Local Transient	80	246	55	0	Nom	Earth
5	Nominal	80	246	55	45	Nom	Earth
6	Nominal-hot	356	246	55	78.5	Max	Sun

*Refers to statistical range only. Seasonal variation will correspond with designated day of year.

ORIENTATION: Sun rays normal to plane of paper. (Into Page)



The data of Table 3-2 was input to an "Orbital Heat Flux" (OHF) computer program to calculate values of incident solar flux (S), incident albedo flux (A) and incident earth flux (E) as functions of orbit time and circumferential position on the EC/LS radiator for the six orbit/orientation sets. The cylindrical radiator was divided into twelve 30⁰ segments for analysis.

The output of the OHF program, along with the absorptance and emittance values stated in Section 3.2.1.2 was input to a Post Processor computer code which calculated and plotted T_{SK} as a function of time. The Post Processor was also set up to determine and plot the instantaneous, cylinder-average sink temperature. Appendix A presents all of the sink temperature graphs generated.

Table 3-3 summarizes the environment study results. In this table, the Orbital average, minimum, and maximum sink temperatures averaged around the cylindrical radiator are tabulated for six orbit/orientation sets and three α/ϵ ratios for series emittance tapes and Z-93 paint. The following conclusions may be drawn about the severity of the Space Station thermal environment:

1. If the tape coating is used, the maximum and minimum orbital average, radiator average sink temperatures will be 329⁰R (orbit number 3, BOL properties) and 451⁰R (orbit number 1, EOL properties), respectively.
2. Corresponding sink temperatures for the Z-93 coating are 329⁰R (with BOL $\alpha/\epsilon = 0.19$, same as tape BOL) and 471⁰R.
3. The most severe transient sink for the radiator as a whole occurs in orbit number 2 (Beta angle 0⁰, sun stabilized).
 - a. If tape is employed, the maximum orbital sink temperature range is 84⁰R (BOL) increasing to 136⁰R as the absorptance of the tape degrades to 0.20.
 - b. If Z-93 is used, this range is 84⁰R (BOL) increasing to 161⁰R as the absorptance of the paint degrades to 0.36.
4. The sink temperatures calculated for orbit numbers 4, 5, and 6 fall within the bounds listed above in both level and transients.

Table 3-3. Environment Summary

Orbit No.	Radiator Average Sink Temperature (^o R)					
	BOL Tape and Z-93 ($\alpha/\epsilon = 0.20$)		EOL Tape ($\alpha/\epsilon = 0.30$)		EOL Z-93 ($\alpha/\epsilon = 0.40$)	
	Ave.	Min/Max	Ave	Min/Max	Ave	Min/Max
1	426	426/426	451	451/451	471	471/471
2	407	342/426	429	342/478	447	342/503
3	329	312/332	332	313/340	334	313/343
4	375	330/408	394	330/434	409	330/457
5	386	330/409	407	330/437	426	330/460
6	423	416/428	449	441/453	470	462/474

It should be noted at this point that the values cited above were determined using worst-case 2-sigma heating constants. In other words, for the anticipated "hot" orbits, +2 sigma limits on solar flux, albedo factor, and earthshine were employed. For "cold" orbits, -2 sigma limits were used. Nominal constants were used for "nominal" orbits. At the conclusion of this study, orbit numbers 1 and 3 (hot and cold) were re-examined using 3 sigma limits. The effect on radiator average sink temperature was found to be negligible, increasing the "hot" temperature by 4^oR in orbit number 1 and decreasing the "cold" temperature by 12^oR in orbit number 3 ($\sigma \cdot T^4$ change is negligible for this swing). It was therefore concluded that the 2 sigma results were acceptable for use in all thermal analyses.

3.2.3 PARAMETRIC RADIATOR STUDY

The purpose of the parametric radiator study was to provide working curves relating heat dissipation, radiator temperature, sink temperature, radiator area and surface emissivity for future tasks. Blockage effects, discussed in Section 3.3.4.2, were not included in this evaluation. Some radiator weight optimization was carried out to indicate preferred approaches to radiator design in system concept generation.

3.2.3.1 Radiator Thermal Balance

An energy balance was written for a plate radiating from one side only as:

$$Q = \eta' \epsilon A (\sigma' T_r^4 - \sigma' T_{sK}^4)$$

The fin effectiveness, η' , is defined as the ratio of heat rejected from the radiator area to that which would be rejected if the radiator temperature were constant at the root temperature value. Figure 3-2, obtained from Reference 9-17, provides a means of calculating the fin effectiveness as a function of the generalized length parameter and source/sink temperature ratio.

A set of curves, based on this equation, that define parametrically the requirements and capabilities of the Space Station radiator are presented on Figures 3-3 to 3-15. The range of each of the variables considered was as shown below.

Variable	Range
Q	0 to 170,000 Btu/hr
$\eta' \epsilon$	0.5 to 0.9
A	0 to 4,000 ft ²
T _r	-40 to +60 ^o F
T _{sK}	250 ^o R to 500 ^o R

Without regard to actual system design, the following conclusions could be drawn by comparing this plotted data to the requirements and constraints as presented in Section 3.2.1.

1. The radiator must be designed to operate at temperatures as high as possible. This implies that the temperature drop between the internal heat dissipators and the radiator must be kept as small as practical.

$$L = \ell \sqrt{\frac{\sigma' \epsilon (10^9)}{K_R t'}} \left(\frac{T_0}{1000} \right)^3$$

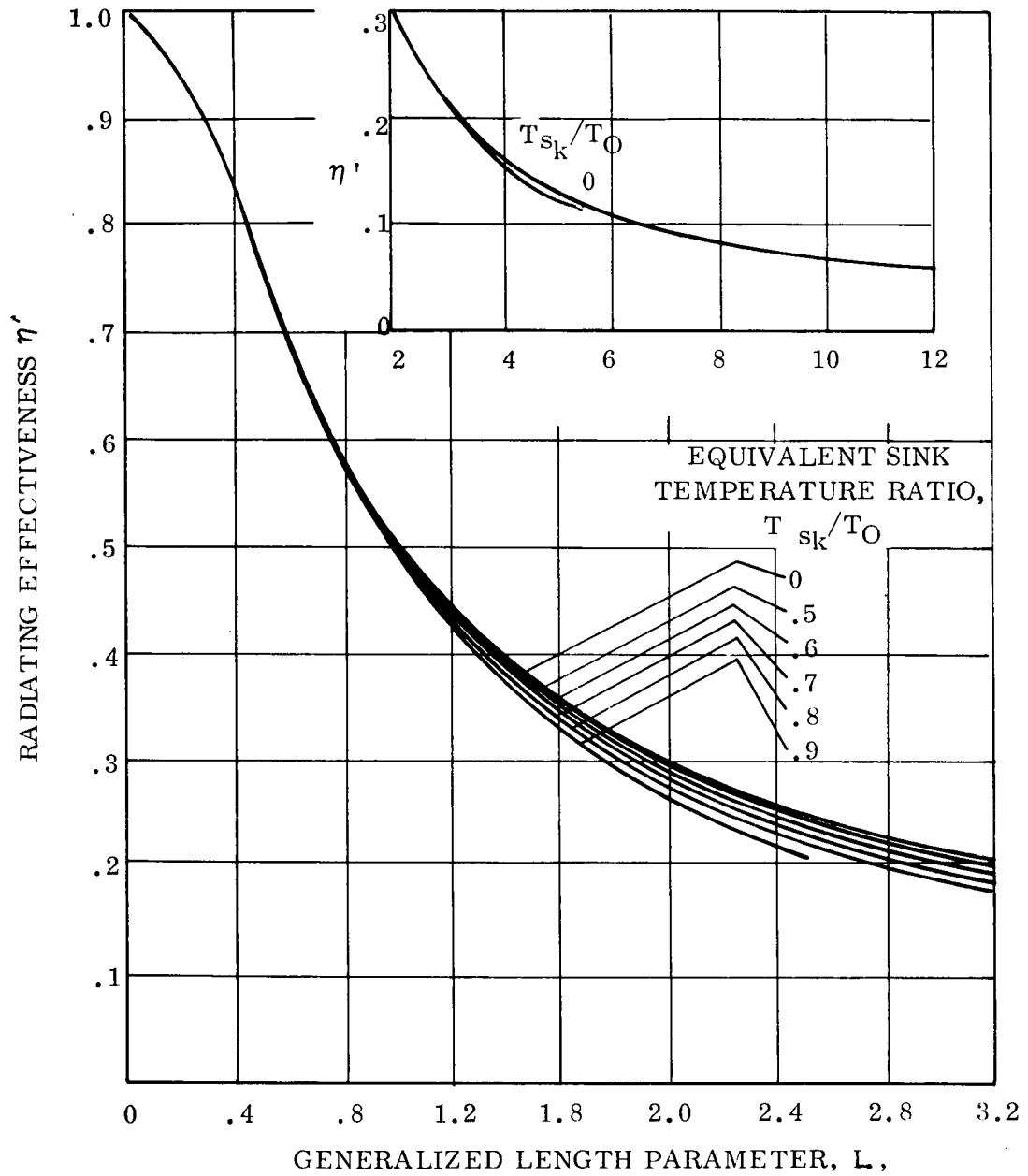


Figure 3-2. Variation of Fin Effectiveness with Length

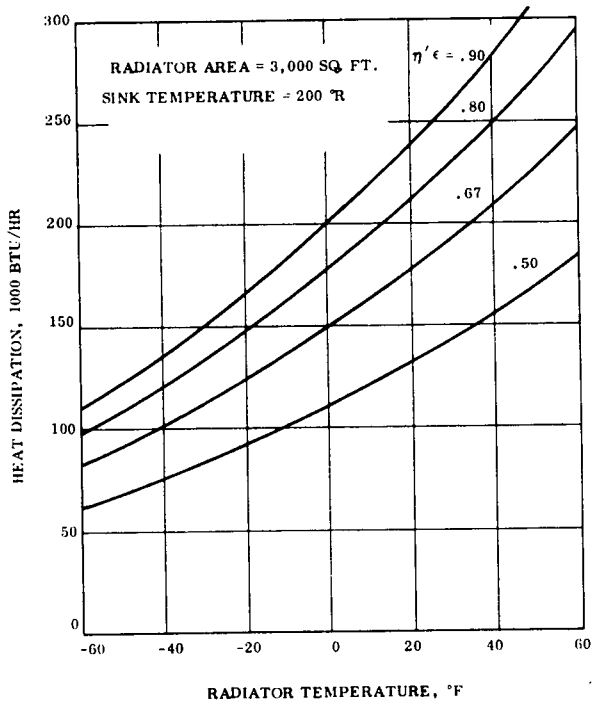


Figure 3-3. Heat Dissipation vs Radiator Temperature and $\eta'\epsilon$ Product - 3000 ft² Area and 200°R Sink

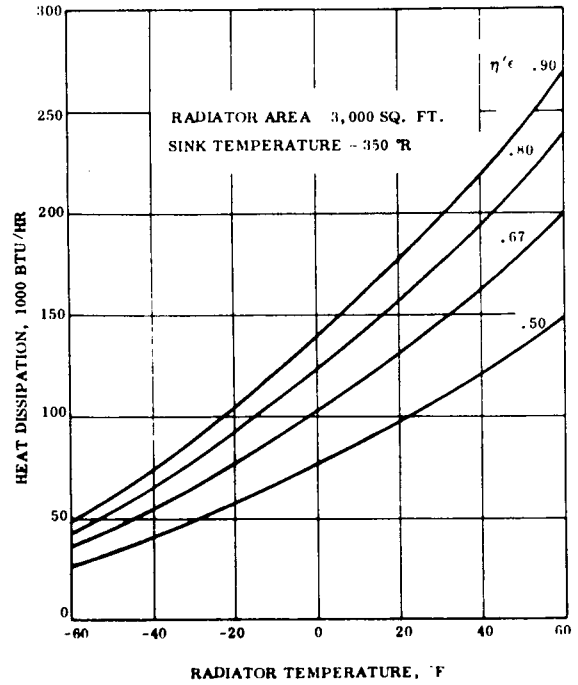


Figure 3-4. Heat Dissipation vs Radiator Temperature and $\eta'\epsilon$ Product - 3000 ft² Area and 350°R Sink

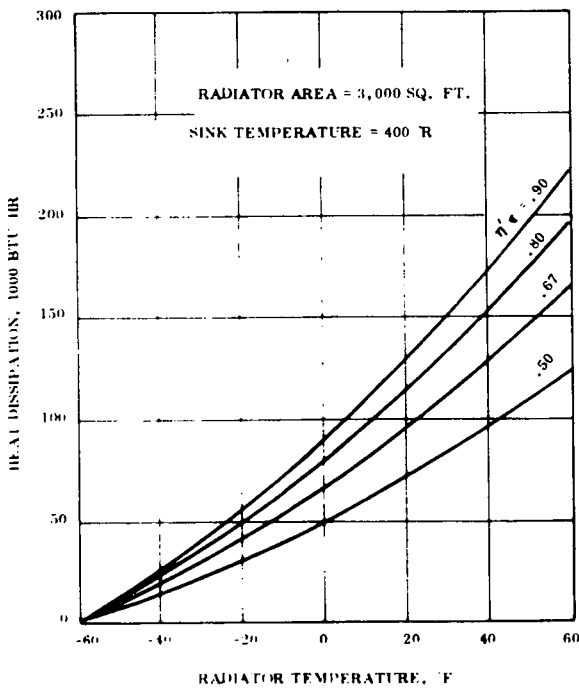


Figure 3-5. Heat Dissipation vs Radiator Temperature and $\eta'\epsilon$ Product - 3000 ft² Area and 400°R Sink

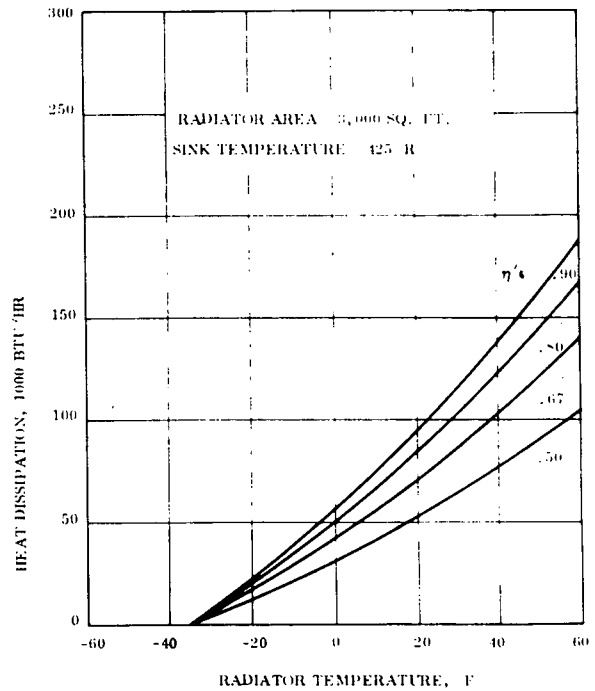


Figure 3-6. Heat Dissipation vs Radiator Temperature and $\eta'\epsilon$ Product - 3000 ft² Area and 425°R Sink

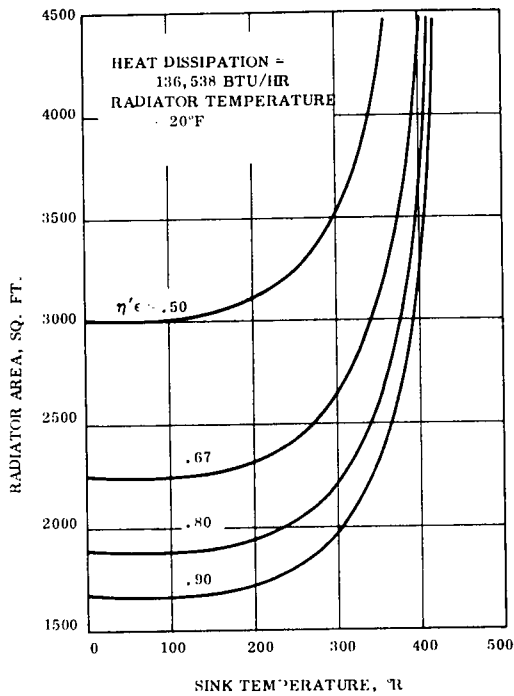


Figure 3-7. Radiator Area vs Sink Temperature and $\eta'\epsilon$ Product - 136,538 Btu/hr and 20°F Radiator

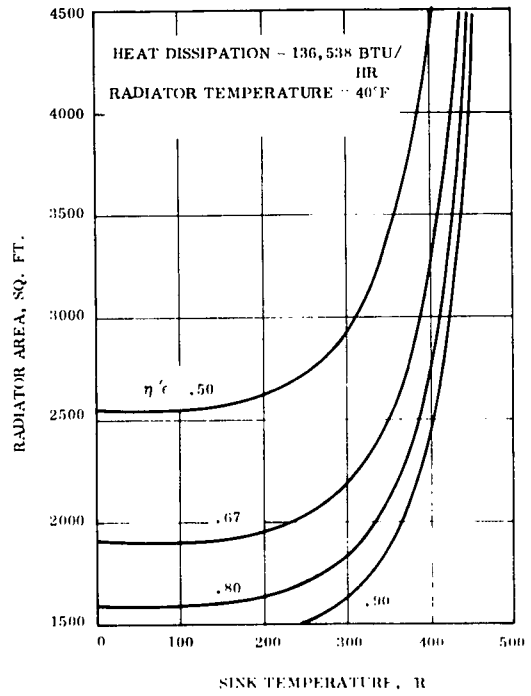


Figure 3-8. Radiator Area vs Sink Temperature and $\eta'\epsilon$ Product - 136,538 Btu/hr and 40°F Radiator

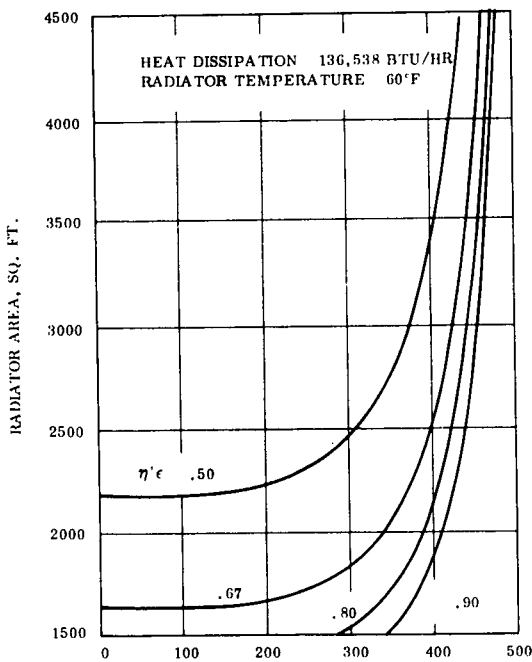


Figure 3-9. Radiator Area vs Sink Temperature and $\eta'\epsilon$ Product - 136,538 Btu/hr and 60°F Radiator

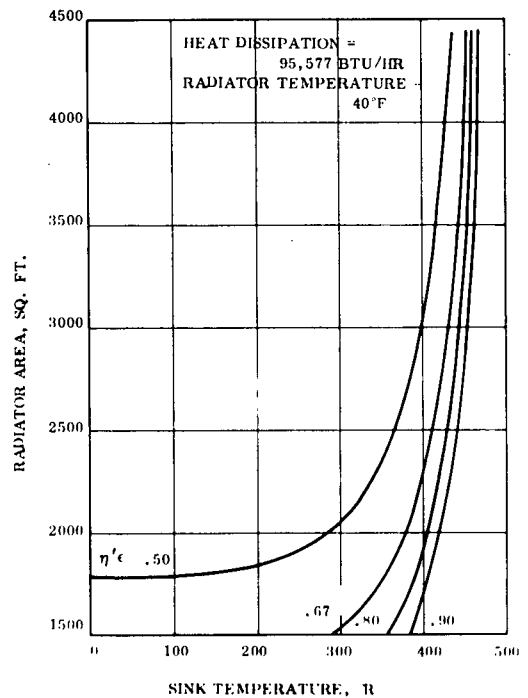


Figure 3-10. Radiator Area vs Sink Temperature and $\eta'\epsilon$ Product - 95,577 Btu/hr and 40°F Radiator

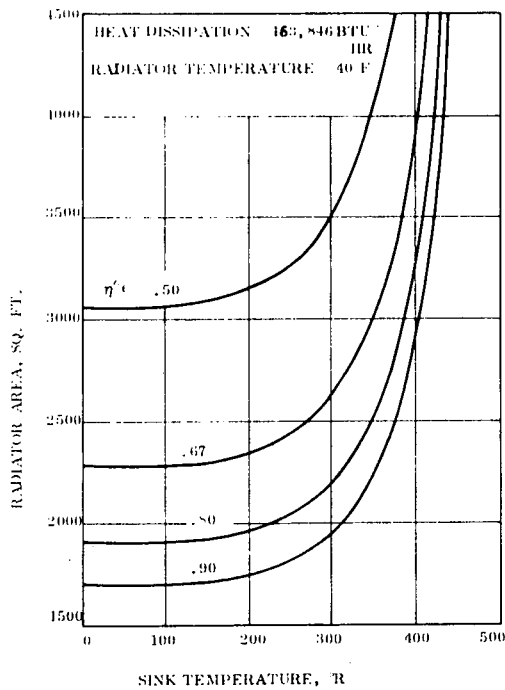


Figure 3-11. Radiator Area vs Sink Temperature and $\eta'\epsilon$ Product - 163,846 Btu/hr and 40°F Radiator

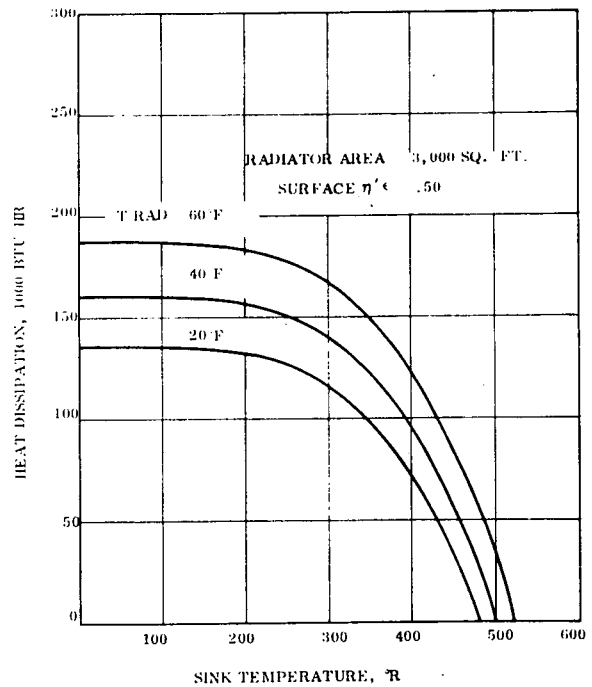


Figure 3-12. Heat Dissipation vs Sink and Radiator Temperature - 3000 ft² and $\eta'\epsilon$ of 0.50

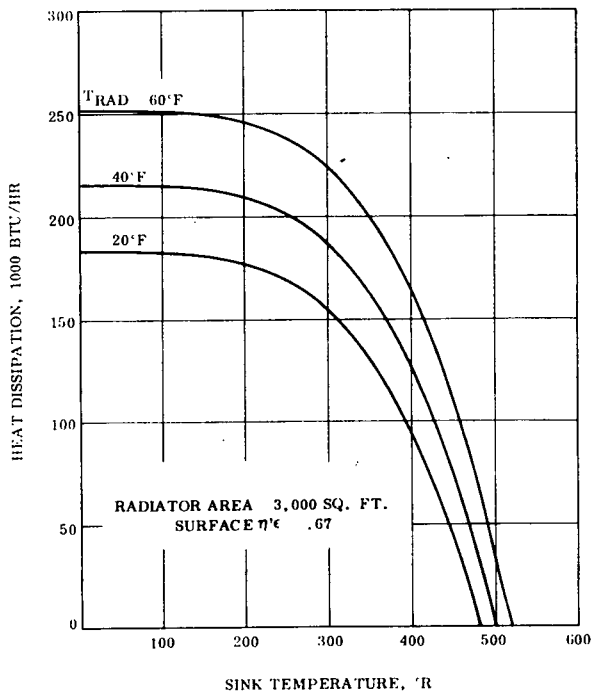


Figure 3-13. Heat Dissipation vs Sink and Radiator Temperature - 3000 ft² and $\eta'\epsilon$ of 0.67

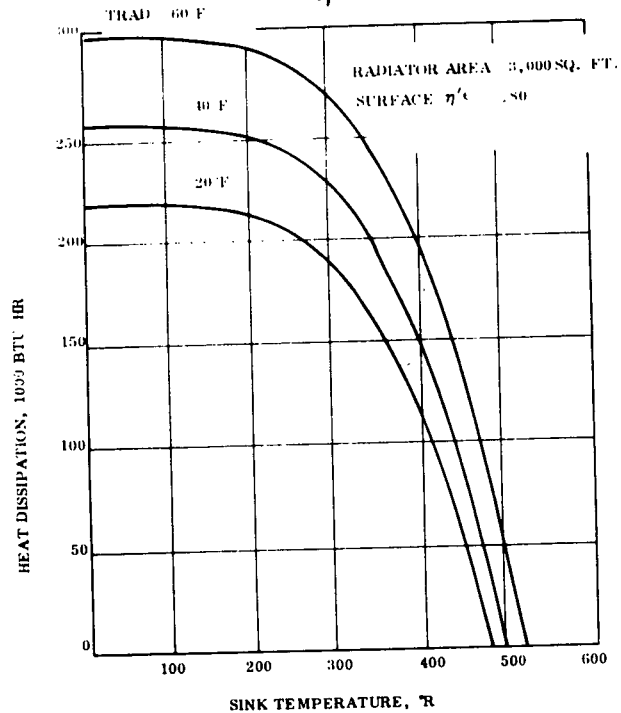


Figure 3-14. Heat Dissipation vs Sink and Radiator Temperature - 3000 ft² and $\eta'\epsilon$ of 0.80

2. The $\eta'\epsilon$ product must be at least 0.7 (which can be achieved with either a 5 mil tape or white paint) and should be 0.8 (which can only be achieved with a white paint).
3. Even with the two above provisions, operation in the "hot" environmental conditions (inclination angle of about 46° or greater, solstice period, sun-oriented vehicle) must be limited by reducing internal dissipation to maintain acceptable component temperatures.

It should be emphasized that these statements are valid with respect to the defined requirements and constraints. Later modification of some of these assumptions permitted more flexibility in the detail design of two preferred system concepts.

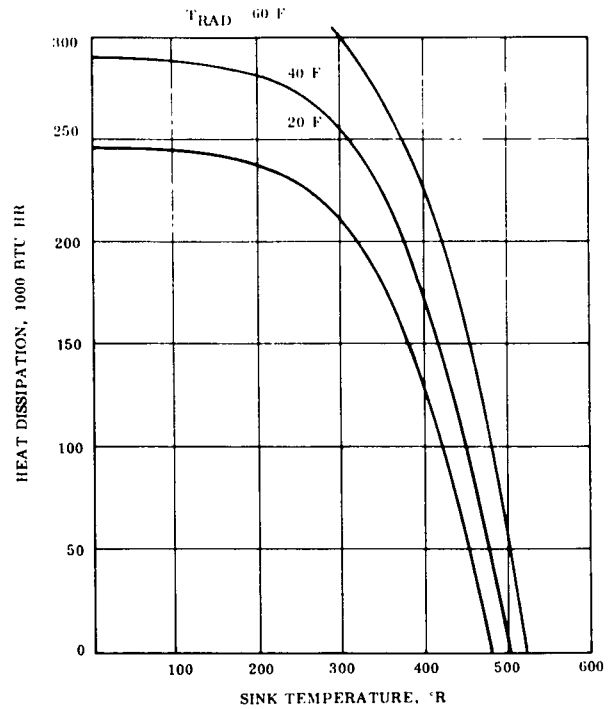


Figure 3-15. Heat Dissipation vs Sink and Radiator Temperature - 3000 ft² and $\eta'\epsilon$ of 0.90

3.2.3.2 Radiator Optimization

Radiator optimization is generally a trade off between required thermal performance and weight. This optimization can only be performed to a limited extent for the Space Station radiator, since:

1. The $\eta'\epsilon$ product requirement is 0.7 minimum over the 3000 ft² (Section 3.2.3.1).
2. A wide variation of thermal sink temperatures exist (Table 3-3) and fin effectiveness is a function of sink temperature (reference Figure 3-2).
3. Manufacturing and assembly difficulties exist with extremely thick or thin radiators.
4. The aluminum radiator also serves as the primary micrometeoroid shield with a required minimum 0.020-inch thickness (Section 3.2.1.4).

Thus, the minimum weight configuration can only be approached and never reached. This ideal fin (from a weight standpoint) is characterized by few sources connected by a thin radiating plate. Approaching this ideal for the station radiator means assuming an aluminum sheet of 0.020 inch thickness (the micrometeoroid shield) and calculating heat source spacing to obtain a minimum acceptance effectiveness.

Effectiveness was calculated as a function of heat source spacing for linear sources. The following conditions were used:

1. Radiator material = 6061-T6 Aluminum alloy ($k = 90 \text{ Btu/hr-ft-}^{\circ}\text{F}$)
2. Coating emissivity = 0.83
3. Radiator thickness = 0.020 inch
4. Effective sink temperature = 407°R (see Table 3-3, Orbit 2 BOL coating)

Analytical procedure was that of Lieblien (Reference 9-17). Results are plotted in Figure 3-16 for two heat source (root) temperatures which were considered to bound anticipated performance of the Space Station radiator. Superimposed on this graph are the tentative 0.7 to 0.8 requirements for the $\eta'\epsilon$ product. It can be seen that a source spacing of 3.5 inches or less will yield an $\eta'\epsilon$ of 0.8 or greater over the expected range of source temperatures, while a spacing of 10.3 inches or more will never yield the desirable minimum $\eta'\epsilon$ of 0.7. Optimum spacing is thus somewhere between 3.5 and 10.3 inches.

Further refinement of heat source spacing for acceptable thermal performance and minimum weight required more detailed system information than had been generated at this point in the program (actual component-to-radiator temperature drops, actual coating properties, acceptable component temperature excursions from nominal). For preliminary concept information, a spacing of about six inches was assumed as near optimum. This spacing was rechecked in the subsequent detailed study of the two preferred system designs.

THICKNESS = 0.020"
 $T_{sk} = 407^{\circ}R$
 $\epsilon = 0.83$
 $K = 90 \text{ BTU/HR-FT } ^{\circ}F$

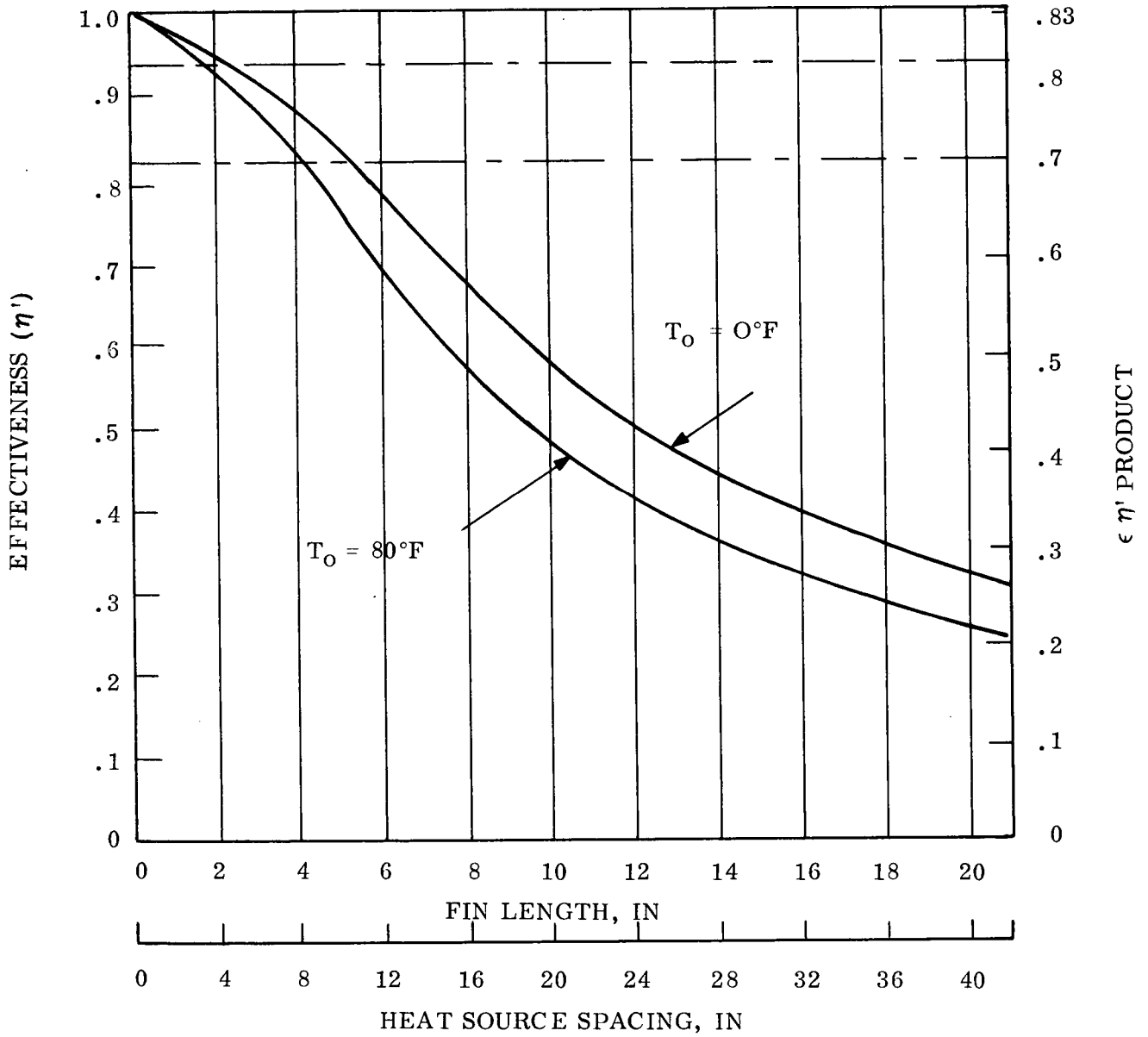


Figure 3-16. Fin Effectiveness vs. Heat Source Spacing and Radiating Temperature

3.2.4 ALTERNATIVE CONCEPTS

This section describes the generation of system concepts for satisfying the thermal control requirement of the Space Station. In keeping with the intent of this project, particular emphasis was placed on highly reliable and long-lived concepts. Such concepts were designed to provide adequate thermal control, and the feasibility of the resultant characteristics was determined.

The following items of the thermal system were considered fixed at the initiation of this task.

1. The location and maximum surface area of the radiator
2. The general location of the heat dissipators
3. The amount of heat generated by each dissipator and its nominal required temperature
4. The range of possible external thermal environments
5. The necessity of a micro-meteroid shield surrounding the Station pressure wall.

These items fairly well fix the heat source and heat sink conditions. Concepts to be generated may therefore vary primarily in heat transmission (source-to-sink) technique and transient temperature control method. System elements and element data used to accomplish these tasks were taken from Phase I. Transport methods considered were conduction, radiation, and heat pipes. Temperature control methods considered initially were louvers, phase change material, boilers, sublimators, and controllable heat pipes. It should be noted that the use of pumped coolant loops for transport and temperature control was specifically omitted for two reasons:

1. Such systems are relatively short-lived and unreliable.
2. A baseline pumped loop concept has been detailed in MDAC studies and may serve as a reference for system comparison.

3.2.4.1 Overall System Characteristics

This subsection describes several schemes which were considered briefly and rejected due to impracticality. The conclusions from these studies led to the details of the concepts discussed in Section 3.2.4.2.

3.2.4.1.1 Heat Distribution Across Radiator

The first fact that was obvious from the environment and radiator studies previously mentioned was that the Station radiator should circumferentially distribute external fluxes to obtain a nearly constant effective sink temperature for the total surface area in each particular orbit. This is a definite requirement during the sun-oriented mode of operation and is also desirable during earth-fixed periods. Without significant circumferential heat transfer, components linked to portions of the radiator which receive high solar loading would experience excessive temperatures. This can be seen by noting that the sink temperatures for some radiator segments in Orbit Number 1 (Appendix A) exceed the nominal 45^oF control temperature. The only practical solution to this problem is to provide heat pipes around the radiator. Pure conduction alone will not suffice for this energy distribution. All concepts will thus utilize circumferential heat pipes on the radiator.

3.2.4.1.2 Directive Radiative Coupling Between Pressure Shell and Outer Skin

Allowing the pressure shell to radiate directly to the meteoroid shield (primary radiator) to avoid the necessity of "hard" thermal ties between the two was studied. See Figure 3-17a. Calculations were made to determine a typical temperature difference requirement for radiation transfer. It was assumed that the total internal heat load was uniformly distributed (by some means) over 3000 sq ft of the pressure shell. A temperature drop of about 55^oF was indicated. This was deemed excessive in light of previous work (see Section 3.2.3). Radiation was thus eliminated as a viable transmission link.

3.2.4.1.3 Pure Conduction Coupling

The feasibility of using pure conduction elements to effect the pressure shell radiator heat transfer was investigated. See Figure 3-17b. It was assumed that the entire internal dissipation was conducted through five inches of aluminum. The total cross-sectional

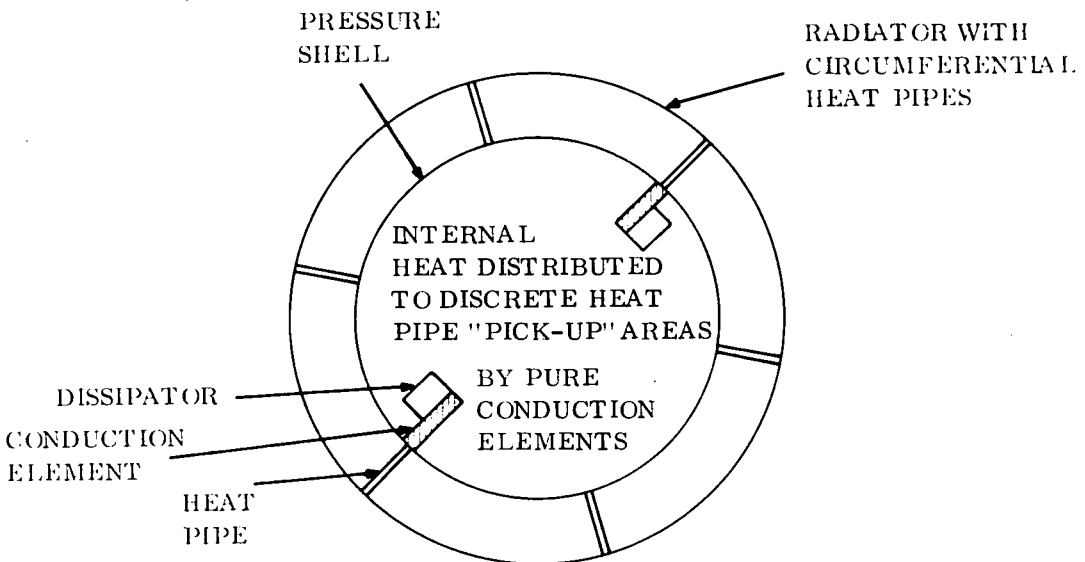
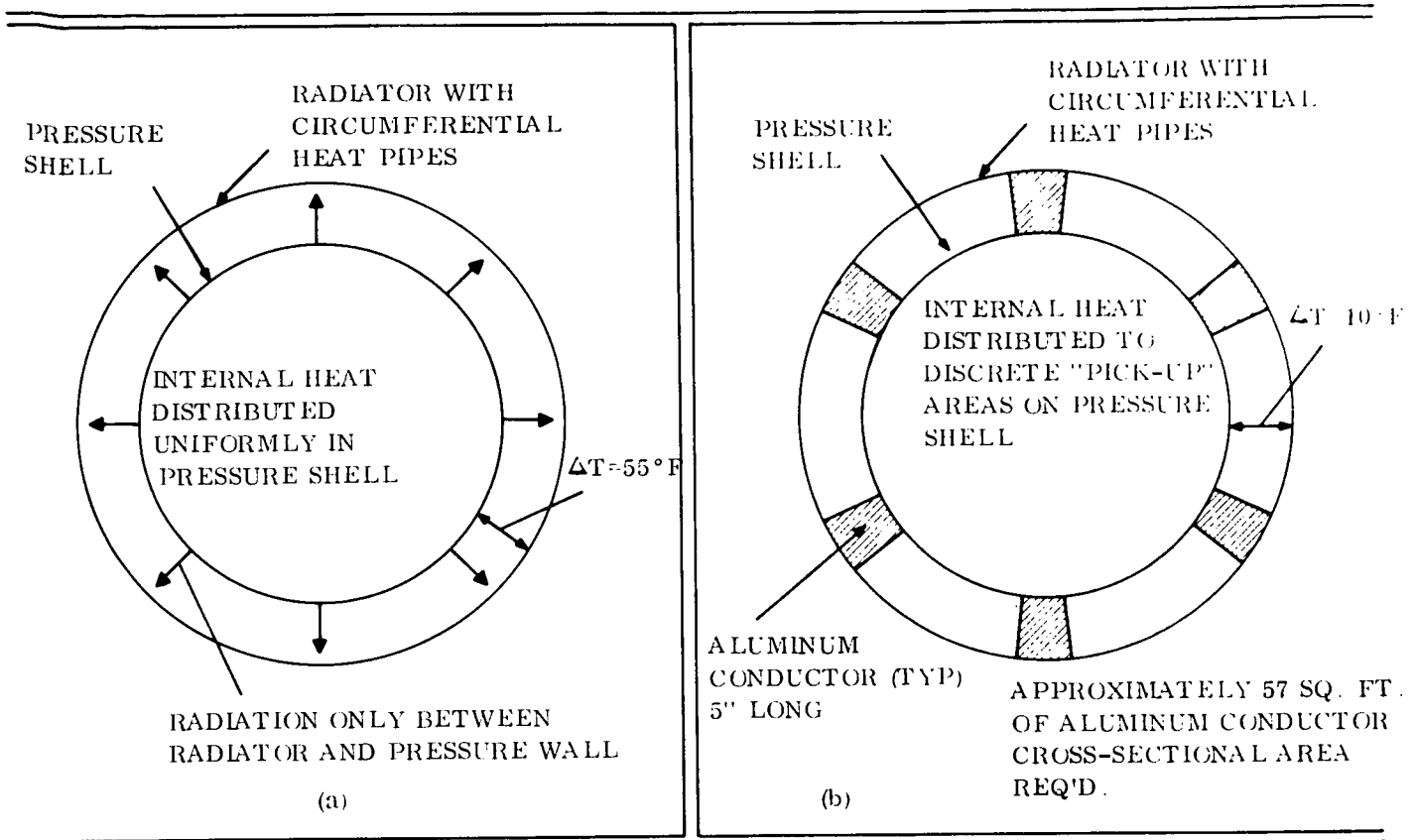


Figure 3-17. Heat Transfer Techniques

area required was calculated based on maintaining a 10°F maximum drop between the shell and the radiator. Temperature drops due to finite contact resistance at the two interfaces introduced were neglected in this calculation.

Approximately 57 sq ft of aluminum cross-sectional area would be required. The resultant weight of aluminum was 4036 pounds. This mass would be distributed to conform to the heat pipe system design on the radiator. The scheme was rejected because of: (a) its weight, (b) the requirement for near-zero interface temperature drops, (c) alignment difficulties over very large areas at both ends of the conduction elements, and (d) the necessity of a complex, internal transmission system to adapt to the design of the heat pipe radiator.

3.2.4.1.4 Internal Conduction

Similar analyses were performed which indicated the futility of employing pure conduction elements for heat transmission in the station interior. See Figure 3-17c. The conclusion was that heat pipes would have to be used to provide transmission links in most of the Space Station thermal subsystem. Of course, there will be very short conduction paths between heat pipes in series.

3.2.4.1.5 Temperature Control Elements

The transient temperature control elements mentioned previously were investigated in the same way to eliminate techniques that were obviously impractical.

A. Boilers and Sublimators. The weight of the expendables required for the operation of these devices is prohibitive. The following assumptions were made in an example which illustrates this point:

1. The radiator is designed to reject minimum internal heat load (70% of nominal) constantly.
2. A water boiler is employed to reject all internal load in excess of this minimum value.
3. For calculation purposes, a daily duty cycle is assumed as follows: 25% of time at minimum load, 50% at nominal load, and 25% at maximum load.

Results indicate that some 1200 pounds of water would be expended per day. This amounts to 108,000 pounds during the nominal 90 day resupply period. Typical Space shuttle payload is less than this weight so the scheme is totally unrealistic.

B. Phase Change. Devices which use a non-expendable solid/fluid phase change material were also considered to provide transient temperature control for the Station. Many drawbacks to this concept were noted. First, the duty cycle of dissipators must be very regular for acceptable control. For example, operation at minimum or maximum dissipation levels for time durations longer than design increments will negate the function of the device. Secondly, an additional temperature drop is incurred through the phase change material (PCM). The magnitude of this drop increases with increasing heat storage requirement and can become very large ($> 20^{\circ}\text{F}$). The third drawback is high weight. Calculations indicate that over 2400 pounds of a relatively good PCM, tetradecane, would be required to damp out temperature excursions caused by the heating pattern defined above (in water boiler example). The final negative aspect of PCM control is that the device still requires significant development to become a viable thermal system component. The PCM device was consequently eliminated as a primary control technique for the station.

3.2.4.1.6 Summary

This Section has considered various heat transmission and transient temperature control schemes proposed for use in the Space Station thermal control system. It should be noted that the techniques rejected for use in the primary system may be required to solve very specific, localized thermal problems on the station. The emphasis in this discussion has been, however, on the overall system characteristics.

By the process of elimination, the following common features of all concepts which are described in Section 3.2.4.2 have been determined.

1. A total heat pipe heat transmission system
2. Circumferential heat pipes around the station radiator
3. Transient temperature control by use of louvers or controllable heat pipes.

3.2.4.2 Concept Detail

The concepts described are variations of a basic thermal control system comprised of heat pipe transmission and louver or variable conductance heat pipe temperature control. Differences between the concepts, other than control technique, are primarily in the configuration of the heat pipe network. The concepts described herein are shown schematically on Figures 3-18 and 3-19 and are ranked in Section 3.2.5.

The various heat pipes within the transmission networks have been classified according to function to avoid confusion in the concept descriptions. Characteristics are shown below:

1. COMHP - component heat pipe. This heat pipe interfaces with a heat dissipating component and carries its energy to some collection point, depending on specific concept.
2. LONHP - longitudinal heat pipe. This pipe is oriented parallel to the axis of the station cylinder, is as long as the station, and is located within the pressure shell. Where used, its primary function is to thermally couple the two otherwise independent common modules of the Station.
3. PENHP - penetration heat pipe. These elements transfer heat through the pressure shell.
4. CIRHP - circumferential heat pipe. The circumferential heat pipe is attached to the station radiator and distributes internal and external heat loads uniformly around the radiator circumference.
5. FINHP - fin heat pipe. Fin heat pipes, when used, extend perpendicularly from the CIRHP on the radiator. Because these pipes are closely spaced, there are many of them, and the required capacity of each is low.

Not every type of heat pipe, as defined above, is employed in all concepts. The combinations considered below were chosen to represent the range of characteristics available and to evolve two concepts for further study.

Concept 1

This scheme used the least complex system possible. COMHP's directly link the individual dissipators to the radiator CIRHP's. The CIRHP's are spaced approximately

six inches apart on the radiator to maintain the necessary efficiency. Each COMHP must penetrate the pressure shell and interface with one particular CIRHP. The transmission systems and radiator for the nominal "45^o F" and "65^o F" components are separate from one another.

Transient temperature control is provided by bimetallically actuated louver systems. Calculation indicates that it is not necessary or desirable to cover the entire 3000 sq ft radiator with louvers. Acceptable control can be obtained with only one-half of this area louvered, as long as louvers present are uniformly distributed over the entire radiator. Because a louver system effectively derates basic coating properties (increasing effective absorptivity by trapping solar energy in cavities, decreasing effective emissivity by baseplate-blade thermal interactions), equivalent louvered and non-louvered performance can be attained only by improving basic coating properties under the louvered area. This is accomplished in Concept 1 by employing Z-93 white paint instead of the series emittance coating in order to obtain the higher base surface emissivity.

Concept 2

The internal configuration of this concept is identical to that of Concept 1. COMHP's are attached to the dissipators and penetrate through the pressure shell. The radiator network, however, consists of both CIRHP's and FINHP's; the FINHP's are spaced every six inches around the circumference and the CIRHP's function as thermal energy heaters for these FINHP's. The COMHP's and CIRHP's interface outside the pressure shell. The radiator is again segmented into "45^o F" and "65^o F" component areas.

Control is provided by making the FINHP's with variable conductance characteristics. A series emittance coating is used.

Concept 3

This concept combines the external configuration of Concept 1 with a more complicated, but more powerful, internal transmission network. Heat from dissipators is transferred by relatively short, straight COMHP's to one of several LONHP's, which are spaced

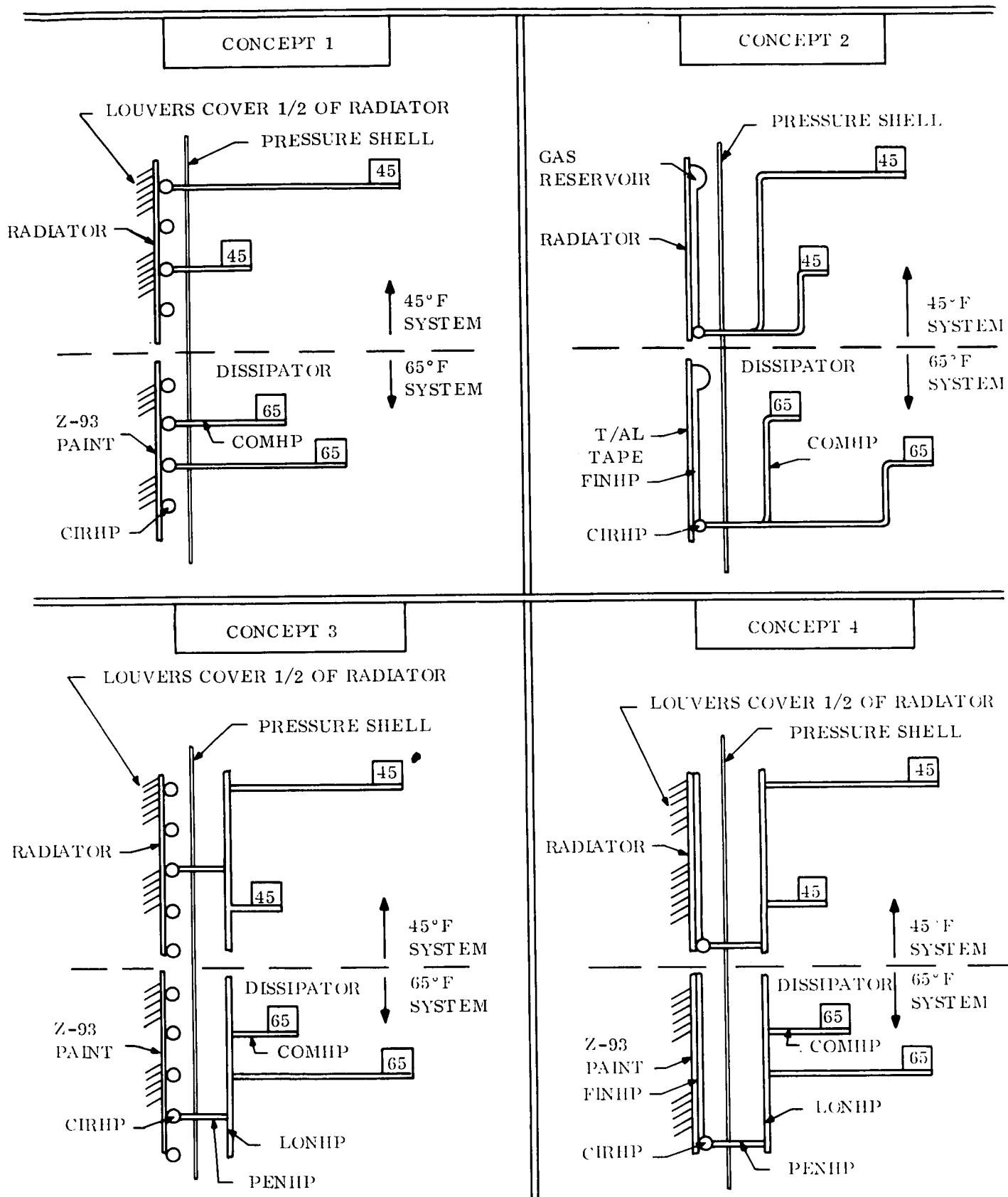


Figure 3-18. System Concepts - Candidates 1 through 4

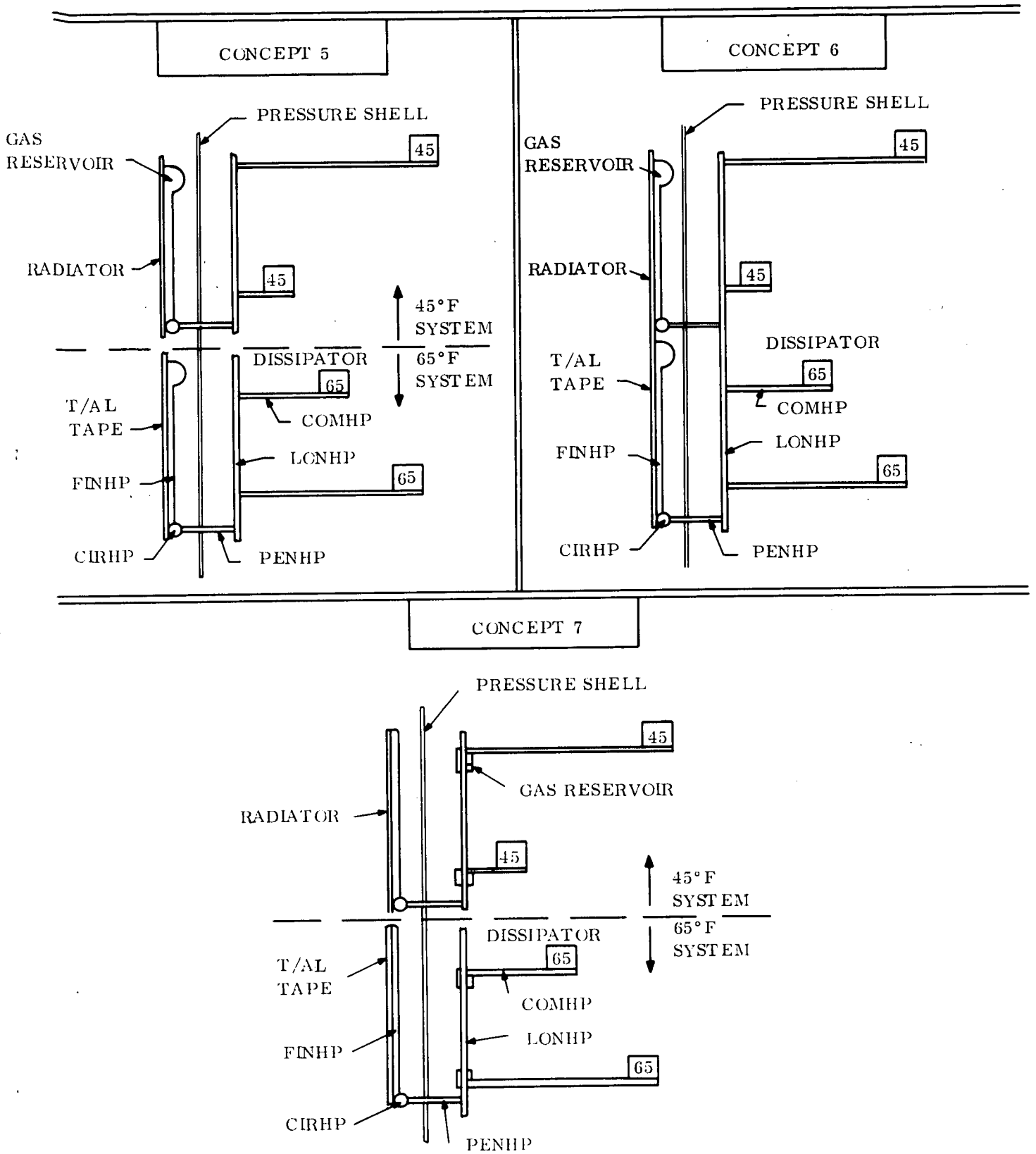


Figure 3-19. System Concepts - Candidates 5 through 7

evenly around the inside circumference of the pressure shell. Each LONHP, in turn is linked to the external CIRHP's through approximately four PENHP's. The "45^oF" and "65^oF" systems are separate. Temperature control is by use of louvers, with Z-93 white paint as the basic coating.

Concept 4

Every type of heat pipe is used in this scheme; the transmission network from source to sink is dissipators, COMHP, LONHP, PENHP, CIRHP, FINHP, radiator. The two temperature systems (i. e. 45^oF and 65^oF) are kept apart and louvers with Z-93 white paint are used for transient control.

Concept 5

The transport system is identical to that of Concept 4. Controllable FINHP's replace louvers as control devices and a series emittance coating is used. It should be noted that controllable circumferential heat pipes were not considered for temperature control since this concept would require circumferential heat pipes both inside and outside the pressure shell with a substantial weight penalty.

Concept 6

In this concept, the radiator is designed to operate at one temperature level (compatible with 45^oF dissipators) instead of two as was the case in all previous concepts. The transmission system is similar to that of Concept 4 and 5, except for the COMHP's whose average lengths are shorter because, in this concept, all LONHP's operate at the same temperature and any COMHP can be attached to any LONHP. The radiator must be made more effective, however, to reject the total internal heat load at the lower temperature. A FINHP spacing of three inches (instead of six inches) is therefore assumed. Temperature control is by controllable FINHP's. A series emittance coating is used.

Concept 7

This system is identical to that of Concept 5 except the COMHP's are controllable instead of the FINHP's.

Significant characteristics of these seven concepts were determined to permit evaluation. First; the number and average length of all heat pipes was estimated based on simplified Space Station geometry. The total required interface area was calculated by assuming a 7 watt/square inch standard and summing areas for each interface type. Table 3-4 shows the results of these first two steps.

Table 3-4. Concept Heat Pipe Definition

Concept Number	Number and Length (in Feet) of Heat Pipes					Interface Area, Sq Ft
	COM	LON	PEN	CIR	FIN	
1	340 (8)	0	0	70 (104)	0	127.5
2	340 (10)	0	0	6 (104)	1272 (6)	145.2
3	340 (7)	36 (35)	140 (2)	70 (104)	0	253.8
4	340 (7)	36 (35)	36 (2)	6 (104)	1272 (6)	271.7
5	340 (7)	36 (35)	36 (2)	6 (104)	1272 (6)	271.7
6	340 (5)	36 (35)	36 (2)	6 (104)	2544 (6)	245.7
7	340 (7)	36 (35)	36 (2)	6 (104)	1272 (6)	271.7

Next weights were determined using the information of Table 3-4 and the following unit weight assumptions:

- COMHP, FINHP - 0.3 lbs/foot of length
- LONHP, CIRHP - 0.4 lbs/foot of length
- PENHP - 0.67 lbs/foot of length
- Interfaces - 0.042 lbs/sq in. of interface area
- Louvers - 0.80 lbs/sq ft of coverage
- Controllable Heat Pipe - Add 0.6 lbs per FINHP, or 3 lbs. per COMHP effected

These weights were modified using more detailed analyses prior to the weight evaluation of the two final selected systems in Section 3.3.4.1. The initial weights computed are shown in Table 3-5.

Table 3-5. Concept Weights

Concept Number	Heat Pipe Weight, (lbs)					Interface Weight (lbs)	Control Weight (lbs)	Total Weight (lbs)
	COM	LON	PEN	CIR	FIN			
1	816	0	0	2912	0	771	1200	5699
2	1020	0	0	250	2290	878	763	5201
3	714	504	188	2912	0	1535	1200	7053
4	714	504	48	250	2290	1643	1200	6649
5	714	504	48	250	2290	1643	763	6212
6	510	504	48	250	4579	1486	1526	8903
7	714	504	48	250	2290	1643	1020	6469

The anticipated thermal performance of each concept was estimated by calculating minimum-to-maximum range of steady state radiator temperature levels under the respective worst-case boundary conditions previously discussed. With the high efficiency transport systems employed, this range will become the expected temperature deviation at the heat dissipators themselves. It should be noted that this range is not an anticipated orbital swing, but is instead a delta between two worst case orbits, orientations, and coating properties. It was found that louvers could not provide as small an overall temperature range as controllable heat pipes.

The total number of heat pipe penetrations through the Station pressure wall, and the number of different types of heat pipe to heat pipe interfaces required in each concept were noted.

All of the data resulting from this concept sizing task is summarized in Table 3-6.

Table 3-6. Concept Characteristics

Concept Number	System Weight, lbs.	Temp. Control, °F	No. of Heat Pipes	No. of Penetrations	No. of H. P. Interface Types
1	5699	+ 17	410	340	1
2	5201	+ 10	1618	340	2
3	7053	+ 17	586	36	3
4	6649	+ 17	1690	36	4
5	6212	+ 10	1690	36	4
6	8903	+ 10	2962	36	4
7	6469	+ 10	1690	36	4

3.2.5 PRELIMINARY SELECTION

The seven concepts for Space Station thermal control which were generated in the previous task were rated against each other to determine the two most promising for further study. This section describes the rating criteria, the method of evaluation, and the selection of the two concepts.

Five major criteria were employed in the concept evaluation; these were (1) anticipated thermal performance, (2) system weight, (3) constraints imposed, (4) reliability, and (5) relative cost. Each of these five items counted equally in the trade-off. Hence, each was worth twenty points on the 100 point scale used. Assessment is described below.

1. Thermal Performance - 20 points. This is a measure of how well the conceptual system can control component temperatures over a wide range of operational conditions. The estimated temperature control shown in Table 3-6 was used as a measure of this performance.
2. System Weight - 20 points. This is self-explanatory.
3. Constraints Imposed - 20 points. Two judgments were made in this category.
 - a. Redundancy - 10 points. In this context, redundancy is provided by thermal coupling between the two common modules. This provision insures a double path through the pressure shell for all component heat. In the systems

considered, the presence of LONHP's supplies this redundancy. Non-redundant systems can impose mission and operational constraints in the event of a single failure.

- b. Packaging - 10 points. The constraints to internal packaging of dissipators imposed by the various concepts were evaluated. Basically this involved noting the average length and complexity of the required COMHP's. Complexity was measured by the approximate number of bends in the COMHP's for routing to their respective sinks.
4. Reliability - 20 points. Reliability was divided into three areas.
 - a. Penetrations - 5 points. Since each pressure shell penetration represents a potential critical failure point, the concepts were penalized according to the number of penetrations required.
 - b. Degradation - 5 points. The most serious life limitations to these concepts is degradation of the thermal control coating. Coating life for Z-93 and series emittance tape was estimated and employed as this criteria.
 - c. Inherent Reliability - 10 points. This was measured by the total number of heat pipes necessary and the presence of moving parts (i. e. louvers) in the system.
 5. Cost - 20 points. Both development and unit costs were considered.
 - a. Development - 10 points. This cost will be a function of the number of different heat pipe/heat pipe interface techniques to be developed. Further, it was assumed that louvers have reached a more advanced stage of development than controllable heat pipes, and this was factored into the assessment.
 - b. Unit - 10 points. Unit cost comparison was based on the number of heat pipes in each system and the control method. Louvers were penalized because of the "tuning" required and their delicacy.

Other possible evaluation criteria (such as safety, volume, power consumption, credibility, possible sources of contamination, life of heat pipes, meteoroid vulnerability, ground test) could have been inserted into this trade-off matrix. It was felt, however, that the seven concepts being considered would have been rated essentially the same in each of these categories. The net effect would be to "damp out" the effects of difference in the five primary categories and confuse the selection process. Consequently, other criteria were neglected.

Table 3-7 shows the completed trade matrix. The ranking system is shown as an equation for determining points assigned in each category, on the basis of factors described above. Characteristics which would yield the maximum number of points in each category are also shown. General conclusions from this study are as follows:

1. There is no one superior concept that rated high in every criteria. This was to be expected since the requirements of some criteria conflict with those of others.
2. Concepts using louvers for temperature control (numbers 1, 3 and 4) rated lower than comparable systems using controllable heat pipes.
3. Concept 6 which employed a single temperature radiator was rated low primarily because of its weight.
4. Concepts 1 and 2, using a minimal internal transmission system, were downgraded due to their lack of redundancy, packaging restrictions, and excessive number of penetrations. These disadvantages more than offset the low weight of these systems.
5. Concepts 5 and 7 were rated highest. These concepts were judged satisfactory in all cases, with the major disadvantage being in the development area. (i. e., controllable heat pipes and interface areas required development).

Concepts 5 and 7 were chosen for further study. These two systems are similar in that they both use all five previously defined types of heat pipes for thermal control. They differ in position of the controllable pipes within the system.

Table 3-7. Concept Trade-Off Matrix*

Concept	Thermal Perform.		System Weight		Redundancy		Imposed Constraints		Reliability			Cost		TOTAL					
	ΔT	P	Lbs.	P	LONHP?	P	#B:	Len.	P	Pene.	Yrs.	P	#HP:		C-L:	HP	P	Unit	
BEST	± 5	20	5000	20	Yes	10	0:	<4	10	50	5	5	5	L:0	10	C:	<200	10	100
1	± 17	8	5700	17	No	0	2:	12	6	340	3	2	2	L:1	6	L:	410	6	57
2	± 10	15	5200	19	No	0	2:	12	6	340	3	5	5	C:2	6	C:	1618	6	66
3	± 17	8	7050	12	Yes	10	1:	7	8	36	5	2	2	L:3	7	L:	586	6	64
4	± 17	8	6650	14	Yes	10	1:	7	8	36	5	2	2	L:4	6	L:	1690	3	59
5	± 10	15	6212	15	Yes	10	1:	7	8	36	5	5	5	C:4	4	C:	1690	6	74
6	± 10	15	8903	4	Yes	10	0:	<6	9	36	5	5	5	C:4	4	C:	1690	6	61
7	± 10	15	6450	14	Yes	10	1:	7	8	36	5	5	5	C:4	4	C:	1690	6	73
P =	$25 - \left \Delta T \right $		$20 \left(\frac{W-5000}{250} \right)$		10-Yes; 0-No		10-Bend-	$\frac{Len}{6}$		5-#/100	Yrs			C ⁺ L ⁺	8-#1 10-#1	C ⁺ L ⁺	10-#HP/400 7-#HP/400		

+ Use if concept uses C
 +- Use if concept uses L.

*Symbols:

Dev = Development
 Pene = Penetration
 P = points assigned
 B = bends in COMHP (one)
 HP = heat pipe

W = Total concept weight
 Len = length (one COMHP)
 C = controllabile heat pipe
 L = louvers
 I = interface type
 # = Number of

3.3 DEFINITION OF PREFERRED SYSTEMS

Section 3.2.4 of this report presented the sequential development and evaluation of seven conceptual "high reliability" systems to provide thermal control for the Space Station. Two of these systems were selected over the others for further study. This section discusses work done to refine these two designs and to assess the characteristics of the finalized configurations.

3.3.1 OVERVIEW

The chosen concepts, designated number 5 and number 7 in Section 3.2.5, were renamed Concepts A and B, respectively, and will be referred to as such hereafter. These concepts are similar in many respects, differing primarily in position of the temperature control device within the system. A network of high capacity heat pipes couples heat sources (internal components which generate heat) to the radiator heat sink. To reiterate, this network consists of COMHP's (component heat pipes) which interface directly with the individual dissipators and transfer their heat to the LONHP's (longitudinal heat pipes). The LONHP's are oriented parallel to the vehicle axis, are located radially just inside the pressure shell, and thermally couple the two common modules of the Station. Heat is transferred from the LONHP's into PENHP's (penetration heat pipes) which penetrate the pressure wall. CIRHP's (circumferential heat pipes) interface with the external end of the PENHP's and function as thermal headers for a large number of FINHP's (fin heat pipes). The CIRHP's and FINHP's distribute internally generated and externally absorbed heat over the radiator area.

The Station thermal system includes two independent networks as described above. One of these networks is sized to maintain its dissipating components at 45⁰F and the other network is sized for 65⁰F components. Since each network must have its own separate radiator, and since circumferential averaging is required on each of these, the total Station radiator is divided into two cylindrical bands, which operate at different temperature levels. Both Concept A and Concept B are so designed.

In Concept A, the FINHP's are variable conductance heat pipes which minimize temperature excursions caused by variations in thermal boundary conditions (heat dissipation, incident external flux, coating degradation, etc.). This function is performed by variable conductance COMHP's in Concept B.

The approach employed to refine these concepts is described below:

1. Update requirements and constraints to more accurately represent actual Space Station parameters.
2. Determine requirements for the individual elements of the thermal system.
3. Design suitable elements to meet these requirements and characterize these elements mathematically.
4. Combine these elements and assemble mathematical thermal model of the total Space Station.
5. Exercise this model with various boundary conditions, modify as necessary to obtain acceptable thermal performance, and finalize design.
6. Determine characteristics of finalized systems.

3.3.2 UPDATED REQUIREMENTS

At the onset of the detailed studies, certain of the requirements and constraints presented in Section 3.2.1 were revised to reflect updated quantities and to correct some of the assumed parameters. The effected items are discussed below.

1. After reviewing reports on the MDAC pumped coolant loop, it was decided to add a third acceptable component temperature level of 90°F to the already established 45°F and 65°F levels. A significant amount of heat is rejected to the MDAC loop at temperatures between 65°F and 110°F. Thus, to limit rejection temperature to 65°F in the heat pipe systems would impose a penalty on these systems and a one-to-one comparison to the active loop system would not be possible. To overcome this, the cold plates in the Station were allowed to operate at 90°F in Concepts A and B. For convenience, the dissipators were designated as follows:

- Class I - Dissipators controlled to 45°F nominal
- Class II - Dissipators controlled to 65°F nominal
- Class III - Dissipators controlled to 90°F nominal

2. The requirement for operation in an artificial-g mode was removed.
3. Thermal performance of Concepts A and B would be evaluated for three worst-case orbit/orientation sets; the "hottest," "largest transient," and "coldest" combinations were chosen. These are described as set numbers 1, 2, and 3, respectively, in Table 3-2.
4. In view of the parametric radiator study undertaken previously, the desirable thickness of the preferred series emittance thermal control tape was changed from 2 mils to 5 mils for increased emissivity. Radiative properties to be considered are shown in Section 3.2.1.2. It should be noted that the α/ϵ ratios for the new tape at both beginning and end of life are identical to those of the thinner tape. Effective sink temperatures for the various orbits thus remain as reported in Table 3-3 and Appendix A.
5. Component dissipation values were reviewed and modified downward to agree more accurately with the anticipated Station energy balance. Nominal case heat sources were found to be,

Electrical	25.5 KW
Metabolic	1.6 KW
Structural (heat leak)	0.6 KW
Nuclear Waste Heat	<u>5.2 KW</u>
Total	32.9 KW

Table 3-8 presents nominal, maximum, and minimum component dissipations to be used in the analysis of concepts A and B. Maximum dissipation occurs for periods of less than one hour per day. Batteries supply the excess and components mounted on the cold plates dissipate the heat. The minimum values were generated by applying a constant -30 percent factor to all nominal case quantities. This factor is rather arbitrary but should be sufficient to demonstrate the effectiveness of the control systems.

The following table summarizes the Station internal heat generation by component classes.

Components (Control Temp)		Dissipation, Btu/Hr		
		<u>Nominal</u>	<u>Maximum</u>	<u>Minimum</u>
Class I	(45 ^o F)	29764	29764	20834
Class II	(65 ^o F)	24276	24276	16993
Class III	(90 ^o F)	<u>58422</u>	<u>101592</u>	<u>40896</u>
		112462	155632	78723

The effects of these modifications on all seven concepts developed in Section 3.2.4.2 were assessed to determine if the conclusions of the trade-off remained valid for the new conditions. The primary effect was a reduction in the weight of all conceptual systems due to the decreased internal generation and the incorporation of the higher temperature control level (90^oF). Other characteristics presented in Table 3-6 did not change significantly. Since the weight reduction effected all systems, the relative rating of the concepts on a weight basis did not change, and therefore, the overall rating of the seven concepts remained as previously stated. In other words, concepts 5 and 7 (now A and B) were retained for detailed study.

3.3.3 ELEMENT DEFINITION

In this section, four major elements of Concepts A and B are defined. These four (the radiator, all heat pipes, interfaces, and control devices), were designed on the basis of preliminary calculations. Thermal characteristics of the elements as described herein were employed in the later system studies.

With the exception of the control device subsection, the discussions below apply to both Concepts A and B.

3.3.3.1 Radiator

3.3.3.1.1 Coating

As already implied in this report, the preferred radiator coating was a 5 mil Teflon over aluminum series emittance thermal control tape. Low α/ϵ coatings were investigated in Phase I and this tape was chosen over other candidates such as white paints, OSR, and an

Table 3-8. Internal Dissipations

Component	Nominal Dissipation, Btu/Hr			Maximum* Dissipation, Btu/Hr			Minimum Dissipation, Btu/Hr		
	Total	Decks		Total	Decks		Total	Decks	
		1&2	3&4		1&2	3&4		1&2	3&4
IVA Support @ 45° F	0	0	0	0	0	0	0	0	0
H ₂ O Chiller @45° F	1200	600	600	1200	600	600	840	420	420
CO ₂ Conversion @ 45° F	1144	572	572	1144	572	572	800	400	400
H ₂ O Electrolysis @ 45° F	2820	1410	1410	2820	1410	1410	1974	987	987
Temp. and Humid Control @45° F	24600	12300	12300	24600	12300	12300	17220	8610	8610
Batteries @ 65° F	4000	2000	2000	4000	2000	2000	2800	1400	1400
Urine Recovery @ 65° F	8100	0	8100	8100	0	8100	5670	0	5670
CO ₂ Removal @ 65° F	12176	0	12176	12176	0	12176	8523	0	8523
Shower/Dishwasher/Cloths-washer @ 65° F	0	0	0	0	0	0	0	0	0
Cold Plates @ 90° F	58422	29211	29211	101592	50796	50796	40895	20448	20448
Total, Btu/Hr	112462	46093	66369	155632	67678	87954	78723	32265	46458
Total, Kw _t	32.9	13.5	19.4	45.6	19.8	25.8	23.0	9.4	13.6

* For one hour only

alternative tape. Early work in Phase II assumed the use of 2 mil tape. This selection was modified during the parametric radiator study when higher emissivity was found necessary. At this point, hereafter, a 5 mil tape was specified with optical radiative properties as shown in Section 3.2.1.2.C.

3.3.3.1.2 Radiator Area Apportionment

A major decision concerning the radiator was how to apportion the total 3000 sq. ft. surface between the Class I, Class II, and Class III dissipators. To do this, heat balances were written for the three radiators, subject to the following conditions:

1. Nominal internal dissipations, as summarized in Section 3.3.2 were employed for each class.
2. A 20^oF temperature drop from the dissipators to the radiator was assumed for the Class III system. Drops for the other systems were scaled from this value according to dissipation. Thus, identical heat transport systems were assumed for all three classes, and the total temperature drop was directly proportional to the heat transport. Class I drop was 10.2^oF and the Class II drop was 8.3^oF.
3. Radiator emissivity was 0.83 with an effectiveness of 0.90 so that the product was 0.75 (midpoint of desired range concluded in Section 3.2.3.1).
4. A maximum average sink temperature of 451^oR was used from Table 3-3. Component temperatures were allowed to be 5^oF above nominal in this "hot-case" condition (Dissipator temperatures were - Class I, 50^oF; Class II, 70^oF; Class III, 95^oF.)

The areas calculated with these values summed to about 2800 sq. ft. The excess 200 sq. ft. available was allotted to the Class I system to provide extra rejection capability for these low-temperature components. Final area distribution was as follows:

Class I radiator	1336 sq. ft.
Class II radiator	564 sq. ft.
Class III radiator	<u>1100 sq. ft.</u>
Total	3000 sq. ft.

Each of these three radiators was, in turn, divided in two and distributed on the Station as shown in Figure 3-20. This was done so that localized radiation and flux blockage would not severely effect any one system.

3.3.3.1.3 Fin Heat Pipe Spacing

Another aspect of radiator design involved determination of FINHP spacing. This decision was made on the basis of total system considerations, not merely radiator requirements. The efficiency of the internal heat transport network was traded-off against radiator effectiveness with weight as the primary criteria. A heavy transport system will yield a low temperature drop from dissipators to radiator, resulting in a relatively high radiating temperature. This, in turn, permits a less effective and therefore lighter radiator to be designed. The converse is also true. The sum of the transport network weight and the radiator weight should thus be considered. The following example is offered to illustrate the procedure. It should be noted that the technique requires information on internal transport characteristics which will be discussed in later sections of this report.

<u>Nominal Component Temperature</u>	Power Module
45° F	Class I Radiator, A = 668 SF
65° F	Class II Radiator, A = 282 SF
90° F	Class III Radiator, A = 550 SF
	Class III Radiator, A = 550 SF
	Class II Radiator, A = 282 SF
	Class I Radiator, A = 668 SF

Figure 3-20. Space Station Radiator Distribution

Consider the Class III dissipators rejecting nominal heat through a transport system and radiator to a constant "hot" sink (451°R), allowing the dissipator temperature to be 95°F . The Class III radiator area is 1100 sq. ft. and has an emissivity of 0.83. Let the radiator root temperature be $(95 - \Delta T)^{\circ}\text{F}$ where 95°F is the component temperature and ΔT is the total system temperature drop to the radiator root. Required radiator effectiveness can now be related to ΔT , as shown in Figure 3-21.

The earlier parametric radiator study indicated the desirability of maintaining radiator thickness at the minimum value (0.020 in.) and varying heat source (FINHP) spacing to obtain necessary effectiveness. Using curves such as shown on Figure 3-16 and Figure 3-21, it is possible to plot required FINHP spacing to system ΔT . This is done on Figure 3-22.

A weight analysis is now performed. Internal interface and external FINHP weights of the Class III system are calculated as a function of ΔT . All other weights are invariant with ΔT . Figure 3-23 shows the data. As expected, internal transport system weight increases sharply with decreasing ΔT , and external weight increases with increasing ΔT (as required effectiveness approaches unity to maintain components at 95°F). The summed weight thus exhibits a minima, which for this case, occurs at a ΔT of about 18°F .

It was in this manner that radiator design was evolved. A certain amount of iteration was necessary to finalize the configuration as follows:

1. FINHP spacing of 6 inches for the entire radiator. Calculated effectiveness is 0.92 and the $\eta'\epsilon$ product with the 5 mil Teflon over aluminum tape is 0.765.
2. Design system maximum ΔT (temperature drop from dissipators to radiator root) of 20°F . This is exhibited by the Class III network since Class III dissipators reject the largest amount of heat. Drops in the Class I and II networks will not be as large.

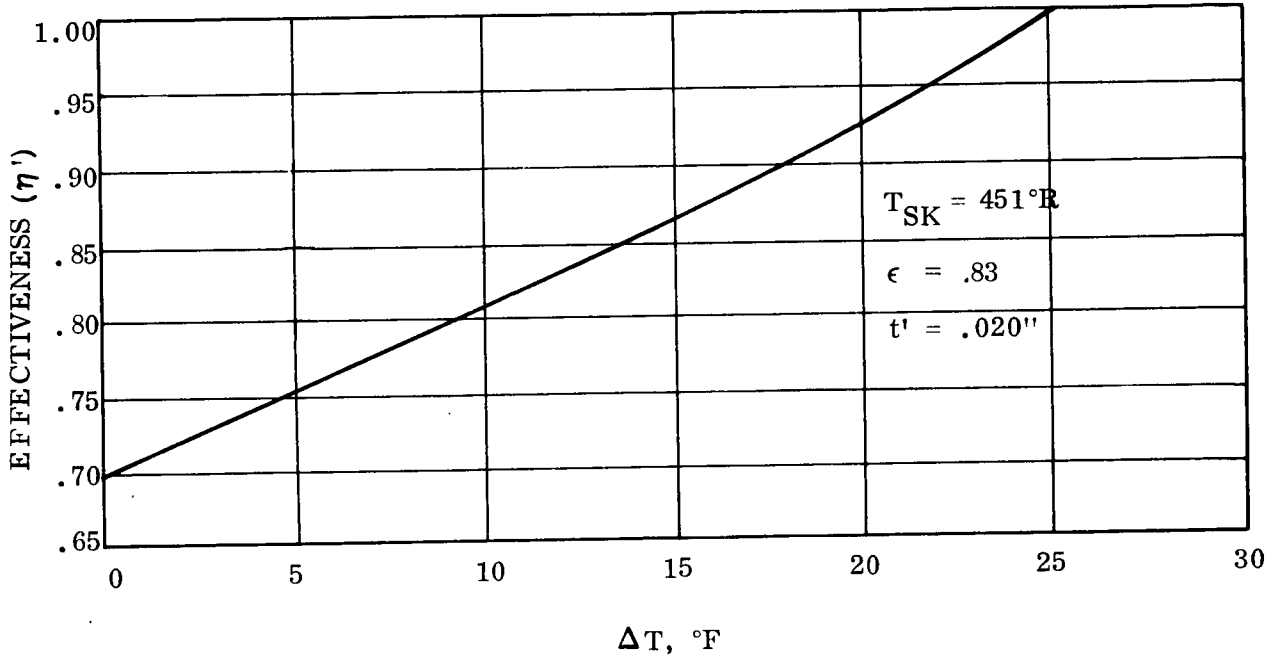


Figure 3-21. Required Effectiveness vs ΔT

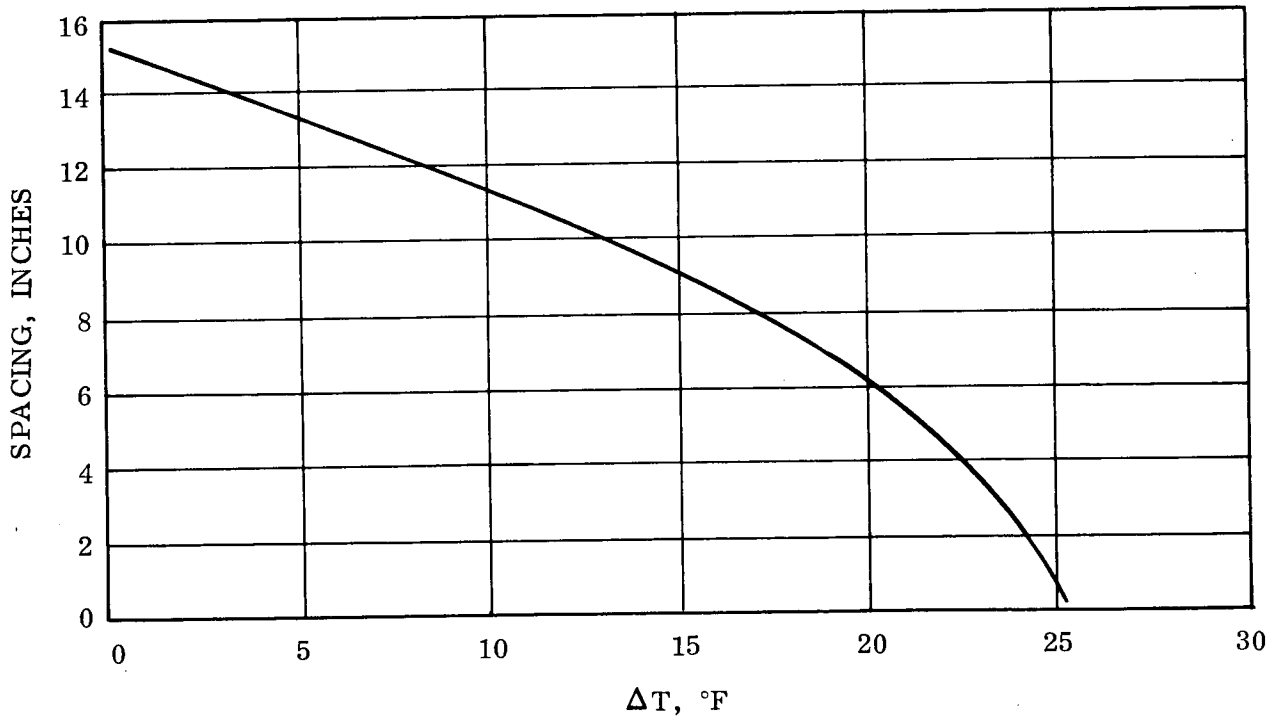


Figure 3-22. Required FINHP Spacing vs ΔT

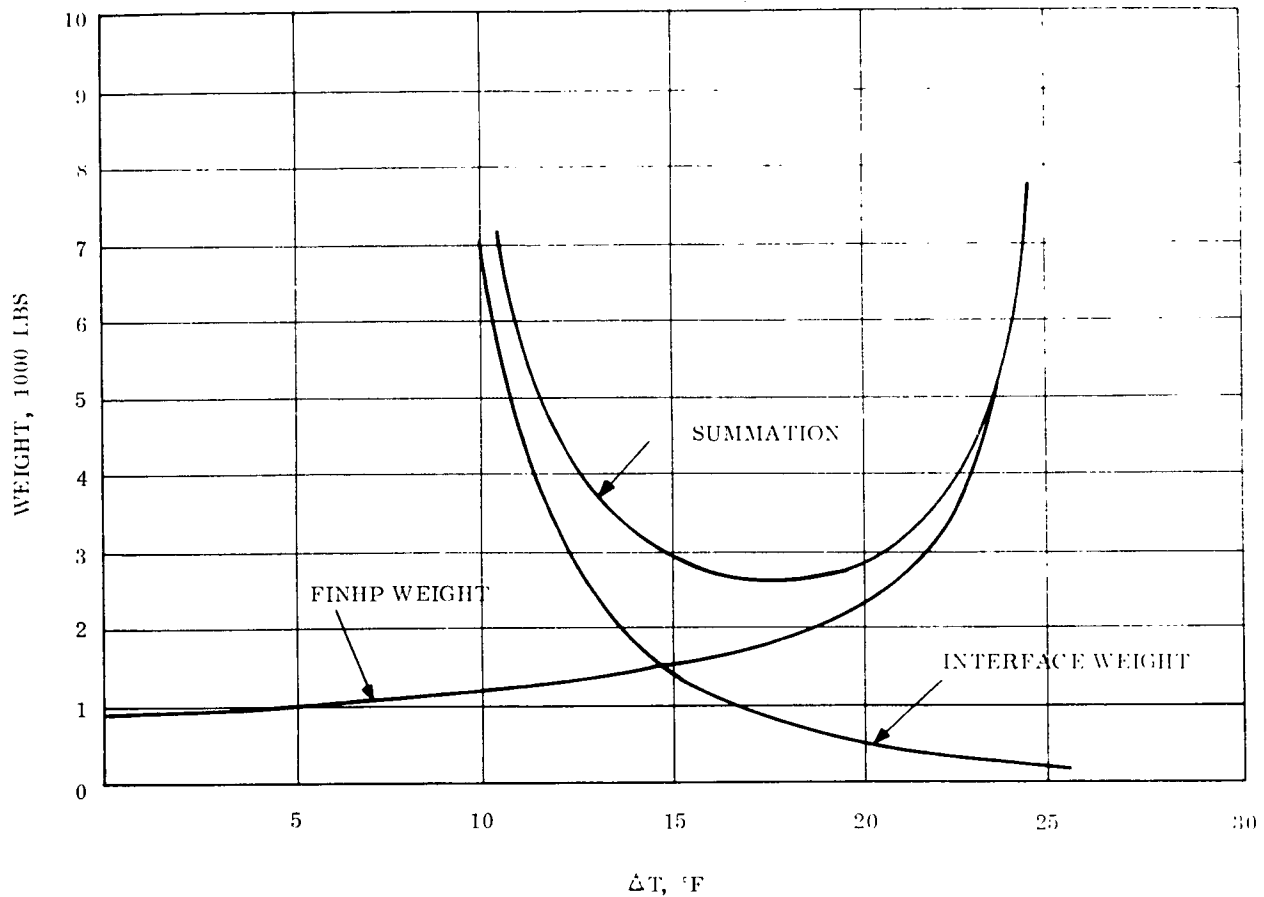


Figure 3-23. System Weight vs ΔT

3.3.3.1.4 Number of CIR HP's

The only remaining question concerning radiator design was how many CIRHP's to use to thermally couple the PENHP's and FINHP's. The minimum number of CIRHP's is 6, one for each of the separate radiating bands shown in Figure 3-20. Increasing this number will have the following effects:

1. The number of required FINHP's will increase. Although the FINHP's would be shorter in this case, total FINHP cost would increase since the cost of such operations as filling and testing depends on the total number of heat pipes involved.
2. The number of CIRHP-FINHP interfaces would increase with attendant alignment and assembly problems.
3. The complexity of the penetration pattern on the pressure shell would increase since PENHP's would be required at more elevations than absolutely necessary.

For these reasons, it was decided to use only six CIRHP's.

3.3.3.2 Heat Pipes

Five types of heat pipes have been specified for Concepts A and B. The thermal requirements of all heat pipes within each of these five functional groups are similar for the Class I, II, and III systems. High performance characteristics have been assumed for all heat pipes to represent optimized networks. This section will discuss these characteristics and describe the tentative heat pipe designs suggested. Evaporator and condenser considerations are omitted from this discussion because they are treated in the Interface Subsection (3.3.3.3).

Table 3-9 presents the approximate requirements of each type of heat pipe. Maximum heat throughput, maximum length, and minimum operating temperature are shown. The maximum heat throughput was determined by designing the COMHP's to transfer 500 Btu/hr (see Section 3.3.3.2.1) and considering the following ratios: twelve COMHP's (maximum) per LONHP; two PENHP's per LONHP; six PENHP's per CIRHP; and 212 FINHP's per CIRHP. Maximum length was calculated from the geometry of the Space Station. Minimum operating temperatures were obtained from system thermal analyses described in Section 3.3.4.2 of this report.

Table 3-9. Heat Pipe Requirements

Type of Heat Pipe	Maximum Heat Input/Pipe, w	Length/Pipe, ft.	No. of Pipes	Minimum Operating Temp, °F					
				Concept A			Concept B		
				Class I	Class II	Class III	Class I	Class II	Class III
COMHP	150	14	340	30	51	71	36	50	80
LONHP	1800	35	36	28	49	68	-62	-21	- 2
PENHP	900	2	36	25	47	64	-63	-22	- 4
CIRHP	5400	104	6	21	45	59	-64	-23	- 6
FINHP	25	6	1272	19	43	55	-66	-25	- 9

Heat pipe design was complicated by the number of constraints to be considered. These are discussed briefly below.

1. Hydrodynamic Performance - Each heat pipe must clearly be able to transfer its maximum heat load. Ranking of room temperature heat pipe fluids (see Section 2.3 of this report) is water, ammonia, methyl alcohol, and Freon.

C-2

2. Toxicity - Heat pipes within the inhabited cabin should contain non-toxic fluids. Water is the obvious choice.
3. Minimum Operating Temperature - No fluid may be used in a heat pipe whose minimum operating temperature is below the freezing point of that fluid. This constraint excluded water from consideration in a number of heat pipes.
4. Controllable Aspects - The FINHP's in Concept A and the COMHP's in Concept B must be designed to obtain acceptable variable conductance properties.

Consideration of these constraints, together with the requirements presented in Table 3-9, yielded the following design guidelines:

1. Water was chosen as the fluid for all heat pipes in the cabin whose operating temperature was never below 50°F. An 18°F safety factor was added to water's freezing point to account for temperature differences between pipes caused by component duty cycles and circumferential gradients.
2. Methanol was selected for all other cabin heat pipes (freezing point - 144°F). It is felt that the small amount of methanol required, combined with the small probability of pipe rupture would make this selection acceptable.
3. Ammonia was chosen for all external heat pipes except the FINHP's of Concept A (freezing point - 108°F). Methanol is used in these elements to obtain proper control characteristics.
4. Stainless steel is the containment vessel material for all heat pipes. Long term compatibility has been demonstrated with methanol and ammonia, and can be obtained with water through proper preparation techniques.
5. Conventional, or isotropic, wicking is employed in the FINHP's of Concept B. All other heat pipes use composite, or arterial, wicks.

3.3.3.2.1 COMHP

Each COMHP has relatively short evaporator and condenser sections at extreme ends of the pipe. These are separated by a long adiabatic section of about 14 ft maximum length (average is approximately 7 ft). In sizing these COMHP's, it was decided to utilize a "standard" design with an invariant throughput capability and group these standard elements as required by each dissipator. A standard capacity of 500 Btu/Hr was chosen on the basis

of system considerations and heat pipe state-of-the-art. With this value and the nominal dissipations of the components shown in Table 3-8, it is possible to determine the minimum number of COMHP's necessary in the Station. Table 3-10 presents this information. Redundancy is provided by increasing the number of COMHP's interfacing with critical components as is also shown in Table 3-10. The additional heat pipes, in general, yield over 30% excess capacity or make one failure per four pipes tolerable (e.g., the other three will not experience wick burnout). The maximum required transport capability of 7,000 Btu-ft/hr (84,000 Btu-in/hr. = 24,600 w-in) can be met with a relatively lightweight heat pipe. Tentative configuration is 1/2 in. OD, 0.020 in. wall stainless steel tubing with an artery wick. Calculated weight is 0.15 lbs/ft length.

Table 3-10. COMHP Distribution

Component	Common Module Nominal Dissipation, Btu/Hr	Number of COMHP's	
		Minimum	Provided
IVA Support	0*	2	2
H ₂ O Chiller	600	2	2
CO ₂ Conversion	572	2	2
H ₂ O Electrolysis	1410	3	4
Temp and Humid. Cont.	12300	25	32
Batteries	2000	4	6
Urine Recovery	8100	17	20
CO ₂ Removal	12176	25	29
Shower/D-wash/ C-wash	0*	3	3
Cold Plates	29211	59	70
	Common Module Total	142	170
	Station Total	284	340

*Not operational in assumed thermal balance.

3.3.3.2.2 LONHP

The LONHP's are long (35 ft.) straight elements which traverse the length of the Station radially inside the pressure wall. Approximately ten COMHP's reject their heat into each LONHP, and two PENHP's act as heat sinks for each LONHP. During nominal operation, the LONHP's will average (for each dissipator class) temperatures of the two common modules of the Station and thus the two sections of each Class radiator shown on Figure 3-20 will be at the same temperature. In the event of failure of one common module, the dissipation in the remaining cabin can be increased above nominal because the LONHP's will still transport heat to the entire radiator. There are six groups of three LONHP's in the Station; the six groups are spaced every 60° around the Station circumference and each group has one Class I LONHP, one Class II LONHP, and one Class III LONHP. These three heat pipes are far enough apart to permit all necessary interfacing. Transport requirements for the individual LONHP's are very high and are beyond the current state-of-the-art. The solution for this study has been to allow a one-inch by one-inch cross-section envelope for each LONHP and to assume a weight of 0.60 lbs/ft length. The LONHP can thus be either a cluster of three or four small, high performance heat pipes similar to the COMHP's, or a single large, multi-artery pipe if available at the time of Station fabrication. From a reliability standpoint, it would probably be better to design each LONHP as two independent pipes so that if one pipe fails, the LONHP can still operate (although at reduced capacity).

3.3.3.2.3 PENHP

As previously mentioned, each of the 18 LONHP's reject their heat to two PENHP's; there are thus 36 PENHP's. There are six PENHP's (evenly spaced) around the Station circumference at each of six elevations over the Station length. The six elevations correspond to the location of the six CIRHP's. Each PENHP must transport about 1,000 watts nominal (1500 watts peak) through the pressure wall, a total distance of one to two feet. In terms of watt-inch transport capability, this requirement is within present technology limits. The major design problem is interfacing with the LONHP and CIRHP, which are at right angles to each other. This will be discussed in the next section of this report.

3.3.3.2.4 CIRHP

The CIRHP's present the most difficult heat pipe design problem. In addition to being mechanically complex (over 100 feet in length, constant curvature, interfacing with six PENHP's and 212 FINHP's), they must distribute internal heat loads and external fluxes with a minimum temperature gradient. To indicate the magnitude of the thermal problem, the heating profile at the orbital subsolar point of Orbit Number 2 (defined in Table A-1, Appendix A) was examined. Figure 3-24 shows the required axial heat flow within the Concept B Class I CIRHP's as a function of circumferential position. This performance is outside of present state-of-the-art, and so a cluster of separate pipes has been assumed to make up each CIRHP. Properties used in system analysis were identical to those of the LONHP's.

3.3.3.2.5 FINHP

The FINHP's are relatively simple elements. Because there are so many of them, the heat load per pipe is low, and conventional (isotropic) wicking can be considered. The longest FINHP's (6.2 feet) are employed on the Class I radiators and must distribute about 25 watts each along their condenser lengths. Tentative size is 1/2 inch OD tubing attached to the radiator as described in the next section. Total FINHP weight (including flanges) is 0.25 lbs/ft length.

3.3.3.2.6 Summary

Table 3-11 summarizes the selected parameters of the five heat pipe types. Two points concerning overall system design concludes this heat pipe discussion. First, 1-g testing of the network in an all-up configuration is not possible. With the Station axis oriented vertically, the LONHP's and FINHP's will be effected by gravity forces. While it is possible to position all of the FINHP's so that gravity aids the condensate return (evaporator below condenser), the LONHP's must provide for evaporation over a large portion of their length, and thus cannot operate against the 1-g field. These pipes can, of course, be ground tested horizontally to verify elemental performance.

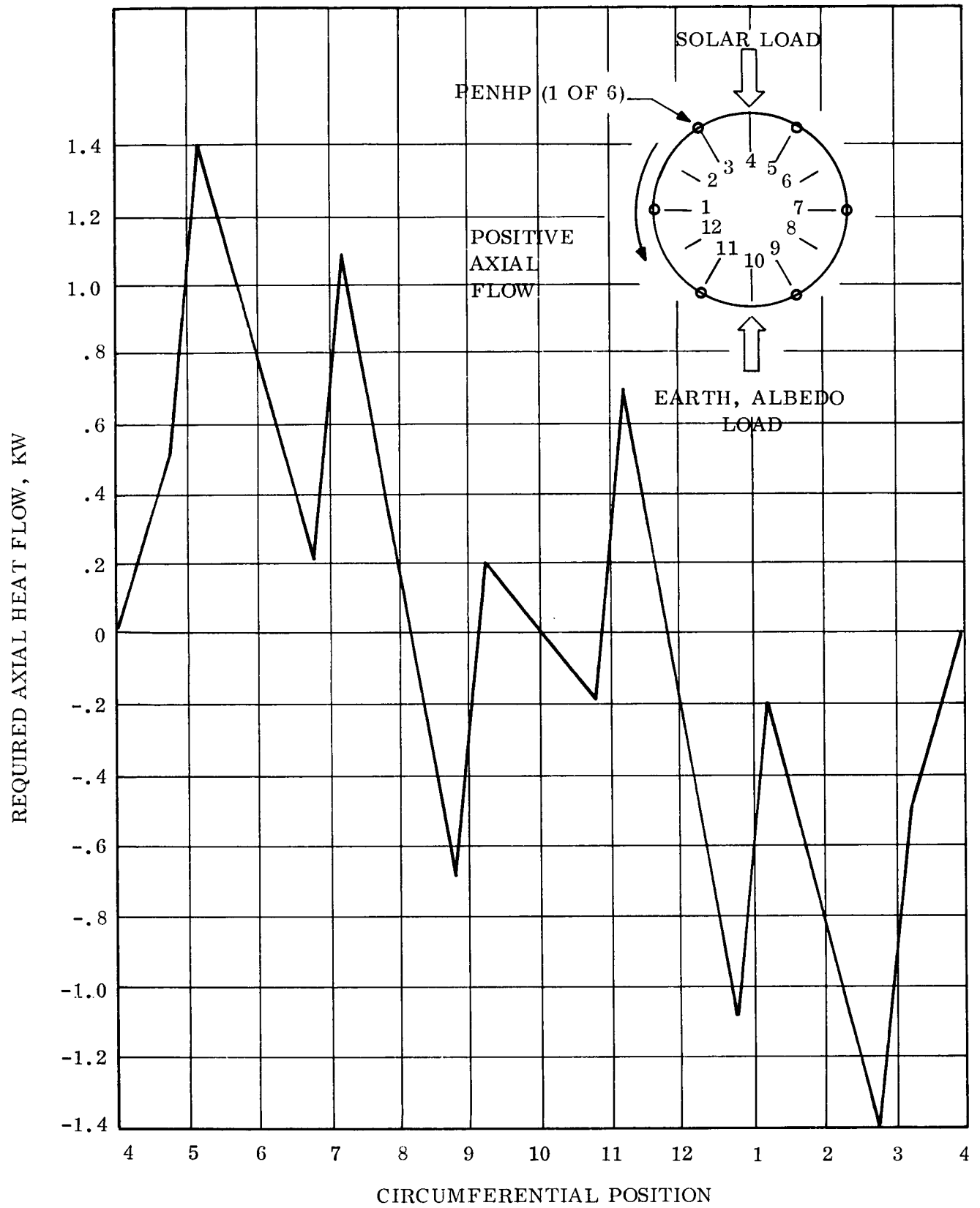


Figure 3-24. Required CIRHP Heat Flow vs Circumferential Position

Table 3-11. Heat Pipe Design Parameters

Type of Heat Pipe	Outer Diameter, in.	Concept A		Concept B	
		Fluid	Wick	Fluid	Wick
COMHP; Class I	0.5	Methanol	Artery	Methanol	Artery
	Class II	0.5	Water	Methanol	Artery
	Class II	0.5	Water	Water	Artery
LONHP; Class I	1.0	Methanol	Artery	Methanol	Artery
	Class II	1.0	Methanol	Methanol	Artery
	Class III	1.0	Water	Methanol	Artery
PENHP; Class I	-	Methanol	Artery	Methanol	Artery
	Class II	-	Methanol	Methanol	Artery
	Class III	-	Water	Methanol	Artery
CIRHP; Class I	1.0	Ammonia	Artery	Ammonia	Artery
	Class II	1.0	Ammonia	Ammonia	Artery
	Class III	1.0	Water	Ammonia	Artery
FINHP; Class I	0.5	Methanol	Artery	Ammonia	Conventional
	Class II	0.5	Methanol	Ammonia	Conventional
	Class III	0.5	Methanol	Ammonia	Conventional

The second point concerns the rigidity of the heat pipe "skeleton." With all five types of pipes hard-mounted to one another, and to dissipators and radiators, it is possible that structural loads will be transmitted to weak points and cause rupture. The incorporation of metallic bellows, or equivalent, into the heat pipes at potential weak spots to absorb the small displacements caused by launch loads, differential thermal expansion, or on-orbit mechanical loads may be required.

3.3.3.3 Interfaces

Thermal interfacing between elements of the proposed thermal systems of Concepts A and B was a major design difficulty. Large amounts of heat must be transferred from the vapor of each heat pipe to the vapor of its mating heat pipe with very little temperature drop. In

addition, the interfaces must be structurally sound, must demonstrate repeatable performance, and should be maintainable to some degree.

An example was prepared to illustrate the thermal problem. A one-square inch segment of a heat pipe-heat pipe interface was considered as shown in Figure 3-25. It was assumed that 7 watts must be conducted from vapor 1 to vapor 2. Temperature drops were calculated for the wick and wall of both pipes and for the contact between the two walls. The wicks were assumed to be two layers of stainless steel mesh saturated with liquid methanol. The effective conductivity of the wick/liquid matrix was calculated as if the two components represented two parallel heat paths through the matrix. It is felt that this approach more accurately simulates experimental data than the alternate technique of a series configuration. Contact conductance for the mechanical joint was taken as 500 Btu/hr-sq. ft. - °F, averaged over the entire contact area. This value can be considered typical of a well-designed, well-prepared bolted joint.

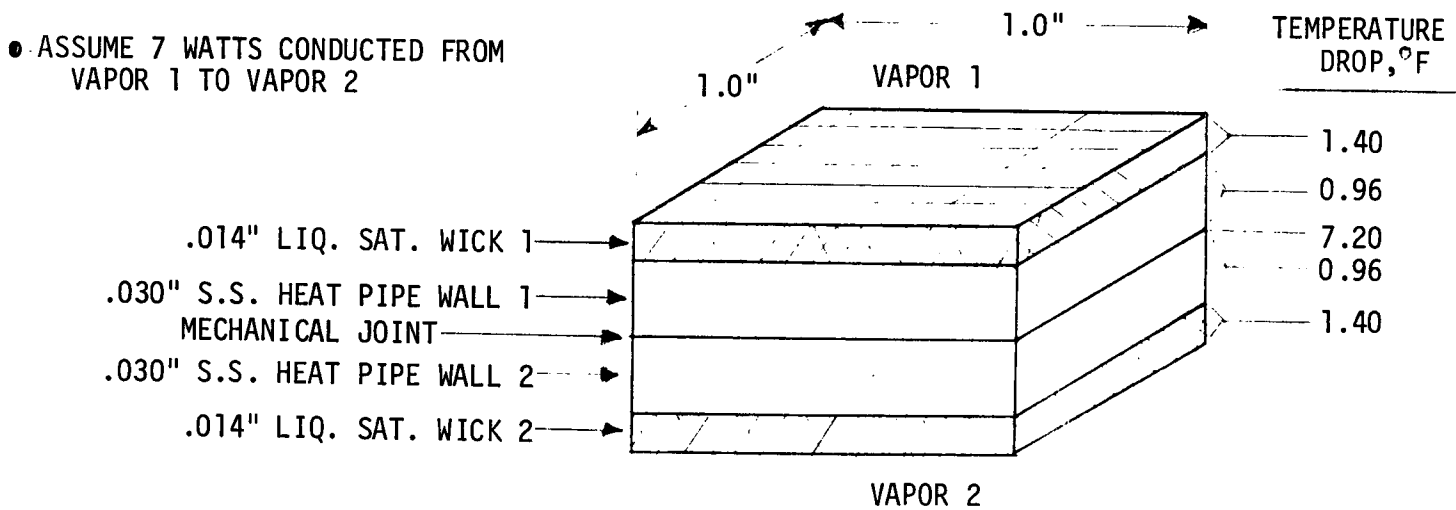


Figure 3-25. Heat Pipe Interface Segment

Temperature drops through each interface component are shown on Figure 3-25. The total drop is 11.92°F , with the largest single drop occurring at the mechanical contact (7.20°F). Since there will be four such interfaces plus two "half interfaces" in the heat pipe transmission networks, the total temperature drop from dissipator to radiator would be about 70°F . This drop would force the Class I radiators to operate at -25°F (435°R) which is below some of the calculated effective sink temperatures for the Station. This is obviously impossible. The total drop must therefore be reduced by either lowering the heat flux density through all interfaces or by eliminating the mechanical joint.

A total temperature drop of 20°F can be obtained with the interface shown in Figure 3-25 if the flux density is reduced to about 2 watts/sq. in. To do this would require very large interfaces; the junction between the LONHP and PENHP, for example, would need about 5 sq. ft. of contact area. If it were possible to design a 5 sq. ft. interface and maintain a contact conductance of 500 Btu/hr-sq. ft. $-^{\circ}\text{F}$ over the entire area, the weight of the structure would be prohibitive. For this reason, the scheme was rejected.

Elimination of the mechanical joint in the interface offers more promise. Brazing or welding the two heat pipe walls together would reduce the joint temperature drop from 7.20°F to virtually zero (for a void-free juncture). Total system drop would be approximately 24°F which is marginally acceptable based on previous work (Section 3.3.3.1). These are two major problems with this approach:

1. It requires the entire heat pipe network to be permanently joined together, which severely reduces the maintainability of the system. Replacing one heat pipe would become a significant task.
2. It may be difficult to obtain void-free welds or brazes over the necessary contact areas, which would still be quite large (about 1.5 sq. ft. in the case of the LONHP-PENHP interface).

The selected technique is based on separation of the mechanical and thermal interfaces at heat pipe junctions. An interface cell or module is fabricated as a single unit to which mating heat pipes are mechanically attached as shown in Figure 3-26.

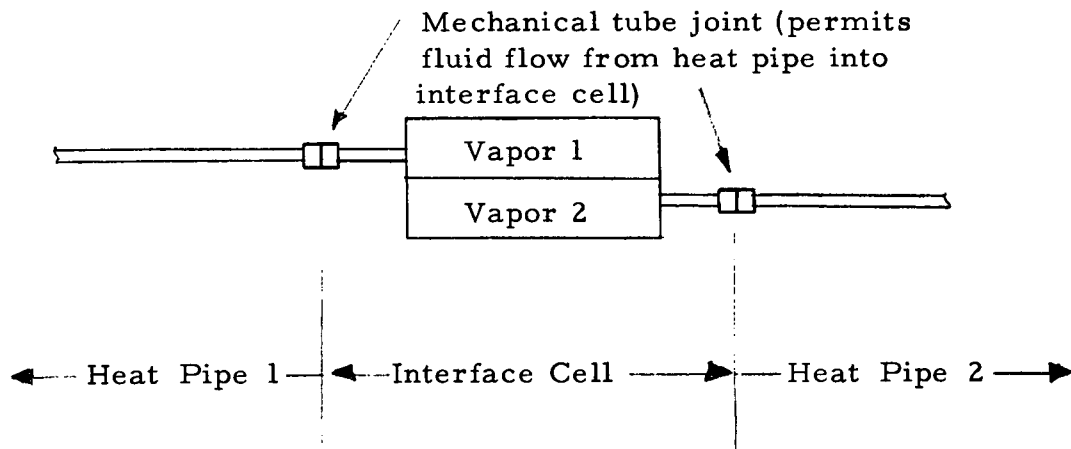


Figure 3-26. Interface Module

Since the mechanical joint occurs in the adiabatic section of each pipe, its thermal characteristics are unimportant. In terms of the example described in Figure 3-25, this method eliminates the mechanical joint shown and one of the heat pipe walls. The remaining wall is common to both pipes and is wicked on both sides. System temperature drop is about 18°F .

It should be pointed out that the use of such interface cells is considered beyond the current state-of-the-art and thus development is required. Specifically, liquid and vapor flow distribution in the region of the abrupt discontinuity in heat pipe cross-section should be examined. Also, a suitable technique for wick joining at the disassembly points should be found. Ideally, this technique would be compatible with joining the heat pipe outer tubing with standard hydraulic/pneumatic unions (AN, MS type). The junction could alternatively be made with an outer sleeve and solder.

Conceptual interface cells have been designed for the heat pipe-heat pipe junctions required for the networks of Concepts A and B. These are:

1. COMHP to LONHP - Shown in Figure 3-27.
2. LONHP to PENHP and PENHP to CIRHP - Shown in Figure 3-28.
3. CIRHP to FINHP - Shown in Figure 3-29.

The first and third of these are similar, varying primarily in size. The basic concept is to surround the larger pipe with an annular volume which is wicked and sealed from the environment and becomes one end of the smaller pipe. The two interfaces shown on Figure 3-28 are more complex because of the magnitude of heat passing through each. Both the LONHP and CIRHP are expanded in cross-section to obtain greater heat transfer area between themselves and the PENHP. The PENHP then consists of annular spaces surrounding these expanded pipes and an interconnecting tube with wick. Bellows are shown in Figure 3-28 to absorb small relative motions between the various heat pipes and the structure of the Station. All four of the interfaces described above were sized to obtain a nominal 4⁰ F temperature drop from vapor to vapor with maximum (Class III) heat loads. Maximum heat flux density is approximately 6 watts/square inch.

The interfaces of the heat pipe system with the dissipators and the radiators can and should be bolted or riveted joints. They "can be" because of the relatively low watt density existent at these points. They "should be" to simplify assembly of the system and to permit removal and replacement of damaged components. Figure 3-30 illustrates three alternative dissipator-to-COMHP interfaces, ranging from simple (flange) to complex (module). It is possible that all three types could be employed in one thermal control system. The selection would depend on accurate thermal interface definition for each dissipating component. It should be noted that the "Module" technique (c in Figure 3-30) could be extrapolated to the point that the vendors of high dissipation boxes could integrate the module into their components and simply supply the necessary outlet to link with the primary control system.

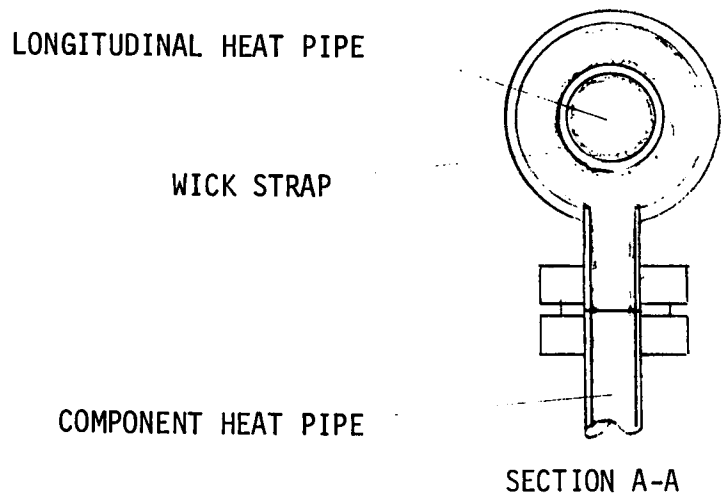
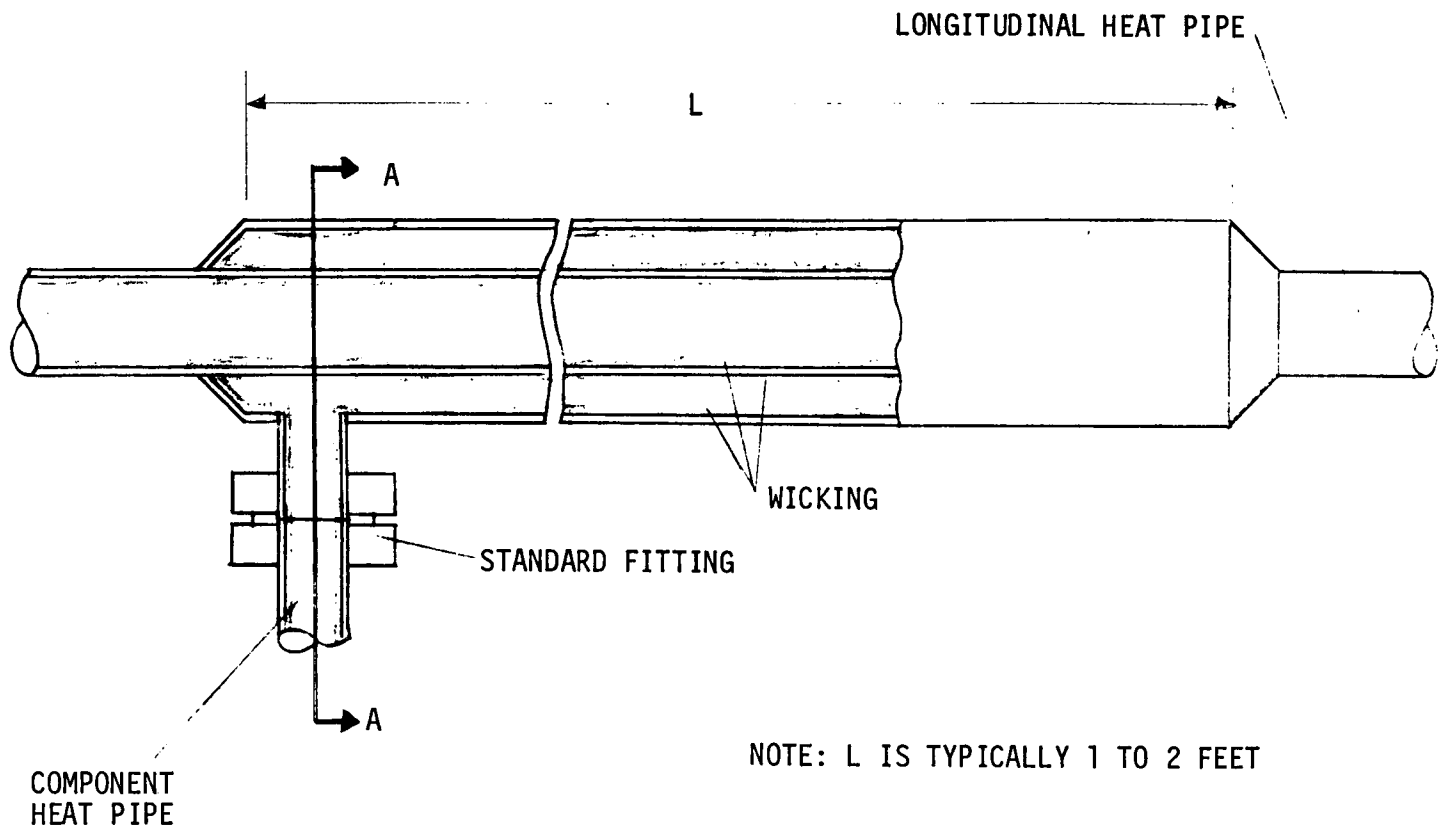
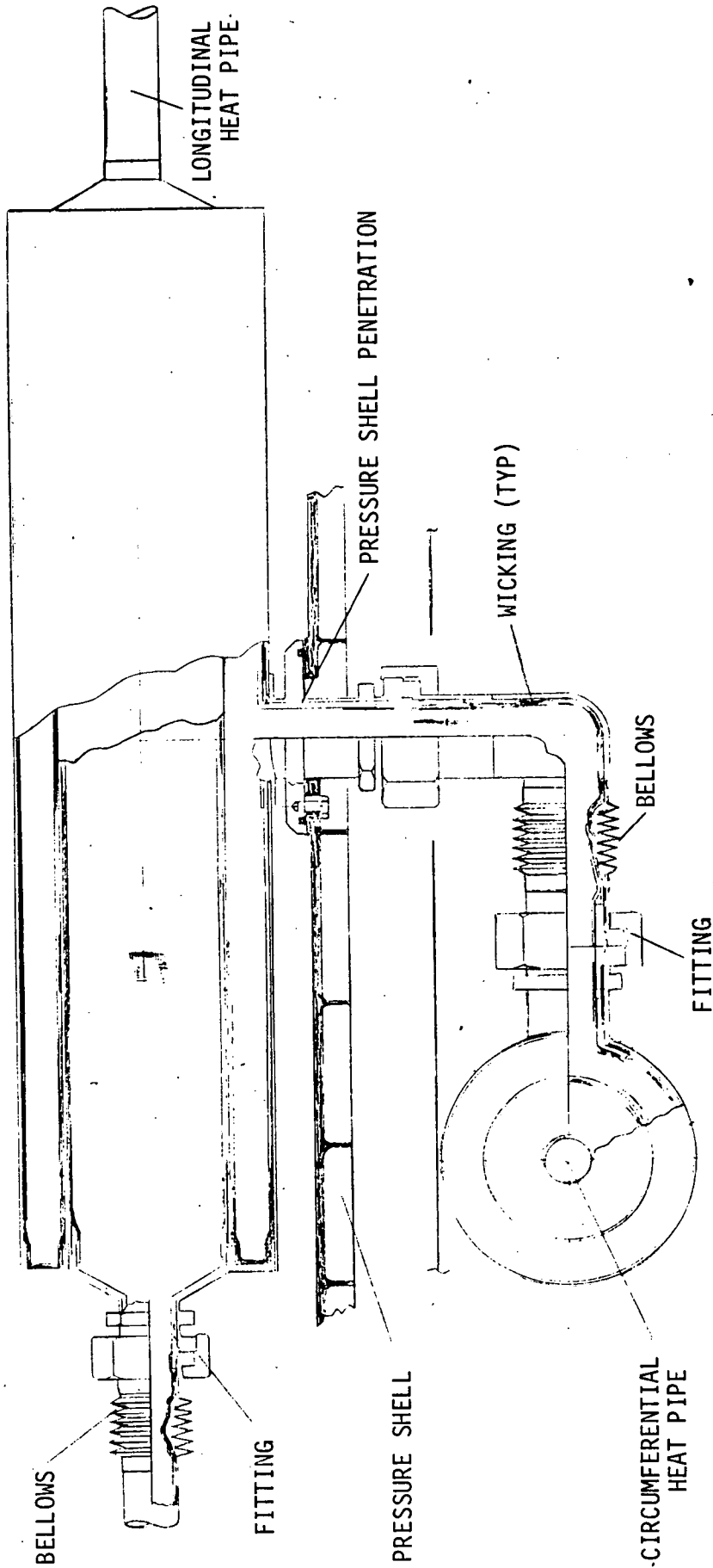


Figure 3-27. Interface - Component Heat Pipe to Longitudinal Heat Pipe



NOTE: CROSS-SECTIONS OF BOTH LONGITUDINAL HEAT PIPE AND CIRCUMFERENTIAL HEAT PIPE ARE EXPANDED AT PENETRATION REGION TO PROVIDE NECESSARY HEAT TRANSFER AREA.

Figure 3-28. Interface - Penetration Element

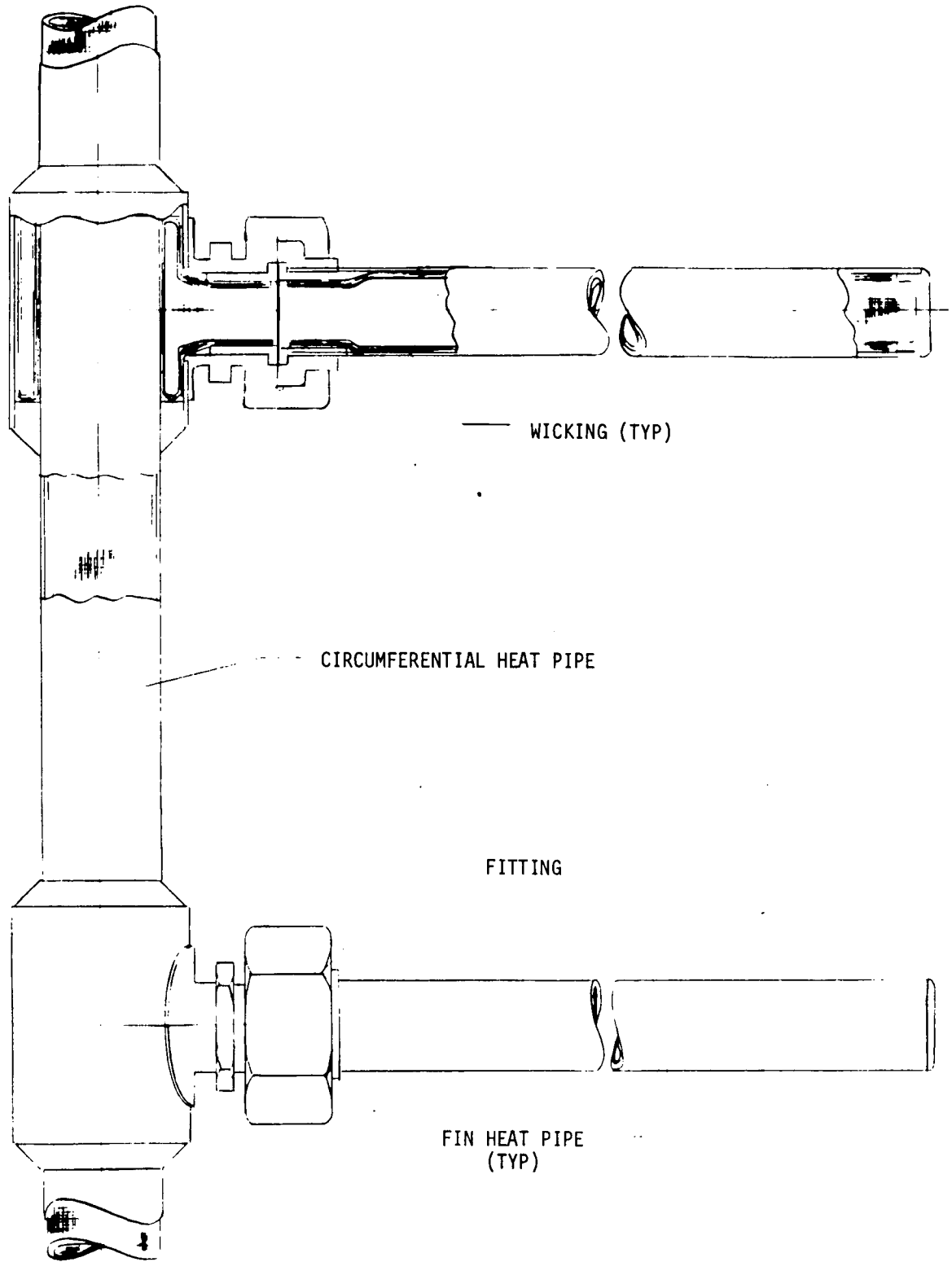


Figure 3-29. Interface - Circumferential Heat Pipe to Fin Heat Pipe

- ALL BOLTED TO PERMIT COMPONENT REMOVAL
- ALTERNATIVES - SELECTION DEPENDS ON DISSIPATION MAGNITUDE AND AVAILABLE AREA

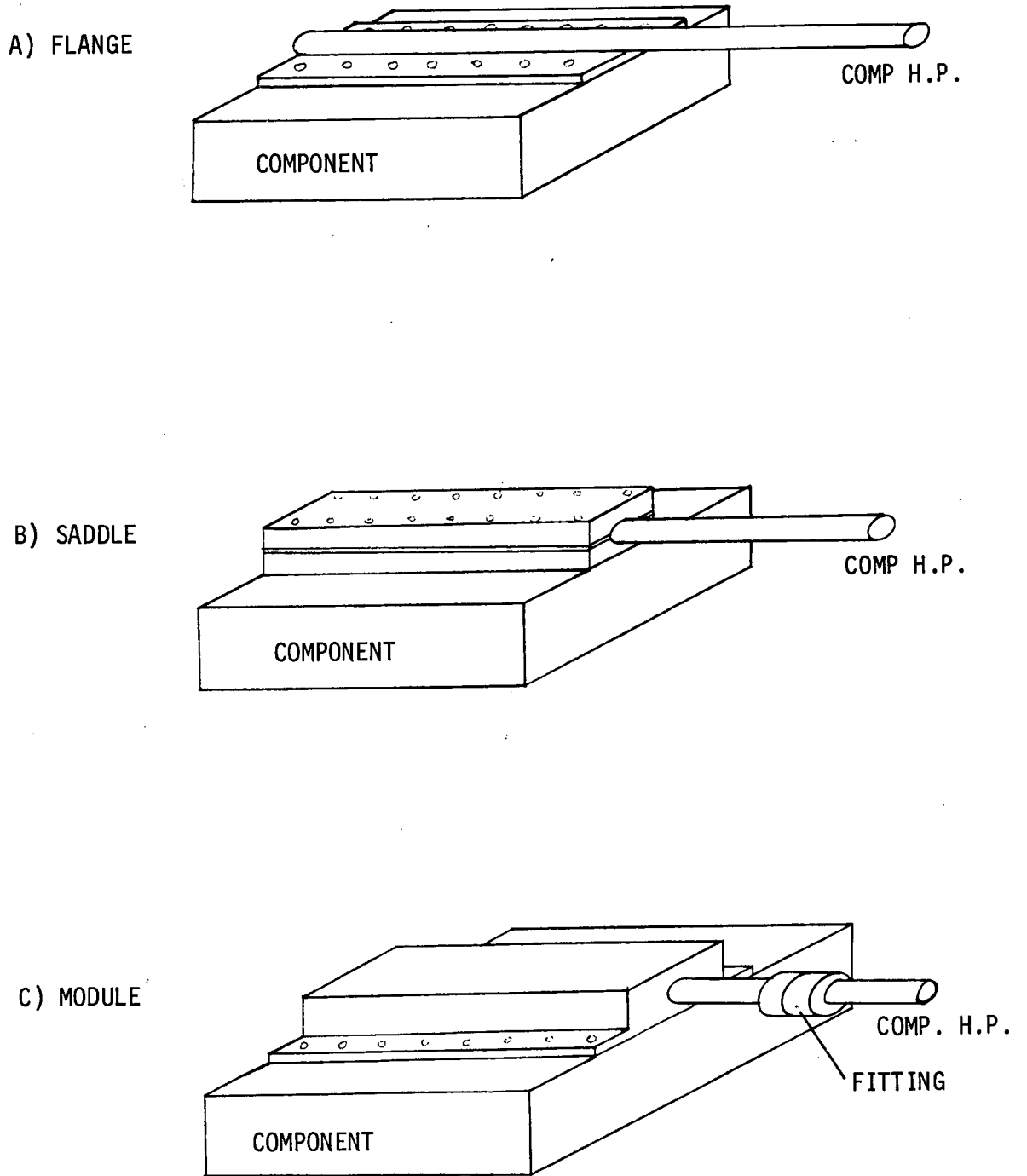


Figure 3-30. Interface - Component to Component Heat Pipe

The FINHP-radiator attachment is shown in Figure 3-31. The FINHP is provided with an integral flange which is bolted or riveted to the 0.020 inch radiator. A "tee-section" is shown on the opposite side of the FINHP cross-section to support the secondary meteoroid shield and multilayer insulation. The overall configuration is thus similar to that proposed by MDAC in their Space Station design. The heat pipe design should be slightly more efficient than MDAC's coolant tube scheme since the heat pipes can be positioned closer to the radiator and a nominal 3⁰ F temperature drop is eliminated. This is possible because the loss of a FINHP by meteoroid penetration is insignificant compared to the loss of a coolant line. The FINHP's therefore require less shielding than the coolant tubes.

The entire FINHP, including flange and tee-section, can be brazed, welded, or soldered together out of standard metallic shapes. As an alternative, the total cross-section could be extruded as one piece, if the final selection of materials permitted.

These then are the interfaces designed for the Space Station heat pipe thermal control system. Admittedly, some require development which could change general configurations from those described above. The basic technique, however, represents a highly effective means of heat transfer of the type that would be required if the heat pipe system were to be feasible.

The discussion of interface cells above introduces the concept of modularized heat pipes. In this scheme, a single heat pipe would be assembled from several standardized parts (interface cells and adiabatic sections) in a "tinker-toy" fashion. After assembly, the unit would be leak checked, evacuated, and charged with working fluid. Figure 3-32 shows a typical arrangement. The advantages of such a system are evident:

1. Individual heat pipes can be tailored to satisfy specific functional and geometric requirements.
2. Comparatively few types of piece parts need be designed and fabricated. This should permit greater optimization of configurations.
3. The fluid and heat transfer functions of the heat pipe are separated into discrete segments of the total pipe. Figure 3-32 lists the primary design criteria for the three major segments. The best wicking arrangement can be used in each segment to meet its particular criterion.

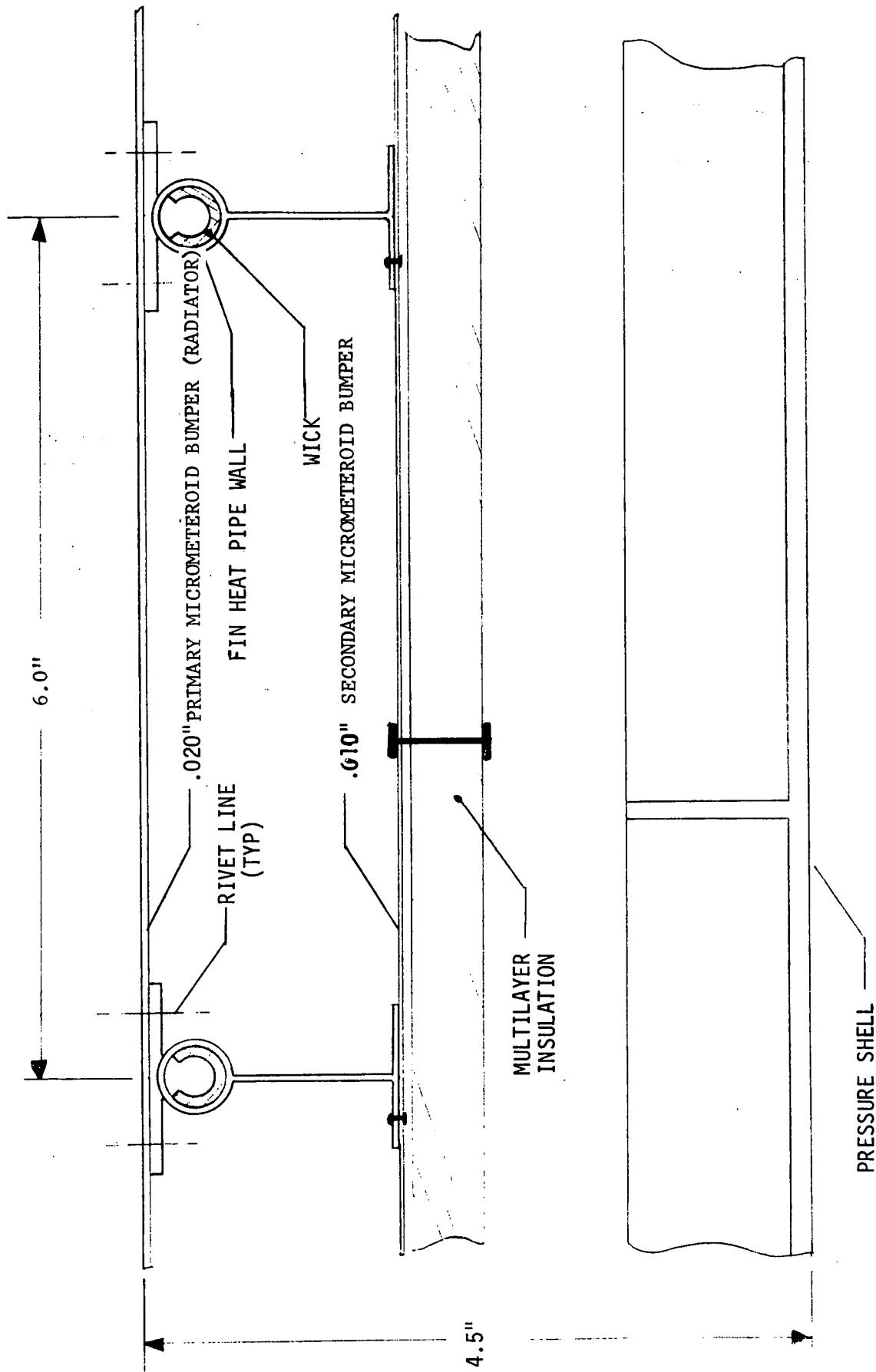
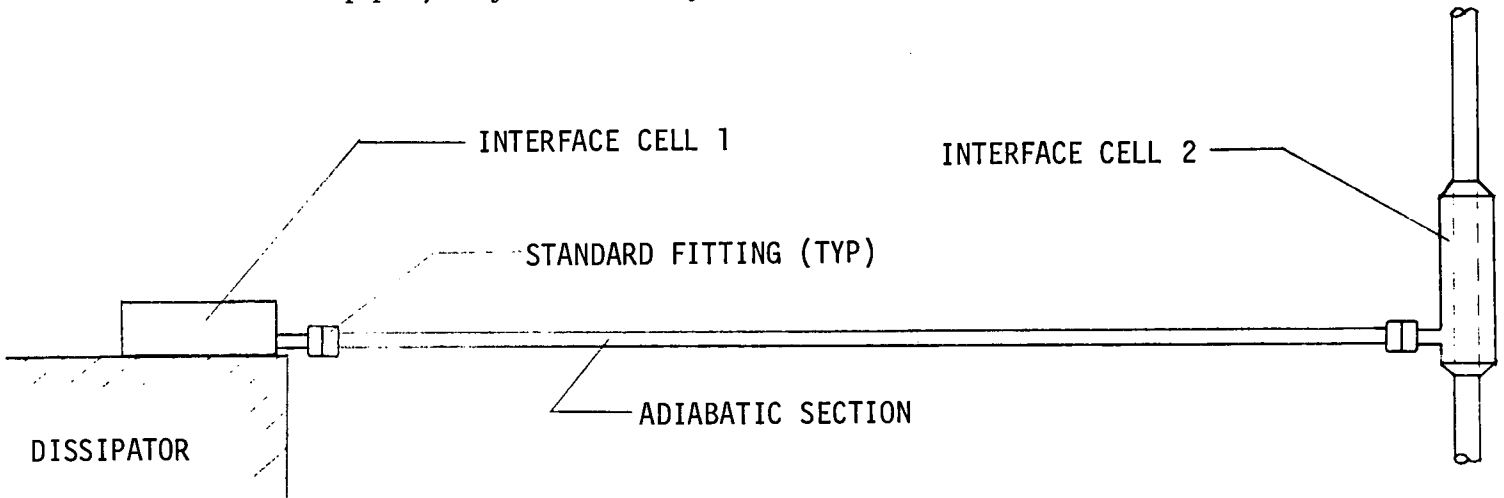


Figure 3-31. Interface - Fin Heat Pipe to Radiator

4. Replacement of damaged portions of the system is comparatively easy.
5. The number of on-board spares required would be reduced to a few standard segments.

The disadvantages, on the other hand are:

1. The technique is beyond the current state-of-the-art and therefore requires development.
2. Weight would increase slightly since only a few standard segments would be available and it would be necessary to choose the "next larger size" for each pipe.
3. The use of mechanical joining techniques suggests leaks into or out of the pipe. Preventive maintenance, such as periodic evacuation and recharging of the pipes, may be necessary.



<u>SEGMENT</u>	<u>PRIMARY DESIGN CRITERION</u>
INTERFACE CELLS	HEAT TRANSFER (ΔT AND BUBBLE FORMATION)
FITTINGS	FLUID FLOW
ADIABATIC SECTION	FLUID FLOW

Figure 3-32. Modular Heat Pipe

It is felt that the advantages of such a scheme outweigh the disadvantages. If the required techniques were developed, either for the Space Station program or independently, the modular approach would enhance the attractiveness of the Station heat pipe system.

3.3.3.4 Controllable Heat Pipes

Space Station temperature control in both Concept A and Concept B is provided by variable conductance, or controllable, heat pipes. These elements effectively vary the thermal coupling between heat source and heat sink to maintain relatively constant source temperature. The heat pipe is a good candidate for such a control device since three of the four basic mechanisms involved (evaporation, vapor flow, condensation, liquid flow) are amenable to modulation.

Both active or passive methods for controlling the flow of working fluid vapor and liquid have been postulated. Unfortunately, the hardware design of such elements becomes fairly involved and a functional heat pipe of this type suitable for consideration for Space Station application has not yet been demonstrated.

The heat pipe condenser is thus the region where control is generally effected. It is not the condensation rate that is varied; it is, instead, the effective condenser area. Again, both active and passive techniques have been suggested. All use either a non-condensable gas or a liquid (excess working fluid or an auxiliary fluid) to block a portion of the total condenser area from the working fluid vapor.

The technique selected for application to Concepts A and B uses a non-condensable gas nominally contained in a cold, wicked reservoir. The gas expands and contracts in the condenser volume passively (in accordance with heat pipe boundary conditions) to maintain acceptable temperature control at the evaporator. This design was selected because:

1. It is completely passive - no moving parts or electrical input is required.
2. Several pipes of this type have been built and tested, and design data is readily available.

3. It can provide the necessary temperature control in this application.
4. It is relatively easy to manufacture.

Several recently published documents discuss the design and performance of cold gas, external reservoir controllable heat pipes (see References 9-18, 9-19 and 9-20). The methods explained in these reports were followed in designing the variable conductance heat pipes for Concepts A and B. It should be noted here that the sizing was performed in conjunction with the system thermal analysis discussed in Section 3.3.4.2. Thus, the control requirements mentioned below were generated to yield acceptable system performance.

3.3.3.4.1 Concept A

The FINHP's are variable conductance devices. As the temperature at the evaporator of the FINHP increases, gas is pushed out of the condenser which has two beneficial effects: 1) the conductance from the heat pipe to the radiator is increased; and 2) a larger portion of the radiator is utilized to reject the heat to space.

System analyses indicate that a turn-down ratio (maximum to minimum conductance) of 5:1 and an overall evaporator temperature change of 20°F ($\pm 10^{\circ}\text{F}$ control) are acceptable characteristics of these controllable FINHP's.

Consideration of these values and the applicable boundary conditions led to the conclusion that ammonia could not be used as the working fluid in the FINHP's. It is virtually impossible to obtain the 20°F control band with ammonia (Reference 9-18). Consequently, methyl alcohol was selected for the FINHP fluid in this concept. This change required a change in wicking schemes also, from isotropic to arterial. Calculations indicated that a reservoir-to-condenser volume ratio of slightly over 3:1 would provide $\pm 10^{\circ}\text{F}$ control with a methanol-nitrogen system. However, since it was impractical to segment the entire Station radiator to achieve minimal axial conduction along the heat pipe (as assumed in the calculation), a wider vapor/gas interface was expected. To allow for this, a volume ratio of 5:1 was used in subsequent design.

The FINHP's for the three different temperature heat transport networks (Class I - 45^o F, Class II - 65^o F, Class III - 90^o F) are of different lengths and therefore have different condenser volumes. Thus, the size to the gas reservoir will vary from system to system. The reservoirs have been designed as cylinders perpendicularly attached to the ends of the FINHP's. Figure 3-33 shows the configuration. All reservoirs have a constant diameter, but the cylinder length is varied to obtain the required volume for each class network. The walls of all reservoirs are made of stainless steel and are thicker than required to contain internal pressure so that additional meteoroid shielding is provided. The performance calculation using controllable heat pipes were based on considerations of transient source and sink conditions.

The nitrogen charges for the three classes of FINHP's are different because the temperature ranges are different. Table 3-12 indicates for each class, the control range, reservoir volume required, reservoir length, and approximate nitrogen charge.

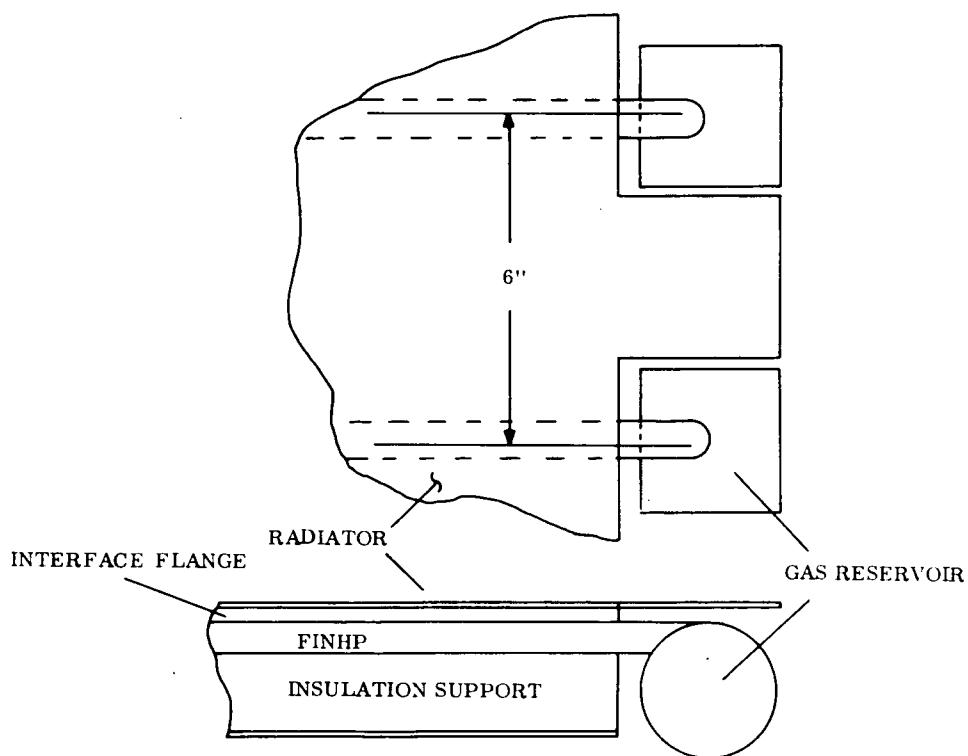


Figure 3-33. Concept A - Gas Reservoir Configuration

Table 3-12. Concept A - Controllable FINHP Requirements

Temperature Class	Control Range, °F	Reservoir Volume, in ³	Reservoir Length, in*	Nitrogen Charge, lbm
I	13-33	14.1	4.07	3.2×10^{-5}
II	35-55	4.3	1.24	1.9×10^{-5}
III	46-66	7.6	2.19	4.7×10^{-5}

*Reservoir diameter = 2.1 in.

Making the FINHP's controllable offers a secondary, but very beneficial, advantage. In certain orbits and at certain circumferential locations around the radiator, high external heat loads can cause the effective sink temperature to rise above the desired radiator temperature. Under these conditions, a fixed conductance heat pipe will operate in reverse; i. e., the external loading will be transferred into the CIRHP (circumferential heat pipe) and cause an overall system temperature rise. Gas-charged FINHP's, on the other hand, will effectively cut this hot radiator section out of the system as the gas is swept to the original evaporator. The loading on the CIRHP is minimized and the overall system can be maintained at lower temperatures than otherwise possible.

3.3.3.4.2 Concept B

The COMHP's are variable conductance devices. As the evaporator temperature increases, the conductance between the COMHP and the LONHP increases, permitting more heat to be transferred.

System studies show that a 20° F total evaporator temperature change ($\pm 10^\circ$ F) will again suffice, but that a very high turn-down ratio is required for these pipes (33:1). This requirement is higher than that of Concept A because in Concept B, interface movement varies conductance only, while in Concept A, interface movement varies conductance and the heat rejection capacity of the heat sink.

Calculations indicate that a reservoir-to-condenser volume ratio of 25:1 is necessary to meet these criteria with a methanol-nitrogen heat pipe. Although the adiabatic length of the

COMHP's vary, the condenser lengths (and volumes) are fixed. Thus, all variable COMHP's have the same reservoir volumes. The volume is calculated to be 265 cu. in. This large reservoir must be thermally coupled to the LONHP and must be wicked. Figure 3-34 shows the tentative configuration.

Again, the amount of nitrogen charge is different for each of the three classes. Table 3-13 presents the approximate charges. Since the reservoirs contain working fluid vapor at temperature just slightly below that of the evaporator, relatively small quantities of nitrogen are required. There is, however, a question regarding the performance of such variable conductance heat pipes. They will be very sensitive to sink temperature changes and, even under constant sink conditions, the length of the vapor/gas interface may be large.

Table 3-13. Concept B - Controllable COMHP Requirements

Temperature Class	Control Range, °F	Nitrogen Charge, lbm
I	35-55	7.8×10^{-5}
II	55-75	15.0×10^{-5}
III	80-100	35.9×10^{-5}

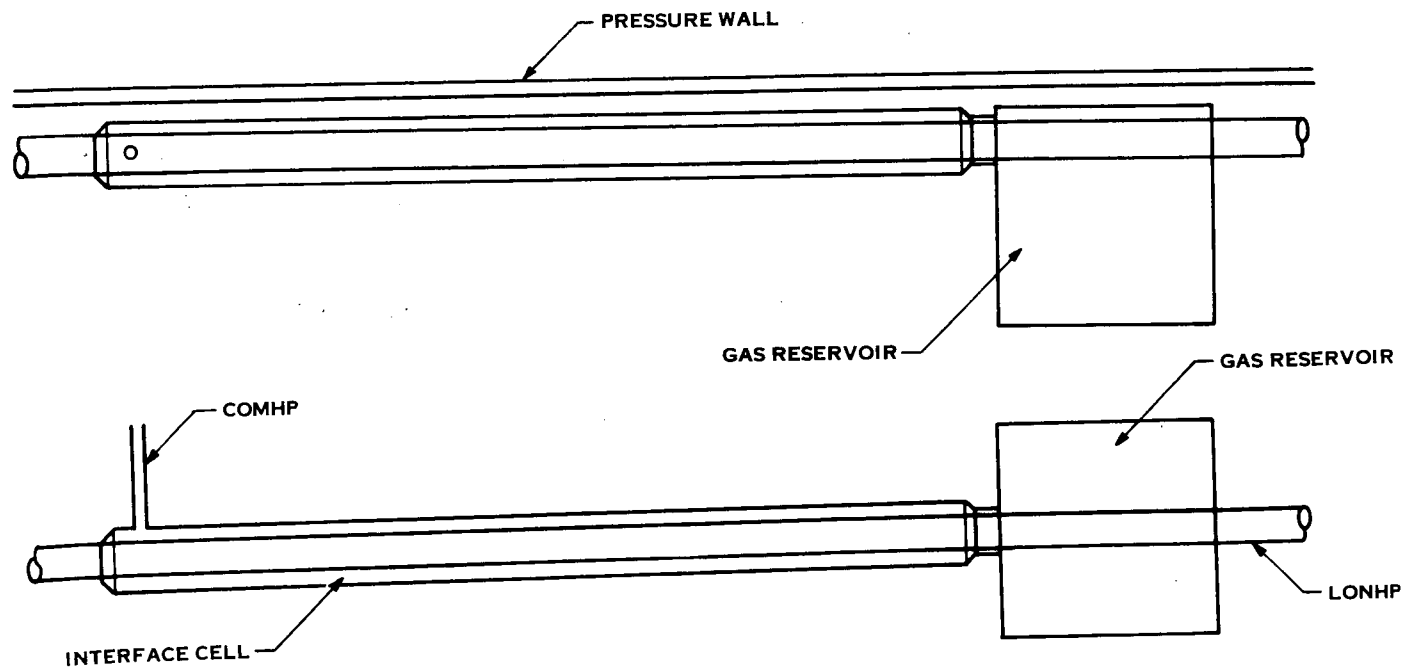


Figure 3-34. Concept B - Gas Reservoir Configuration

3.3.4 SYSTEM CHARACTERISTICS

3.3.4.1 Weight Summary

This section presents a weight summary for Concepts A and B, and compares these weights to that of a pumped liquid loop system providing equivalent thermal control for the Space Station. Each of the three systems included all primary hardware required to collect, transport, and reject to space the heat generated within the pressurized cabin, and to provide temperature control under varying thermal boundary conditions.

Specifically omitted from consideration in this analysis were such items as support structure, monitoring equipment, and on-board spares. This was done for three reasons:

1. The weights of these elements were difficult to ascertain at this stage of system definition.
2. At any rate, the weights involved will be only a small portion of the total system weights.
3. Each of the three systems would most likely require roughly equivalent equipment weight to perform these functions.

The weight breakdown is shown in Table 3-14. The following comments are offered in explanation of the entries.

1. All item weights for the pumped loop system except the first and last (0.020 inch aluminum radiator and power weight penalty) were obtained from McDonnell Douglas Space Station documents (References 9-12 to 9-16).
2. The 0.020 inch aluminum radiator has been included in the weight of each system, even though it is, in fact, the primary meteoroid shield for the Station.
3. A weight penalty for supplying electrical power to the thermal subsystem was assigned to each of the three designs. A weight of 0.57 pounds per electrical watt was used for a Brayton/Isotope EPS. A total power requirement of 758 watts (average) for the pumped loop system was found in the previously mentioned McDonnell Douglas reports.

Table 3-14. Weight Summary
(Pounds)

Item	Pumped Loop Total Item Wt.	Concept A			Concept B		
		No. Units	Factor	Total	No. Units	Factor	Total
<u>External</u>							
.020" Alum. Radiator	850	--	--	850	--	--	850
Freon Tubes	2811	--	--	0	--	--	0
Manifolds	92	--	--	0	--	--	0
Freon	301	--	--	0	--	--	0
FINHP	0	6106 ft	.25#/ft	1527	6106 ft	.25#/ft	1527
CIRHP	0	624 ft	.60#/ft	374	624 ft	.60#/ft	374
Control Gas Reservoir	0	1272	.61	776	--	--	0
Interfaces	0	1272	.11	140	1272	.11	140
Coating	239	--	--	359	--	--	359
Insulation	929	--	--	929	--	--	929
Total External	5222			4955			4179
<u>Internal</u>							
Heating Water Loop	48	--	--	48	--	--	48
Freon Loop	1048	--	--	0	--	--	0
Cooling Water Loop	40	--	--	0	--	--	0
Fluids	860	--	--	0	--	--	0
Cold Plates	700	--	--	630	--	--	630
COMHP	0	2380 ft	.15#/ft	357	2380 ft	.15#/ft	357
LONHP	0	630 ft	.60#/ft	378	630 ft	.60#/ft	378
PENHP	0	36	9.54	343	36	9.54	343
Control Gas Reservoir	0	--	--	0	340	2.39	813
Interfaces	0	680	.83	564	680	.83	564
Pwr Wt Penalty	432	--	--	75	--	--	75
Total Internal	3128			2395			3208
TOTAL STATION	8350			7350			7387

Note: 1) Heat pipes not weight optimized
2) Stainless steel used as heat pipe material; other materials may be used if required.

4. All three systems employ a pumped loop heating water supply from the electrical power subsystem. The power drain for this loop is 132 watts, which is included in the 758 watt figure for the active system in 3 above.
5. Identical insulation schemes (and therefore weights) were assumed for all systems.
6. Per the Data Handbook prepared earlier in this project, the weight of the series emittance thermal control tape employed on Concepts A and B was assumed to be 1.5 times that of the Z-93 white paint used on the pumped loop system.
7. Heat pipe weights per unit length were cited previously in this report. All heat pipes are fabricated using stainless steel as the containment vessel material. Total pipe lengths were calculated as follows:

COMHP	340 pipes @ 7 ft/pipe (avg.) = 2380 ft.
LONHP	18 pipes @ 35 ft/pipe = 630 ft.
CIRHP	6 pipes @ 104 ft/pipe = 624 ft.
FINHP	1272 pipes @ 4.8 ft/pipe (avg.) = 6106 ft.

8. The PENHP's were treated as units weighing 9.54 pounds each.
9. All heat pipe weights include containment vessel, wicking, and working fluid.
10. The weight of the cold plates (both integral and separate) in the heat pipe systems was assumed to be 10% lighter than that associated with the pumped loop system.
11. Weights for the control gas reservoirs on the variable conductance heat pipes were calculated based on internal volume requirement shape, and from 0.030 inch to 0.040 inch thick stainless steel walls depending on stress calculations.
12. Interface weights were based on heat transfer area required, interface configuration, and from 0.025 inch to 0.035 inch thick stainless steel wall.

Summarizing Table 3-14, it can be seen that both heat pipe system concepts offer weight savings over the pumped loop design. The reduction is about 12% for both Concept A and Concept B. Weights for the heat pipe networks are almost identical for either internal or external variable conductance devices.

3.3.4.2 Thermal Performance

Mathematical thermal models of Concept A and Concept B thermal control systems were generated and used to predict on-orbit temperatures with a variety of Space Station boundary conditions. These models were run with the THTD (Transient Heat Transfer-Version D) computer code. A total of forty-two cases were run to assess the effects of 1) Space Station orbit/orientation, (2) internal heat dissipation, (3) radiator coating properties, (4) radiator blockage, and (5) variable conductance heat pipe characteristics.

Because Concept A and Concept B were similar except for the position of the controllable heat pipes, the basic modeling technique was the same for both. The next subsection describes methods used that were common to the two models.

3.3.4.2.1 General Modeling Technique

The THTD program computes both transient and steady-state temperature solutions for large, three dimensional problems which can include conduction, convection, thermal radiation, and isothermal phase change with materials whose thermal properties are temperature dependent. Program information can be found in Reference 9-21. Only one of the two Common Modules of the Space Station was modeled since the longitudinal heat pipes will average heat inputs from the two sections and present one "source" temperature to the remainder of the heat transport and rejection system. Originally, a 108 node model was developed for the Common Module, which consisted of three independent 36 node networks, one each for the three temperature classes. The 36 nodes included 12 circumferential radiator nodes, 12 CIRHP nodes, 6 LONHP nodes, and 6 internal dissipator nodes. Intervening heat pipes (COMHP's and PENHP's) were simulated as conductance elements, and were not designated as nodes. Figure 3-35 presents a sample data sheet showing one 36 node temperature class system.

Runs made with this model showed that very little error would be introduced in the temperature profile by assuming that the radiator of each class system operated at its circumferentially averaged temperature. In other words, because of the CIRHP's, circumferential gradients were small and had an insignificant effect on overall system performance. The

INSTANTANEOUS TEMPERATURE DISTRIBUTION

CLASS I SYSTEM

- MAX. POINT IN ORBIT 2
- $\alpha / \epsilon = .21 / .83$
- NOMINAL DISSIPATION
- TEMPERATURES IN °F

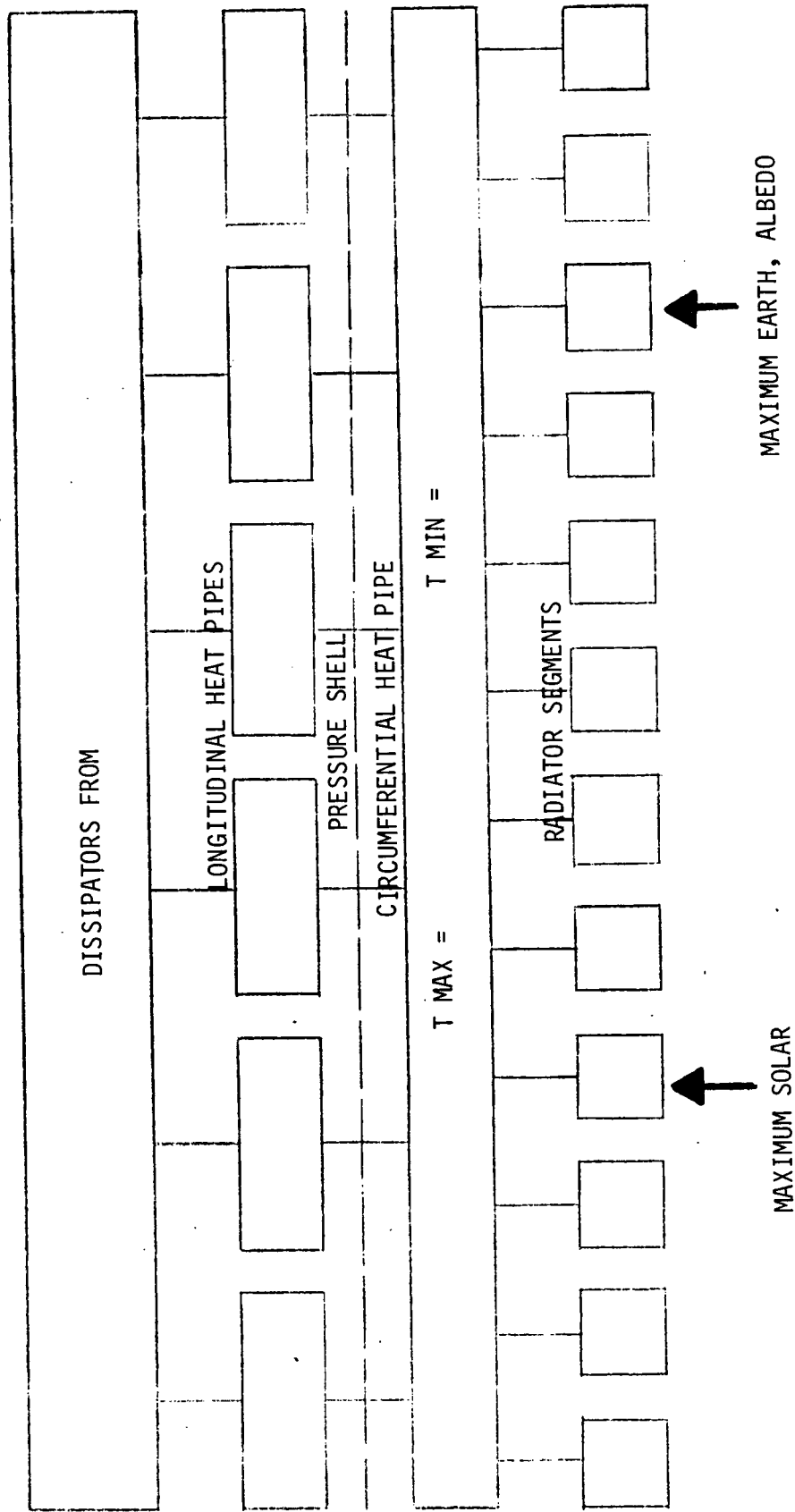


Figure 3-35. Nodal Breakdown - Segment of Detailed Model

model was simplified at this point to 12 nodes, three systems of four nodes each (component, LONHP, CIRHP, radiator). Figure 3-36 shows this model. In one specific case -- Concept A, Orbit 1 - the simplified model led to inaccuracies of approximately 6-8° F based on detailed model results. Consequently, all runs involving this combination were made with the larger model.

In the simplified model, the vapor of all heat pipes was assumed isothermal and conductance between nodes was determined based on interface designs previously presented. Calculation of the total internode conduction terms included consideration of the number of parallel heat paths connecting the nodes. Internode radiation was ignored, but radiation coupling to the space boundary was calculated for the three radiators. Conduction and radiation terms used in the 12 node model are shown in Table 3-15.

Table 3-15. Internode Conductances

Node-Node	Conductance Btu/hr - °F		
	Class I	Class II	Class III
Comp - LONHP	2731	3959	4915
LONHP-CIRHP	5001	5001	5001
CIRHP-Rad	5652	3960	5310

Radiation

Radiator	Radiation to Space*, Ft ²
Class I	511
Class II	216
Class III	421

* Term is $\eta' \in AF_A$ radiator \rightarrow space

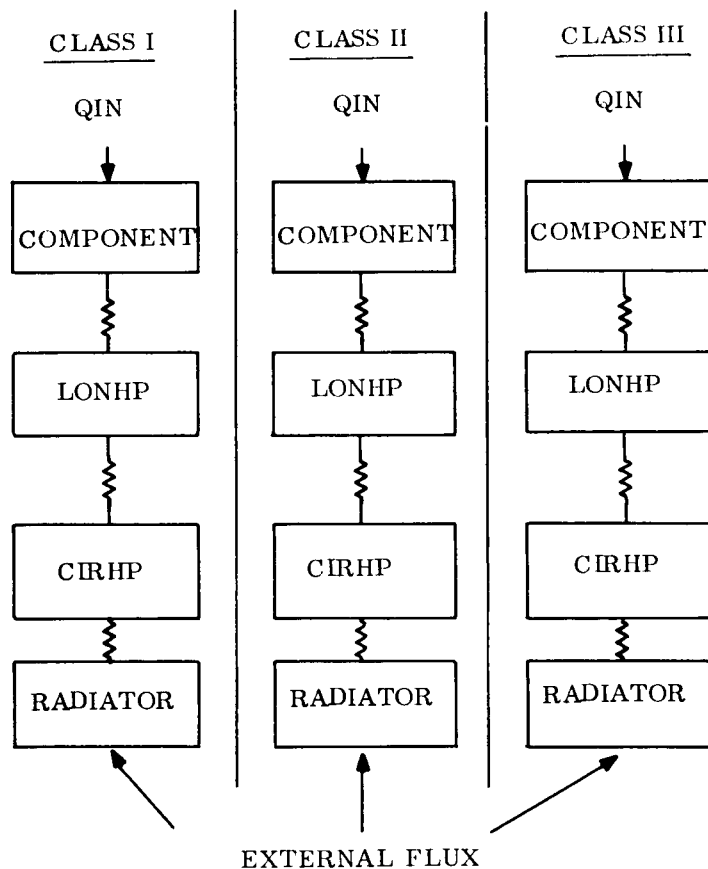


Figure 3-36. Nodal Breakdown - Simplified Model

Thermal capacity for all nodes was determined from calculated weights and an assumed specific heat of $0.2 \text{ Btu/lb} - ^\circ\text{F}$ constant. Heat pipe and radiator weights were divided between applicable nodes. (In other words, 50% of the PENHP weight was assigned to the LONHP, 50% to the CIRHP, etc.). Component weight was determined by summing the weights of the individual dissipators of each class. This results in very conservative transient response predictions since, in essence, the model includes the full Common Module heat rejection capability but only a small portion of its actual mass. Orbital temperature swings presented later in this section should thus be regarded as extreme variations which will probably not occur. Table 3-16 lists the weights used in constructing the 12 node model. Class II component weight is large since it includes a number of heavy batteries.

The effect of radiator blockage on system temperatures was determined by assuming that both external flux into and radiation from the radiators were reduced by a constant percentage. Admittedly, this is a gross assumption but it should suffice to predict trends.

Table 3-16. Component Weights

Node	Total Assigned Weight, lbs		
	Class I	Class II	Class III
Component	800	3955	322
LONHP	147	156	162
CIRHP	138	138	138
Radiator	726	300	592

Internal and external heating profiles were assumed as stated previously in this report.

3.3.4.2.2 Concept A

Both the conductance from the FINHP's to the radiator and the effective radiator area to space were varied as functions of the temperature of the vapor of the FINHP's. Figure 3-37 shows that the dependent variable was assumed to vary linearly with temperature and describes the nomenclature used to characterize the variable conductance heat pipes.

Choosing the correct band midpoint and control band to use was performed by exercising the model with assumed values and noting the results. Runs with 10°F and 20°F control bands showed little difference in average component temperatures and consequently the 20°F band was selected, being easier to obtain with lightweight gas reservoirs. The minimum value of the dependent variable was initially set at 20% of the full value and was not changed in

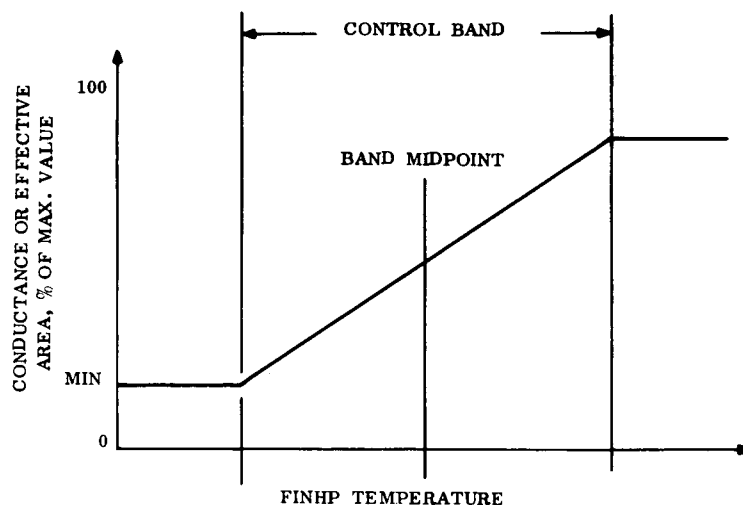


Figure 3-37. Concept A - Controllable Heat Pipe Characteristics

subsequent runs. Parametric curves aided in the setting of the band midpoints. Figure 3-38 shows the graph which was used for final midpoint definition. The intersection of the performance line with the desired temperature of each Class (45, 65, and 90°F, respectively) yielded the optimum midpoint of each Class (23, 45 and 56°F, respectively). Table 3-17 presents the data for all 31 runs made for Concept A. Information to the left of this Table is identification/input data and results are shown to the right. Output quantities consist of the minimum and maximum orbital temperatures for the radiator and components of Classes I, II and III. The average of the minimum and maximum is very nearly the orbital average temperature for each item.

A series of graphs were prepared from the basic data on Table 3-17 to depict overall Concept A thermal performance. The applicable figures are described on the page following

Table 3-17.

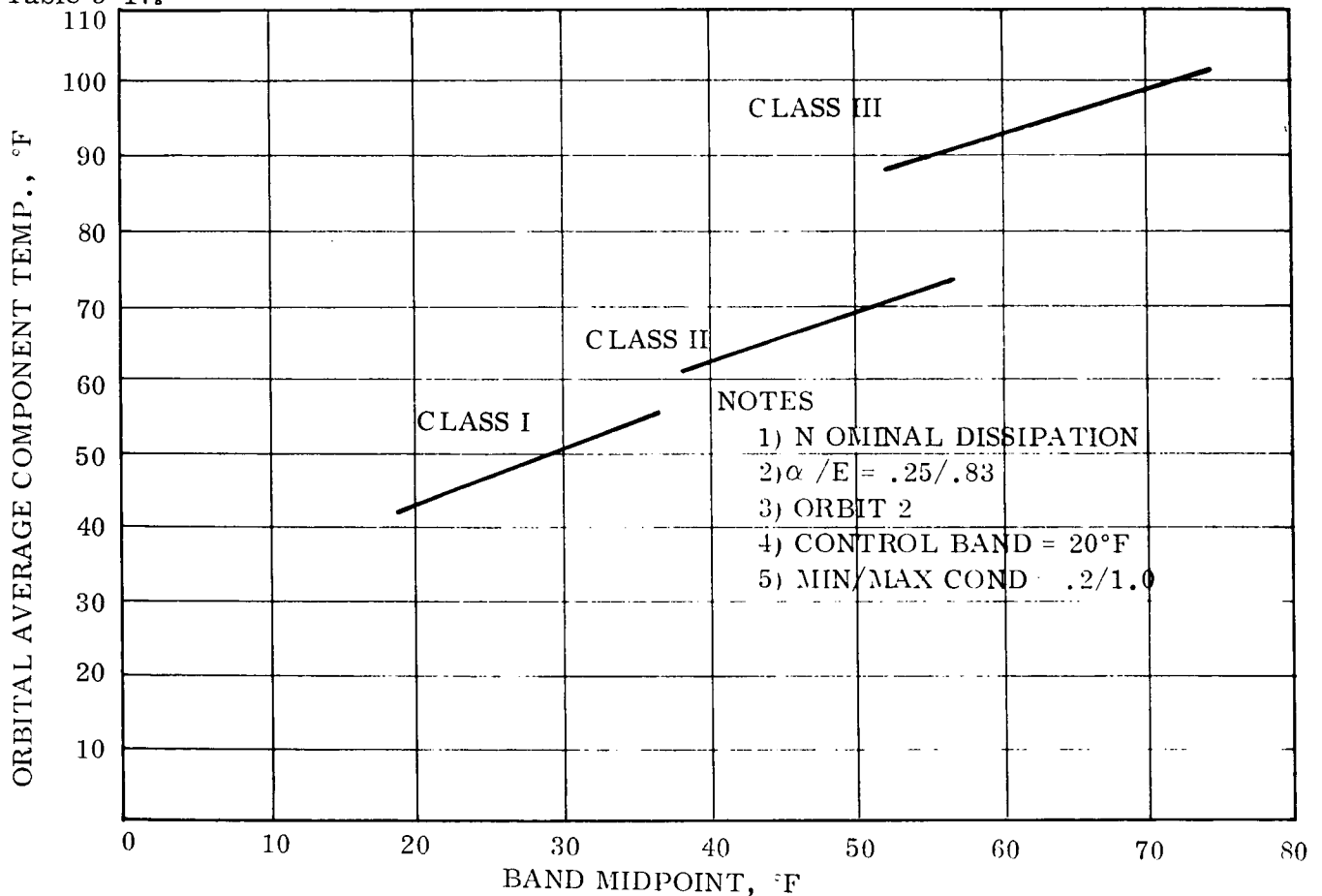


Figure 3-38. Concept A - Control Midpoint Sensitivity

Table 3-17. Space Station Heat Pipe
 Concept A Analytical Results
 (Temperature in °F)

Run No.	Size of Model ~ Nodes	Orbit No.	Internal Generation	α/ϵ	Control Band ~ °F	Class I				Class II				Class III			
						Radiator		Components		Radiator		Components		Radiator		Components	
						T _{max}	T _{min}	T _{max}	T _{min}	T _{max}	T _{min}	T _{max}	T _{min}	T _{max}	T _{min}	T _{max}	T _{min}
1	108	Hottest 1 Average	Nominal	.25/.83	I 30-40 II 50-60 III 65-75	48.7	60.7	60.7	67.6	67.6	76.3	76.3	84.6	84.6	102.8	102.8	
2	108	Largest 2 Transient	Nominal	.25/.83	I 30-40 II 50-60 III 65-75	49.6	60.0	49.1	66.0	57.7	72.7	69.9	88.8	71.4	106.5	91.8	
3	108	Coldest 3 Average	Nominal	.25/.83	I 30-40 II 50-60 III 65-75	34.3	48.5	47.9	55.9	55.3	66.2	66.1	71.2	70.6	91.8	91.4	
4	108	Hottest 1 Average	Nominal	.21/.83	I 30-40 II 50-60 III 65-75	45.1	57.4	57.4	64.7	64.7	73.6	73.6	81.7	81.7	100.2	100.2	
5	108	Largest 2 Transient	Nominal	.21/.83	I 30-40 II 50-60 III 65-75	44.7	55.5	49.0	63.0	57.1	70.4	62.7	83.1	71.4	100.7	91.8	
6	108	Coldest 3 Average	Nominal	.21/.83	I 30-40 II 50-60 III 65-75	34.2	48.4	47.9	55.8	55.3	66.2	66.1	71.2	70.6	91.7	91.4	
7	108	Hottest 1 Average	Nominal	.17/.83	I 30-40 II 50-60 III 65-75	41.8	54.5	54.5	62.2	62.2	71.4	71.4	78.7	78.7	97.5	97.5	
8	108	Largest 2 Transient	Nominal	.17/.83	I 30-40 II 50-60 III 65-75	40.9	52.1	48.8	60.9	56.8	68.9	67.8	78.4	71.4	96.3	91.8	
9	108	Coldest 3 Average	Nominal	.17/.83	I 30-40 II 50-60 III 65-75	34.0	48.4	47.9	55.7	55.3	66.2	66.1	71.1	70.6	91.8	91.4	
10	108	Largest 2 Transient	Nominal	.21/.83	I 20-30 II 40-50 III 55-65	38.6	49.0	39.4	56.7	48.9	63.6	60.9	79.1	62.1	96.8	82.0	
11	108	Coldest 3 Average	Minimum	.17/.83	I 20-30 II 40-50 III 55-65	23.4	34.1	33.5	44.6	44.2	52.5	52.4	59.8	59.2	75.6	75.1	
12	12	Hottest 1 Average	Nominal	.21/.83	I 20-40 II 40-50 III 65-75	39.2	50.4	50.4	61.5	61.5	70.2	70.2	74.9	74.9	92.3	92.3	
13	12	Largest 2 Transient	Nominal	.21/.83	I 20-30 II 40-50 III 55-65	35.7	46.0	39.2	55.3	48.1	62.0	59.4	76.9	62.0	93.9	81.0	
14	12	Coldest 3 Average	Minimum	.17/.83	I 20-30 II 40-50 III 55-65	23.4	33.2	33.1	44.6	44.1	52.2	52.1	59.7	59.2	74.7	74.6	
15	12	No Ext. Flux	Minimum	.83	I 20-30 II 40-50 III 55-65	20.3	34.5	34.5	42.0	42.0	51.8	51.8	57.4	57.4	75.5	75.5	

Table 3-17. Space Station Heat Pipe
Concept A Analytical Results
(Temperature in °F) (Cont)

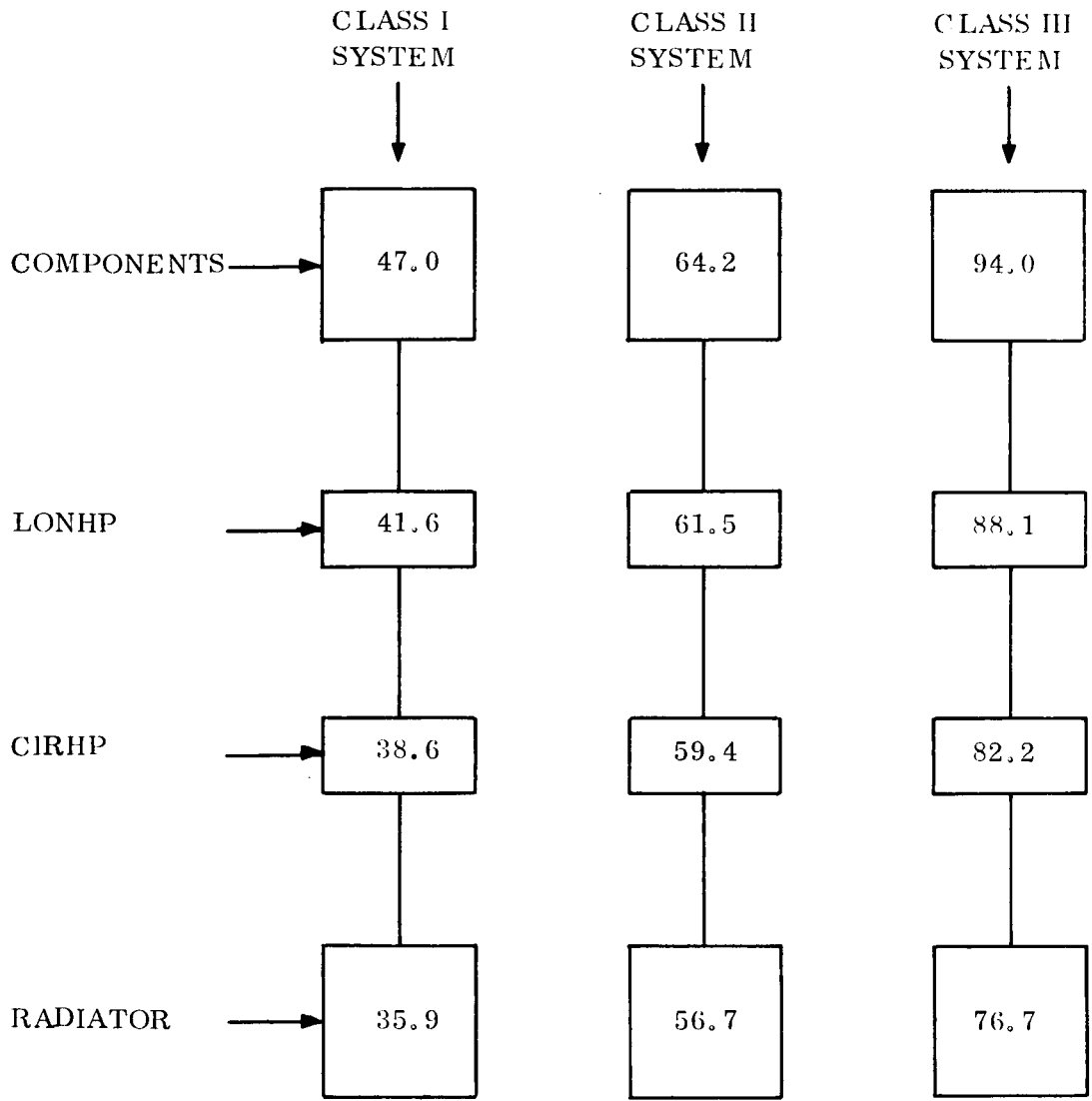
Run No.	Size of Model - Nodes	Orbit No.	Internal Generation	c/k	Control Band ~ F	Class I				Class II				Class III			
						Radiator		Components		Radiator		Components		Radiator		Components	
						T _{max}	T _{min}	T _{max}	T _{min}	T _{max}	T _{min}	T _{max}	T _{min}	T _{max}	T _{min}	T _{max}	T _{min}
16	12	2 Largest Transient	Nominal	.25/.83	I 20-30 II 40-50 III 55-65	41.3	25.2	51.4	38.6	58.3	48.9	64.6	60.9	83.2	62.0	100.3	81.1
17	12	2 Largest Transient	Nominal	.25/.83	I 23-33 II 43-53 III 55-68	42.7	27.9	52.8	41.3	59.8	51.2	66.1	62.9	84.0	64.7	101.1	84.0
18	12	2 Largest Transient	Nominal	.25/.83	I 30-40 II 50-60 III 65-75	46.3	34.5	56.4	48.0	64.0	57.1	70.5	68.4	85.9	71.3	103.1	90.9
19	12	2 Largest Transient	Nominal	.25/.83	I 15-35 II 35-55 III 50-70	42.8	25.9	53.0	39.6	60.1	51.7	66.5	63.5	84.2	63.9	101.2	83.1
20	12	2 Largest Transient	Nominal	.25/.83	I 18-38 II 38-58 III 53-73	44.4	28.4	54.5	42.2	61.6	53.8	68.1	65.5	85.1	66.5	102.1	85.8
21	12	2 Largest Transient	Nominal	.25/.83	I 25-45 II 45-65 III 60-80	48.3	34.4	58.4	48.3	66.2	59.3	72.8	70.8	87.5	72.6	104.7	92.4
22	108	1 Hottest Average	Nominal	.25/.83	I 13-33 II 35-55 III 46-66	43.1	43.1	54.7	54.7	66.4	66.4	74.9	74.9	80.6	80.6	98.4	98.4
23	12	2 Largest Transient	Minimum	.17/.83	I 13-33 II 35-55 III 46-66	31.0	21.6	38.3	31.7	52.3	47.1	57.6	55.8	64.6	56.8	76.9	71.3
24	12	3 Coldest Average	Minimum	.17/.83	I 13-33 II 35-55 III 46-66	20.0	19.0	29.7	39.2	43.9	43.3	51.4	51.1	55.8	55.1	70.7	70.2
25	12	2 Largest Transient	Nominal	.21/.83	I 13-33 II 35-55 III 46-66	36.7	23.8	46.9	37.3	57.5	50.8	64.3	62.1	76.8	60.3	93.9	79.4
26	12	3 Coldest Average	Nominal	.17/.83	I 13-33 II 35-55 III 46-66	22.2	21.2	35.2	34.7	47.4	46.8	57.2	57.2	59.6	58.7	78.9	78.4
27	108	1 Hottest Average	Nominal	.17/.83	I 13-33 II 35-55 III 46-66	34.4	34.4	46.6	46.6	58.3	58.3	67.4	67.4	71.7	71.7	89.9	89.9
28	12	2 Largest Transient 10 ⁷ Blockage	Nominal	.21/.83	I 13-38 II 35-55 III 46-66	37.8	24.8	48.2	38.2	60.6	53.1	67.4	64.5	81.1	61.9	98.4	80.6
29	12	1 Hottest Average	I Nominal II Nominal III (Max (1hr Spike.))	.25/.93	I 13-33 II 35-55 III 46-66	43.1	43.1	54.7	54.7	66.4	66.4	74.9	74.9	118.2	80.6	147.7	98.3
30	12	2 Largest Transient 20 ⁷ Blockage	Nominal	.21/.83	I 13-33 II 35-55 III 46-66	39.4	26.0	49.7	39.2	64.0	57.2	70.9	68.4	87.5	66.7	104.7	85.5
31	12	2 Largest Transient	Nominal	.36/.90	I 13-33 II 35-55 III 46-66	54.0	24.3	63.7	39.2	68.4	54.0	73.9	68.2	93.4	59.7	110.4	79.2

1. Figure 3-39 shows the 12 node temperature distribution at a particular instant in Orbit 2 for an otherwise nominal case. This indicates the magnitude of anticipated instantaneous temperature gradients within the system.
2. Figure 3-40 traces the temperature-time history of the Class I, II and III components for a dynamically stable Orbit 2 condition.
3. Figure 3-41 illustrates the sensitivity of the system to radiator coating properties. System performance with a degraded coating may be inferred from this graph.
4. Figure 3-42 indicates radiator blockage effect.
5. Figure 3-43 depicts component temperatures with off-design internal heat dissipations.
6. Figure 3-44 shows the transient temperature response of the Class III components when dissipating 150% of their nominal heat load for one hour. This performance is clearly unacceptable and the use of a thermal capacitor (of phase change material) was suggested to minimize the temperature rise. In view of the conservative assumptions in assigning nodal weights when constructing the model, however, it was felt that the predicted response was not a true indication of transient behavior. Further definition of Class III component thermal environment and weight is required to assess the problem.

In addition, Table 3-18 was prepared to demonstrate the effect of orbit/orientation changes on the system.

Overall, the thermal performance was judged acceptable. Temperature levels and gradients under nominal Space Station conditions are very good. Sensitivity studies demonstrate temperature control to within about $\pm 10^{\circ}\text{F}$ at the components when variables such as coating properties, blockage, internal dissipation, and orbit/orientations are varied singly over credible ranges. The effects of "stacking" minimum or maximum values of these parameters will be more severe, but any devised Space Station thermal control system would have difficulties under these conditions. Corrective actions such as increased/decreased internal generation or orientation change would be warranted.

(TEMPERATURES IN °F)



NOTES

- 1.) NOMINAL DISSIPATION
- 2.) $\alpha/\epsilon = .21/.83$
- 3.) ORBIT 2 (TIME = 17.5 MIN)

Figure 3-39. Concept A - Nominal Temperature Profile

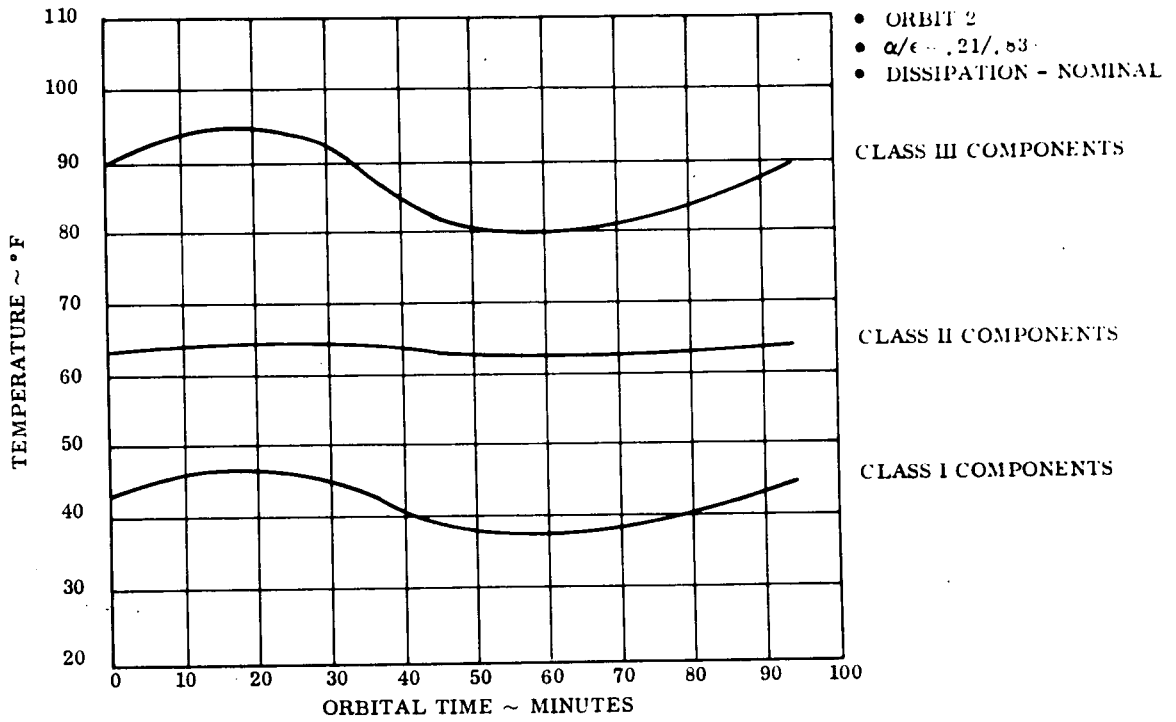


Figure 3-40. Concept A - Orbital Temperature-Time History

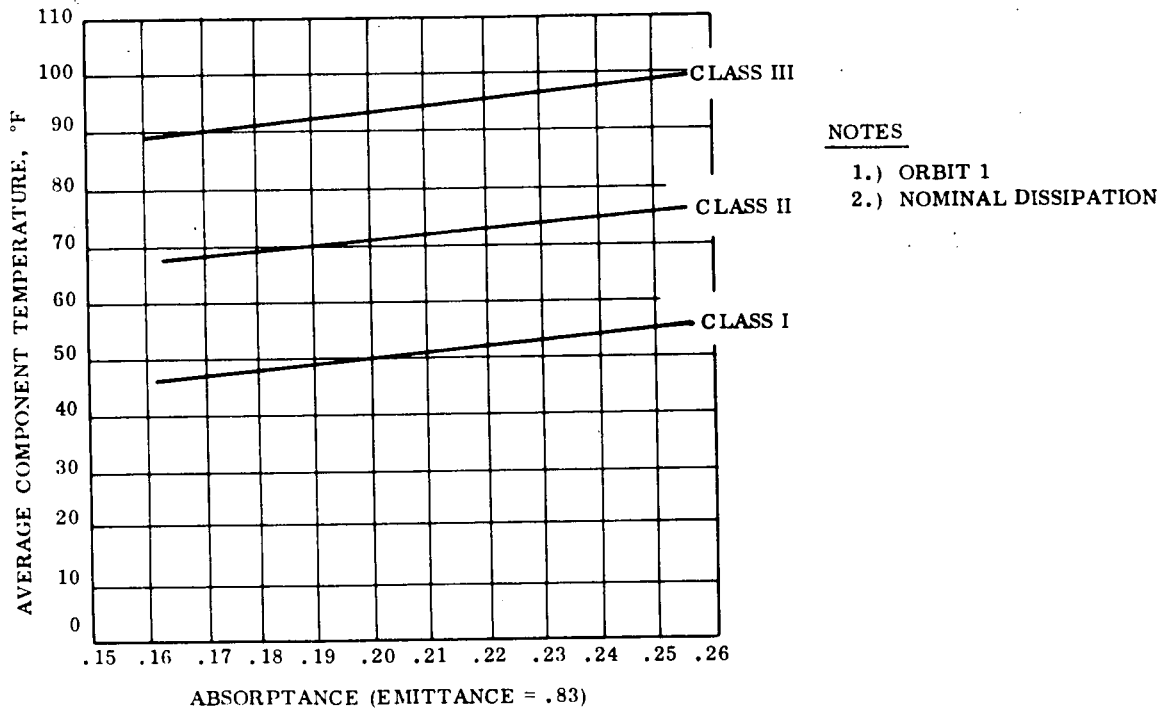


Figure 3-41. Concept A - α/ϵ Sensitivity

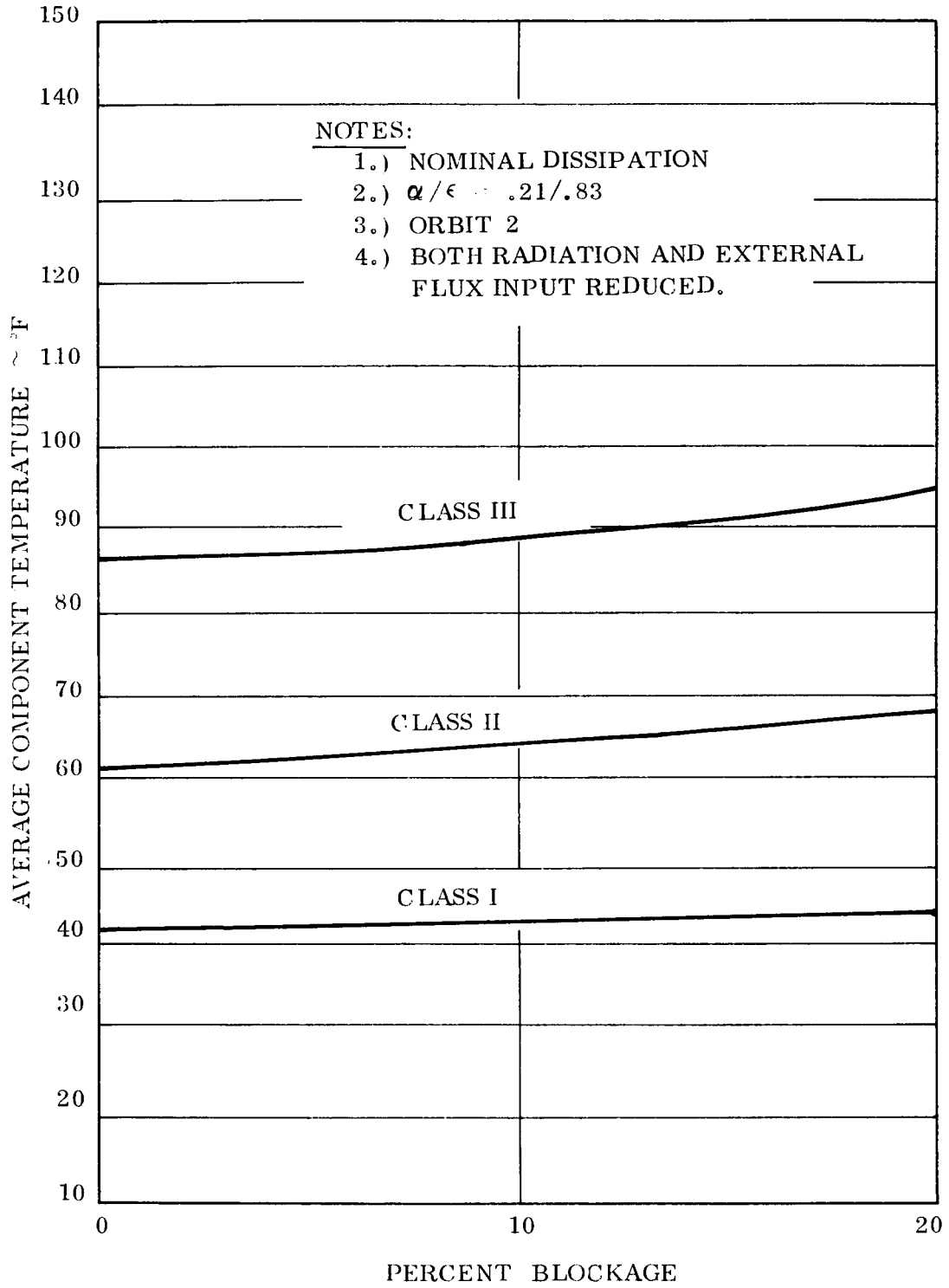
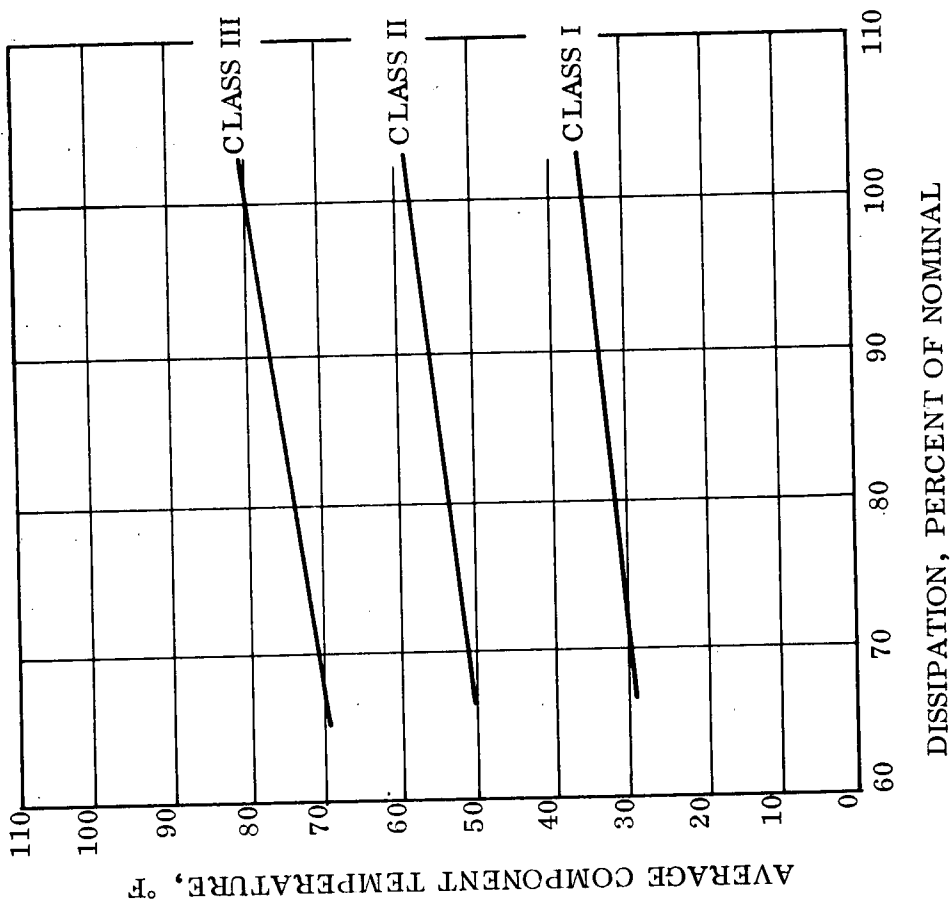


Figure 3-42. Concept A - Blockage Sensitivity



NOTES

- 1.) $\alpha/\epsilon = .17/.83$
- 2.) ORBIT 3

Figure 3-43. Concept A - Internal Dissipation Sensitivity

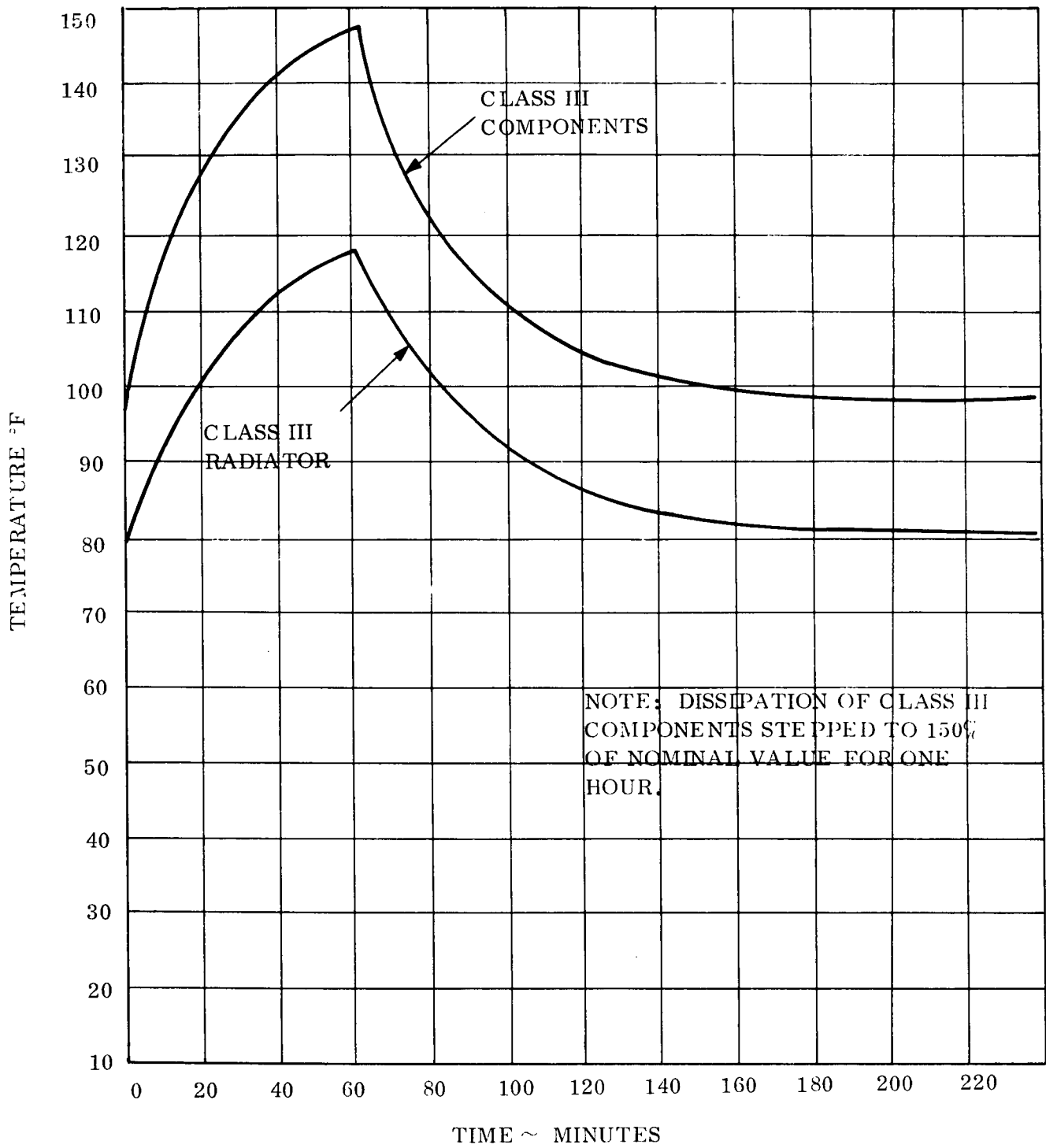


Figure 3-44. Concept A - Maximum Dissipation Response

Table 3-18. Concept A - Temperature Variation with Orbit

- Temperatures in °F
- $\alpha/\epsilon = .17/.83$

Class	Average Component Temperature	
	Orbit 3 "Coldest"	Orbit 1 "Hottest"
	I	34.9
II	57.2	67.4
III	78.6	89.9

3.3.4.2.3 Concept B

The thermal analysis of Concept B was not as extensive as that of Concept A. A total of eleven computer runs were made, of which the first four fixed the controllable heat pipe characteristics and the remaining seven were performance runs. Experience gained in Concept A analysis permitted this reduction in scope for Concept B.

The COMHP's are made to vary the conductance between the components and the LONHP's for each Class as functions of component temperatures. The sketch on Figure 3-45 again illustrates the linear proportionality assumed, but not that there is no corollary to effective area change in Concept B.

Setting the control characteristics was again difficult. Initial runs with varying midpoints and control bands, but with 20% to 100% conductance changes, resulted in cold component temperatures. The minimum conductance value was dropped to 4% and then 3%, and satisfactory performance was obtained. A 20° F total control band was again employed and Figure 3-46 shows midpoint sensitivity. Midpoints were set at desired component temperatures in the remaining runs.

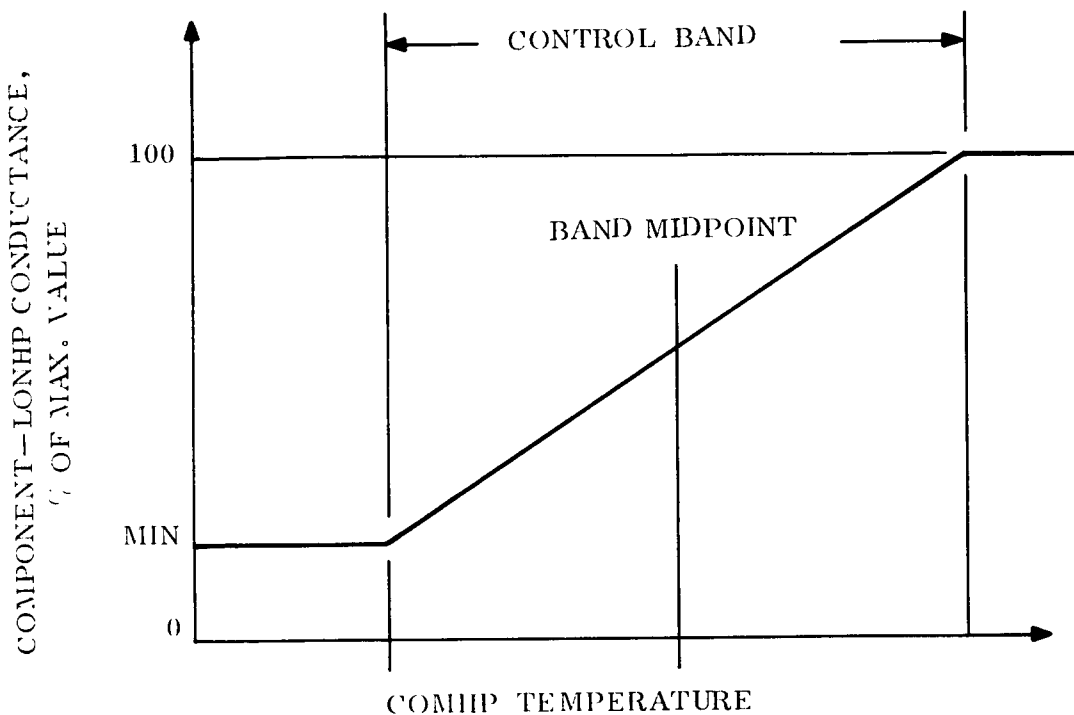


Figure 3-45. Concept B - Controllable Heat Pipe Characteristics

Table 3-19 presents the input data and summarizes the results for the eleven Concept B cases. The format is similar to that employed for Concept A (Table 3-17). Figures 3-47 to 3-50 graphically show thermal performance and sensitivity of the system using previously employed parameters. No Class III maximum dissipation cases were run for Concept B since response would be the same as that obtained in Concept A. Table 3-20 shows temperature variation with orbit/orientation.

In some of the Concept B runs, it was difficult to obtain a temperature solution as the component approached at minimum temperature of the control band. The problem was solved analytically by decreasing the time increment (thus limiting the temperature rise/drop between successive iterations) but it did point out a distinctive feature of the Concept B system. The linear conductance-temperature characteristic requires, for Concept B, a change of 4.8% of maximum conductance per 1°F change in component temperature. Thus, the conductance

Table 3-19. Space Station Heat Pipe
Concept B
(Temperatures in °F)

Run No.	Size of Model - Nodes	Orbit No.	Internal Generation	α/c	Control Band - °F	Class I				Class II				Class III			
						Radiator		Components		Radiator		Components		Radiator		Components	
						T _{max}	T _{min}	T _{max}	T _{min}	T _{max}	T _{min}	T _{max}	T _{min}	T _{max}	T _{min}	T _{max}	T _{min}
1	12	2 Largest Transient	Nominal	.21/.83	I 25-45 II 45-65 III 70-90 (.20-1.0)	25.7	-2.4	38.2	26.7	51.7	42.0	59.1	56.0	73.2	45.6	90.4	74.1
2	12	2 Largest Transient	Nominal	.21/.83	I 30-45 II 50-65 III 75-90 (.20-1.0)	26.5	-3.4	39.3	30.2	52.7	42.6	60.3	57.2	73.5	45.1	90.7	76.9
3	12	2 Largest Transient	Nominal	.21/.83	I 25-45 II 45-65 III 70-90 (.04-1.0)	26.2	-3.0	38.9	28.9	54.8	44.8	62.1	58.6	73.4	45.3	90.6	75.9
4	12	2 Largest Transient	Nominal	.21/.83	I 35-55 II 55-75 III 80-100 (.04-1.0)	27.4	-4.3	44.0	37.5	54.1	41.9	63.9	61.1	74.0	44.6	93.8	23.7
5	12	1 Hottest Average	Nominal	.25/.83	I 35-55 II 55-75 III 80-100 (.03-1.0)	39.1	39.1	51.4	51.4	68.0	68.0	76.6	76.6	80.9	80.9	98.7	98.7
6	12	2 Largest Transient	Nominal	.21/.83	I 35-55 II 55-75 III 80-100 (.03-1.0)	27.4	-4.3	44.1	37.6	54.1	41.8	64.0	61.1	74.0	44.6	93.8	83.7
7	12	1 Hottest Average	Nominal	.17/.83	I 35-55 II 55-75 III 80-100 (.03-1.0)	21.5	21.5	42.0	42.0	52.5	52.5	64.3	64.3	67.2	67.2	90.0	90.0
8	12	2 Largest Transient 20° Blockage	Nominal	.21/.83	I 35-55 II 55-75 III 80-100 (.03-1.0)	33.7	9.2	47.4	30.4	63.5	53.0	70.0	67.5	87.9	65.4	105.2	89.7
9	12	2 Largest Transient	Minimum	.21/.83	I 35-55 II 55-75 III 80-100 (.03-1.0)	16.5	-19.0	38.6	36.0	36.2	14.9	56.8	55.7	52.8	18.0	83.2	80.7
10	12	3 Coldest Average	Minimum	.17/.83	I 35-55 II 55-75 III 80-100 (.03-1.0)	-61.8	-65.7	35.7	35.3	-24.0	-26.4	50.1	50.1	-7.5	-11.4	80.9	80.5
11	12	3 Coldest Average	Nominal	.17/.83	I 35-55 II 55-75 III 80-100 (.03-1.0)	-42.7	-46.6	36.5	36.0	3.2	1.0	55.6	55.6	22.6	18.2	81.9	81.4

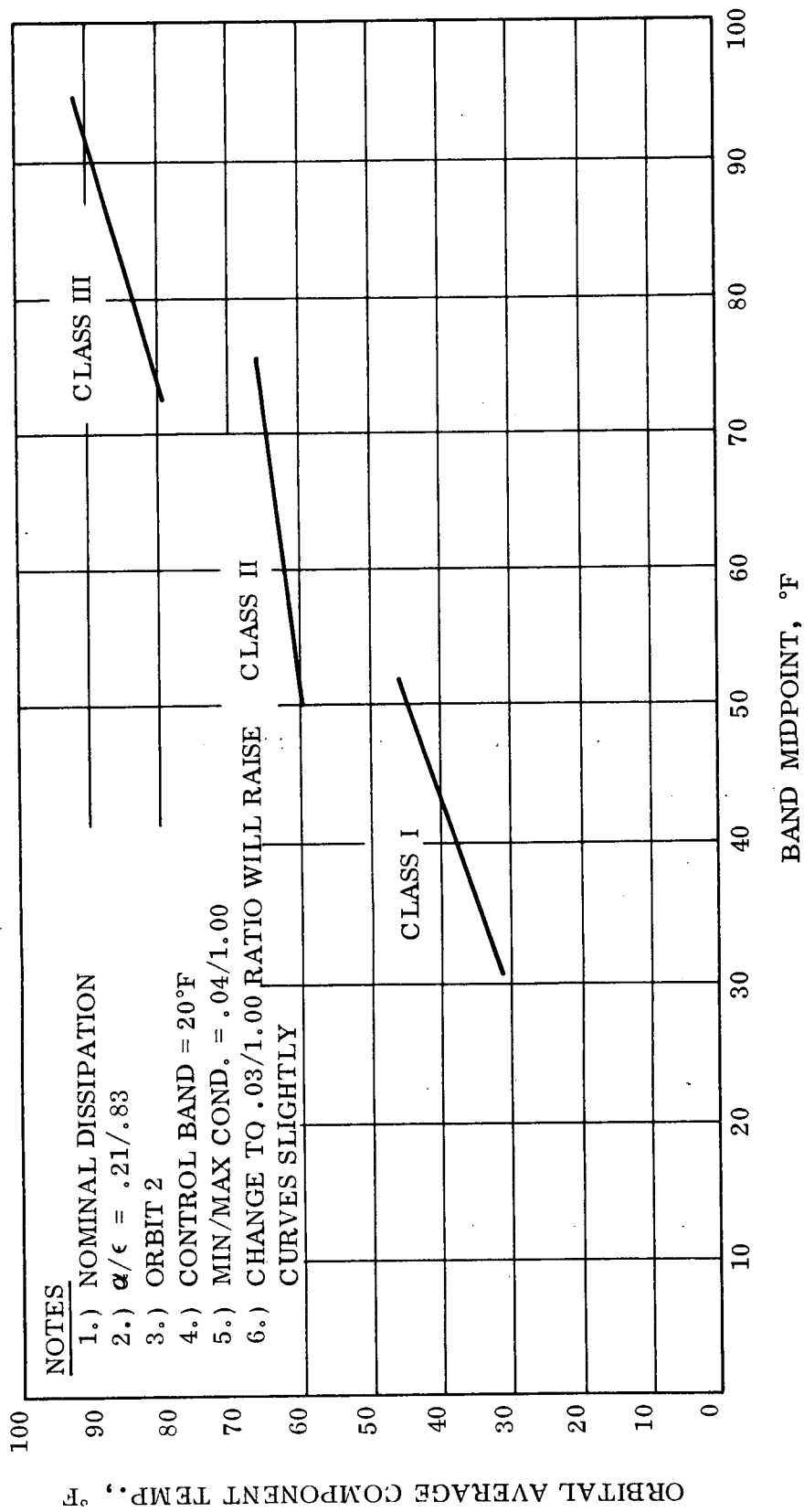
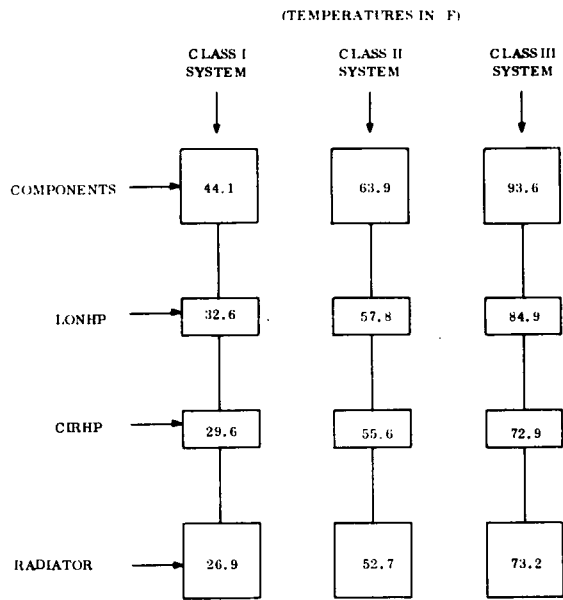


Figure 3-46. Concept B - Control Midpoint Sensitivity



- NOTES
- 1.) Nominal dissipation
 - 2.) $\alpha/\epsilon = .21/.83$
 - 3.) Orbit 2 (Time = 25 min)

Figure 3-47. Concept B - Nominal Temperature Profile

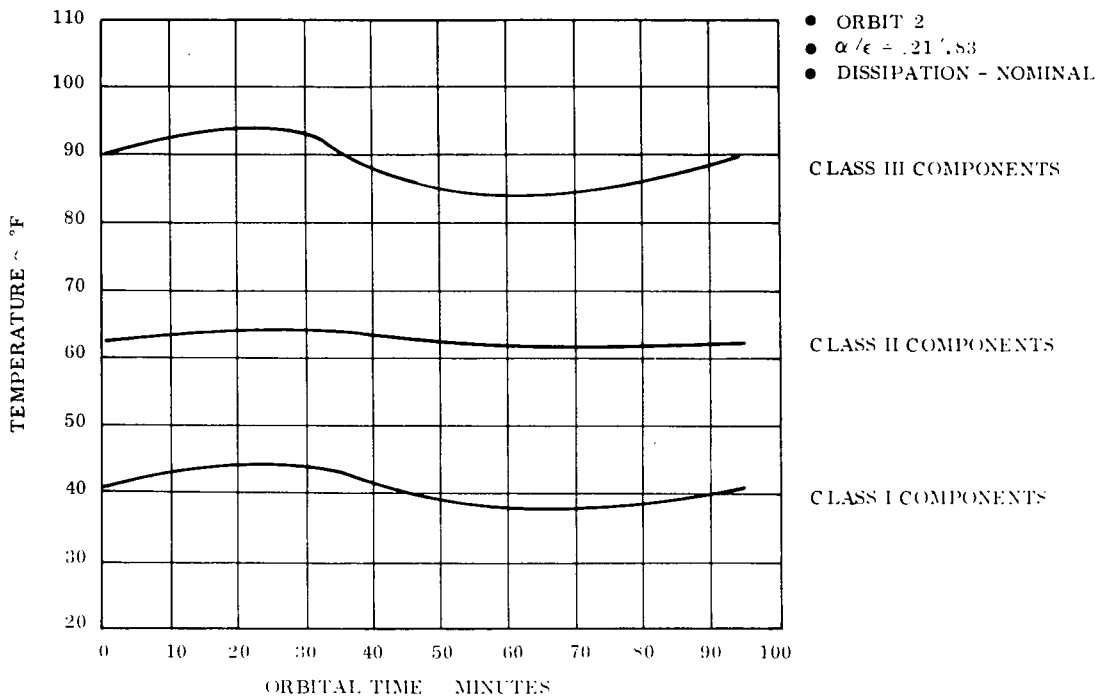
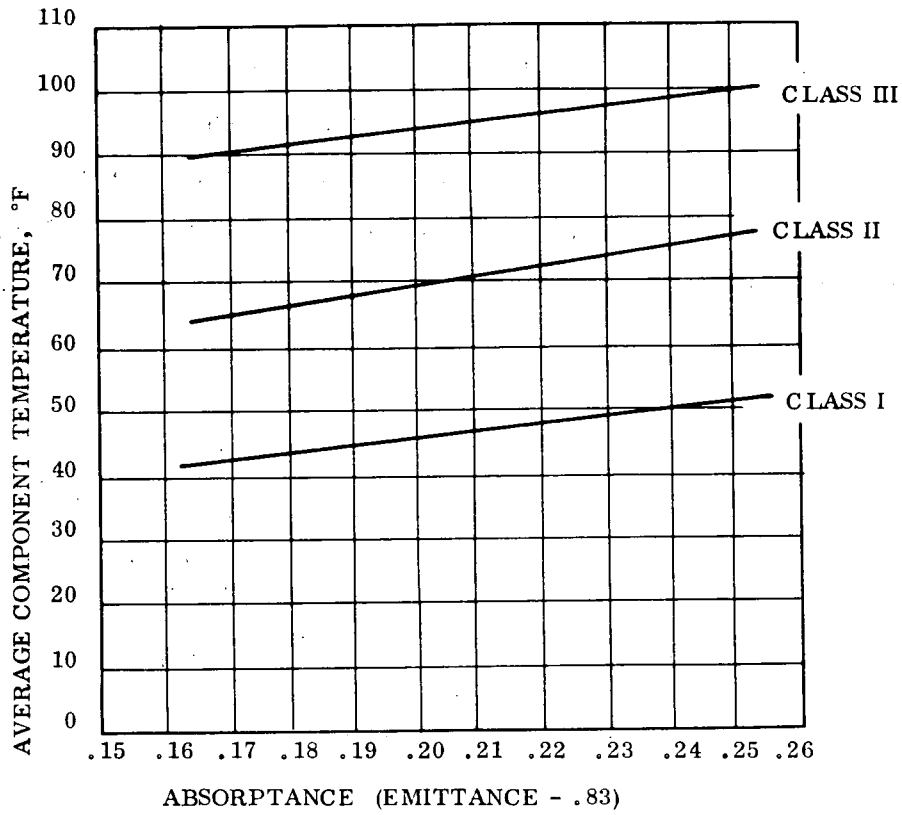


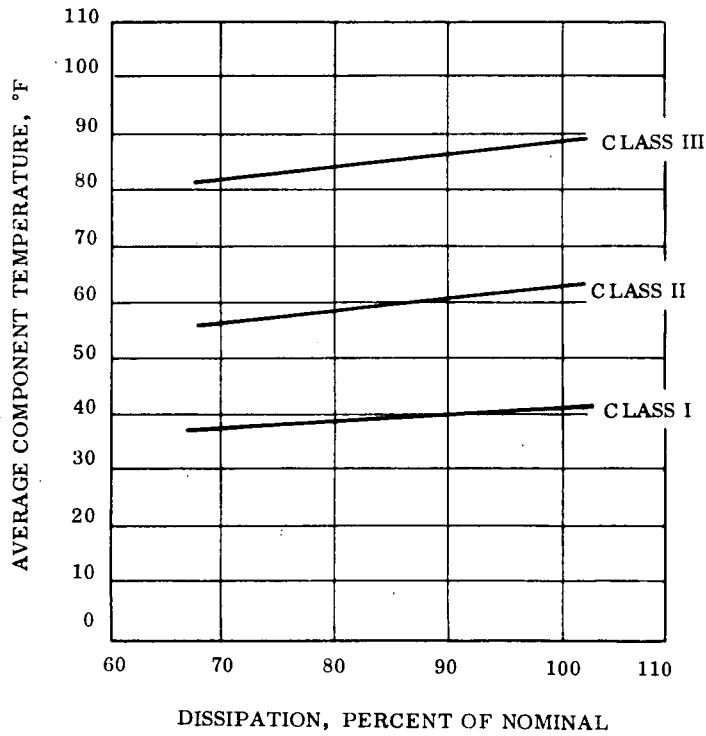
Figure 3-48. Concept B - Orbital Temperature - Time History



NOTES

- 1.) ORBIT 1
- 2.) NOMINAL DISSIPATION

Figure 3-49. Concept B - α/ϵ Sensitivity



NOTES

- 1.) $\alpha/\epsilon = .21/.83$
- 2.) ORBIT 2

Figure 3-50. Concept B - Internal Dissipation Sensitivity

changes from 3% to 7.8% of full value in the first degree rise above the minimum point. The conductance value more than doubles for a single degree variation. This is the point that the computer technique had trouble obtaining a heat balance. It seems logical that the heat pipe itself would have the same stability difficulty. (By way of comparison, the FINHP's of Concept A would alter parameters from 20% to 24% of full values in the first degree above minimum.)

Table 3-20. Concept B - Temperature Variation with Orbit

- ◊ Temperatures in °F
- $\alpha/\epsilon = .17/.83$

Class	Average Component Temperature	
	Orbit 3 "Coldest"	Orbit 1 "Hottest"
I	36.2	42.0
II	55.6	64.3
III	81.6	90.0

Thus, although system performance is satisfactory for Concept B, there is some question concerning the thermal stability of the controllable COMHP's at the low end of their control bands.

3.3.4.3 Reliability Assessment

This section contains a reliability evaluation of the conceptual heat pipe thermal control system described in Section 3.3.3 of this report. The study includes an analysis of potential failure mode, effects, and safety hazards. In addition, the inherent reliability of the heat pipe system is compared to that of a typical pumped liquid loop system.

All evaluations are performed on a qualitative basis only. More refined detail of the heat pipe system would be required to assign quantitative values to its reliability.

3.3.4.3.1 Overall Assessment - Heat Pipe System

A preliminary evaluation of the heat pipe system resulted in the identification of the favorable and unfavorable reliability and safety features inherent in the design as described below.

Favorable Features

- The passive (non-mechanical) nature of the system is the major favorable influence for achieving long life reliability and safety.
- Provisions for redundancy in the heat pipe system configuration result in additional assurance of realizing the desired reliability and safety characteristics.
- Opportunities for scheduled and preventive maintenance during operations further enhances system reliability and safety. The modular approach in system design means that the crew will be able to perform maintenance actions in a timely and effective manner.
- Repair can be done at the element level without significantly disturbing the overall Space Station thermal profile.

Unfavorable Features

- The system is complex, involving a large number of heat pipes and interconnections. Vibration and shock within the Station may result in degraded performance and/or safety hazard.
- Long-term contamination and non-condensable gas build-up within the heat pipe would adversely effect thermal performance.
- Leakage through welded joints and fittings used in modular design could degrade performance and present safety hazard.
- Bursting of heat pipe pressure vessel within the cabin is a distinct safety hazard.
- Introduction of semi-toxic working fluid vapor into cabin atmosphere would represent an additional safety hazard.

It should be noted at this point that design or process control solutions are available for the unfavorable features enumerated above (with the exception of system complexity).

3.3.4.3.2 Failure Mode, Effects, and Safety Analysis

The previous section presented a partial evaluation of reliability and safety features of the heat pipe system. The present section was prepared to expand the reliability evaluation to a combined Failure Mode, Effects and Safety Analysis with the purpose of identifying areas of the system which require design and/or development effort to ensure the desired long life reliability goal.

Table 3-21 presents the Failure Mode, Effects and Safety Analysis worksheets prepared for the current system design approach. It lists each type of functional element in the system, gives the quantity used, describes its function, identifies the most probable failure modes and the resulting failure effects on the thermal control system, identifies safety hazards associated with each element and the resulting effects on the crew, and provides clarifying comments relative to existing design features or recommended effort to minimize the effects of assumed failure modes and safety hazards.

The analysis considers each item independently and assumes that only the single failure or hazard under consideration has occurred. The significant features that appear in Table 3-21 are discussed in the next paragraphs.

The passive (non-mechanical) nature of the heat pipe approach to the design of the heat pipe control system provides an inherent long life, high reliability and safety characteristic. This is further enhanced by existing design features such as redundancy and operational provisions for maintenance.

There are, however, certain features of the proposed heat pipe system which are identified as potential failure mode and hazard areas. The effort required to overcome these weaknesses will not fall so much in the design phase as in the fabrication/processing and testing phase of the development program.

The system is a complex one in terms of the number of heat pipe units and the interconnections which are required to transfer heat load from one type of heat pipe to a heat pipe of

Table 3-21. Failure Mode, Effects and Safety Analysis Summary

Item Qty	Function	FMEA		Safety Analysis		Remarks and Hazard Category	
		Failure Mode	Failure Effect	Hazard	Effect		
1. Component Heat Pipe (COMHP) 340	Removes heat from component (heat source) and transports it to Longitudinal Heat Pipe	Loss of Fluid - at fitting or puncture Wicking Damage - due to puncture Rupture - due to pressure Loose Wicking - due to shock vibration, etc.	None - Redundancy None - Redundancy None - Redundancy None - Redundancy	Toxicity - Methanol Toxicity - fluid maybe released Toxicity Exposed Heat Pipes in crew compartment	Crew exposed to toxic vapors Same as above Same as above None - Pipes will be insulated for thermal control	<u>Failure Effects</u> <ul style="list-style-type: none"> Thermal system is protected by redundancy Tight process control will be established for wicking process Puncture, ruptures prevented by safety margin >4:1 Loss of a single COMHP is a minor effect Thermal sensing devices will be used to detect failure conditions <u>Safety Effects</u> <ul style="list-style-type: none"> Effect of toxic hazard will be temporary due to maintenance section (patching, replacement) - use of toxic vapor detection - determine exposure limit values for thermal fluid Crew can enter other compartment to escape hazards 	
2. Interface (COMHP-LONHP) 340	Transfer heat load from Component Heat Pipe (COMHP) to Longitudinal Heat Pipe (LONHP)	← Same as for Item No. 1 →				This item connects to redundant pair of LONHP's	
3. Longitudinal Heat Pipe (LONHP) 18	Accepts heat from a number of COMHP's (~10-12) via Interface element (COMHP-LONHP) and distributes heat to interface units (LONHP-PENHP) along its length	← Same as for Item No. 1 →				<ul style="list-style-type: none"> Redundancy present in the form of 18 redundant pairs of LONHP's. Maintenance and modular replacement sections available to renew redundancy and recover from safety hazards. 	
4. Interface (LONHP-PENHP) 36	Transfers heat load from LONHP to Penetration Heat Pipe (PENHP)	<ul style="list-style-type: none"> Loss of Fluid Wicking Damage 	Degradation of thermal control - Temperature increase in crew compartment	Toxic Vapors -methanol released in cabin	Crew exposed to toxic vapors	<ul style="list-style-type: none"> Welded interface joints and strength-stress safety margin >4:1 are design features which will minimize both failure modes and safety hazards related to fluid loss Interface configuration relative to redundant LONHP being designed Maintenance 	
5. Penetration Heat Pipe (PENHP) 36	Accepts heat from LONHP via interface (LONHP-PENHP) and carries heat external to cabin	← Same as above plus: →			Decrease cabin pressure	Not serious if pressure does not drop sharply	<ul style="list-style-type: none"> Vapors, if any, will be external to cabin. - EVA repair. Bottled gas available to maintain pressure Leakage can be corrected by maintenance action
6. Interface (PENHP-CIRHP) 36	Transfers heat load from PENHP to Circumferential Heat Pipe (CIRHP)	Loss of Fluid or Wicking Damage - due to meteoroid damage Rupture - due to pressure Loose Wicking	Degradation of thermal control system - not serious if single interface	Temperature increase in crew cabin	Crew fatigue and discomfort if Temp. > 75°F	<ul style="list-style-type: none"> Vapor external to cabin Welded interface joints and pipe safety margin minimize failure modes EVA repair required to correct failure 	
7. Circumferential Heat Pipe (CIRHP) 6	Accepts heat from 18 PENHP's via Item No. 6 and distributes heat to Fin Heat Pipe (FINHP) along its circumference	(Same as above)	Critical degradation	Temperature increase in crew cabin	Short term crew tolerance to Temp. ~ 120°F	(Same as above)	
8. Interface (CIRHP-FINHP) 1272	Transfers heat load from CIRHP to FINHP	(Same as above)	Degradation (Not serious if one interface)	Insignificant temperature increase in crew cabin	Not serious	(Same as above)	
9. Fin Heat Pipe (FINHP) 1272	212 FINHP's accepts heat from each of 6 CIRHP's and distributes heat to external radiator	← Same as for Item No. 8 →					

higher (or lower) capacity. To ensure the integrity of interconnections tight process control and inspection must be established and maintained during fabrication. Adequate qualification testing (vibration, shock) must be provided for and conducted on a system model to determine the effects of operational stresses on critical elements (joints, wicking). In addition, after the system has been assembled in its flight configuration, sufficient acceptance testing must be accomplished to remove residual sources of unreliability and to provide confidence in successful operational performance in the Space Station application.

Although emphasis for reliability control is placed on the fabrication and testing phase, effort is also required during the design and planning stages of the system development. The heat pipe and interface units have design features which are critical to reliable thermal control operation and safety such as wicking, fluid, and pipe strength. Important design considerations in this regard are the selection of wicking technique and its ability to adhere to the inner wall of the heat pipe and interface paths; the working fluid and its compatibility with heat pipe materials; and providing heat pipes with sufficient safety margin to resist punctures and rupture.

Thus, an overall interpretation of Table 3-21 indicates that failure potentials do exist that could degrade thermal control and affect crew safety to various degrees of severity. However, presently proposed design features, development activities and operational provisions will significantly reduce the probability of occurrence of these failure and hazard conditions.

3.3.4.3.3 Heat Pipe - Active Loop Comparison

The purpose of this section is to qualitatively analyze the reliability of the pumped liquid loop system proposed by MDAC for the Space Station and to make a comparison to the reliability of the heat pipe design. Five criteria were employed in the analysis:

- Complexity - Heat Pipe System - High
Pump Loop - High

Both systems are highly complex, but the complexity of each takes a different form. The pumped liquid loop requires such items as pumps, valves, controls, continuous tubing, resupply tanks, etc.; while the heat pipe system is made up of a number of passive pipe sections and many interconnections.

- Component Type - Heat Pipe System - Passive
Pumped Loop - Active

The mechanical items of the pumped liquid loop system have a higher failure mode potential during operation than the passive components of the heat pipe system. The failure modes of these latter items are associated with the fabrication process and therefore their occurrence during operation can be significantly reduced or eliminated by good process control and a well-planned test program.

- Redundancy - Heat Pipe System - Component Level
Pumped Loop - System Level

Both design approaches provide redundancy to protect the system against catastrophic failure effects. However, it appears that the pumped liquid loop approach provides more extensive but less effective redundancy than the heat pipe approach. Tubing redundancy in the liquid loop is applied at the system level, while in the heat pipe approach redundancy is applied at the component (pipe) level, which is considered to be a more effective level for redundancy.

- Maintenance Requirement - Heat Pipe System - Low
Pumped Loop - High

On-board and EVA maintenance will be available for both systems as a means of extending the operational life of the heat pipe control system. The frequency of maintenance would appear to be much greater for the pumped liquid system than for the heat pipe system. This is primarily due to system adjustments of control units required for the pumped liquid loop but also repair and replacement of failed or degraded mechanical units. The passive components and the natural physical mechanism of the heat pipe system operation will tend to minimize the maintenance required. It is expected that a more extensive system for failure detection and isolation will be required for the pumped liquid loop system than for the heat pipe system due to level of complexity and greater likelihood of failure of mechanical items.

- Failure Effects - Heat Pipe System - Degrading
Pumped Loop - Serious

Failure occurrences in both systems will generally result in only a temporary effect on thermal control due to redundancy and maintenance. However, it is considered that certain failure occurrences will result in more serious failure effects on the pumped liquid loop system. The immediate effect of a line puncture on the pumped liquid loop system would be a loss of fluid from a large portion of the system. The effect of a line puncture on the heat pipe system would be less serious because of the isolated nature of the heat pipe segments or components. This difference also provides the heat pipe approach with a maintenance advantage and a capability for faster failure recovery.

Thus, the heat pipe approach to the Space Station thermal control system appears to have a distinct reliability advantage over the pumped liquid loop approach. The completely passive nature of the heat pipe system will provide a greater long life potential than the mechanical pumped liquid loop system. Effective redundancy, low maintenance frequency and less serious failure effects are additional reliability advantages provided by the heat pipe approach.

3.3.4.3.4 Reliability Summary

In summary, the passive nature of the heat pipe system establishes a basic long life reliability characteristic for the design approach. The application of redundancy and provision for operational maintenance markedly enhances reliability and lifetime potential. System development tasks such as reliability design techniques, process control, qualification and acceptance testing will provide assurance that the reliability and system safety goals will be met. Also, on the basis of the superficial comparison performed, it is apparent that the heat pipe system demonstrates a higher inherent reliability potential than the pumped fluid loop approach. This is primarily due to the completely passive nature of the heat pipe concept and the maintenance features of the modularized design.

3.3.5 SUMMARY

Phase II work included defining Space Station boundary conditions and constraints, performing preliminary analyses to determine desirable features of a thermal control system for this vehicle, formulating seven system concepts possessing these features, and selecting of two concepts for further study. These two systems were defined sufficiently to evaluate thermal performance, approximate weights and qualitative reliability. Selection and description of the favored concept is presented below.

It is perhaps obvious that Concept A has three distinct advantages over Concept B. Although the weights of the two were practically identical, and the reliability analysis was performed for a general heat pipe system, the following deficiencies were noted in the Concept B design:

1. Thermal loading on the circumferential heat pipes was significantly higher in Concept B. Absorbed external heat from hot radiator sections must be transferred into these heat pipes for transport around the radiator circumference. This is not the case in Concept A, which cuts out hot radiator segments automatically.
2. Thermal stability problems near the low end of the control band of the variable conductance heat pipes employed in Concept B may be real, and not just analytical, difficulties.
3. The formation of a distinct working fluid vapor/non-condensable gas interface in the variable conductance heat pipes of Concept B is questionable. At any rate, its performance would be very sensitive to variations in the temperature of its heat sink.

Concept A is therefore selected as the preferred totally passive system for Space Station thermal control. Figure 3-51 shows a schematic of the system. It combines a series-parallel network of high performance heat pipes, advanced thermal interfacing techniques, and radiator-mounted variable conductance heat pipes to provide a lightweight, reliable, and thermally effective overall system.

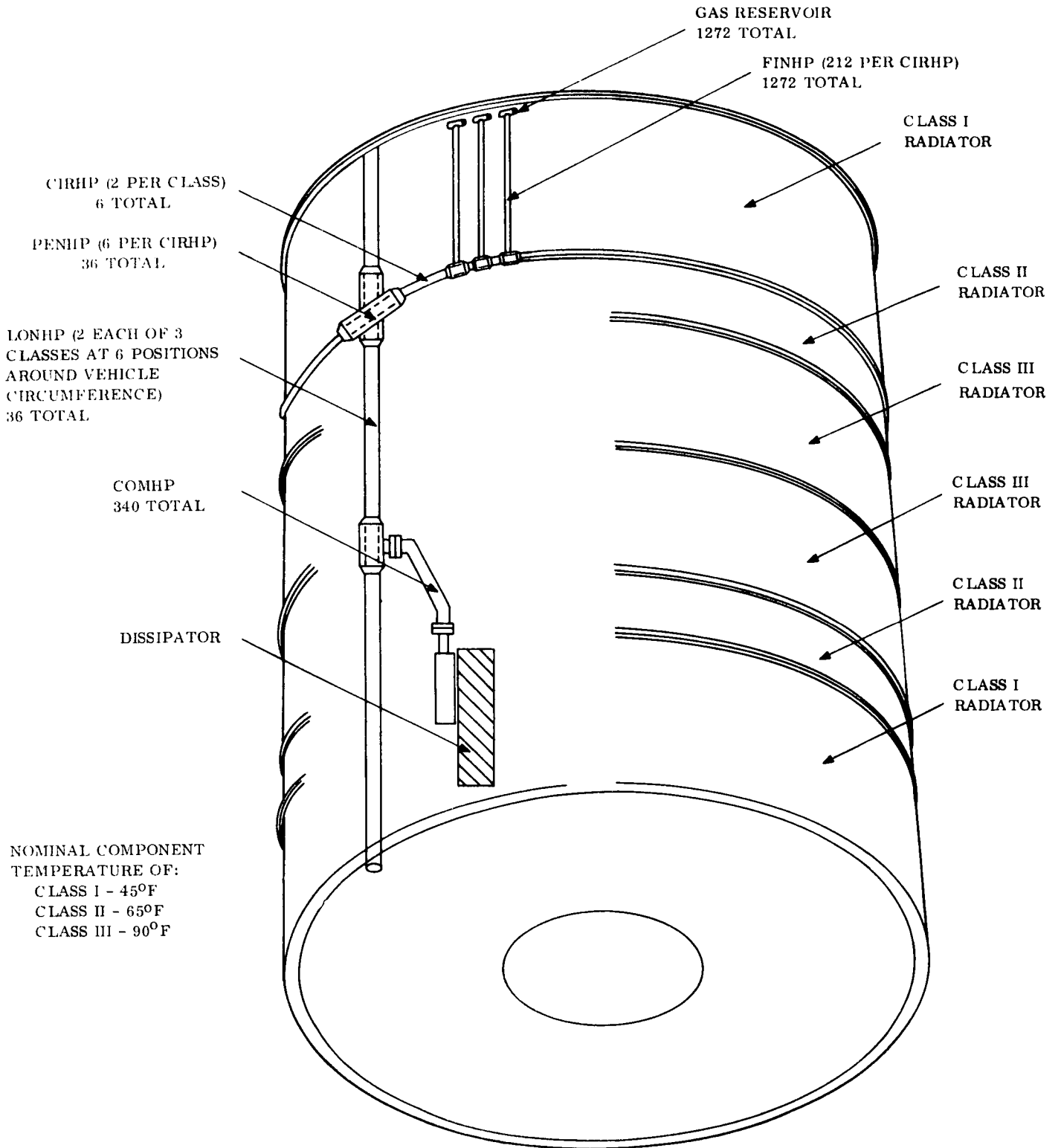


Figure 3-51. Selected Configuration

SECTION 4

PHASE III

4.1 OBJECTIVE

The objective of Phase III was to demonstrate the adequacy of the thermal control system chosen in Phase II by means of a thermal balance test of a mock-up segment of the proposed system. Boundary conditions would be varied to verify both steady state and transient performance of the heat transport and temperature control features.

4.2 SCOPE

Phase II work (Section 3) indicated the superiority of a total heat pipe thermal control system with external variable conductance heat pipes for Space Station application. A network of heat pipes was devised to transfer internally generated heat to the controllable pipes on the space radiator. Typically, heat from a dissipating component would pass through five heat pipes (and associated interfaces) before being rejected to space.

The Phase III test article was designed to represent a scaled-down portion of the system described above. Its salient design features were:

1. Transfer of heat from electrical resistance heaters (simulating dissipating components) through a series of five distinct heat pipes to a simulated space radiator.
2. Transfer of heat from a room ambient environment to a thermal vacuum environment.
3. Variable conductance heat pipes mounted on the radiating surface.
4. Minimal temperature drop from the simulated dissipators to the radiator.

Since Phase II studies had indicated the desirability of maintaining separate control systems for each of three temperature bands, the test article was designed to control both simulated components at only one temperature level. Performance of this one system could be directly extrapolated for the other two because all three are identical in all respects except operating temperature.

4.3 DESCRIPTION OF TEST ARTICLE

The system shown schematically in Figure 4-1 was designed to satisfy the four goals stated above. One additional fact could be verified by this article; because two components and two radiator panels are provided, the temperature averaging effect of the simulated longitudinal and circumferential heat pipes would be observable.

The heat pipes of the test article were assigned numbers instead of names to avoid confusion with the heat pipes designated in Phase II. As can be seen in Figure 4-1, pipes of similar construction and function are given the same number and are differentiated by the letter following that number.

General assumptions used in sizing the overall system and the individual elements were:

1. Transfer of 30 watts of heat from each component heater to the radiators with an overall temperature drop of about 20 to 25^oF.
2. Control of component heater temperature to 45^oF \pm 10^oF for all test cases.
3. Rejection of 30 watts per radiator to an effective sink of 400^oR.
4. Size and orientation limitations of the thermal vacuum chamber chosen for article testing.

The nominal 60 watt capability of the system was selected for two reasons; first, to yield a reasonably sized radiator section; and second, to allow the use of isotropic wicking in all heat pipes. The total article would thus be less sensitive to tilt than if any of the composite wicking schemes available had been selected.

Chamber constraints required a mechanical joint between heat pipes #2 and #3. The total article was thus fabricated in two halves which were joined after insertion in the vacuum chamber (but before closing the chamber door).

Specific elements of the test article will be discussed in the following subsections.

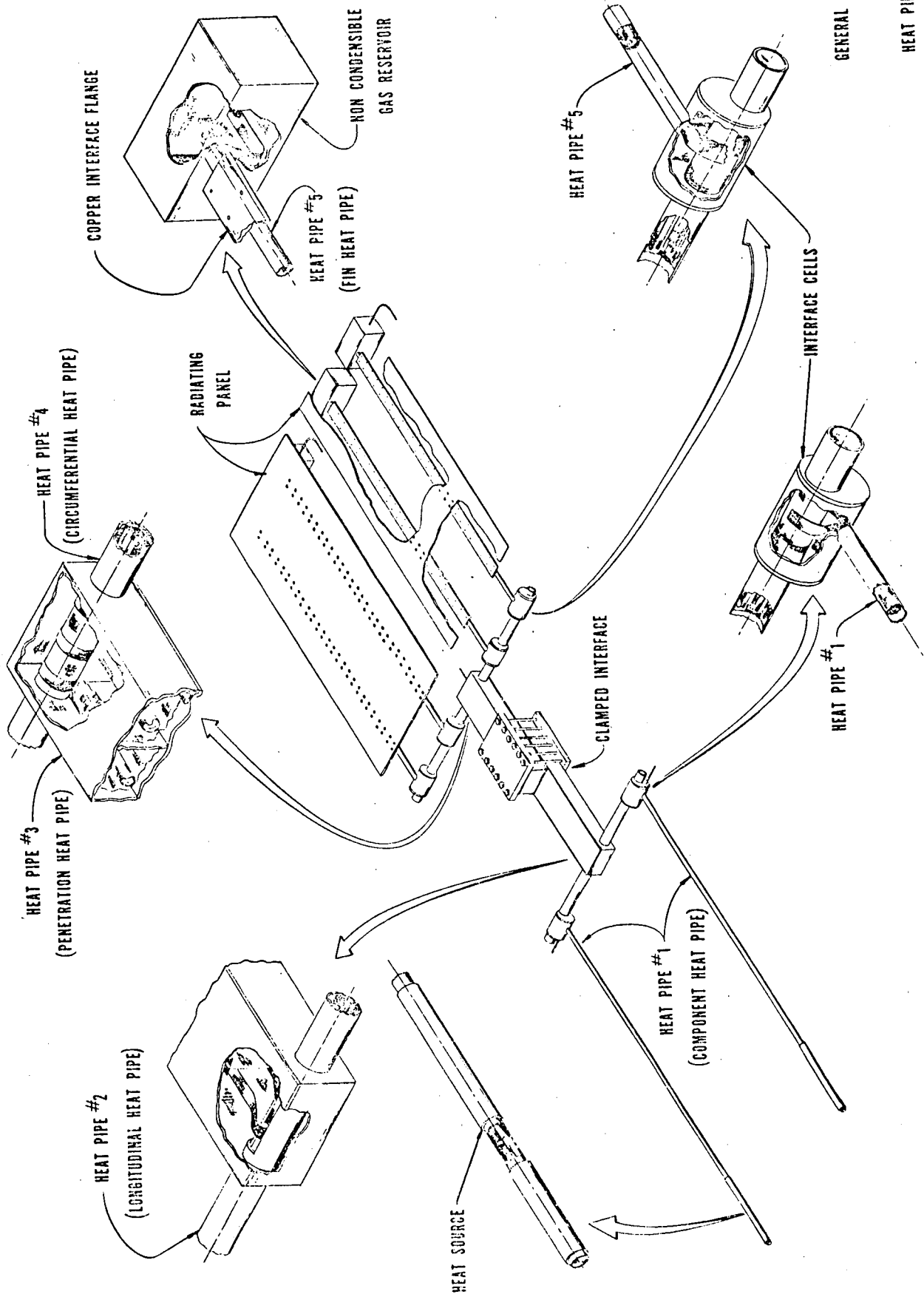


Figure 4-1. Heat Pipe System Segment Test Article

4.3.1 HEAT PIPES

The working fluid in all pipes was methyl alcohol. Control gas in the four variable conductance (#5) heat pipes was nitrogen. All containment vessels were fabricated from type 304 stainless steel and wicks were formed from 100 to 200 mesh stainless steel wire cloth.

4.3.1.1 Containment Vessels

Dimensions of the heat pipe containment vessels are given in Table 4-1. It should be noted that heat pipe #2 is composed of two geometrical shapes, a tube and a rectangular box. The tube is 50% cut away within the box to allow vapor flow from tube to box sections. The wicks of both sections are joined at the intersection to provide liquid return to the evaporator. The tube and box are welded together to form an integral containment vessel.

The box shapes of heat pipes #2 and #3 were fabricated by bending stainless steel sheet into a "U" channel and welding end-caps and top-plate onto this channel. A bulkhead was welded down the center of each channel prior to wick insertion to minimize top deflections and provide structural support.

Table 4-1. Containment Vessel Dimensions

Heat Pipe	Outer Diameter or W x D, In.	Length, In.	Wall Thickness, In.
#1	0.5	40	0.035
#2 (circ)	1.0	20	0.065
#2 (rect)	3.0 x 1.5	16	0.063 (0.093 top)
#3	3.0 x 1.5	12	0.063 (0.093 bottom)
#4	1.0	25	0.065
#5	0.5	30	0.035

NOTE: All Type 304 Stainless Steel

4.3.1.2 Wicking

As previously mentioned, isotropic wicking was employed throughout the system. The scheme, in general, was to surround the inner perimeter of all heat pipes with two layers of 200-mesh stainless screen for surface distribution and capillary pumping, and to spot-weld "transport" wicks formed of 100-mesh screen as required to these base layers. The transport wick provides a liquid flow path of less resistance than the surface wicking and therefore carries the bulk of the axial flow. By restricting the surface wick to the two layer thickness, the temperature drop through the liquid/wick matrix over heat transfer areas could be minimized, while surface distribution could be assured.

The transport wicks were made by first rolling a single piece of screen around a one-eighth inch mandril and spot-welding the wick annulus closed with an outer diameter of three-eighths inch. The mandril was removed and the annulus was pressed into a bulky C-shape. The empirically determined porosity of the transport wick was 0.56.

The two #1 heat pipes did not use the transport wick as described above because of their unique constraints. It was only necessary to provide 200-mesh screen (for high capillary pumping) over the six-inch long evaporator in each case. The adiabatic length of the pipe was consequently wicked with an annulus of 100-mesh screen with 0.43 inch outer diameter and 0.125 inch inner diameter. The transition from the evaporator to adiabatic wicking was made by overlapping the 200 and 100 mesh screens approximately one-half inch before rolling. A wick strap of six layers of 100-mesh screen one-eighth inch wide was spot-welded inside the length of the evaporator to augment liquid flow.

Figure 4-2 shows the wick configurations for all heat pipes. A following section will discuss thermal interfacing between evaporators and condensers of adjacent pipes in the system.

4.3.2 CONTROL VOLUMES

The four #5 heat pipes were made to exhibit variable conductance as a function of boundary conditions by providing a gas reservoir on the end of each, and by charging each with a controlled amount of dry nitrogen subsequent to methanol fill. The reservoirs, or control

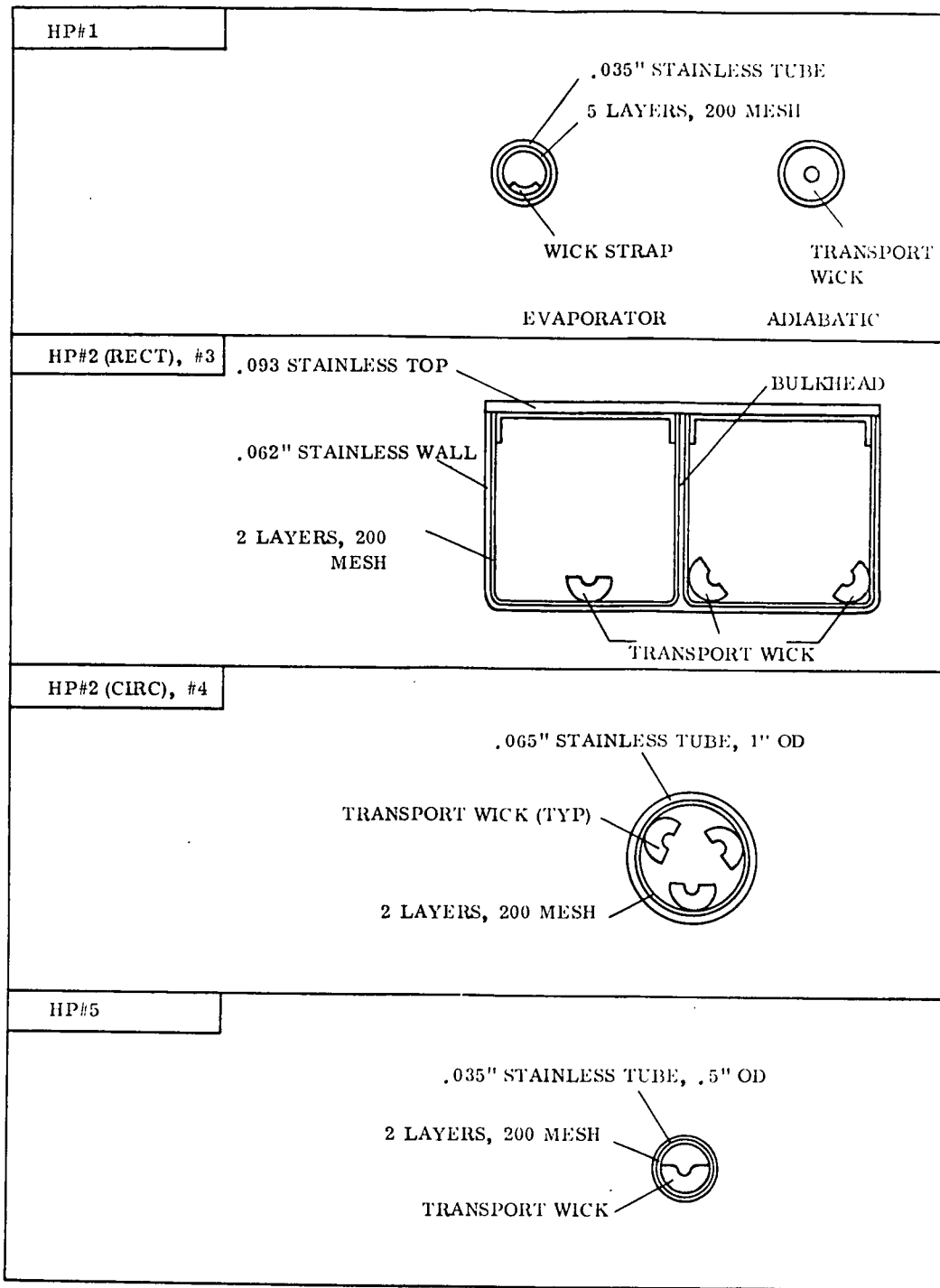
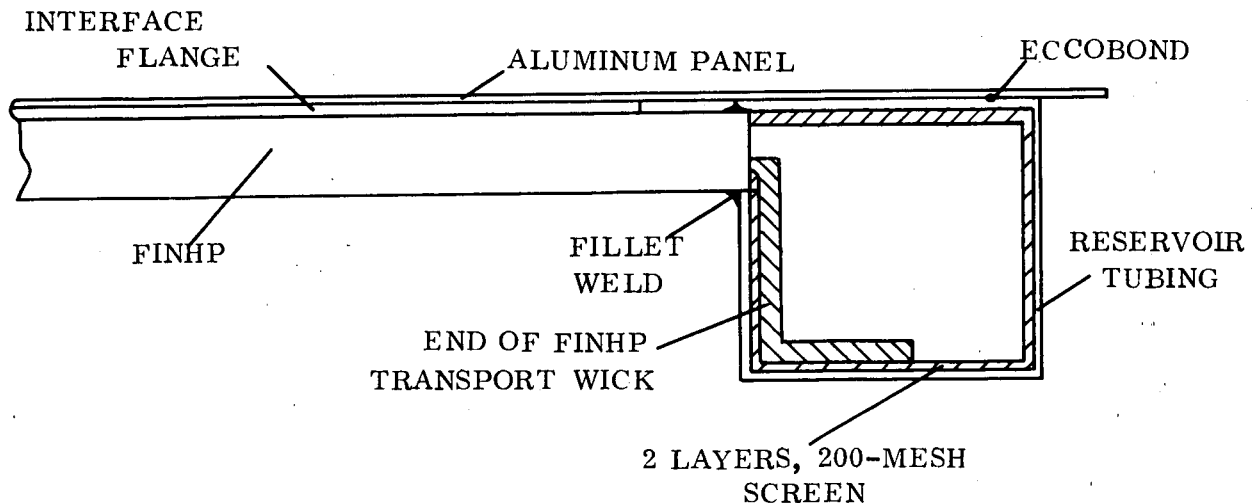


Figure 4-2. Wick Configurations

volumes, were thermally coupled to the radiating panels through heat conductive epoxy (Eccobond 57C) so the controllable pipes were of the cold gas variety. Wicking was thus required in the reservoirs to prevent excess accumulation of working fluid within these volumes.

Square tubing was chosen for reservoir fabrication to facilitate bonding to the heat sink. The tubing was stainless steel (type 304) nominally two inches by two inches with a 0.065-inch wall. Each reservoir was made four inches long. Two layers of 200-mesh screen were spot-welded on all internal surfaces of the reservoirs prior to assembly with the heat pipes themselves.

The sketch below shows the method of joining the heat pipes and the gas reservoirs. The transport wick of the heat pipe extended about three inches beyond the end of the tubing. The tube was inserted into a one-half inch hole bored in the side of the reservoir and the three-inch wick strap was then spot-welded onto the 200-mesh covering the reservoir inner surface as shown (the reservoir end-caps were not yet in place). The tube was welded to the reservoir and finally, the reservoir end plates were welded to the square tubing, completing the structure.



Calculated volume of each reservoir was 14.06 cu. in. (0.008138 cu. ft.). The ratio of reservoir volume to heat pipe condenser vapor volume was 5.47.

4.3.3 INTERFACES

Heat from two simulated components shown in Figure 4-1 must be transferred through six types of interfaces to reach the radiator panels. Adjacent pairs of each type are listed below, along with the number of times the interface occurs in the total system.

Types

1	Heater - HP #1	(2)
2	HP #1 - HP #2	(2)
3	HP #2 - HP #3	(1)
4	HP #3 - HP #4	(1)
5	HP #4 - HP #5	(4)
6	HP #5 - Radiator	(4)

Types 1, 3, and 6 are relatively straightforward and will be discussed first.

Electrical resistance tape wrapped around and bonded to heat pipe #1 made up type 1. The tape was obtained with a suitable pressure sensitive adhesive and was wound tightly around the six-inch evaporator end of the heat pipe. Calculated conductance from the tape to the vapor in the pipe was $60 \text{ Btu/hr-}^{\circ}\text{F}$.

As previously mentioned, the interface between heat pipes #2 and #3 (which is interface type 3) had to be a mechanical joint to get the test article into the thermal vacuum chamber. The joint occurred just inside the chamber door. Figure 4-3 depicts the joint configuration. As can be seen, mating surface area was 18 sq. in. Silver-filled silicone grease was applied to the interface area to enhance the joint heat transfer. The aluminum plates and twelve bolts were provided in an attempt to obtain uniform and high contact pressure between the mating surfaces of the heat pipes. A contact conductance of $500 \text{ Btu/hr-sq. ft. -}^{\circ}\text{F}$ was assumed for these conditions and the total conductance from heat pipe #2 vapor to heat pipe #3 vapor was determined to be $36 \text{ Btu/hr-}^{\circ}\text{F}$. The mating surfaces were left in an "as received" condition.

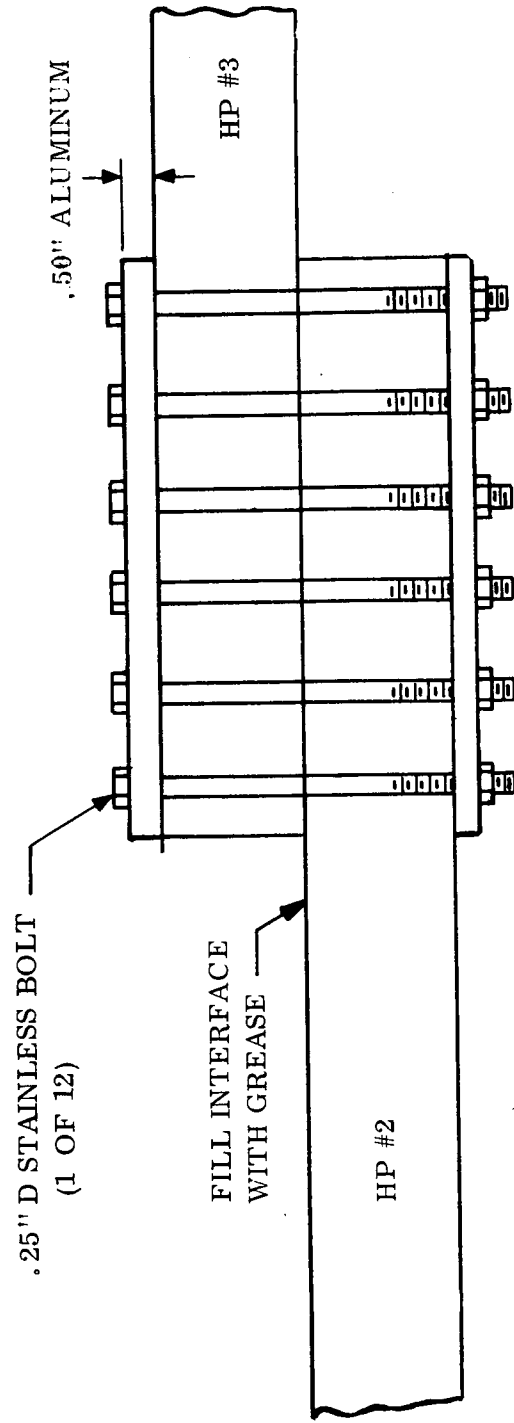
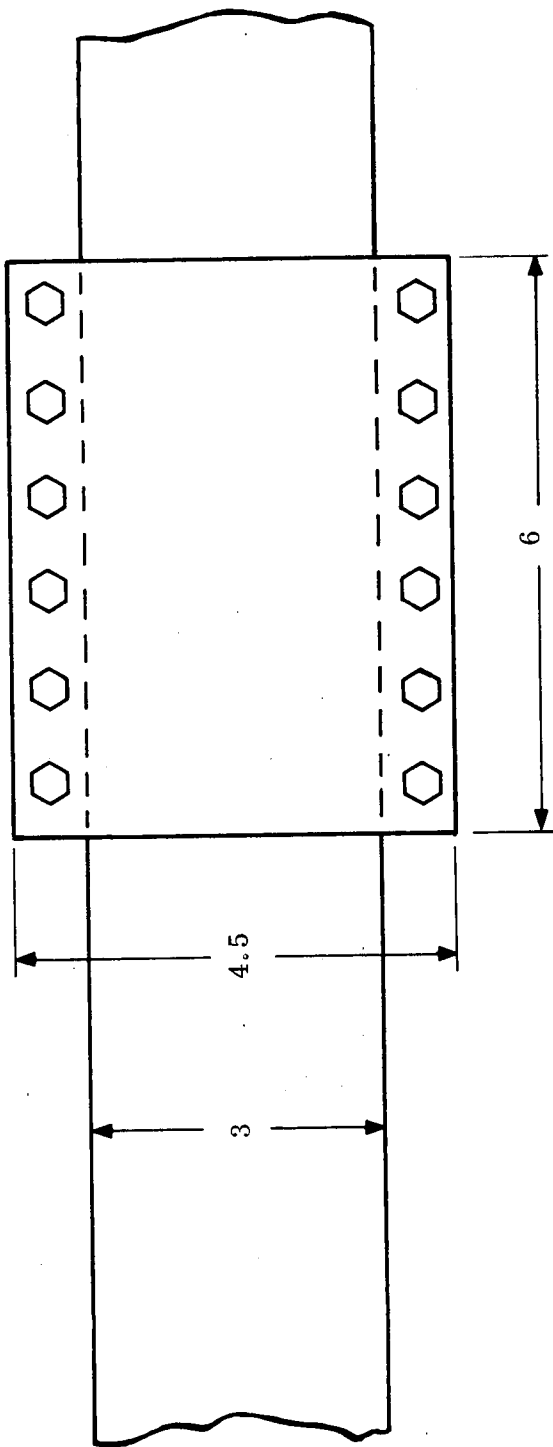
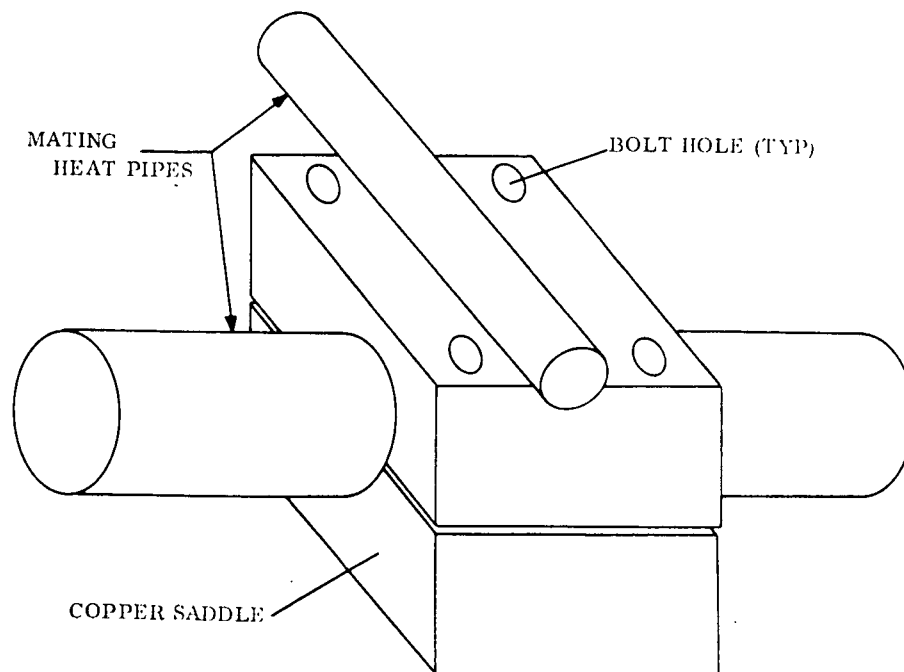


Figure 4-3. Mechanical Interface

Figure 4-4 shows details of the type 6 interface. The one-half inch heat pipe was first silver-soldered to a copper strip which had been previously ball-milled. The heat pipe was then positioned on the radiator panel and holes were match-drilled through the copper strip and aluminum radiator for bolts. Bolt spacing was two inches on both sides of the pipe with each bolt in one line being offset one inch from a bolt on the other. Again, silver-filled grease was spread over the contacting surfaces. The conductance from the vapor of the heat pipe into the radiator was calculated to be $46 \text{ Btu/hr-}^{\circ}\text{F}$.

The remaining interfaces (types 2, 4, and 5) require transport of heat from the vapor of one heat pipe to the vapor of another heat pipe. As discussed in the Phase II section of this report, conventional interfacing techniques yield relatively large temperature drops when applied to this condition. Phase II system studies indicated that these drops were excessive for adequate thermal control and an alternate solution to the interface problem was found.

Because of the scaled down heat loads to be imposed on the Phase III test article, conventional interfaces (bolted joints with saddles) were considered for use. A tentative saddle design was generated (see sketch below) to thermal couple two heat pipes perpendicular to each other. The vapor-to-vapor conductance was calculated with 1) a copper saddle, and 2) contact conductances of $1,000 \text{ Btu/hr-}^{\circ}\text{F}$ at the heat pipe/saddle interface. The total value was found to be $3.3 \text{ Btu/hr-}^{\circ}\text{F}$ or about $1 \text{ W/}^{\circ}\text{F}$.



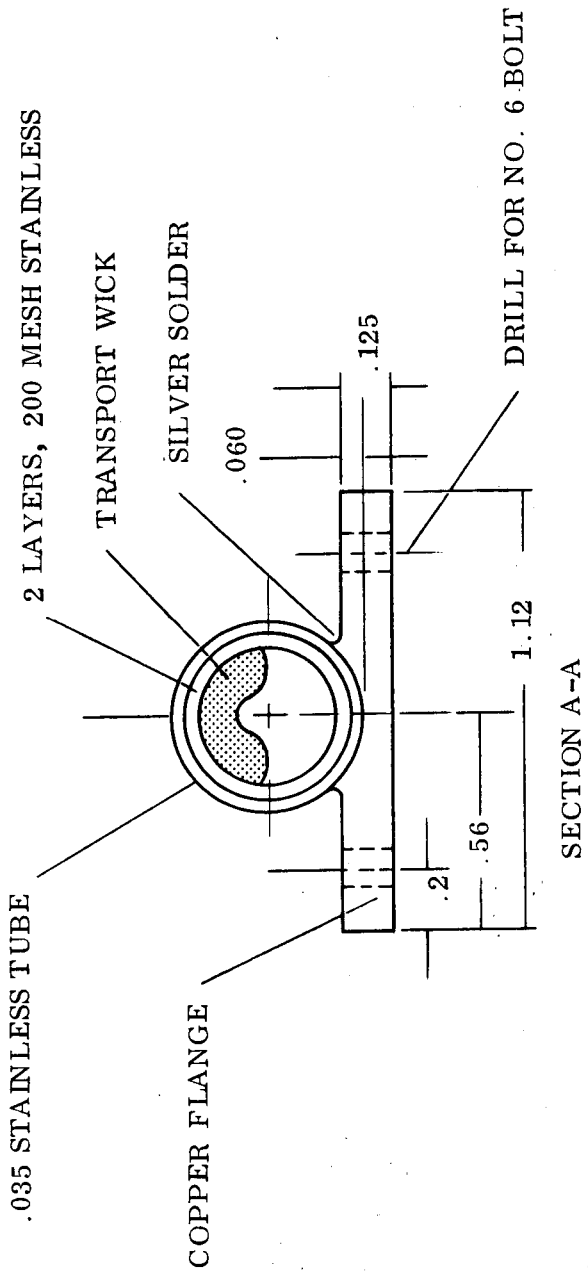
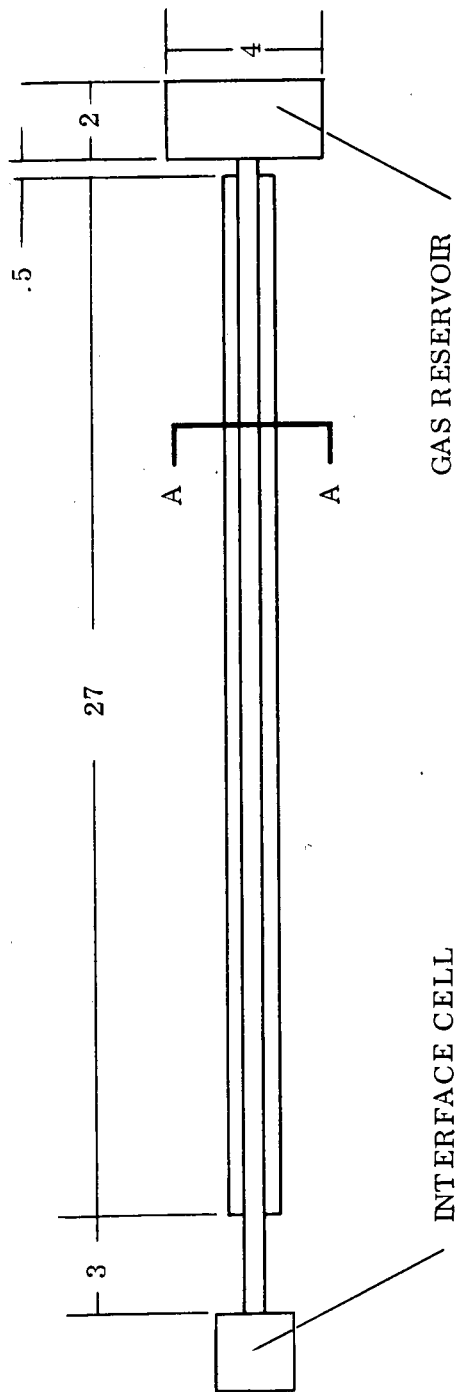


Figure 4-4. Heat Pipe #5 Design

Thus, for the 30W nominal case, the temperature drop through one such interface would be about 30°F , and extrapolating using similar saddles for all types 2, 4, and 5 junctions, the overall heater-to-radiator drop was calculated to be in excess of 100°F . This was judged excessive and the interface cell method was consequently adapted to the test article.

Figure 4-5 illustrates the method used for type 2 and 5 interfaces. Basically, a two-inch length of two-inch outer diameter tubing surrounds the larger heat pipe of each pair. Both the inside of the cell (two-inch tubing) and the outside of the heat pipe are covered with two layers of 200-mesh screen. The transport wick of the smaller pipe extends about two inches beyond its tubing and is split in half. One half of this wick is spot-welded to the inner surface of the cell and the other half is wrapped around and spot-welded to the outer surface of the large heat pipe. End-caps are added and the entire cell is welded to both pipes. The annulus formed by the larger heat pipe and the two-inch diameter tube becomes vapor space for the smaller heat pipe. The axis of the cell is offset from the axis of the larger heat pipe to facilitate wick placement.

Total conductance for this interface was determined as $21 \text{ Btu/hr-}^{\circ}\text{F}$.

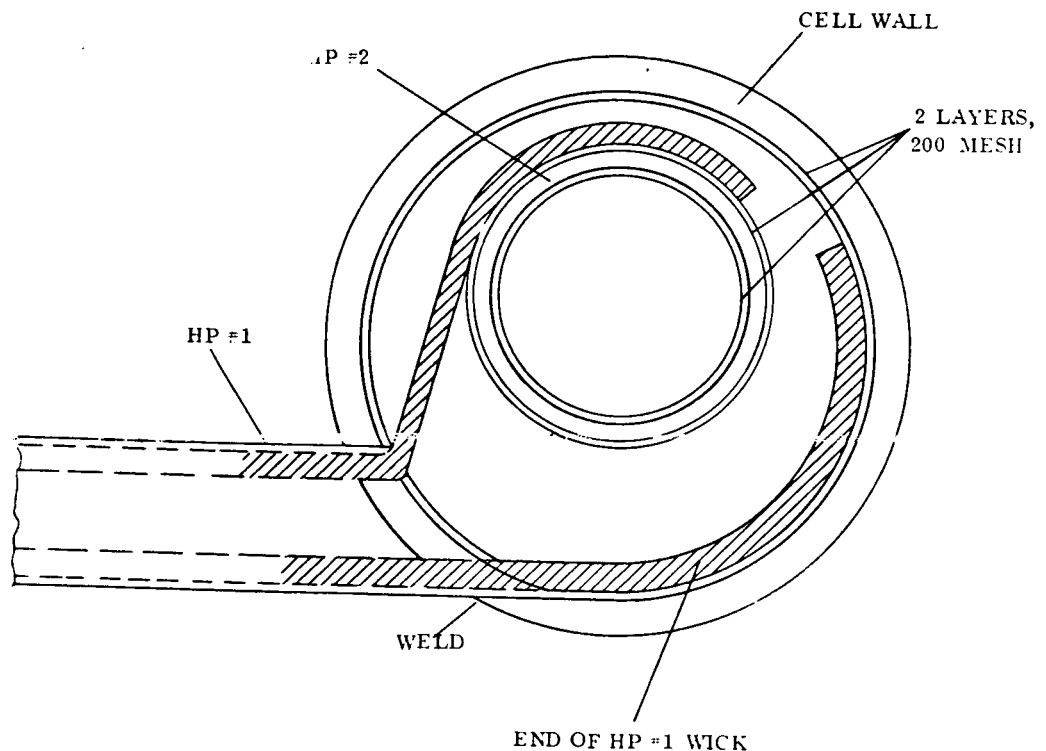


Figure 4-5. Interface Cell Cross-Section

The last interface type (number 4) was similar in principle to the interface cell method described above but was simpler to implement. In this case, the tubing of heat pipe #4 was run directly through the box forming heat pipe #3. The outside of pipe #4 was again wrapped with two layers of 200-mesh screen and the ends of the three transport wicks of heat pipe #3 were wrapped around this two-layer covering. The pipes were then welded together. A conductance of 32 Btu/hr-°F was determined from vapor-to-vapor.

It should be noted that heat pipe #4 is not open within heat pipe #3 as is the case with the two pieces of heat pipe #2.

Table 4-2 summarizes the conductances of each type of interface and presents predicted temperature drops for a nominal case of 30 watts/simulated component and balanced sinks.

Table 4-2. Theoretical Interface Performance

Type	Conductance Btu/hr-°F	Nominal Heat Transferred		Temperature Drop, °F
		W	Btu/hr	
1	60	30	102.4	1.7
2	21	30	102.4	4.9
3	36	60	204.8	5.7
4	32	60	204.8	6.4
5	21	15	51.2	2.4
6	46	15	51.2	1.1
			Total Drop	22.2 °F

4.3.4 RADIATORS

Each of the two radiator panels measured 12" x 30" (2.5 sq. ft./panel) and was fabricated of 0.020-inch aluminum 6061-T6 sheet. Heat pipe spacing on these panels was six inches. The radiating surface of each panel was sprayed with a white paint whose emissivity has been previously measured at 0.87. The opposite surface was insulated from the thermal

vacuum environment of the chamber as described in the next subsection. In total then, the radiators designed for the test article modeled quite accurately the radiator design suggested in Phase II for the Space Station.

4.3.5 INSULATION

The entire test article (with the exception of one side of each radiating panel) was thermally insulated from its environment. Within the thermal vacuum chamber, blankets of 24 layers of aluminized mylar were wrapped around and secured to 1) the underside of each radiator; and 2) the entire heat pipe network including the clamping hardware for joining heat pipes #2 and #3.

Heat pipes which extended from the chamber door into the room ambient environment were insulated with at least one-half inch thick flexible foam insulation. This, in turn, was wrapped with aluminized mylar sheet and tape to form a vapor barrier since it was anticipated that the heat pipe temperatures could fall below the room dew point.

4.3.6 ARTICLE MOUNTING

Figure 4-6 shows the method by which heat pipe #2 penetrated into the vacuum environment. A rectangular hole was machined in a blank flange which covered the chosen port in the vacuum chamber. The hole was sized to leave a gap of about one-quarter inch around the heat pipe. A piece of 0.062-inch stainless sheet was double-bent to structurally couple the flange and the heat pipe. The channel groove shown milled in the flange was merely to aid the final welding operation. The 0.25-inch air gap was sealed at its opening with mylar tape.

The total conductance from the vapor of heat pipe #2 to the flange (including conduction through the stainless bracket and the air) was found to be $0.34 \text{ Btu/hr-}^{\circ}\text{F}$. Since the anticipated temperatures of the flange and heat pipe #2 were 70°F and 40°F , respectively, a heat leak of about 3 watts into the heat pipe system was expected.

The total article was supported at two additional points during testing. Textolite bars were fastened to the article at the two extreme ends of the system. The article was suspended

from the chamber door with nylon cord which attached to these textolite bars. The heat leak through these two support structures was negligibly small.

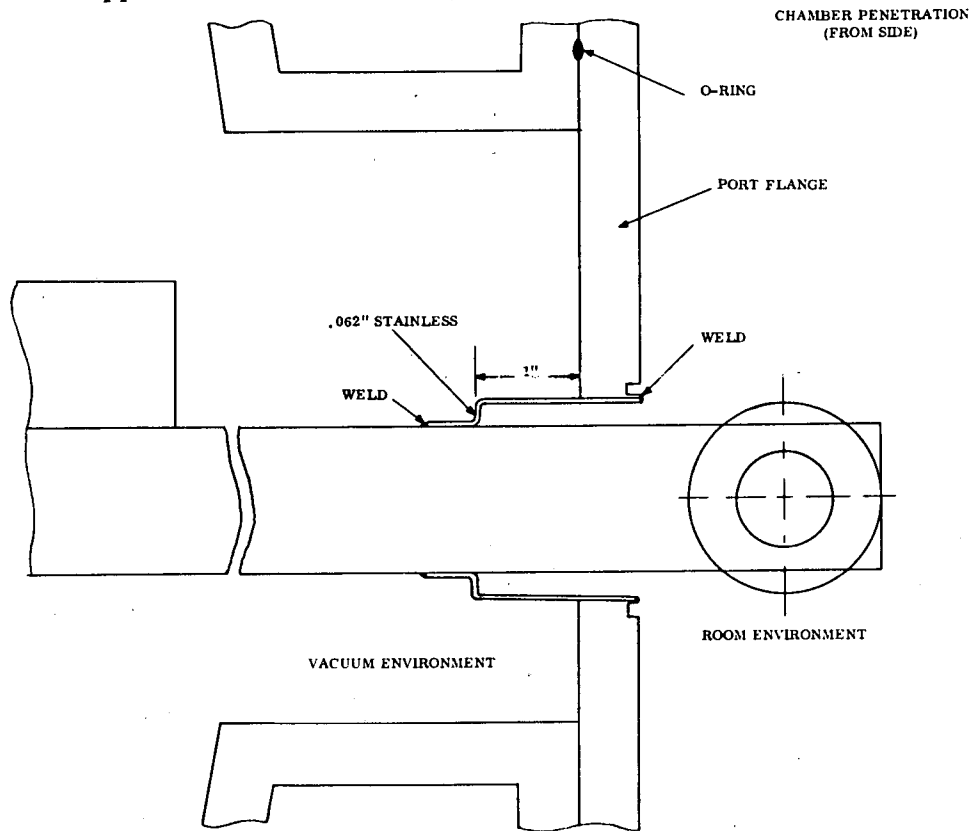


Figure 4-6. Chamber Penetration

4.4 INSTRUMENTATION

Test article instrumentation consisted of forty thermocouples, two multi-channel temperature recorders, four electrical resistance heaters, and four DC power supplies.

Copper/constantan twisted pair thermocouples were employed throughout the system. Figure 4-7 shows the forty locations selected. The four beads attached to the aluminum radiator panels were attached with heat conductive Eccobond 57C. The rest of the beads were sandwiched between the subject surface and a small ribbon of 0.003-inch stainless steel shim stock which was spot-welded to the surface. Twenty-four channel Honeywell recorders monitored thermocouple output. The recorders were calibrated to $\pm 2^{\circ}\text{F}$ just prior to test.

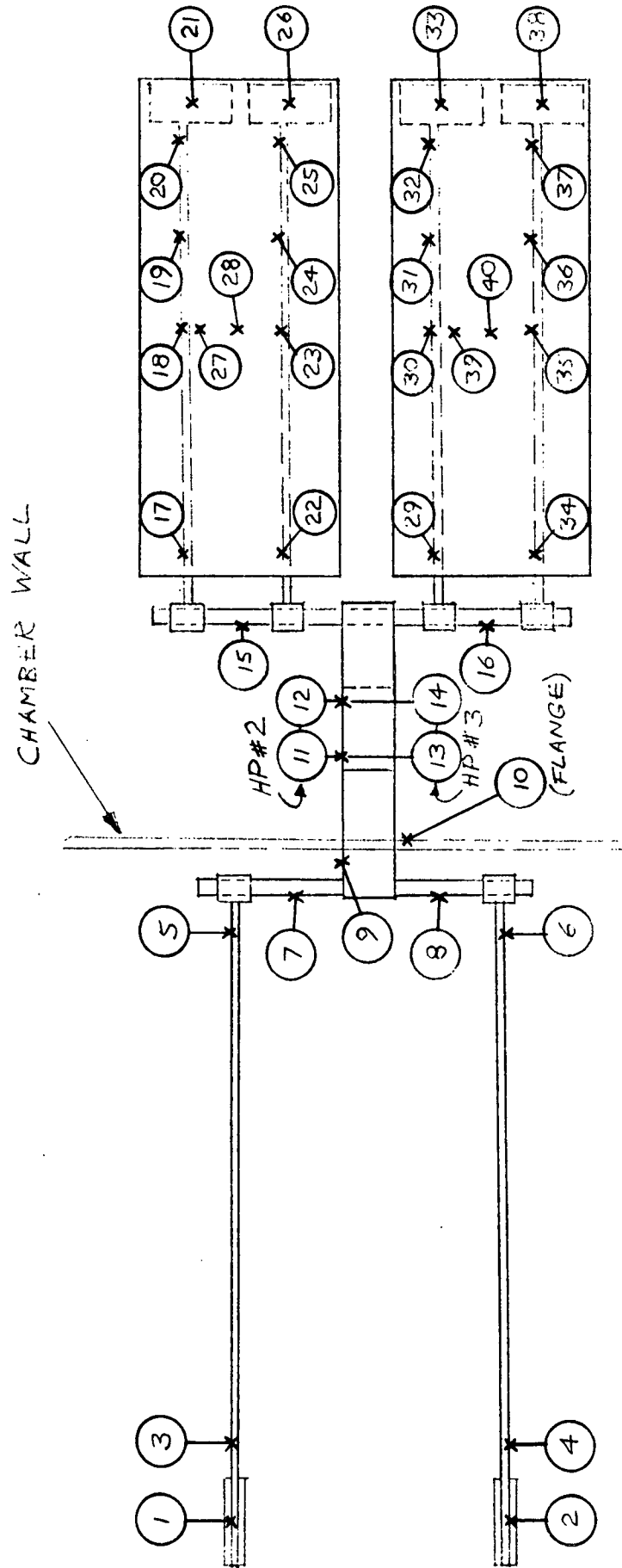


Figure 4-7. Thermocouple Locations

Two of the four electrical heaters simulated dissipators on heat pipes #1A and #1B. The other two were bonded to the two radiating panels and were used to simulate absorbed external flux on the panel. The simulated component heaters were designated COMP 1 and COMP 2, while the panel heaters were SINK 1 and SINK 2. Physically, all four heaters were made up of lengths of four-conductor heater tape. The COMP heaters were wound around the #1 heat pipes as previously discussed. Each SINK heater consisted of four lengths of the tape, spaced 1.5 inches on each side of each heat pipe on the panel, and wired in a series-parallel arrangement to yield the necessary total electrical resistance. Listed below are the measured resistance of each heater and the maximum output required from each associated power supply.

<u>Heater</u>	<u>R, Ω</u>	<u>Power Supply Requirements</u>	
		<u>Max Volts</u>	<u>Max Amps</u>
COMP 1	6.9	18.6	2.7
COMP 2	6.9	18.6	2.7
SINK 1	7.9	18.0	2.3
SINK 2	7.9	18.0	2.3

With these conditions, it is possible to put 50 watts on each COMP heater and 40 watts on each sink. This sink heat load corresponds to a maximum effective sink temperature of 450° R.

4.5 INTEGRATED ARTICLE CONFIGURATION

Figures 4-8 through 4-12 show photographs of the integrated test article prior to installation of the room and multilayer insulation. The white spots that appear on the radiator panels near pipe #4 are volumes of RTV over the ends of the SINK heaters to maintain electrical insulation from the panels.

4.6 HEAT PIPE CHARGING

The void volume within the isotropic wicks of all heat pipes was calculated based on empirically determined porosities and measured wick dimensions. The pipes were charged to 110%

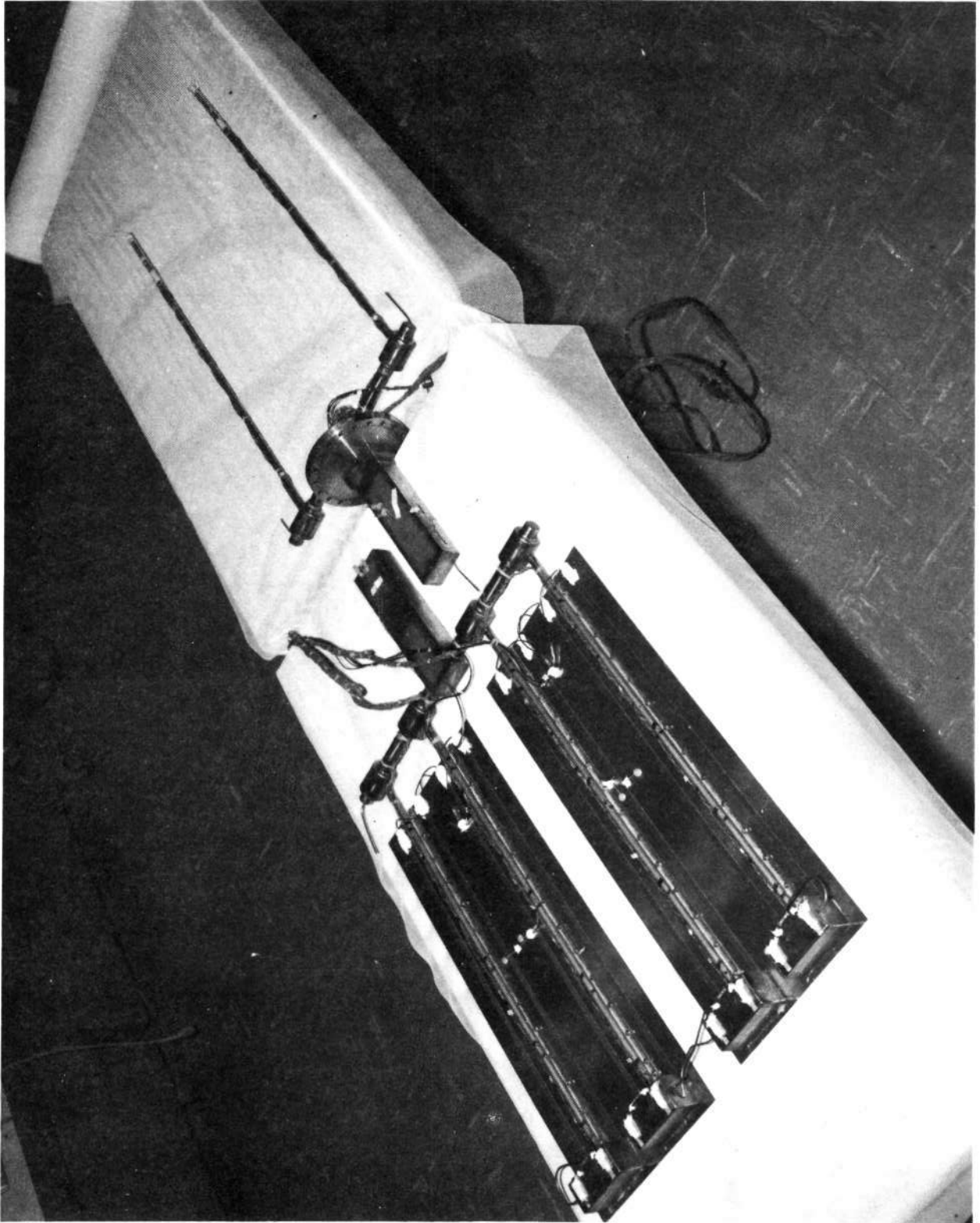


Figure 4-8. Photograph - Overall Test Article

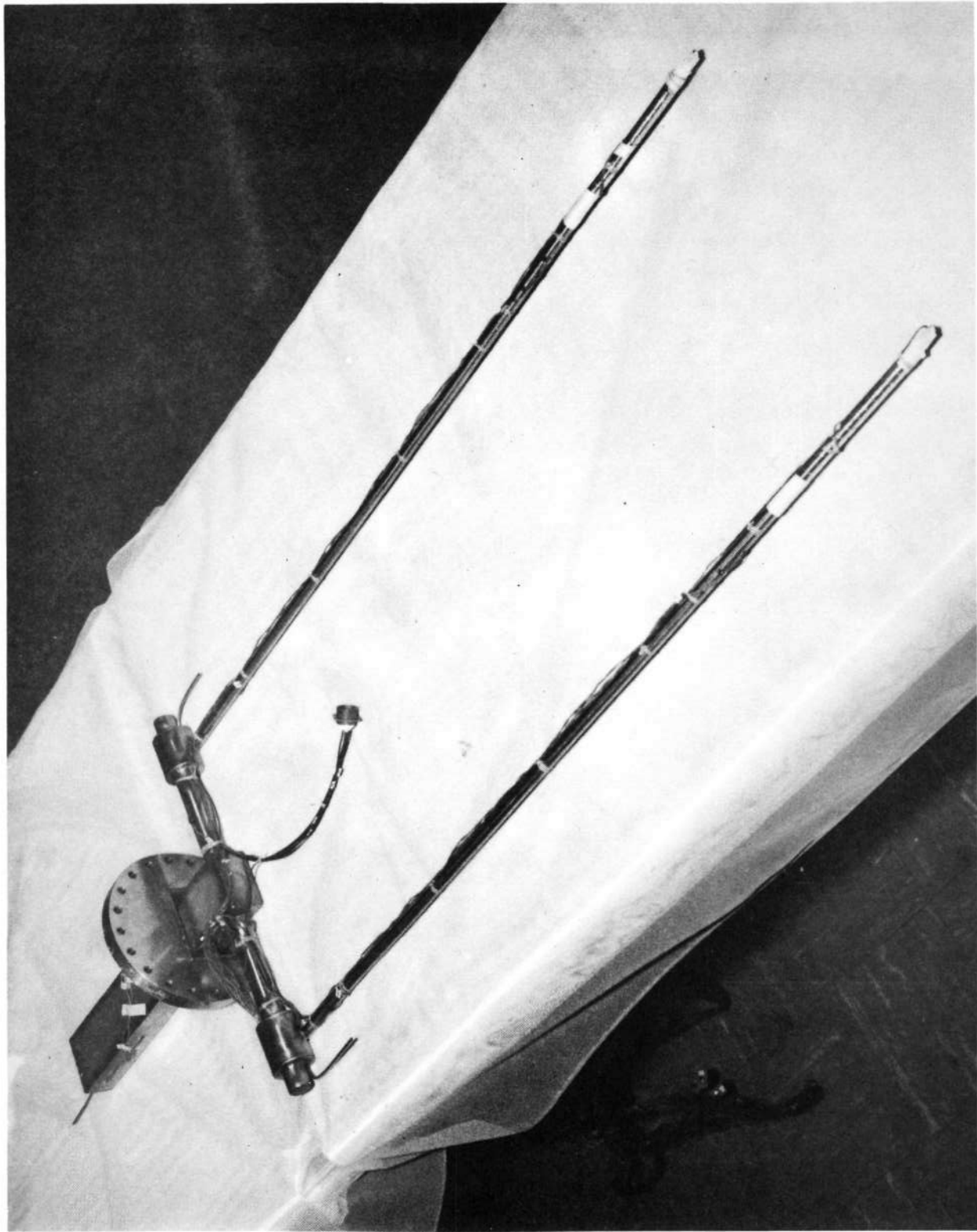


Figure 4-9. Photograph - Bottom of Radiator Assembly (Side View)

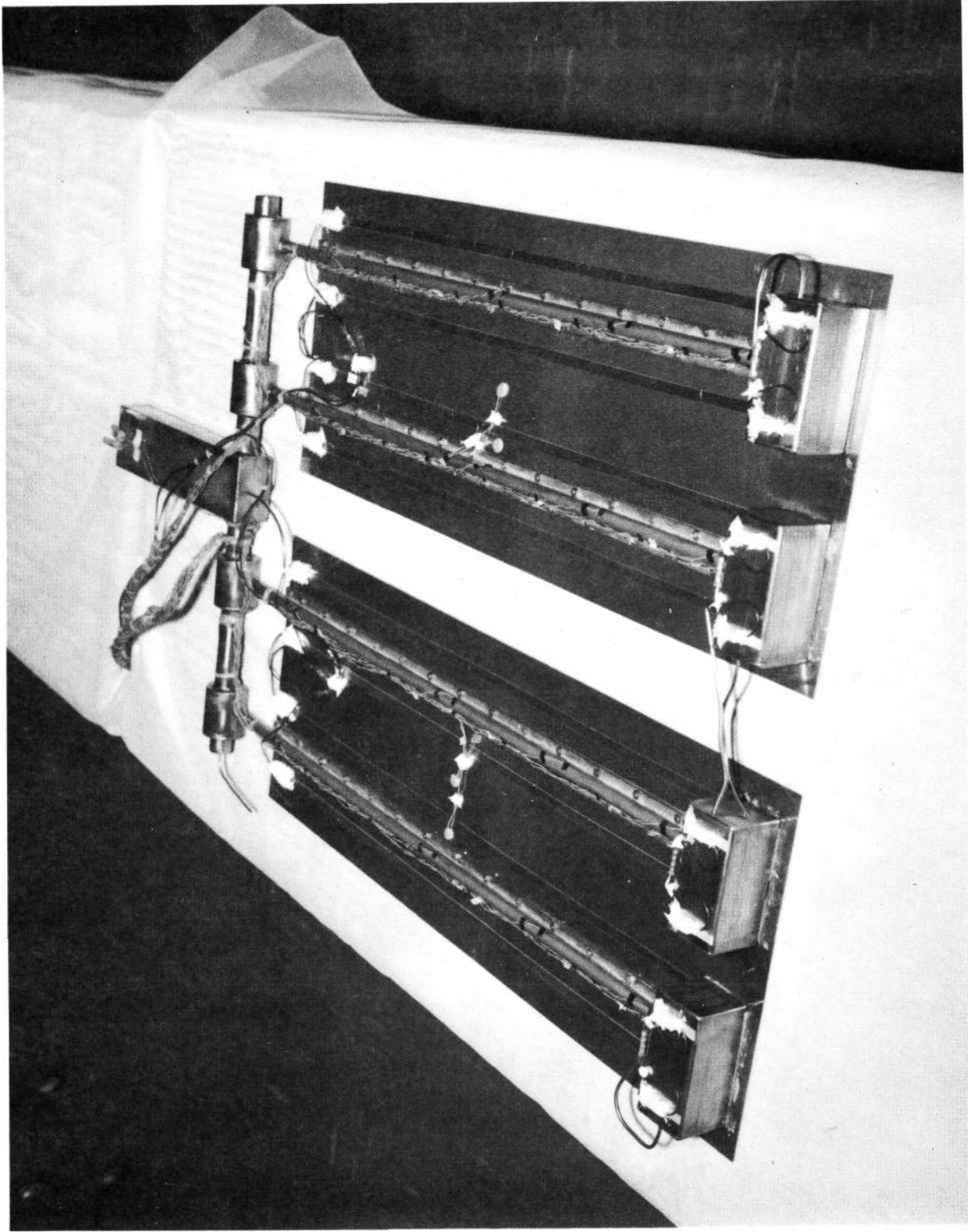


Figure 4-10. Photograph - Bottom of Radiator Assembly (End View)

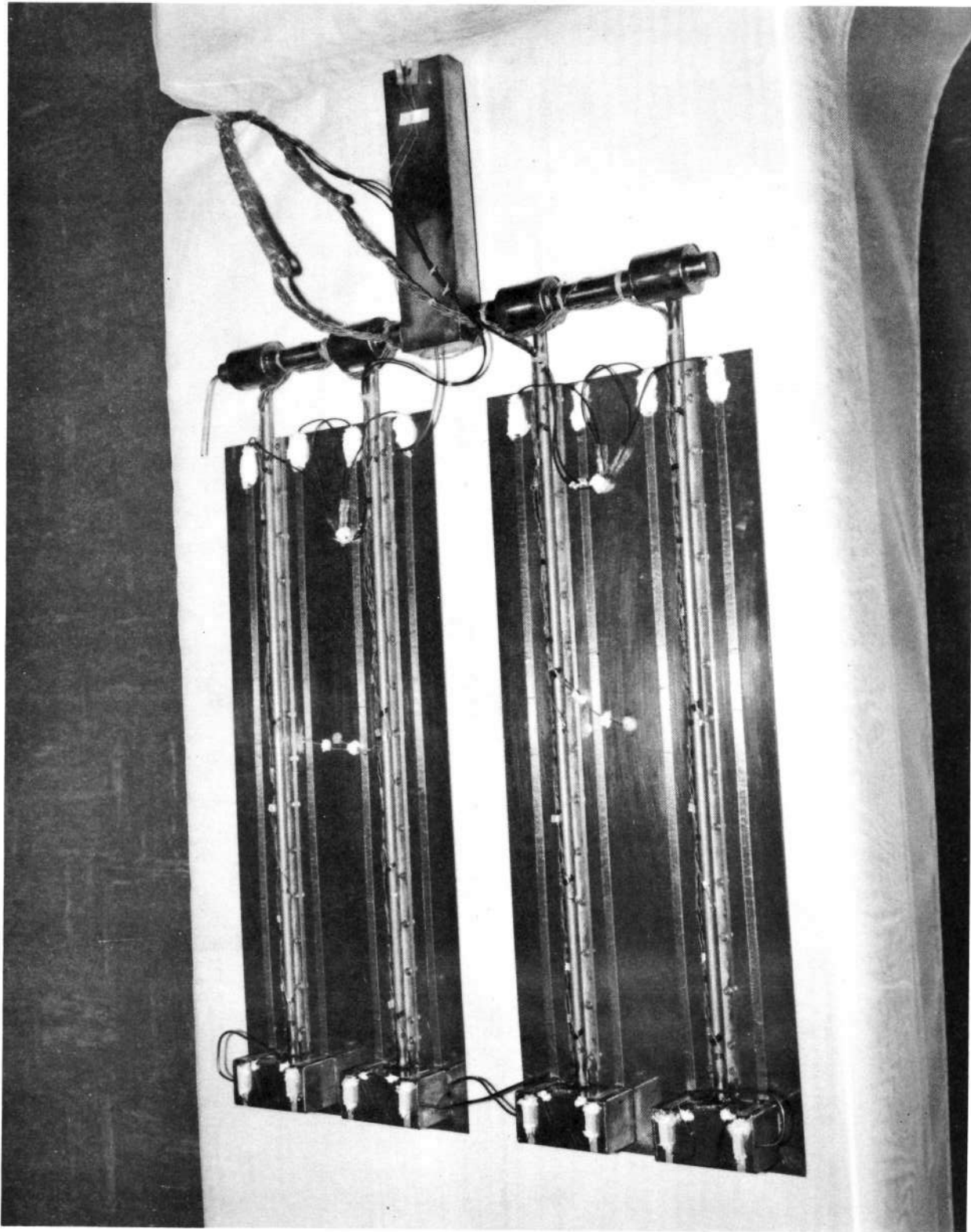


Figure 4-11. Photograph - Room Ambient Assembly

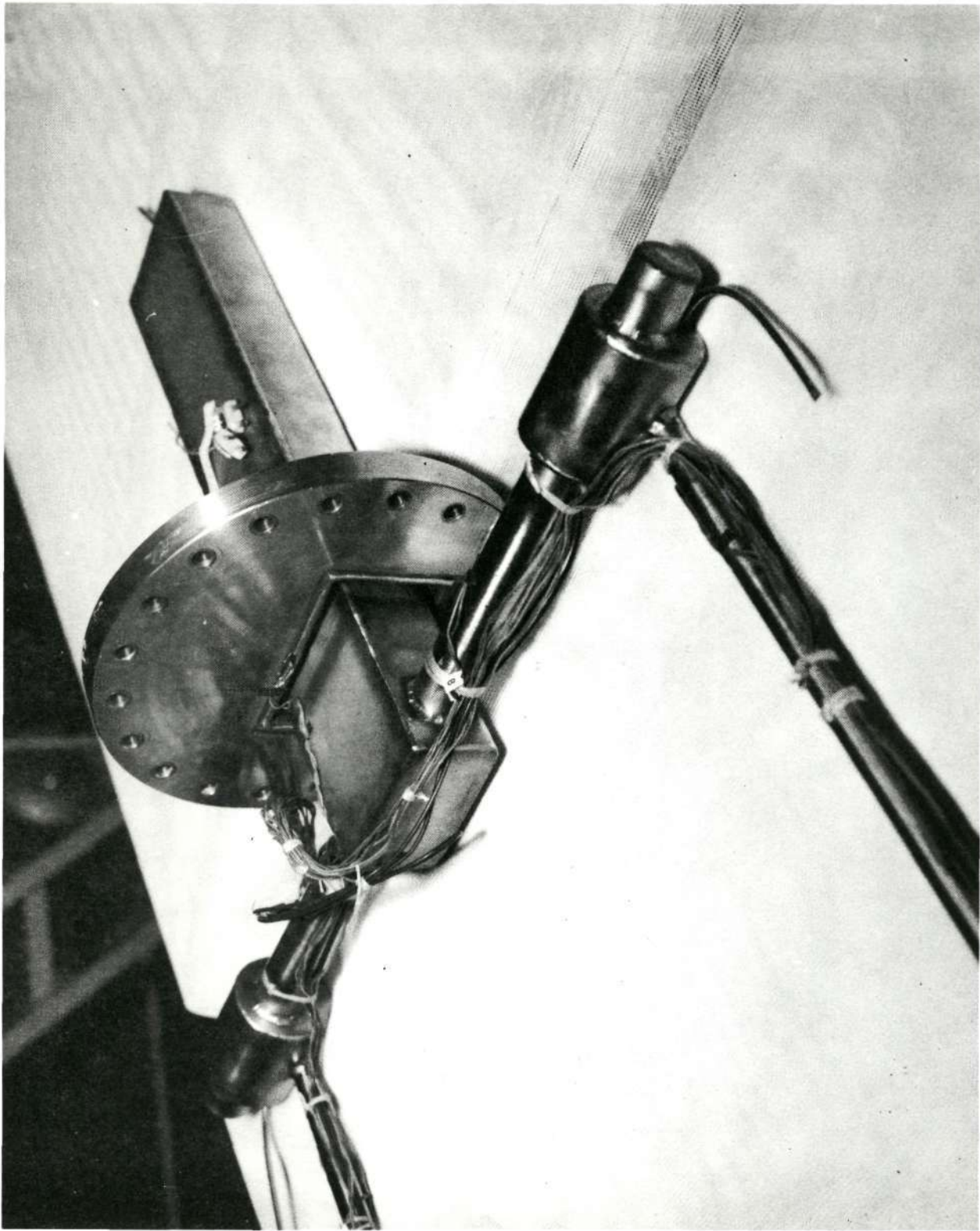


Figure 4-12. Photograph - Interface and Feed Through Detail

overflow based on this theoretical void volume for two reasons: (1) about 5% of the excess was provided to account for uncertainties in the calculation, and (2) the other 5% excess provided for liquid density change from fill conditions (room temperature) to the lowest operating temperature expected (-50°F). The pipes could thus function at -50°F with no deficiency of liquid in the wicks. Because of the configuration of the condensers of all heat pipes, the excess liquid of temperatures higher than -50°F would not significantly block transfer surfaces. Table 4-3 lists the actual charge volume for room temperature liquid methyl alcohol for all heat pipes.

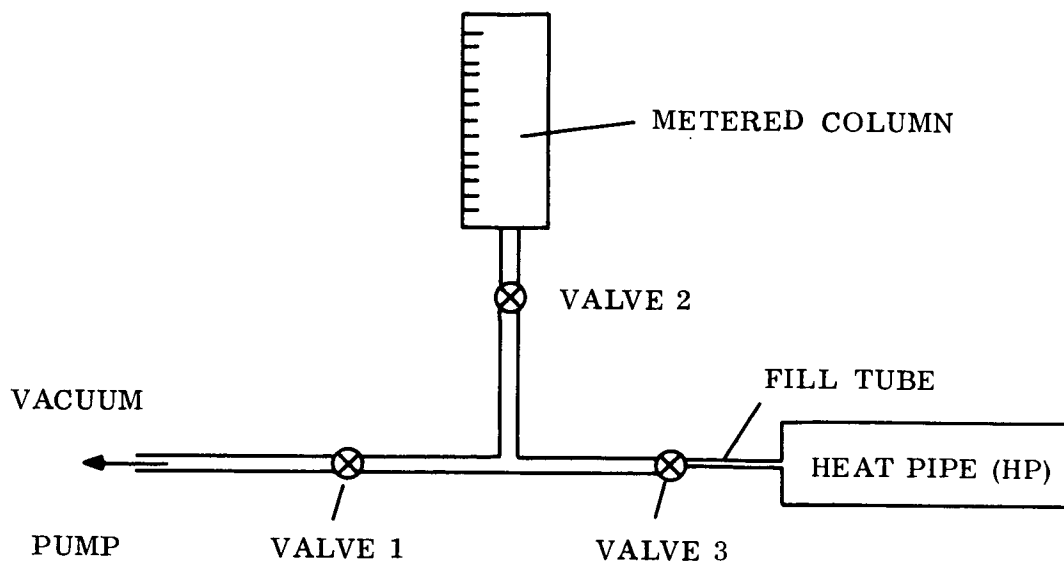
Table 4-3. Heat Pipe Methanol Charges

Heat Pipe	Charge, Milliliters*
#1	47
#2	93
#3	44
#4	53
#5	26

*At room temperature (70°F)

A fill tube of one-eighth inch outer diameter (one-sixteenth inch inner diameter) annealed nickel tubing was welded into the condenser (cold) end of each of the nine distinct heat pipes of the test article. The open end of this fill tube was flared for an AN fitting for attaching the heat pipe to the fill station. The fill tube was pinched-off after charging the heat pipe.

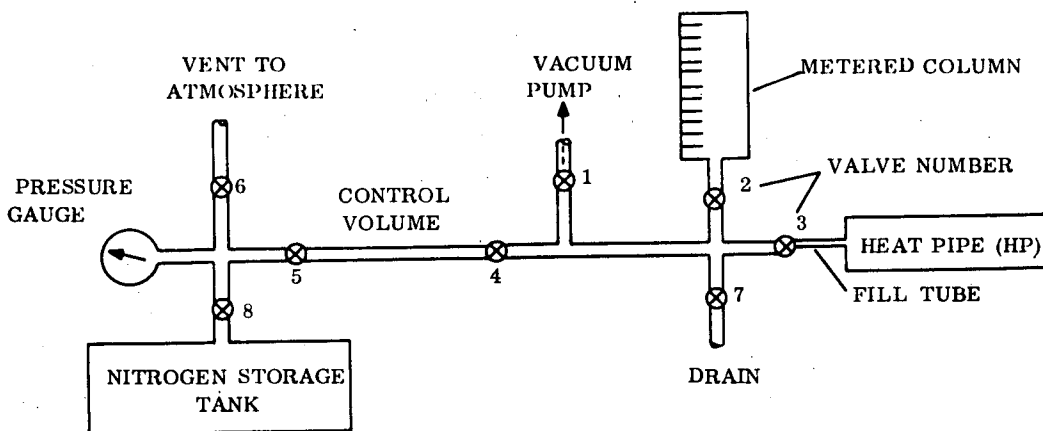
The actual fill procedure is detailed into Figure 4-13 (fixed conductance heat pipes) and Figure 4-14 (variable conductance heat pipes). Both begin with evacuation of the pipe and direct liquid phase transferral of a metered quantity of methanol into the pipe. For heat pipes #1, #2, #3 and #4 the procedure ended here, with a fill tube-pinch off. For the four #5 heat pipes, additional hardware and steps were necessary for non-condensable (nitrogen) charging.



Step	Operation	Valves*			Comments
		1	2	3	
1	Evacuate	0	C	0	Rough/diffusion pump for 3 hours. Heat HP periodically with heat gun.
2	End Evacuation	C	C	0	
3	Set-up	C	C	C	Fill metered column with liquid methanol.
4	Tare Fill	C	0	C	When column is stable, establish zero liquid level.
5	HP Fill	C	0	0	Until desired quantity of methanol is withdrawn from column.
6	End Fill	C	0	C	
7	Pinch-Off	C	0	C	Pinch fill tube between valve 3 and HP.

*0 is open; C is closed.

Figure 4-13. Fill Procedure - Fixed Conductance Heat Pipes



Step	Operation	Valve*								Comment
		1	2	3	4	5	6	7	8	
1	Preliminary	0	C	0	0	0	C	C	C	Evacuate and fill nitrogen storage tank to at least 60 psig. Fill metered column with liquid methanol.
2	Evacuate	0	C	0	0	0	C	C	C	Rough/diffusion pump for 3 hrs. Heat HP periodically with heat gun.
3	End Evacuation	C	C	C	C	0	C	C	C	
4	Tare Fill (Methanol)	C	0	C	C	0	C	C	C	When column is stable, establish zero liquid level.
5	HP Fill (Methanol)	C	0	0	C	0	C	C	C	Until desired quantity of methanol is withdrawn from column. Then close valve 3.
6	Tare Drain	C	C	C	C	0	C	0	C	Heat volume enclosed by valves 1, 2, 3, 4, 7 to drive out liquid methanol. Then close valve 7.
7	Tare Evacuation	0	C	C	C	0	C	C	C	For 20 minutes.
8	Nitrogen Set-Up	C	C	C	C	0	C	C	0	Fill volume enclosed by valves 4, 6, 8 to at least 60 psig from tank. Then close valve 8.
9	Set Pressure	C	C	C	C	0	0	C	C	Bleed pressure in volume enclosed by valves 4, 6, 8 to 52.4 psig. Then close valve 6.
10	Trap Nitrogen	C	C	C	C	C	C	C	C	
11	HP Fill (Nitrogen)	C	C	0	0	C	C	C	C	Until equilibrium is reached. Then close valve 3.
12	Pinch-Off	C	C	C	0	C	C	C	C	Pinch fill tube between valve 3 and HP.

*0 is open, C is closed.

Figure 4-14. Fill Procedure - Variable Conductance Heat Pipes

The quantity of nitrogen required in the variable conductance heat pipes was calculated based on the following conditions and/or assumptions.

1. Reservoir volume of 14.06 cu. in. and a total condenser vapor volume of 2.57 cu. in.
2. Condenser fully active when working fluid vapor at 25^oF and reservoir at a sink temperature of 390^oR. This implies that the vapor/gas interface is at the reservoir entrance under the stated conditions.
3. No axial conduction through the heat pipe wall.
4. No mass diffusion axially through the vapor/gas interface.
5. Working fluid present in the gas reservoir at all times. Pressure corresponds to saturation pressure of methanol at sink temperature.

Nitrogen charge was thus calculated to be 2.42×10^{-5} lbm. Analysis of heat pipe performance with this nitrogen mass at other conditions revealed that the theoretical total control band (range of vapor temperature) was 17^oF to 31^oF while the heat throughput varied from 20 to 60 watts system total and the sink temperatures varied from 330^oR to 410^oR.

The technique used to transfer the calculated mass of nitrogen into the pipes is presented in Figure 4-14. Basically, it involves trapping nitrogen in an accurately determined control volume (2.2 ± 0.1 ml) at a predetermined pressure (52.4 ± 2 psig). The control volume is then opened to the heat pipe. At equilibrium, 2.42×10^{-5} lbm of nitrogen ($\pm 5\%$) will be present in the heat pipe. It should be pointed out that the pressure stated above includes consideration of tare volumes within the fill set-up.

4.7 TEST SEQUENCE/ANTICIPATED RESULTS

A test sequence was planned to determine both steady state and transient thermal performance of the test article. Of primary interest, of course, were the system temperature drops, the averaging effects of the #2 and #4 heat pipes, and the control characteristics of the variable conductance heat pipes. The sequence shown in Table 4-4 was generated to evaluate these three points. Case 10 was inserted to determine the "weak link" heat pipe in the system.

Table 4-4. Planned Test Sequence

Case No.	Steady State or Transient	Comp Heat, W		Sinks, °R	
		C1	C2	S1	S2
1	SS	20	20	330	330
2	SS	30	20	330	330
3	SS	30	30	330	330
4	SS	30	30	400	400
5	SS	30	30	450	330
6	SS	30	20	450	330
7	Trans	20	20	Vary	Vary
8	Trans	30	30	Vary	Vary
9	Trans	36	36	Vary	Vary
10	SS	30+*	30	400	400

*Increase until a heat pipe burnout occurs

An analytical model of the total test article was set up to predict temperatures at several system points during test. The computer code used for Phase II analysis of the Space Station thermal control system was again employed. The model consisted of eleven (11) nodes including the two COMP heaters, seven heat pipe vapor passages (only one variable conductance heat pipe was monitored per panel -- the other would theoretically exhibit identical characteristics), and the two radiating panels. The conductance terms between these nodes were presented in Table 4-2. An emissivity times effectiveness product of 0.765 was assumed for calculation of the two panel radiation terms. Estimated weights were used to generate nodal thermal inertia terms. Variable conductance was included between the #5 heat pipes and the radiators.

This model was run for steady state cases 1 through 6 shown in Table 4-4. No predictions were made for the transient cases (7, 8 and 9) because the hardware testing had been initiated at the time. Results for the steady state cases are shown in Table 4-5. Listed are the

input conditions and the output temperatures at the two COMP heaters and the two radiating panels. As can be seen, expected heater temperatures were very close to the $45^{\circ}\text{F} \pm 10^{\circ}\text{F}$ design goal for these cases. Element sizing was thus verified analytically

Table 4-5. Analytically Predicted Test Results

Case No.	Heating, W		Sink Temp, $^{\circ}\text{R}$		Predicted Temperatures, $^{\circ}\text{F}$			
	COMP 1	COMP 2	SINK 1	SINK 2	COMP 1	COMP 2	SINK 1	SINK 2
1	20	20	330	330	32	32	16	16
2	30	20	330	330	39	37	18	18
3	30	30	330	330	44	44	20	20
4	30	30	400	400	53	53	29	29
5	30	30	450	330	55	55	33	29
6	30	20	450	330	43	40	23	19

Based on the profiles generated by the above study, approximate operating temperature levels for all system heat pipes were designated. These levels were employed to calculate burn-out heat loads for all of the pipes. The computer code written in Phase I was used. Results are given below, along with the nominal heat transport capacity required. Clearly, the two #1 heat pipes are the most highly stressed but each should be capable of carrying its nominal heat load.

<u>Heat Pipe</u>	<u>Operating Temp, $^{\circ}\text{F}$</u>	<u>Calculated Burn-out, W</u>	<u>Nominal Heat Load, W</u>
#1	45	36	30
#2	39	77	60
#3	31	228	60
#4	22	248	60
#5*	20	26	15

*Assumed fully active condenser length

4.8 TEST DESCRIPTION AND RESULTS

The chamber used for testing was a horizontal-axis, cylindrical vessel, four feet in diameter and five feet long. One end-dome of the chamber was a dolly-mounted door. The test article was fixed to this door by bolting the flange on heat pipe #2 to a port in the center of the door. Additional support was provided by nylon cords from the door to the ends of the article. A series of three overlapping liquid nitrogen shrouds surrounded the radiating panels of the system.

Prior to the chamber pump-down, all control and monitoring equipment was checked out and found satisfactory.

The heating profile of test case 1 was imposed on the system after pump-down to 5×10^{-4} torr and while the cryowalls were cooling. Very large system temperature drops were immediately observed. It was decided to let the system temperatures stabilize and use the data from this case to suggest a subsequent course of action. Thermal equilibrium was reached after about seven hours and the temperature profile shown on Figure 4-15 was recorded.

RUN #1 - 20W COMPONENT LOAD EACH; 330°R SINK EACH
 MAIN SHROUD - 260°F
 2.4×10^{-4} TORR

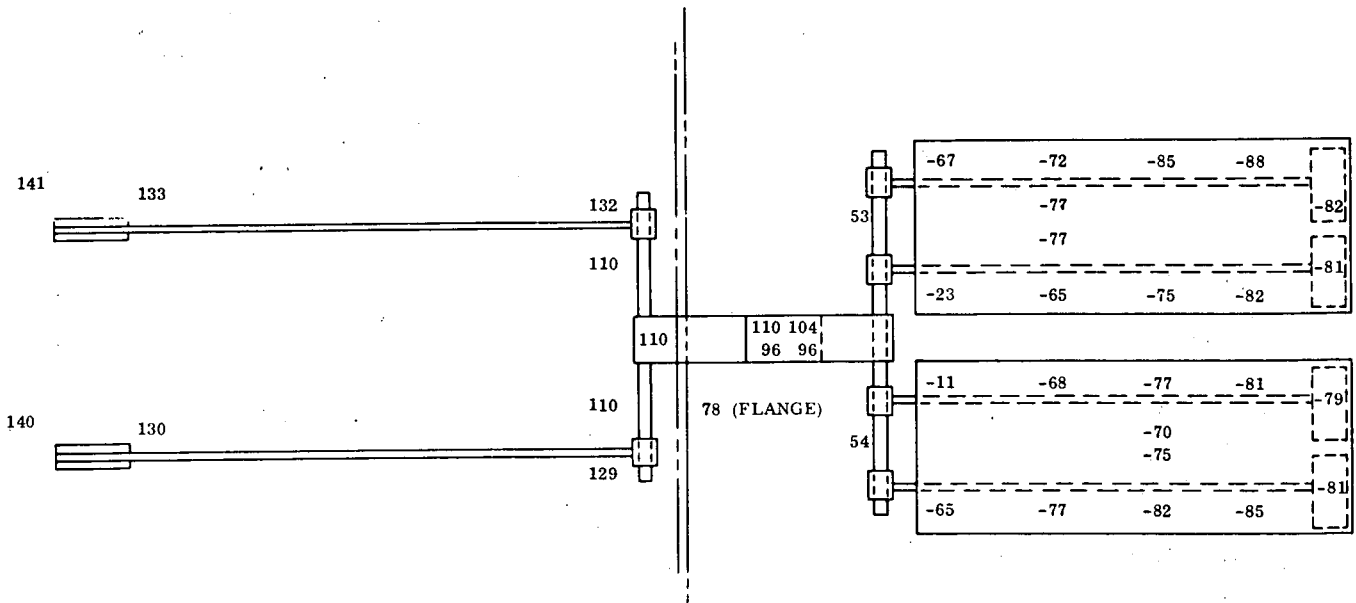


Figure 4-15. Test Data Profile - Case #1

As can be seen on Figure 4-15, the overall system temperature drop was significantly higher than anticipated. Where a calculated drop of about 20°F was predicted from the COMP heaters to the action portion of the radiators, a drop of about 163°F ($=140-(-23)$) was noted. Further examination of the profile revealed that the major drops occurred not in the heat pipes but in the interface region where the heat pipes were joined together.

Because of the large interface temperature differences, the system thermal balance shifted to the point where heat leaks became significant. Primary heat leaks occur in the room ambient section of the article, up to and including the feed-through structure. Since this half of the system was expected to operate below room temperature, a leak into the system was anticipated. A theoretical value of +8.8 watts was calculated and its effect on the system would have been to raise temperatures a few degrees. During test, the outer half of the article was well above room temperature and, based on the data of Figure 4-15, an actual heat leak of 17.8 watts out of the system was calculated. The radiating panels were thus at colder temperatures than planned, which represented an off-design condition for the variable conductance heat pipes and degraded their intended performance.

It was realized at this point that none of the quantitative design goals for the article could be verified. Specifically,

1. The COMP heaters could not be held at 45°F .
2. $\pm 10^{\circ}\text{F}$ control at these heaters could not be demonstrated because the variable conductance heat pipes were not operating in their optimum control temperature band
3. An overall temperature drop of 20°F to 30°F could not be shown.

The planned test sequence was consequently modified. The possible causes of the large interface drops were discussed (see Section 4.9), and the corrective action in each case was determined. It was decided that further testing was necessary to evaluate the characteristics of the interfaces under different heat load conditions so that the cause could be identified. Since the article was still in the chamber, a series of six new test cases was generated to be performed with the set-up as it was.

Table 4-6 shows the conditions for the seven cases actually run. All cases were steady state since it was felt that transient performance would be washed out by the interface losses. Temperatures were monitored every hour during these tests, and equilibrium was attained in from five to seven hours in each case. Figures 4-16 through 4-21 present the stable temperature distributions for cases 2 through 7 of Table 4-6.

Table 4-6. Test Sequence

New Case No.	Comp Heat, W		Sink Temperature, °R	
	COMP 1	COMP 2	SINK 1	SINK 2
1	20	20	330	330
2	10	10	330	330
3	30	30	330	330
4	30	20	330	330
5	30	20	450	330
6	30	30	450	330
7	0	10	450	330

RUN #2 - 10W LOAD EACH COMPONENT HEATER

330°R SINK

MAIN SHROUD - 230°F (#3); -120°F (#6); -220°F (#2)

PRESSURE 2.4×10^{-4}

ROOM TEMPERATURE 70°F

COMP #1 9.0 V (12W)

COMP #2 8.2 V (10W)

SINK #1 8.8 V (9.5W)

SINK #2 8.5 V (9.1W)

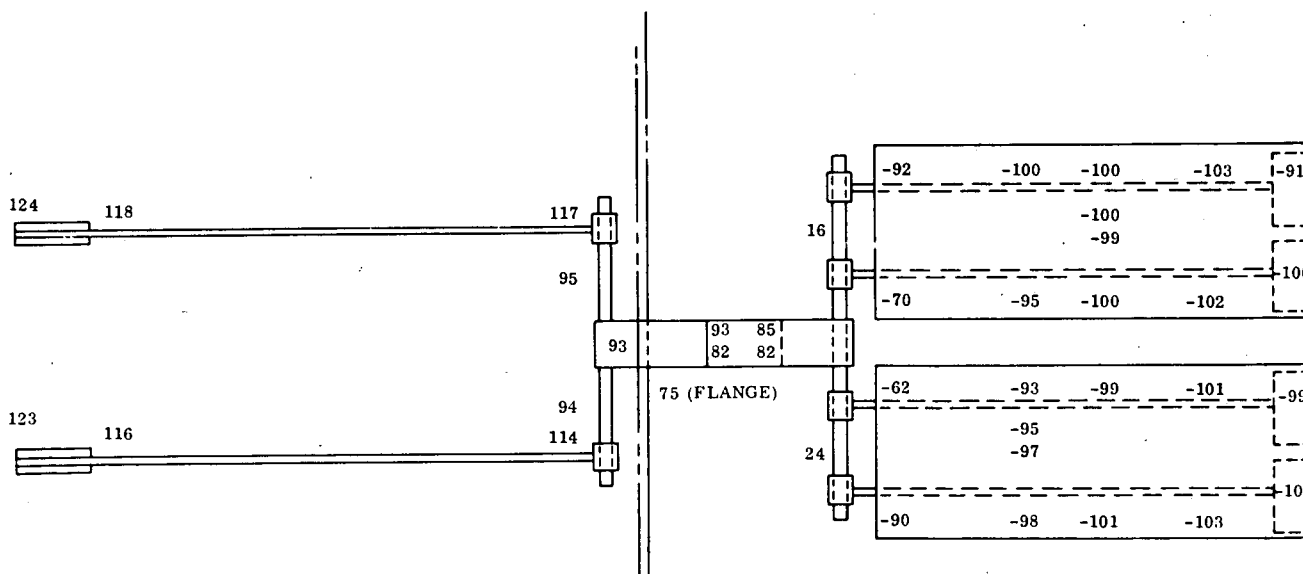


Figure 4-16. Test Data Profile - Case #2

RUN #3 30 W LOAD EACH COMPONENT HEATER
 330°R SINKS
 SHROUD #2 -225°F
 #3 -280°F
 #6 -125°F
 Room 75°F
 4.0×10^{-4} TORR

COMP #1 - 14.0 V (28.9 W)
 #2 - 14.7 V (3.8 W)
 SINK #1 - 9.1 V (10.5 W)
 #2 - 8.8 V (9.5 W)

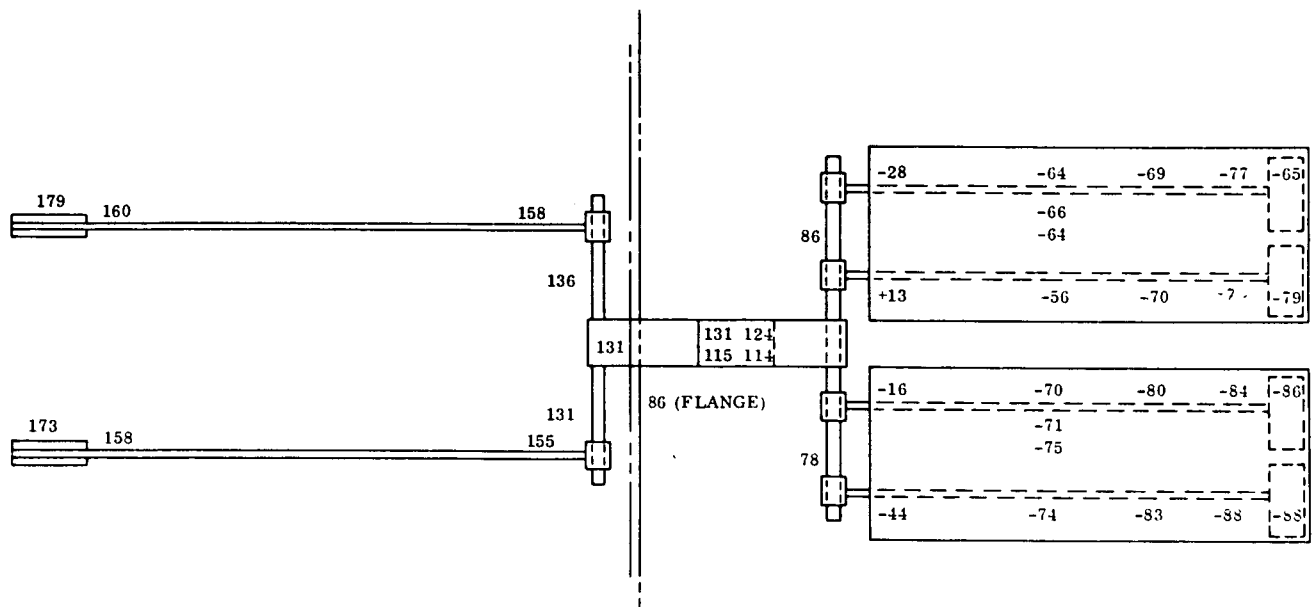


Figure 4-17. Test Data Profile - Case #3

RUN #4 30 W COMP 1
 20 W COMP 2
 BOTH SINKS 330°R
 SHROUD #2 -218°F
 #3 -255°F
 #6 -125°F
 ROOM 71°F
 3.9×10^{-4} TORR

COMP 1 - 14.2 V (29.4 W)
 2 - 12.1 V (21.1 W)
 SINK 1 - 9.4 V (11.0 W)
 2 - 9.1 V (10.5 W)

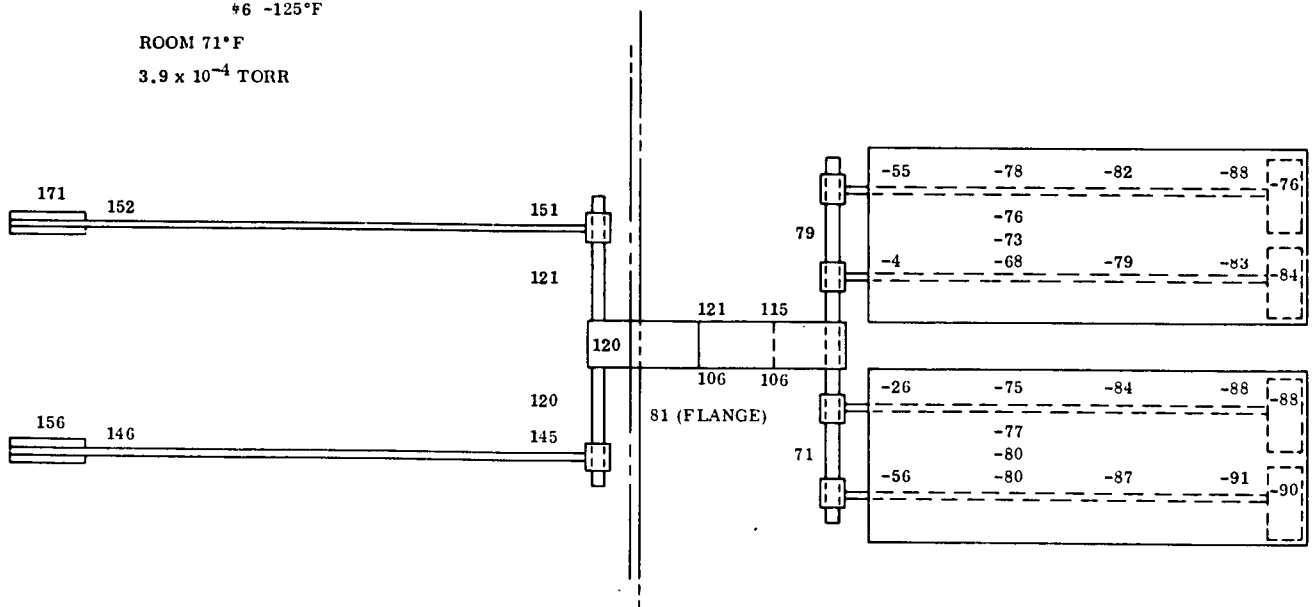


Figure 4-18. Test Data Profile - Case #4

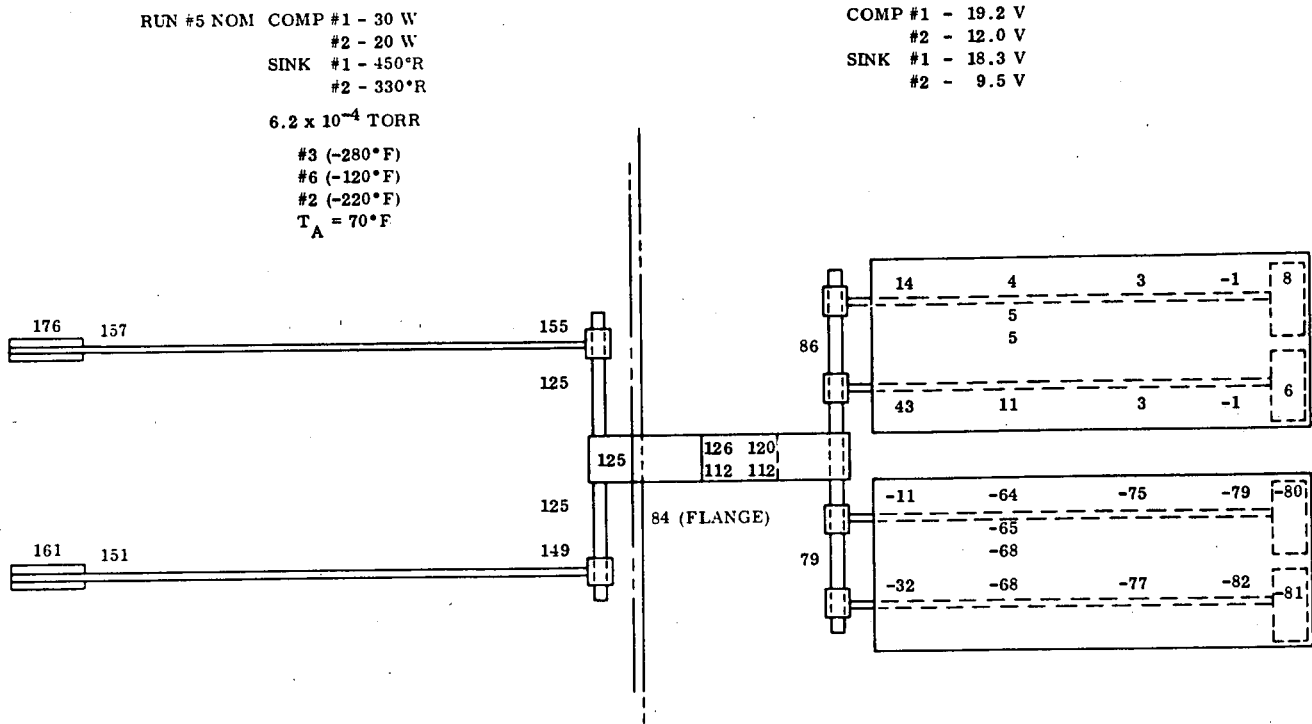


Figure 4-19. Test Data Profile - Case #5

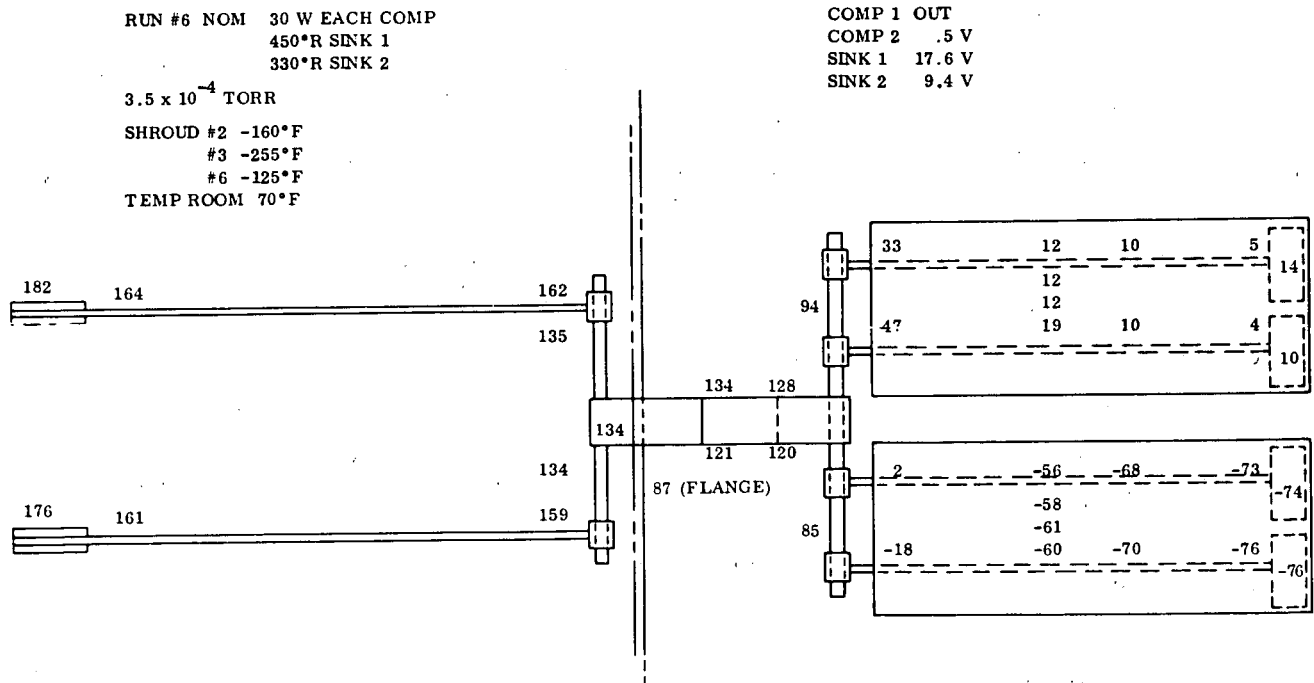


Figure 4-20. Test Data Profile - Case #6

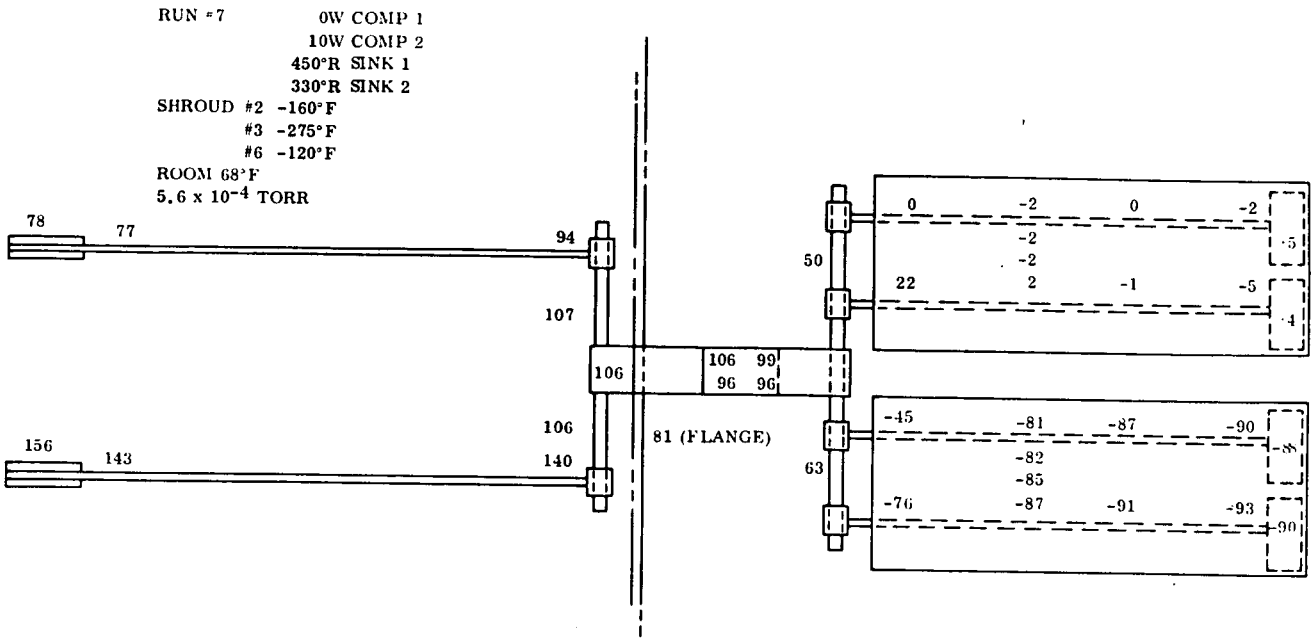


Figure 4-21. Test Data Profile - Case #7

Tables 4-7 and 4-8 summarize the observed temperature drops through all interfaces and all heat pipes, respectively, for each of the seven test cases. With reference to Table 4-8, it should be noted that very high end-to-end drops are expected in variable conductance heat pipes such as #5A, #5B, #5C and #5D.

4.9 TEST DATA EVALUATION

In trying to analyze the test results presented in the previous section, several conclusions can be reached immediately. On the positive side, no heat pipe burn-out was observed and consequently the integrity of all wicking and wick joining schemes was proven. Sufficient condensate did return to the evaporator of each pipe. Also on the positive side, vapor/gas fronts were definitely established in the variable conductance heat pipes and these fronts did move as expected due to varying boundary conditions. Off-design temperature levels prevented the attainment of $\pm 10^{\circ}$ F control desired.

Table 4-7. Interface Temperature Drops

Interface Pair	Temperature Drop in °F						
	Case 1	Case 2	Case 3	Case 4	Case 5	Case 6	Case 7
COMP 1-HP#1A	8	6	19	19	19	18	1
COMP 2-HP#1B	10	7	15	10	10	15	13
HP#1A-HP#2	22	22	26	30	30	27	-13
HP#1B-HP#2	19	20	24	25	24	25	34
HP#2-HP#3 (Ave.)	11	7	13	12	11	10	7
HP#3-HP#4	53	62	33	31	29	30	39
HP#4-HP#5A	120	108	114	134	72	61	50
HP#4-HP#5B	76	86	73	83	43	47	28
HP#4-HP#5C	65	86	94	97	90	83	108
HP#4-HP#5D	119	114	122	127	111	103	139
HP#5A-SINK 1	3	0	2	2	-1	0	0
HP#5C-SINK 2	2	2	1	-2	1	2	1

Table 4-8. Maximum Heat Pipe Temperature Drops

Heat Pipe	Temperature Drop in °F						
	Case 1	Case 2	Case 3	Case 4	Case 5	Case 6	Case 7
#1A	1	1	2	1	2	2	-17
#1B	1	2	3	1	2	2	3
#2	6	10	8	6	5	7	8
#3	0	0	1	0	0	1	0
#4	1	8	8	8	7	9	13
#5A	21	11	49	33	15	28	5
#5B	59	32	92	80	44	43	27
#5C	70	39	70	62	69	76	45
#5D	20	13	44	35	50	58	17

The major negative conclusion drawn was that the "high performance" interface technique did not perform as expected. This, in turn, caused modification of the system thermal balance to the extent that unplanned heat leaks became significant items and meaningful system performance could not be observed.

The cause of the large interface temperature drops has not been firmly established. Evidence points, however, to the presence of non-condensable gas in the heat pipe condensers (interface cells). Three other possible explanations were discussed; these were:

1. Theoretical calculations were very optimistic with respect to wick/liquid conductivity and thickness, and all interfaces were vastly undersized from the start.
2. Momentum considerations did not permit all the vapor of the hotter heat pipe to completely surround and condense on the total planned heat transfer area.
3. Excess liquid methanol collected on the condenser surface and represented another thermal resistance in the heat flow path.

The excess fluid theory was rejected primarily because the condenser wicks would not support a sufficient thickness of liquid to cause the measured drops. The momentum explanation was deemed unlikely since vapor velocities ranged from about 0.2 feet/second to 30 feet/second at the entrance to the various interface cells which exhibited poor performance. The possibility of undersizing is discussed in the next paragraphs.

As an aid to understanding the behavior of the interface cells, the conductance of three selected cells was calculated for each test case. Heat actually transferred through these interfaces was determined from a thermal balance for each case (including heat leaks based on monitored test data). These conductances were plotted against the temperature of the "upstream" heat pipe. Figure 4-22 shows the result. Data from Case 2 was plotted, but omitted in drawing the curves. Data from Case 7 was not shown since heat pipe #1A was acting as a heat sink and gradients were reversed.

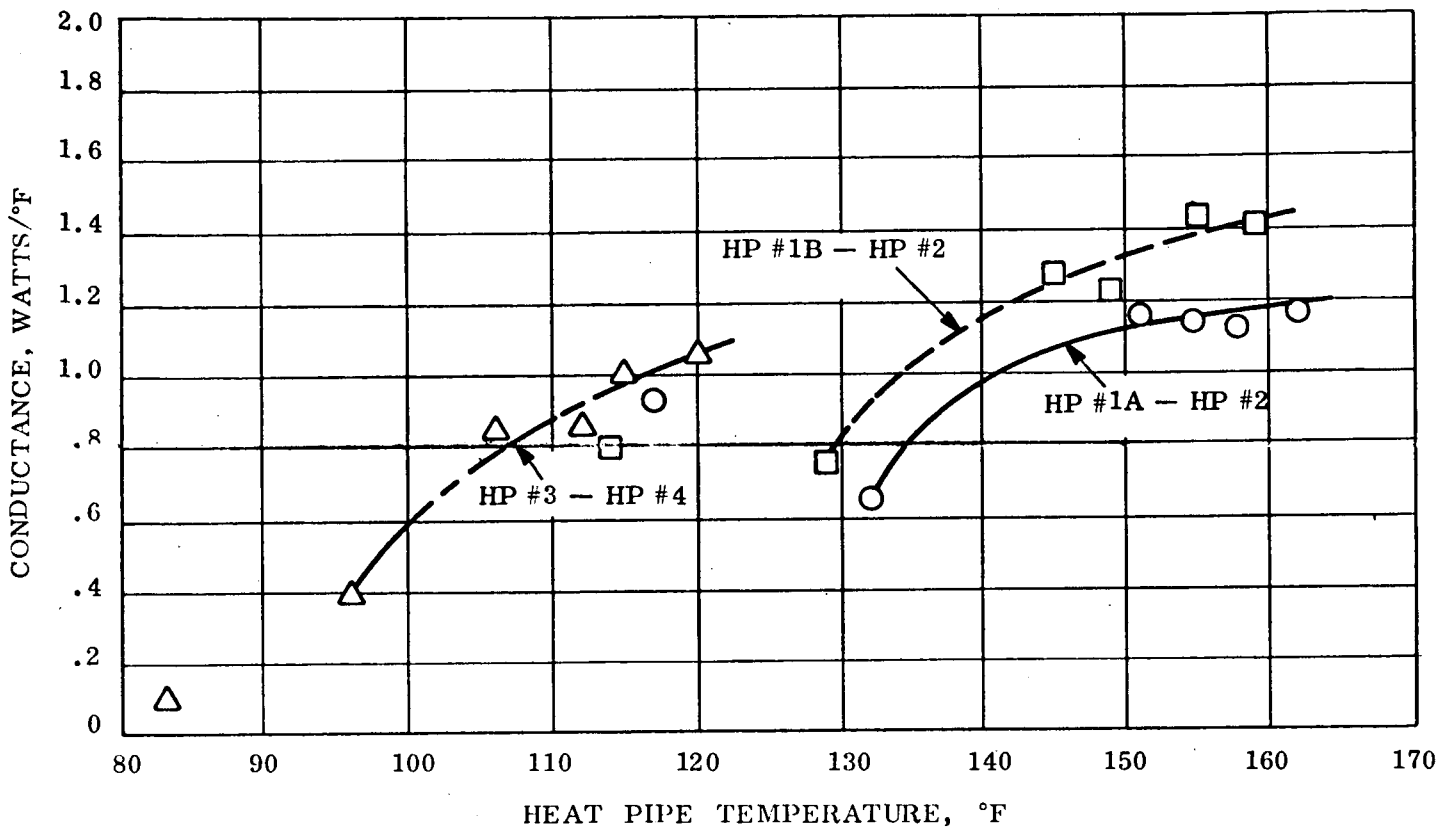


Figure 4-22. "Advanced" Interface Conductance Detail

The most significant feature of Figure 4-22 is that the conductance of all three interfaces varied greatly with heat pipe temperature. The profiles are very similar to the characteristics of variable conductance heat pipes with non-condensable gas charges. This fact lends credence to the non-condensable gas theory. If the interfaces had merely been undersized, conductance would have been invariant with pipe temperatures.

Heat pipe #4 presents the only difficulty in the acceptance of the presence of non-condensable gas. Because four interface cells are attached to this heat pipe, it would be necessary for the non-condensable to at least partially cover each of these four heat transfer areas. To do this, the gas (non-condensable) would have to defy the momentum of the working fluid vapor trying to force it (the gas) to the ends of the heat pipe. This anomaly has not been resolved.

If the presence of gas is accepted, the question becomes where did it come from and how can the problem be avoided in the future. Four sources of gas are readily apparent:

1. inadequate evacuation prior to charging,
2. inadequate fill techniques,
3. leakage of room air into the pipes after charging, and
4. a chemical reaction between wick, wall and fluid producing a non-condensable.

For the latter two of these, leakage and chemical reaction, the quantity of gas in the heat pipes would have been time-dependent. Furthermore, the rate of gas build-up would have to be relatively high to affect Case 1 as observed (approximately five days elapsed between heat pipe charging and the onset of test Case 1). It is felt that, at such a rate, interface performance would have degraded significantly during the three day test. This degradation was not noted. Therefore, leakage and chemical reaction were rejected as the primary sources of non-condensable gas.

Three additional comments about heat pipe leaks are warranted;

1. For leakage to have been the primary source of gas, five heat pipes would have had to leak to justify the measured performance. This is deemed unlikely.
2. Test technicians suspected a small leak into the chamber of a substance other than nitrogen or oxygen. This was based on observation of pump characteristics and chamber pressure. It is probable that a small leak existed in one of the heat pipes within the chamber, but it is not possible for this one leak to have caused significant thermal effect on that pipe during this short-term test.
3. All heat pipes were pressure checked prior to evacuation using standard air-flow techniques. They were not, however, checked with helium leak detection equipment.

Although facts (2) and (3) indicate the possibility of heat pipe leakage, fact (1) tends to confirm the assumption that leakage was not responsible for the noted temperature drops.

Thus, logic leads to the conclusion that the gas in the heat pipes was either residual after evacuation or was transferred during the fill operation. The procedures used to evacuate and fill these heat pipes were identical to those used for many other heat pipes in the past, and have proven very acceptable. The only significant difference between the past and present heat pipes was the perpendicular condenser design employed on the latter. It was therefore felt that a small amount of gas existed in both past and present heat pipes after charging with working fluid and that this amount, although insignificant in heat pipes of normal condenser design, severely reduced the effective heat transfer in the crossed-condenser design.

4.10 SUBSEQUENT TESTING

Three small-scale tests were performed on one-half of the test article subsequent to thermal vacuum runs. The section of the system which was originally designated the "room ambient" half (that is, heat pipes 1A, 1B, 2, and associated interface cells) was employed for these tests. The purpose was to verify the presence of non-condensable gas in the system heat pipes.

The first case, P1, was set up to reverse the heat flow through the segment in an attempt to drive any gas present in heat pipes 1A and 1B away from their respective interface cells. It was hoped that a vapor/gas interface would become obvious in these two pipes and also that the conductance of each interface cell would be increased. The following steps were taken to prepare the segment after testing.

1. The flexible foam thermal insulation was removed from most of heat pipe 1A. Only the eight inches nearest its interface cell remained insulated.
2. The heater tape previously called COMP 1 was removed from heat pipe 1A.
3. Thermocouples #1 and #3 were repositioned on the now exposed portion of heat pipe 1A. All other thermocouple locations and readout equipment were identical to those employed during thermal vacuum testing.
4. A silicone rubber heater was clamped to the bottom of the rectangular section of heat pipe 2. This heater measured 3" x 6" and was positioned on the last 6" of heat pipe 2.

Figure 4-23 shows the resultant segment configuration for test case P1. A variac was employed for heater power input.

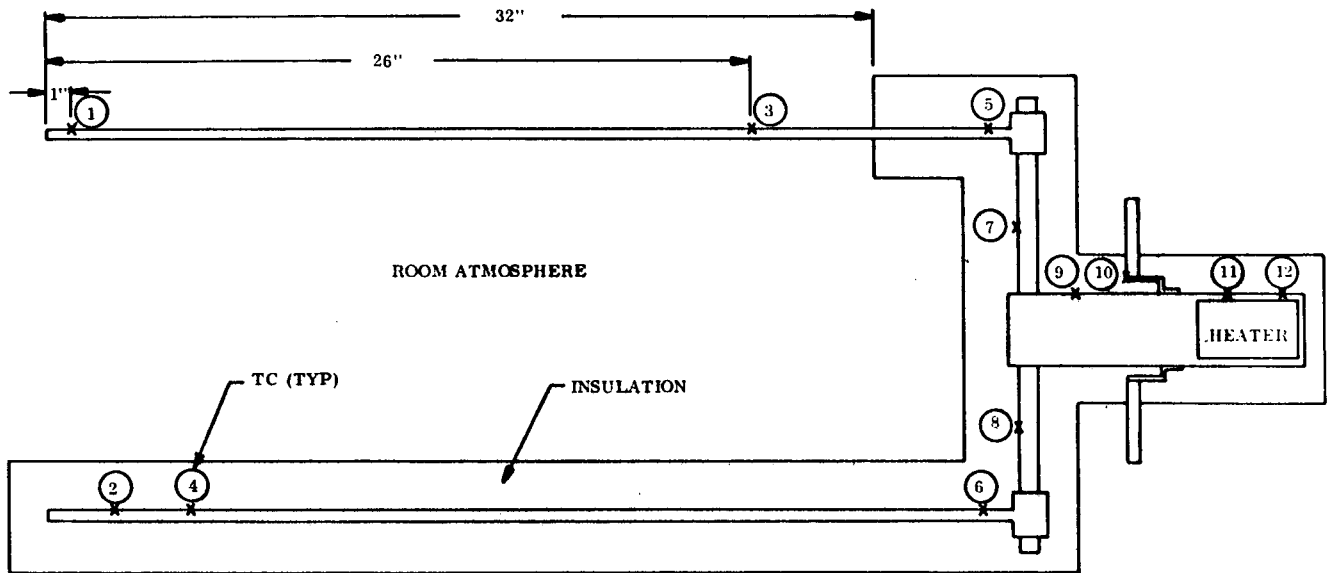


Figure 4-23. Case P1 Configuration

Case P1 was performed with the segment horizontal in a room environment and a nominal 20 watt input to the added heater. At the end of six hours, system temperatures were rising at a rate of approximately $1.5^{\circ}\text{F}/\text{hour}$ and the test was ended. Accurately determined heater resistance and voltage measurements during the test indicated that heater power was actually 20.71 watts. Figure 4-24 shows the test results, including both temperatures monitored at the end of six hours and heat flow through the various elements calculated on the basis of these temperatures. The overall heat balance includes 1.20 watts of thermal energy being stored at the conclusion of the test.

The setup was modified for test cases P2 and P3. In these runs, heat was applied directly to the outer wall of the interface cell between heat pipes 1A and 2. The following changes were made:

93 POST TV TEST
CASE I

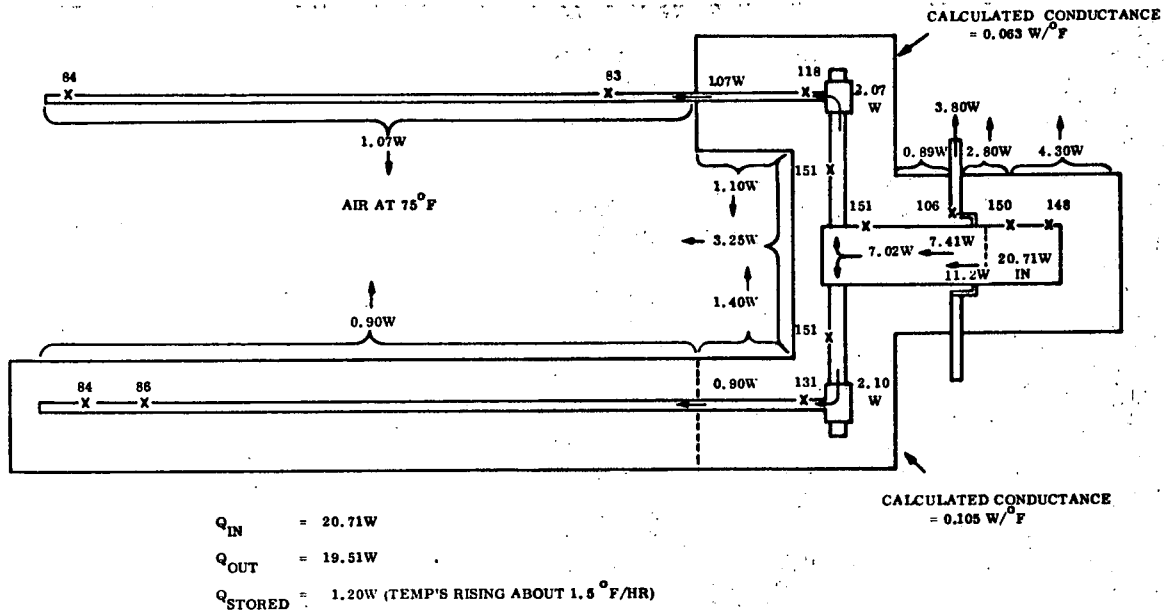


Figure 4-24. Case P1 Results

1. All insulation was removed from heat pipe 1A and the subject interface cell.
2. A 2" x 2" silicone rubber heater was wrapped around a portion of the outer wall of the interface cell and was clamped in place.
3. Three additional thermocouples were installed on the test article; two on the heated interface cell and one on heat pipe 1A.
4. The interface cell region was re-insulated with 2" thickness of flexible foam.

The final configuration for cases P2 and P3 is shown in Figure 4-25. It should be noted that the heater and insulation added for test P1 remained in place during the P2 and P3 tests.

Cases P2 and P3 differed only in the amount of heat supplied to the interface cell (nominally 15 to 20 watts, respectively). Both tests were allowed to run six hours, after which time the heat storage term in the heat balance accounted for less than 5% of the heat input. Figures 4-26 and 4-27 show the results of cases P2 and P3 in a manner similar to that already presented for case P1 (Figure 4-24).

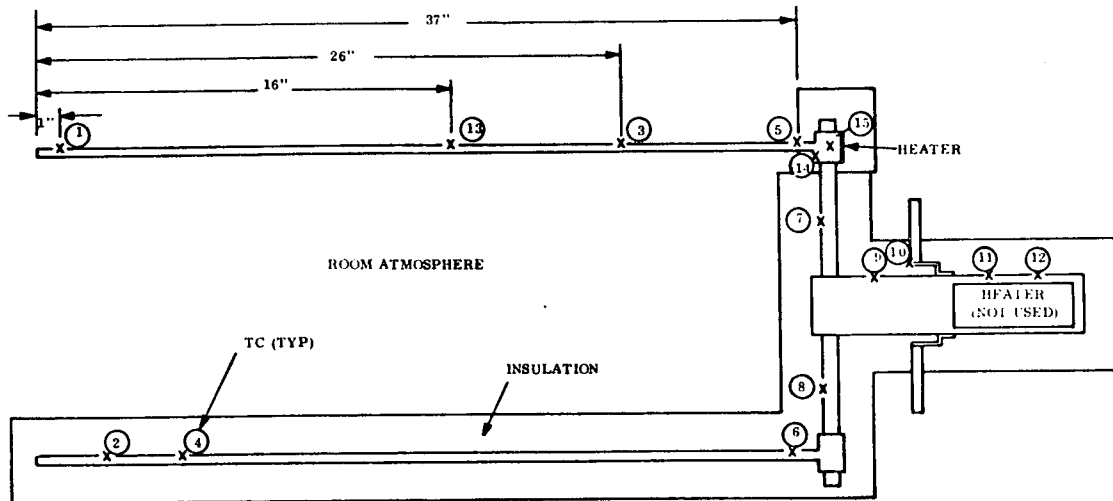


Figure 4-25. Cases P2 and P3 Configuration

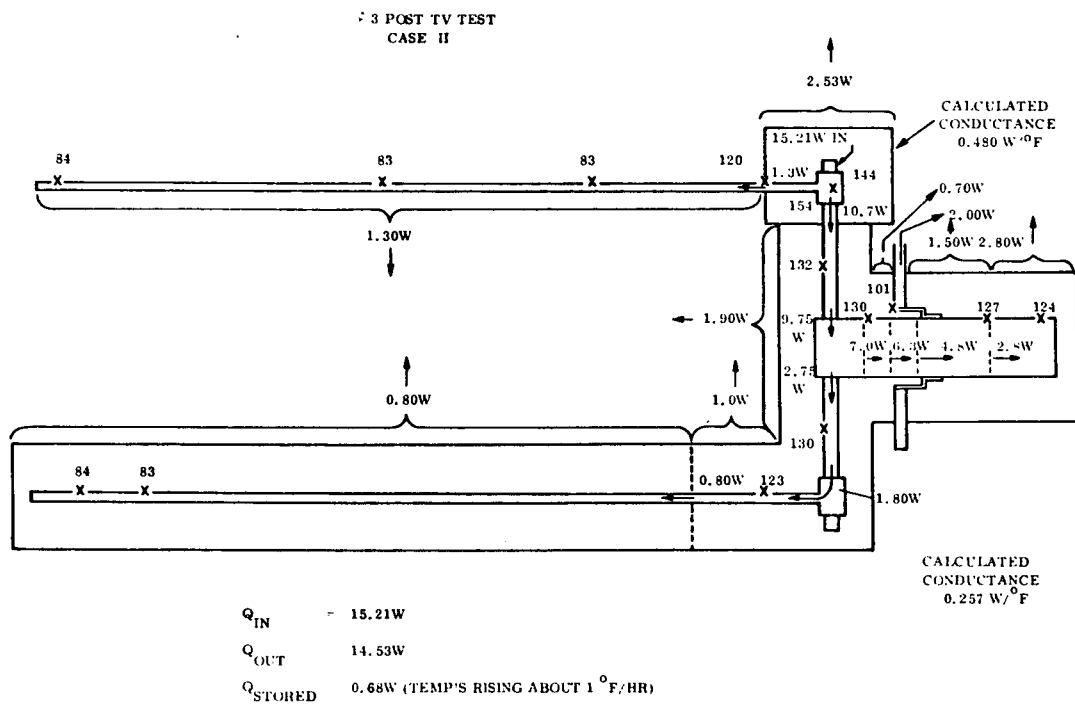


Figure 4-26. Case P2 Results

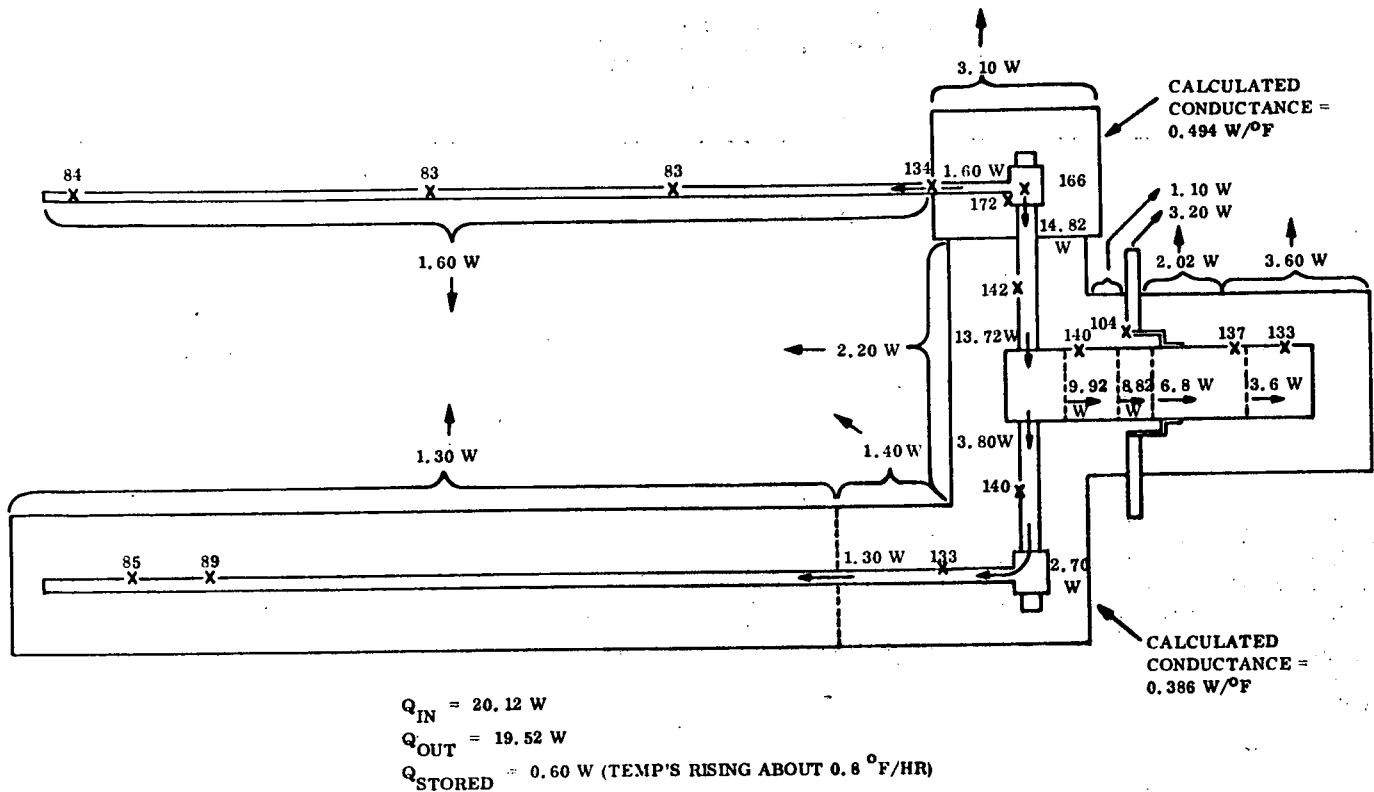


Figure 4-27. Case P3 Results

Taken together, the results of tests P1, P2, and P3 provide some insight concerning the system anomaly. The large temperature gradients observed in heat pipes 1A and 1B during all tests clearly indicate abnormal operation. Also, the apparent conductance from vapor to vapor in the interface cells was not improved over those calculated for the thermal vacuum tests.

Two possible mechanism have been defined to explain the noted performance. One of these requires the presence of non-condensable gas in the system heat pipes. The second, which does not require this assumption, is somewhat contradicted by data other than that obtained during tests P1, P2, and P3. The mechanisms are discussed below:

- A. A large quantity of non-condensable gas in the three heat pipes could cause temperature profiles such as those observed during testing. The P2 and P3 tests indicate that the vapor/gas interface of heat pipe 1A was spread around thermocouple #5 and the interface zone began very near, if not within, the interface cell. Indeed, to explain the small conductance from the vapor within

50

the annulus of the interface cell to the vapor of heat pipe 2, it is necessary to assume gas in the interface cell annular volume. It should be noted that of the total vapor volume of heat pipe 1A, 29% is in the 40-inch long, one-half inch tube and the remaining 71% is in the interface cell.

Although temperatures on the interface cell between heat pipes 1B and 2 were not measured during the tests, it can be postulated that the total profile of pipe 1B was similar to that measured on pipe 1A and the same non-condensable assumption can explain this performance.

The presence of some gas in heat pipe 2 is evidenced by the 8-9^o F gradient along its length in tests P2 and P3. This anomaly was not observed in test P1, as could be anticipated since gas would be driven to the interface cell regions in this case. Temperatures on heat pipe 2 were not monitored in these regions.

In summary, all observed test results can be explained by assuming the presence of a large quantity of non-condensable gas in heat pipes 1A and 1B, and some gas in heat pipe 2. The low conductance of each interface cell in tests P2 and P3 could have been caused by gas in the annular volume of the cell. These conductances could have been further reduced in test P1 by gas in the inner heat pipe (2) of each cell.

- B. The temperature profiles can also be explained by assuming burnout of heat pipes 1A and 1B in all three test runs. The burnout would occur between thermocouples 3 and 5 on heat pipe 1A, and at the corresponding position on pipe 1B. Figure 4-28 shows a schematic of the assumed burnout condition for heat pipe 1A. The heat necessary to burn out the one-half inch OD pipe is supplied by solid and gaseous conduction through the tube wall, wick, and superheated vapor. In tests P2 and P3, the same mechanisms would transfer heat from the heated cell wall to the vapor of heat pipe 2.

It is again necessary to assume non-condensable gas in the heat pipe 2 to explain the temperature gradients observed in this pipe in tests P2 and P3.

The credibility of the burnout theory (B above) is tempered somewhat by the following three facts:

1. No burnout was observed during thermal vacuum testing at substantial higher values of throughput than during the post-tests.
2. After the equilibrium temperatures of case P1 were recorded, the entire system was tilted so that gravity would aid condensate return to the heated end of the pipes. No change was noted in temperature profiles.

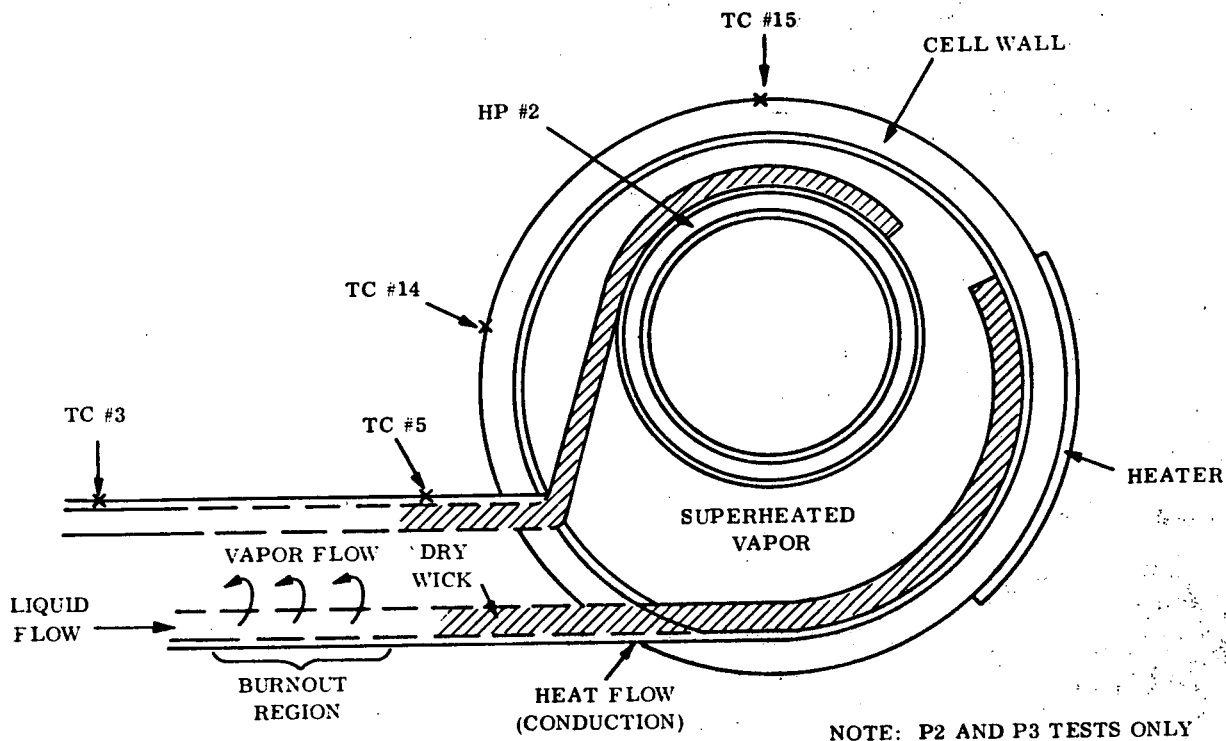


Figure 4-28. Schematic of Burnout Theory

3. Calculations indicate that conduction alone could not transport heat from the interface cell to the burnout point and yield the measured temperatures and apparent heat flows.

For these reasons, the non-condensable gas explanation is favored to justify the system behavior during the small-scale tests.

4.11 MODIFICATION OF INTERFACE CELL SYSTEM

An effort was undertaken to improve the thermal conductance of the interface cells of the test article. It was assumed that non-condensable gas present in the cells added resistance of heat flow by either blanketing the entire condensing surface with a thin layer of gas (acting as a diffusion barrier to the methanol vapor) or that pockets of the gas effectively closed off some portion of this surface. The effort was thus aimed at removing all gas from the heat pipes.

As a first step, all insulation, thermocouples, and wiring were removed from the room ambient section (heat pipes 1A, 1B, and 2) of the system. The pinch-off seals of all three heat pipes were then sawed off. The section was placed in an oven and baked at 430°F for 24 hours to remove the original methanol charges from the pipes.

Each of the three heat pipes was connected to a helium leak detection unit and was examined for leaks. No leaks were found in any of the pipes within the sensitivity of the detection unit (10^{-9} std. cc/sec). Valves were installed on the three heat pipe fill tubes. As a further check, heat pipes 1A and 1B were pressurized to 200 psia and tested with LEK-TEC[®] fluid just prior to re-filling. Again, no leak could be found.

Heat pipe 1A was re-charged first; fill was 47 ml of methanol. The procedure was the same as that described on Figure 4-13, except that the methanol was de-aerated just prior to fill by drawing a vacuum over it in the metered column. The fill station was checked for leaks before the charging operation. The valve was left in place after filling and the exit port was capped.

At this point, heat was applied to first one end of heat pipe 1A and then the other to determine if non-condensibles were present. While no gas interface could be detected when the normal evaporator end was heated, a very distinct interface was found about two inches from the evaporator end of the pipe when heat was applied to the interface cell end. The presence of gas was thus indicated.

An arrangement was set up to permit bleeding this gas from the heat pipe. An evacuated tank was attached to the exit port of the heat pipe valve. An ice bath was applied to that portion of the interface cell end-cap to which the fill tube was welded. The pipe was then heated to approximately 100°F . The valve was then cracked intermittently to allow the gas to accumulate around the fill tube region and be forced into the evacuated tank. This procedure was repeated twice, until the subsequent application of heat to the interface cell caused no discernable temperature drop-off at the evaporator end of the pipe. Thus, no gas could be detected in heat pipe 1A.

Heat pipe 2 was now refilled with 93 ml of methanol. Procedure was the same as indicated above.

Tests were conducted to determine the performance of the interface cell between heat pipes 1A and 2. Temporary instrumentation (heater, thermocouples, and insulation) was positioned as located during original thermal vacuum testing. The portion of heat pipe 2 which was inside the vacuum chamber was left uninsulated and was the system heat sink (by convection and radiation to the lab environment).

The primary parameter for measuring interface cell performance was its conductance in watts/^oF. Computation of this parameter involved: 1) establishing a steady-state temperature profile on the system, 2) calculating heat leaks throughout the segment, 3) calculating the heat actually flowing through the interface cell, and 4) dividing this flow rate by the measured temperature drop from one heat pipe to the other. By way of background, the theoretical conductance of the subject cell was 6.18 W/^oF. The range of conductances observed during thermal vacuum tests (see Figure 4-22) was 0.65 to 1.15 W/^oF. Post T/V tests revealed a conductance of about 0.49 W/^oF.

The first test of the recharged segment indicated a conductance of about 0.8 W/^oF at 100^oF heat pipe 1A vapor temperature. Because this value was low, heat pipe 1A was re-bled, using the ice-bath procedure outlined above. The next system test revealed a jump in conductance to 2.32 W/^oF @ 100^oF). This indicated the definite presence of gas in the first test. A period of four days was allowed to pass and the segment was tested again. The conductance was determined to be 2.19 W/^oF. The slight reduction could very possibly have been caused by instrumental uncertainty (thermocouple error, recorder error, computation of heat leaks). A further bleed of heat pipe 1A resulted in a conductance of 2.53 W/^oF, the highest value obtained in an interface cell.

During the course of this testing, a gas interface was noted near the end of heat pipe 2. An evacuated tank was attached to its valve and the gas was bled from this pipe. The use of an ice-bath was not required since the gas was naturally forced to the fill tube region.

It was now apparent that the design conductance value could not be attained in the interface cell. Although one bleed of gas in heat pipe 1A had raised the conductance from 0.8 to 2.32 W/°F, a second bleed had a much less significant effect (to 2.53 W/°F). It was considered very doubtful that subsequent bleeding operations could increase the value substantially. The valve of heat pipe 1A was therefore pinched-off and attention was turned to heat pipe 1B (which had not yet been recharged).

Still assuming that non-condensable gas was the cause of poor interface cell conductance, the best method of negating its effect in the existing hardware was thought to be charging heat pipe 1B with ammonia. Its higher vapor pressure at test temperatures would compress any small quantity of gas in the pipe, and would open more of the condensing surface in the interface cell for active heat transfer. A significant increase in conductance would be anticipated. Accordingly, a 47 ml ammonia charge was added to heat pipe 1B. Figure 4-29 shows a schematic of the ammonia fill setup.

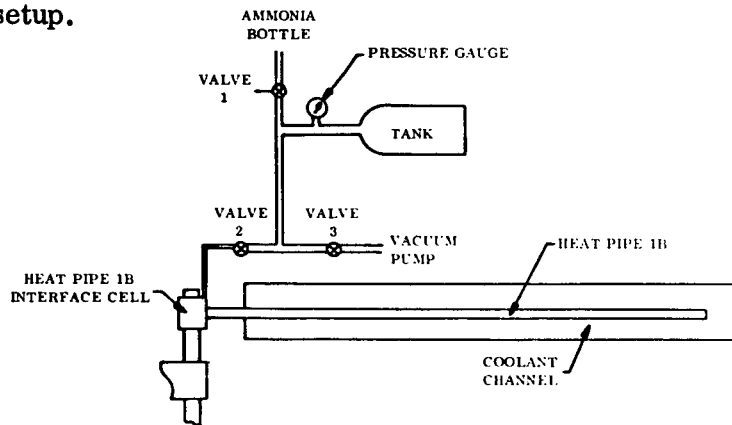


Figure 4-29. Ammonia Fill Setup

The procedure was as follows:

1. With valve 1 closed, the heat pipe, tank, and interconnecting tubing were evacuated.
2. Valves 2 and 3 were closed.
3. Valve 1 was opened to admit ammonia vapor to the tank. Valve 1 was closed and the tank pressure stabilized at 138 psia.
4. Most of the length of heat pipe 1B was cooled to below 0°F by placing a mixture of dry ice and isopropanol in the coolant channel.

5. Valve 2 was opened and, as ammonia vapor from the tank condensed in the heat pipe, tank pressure decreased.
6. Valve 2 was closed when the tank pressure reached a predetermined value (based on desired charge, tank and tubing volumes, initial conditions - 26 psia in this case).
7. The heat pipe (with valve 2 attached) was removed from the setup.

Brief applications of heat to various portions of heat pipe 1B revealed no gas interface. The valve was consequently pinched-off. Further testing of heat pipe 1B was done simultaneously with heat pipes 1A and 2 as described in the next section.

4.12 RE-TEST

New thermocouples were made and attached to the room ambient segment of the test article. Thermocouple locations were identical to those used in thermal vacuum testing (TC's 1 through 12 on Figure 4-7). This time, however, the beads were bonded to surfaces with Eccobond 57C silver-filled epoxy. Readout was again on a 24-channel Honeywell recorder.

Heater blocks were machined to accept long, thin cartridge heaters which provided the heat input to the two component heat pipes (1A and 1B). Figure 4-30 shows heater details. Measured resistance of each cartridge heater was 10.43 ohms. Two variacs were employed to allow independent control of the heaters.

The entire segment, with the exception of that portion of heat pipe 2 which was in the thermal vacuum chamber, was insulated with 2-inch thick semi-rigid foam. All testing was done with the segment horizontal.

The first test performed was a check-out case. The uninsulated section of heat pipe 2 was allowed to convect and radiate heat to the lab environment, and 2.5 watts were input to each heater. The temperatures were allowed to stabilize, and a 0.5^oF to 1.0^oF temperature drop was noted across each interface cell. The data was not reduced (to yield conductances) because it was felt that inaccuracy in reading data would make the results questionable.

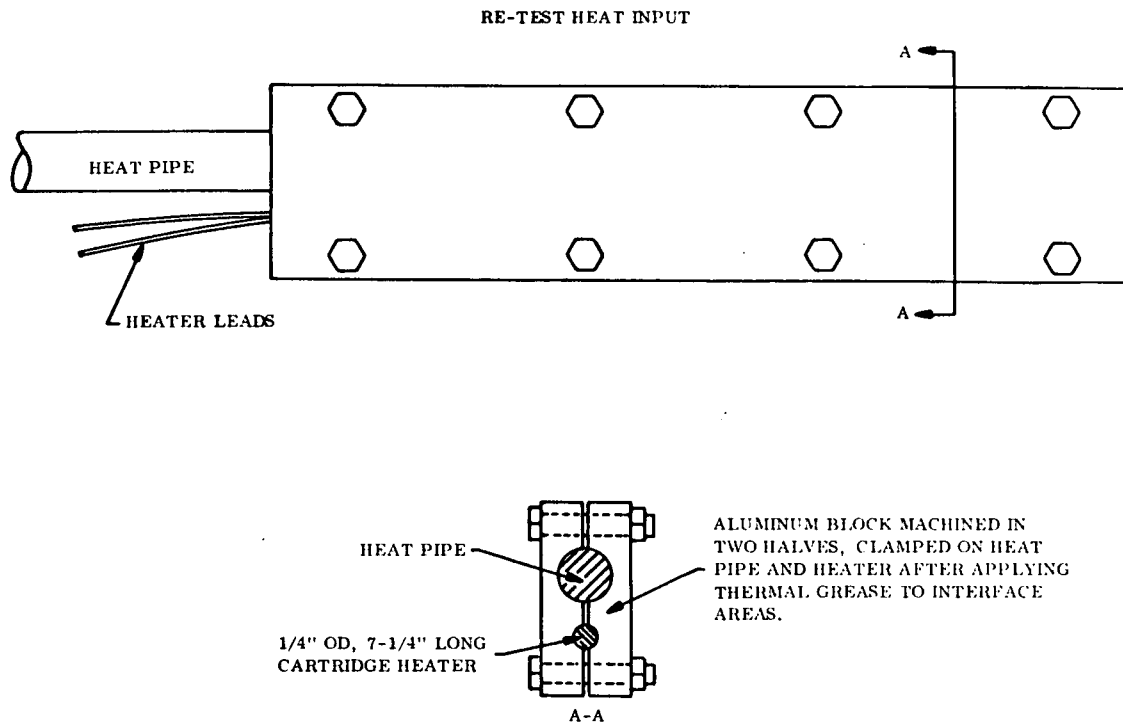


Figure 4-30. Heater Details

A 7-inch long ice bath container was clamped to the top of heat pipe 2 to act as a heat sink for case R1. A nominal 16 watt heat dissipation was input to each heater.

It soon became apparent that heat pipe 1A was at least partially burned out at this heat flow, since the temperature of its heater block rose substantially above that of the heat pipe adiabatic section. Nonetheless, the case was allowed to run until all other system temperatures stabilized. Figure 4-31 shows the temperature profile at this point. Also shown on this figure are:

1. Calculated heat leaks into or out of various parts of the system
2. Calculated heat storage term for the burned out heater block
3. Derived heat flows through the system
4. Calculation of the conductance value for each interface cell.

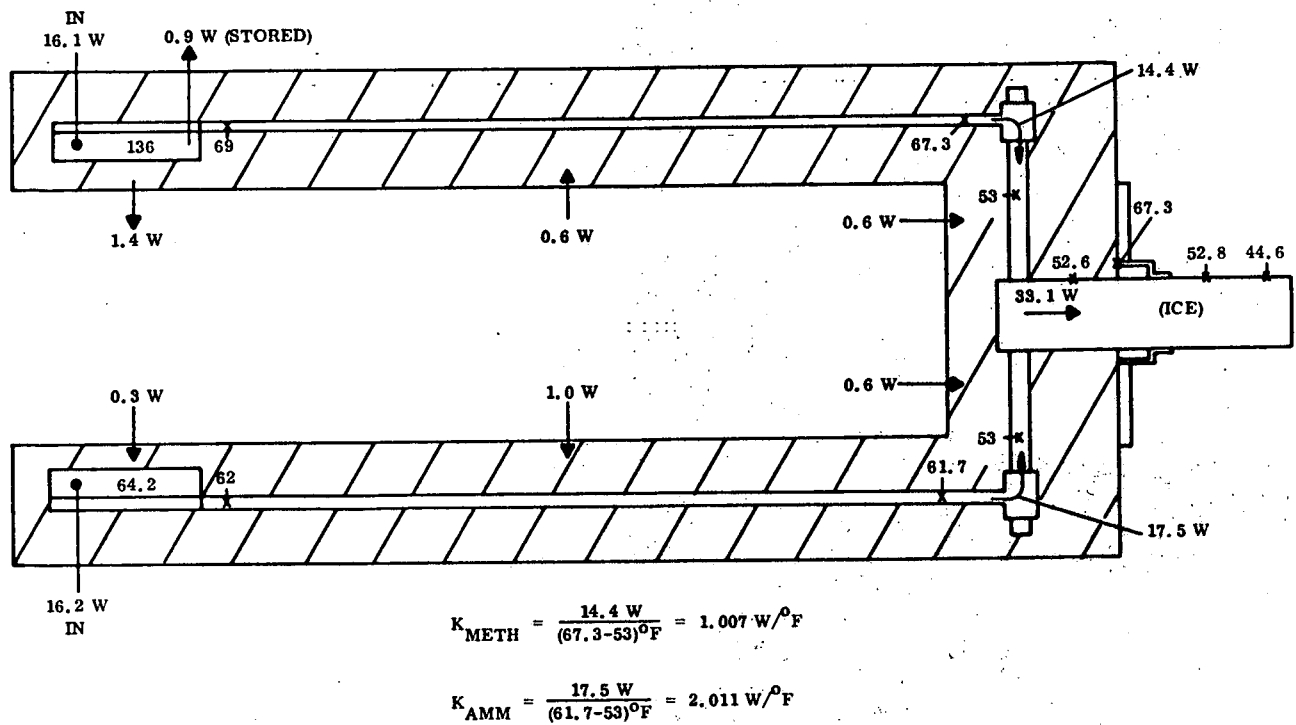


Figure 4-31. Case R1 Results

As can be seen, the conductance of the ammonia-filled interface cell is twice that of the methanol-filled cell, but is less than that previously obtained in the methanol cell ($2.53 \text{ W}/^{\circ}\text{F}$, see Section 4.11). Further, the conductance of the methanol cell decreased significantly from the last time it was measured (2.53 to $1.01 \text{ W}/^{\circ}\text{F}$).

Case R2 was thus an attempt to re-create the conditions which yielded the $2.53 \text{ W}/^{\circ}\text{F}$ conductance of the methanol cell. The ice bath was removed and a nominal 10 watts of heat was applied to the methanol pipe (1A). The ammonia pipe was not heated. A quasi-steady state was reached in about two hours, at which time the temperatures shown on Figure 4-32 were recorded. True equilibrium was not attained because the temperature of the massive vacuum chamber port flange was still increasing slightly. This condition would not affect cell performance. The data indicates a conductance of $1.53 \text{ W}/^{\circ}\text{F}$ for the methanol interface cell.

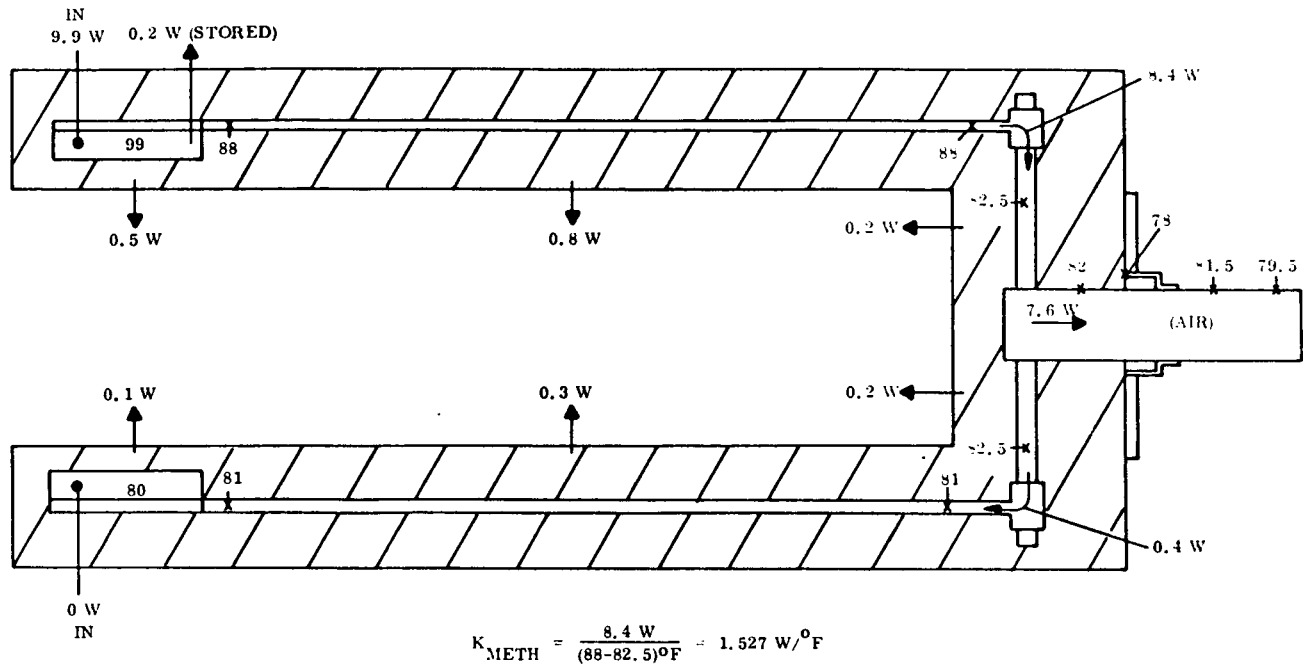
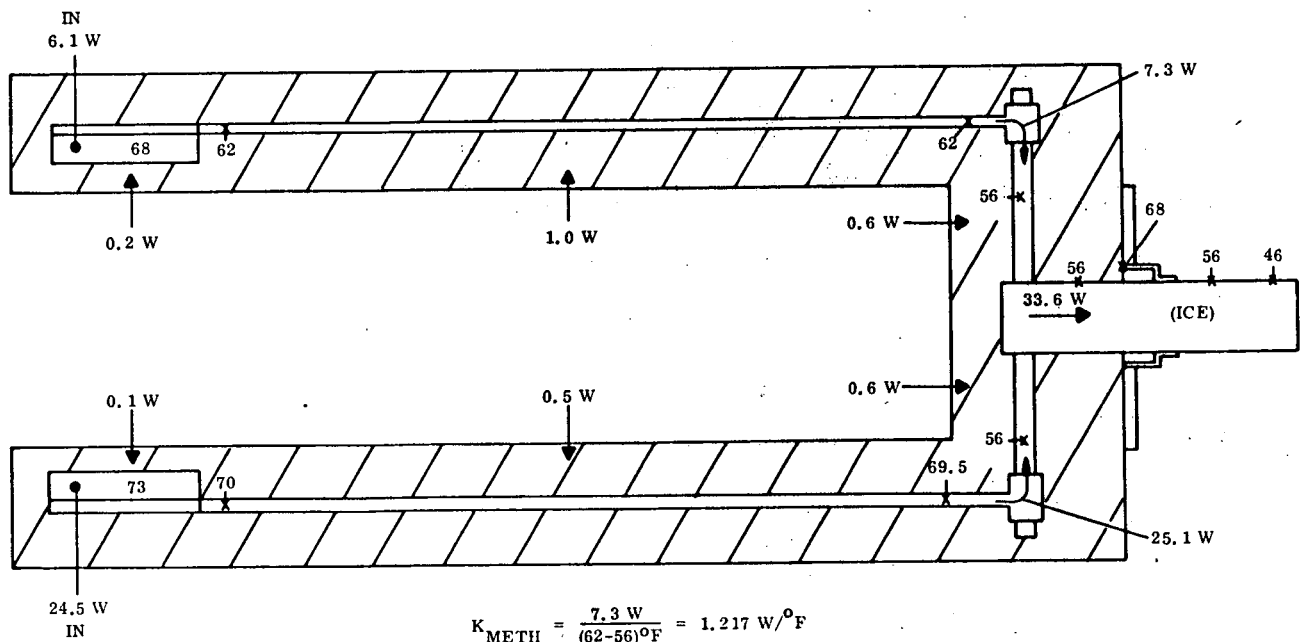


Figure 4-32. Case R2 Results

Cases R3, R4, and R5 were run to accumulate more data which might aid in understanding the interface cell behavior. Figures 4-33 through 4-35 presents the results of these runs.

4.13 INTERFACE CELL SYSTEM DISCUSSION AND CONCLUSIONS

By this time, a large amount of data had been compiled concerning the performance of the interface cell at the end of heat pipe 1A. Information was available from the original thermal vacuum test, the initial trouble-shooting tests (P series - Section 4.10), tests performed immediately following the refill (Section 4.11), and the ambient retest (R series - Section 4.12). Through all of this testing, the physical configuration of the interface cell did not change; it was not opened for inspection or rework and it received no shocks capable of distorting the wick structure.



$$K_{\text{METH}} = \frac{7.3 \text{ W}}{(62-56)^{\circ}\text{F}} = 1.217 \text{ W}/^{\circ}\text{F}$$

$$K_{\text{AMM}} = \frac{25.1 \text{ W}}{(69.5-56)^{\circ}\text{F}} = 1.559 \text{ W}/^{\circ}\text{F}$$

Figure 4-33. Case R3 Results

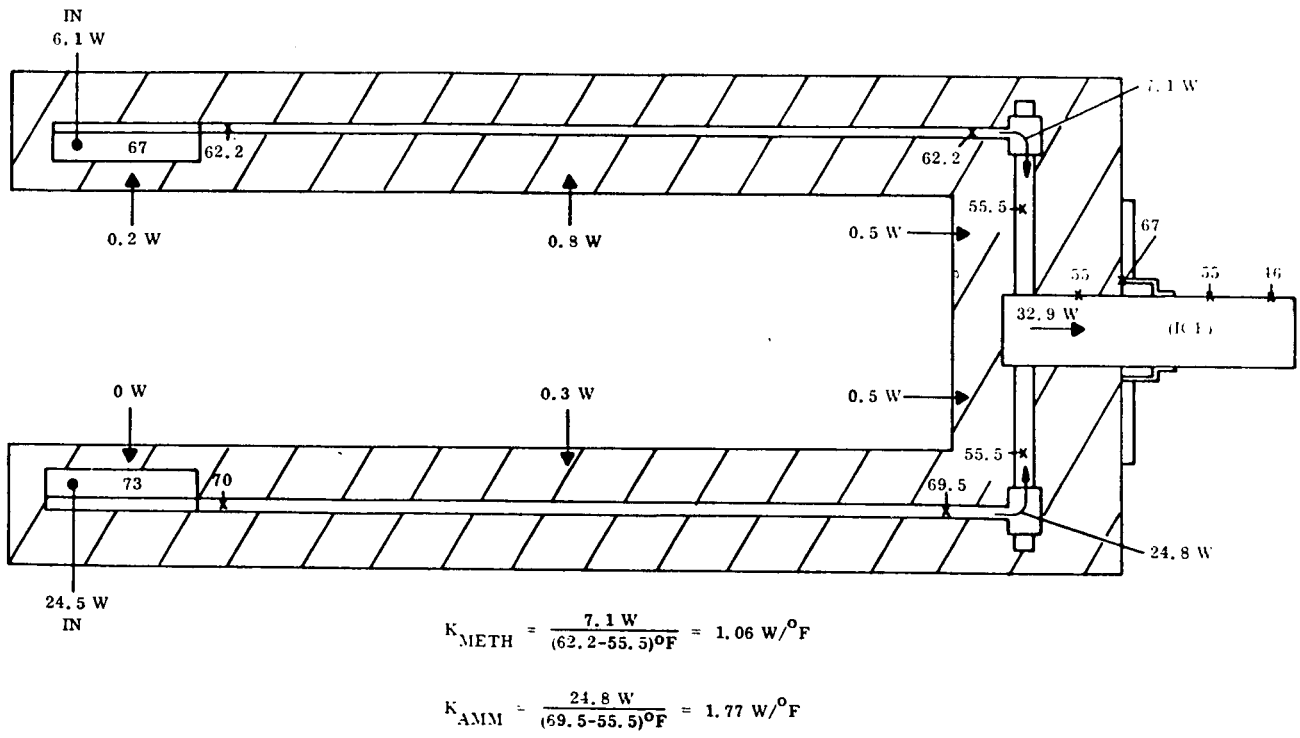


Figure 4-34. Case R4 Results

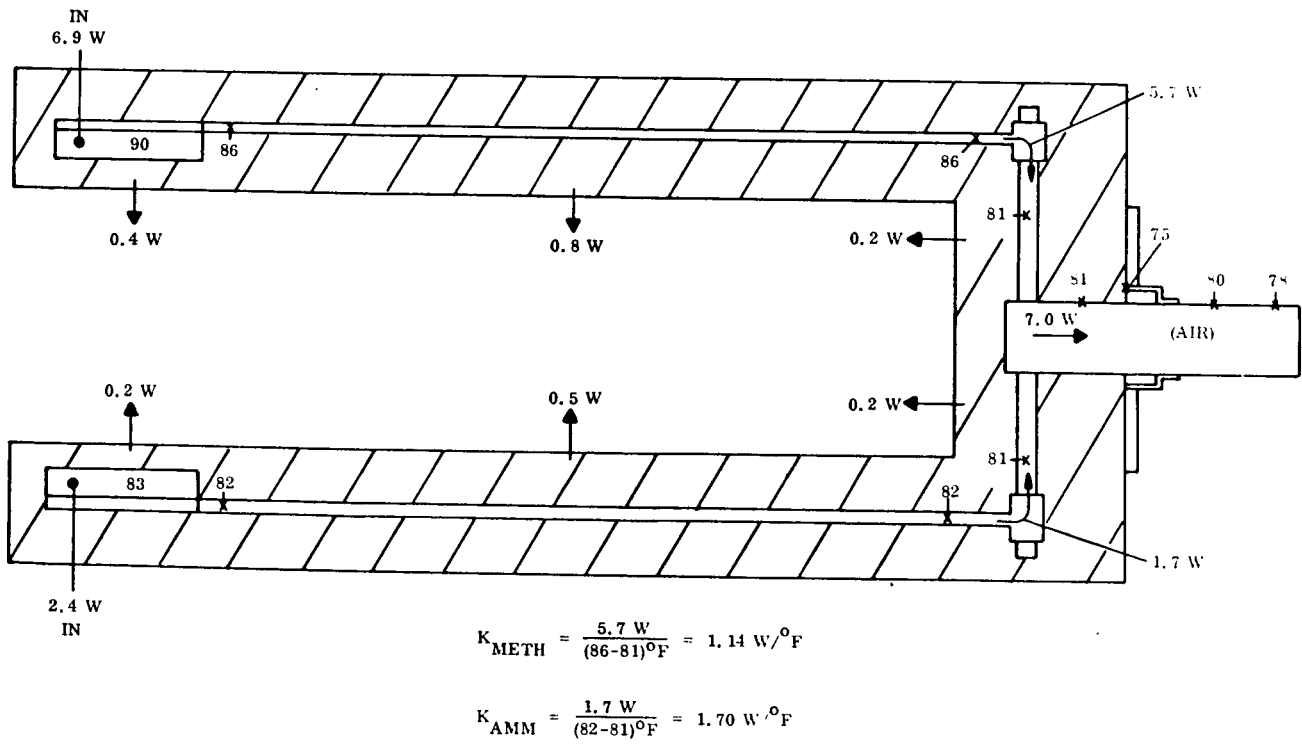


Figure 4-35. Case R5 Results

Table 4-9 lists the applicable data for each of the tests. It quantifies the three recognized variables which could effect conductance;

1. Charge - The two methanol charges (1 and 2) were taken from the same bottle, so chemically they should be identical. However, differences in the fill procedure may have admitted more non-condensable gas in the first charge.
2. Date - It was realized that internal degradation within the heat pipe would cause changes in conductance as a function of time.
3. Heat Pipe Temperature - Cell conductance would be a function of heat pipe temperature if gas were present.

Table 4-9. Summary of Methanol Interface Cell Data

Series	No.	Charge	Date	Heat Pipe Temp, °F	Calc. K, W/°F	Comment
TV (Thermal Vacuum)	1	1	11/2/71	132	0.65	
	2	1	11/2/71	117	0.92	
	3	1	11/2/71	158	1.13	
	4	1	11/3/71	151	1.16	
	5	1	11/3/71	155	1.14	
	6	1	11/3/71	162	1.17	
	7	1	11/4/71	---	---	Reversed mode
P	1	1	12/3/71	---	---	Reversed mode
	2	1	12/22/71	144	0.48	IC** Heated
	3	1	12/23/71	166	0.49	IC** Heated
D (During Refill)	1	2	7/5/72	110	0.80	Prior to 1st bleed
	2	2	7/7/72	107	2.32	After 1st bleed
	3	2	7/10/72	103	2.19	(Repeat D2)
	4	2	7/10/72	103	2.53	After 2nd bleed
R	1	2	7/17/72	67	1.01	
	2	2	7/18/72	88	1.53	
	3	2	7/18/72	62	1.22	
	4	2	7/26/72	62	1.06	
	5	2	7/26/72	86	1.14	

*Charge 1 on 10/18/71, Charge 2 on 7/5/72

**IC = Interface Cell

It should be noted that, ideally, the conductance of the interface cell should not vary with charge, time, or temperature. It should be a function of cell geometry, dimensions and materials only. This is not the case with the present hardware. In fact, the data suggests that the conductance was a function of all three variables. This fact is confirmed when the information on Table 4-9 is plotted against temperature and points of the same charge and date are interconnected, as has been done on Figure 4-36.

Data from runs D1, D2, and D3 were omitted from this figure so that a uniform second charge could be defined. It can be seen that conductance increased with temperature, decreased with time, and was greater for the second charge than the first. The apparent explanation is three-fold; 1) there was a non-condensable gas in the cell during all tests, with the possible exception of run D4, 2) the quantity of gas increased with time, and 3) there was more gas in the first charge than the second. The presence of gas must be assumed to explain all of the trends shown on Figure 4-36.

De-aeration of the methanol prior to the second charge would account for a greater quantity of gas (less conductance) in the first charge.

The build up of gas with time is more puzzling in view of the extensive (and negative) leak-testing performed between the two charges. Two possible gas sources remain; the final pinch-off seal (which could not be helium leak-tested) or gas generation as a result of chemical reaction within the pipe. Because pinch-offs have proven leak-tight several times in the past, generation is considered the more likely source.

One additional plot of interface cell performance is shown on Figure 4-37. In preparing this graph, the data on Figure 4-36 was extrapolated to estimate the conductance at 100^oF on each of the five test dates. These five conductances were reciprocated to yield thermal resistance in ^oF/watt which were then plotted against time after sealing the two charges. Also shown on the figure are the calculated "solid" components of the total resistance (wicks and tube wall).

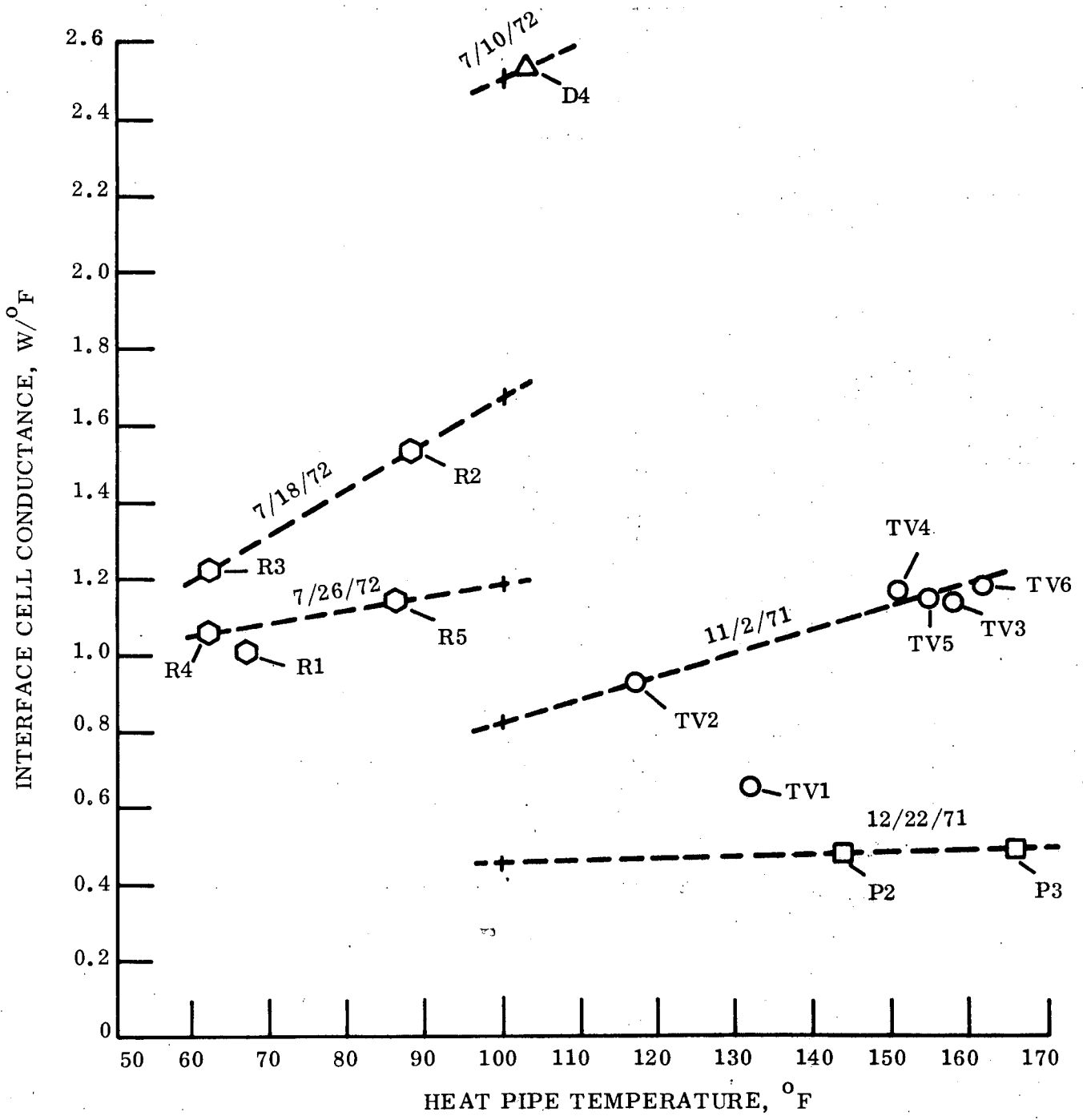


Figure 4-36. Methanol Interface Cell Data

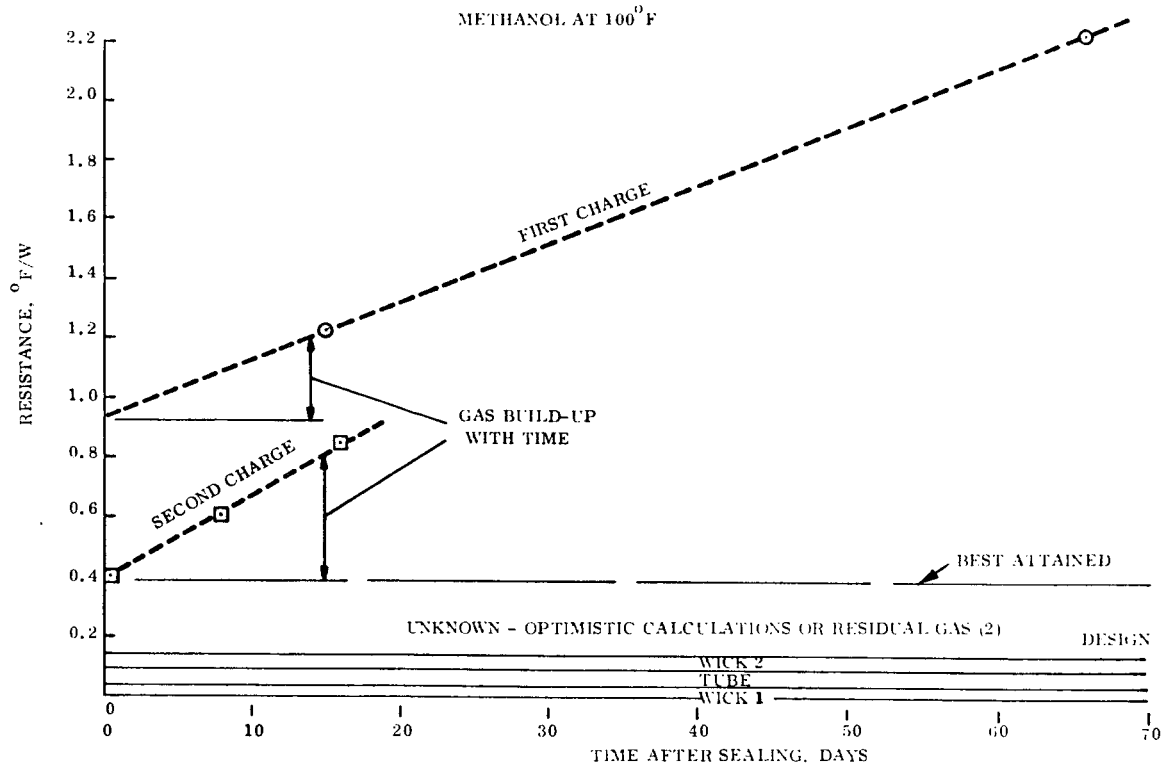


Figure 4-37. Thermal Resistance of Interface Cell

Figure 4-37 shows the tremendous effect of gas on cell heat transfer. In a relatively short period of time, the resistance component caused by the gas dominates that of the solid thermal path. This could be due to a large rate of gas accumulation or could indicate extreme sensitivity to even a small quantity of gas, as was suggested previously (Section 4.9). Consideration of the cell geometry suggests the latter is the case. Whereas in a "normal" heat pipe (pipe and condenser axes coincident) gas can accumulate at the end of the condenser, the interface cell condenser offers no such convenient pocket for gas. All gas present in the cell must adjoin the heat transfer surface. Thus a small quantity of non-condensable may spread over this surface to form a very thin, but effective, barrier between the vapor volume and the condensing area.

This gas location plus the location of the fill tube on the end-cap of the cell, makes it virtually impossible to remove all traces of gas once in the pipe. It is therefore difficult to determine the cause of the difference between the design resistance and the best value

attained during tests (shown on Figure 4-37). It could be explained by either residual gas in the cell after sealing or overly optimistic initial calculation of "solid" resistances. It is suspected that both factors contributed to the difference because 1) it is doubtful that all gas was removed during the bleed operation of the second charge, and 2) low values of resistance were not obtained in the ammonia-filled interface cell. The use of ammonia should have minimized the effect of residual gas, but, as Table 4-10 shows, conductances never approached the design value ($6.18 \text{ W}/^{\circ}\text{F}$).

In summary, the following conclusions have been drawn concerning the test article employing interface cells for heat pipe vapor-to-vapor heat transfer:

1. The calculated conductance for the interface cells was optimistic.
2. The presence of non-condensable gas in the cells during tests never permitted even this derated conductance to be attained.
3. The design of these interface cells made their performance sensitive to even a small amount of gas and made post-charge removal of gas very difficult.
4. Decreasing conductance suggests an accumulation of gas with time. It is felt that this gas represents generation within the pipe instead of leakage.
5. For the reasons above, further testing of the interface cell system would be warranted only if an independent development program (see next item) is successful and suggests an easy fix to the existing design.
6. The interface cell concept requires more development to yield a better understanding of localized liquid and vapor flows and to suggest a method of significantly decreasing its sensitivity to gas. This is best done with small-scale units instead of a system built on the current program.

Table 4-10. Summary of Ammonia Interface Cell Data

Test	Date*	Heat Pipe Temp, $^{\circ}\text{F}$	Calc. K, $\text{W}/^{\circ}\text{F}$	Calc. R, $^{\circ}\text{F}/\text{W}$
R1	7/17/72	62	2.01	0.50
R3	7/18/72	70	1.86	0.54
R4	7/26/72	69	1.77	0.56
R5	7/26/72	82	1.70	0.59

*Charged on 7/13/72

4.14 SADDLE SYSTEM

At this point in the hardware program, it was decided to build and test a heat pipe system employing more conventional interfacing techniques. Accordingly, a second test article was designed in which copper "saddles" effected the heat transfer between heat pipes. It was felt that acceptable system thermal performance could be demonstrated with this "minimum risk" article.

Two alternative designs were generated using saddle interfaces. The first, shown in Figure 4-38, employed mitered heat pipes so that the overall article geometry resembled that of the original unit. The second (Figure 4-39) eliminated the mitered joints and replaced them with large radius bends where straight pipes could not be used. In keeping with the minimum risk policy of this task, the second design was selected for fabrication and test. The following discussion describes design, fabrication, and test of this unit.

4.14.1 SYSTEM DESIGN

As can be seen in Figure 4-39, the saddle system consists of nine separate heat pipes, five of which are "in-line" and the remaining four are bent to attach to radiating panels. These four "fin" heat pipes are shown with non-condensable gas reservoirs at their ends. The fin pipes and the two parallel heat pipes at the other end of the system (which represent "component" heat pipes) are made from 0.50 inch OD stainless steel 304 tubing with a 0.035 inch wall. The other three heat pipes (longitudinal, penetration, and circumferential) are fabricated of 1.00 inch OD stainless steel 304 tubing with a 0.065 inch wall. The total length of all heat pipes is 30 inches, except the penetration pipe which is 22 inches long. Flat end-caps are employed and fill tubes are provided at the condenser end of each heat pipe. The gas reservoirs are again made from type 304 stainless steel tubing, 2 inch OD, and 0.125 inch wall. They are 5 inches long and each has a calculated internal volume of 11.42 cu. in. All heat pipe elements were sized to support an internal pressure of at least 500 psia.

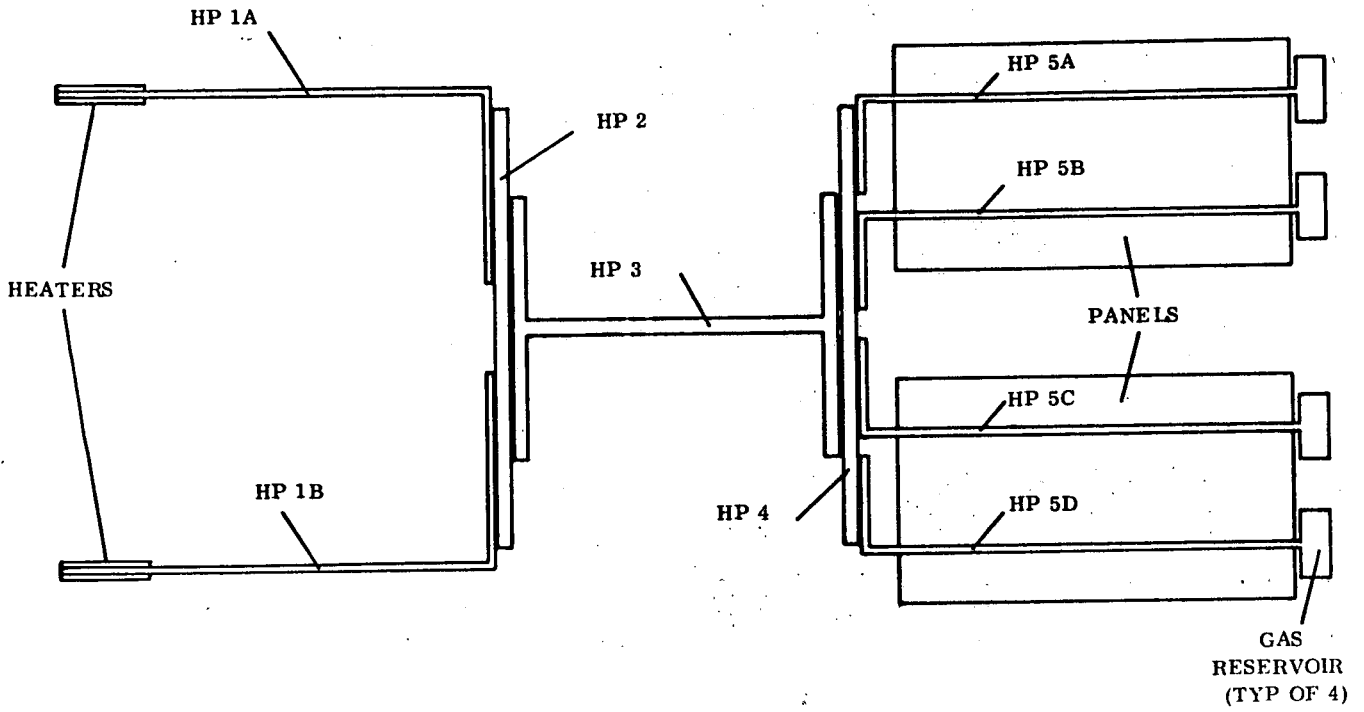


Figure 4-38. Saddle System #1

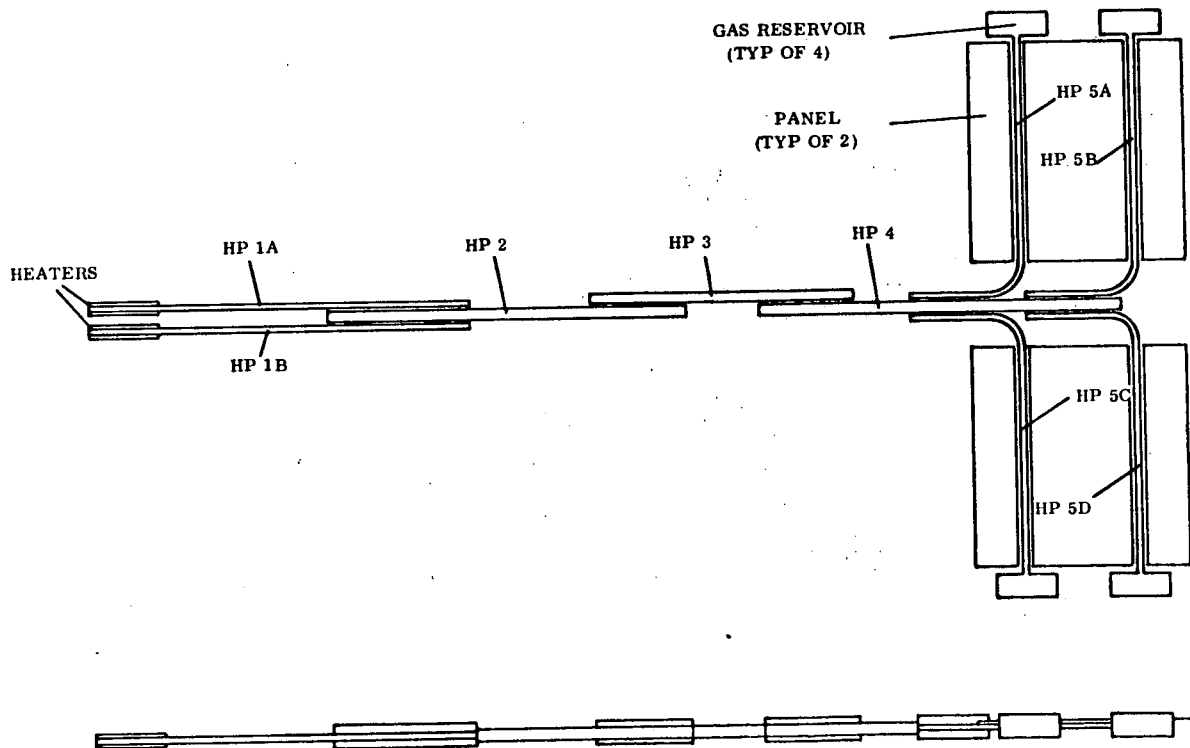
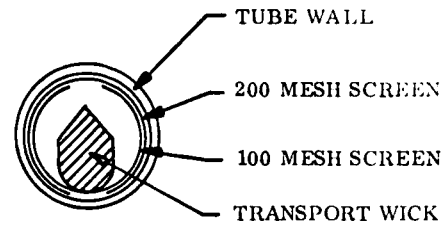
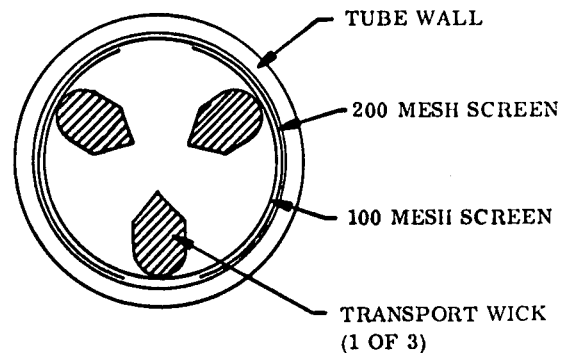


Figure 4-39. Saddle System #2

Isotropic wicking was used throughout and the wick cross-section of each heat pipe was uniform over its total length. As in the original test article, wicks consisted of "transport" and "circumferential" structures, both fabricated of stainless steel mesh. The transport wicks had a calculated cross-sectional area of 0.061 sq. in. and an empirically determined porosity of about 43%. These were spot-welded securely to a single layer of 100 mesh screen whose width was determined to very nearly cover the tube ID. A single layer of 200 mesh screen was inserted and spot-welded into the tube prior to installation of the transport wick. After assembly, the 100 mesh support screen was spot-welded to the 200 mesh screen and the tube ID, and thus became the second component of the circumferential wicking. Figure 4-40 shows the cross-sections for the 0.5 inch and 1.0 inch heat pipes.



(a) ONE-HALF INCH PIPE



(b) ONE INCH PIPE

Figure 4-40. Saddle System Heat Pipe Cross Sections

The working fluid for all heat pipes was methanol. With this fluid and the wicking as described above, the maximum heat throughput for each pipe was calculated. Table 4-1 presents this information along with other characteristics of the pipes.

Table 4-11. Saddle System Heat Pipes

Heat Pipe	Number Used	Pipe OD, In.	Pipe Length, In.	Calculated Q_{max} , watts
Component	2	0.5	30	24
Longitudinal	1	1.0	30	145
Penetration	1	1.0	22	193
Circumferential	1	1.0	30	145
Fin	4	0.5	30	24

Figure 4-41 describes the three types of interface saddles employed to join the heat pipes of the system. They consisted of ETP copper which had been ball-milled (to a depth slightly less than the ball radius) to accept the subject heat pipe(s). In each case, one of the mating pipes was silver soldered into the saddle, while the other thermal interface was a mechanically clamped joint. Bolt holes were provided at 1-inch spacing along both sides of the heat pipes for the saddles shown in Figure 4-41(a) and (b), and at 2-inch spacing for the flange of Figure (c). The lengths of the various saddles employed in the system are given below. The calculated total interface temperature drop was from 3° F to 5° F in each saddle. A contact conductance of 1000 BTU/hr-ft-° F was assumed for the mechanical joint in this calculation.

<u>Saddle Between</u>	<u>Saddle Length, In.</u>
Component-Longitudinal HP's	12
Longitudinal-Penetration HP's	8
Penetration-Circumferential HP's	8
Circumferential-Fin HP's	6
Fin HP-Radiator	20

Each of the two radiating panels had a surface area of 2.5 sq. ft. (18" x 20") and was painted white on the top surface. The panels were fabricated from 0.032-inch aluminum alloy 6061-T6. Heat pipe spacing was 9 inches, so that the effective fin length was 4.5 inches. The effectiveness of these radiators was determined to be approximately equal to that of the original test article (0.020-inch thick panels, heat pipe spacing of 6 inches).

4.14.2 SYSTEM FABRICATION

All piece parts of the system were cut and checked for fit. Assembly began with the insertion and securing (i. e., spot-welding) of the wicks in all heat pipes. These units were then cleaned using an acid etch technique. In this technique, the stainless steel is passivated by replacing the pre-existing uncertain surface with one of known characteristics. Following cleaning, end-caps (and gas reservoirs) were welded in place. The interface saddles were then silver-soldered to the applicable heat pipes.

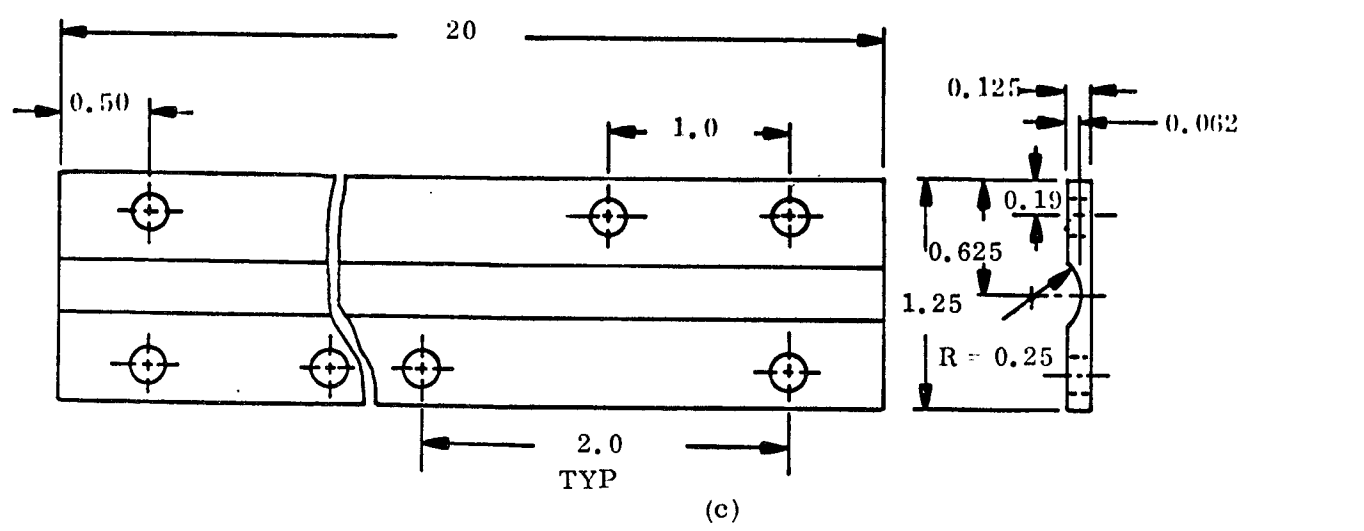
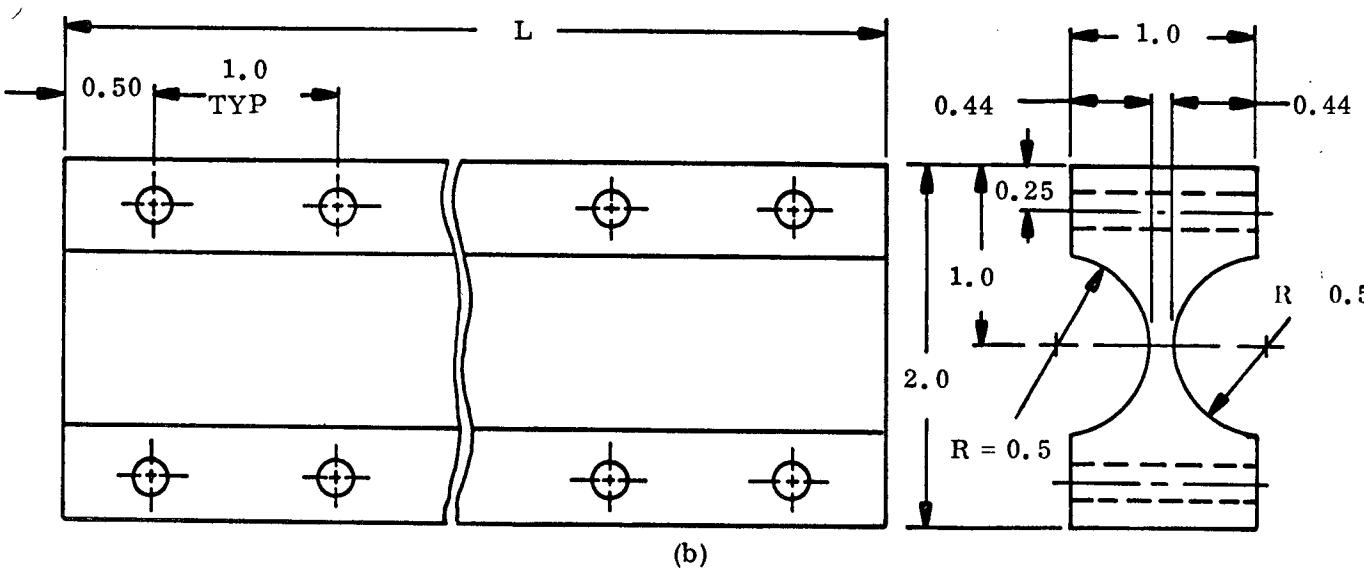
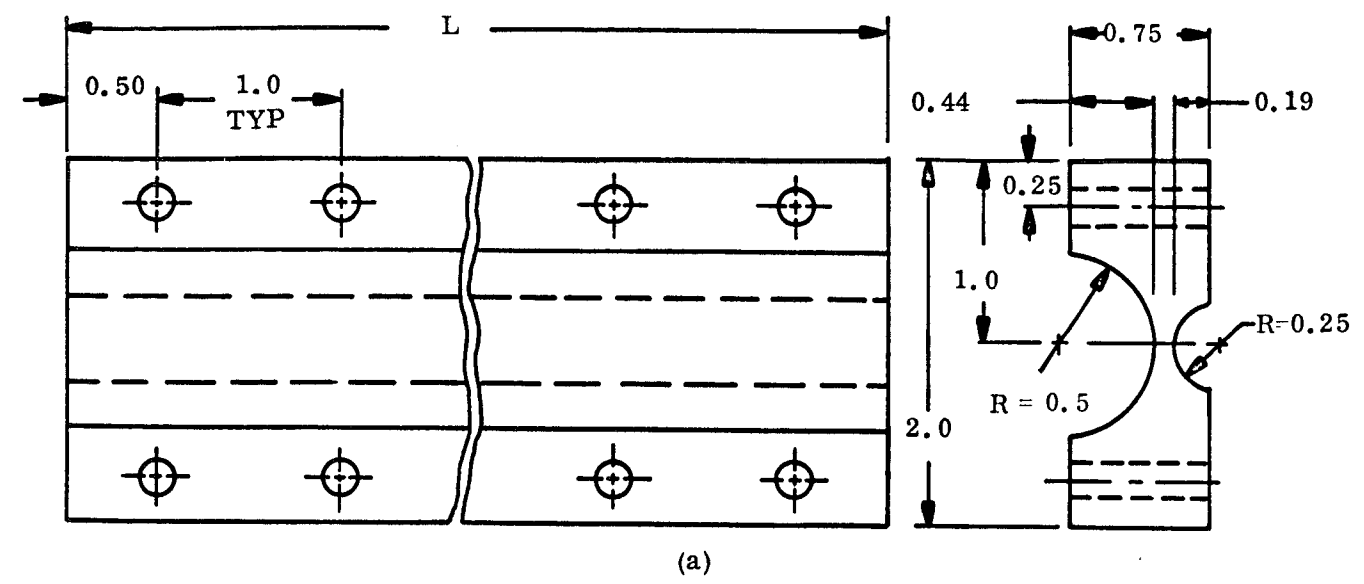


Figure 4-41. Saddle System Interface

All heat pipes were leak-checked and pressure-checked at 200 psia. Fill procedure was nearly identical to that described by Figures 4-13 and 4-14. The two exceptions were:

1. The methanol working fluid was de-aerated in place prior to fill by drawing a vacuum over it while in the metered column.
2. The calculated nitrogen charge for the four fin heat pipes of the saddle system was 1.187×10^{-4} lbm. A control gas volume of 22.0 ml was fabricated to replace the previously used 2.2 ml volume in the fill setup (Figure 4-14). The required initial pressure of nitrogen in this volume was determined to be 65.0 psig (Step 9), (Figure 4-14). The pressure in the nitrogen storage tank was about 80 psig (Step 8, Figure 4-14).

Table 4-12 shows the amount of methanol charge for each of the system heat pipes.

Table 4-12. Saddle System Heat Pipe Charges

<u>Heat Pipe</u>	<u>Methanol Charge, ml</u>
Component	10.5
Longitudinal	26.2
Penetration	19.2
Circumferential	26.2
Fin	19.0

Thermal grease was applied to all mechanical interface surfaces and the system was bolted together.

4.14.3 TEST PLAN

Thermal testing of the saddle system was performed in a laboratory environment. The objectives of the test were to demonstrate:

1. A predictable overall temperature drop
2. Acceptable temperature control provided by the variable conductance fin heat pipes.

Heat input for the saddle system was provided in the same manner as was employed for the interface cell system retest. That is, machined blocks identical to those shown in Figure 4-30 were clamped around the component heat pipes and cartridge heaters. Measured heater resistance was 10.0 ohms and two variacs were again used for electrical input.

The heat sinks for the system were the top surfaces of the two radiating panels. The ultimate sink was, of course, the laboratory environment and the coupling between the panels and this sink was both convective and radiative.

The entire system was insulated from the surroundings, with the exception of the tops of the two panels. Figure 4-42 shows a cross-section of the insulation scheme. As can be seen, a "box" is formed from 2-inch thick semi-rigid foam and all "in-line" heat pipes are encased in this box. Prior to installation of the heat pipe system, the 91-inch long box was calibrated for heat leak. A single resistance wire was stretched over the length of the box in the center of the void volume. A known quantity of heat was dissipated by this wire, and thermocouples monitored inside box temperature. Results of this test indicated an overall conductance from the internal volume to the room atmosphere of 0.00285 watts/^oF differential per inch of box length. It was also found that this value could be reduced about 6% by stretching a single layer of aluminized mylar over the box top and sides. The undersides of the two radiating panels were also insulated with the 2-inch foam.

Forty-eight copper-constantan thermocouples were located as shown in Figure 4-43 to measure temperatures of the elements of the system. The thermocouple beads were bonded to the subject surface with Eccobond 57C. Temperatures were read-out on two 24-channel Honeywell recorders calibrated to $\pm 2^{\circ}\text{F}$.

A minimum of three test points were to be obtained. All would be allowed to run until thermal equilibrium was obtained (steady-state conditions). The first two cases would be balanced load conditions, with equal amounts of heat applied to each of the two component heat pipes. They would differ in total system heat load, which would show the effect of the variable conductance heat pipes. The third case would be run with imbalanced loads and

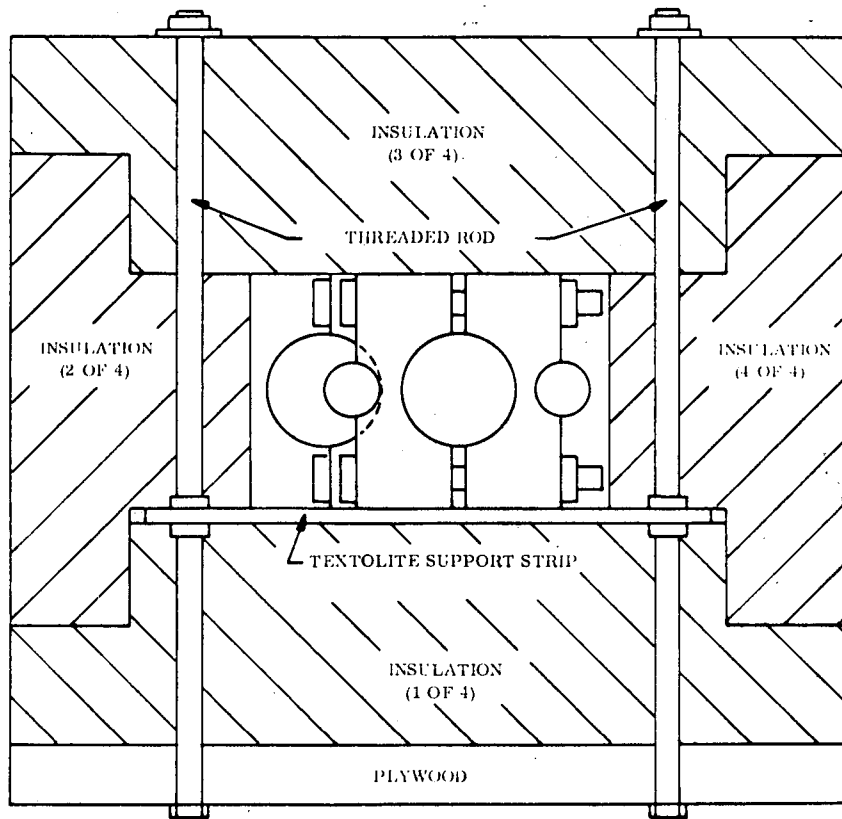


Figure 4-42. Saddle System Insulation

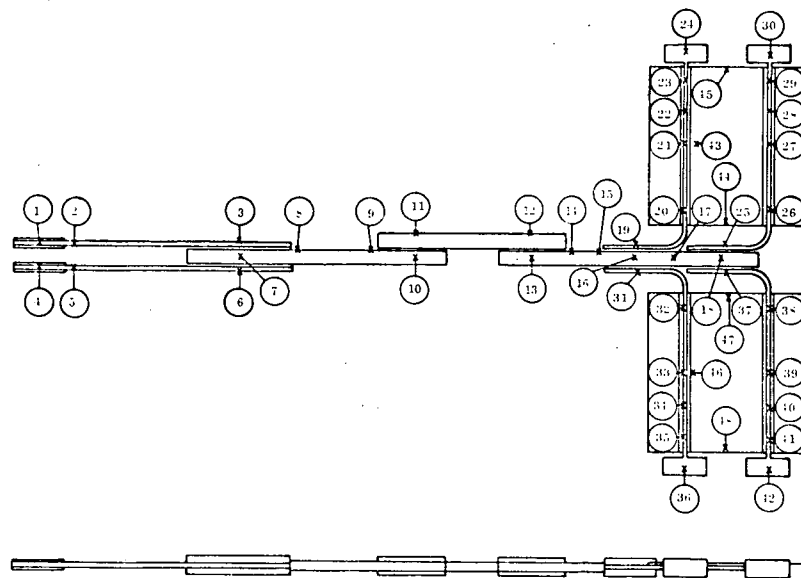


Figure 4-43. Saddle System Thermocouple Locations

still another total system load. It was felt that these cases would allow the thermal transport and control characteristics of the system to be ascertained.

4.14.4 INTEGRATED SADDLE SYSTEM

Figures 4-44, 4-45, and 4-46 are photographs showing the assembled and instrumented saddle system prior to test. Heat pipe valve pinch-off, and installation of the sides and top of the insulation box completed the pretest tasks.

4.14.5 TEST

Test Case S1 was run with 10 watts on each of the two heaters. Temperatures were recorded every hour and after eight hours, no temperature was changing by more than $1^{\circ}\text{F}/\text{hour}$. Data was recorded at this point and Figure 4-47 shows the profile. As can be seen, heat pipe 1B exhibited a very large temperature drop along its length. Also, because the amount of heat reaching the controllable heat pipes was small, a large portion of their lengths was inactive (gas-filled). In an attempt to force more heat through the system, while limiting

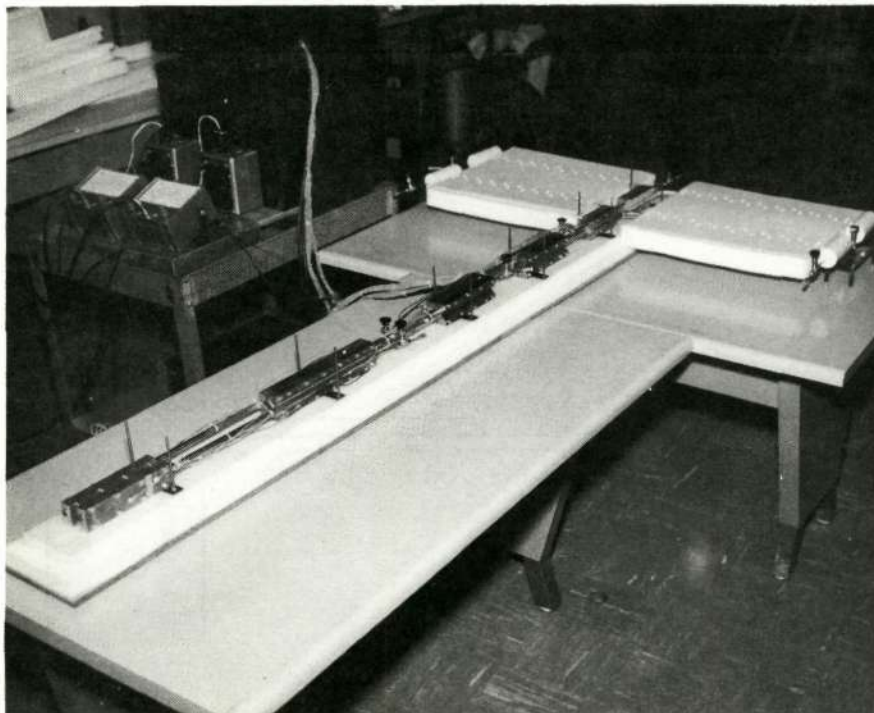


Figure 4-44. Photograph - Overall Saddle System

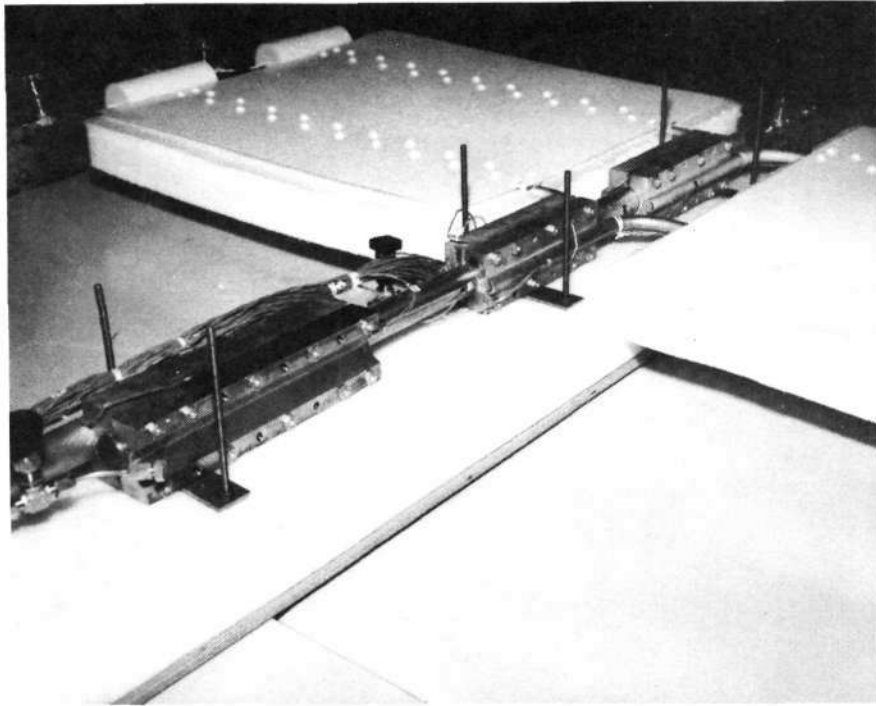


Figure 4-45. Photograph - Saddle System Detail (1)

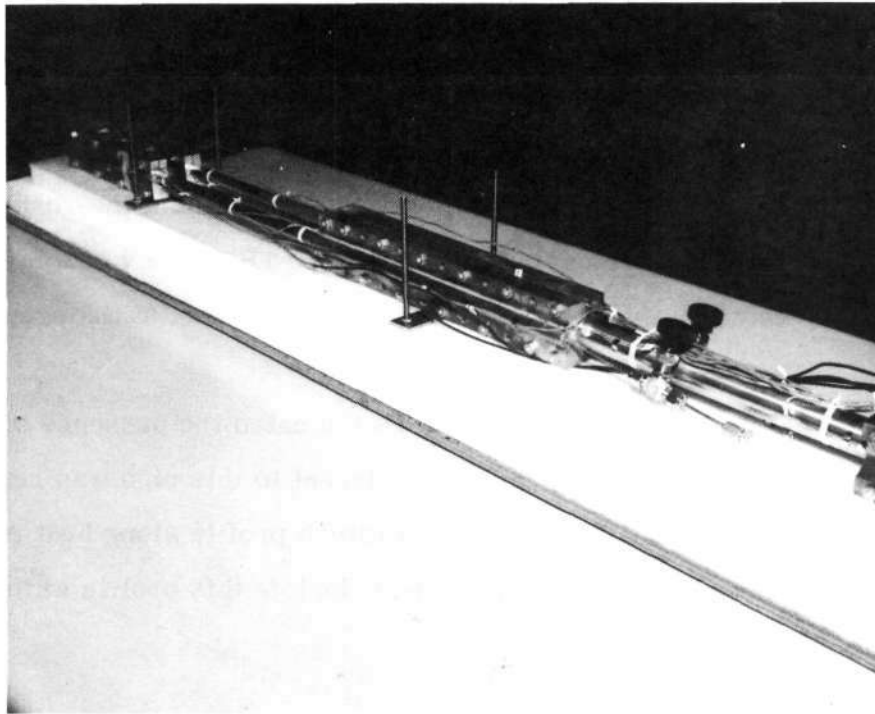


Figure 4-46. Photograph - Saddle System Detail (2)

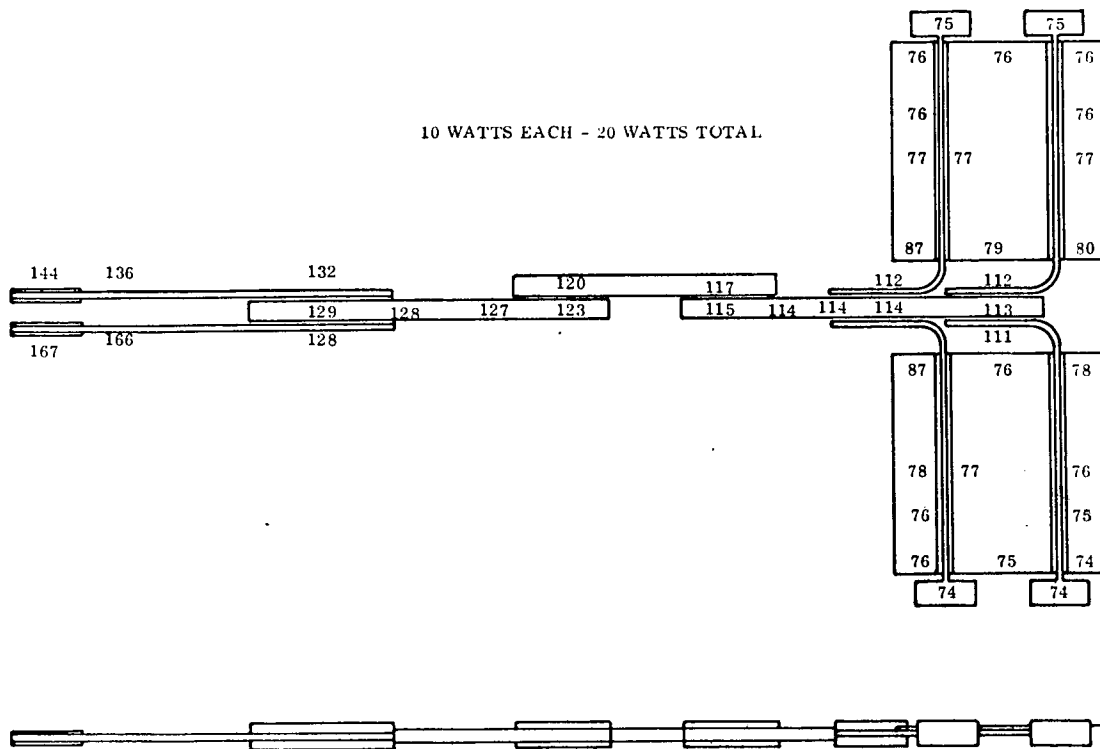


Figure 4-47. Case S1 Profile

the maximum heater temperature to below about 180°F , the heaters on both component heat pipes were moved to within 1 inch of their (condenser end) saddles. Cases S2 and S3 were run with this configuration and Figures 4-48 and 4-49 present the results. In each case, high temperature drops were observed in heat pipe 1B. The variable conductance heat pipes performed well, however, demonstrating $\pm 2^{\circ}\text{F}$ control at the evaporators.

The temperature differentials noted in heat pipe 1B indicated the presence of non-condensable gas in the pipe. To confirm this, the insulation adjacent to this pipe was removed at the end of Case S3 and, with the power still on, the temperature profile along heat pipe 1B was monitored with a thermocouple probe. Figure 4-50 depicts this profile which clearly indicates gas on both sides of the heater.

An attempt was made to bleed the gas from this pipe without recharging. The fill tube was reopened (allowing air to enter) and the valve was replaced. An evacuated tank was attached

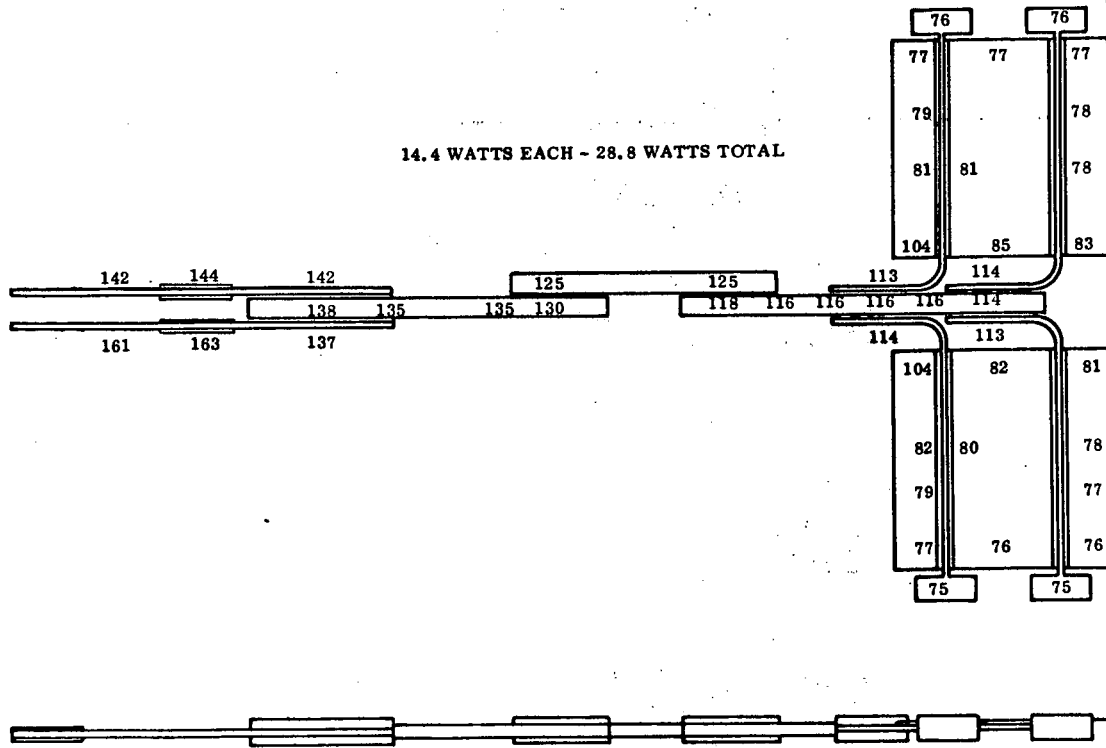


Figure 4-48. Case S2 Profile

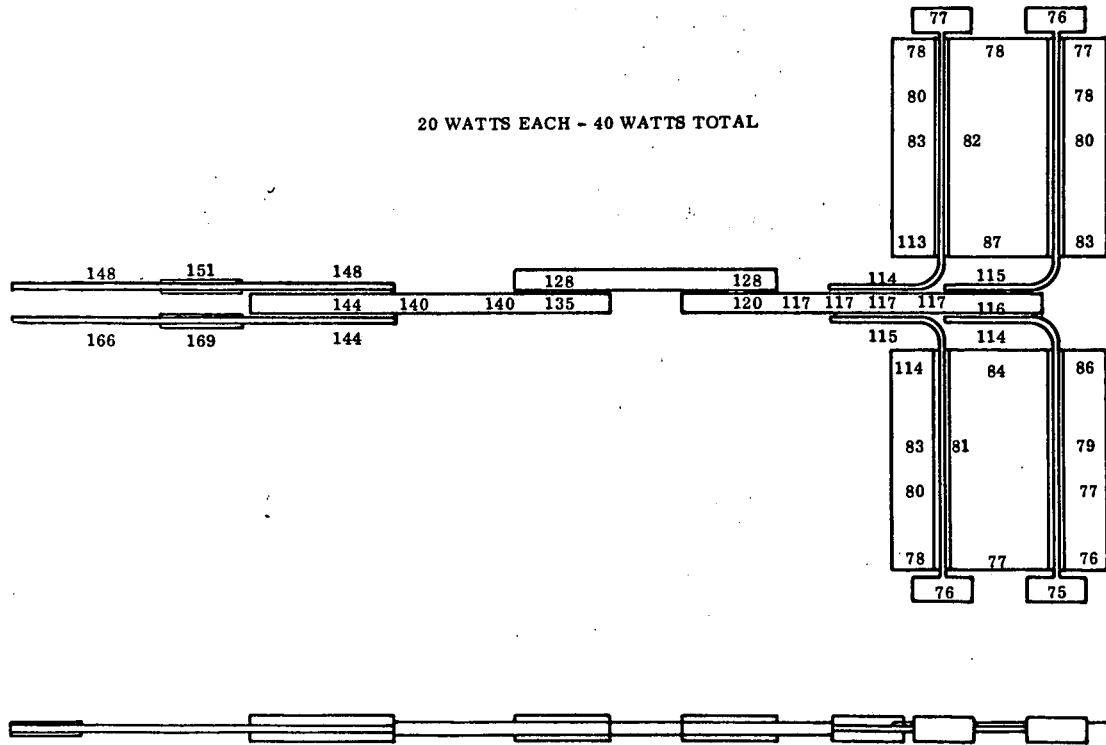


Figure 4-49. Case S3 Profile

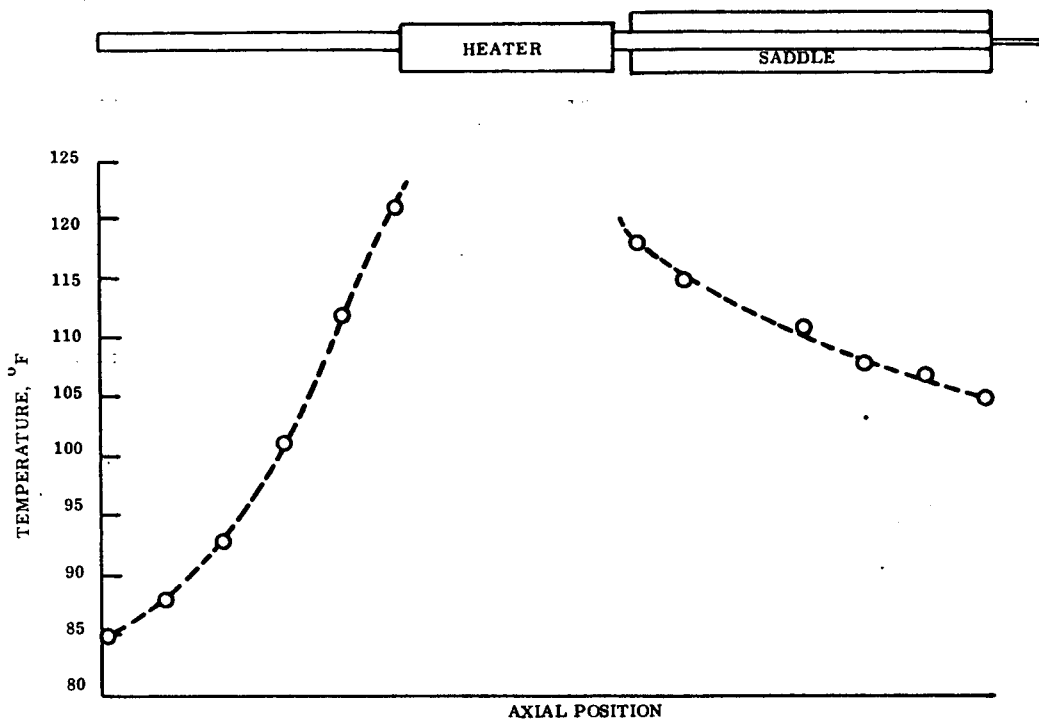


Figure 4-50. Heat Pipe 1B Profile

to the valve. The heater block was moved back to its original position at the end of the pipe. Heater power was turned on and increased until a distinct thermal interface was noted on the pipe. The valve was then opened intermittently to allow the gas to escape into the tank. This was continued until no temperature differential could be detected (with the thermocouple probe) along the total length of the pipe. When the pipe was rechecked about one hour later however, an interface was found. It was concluded that in removing the original pinch-off, the weld between the end cap and fill tube had been broken and air was leaking into the pipe. The only recourse was to remove the pipe from the system, drill out the fill tube, bake the pipe to dump the initial charge, weld a new fill tube in place, and refill with methanol. Tests of heat pipe 1B after this modification revealed no interface and the fill valve was pinched off.

Heat pipe 1B was attached to the remainder of the system and was re-instrumented. The heater on heat pipe 1A was returned to its initial position prior to running Case S4. Twenty (20) watts were input to each heater at the start of Case S4. It soon became evident that both

heat pipe 1A and 1B were burned out at this setting. This fact was confirmed by tilting the entire system so that all heat pipe evaporators were down and noting the decreasing heater temperatures and increasing system temperatures. It was decided to leave the system tilted (about 7.2°) and increase the dissipation of each heater to 30 watts. The profile shown on Figure 4-51 is the resultant steady state data.

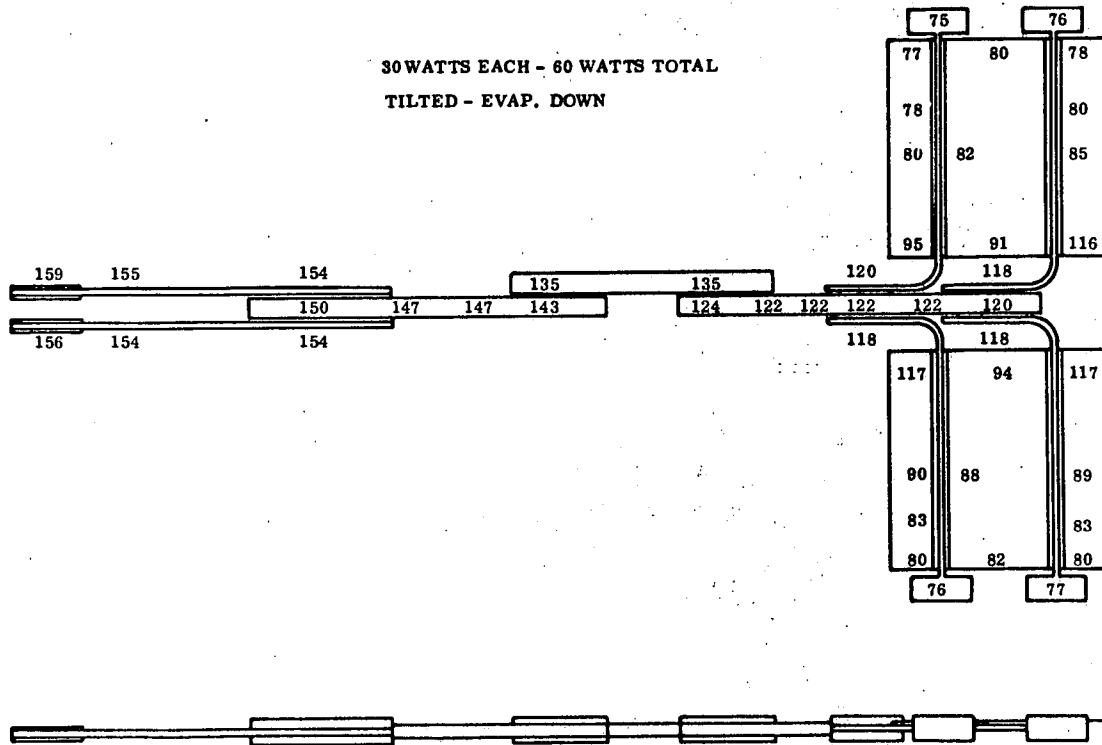


Figure 4-51. Case S4 Profile

Case S5 was run with the system horizontal and with approximately 12 watts on each heater. No burn-out occurred, as the results on Figure 4-52 indicate.

4.14.6 CONCLUSIONS

Data from the five tests run on the saddle system is summarized in Table 4-13. Heat leaks were calculated based on the empirically determined leak rate and the temperatures monitored at equilibrium. The "Thru System" heat is the difference between the heat input and heat leak, and represents the energy actually rejected at the radiating panels. It should be recalled that

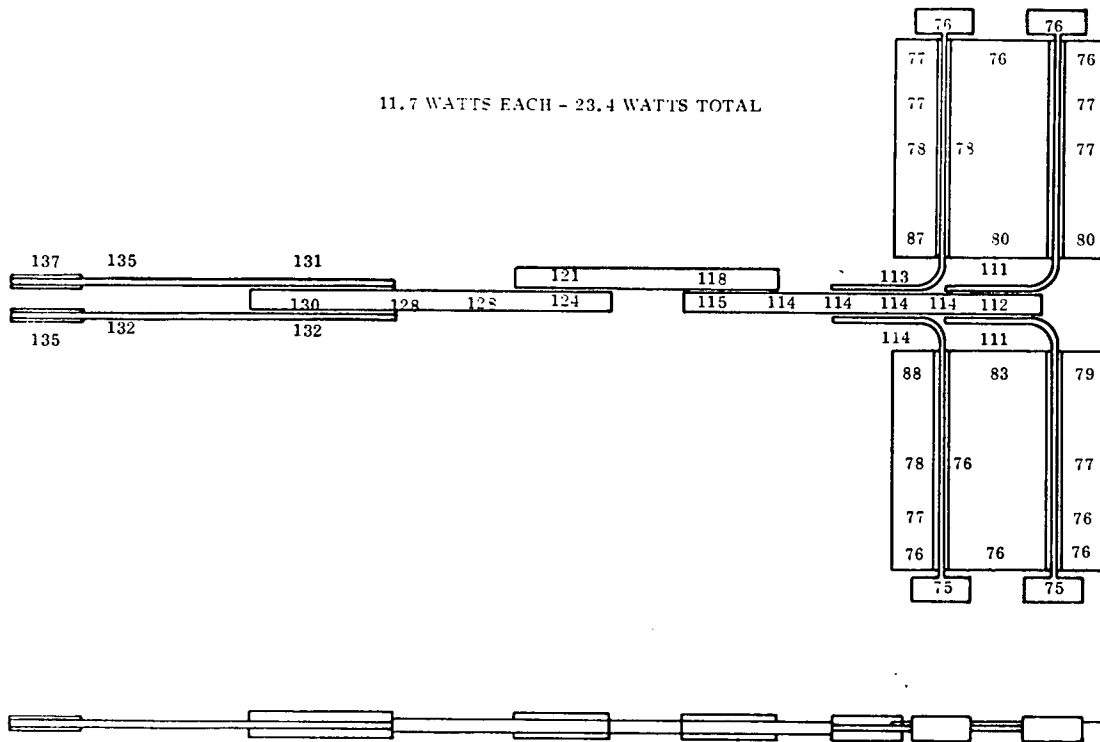


Figure 4-52. Case S5 Profile

in the first three tests, the temperature of the evaporator of heat pipe 1B was inordinately high due to the presence of non-condensable gas. This problem was corrected before running test S4.

The following conclusions were drawn from the data in Table 4-13.

1. System performance after modification of heat pipe 1B was satisfactory.
2. Overall system temperature drop from the evaporator of the component pipes (1A, 1B after modification) to that of the fin pipes (5A through 5D) averaged about $1^{\circ}\text{F}/\text{watt}$ input for the horizontal cases. A lower value, $0.6^{\circ}\text{F}/\text{watt}$ input, was obtained for Case S4.
3. The four variable conductance fin heat pipes showed evaporator temperature control at about $115 \pm 4^{\circ}\text{F}$ over a 4:1 range of heat rejection.
4. Typical conductances for the copper "saddle" interfaces were in the $4\text{-}5 \text{ watts}/^{\circ}\text{F}$ range. In comparing this to the "interface cell" conductances (see Section 4.13), it should be pointed out that the weight of the saddles was over five times that of the interface cells.

5. Heat pipe burnout will occur in the component pipes (1A and 1B) at somewhere between 12 and 20 watts on each, or 24 to 40 watts total. This limit can be increased by moving the heater blocks closer to the condensers of the pipes (thus reducing the effective heat pipe length).

Table 4-13. Summary of Saddle System Data

Case	Heat Values, W			Heat Pipe Evaporator Temp's, °F					
	Input	Leak	Thru System	1A	1B	5A	5B	5C	5D
S1	20	9.6	10.4	136	166	112	112	111	111
S2	29	11.2	17.8	142	161	113	114	114	113
S3	40	13.0	27.0	148	166	114	115	115	114
S4*	60	17.5	42.5	155	154	120	118	118	118
S5	23	9.1	13.9	135	132	113	111	114	111

*System Titled

SECTION 5

PHASE IV

5.1 SCOPE

Successful operation of the Space Station will require continual generation of large quantities of electrical energy over an extensive period of time. The exceptional power requirements have led to the consideration of a nuclear system as the primary energy source. Leading contenders for this purpose are the:

- Isotope/Brayton Cycle
- SNAP-8/Brayton Cycle
- SNAP-8/Organic Rankine Cycle
- SNAP-8/Thermoelectric

An important characteristic of these systems is the fact that the amount of waste heat generated ranges between 4 and 20 times the electrical energy produced. Normally, system concepts show all of this waste heat rejected from an active fluid radiator system. Consideration will be given in this portion of the study to the utilization of this waste heat aboard the space station.

Effective utilization of waste heat has the potential of lowering overall system weight by eliminating the requirements for additional electrical heating energy and/or secondary power sources. In addition, substantial savings in the power system radiator weight and area may also be realized. The alternate concepts investigated were: electrical heaters, individual isotope clusters and a central isotope unit.

In order to achieve a realistic assessment of the attractiveness of waste heat utilization, it is necessary to investigate the following areas:

1. Method of removal of heat from the power cycle
2. Transmission of waste heat from source to user
3. Interfacing of the transmission line with the user.

Removal of waste heat from the power cycles can be made at various locations. The effect of the waste heat system upon cycle weight, efficiency, and pumping requirements is included in the final evaluation.

Two methods of heat transmission were considered: active fluid loops and heat pipes. Conventional fluid loops offer greater design flexibility; however, heat pipes eliminate pumping power requirements and may be lighter in weight. Both concepts are susceptible to meteoroid damage.

Interfacing of the waste heat distribution system with various users may constitute the most difficult aspect of the entire waste heat utilization concept. Each user has a specific geometry, duty cycle and power need; these characteristics require a highly flexible and reliable system design.

5.2 REQUIREMENTS

5.2.1 GENERAL

The Space Station requirements and constraints established for Phase II concept generation as stated in Sections 3.2.1 and 3.3.2 also apply for the waste heat utilization study. All design based parameters concerning the power systems and Space Station configuration reflect the MDAC Phase B studies.

5.2.2 POTENTIAL USERS OF WASTE HEAT

At the present time, several uses of waste heat have been identified whose power and temperature requirements are known. These uses, basic to the life support and well being of the astronauts, include the following:

1. Urine recovery unit
2. Carbon dioxide removal system
3. Water storage assembly
4. Fecal collection unit
5. Clothes washer
6. Dishwasher
7. Shower

These systems will be used as a basis for determining the requirements, characteristics, and attractiveness of the waste heat utilization concept. The systems cited above have a variety of temperature and duty cycle requirements as well as individual interfacing problems with waste heat sources. Consequently, if found attractive for the units mentioned, it can be anticipated that the concept of waste heat utilization will be extended to other systems. Although the definition of the Space Station and Base is still in the formative stages, many other potential uses of waste heat can be suggested. Examples of these are:

1. Trash sterilization
2. Warming of food
3. Sterilization of medical utensils
4. Heat source for laboratory equipment
5. Heating of incubators, cultures, etc.
6. Isothermalization of operating components
7. Warming of ports and penetrations
8. Warming of propellant tankage

Undoubtedly, as a more detailed definition of the Space Base is acquired, other uses of waste heat will become apparent.

5.2.3 DESCRIPTION OF WASTE HEAT USERS

A brief description of the way in which waste heat may be utilized in each of the life support systems is given below. This information is based on the concept definition provided by the

McDonnell/Douglas Space Station effort (References 9-12 to 9-16). A summary of the waste heat users and their requirements is provided in Table 5-1.

5.2.3.1 Urine Recovery Assembly

The urine recovery unit is based on an air evaporation process. Urine and waste wash water are chemically treated and collected by wicks. Air passes over the saturated wicks and carries the evaporated moisture to a condensing heat exchanger. Product water is passed through a series of filters and finally to the water storage assembly.

Waste heat is primarily used to heat the saturated wicks in order to enhance water evaporation. In addition, waste heat may be used to sterilize the air evaporation loop in the event of bacteria contamination.

Two urine recovery units are used, each of which utilizes 7660 Btu/Hr at 270^oF on a 75 percent duty cycle basis.

5.2.3.2 Carbon Dioxide Removal System

Air is drawn into the assembly where it is dehumidified in a dessicant bed; from this point, the air stream is directed to one of a series of absorbing molecular sieve canisters where CO₂ is removed by absorption on zeolite. Effluent air returns to the cabin through the desiccant bed where the air is rehumidified with consequent regeneration of the dessicant. Next the canister which had been recovering carbon dioxide from the cabin air undergoes a desorption process. This is accomplished by a simultaneous reduction in pressure and heating of the canister to approximately 250^oF.

Therefore, waste heat will be used in the CO₂ removal operation to supply heat to a group of canisters in a sequenced manner. It is estimated that 9956 Btu/Hr must be supplied at 250^oF to each of two CO₂ removal assemblies on a 63 percent duty cycle basis.

①

Table 5-1. Summary of Waste Heat User Requirements

User (Number of Units)	Temperature Requirement °F	Individual Unit Power Requirement Btu/Hr	Total Power Requirement Btu/Hr	Individual Duty Cycle % Use	Average Power Btu/Hr
Urine Recovery (2)	270	7660	15,320	75.0	11,500
CO ₂ Recovery (2)	250	9956	19,912	63.0	13,560
Water Storage (2)	160*	1700	3,400	53.0	1,802
Fecal Collection (4)	120	119	476	100.0	476
Clothes Washer/Dryer (2)	100	2560	5,120	2.4	123
Dishwasher/Dryer (2)	170	1710	3,420	4.1	142
Shower (2)	110	1080	2,160	0.6	13

* Capability of 250° F required for sterilization if contamination occurs.

5.2.3.3 Water Storage Assembly

In order to prevent the growth of bacteria all potable water and processed washwater is stored at pasteurization temperature. Therefore, waste heat is utilized to maintain the storage tanks and washwater holding tanks at 160^o F during normal operation.

Two water storage assemblies are provided; each assembly contains three tanks with a capacity of 131 pounds of water per tank. These tanks are designed for a 24-hour use period and are alternately cycled through the collecting, test and use functions.

Two washwater holding tank assemblies are also provided; they consist of a fill tank and a use tank with an individual capacity of 175 pounds of water.

In the event that the system becomes contaminated with bacteria, the design allows for complete sterilization of the water storage, urine water recovery, and washwater and condensate recovery assemblies. This is achieved by circulating these loops in a closed cycle mode while raising the temperature to 250^o F.

It is estimated that 1700 Btu/Hr must be supplied to each of two water storage assemblies at 160^o F on a 53 percent duty cycle basis. Also, the emergency sterilization mode requires a waste heat temperature capability of 250^o F.

5.2.3.4 Fecal Waste Collection Assembly

Fecal waste is drawn into a cylindrical container by forced air where the waste matter is diced and deflected evenly about the interior of a lined wall. The container is heated externally to provide optimum drying conditions for the fecal material; this is accomplished by wrapping coils from the waste heat loop around the collector. Continuous heating of the unit is required with each of four units needing 119 Btu/Hr at 120^o F.

5.2.3.5 Clothes Washer/Dryer

The clothes washer utilizes mechanical agitation and centrifugal force to provide washing and semi-drying of soiled clothing. The final drying operation is conducted under a partial

vacuum, utilizing waste heat at 100^oF. Power requirements for this operation will be substantial. Assuming a wash load of 10 pounds, it can be expected that an additional 10 pounds of water will be retained at the completion of the semi-drying operation. It is desired to complete the drying operation within 15 minutes; therefore, approximately 12 KW of power are required. This demand appears unreasonable and unnecessary. Either of two changes are recommended: reduce the amount of wash per cycle or increase the drying time. Reducing the amount of wash/cycle will increase the crewman's work load; therefore, it appears judicious to lengthen the drying time. Increasing the drying time to four hours will drop the power demand to 0.75 KW or 2560 Btu/Hr. This increase will not interfere with the ability of each crewman to perform one wash per week and is a more reasonable demand for space operations.

5.2.3.6 Dishwasher and Dryer Subassembly

The dishwasher will utilize water at 170^oF to clean and sterilize dishes and utensils. During the wash cycle, waste heat is used to raise and hold the water temperature at 170^oF. The sterilization temperature of 170^oF is required for a minimum of five minutes out of a total wash time of 10 minutes. Dishes and utensils are dried with a warm air flow for a duration of 15 minutes.

An estimate of the required power indicates 1700 Btu/Hr for five minutes, at 170^oF, during the cleaning cycle for each of two assemblies. The drying cycle will require a nominal amount of waste heat energy if proper draining is provided.

5.2.3.7 Shower Assembly

The shower is a closed compartment designed for wetting, washing, rinsing, and drying of the body. Water is introduced into the shower in the form of a warm air/water spray by a fixed or hand-held shower head. The air stream carries the spray to the bottom of the shower where the water is collected and the air recycled. Water temperature is manually regulated by the appropriate mixing of hot water (at the storage temperature of 160^oF) and a 72^oF water supply.

Drying is accomplished by an overhead warm air stream, heated by the waste heat supply. Drying may be completed by toweling.

Since the washing procedure will use preheated water, the drying operation will constitute the only waste heat requirement. The energy required to dry the body by air evaporation is estimated to be 1080 Btu. It is expected that five minutes will be needed to complete the drying portion of the shower.

5.3 EVALUATION OF POWER SYSTEM WASTE HEAT SOURCES

Each of the four power systems considered in this section generates sufficient waste heat to supply the space station with the user heat requirements listed in Table 5-1. However, the attractiveness of the waste heat utilization concept will depend in part on the temperature at which the waste heat is available and the feasibility of removing the energy without a major disturbance of the cycle efficiency. In general, three locations within a nuclear power system are available for the extraction of waste heat: the nuclear radiation shielding, the heat rejection portion of the working fluid loop and the waste heat rejection loop. Typically, the highest available temperature will occur in the shield and the lowest in the heat rejection loop. Exceptions to these generalizations will be pointed out as each power system is discussed.

The effect of the location of the waste heat removal unit on the system control philosophy and radiator size will be discussed in Section 5.4.

5.3.1 POWER SYSTEM DEFINITION

Cycle diagrams for the Isotope/Brayton, Reactor/Brayton and Reactor/Thermoelectric power systems are shown in Figures 5-1 through 5-3 as defined by the McDonnell Douglas Corporation. Although the Reactor/Organic Rankine is not considered to be a leading contender for the Space Station at the present time, it will be considered in this effort to evaluate its compatibility with the waste heat utilization concept. Typical cycle conditions for this system are given in Figure 5-4. Characteristics of each cycle are discussed as follows:

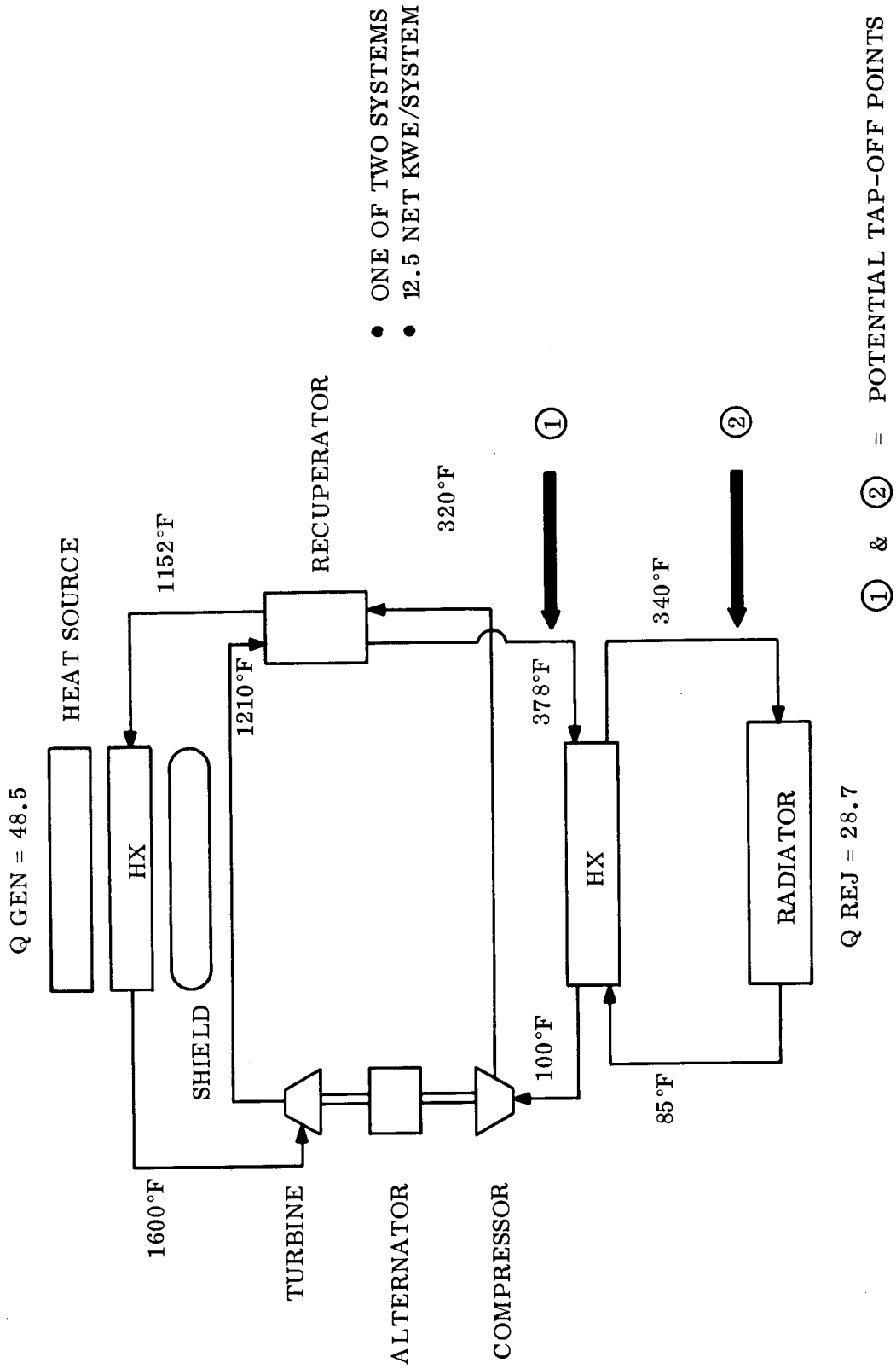
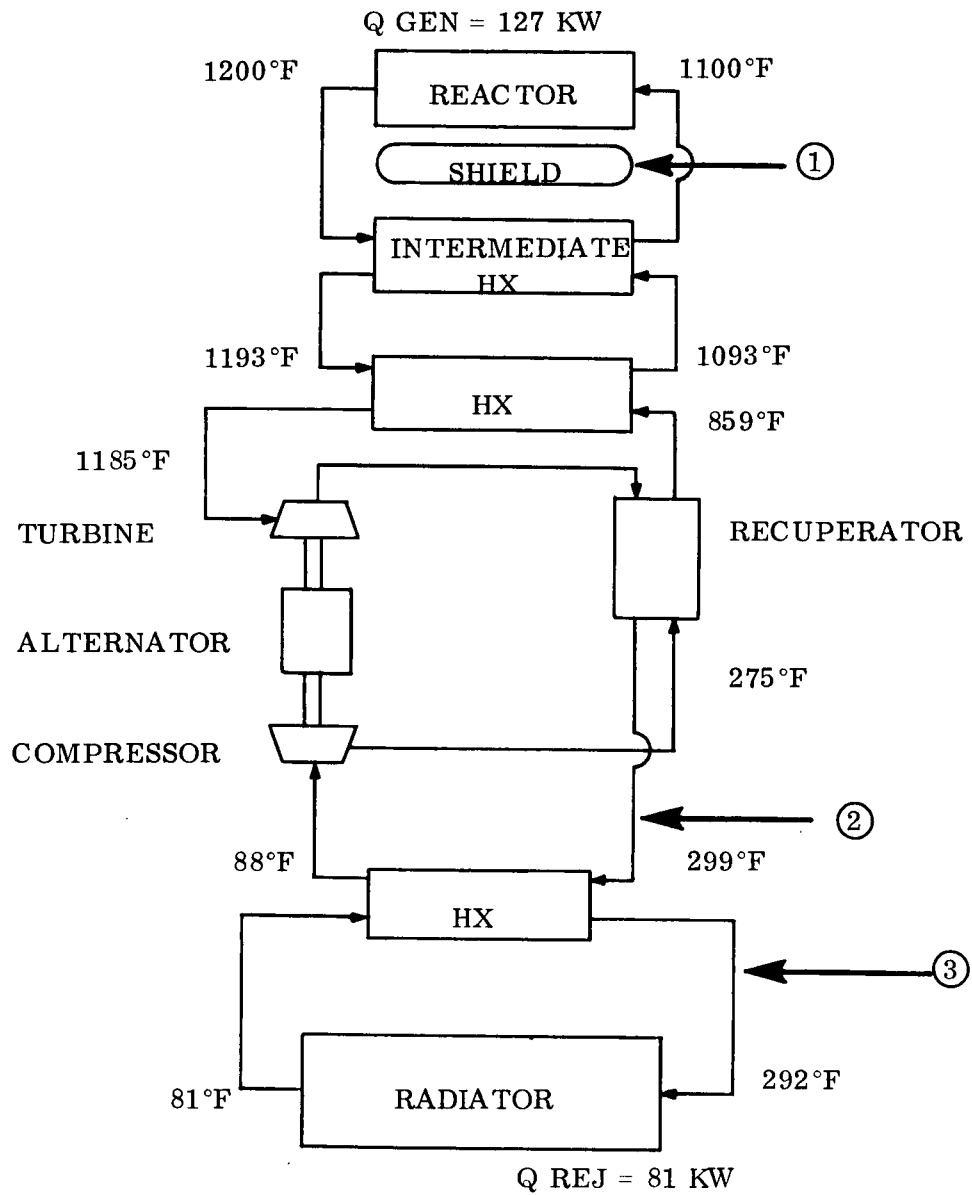


Figure 5-1. Simplified Isotope/Brayton Cycle



① ② & ③ = POTENTIAL TAP-OFF POINTS

Figure 5-2. Simplified Reactor/Brayton Cycle

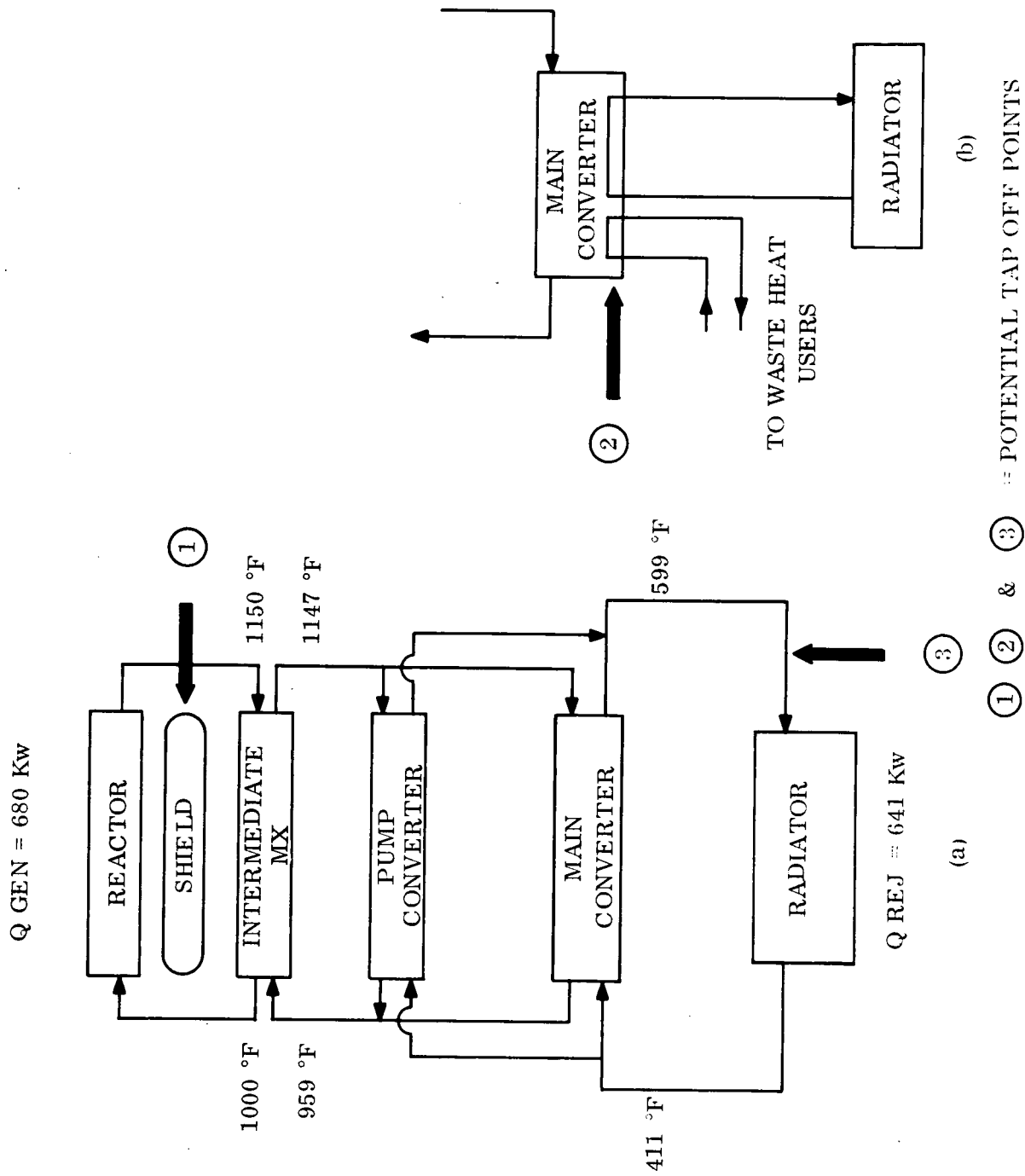


Figure 5-3. Simplified Reactor/Thermoelectric Cycle

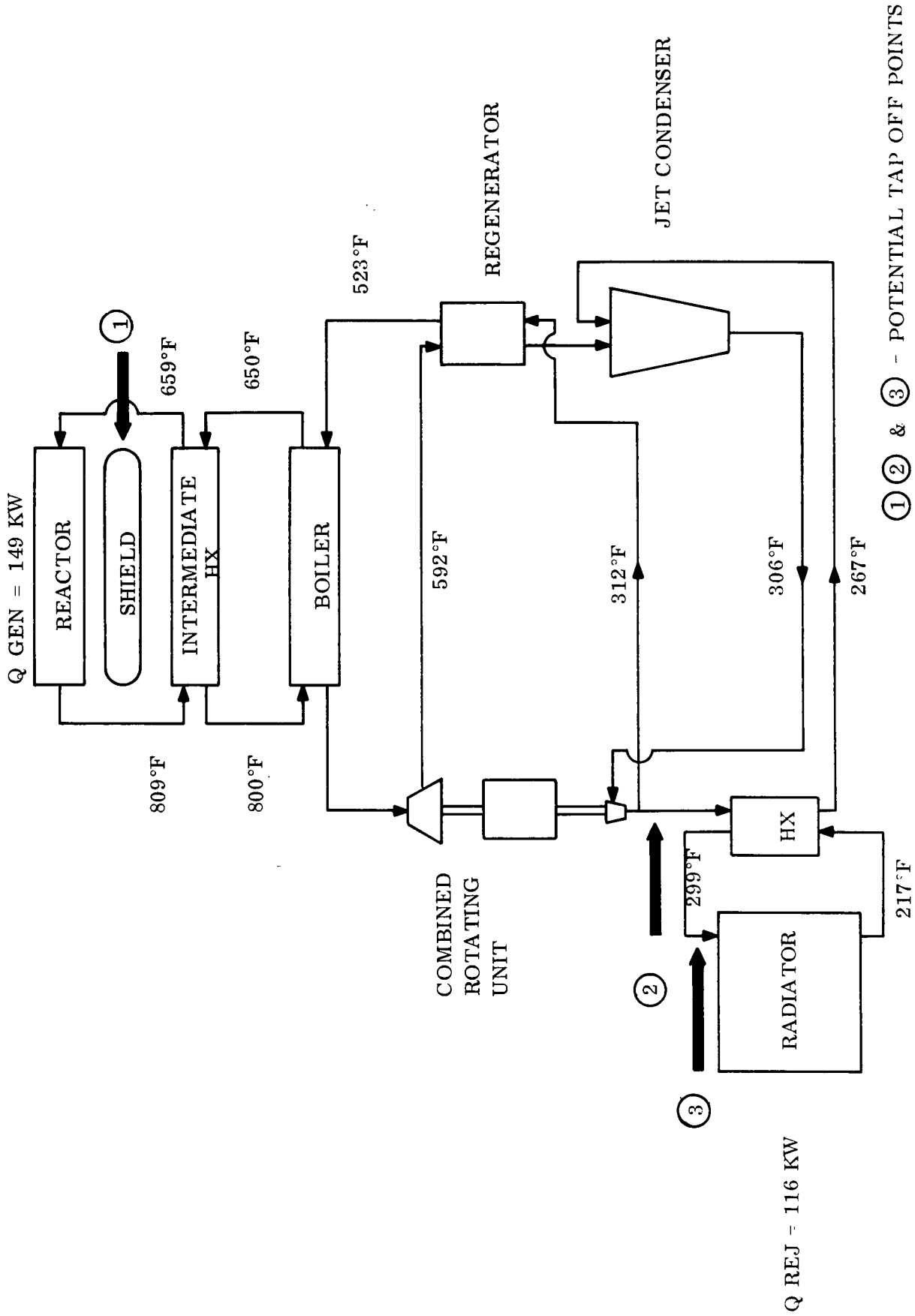


Figure 5-4. Simplified Reactor/Organic Rankine Cycle

5.3.1.1 Isotope/Brayton

This system uses the decay heat energy from Pu^{238} to power a high temperature Brayton cycle using a He/Xe mixture of gas as the working fluid. Two individual systems are provided, each of which produces 12.5 Kwe.

Heat is radiated from the isotope capsules to the main heat exchanger of the gas cycle loop. The heated gas is expanded through a turbine, passes through a recuperator and rejects the cycle waste heat in a silicone fluid cooled (DC-200) heat exchanger. Waste heat is rejected to space by the DC-200 by means of a radiator system. Approximately five inches of lithium hydride is provided to reduce the neutron dose to the manned compartments.

The neutron generation rate for a Pu^{238} radioisotope heat source is orders of magnitude less than for a reactor system. Therefore, neutron moderation and absorption in the shield generates an insignificant amount of heat. Assuming that the lithium hydride shield is well insulated from the Brayton heat exchanger (see Figure 5-5) it will be unable to provide energy to the waste heat users.

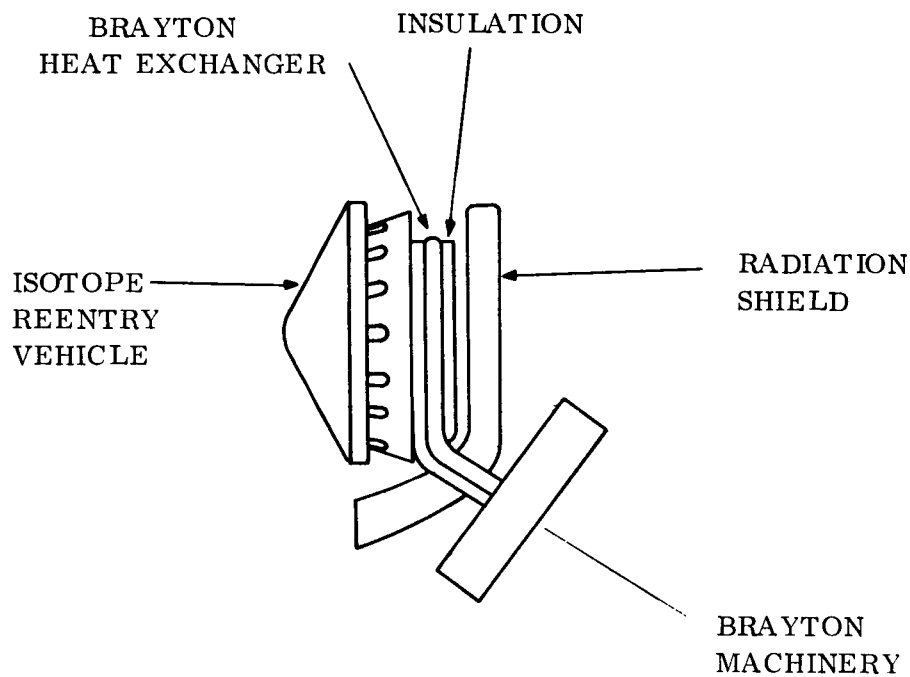


Figure 5-5. Isotope/Brayton System Configuration

The He/Xe gas loop provides a source of waste heat prior to its entry into the waste heat exchanger. A maximum power of 28.7 Kw is available per system at a maximum gas temperature of 378^oF. Removal of waste heat from this location appears entirely feasible with the present cycle conditions and user requirements.

The second possible location for the removal of waste heat occurs in the radiator loop. As before, the maximum power available per loop is 28.7 Kw; however, the radiator fluid is at a maximum temperature of 340^oF.

5.3.1.2 Reactor/Brayton

In this system, the proposed SNAP-8 reactor operates at a power level of 127 Kw to yield a net power of 29 Kwe to the space station. Energy is transferred from the reactor loop to the Brayton cycle by means of an intermediate fluid loop. However, since the reactor temperature is considerably less than the radioisotope temperature level, this Brayton cycle operates at a lower temperature and efficiency than the Isotope/Brayton cycle.

Due to the high neutron and gamma fluxes generated, the entire reactor assembly is surrounded by tungsten and lithium hydride shielding. One potential concept of the reactor, radiation shield and reentry protection arrangement is shown in Figure 5-6. It is estimated that 2.5 to 6.2 Kw will be generated in the shield due to radiation effects. The advisability of utilizing this power is complicated by several considerations.

Of primary importance is the necessity to maintain the lithium hydride temperature below 1000^oF in order to prevent lithium hydride dissociation. Although it is recognized that this requirement may require an active loop system, present plans depend upon passive radiation to space to maintain the desired temperature level.

If it is deemed feasible to accomplish the necessary cooling by passive means, the possibility of introducing an active loop into the shield system for waste heat utilization may be hampered by the following factors:

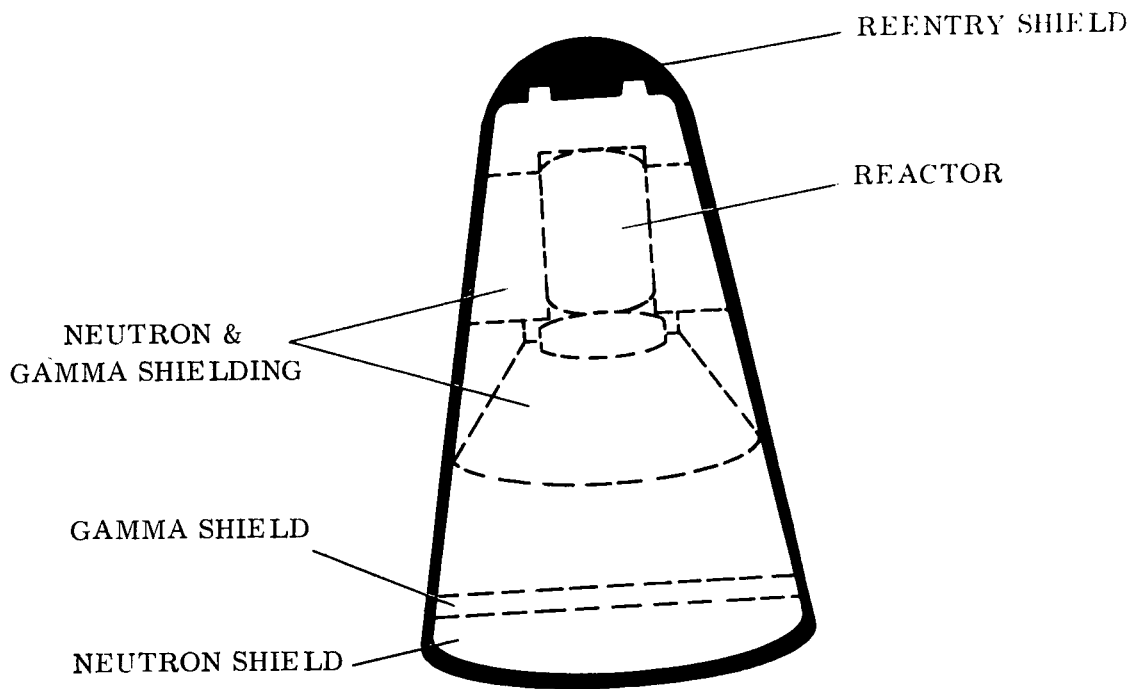


Figure 5-6. SNAP-8 Reactor Assembly

1. Aggravation of the reentry safety problem by increasing the number of reentry shield penetrations
2. Potential nuclear radiation hazard due to removal of activated fluid
3. Increase in reactor envelope resulting from the introduction of piping in the shield

Therefore, in this situation, the desirability of utilizing the absorbed radiation energy must consider the effect on the reactor assembly design. However, if it is found to be necessary to cool the reactor shield by active techniques, space station utilization of this energy may appear attractive. For the purposes of this investigation, it will be assumed that 4.0 Kw of thermal power is available in the shield at a temperature level of 1000^oF.

The second possible location for the removal of waste heat occurs in the Brayton cycle working fluid loop as shown in Figure 5-2. Approximately 81 Kw of heat is available at this location at maximum temperature of 299^oF.

The third location is the DC-200 heat rejection loop where it is also assumed that 81 Kw of heat is being transferred. Maximum temperature level in this loop is 292^oF.

5.3.1.3 Reactor/Thermoelectric

This is a completely static system which utilizes the SNAP-8 reactor as the heat source. As shown in Figure 5-3, approximately 680 Kw of reactor heat is required to produce 29 Kwe; growth versions of this system which employ supplemental radiator loops will not be considered here. Figure 5-3B illustrates a possible modification to the current reactor/thermoelectric system.

Heat is transferred from the reactor by a liquid metal coolant loop to an intermediate heat transfer loop. The intermediate loop is used to heat an array of lead-telluride thermoelectric converters. The cold junction of the thermoelectric converter assembly is cooled by an active loop radiator system. Pumping power for all three loops is provided by a three-throated thermoelectric pump converter using four TE modules.

Three locations are available for the removal of waste heat without disturbing the system efficiency: the reactor radiation shield, the cold side of the converter loop, and the waste heat rejection loop. The shield provides a large source of energy due to the very high operating power of the reactor. Depending upon the final design geometry and radiation dose limits, it is estimated that between 15 and 35 Kw of thermal power will be generated in the shield from radiation absorption. For this system, it can be assumed that active cooling of the shield will be required to maintain a maximum lithium hydride temperature of 1000^oF.

The second location from which heat can be removed is shown in Figure 5-3B. In this approach, the function of waste heat removal from the thermoelectrics is divided into two separate loops. Although this concept involves a change in the system layout, the efficiency of the cycle is unaffected. The 641 Kw of power which must be removed from the thermoelectric cold side at a maximum temperature of about 605^oF provides wide flexibility in the number of waste heat uses.

The heat rejection loop is the third source of waste heat; approximately 641 Kw are available at a maximum temperature of 599^o F.

5.3.1.4 Reactor/Organic Rankine

Figure 5-4 illustrates a reactor/organic Rankine cycle modeled from a North American Rockwell version of potential Space Base power system. In this system, the SNAP-8 reactor transfers heat from the primary loop to an intermediate heat transfer loop. The intermediate loop provides energy to a boiler in which an organic fluid is vaporized and superheated prior to expansion in a turbine. The net power output from the combined rotating unit is 29 Kwe. The expanded gas passes through a regenerator and into a jet condenser. Use of a jet condenser enables low turbine exit pressures and high system efficiencies to be achieved. After exiting from the jet condenser, the loop is split into two streams. One portion is passed through a heat exchanger in which the waste heat is rejected to a radiator loop. The other stream is recycled through the jet condenser to sustain its operation. The level of the jet condenser exit pressure is a trade-off between system efficiency and radiator area.

As in the previous reactor systems discussed, waste heat is available in the neutron and gamma shield. At a reactor power level of 149 Kw, however, it is questionable whether an active cooling loop is required. For the purposes of this study, it will be assumed that 5.0 Kw of power is available in the shield at a maximum temperature level of 1000^o F.

Prior to entering the waste heat exchanger, 116 Kw of power at a maximum temperature of 306^o F is available in the Dowtherm A loop. Removal of waste heat from the radiator loop can provide the same amount of power at a maximum temperature of 299^o F.

5.3.1.5 Summary of Waste Heat Sources

A tabulation of the candidate power systems is given in Table 5-2; all of these have the potential of satisfying the waste heat user power and temperature requirements. The reactor systems differ from the isotope system in that they are able to deliver a higher waste heat temperature to the manned areas (1000^o F from the shield). For the reactor/Brayton and

Table 5-2. Candidate Power System Characteristics

System	Power Level, Kw	Power Output, Kwe	System Efficiency %	Available Locations	Waste Energy Available, Kw	Maximum Available Waste Heat Temperature, °F
Isotope/ Brayton	97	25	26	Working Fluid Loop	57.4	378
				Heat Rejection Loop	57.4	340
Reactor/ Brayton	127	29	23	Shield	~4.0	~1000
				Working Fluid Loop	81.0	299
				Heat Rejection Loop	81.0	292
Reactor/ Thermo- electric	680	29	4.2	Shield	~25.0	~1000
				Thermoelectric Cold Junction	641.0	605
				Heat Rejection Loop	641.0	599
Reactor/ Organic Rankine	149	29	19	Shield	~5.0	~1000
				Working Fluid Loop	116.0	306
				Heat Rejection Loop	116.0	299

reactor/Organic Rankine systems, the attractiveness of removing waste heat from the shield will depend to a large extent on the magnitude of the nuclear irradiation and other design problems. However, the high reactor power level of the thermoelectric system will necessitate an active shield cooling system, making the concept of shield heat utilization more acceptable.

Heat removal from the working fluid loops of the candidate systems is considered feasible, although redesign may be required to accommodate the additional heat exchanger. Waste heat removal from the waste heat rejection loop should have the least impact on the present system designs.

The power output of any isotope system cannot be varied at will; of course, the power will decrease over the lifetime of the mission in accordance with the half-life of the particular radioisotope. Theoretically, the power output of a nuclear reactor power system can be varied between its maximum rated power and zero. In practice, however, the power of the reactor can be reduced to some fraction of its operation power at which point its heat-to-electrical conversion system will cease to function. The value of the minimum power output depends upon the type of energy conversion system employed. Further study would be required to estimate this value for the power systems considered.

5.4 HEAT TRANSMISSION ANALYSIS

The transfer of power from the sources of heat to the Space Station users can be divided into three design areas: waste heat removal, energy transport and power distribution. Each of these activities is discussed with respect to each power system heat source location in the subsections below.

5.4.1 WASTE HEAT REMOVAL

One effect of the location of the waste heat removal system is the impact on required radiator area. If waste heat is removed from the shield, no reduction in cycle radiator area is possible; however, removal of waste heat from the working fluid or heat rejection loops can decrease the radiator area. In addition, the waste heat removal location can affect system

control due to the fluctuations in user requirements. The parts of the system from which the removal of waste heat has been considered are restricted to those identified in Section 5.3.

5.4.1.1 Isotope/Brayton

Figure 5-7 shows four alternatives for the removal of energy from the Isotope/Brayton power system. Figure 5-7A illustrates a design in which an auxiliary heat exchanger has been provided in the working fluid loop. With this approach, the gas inlet temperature to the waste heat exchanger is lowered, but the overall radiator area requirement will be decreased due to the smaller heat load. Obviously, the size of the waste heat exchanger can be decreased as well. Control of the compressor fluid inlet temperature can be accomplished by varying the radiator fluid flow rate through the waste heat exchanger. Control must also be provided to regulate the amount of energy transferred to the waste heat users.

Figure 5-7B illustrates a variation of the former concept; in this design, the auxiliary heat exchanger has been placed in parallel with the Brayton waste heat exchanger. This configuration has the advantage of keeping the radiator fluid inlet temperature at its original level, thereby affording larger reductions in the radiator area. A reduction in the waste heat exchanger size can again be realized.

Figures 5-7C and 5-7D show concepts in which the auxiliary heat exchanger has been placed in the heat rejection loop. The former approach, 5-7C, results in a reduction of the radiator fluid inlet temperature while the second approach avoids this by a parallel loop arrangement. Control of the compressor fluid inlet temperature is again accomplished by a variable heat rejection loop flow rate.

The required radiator area for each of these system variations will be determined by the maximum heat load/heat sink conditions on the system. Figure 5-8 plots the required radiator area for the Isotope/Brayton cycle as a function of the waste heat utilized by the space station; each of the four removal concepts are shown. Results shown in Figure 5-8 illustrate the advantage of placing the auxiliary heat exchanger in parallel with either cycle

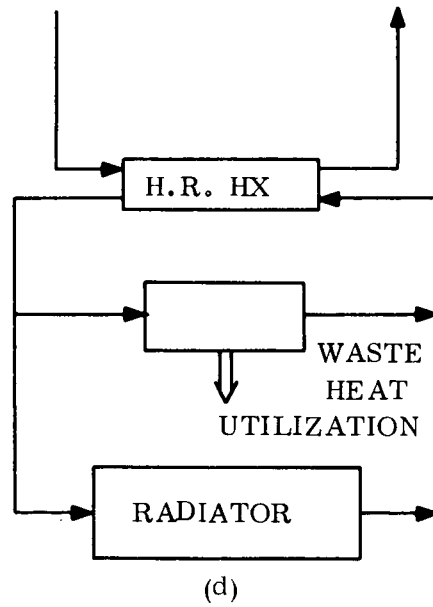
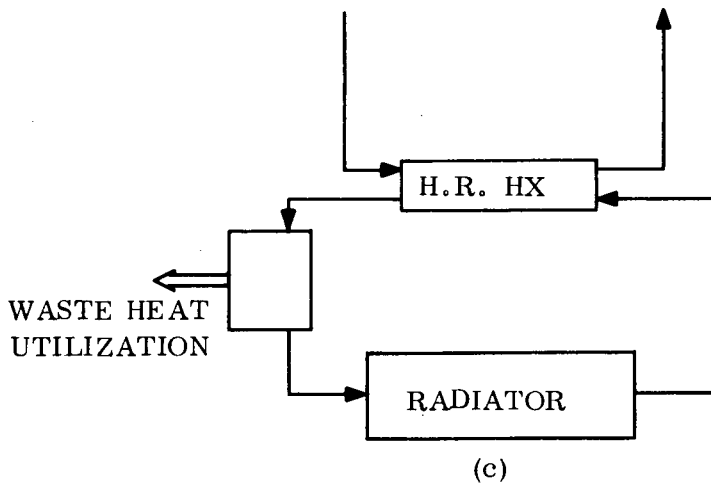
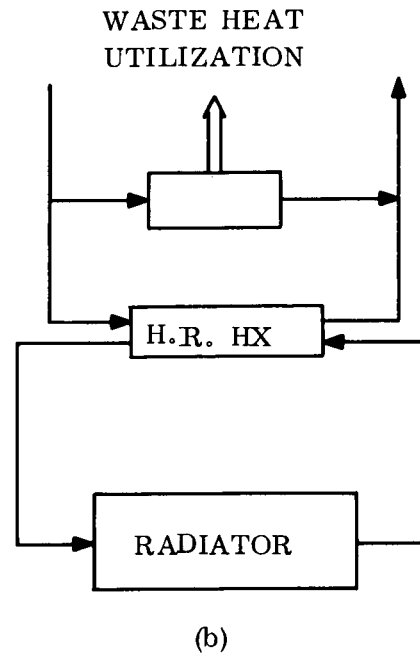
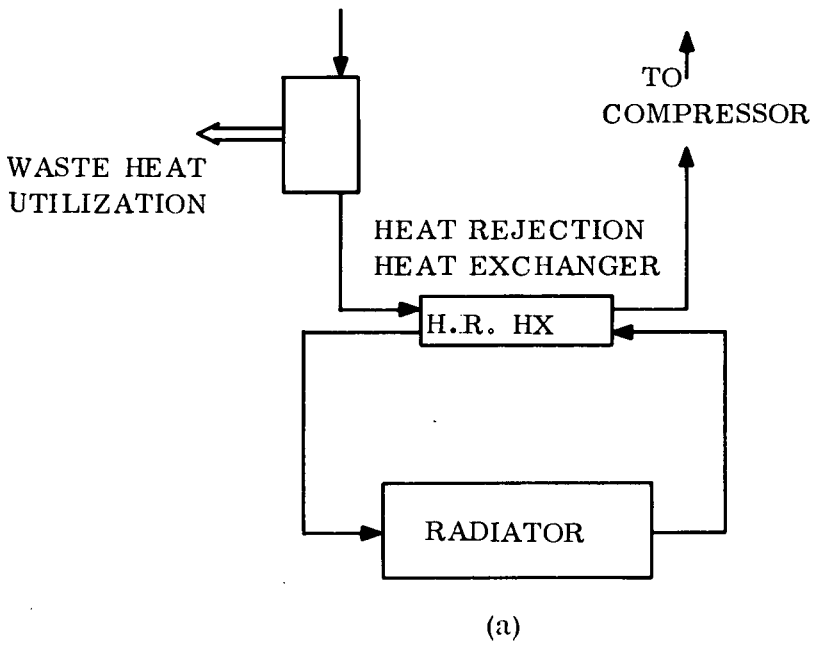


Figure 5-7. Energy Removal Alternatives - Isotope/Brayton Cycle

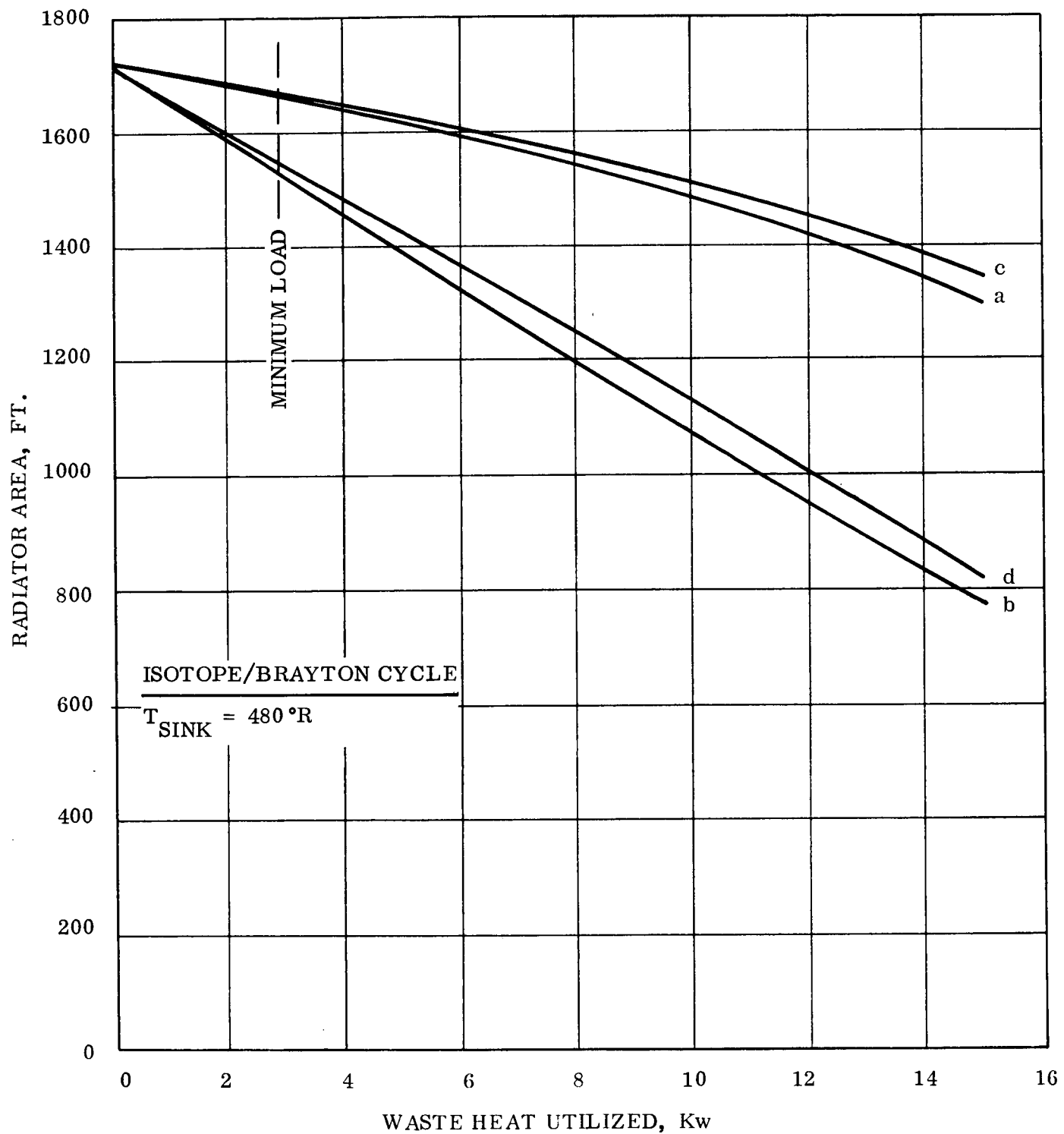


Figure 5-8. Required Radiator Area vs Waste Heat Utilized - Isotope/Brayton Cycle

loop as opposed to the series arrangement. Considering just radiator and heat exchanger weight, the minimum weight approach is provided by the parallel configuration, working fluid loop waste heat removal.

Since the radiator area is determined by the maximum heat load/heat sink condition, it is necessary to evaluate the response of the radiator under a minimum heat load/heat sink condition. The maximum heat load for the radiator occurs when waste heat utilization is at a minimum.

The minimum power requirement for the WHU system was assumed to consist of 1 urine recovery unit (7660 Btu/Hr), 4 fecal collection units (476 Btu/Hr) and 1 water storage unit (1700 Btu/Hr). This results in a total minimum power requirement of 9836 Btu/Hr or 2.88 Kw. An equally valid assumption would have been to assume 1 CO₂ recovery unit in place of the urine recovery system to yield a total minimum power requirement of 12,132 Btu/Hr or 3.56 Kw. In light of the duty cycles (see Table 5-1) it is necessary to assume 1 water storage and 4 fecal collection units in operation at all times. Energy management considerations indicate that it is unreasonable to assume all urine and CO₂ recovery systems inoperative simultaneously. Therefore one urine recovery unit has been assumed functioning in the minimum power mode.

Examination of Figure 5-8, indicates that a 5 percent reduction in radiator area is obtained by the utilization of waste heat with concepts b or d.

Using the reduced radiator area and heat load, it is possible to estimate the effect on radiator outlet temperature as a lower heat load/heat sink condition is attained. Figure 5-9 illustrates the steady state behavior of the Isotope/Brayton radiator as the sink temperature drops to 312°R and Space Station waste heat utilization is increased from the minimum amount of 2.88 Kw. For concepts a and c (Figure 5-7) the radiator outlet temperature remains relatively constant for various levels of waste heat utilization. This is due to the fact that as the power to the radiator is decreased, the radiator inlet temperature also decreases for these

E

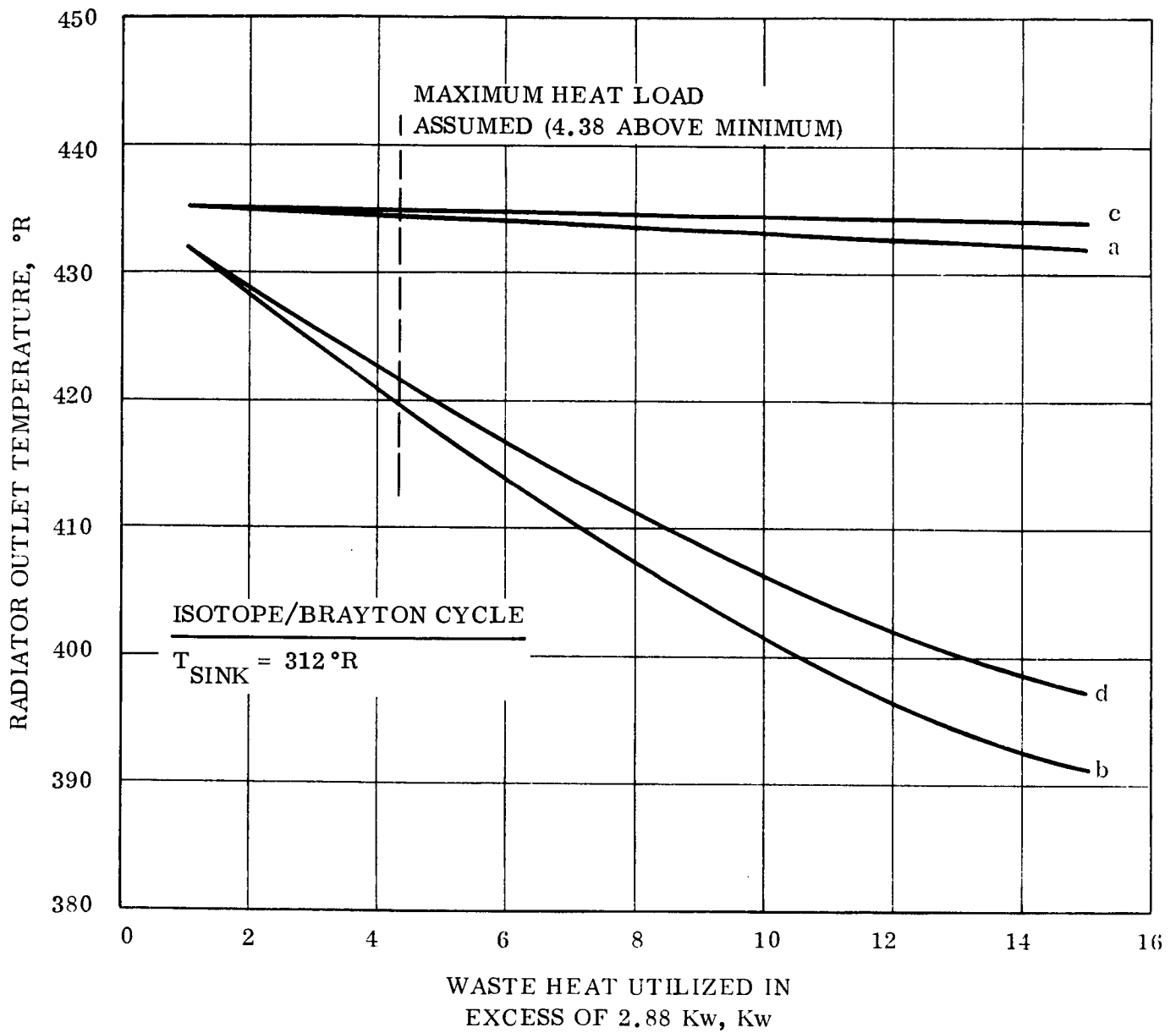


Figure 5-9. Radiator Outlet Temperature vs Waste Heat Utilized - Isotope/Brayton Cycle

configurations. The result is a lower inlet temperature and effective radiator temperature, but a stable exit temperature. Concepts b and d, which were attractive from the standpoint of reducing radiator area, exhibit substantial decreases in radiator outlet temperature as waste heat utilization increases. This phenomena is cause for concern because of the rapidly changing radiator fluid flow properties at these temperatures. Figure 5-10 shows the variation in kinematic viscosity with temperature for FC-75. During normal operation, the outlet fluid will have a kinematic viscosity of 0.8 centistokes (85°F). Assuming a worst case condition in which 7.26 Kw is being directed to the Space Station and the sink temperature has fallen to 312°R , the radiator fluid outlet temperature will have dropped to between 420°R and 435°R (Figure 5-9). This results in a factor of 6 increase in fluid viscosity. The implications of this change as to fluid flow stability, maldistribution, and pumping power requirements must be investigated further.

5.4.1.2 Reactor/Brayton

The radiation shield of the Reactor/Brayton system provides a high temperature source of energy which can be used aboard the space station. This heat is generated by the slowing down and absorption of neutrons and gamma rays escaping from the reactor. The problems of removing power from the shield are related to the possibility of compromising the integrity of the reentry protection shield surrounding the reactor, removing activated fluid and the more conventional concerns of heat transfer design and fabrication techniques.

Figure 5-11 provides an estimate of the heat transfer area required to remove various amounts of power from the shield at 300°F by a liquid metal cooling loop. At a nominal power level of 4 Kw, approximately 4 ft^2 of area is needed. This amount of area must be provided by some type of extended surface design such as pictured in Figure 5-11. Obviously, this concept entails a development of a fabrication procedure which would provide adequate thermal contact between the LiH and the heat acceptance surfaces and in addition, maintain a uniform LiH structure.

It is important that the shield heat removal design does not induce an increase in the amount of heat lost from the reactor to the shield, thereby reducing system efficiency. Also of

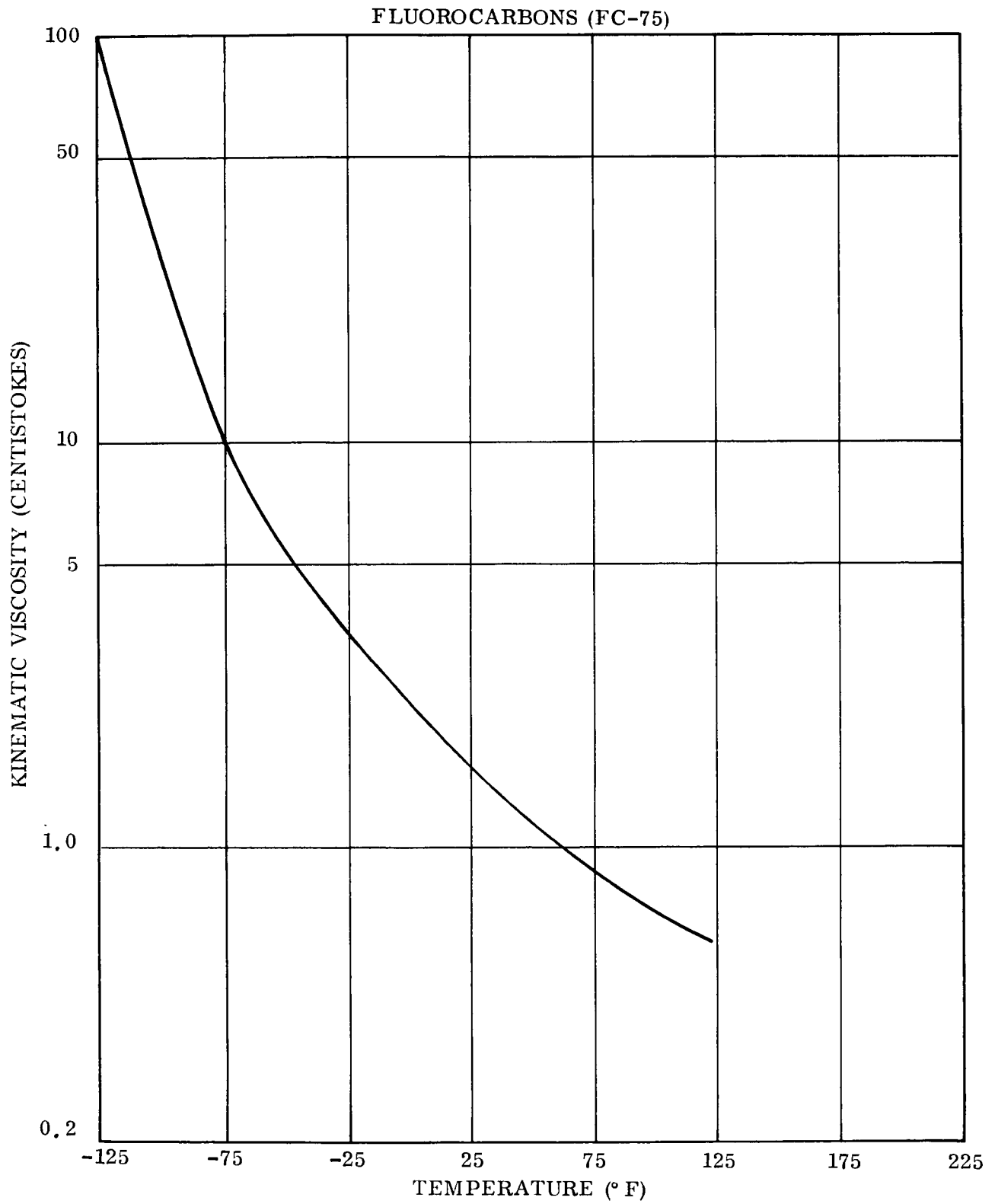


Figure 5-10. Kinematic Viscosity vs Temperature -
Fluorocarbons (FC-75)

REQUIRED HEAT TRANSFER AREA
FOR HEAT REMOVAL FROM THE
REACTOR SHIELD

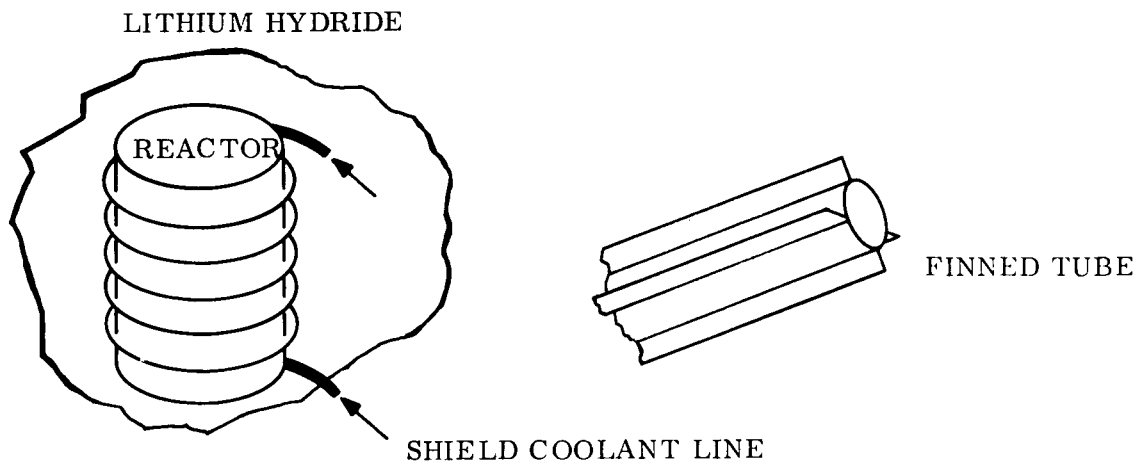
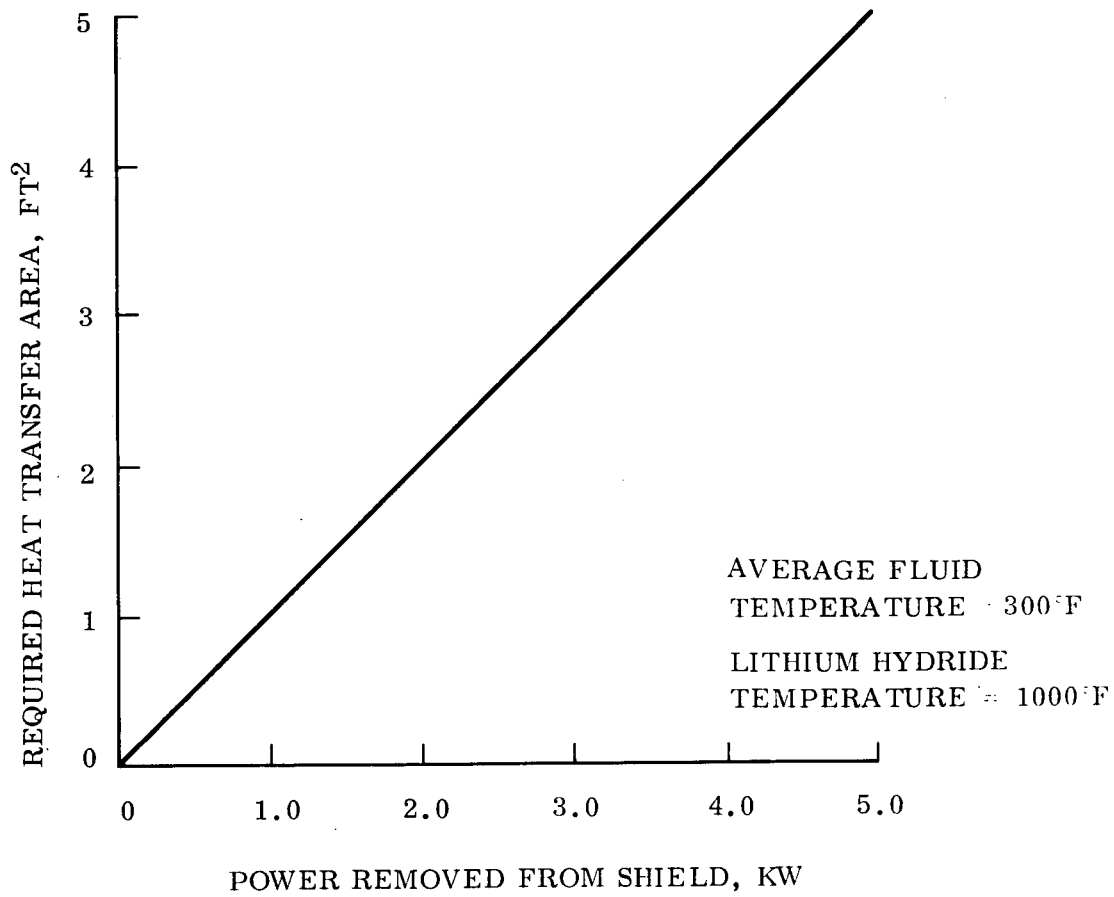


Figure 5-11. Shield Waste Heat Removal Concept and Heat Transfer Area Requirements

significance is the fact that no area reduction in the power system radiator is derived from use of the shield waste heat.

The second and third locations for heat removal in the Reactor/Brayton cycle are analogous to those offered by the Isotope/Brayton cycle -- the four approaches considered are shown in Figure 5-7. However, since the Reactor/Brayton system is less efficient than the Isotope/Brayton system the effect of waste heat utilization on the required radiator area is less pronounced. This is illustrated in Figure 5-12.

Figure 5-13 shows the radiator outlet temperature as a function of the amount of waste heat utilized for the low sink temperature condition. The drop in the radiator outlet temperature is more severe than for the Isotope/Brayton cycle due to the difference in cycle efficiency and operating conditions.

5.4.1.3 Reactor/Thermoelectric

The salient characteristics of this nuclear power system is its lack of moving parts and also its low efficiency, which implies a large availability of waste heat. Consequently, the manner in which waste heat is removed from the system, in the amounts shown here, will not affect the radiator area or system weight to any measurable degree, nor will it induce a radiator fluid freezing problem.

At a reactor power level of 680 Kw, active shield cooling must be considered as a probable design feature. Therefore, a design concept similar to that shown in Figure 5-11 can be used for this system.

The other likely approach is to remove energy from the heat rejection loop before the fluid enters the radiator. Since the heat rejected is 641 Kw, removal of 7.26 Kw would drop the inlet temperature to the converter only 2^o F.

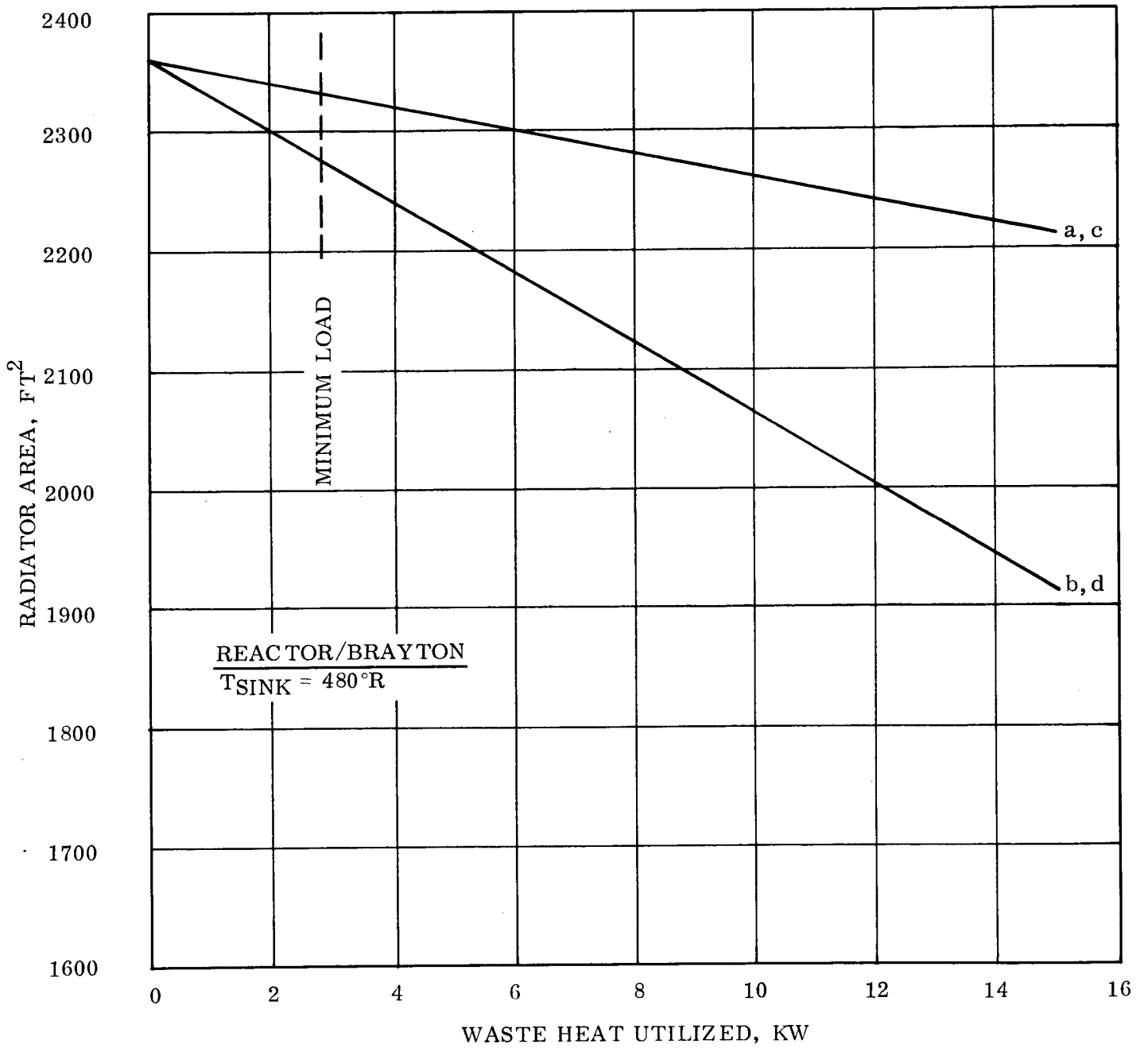


Figure 5-12. Required Radiator Area vs Waste Heat Utilized - Reactor/Brayton Cycle

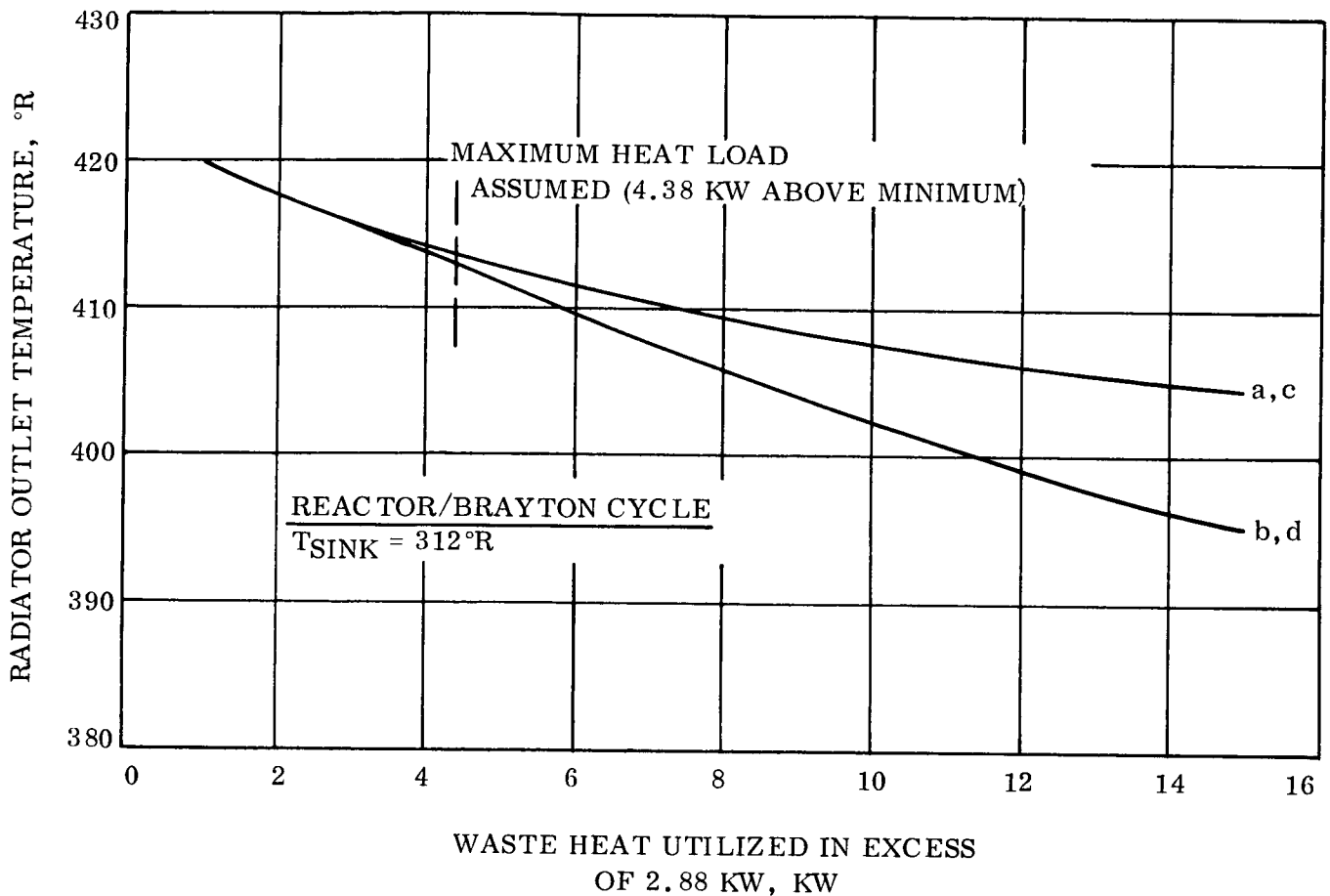


Figure 5-13. Radiator Outlet Temperature vs Waste Heat Utilized - Reactor/Brayton Cycle

While integrating the waste heat removal system with the main converter is possible, as shown in Figure 5-3, the design problems entailed appear considerably greater as compared to the previous approach.

5.4.1.4 Reactor/Organic Rankine

The options available for waste heat removal in the Reactor/Organic Rankine cycle are analogous to those identified in the Reactor/Brayton cycle. Like the Reactor/Brayton cycle, only a small reduction in radiator area can be realized (Figure 5-14). However, unlike the Brayton cycles, excessively low radiator fluid outlet temperatures are not experienced; this conclusion is illustrated in Figure 5-15.

5.4.2 ENERGY TRANSPORT

In each of the candidate systems the source of waste heat is located away from the habitable areas of the Space Station, therefore, an energy transport system is required. In the

Isotope/Brayton system, however, the power conversion system is situated at a relatively close distance to the waste heat users -- an average distance of 25 feet will be assumed. Due to the higher neutron and gamma fluxes generated by reactor systems, a transmission distance of approximately 200 feet (400 feet to complete loop) will exist between the sources and users.

Heat transmission by an active fluid loop system and heat pipes are considered in this analysis. Other means, such as radiation heat transfer, were considered to be impractical.

5.4.2.1 Active Fluid Loop Transmission

Three fluids were considered as heat transmission candidates in this analyses: water, DC-200 (2 cs.) and NaK-78. Containment materials were stainless steel for water and NaK while DC-200 permitted the use of aluminum.

A computer program was used to calculate the weight of the transmission system using each fluid. For this analysis, it was assumed that heat was being removed from the working fluid loop of the Isotope/Brayton cycle; other important assumptions were:

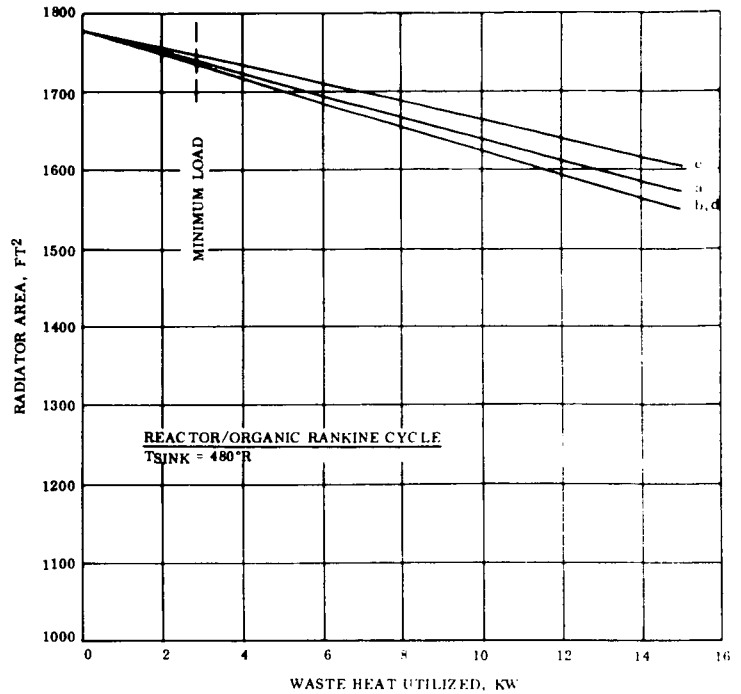


Figure 5-14. Required Radiator Area vs Waste Heat Utilized - Reactor/Organic Rankine Cycle

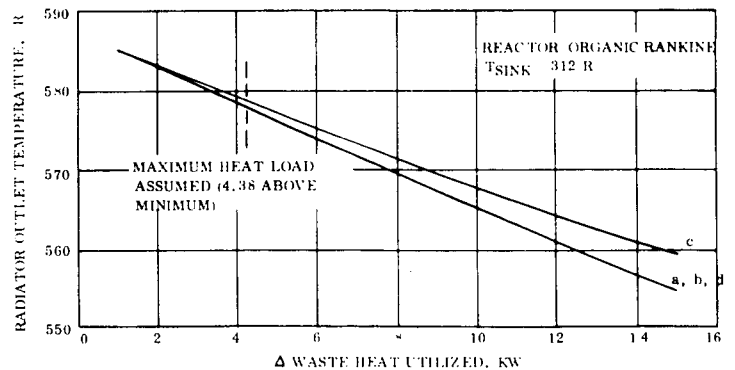


Figure 5-15. Radiator Outlet Temperature vs Waste Heat Utilized - Reactor/Organic Rankine Cycle

1. Waste heat utilized = 4.0 Kw
2. Maximum fluid temperature = 350°F
3. Pipe wall thickness = 0.030 inches
4. Pump efficiency = 15 percent
5. System specific weight = 600 lbs/Kwe

The flow rate for each fluid was based on an outlet temperature of 270°F from the CO₂ recovery unit and an average power of 3.67 Kw in the urine and CO₂ recovery units. This assumption was found to provide a sufficiently high fluid temperature for subsequent users. Figure 5-16 through 5-18 illustrate the weight of the active loop transmission system for various pipe diameters and lengths. An electromagnetic pump was assumed for the NaK fluid case while a reciprocating pump concept was used for the water and DC-200 cases. System weight consists of fluid weight, piping weight, system pumping power weight penalty and pump weight. The pump was found to constitute a small portion (~2 lbs) of the total system weight. Insulation was assumed to be unwarranted since the fluid lines will run inside the power system radiator envelope.

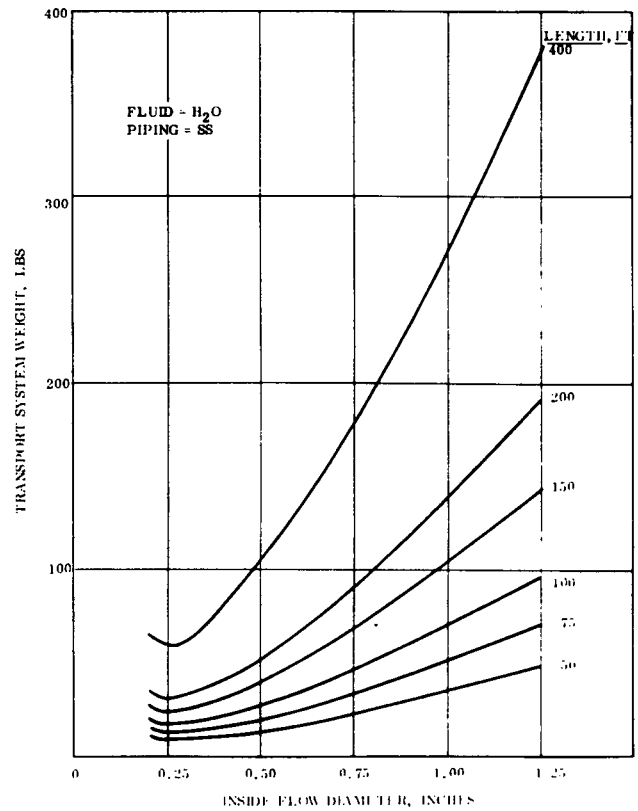


Figure 5-16. Energy Transport System Weight as a Function of Flow Path Length and Tube Diameter - H₂O

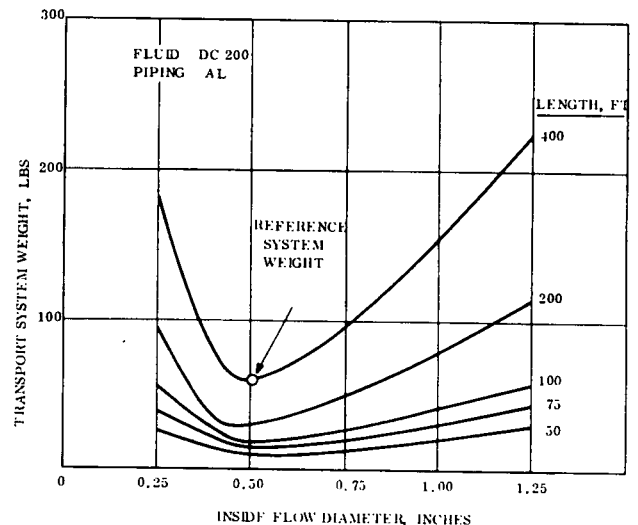


Figure 5-17. Energy Transport System Weight as a Function of Flow Path Length and Tube Diameter - DC 200

For this application, the DC-200 and water flow systems provided the lowest weights. From the standpoint of safety, however, the DC-200 could have a definite advantage over water due to its low vapor pressure. At 350° F, the vapor pressures of water and DC-200 are 135 and 3.6 psia, respectively. The pressurized water line has a higher probability of causing damage to the spacecraft and crew in the event of a puncture. In the weightless environment of space, a punctured DC-200 line within the cabin would be relatively simple to repair if the cabin pressure were higher than the fluid vapor pressure.

Although the fluid selection analysis assumed the use of the Isotope/Brayton cycle at a waste heat utilization load of 4.0 Kw, the results can be extended to the remaining candidate power conversion systems at various power levels. In the case of waste heat removal from the shield, however, radiation damage and fluid activation must be considered. On this basis, either NaK or H₂O would be preferable to DC-200 as a shield coolant.

5.4.2.2 Heat Pipe

The concept of transferring power with heat pipes from the waste heat sources to the various users was investigated. In order to arrive at an attractive a system as possible, it was necessary to select the heat pipe fluid and heat pipe transmission configuration most suitable for this application. For waste heat removal from the working fluid and heat rejection loops the heat pipe fluids are restricted to the organic fluids, water and ammonia. In the case of waste heat removal from the reactor shield, alkali metal heat pipes are a possibility.

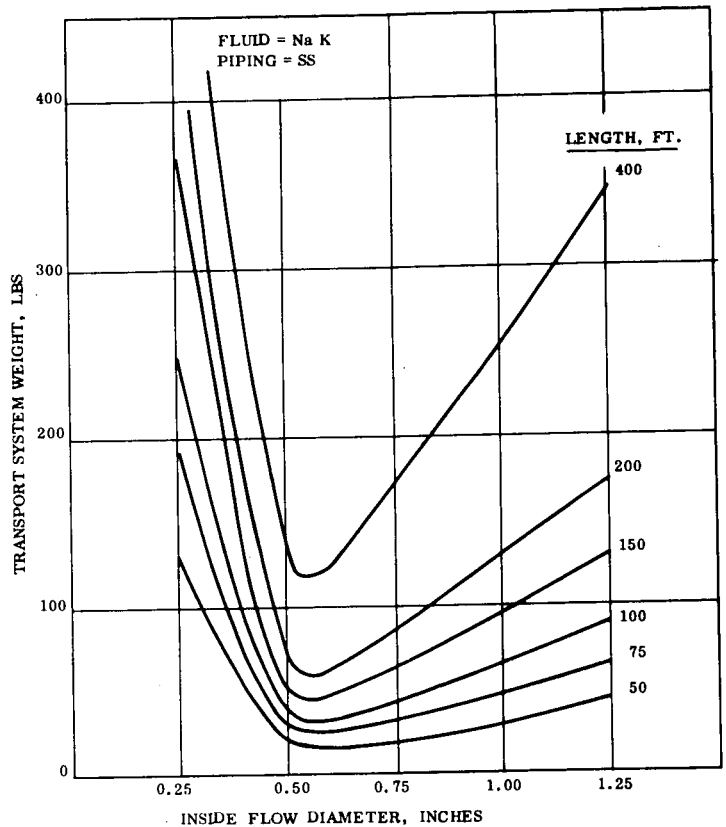


Figure 5-18. Energy Transport System Weight as a Function of Flow Path Length and Tube Diameter - NaK

First, heat pipe transport at lower temperatures is considered while shield waste heat removal is treated later.

5.4.2.2.1 Waste Heat Removal from Power Conversion Loops

In view of the large transport distance involved, the capillary pumping and vapor flow properties of the heat pipe fluid are of particular importance. Figures 5-19 and 5-20 illustrate the vapor energy transport and capillary pumping capability of various fluids, respectively. The vapor flow parameter indicates the ability of a vapor to transport energy through a given flow diameter without suffering a large pressure (and temperature) drop. At the higher end of the temperature range methyl alcohol, ethyl alcohol and water appear to offer exceptional performance in this regard. The capillary flow parameter offers a quantitative measure of the ability of a particular fluid to be pumped by capillary action. On this basis, water is the outstanding choice with the alcohols providing a poor second choice.

Due to its superior capillary pumping and vapor flow properties, water was selected as the heat pipe working fluid. Materials found to be compatible with water for heat pipe applications are nickel and copper; the higher thermal conductivity, workability and lower cost of copper makes this material the preferred choice.

Several basic parameters are of importance in determining a minimum weight heat pipe system, specifically: the number of heat pipes, length of the heat pipes and heat pipe diameter. Obviously, the number of heat pipes and individual length are interdependent.

Theoretically, heat pipes can be designed to operate with extremely long lengths; however, in view of the practical experience accumulated by various investigators over the past several years, it was decided to limit the heat pipe lengths to a maximum of 30 feet. Therefore, in the case of the Isotope/Brayton system, the transmission distance may be traversed with a single heat pipe length. However, the long distances, characteristic of the reactor power systems, require a number of heat pipes thermally coupled in series. Two means of accomplishing this are shown in Figure 5-21. Of the two concepts shown, concept (a) offers less heat transfer resistance at the expense of system redundancy; due to the importance of maintaining a high temperature, this configuration will be used.

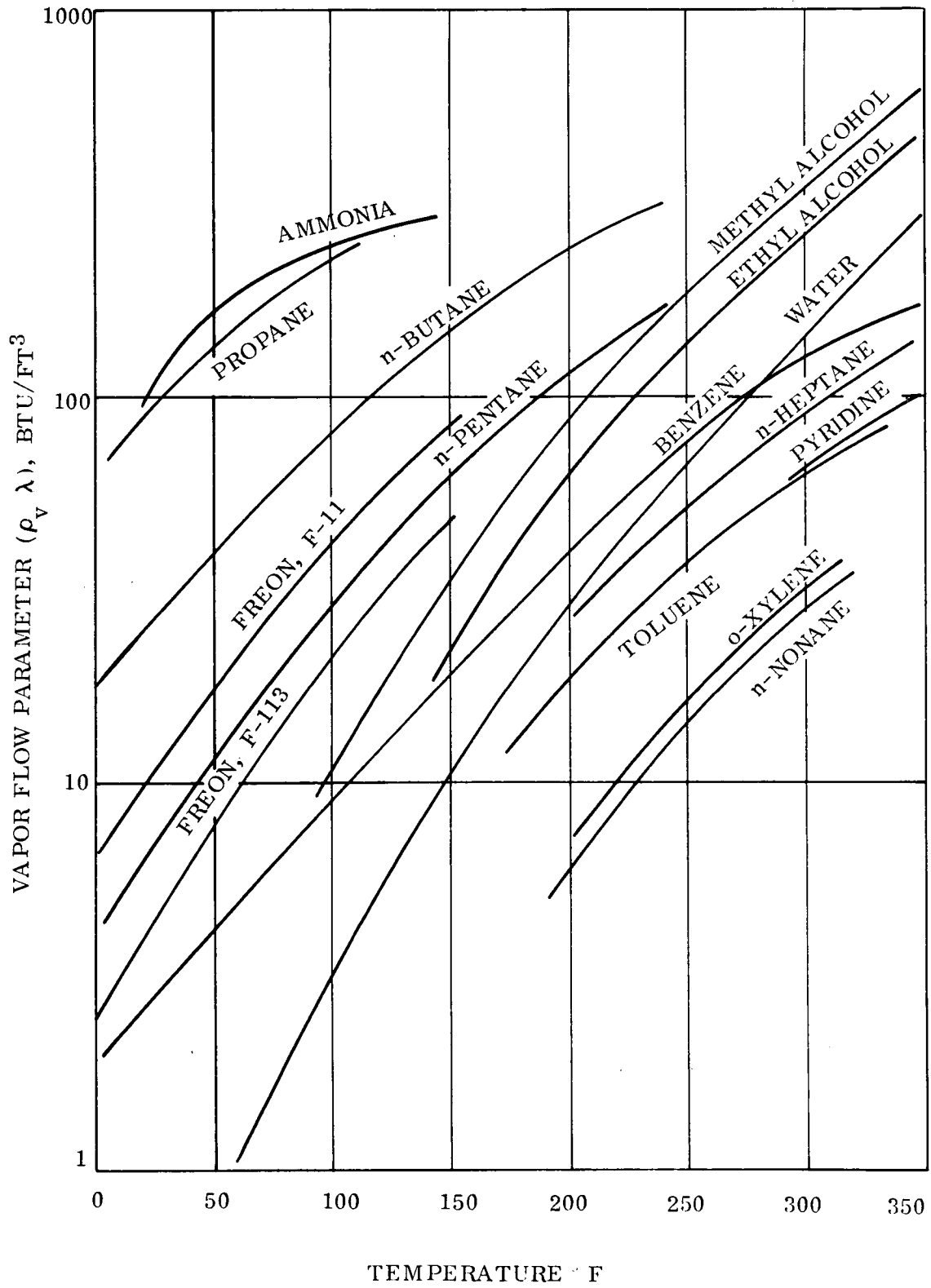


Figure 5-19. Vapor Flow Parameter vs Temperature for Various Fluids

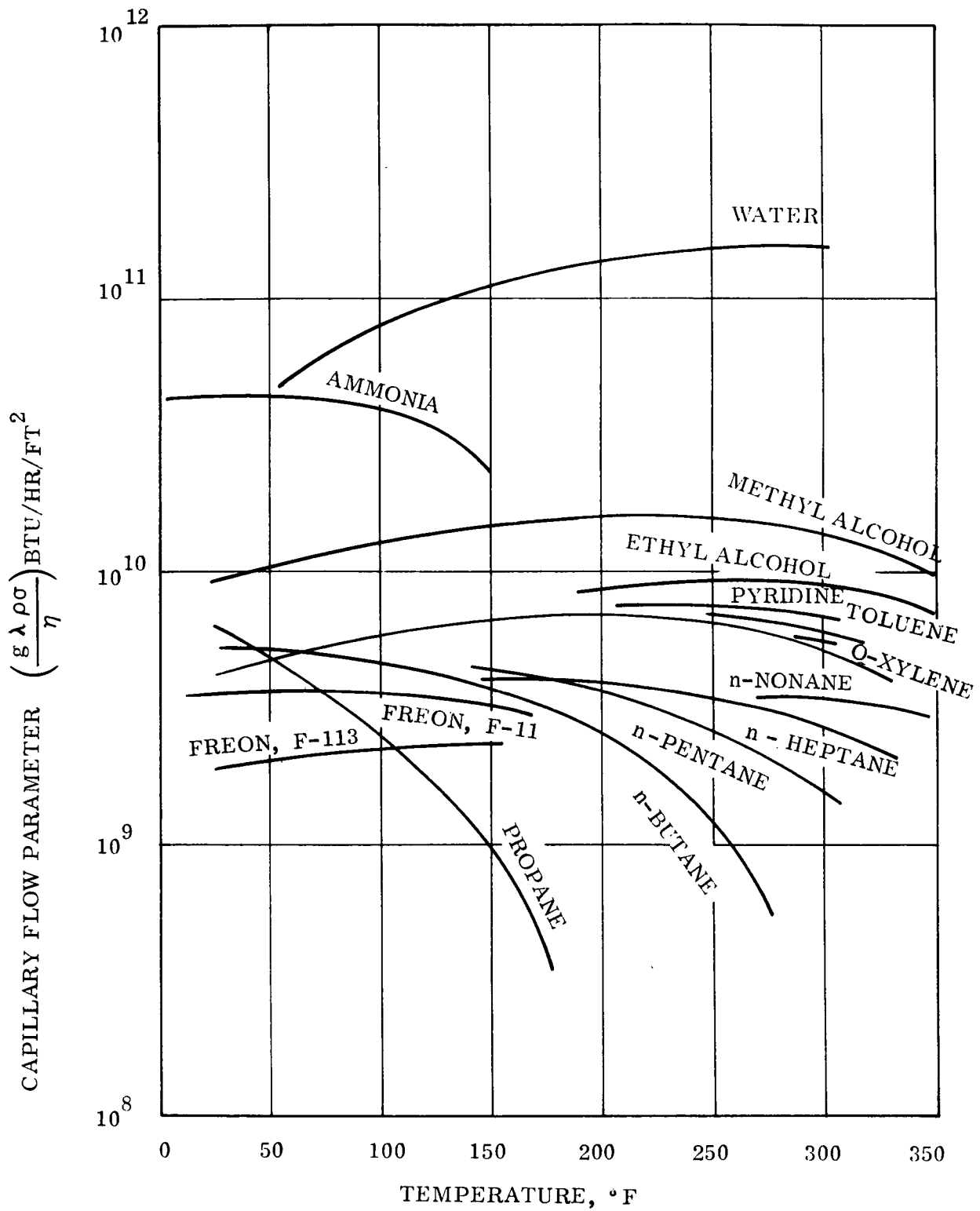


Figure 5-20. Capillary Flow Parameter vs Temperature for Various Fluids

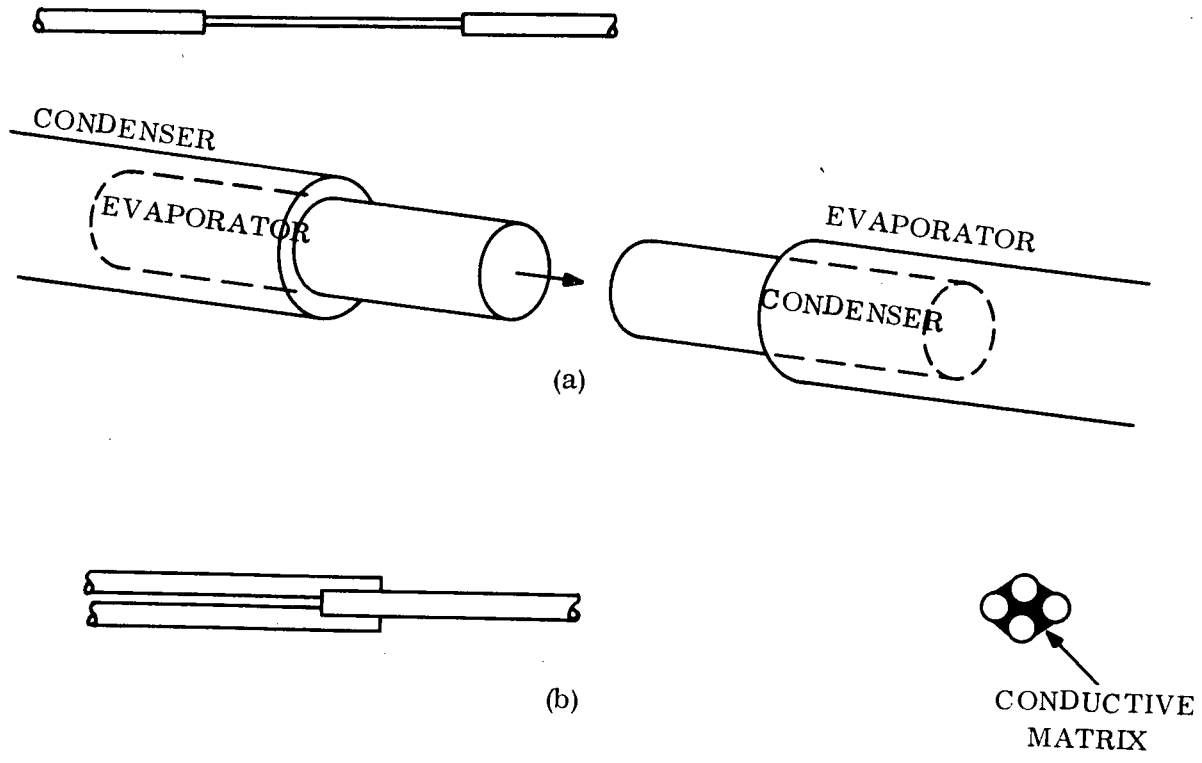


Figure 5-21. Schematic of Heat Pipe Concepts

The next consideration is to determine if any weight advantages accrue by providing parallel heat pipe paths for concept (a). This requires a determination of optimum heat pipe lengths, vapor space diameter and liquid return flow diameter as a function of heat pipe power level.

The heat pipe diameter is determined by the following factors:

1. Size of the vapor flow passage
2. Size of the liquid return passage
3. Heat pipe wall thickness

The inside pipe diameter must be large enough to transfer the required vapor flow rate without any appreciable pressure drop. Since the vapor temperature is exponentially dependent upon vapor pressure, even small vapor pressure drops can seriously reduce the heat pipe effective conductivity.

F

Required vapor passage diameters as a function of heat pipe temperature and power level are shown in Figure 5-22 for water. These values were obtained by means of the following relationship:

$$D_v \approx \eta \cdot 0.042 \left(\frac{Q}{\lambda} \right)^{0.375} \left(g_c \rho_v \frac{\Delta P_v}{\ell} \right)^{-0.208} \quad (5-1)$$

The possibility of a vapor temperature drop was eliminated by fixing $(\Delta P/\ell)$ at $1 \text{ lb/ft}^2\text{-ft}$. Of interest is the fact that small diameters are required at higher temperatures due to an increase in vapor density. Also of importance is the observation that large increases in the heat transferred can be accomplished by relatively small changes in flow diameter. This fact indicates that a number of small heat pipes may be heavier than one larger heat pipe carrying an equivalent heat load. Examination of equation 5-1, also implies that the heat pipe diameter is relatively insensitive to length.

In order to achieve the required liquid return flow characteristics over long distances, a composite wick was assumed. The heat pipe evaporator wick was assigned an effective pore size of 0.0014 inches (Reference 9-6); at 350°F the capillary pump rise for water was calculated to be 0.381 lb/in.^2 . An annular liquid return passage, covered by one layer of screen, was assumed for the condenser wicking configuration. The size of the annulus was calculated by equating the capillary pressure rise to the frictional pressure drop in the return annulus. Using the expression below, the results presented in Table 5-3 were obtained.

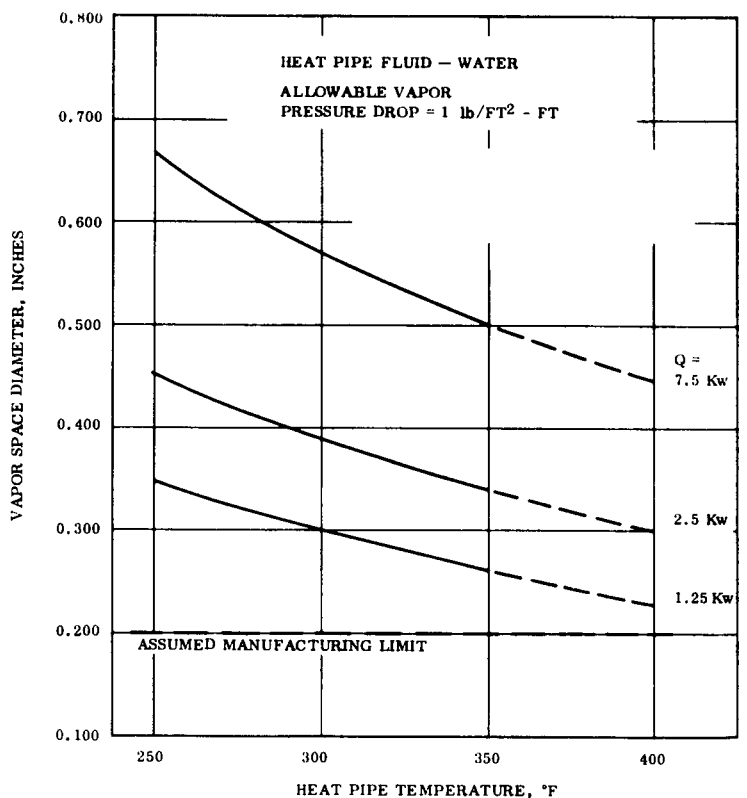


Figure 5-22. Required Vapor Space Diameters vs Heat Pipe Temperature at Various Power Levels

Table 5-3. Return Liquid Flow Annulus Width as a Function of Heat Pipe Length and Power Load

Power Level (kw)	Heat Pipe Length (ft)	Required Flow Annulus Width, $(D_v - D_p)/2$ (in.)
1.25	10	0.0080
	20	0.0101
	30	0.0115
	40	0.0127
2.50	10	0.0093
	20	0.0117
	30	0.0133
	40	0.0147
3.75	10	0.0401
	20	0.0427
	30	0.0445
	40	0.0460
7.50	10	0.0403
	20	0.0430
	30	0.0450
	40	0.0463

$$\frac{(D_v^2 - D_p^2)^3}{(D_v + D_p)^2} \sim \frac{\eta W}{p (\Delta P / l)} \quad (5-2)$$

The increase in pipe diameter with increasing heat pipe length is shown to be modest; this fact indicates that for a given total length, a series of fewer, longer pipes will be lighter than a series of many, shorter pipes.

Using the results for the vapor and liquid flow passages, weights were calculated for various transmission configurations. The following groundrules were used:

1. Heat pipe temperature = 350°F
2. Power transferred = 7.5 Kw
3. Overall distance = 25 ft., 200 ft.
4. Individual heat pipe power = 1.25 to 7.5 Kw

Figure 5-23 summarizes individual heat pipe weights as a function of power level and length.

Isotope/Brayton Cycle

Figure 5-24 illustrates the variation of heat pipe weight for situations where 1 to 4 heat pipes are used to transfer 7.5 Kw the required distance. As shown, utilizing a single heat pipe with a heat load of 7.5 Kw is lighter than using two heat pipes operating at 3.75 Kw each; this trend continues for larger number of heat pipes.

Two considerations, however, may suggest the selection of a multiple number of heat pipes as opposed to a single heat pipe. First, in the event of a heat pipe failure, the multiple concept would allow operation to continue at a reduced level. Secondly, the problem of transferring heat in and out of the heat pipe may be simplified by providing more than one heat pipe.

Reactor Conversion Systems

The reactor conversion systems require an energy transmission distance of 200 feet; this requires a minimum of 8 heat pipes in series. Therefore, the heat pipe temperature at the waste heat source will be higher than the heat pipe temperature at the user end due to the thermal resistances between heat pipes. Three principal resistances are present: the condensing liquid film, the pipe wall and the evaporator wick matrix. Of these, the high conductivity of the copper pipe and wick makes the latter two resistances small; however, the low conductivity of the liquid film can cause substantial temperature drops. Figure 5-25 plots the required heat transfer area between heat pipes in series for each of the reactor systems as a function of the power transferred per heat pipe. The following was assumed:

1. Total heat transferred = 7.5 Kw
2. Source temperature:
 - a. Reactor/Brayton = 299°F
 - b. Reactor/Organic Rankine = 306°F
 - c. Reactor/Thermoelectric = 599°F
3. User temperature = 270°F
4. Condensing film thickness = 0.005 inches
5. Number of heat pipes in series = 8

The reactor/thermoelectric system requires the least heat transfer area per junction due to the larger temperature drop allowable; however, a fluid other than water must be used in the first three heat pipes emanating

from the source due to the excessively high temperatures. Even with the optimistic assumption of a 0.005 inch condensing water film, significant amounts of heat transfer area are required per junction. For example, with a 0.50 inch pipe diameter, the 0.676 ft² of heat transfer area required for the reactor/thermoelectric system translates into an interface length (Figure 5-21a) of over 5.0 feet or an extended surface area design. Heat transfer area requirements for the Reactor/Brayton and Reactor/Organic Rankine appear prohibitive. Using the results shown in Figure 5-23, the minimum heat pipe system weight, assuming no temperature drop between heat pipes, is 45 lbs. Comparison of this highly optimistic number with the 60 pounds calculated for the DC-200 active loop indicates that there is no incentive for attempting to further the state-of-the-art for the heat pipe transmission concept.

5.4.2.2.2 Waste Heat Removal from Reactor Shields

Two alternatives were investigated for the transmission of waste heat from the reactor shield by pipes -- neither of these options appeared attractive.

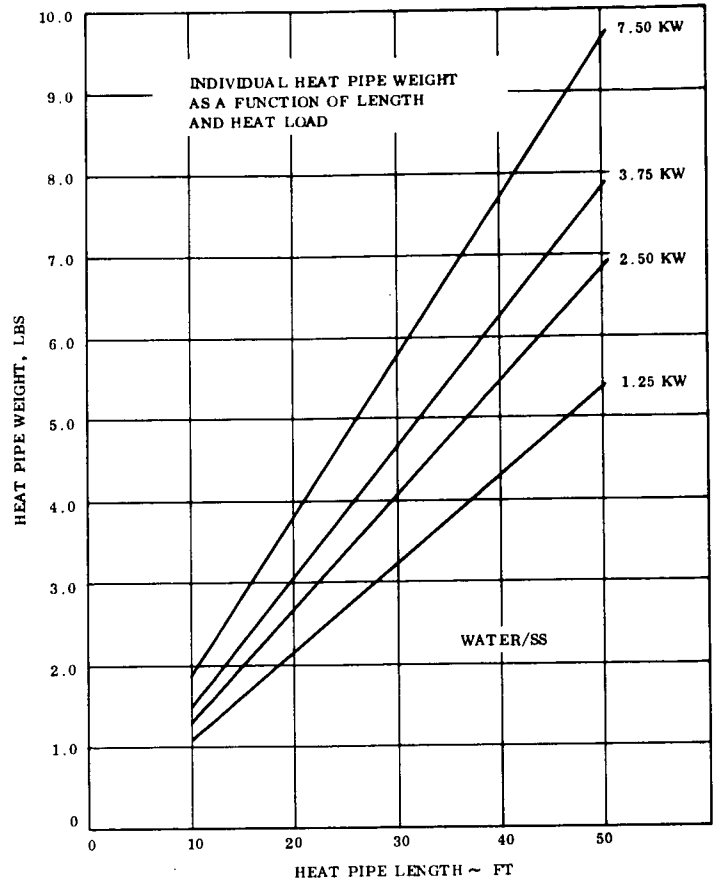


Figure 5-23. Individual Heat Pipe Weight as a Function of Length and Heat Load

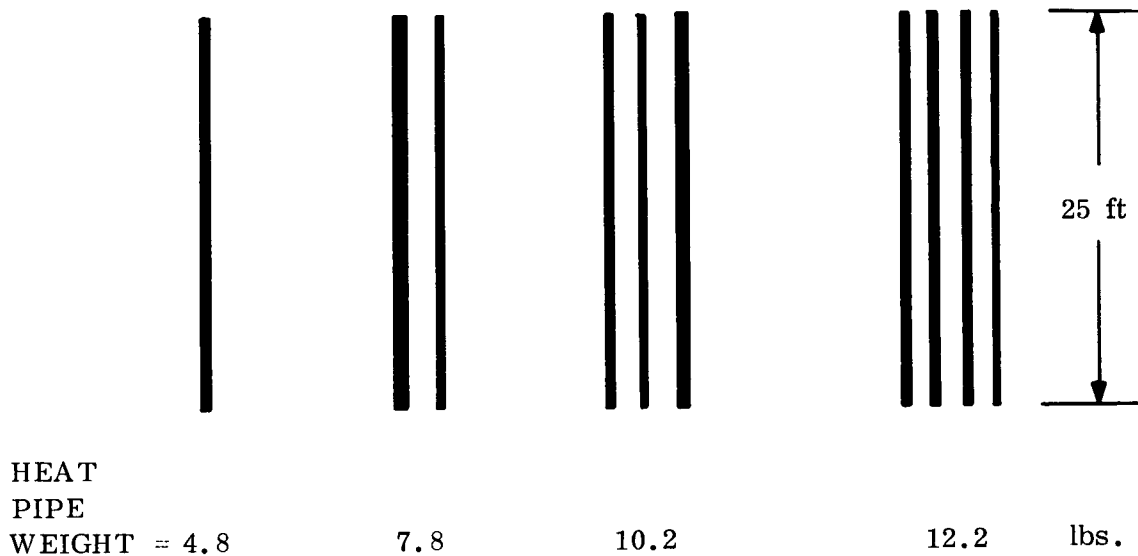


Figure 5-24. Variation of Heat Pipe Weight with Multiple, Parallel Paths - Isotope/Brayton Cycle

The first option was to utilize a water heat pipe concept. However, since the upper temperature limit for a water heat pipe is 450^oF, it is impossible to utilize the higher source temperature of the shield to overcome the temperature drop problem at the heat pipe series interfaces.

The second alternative is to utilize an alkali metal heat pipe transmission system, such as potassium to receive heat from the shield at 900^oF. This provides an available series transmission ΔT of approximately 630^oF to the highest temperature user. Calculation of the required heat pipe diameters for potassium at 900^oF indicates a factor of 3 increase over the water heat pipe diameter at 350^oF. Secondly, as the heat pipe temperature decreases along the series path, other fluids must be used which have a higher vapor density. This approach offers additional complexity and weight as compared to the active loop transmission system. The use of heat pipes does not lend itself to taking advantage of the higher

shield temperature without introducing additional developmental problems and higher waste heat utilization system weight. Consequently, the active loop approach seems more desirable for heat removal from reactor shields.

5.4.3 POWER DISTRIBUTION

The factors of importance in the design of the waste heat distribution system are the relative location of the users, the flow rate requirements and the reliability of the flow system. Relative location of each user is not defined at the present time; however, several of the waste heat users such as the urine recovery, fecal collection, shower and laundry facilities can be assumed to be in close proximity. The power distribution system is envisioned as being a fluid loop.

Figure 5-26 illustrates a power distribution system in which the active fluid loop is connected in series with the individual users. The indicated valving arrangements make it possible to separate one or more of the users from the loop when waste heat is not desired. In this approach, the fluid temperature decreases along the loop, therefore the users are inserted in the line in order of decreasing temperature. This characteristic may result in an excessively long flow path if the consecutive location of the users is far apart. The emergency mode operational requirement of the water storage ($\geq 250^{\circ}\text{F}$ source) necessitates a separate line from an upstream location. Table 5-4 lists the maximum and minimum flow rate requirements along with inlet and outlet temperatures for each of the power conversion systems assuming waste heat removal from the working fluid loops. Required flow rates were obtained by assuming operation of one urine and one CO_2 recovery unit at the maximum

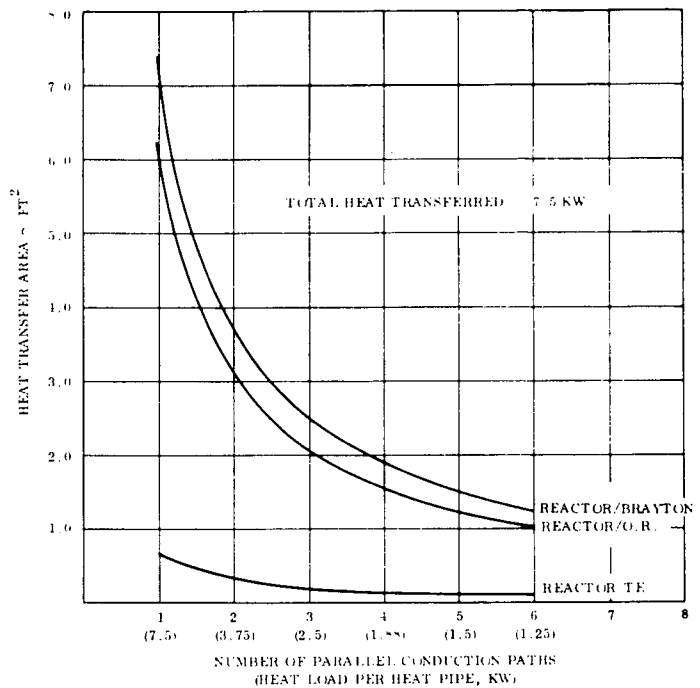


Figure 5-25. Required Heat Transfer Area Between Heat Pipes in Series as a Function of Heat Load

waste heat utilization condition and the urine recovery unit at the minimum condition. The reactor/thermoelectric system requires the lowest flow rate due to the availability of a higher temperature heat source. As a direct consequence of the low operating temperature of its working fluid loop, the reactor/Brayton cycle requires significantly higher flow rates.

Figure 5-27 illustrates a parallel power distribution system in which all users receive energy at the same temperature. Power requirements are regulated by controlling the flow rate through each user. Comparison of Table 5-4 with Table 5-5 illustrates that at the maximum level of waste heat utilization significantly higher flow rates are required by the parallel configuration; however, at the minimum waste heat utilization case, the results vary with power system. In general, it is observed that the series configuration has a lower outlet temperature than the parallel concept; this characteristic will tend to reduce the size of the auxiliary heat exchanger.

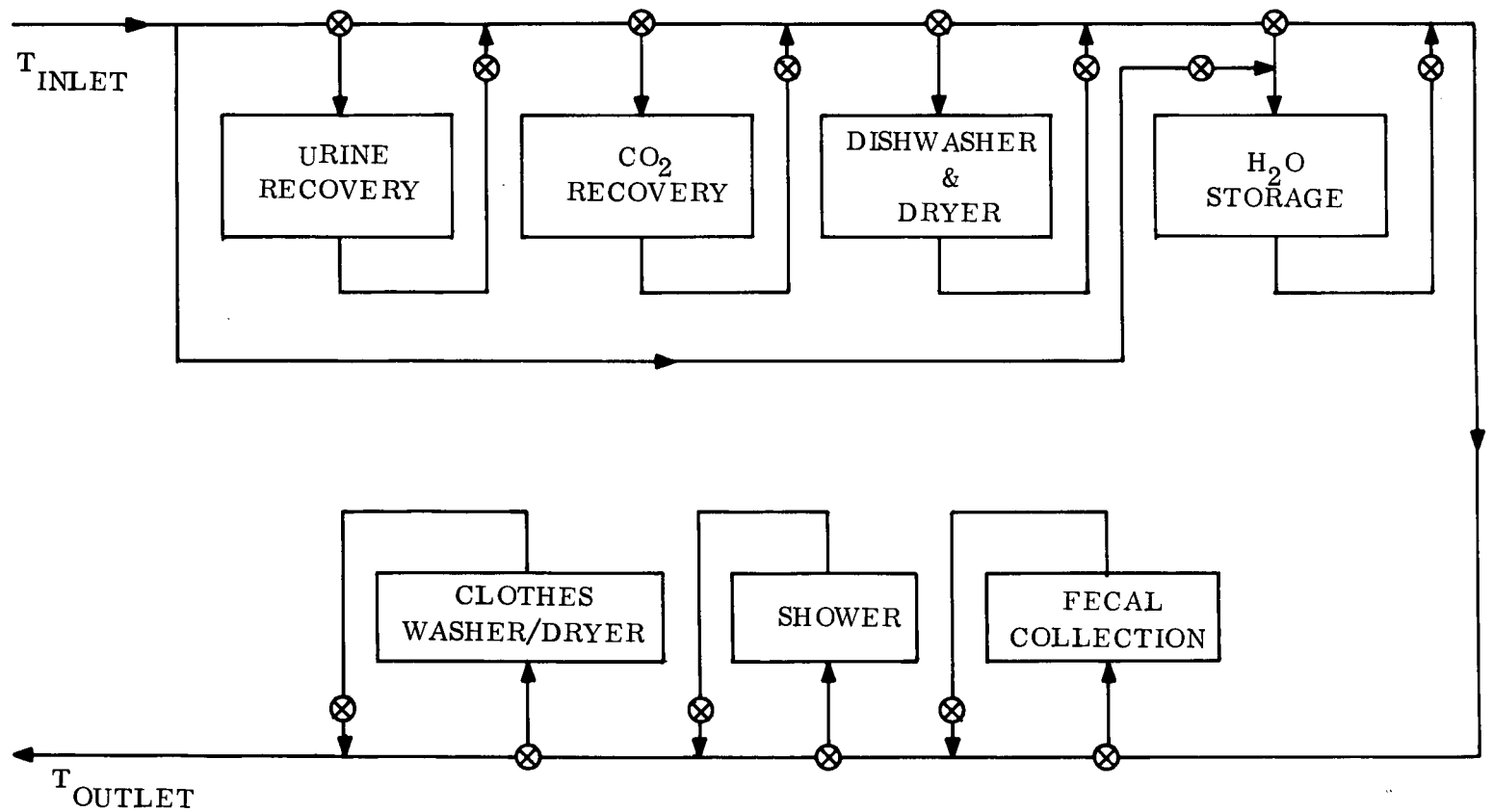


Figure 5-26. Layout of Series Power Distribution Concept

Table 5-4. Power Distribution System Characteristics for Series Configuration

System	Maximum WHU (7.5 kw)			Minimum WHU (2.9 kw)		
	Flow Rate (lb/hr)	T Inlet (°F)	T Outlet (°F)	Flow Rate (lb/hr)	T Inlet (°F)	T Outlet (°F)
Isotope/Brayton	462	343	223	245	343	256
Reactor/Brayton	1200	292	246	980	292	270
Reactor/T. E.	116	590	111	54	590	193
Reactor/O. R.	980	299	242	694	299	268

Table 5-5. Power Distribution System Characteristics for Parallel Configuration

System	Maximum WHU (7.5 kw)			Minimum WHU (2.9 kw)		
	Flow Rate (lb/hr)	T Inlet (°F)	T Outlet (°F)	Flow Rate (lb/hr)	T Inlet (°F)	T Outlet (°F)
Isotope/Brayton	623	343	254	239	343	254
Reactor/Brayton	1820	292	262	699	292	262
Reactor/T. E.	160	510	242	62	590	242
Reactor/O. R.	1400	299	259	538	299	259

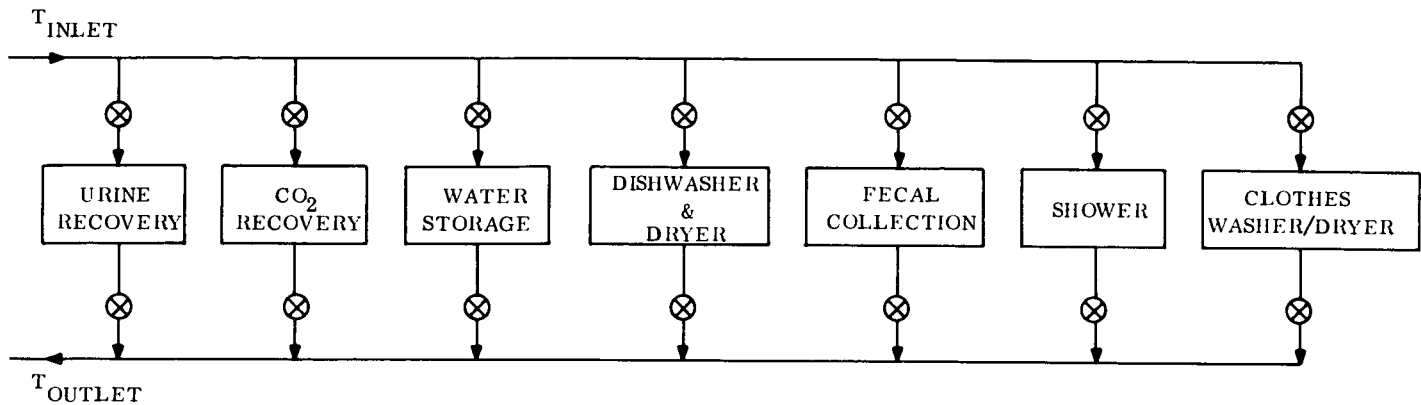


Figure 5-27. Layout of Parallel Power Distribution Concept

For an active loop transmission system, the power distribution system is integrated directly into the loop. In the case of a heat pipe transmission system, the power distribution loop can be convectively coupled to the heat pipe condenser sections.

From the standpoint of reliability, the two power distribution concepts are equivalent. In the event of a component failure, the affected user can be separated from the system by the appropriate valve action. Each system has the same number of valves and control of the power distribution is essentially the same.

In total, it appears that the series configuration may offer a small advantage due to its lower flow rate requirements at the higher power levels; however, this conclusion may be tempered by a comparison of total flow path length required for each system. A more detailed system definition would be required to assess this factor.

5.4.4 HEAT REMOVAL, TRANSPORT, AND DISTRIBUTION SUMMARY

The following conclusions can be drawn from the work presented in this section:

1. None of the power systems exhibit a large reduction in required radiator due to the utilization of waste heat

2. Use of configuration (a) or (d) (Figure 5-7) for the Isotope/Brayton cycle may lower the radiator fluid outlet temperature to the point where flow problems are induced.
3. No coolant flow problems at the lower heat sink conditions are present with either the reactor/thermoelectric or reactor/organic Rankine cycles.
4. Removal of heat from a reactor radiation shield using an active fluid loop may be attractive. A more detailed investigation is required to assess the overall impact on the reactor system design.
5. The active fluid loop concept using DC-200 is chosen to provide an effective, light-weight and safe approach to waste heat transport. A heat pipe transport system promotes developmental problems without a significant weight advantage.
6. Either a series or parallel power distribution system is compatible with the utilization of waste heat.

5.5 MAINTENANCE REQUIREMENTS

The long duration of the Space Station mission, 10 years, requires that attention be given to the maintainability of proposed systems in addition to a basic design philosophy of redundancy. For systems which are critical to life aboard the Space Station, such as the waste heat utilization loop, maintainability is particularly important.

Figure 5-28 pictures the waste heat utilization system defined in Section 5.4 as integrated with the working fluid loop of the Isotope/Brayton cycle. This system consists of two operating power conversion units; a standby power conversion unit is also available. Each operating power conversion loop is linked to the waste heat utilization loop by means of an auxiliary heat exchanger. During normal operation, each waste heat utilization loop would provide energy to two of the four space station decks. In the event of a failure in one of the waste heat utilization loops, the second loop can provide the necessary life supporting functions until repair or replacement of the inoperative system is effected.

The waste heat utilization loop consisted of the following components:

1. Auxiliary heat exchanger
2. Temperature balancing heat exchanger

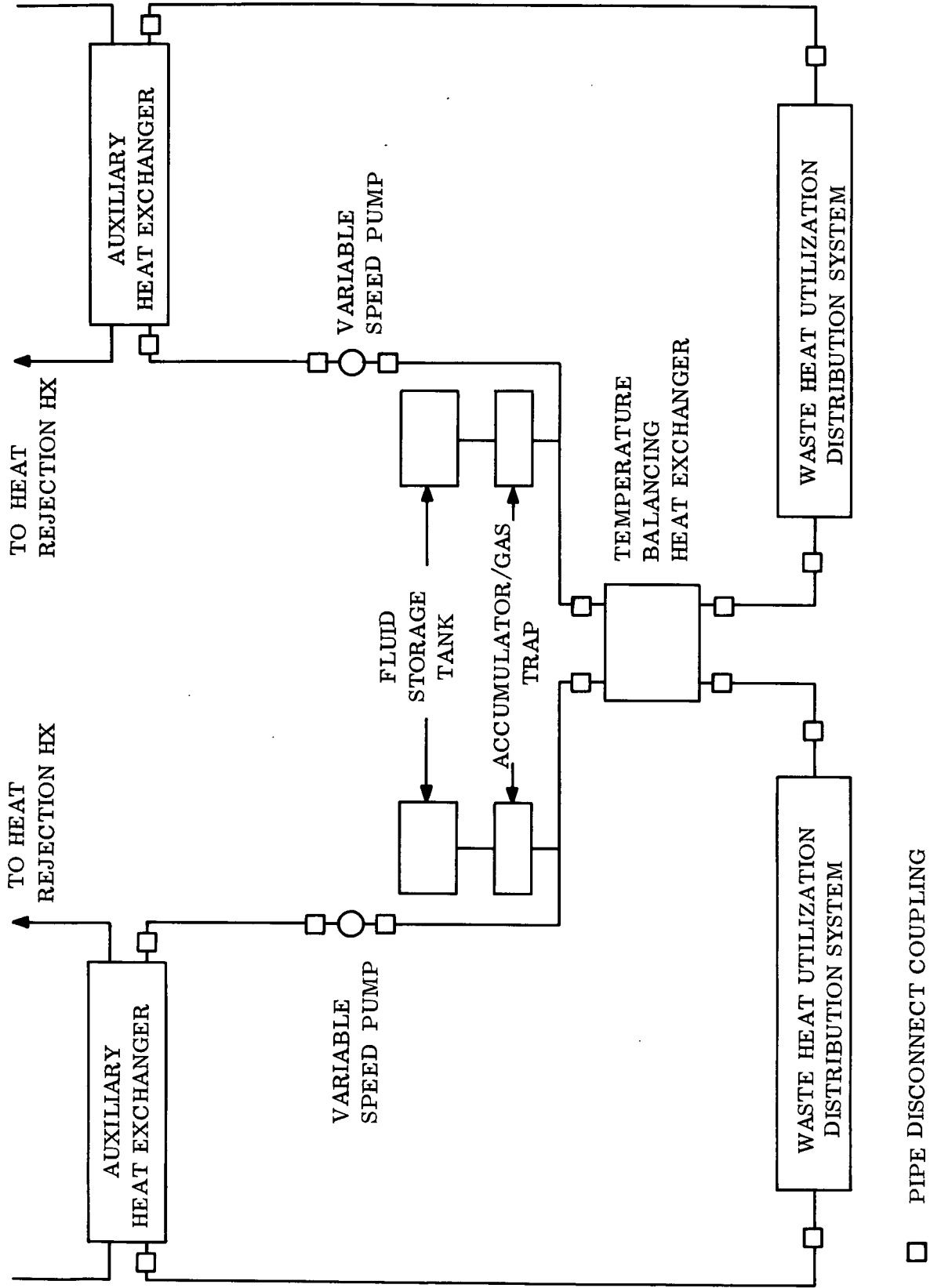


Figure 5-28. Isotope/Brayton Waste Heat Utilization System

3. Pump
4. Piping
5. Waste heat utilization power distribution system (see Figure 5-26).

The overall power demand of the waste heat utilization system is regulated by the flow rate of the DC-200 through the auxiliary heat exchanger. Temperature (and power) requirements of individual users are controlled by the valves shown in the distribution system.

The types of failures which can be anticipated in the waste heat distribution system are:

1. Leaks in the heat exchangers due to manufacturing
2. Leaks in the accumulator/gas trap and make-up tank assembly
3. Pump failures
4. Valve failures
5. Piping ruptures

The most probable source of failures will be in the pump and proportional control valves. The probability of meteoroid punctures in the piping, heat exchangers and storage tank is negligible due to the fact that in the Isotope/Brayton design the vehicle provides complete meteoroid protection.

Maintainability of the waste heat utilization loop can be enhanced by the use of quick-disconnects in the piping system. These fittings allow for separation and removal of components from the loop with only small losses of fluid. The use of DC-200, which is innocuous to human life, reinforces the feasibility of this approach. Use of quick-disconnects offers the following options to maintainability of the waste heat utilization system:

1. Replacement of critical parts at opportune periods prior to failure
2. Replacement at time of failure
3. Removal and repair of a failed component while loop is temporarily shutdown

The flow schematic shown in Figure 5-28 illustrates the proposed waste heat utilization loop with the appropriate locations for the quick-disconnects. This design allows for removal of the power conversion system, pump or temperature balancing heat exchanger.

If a difficulty arises which necessitates replacement of the piping, disconnects on the inlet and outlet to the waste heat utilization distribution system simplify this procedure. Replacement of individual users can also be accomplished by the use of disconnect fittings as illustrated in Figure 5-29.

The remaining portion of the waste heat utilization system which does not lend itself to replacement or repair, due to its inaccessibility, is the piping associated with the power distribution system. If reliability requirements indicate the necessity to do so, a dual circuit can be installed during vehicle construction to provide a redundant path for the DC-200 distribution system.

5.6 NUCLEAR HAZARDS

The incorporation of the WHU system into the Space Station design was assessed with respect to the nuclear safety impact on the crew. The effect of a nuclear radiation environment on the WHU system is potentially hazardous in two ways:

1. Irradiation damage to the coolant (DC-200) can result in an increase in fluid viscosity and a loss in the effectiveness of the WHU system.
2. Activation of DC-200 can transform the coolant into a hazardous source of radiation.

Both of these effects are amenable to early detection and as such, are able to be corrected before serious damage results. However, if these conditions can be anticipated, the problem can be avoided by selecting a different fluid.

Chemically, DC-200 is a dimethyl siloxane polymer; the elemental constituents of the fluid are: silicon, carbon, oxygen and hydrogen. The possibility of radiation damage to the fluid can be initiated by ionizing radiation from space as well as from the nuclear system. The

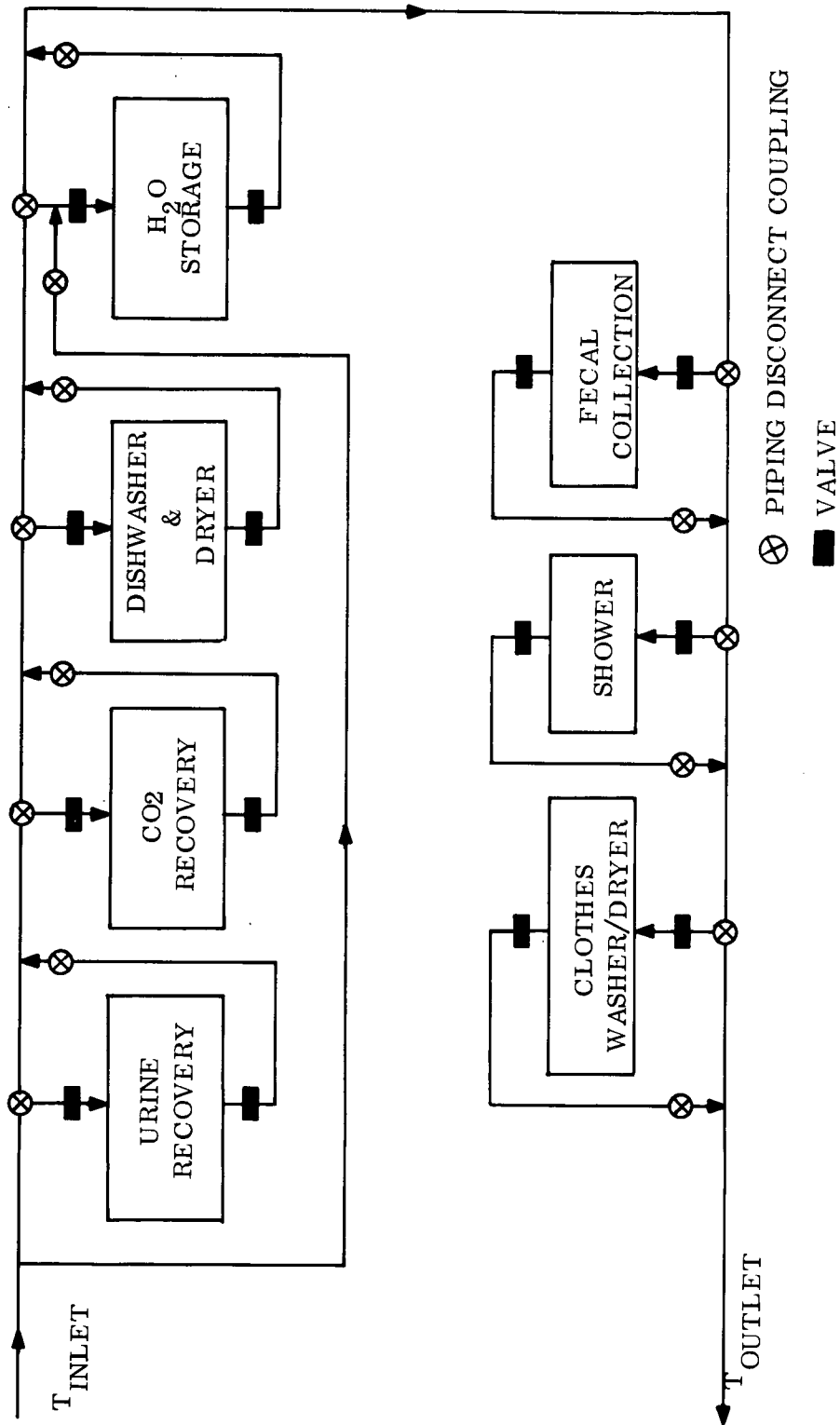


Figure 5-29. Layout of Series Power Distribution Concept Showing Quick Disconnect Coupling Locations

G

levels of radiation which are capable of causing damage to DC-200 are shown in Figure 5-30. Figure 5-30 indicates that ionizing radiation such as gamma rays and protons in excess of 10^6 rads will cause severe damage in DC-200. For fast neutrons (1 Mev equivalent) severe damage to DC-200 can occur at dose levels higher than 0.5×10^{15} neutrons/cm².

In the Isotope/Brayton system, the dose rate received by the DC-200 will depend upon the position of the DC-200 accumulator, the type of fuel and shielding provided. For the McDonnell/Douglas reference design, the combined neutron and gamma dose rate in the vicinity of the power conversion system is approximately 200 mr/hr which results in a neutron dose of 1.5×10^{11} n/cm² and a gamma dose of 3.55×10^3 rads over a five-year period. An additional dose of 2.8×10^3 rads will be contributed by geomagnetically trapped radiation, solar proton events and galactic cosmic rays.

In summary, the integrated neutron dose is 4 orders of magnitude less than that necessary to induce severe damage in DC-200 and 3 orders of magnitude less than that required to result in moderate damage. The level of the combined background and isotope source ionizing radiation dose is approximately 2-3 orders of magnitude lower than that required to induce moderate to severe damage after five years.

The second problem, fluid activation, is most likely to occur in DC-200 by neutron capture of Si³⁰ to yield Si³¹ (η, γ reaction). In order to assess the possibility of DC-200 being a secondary radiation hazard source, it was assumed that 25 pounds of DC-200 was located within a neutron flux of

$$10^3 \frac{\eta}{\text{Cm}^2 \text{-sec}}.$$

As a conservative measure,

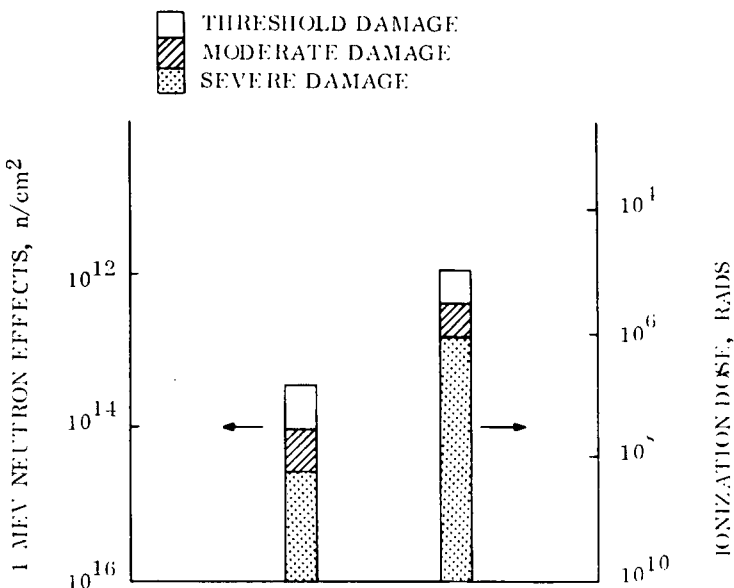


Figure 5-30. Radiation Damage Effects in DC-200

the DC-200 was assumed to consist solely of Si^{30} atoms. At a distance of 10 cm from the DC-200 the dose rate was $10^{-4} \frac{\text{mr}}{\text{hr}}$ which is several orders of magnitude below allowable levels.

It can be concluded that the use of a DC-200 WHU system, coupled with the Isotope/Brayton cycle, will not be subject to radiation damage, nor will it become a serious source of radiation to the crew.

Current designs of reactor power systems show lower dose rates in the power conversion equipment area than is present in the Isotope/Brayton cycle. Therefore, no nuclear hazard will be introduced by use of a DC-200 WHU system for these reactor system designs. The use of a shield cooled WHU system, discussed in Sections 5.3 and 5.4, however, could result in fluid activation to the degree where a hazard would be induced.

5.7 ALTERNATE APPROACHES TO WASTE HEAT UTILIZATION

Results of Section 5.4 have shown the utilization of power system waste heat for various life support functions to be a feasible concept. In order to determine its overall attractiveness, an evaluation of alternate approaches to the waste heat utilization (WHU) concept is provided in this section.

The obvious alternative to the WHU approach is to increase the electrical power output of the primary power system. The required heat energy can then be supplied upon demand by means of electrical resistance heaters. This approach, however, involves the conversion of heat energy into electrical energy and finally, back to heat energy.

Another possibility, which converts nuclear energy into heat energy, is the use of radio-isotope power. This technique can be designed either as one central unit or several individual heating units for one or more user.

Other approaches to supplying power to waste heat users were also considered; however, because of their relative unattractiveness these are mentioned only briefly.

5.7.1 PRIMARY POWER SYSTEM CONCEPT

Each of the power systems is capable of providing power to the waste heat users by electrical heaters. The increase in the system weight necessitated by this additional function is discussed below for each power system.

The total weight of the Isotope/Brayton power system is shown in Table 5-6. This weight includes 2 complete power systems with a reserve Brayton power conversion unit; net electrical power output from this system is estimated to be 25.0 kWe. Increasing the power level of the system can be expected to increase the subsystem weights proportionately, with the exception of the shield weight. Relatively large changes in nuclear power sources can be achieved without necessitating a substantial increment to the shield thickness. Therefore, the total power system weight is estimated to increase at 448 lbs/kWe of output.

Assuming no heat losses, the net power output capability of the system must be increased 7.5 kWe to satisfy peak user demand. Total increase in the power system weight is calculated to be 3360 pounds. Additional weight requirements in the form of heating coils, controls and insulation is expected to be comparatively negligible.

A weight breakdown for the reactor/Brayton, reactor/thermoelectric and reactor/organic Rankine cycles is given in Tables 5-7, 5-8 and 5-9, respectively. Using the reasoning previously stated, the shield, docking adapter and EOL disposal system weights can be subtracted from the total system weight before calculating the expected power system specific weight increases.

For a base power level of 29 kWe the reactor/Brayton power system weight is 478 lbs/kWe. By increasing the reactor power level, it is estimated that the system output can be raised to 54.0 kWe or a system specific weight of 257 lbs/kWe. Consequently, the power system weight penalty is estimated to be 3590 and 1920 pounds for the 29 kWe and 54.0 cases, respectively.

Table 5-6. Isotope/Brayton Weight Summary

System	Weight
Heat Source (2 at 1710)	3,420
IRV (2 at 750)	1,500
Shielding (2 at 1500)	3,000
Brayton Cycle PCS (3 at 998)	2,994
PCS Electrical and Support (2 at 275)	550
Heat Rejection and Radiator	1,737
Structural-Mechanical Integration	<u>1,000</u>
Power Source Subtotal	14,201

Using the data in Table 5-8, the reactor/thermoelectric specific weight is calculated to be 388 lbs/kWe for a net power output of 29 kWe. However, by including a supplemental radiator which allows an increase in power level to 41.4 kWe, this figure can be reduced to 342 lbs/kWe. For a maximum user load of 7.5 kWe, the respective increases in power system weight amounts to 2560 and 2910 pounds for the 342 and 388 lbs/kWe examples.

A summary of the reactor/organic Rankine system weight is shown in Table 5-9 for a 50 kWe power output. The effective power system specific weight is calculated to be 370 lbs/kWe for a weight increase of 2770 pounds.

The weight increases cited represent a base to which the weight of insulation, controls and heater units must be added. These additions are expected to be relatively small.

Table 5-7. Reactor/Brayton Weight Summary

Item	Weight (lb)
Reactor	1,650
Primary Loop	479
Intermediate Loops	1,359
IHX	130
BHX (3)	450
Structure	500
Docking Adapter	200
Radiation Shield	8,930
Radiator	2,732
HRL Pumps and Valves	96
Power Conversion Units (3)	5,580
Controls and Auxiliaries	<u>950</u>
Total NRM	23,056
EOL Disposal System	<u>3,250</u>
Total NRM with EOL Disposal System	26,306

5.7.2 RADIOISOTOPE HEATERS

The radioisotope heater concept is envisioned as a fuel matrix surrounded by appropriate shielding material and insulation. An active fluid loop, passing through the fuel/shield assembly, transfers the necessary power to the users; for simplicity the entire configuration is assumed to be spherical in shape. Excess radioisotope heat is rejected by a radiator system as shown in Figure 5-31.

Table 5-8. Reactor Thermoelectric System Weight Summary

Item	Weight (lb)
Reactor	1,650
Primary Loop Piping and Accumulator	400
IHX + HX	300
Intermediate Loop Piping and Accumulator	650
TE Modules	2,300
TE Pumps	680
NaK HRL Piping and Accumulator	1,250
NaK Radiator	2,430
Basic Structure	500
Controls and Wiring	420
Bus to Patchboard	300
Thermal Shroud	380
Docking Adapter	200
Radiator Shield	<u>13,060</u>
Nuclear Reactor Module (NRM)	24,520
EOL Disposal System	<u>3,250</u>
NRM with Disposal System	27,770
Supplemental Loop Piping, Accumulator and Pump	700

In order to evaluate the relative attractiveness between the use of a radioisotope heater and WHU five candidate radioisotopes were investigated: cobalt-60 (Co^{60}), strontium-90 (Sr^{90}), actinium-227 (Act^{227}), plutonium-238 (Pu^{238}) and curium-244 (Cm^{244}). The important parameters used in determining the desirability of these fuels are the weight of the fuel, weight of the required shielding and the cost of using such a system.

Table 5-9. Reactor/Organic Rankine System Weight

Item	Weight (lb)
Reference Reactor	1, 830
Primary Loop	489
Shield	40, 600
Intermediate Loop (includes heat rejection loop)	562
Power Conversion System (3 at 1784 lb each)	5, 352
Electrical/Electronics (3 at 563 lb each)	1, 688
Radiator/radiator Structure	5, 610
Structural Cone and Mounting Brackets	1, 000
Thermal Shroud and Actuators (0.5 lb/ft^2)	1, 875
Docking Equipment	300
Disposal Propulsion (15%)	<u>8, 895</u>
Subtotal	68, 201
Contingency (10%)	<u>6, 820</u>
Total Space Base Power Source Weight	75, 021

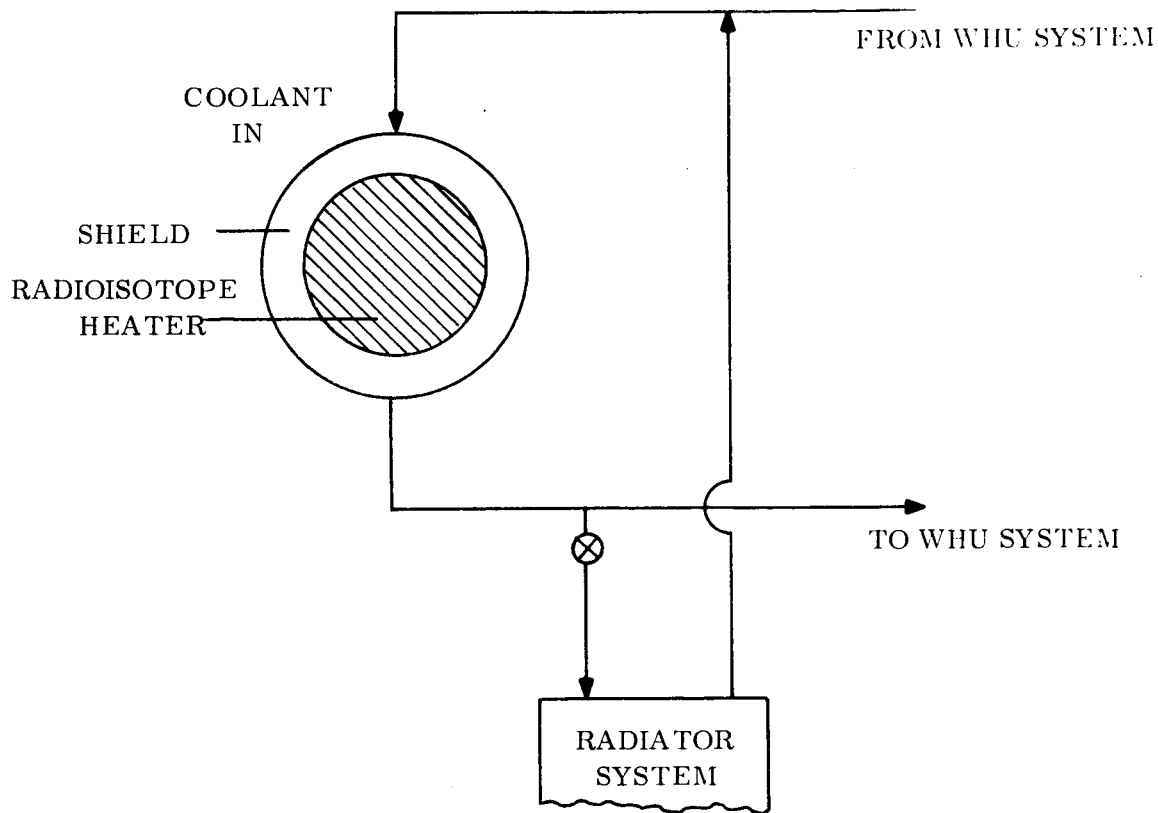


Figure 5-31. Isotope Heater Concept

Table 5-10 lists the characteristics of interest for each of the fuels. The half-life of the radioisotope is of importance since it determines the rate of power decay. Figure 5-32 illustrates the fraction of initial power available as a function of time for the radioisotope of interest. Assuming a power requirement of 7.5 Kw at the end of ten years, the BOL fuel inventories, given in Table 5-11 were calculated; also shown are the weight and volume of the fuel.

All of the radioisotopes emit gamma radiation, however, plutonium and curium require neutron shielding as well. The gamma shield was assumed to be made from depleted uranium except for Pu^{238} where lead was used to minimize the likelihood of criticality. Lithium hydride was used as the neutron shield. Shielding thicknesses were calculated assuming an arbitrary dose rate of 1.0 Mr/hr at a distance of 1.0 meter. In situations where a neutron and gamma dose was present, each dose rate was maintained at 0.5 Mr/hr at a distance of 1 meter.

Table 5-10. Radioisotope Fuel Characteristics

Fuel	Half Life, Yrs.	Power Density, W/cc	Density, g/cc
Co ⁶⁰	5.3	65.0	8.9
Sr ⁹⁰	28.8	1.5	4.5
Act ²²⁷	22.0	118.0	9.8
Pu ²³⁸	87.0	43.0	10.0
Cm ²⁴⁴	18.0	24.5	9.8

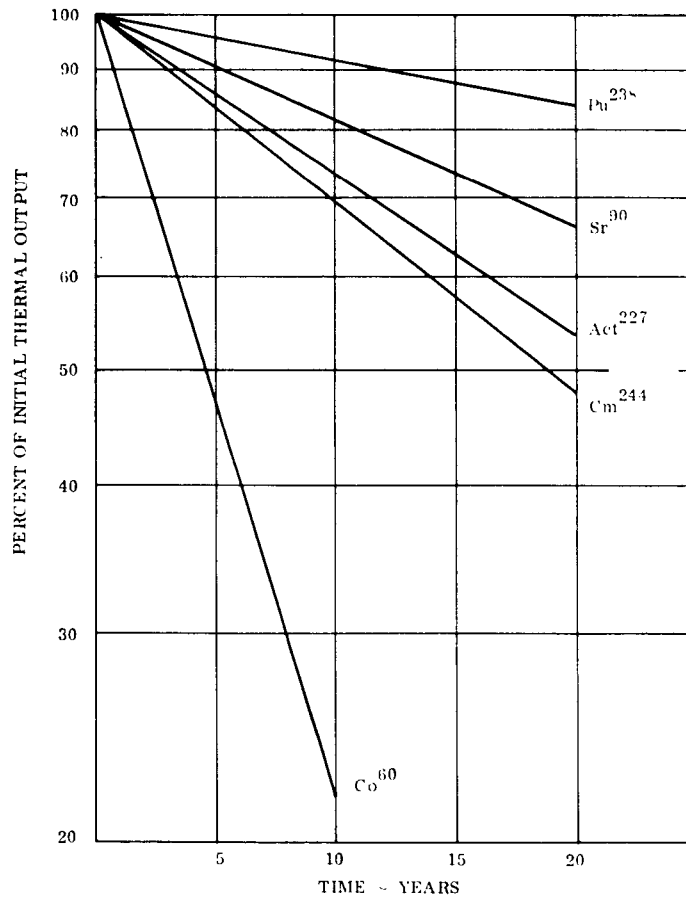


Figure 5-32. Fraction of Isotope Power Remaining as a Function of Time

Table 5-11. Required Radioisotope Fuel Inventories

Fuel	BOL Power, Kw	Fuel Weight, Kg	Fuel Volume, cc
Co ⁶⁰	28.0	3.8	430
Sr ⁹⁰	9.5	28.0	6400
Act ²²⁷	10.0	0.86	87
Pu ²³⁸	8.1	20.0	1900
Cm ²⁴⁴	11.0	4.4	450

Table 5-12. Radioisotope Shield Weight

Fuel	γ Shield Thickness, cm	γ Shield Weight lbs	n Shield Thickness, cm	n Shield Weight, lbs	Total Shield Weight, lbs
Co ⁶⁰	17.0	1760.0	--	--	1760
Sr ⁹⁰	12.0	2010.0	--	--	2010
Act ²²⁷	6.1	117.0	--	--	117
Pu ²³⁸	2.5	64.0	41.0	1000	1064
Cm ²⁴⁴	8.9	410.0	72.0	4510	4920

Table 5-12 summarizes the required shield thicknesses and weights. In order to achieve minimum weight the dense gamma shielding was assumed to be in closest proximity to the fuel. Actinium required the least shielding weight while curium exhibited the heaviest.

An estimate of the comparative costs for each of the radioisotope heaters can be obtained by adding the cost of the fuel to the cost required to orbit the heater. Assuming launch costs of $\$10^3$ /lb and the radioisotope costs listed in Table 5-13, approximate costs for each radioisotope heater were calculated. Cobalt-60 and strontium-90 provide the least expensive radioisotope heaters. The attractiveness of Co^{60} is however tempered by its short half-life which necessitates an initial power level of 28 Kw. This excess power, which must be rejected by the Space Station, results in an increase in the required radiator area.

Actinium is a promising radioisotope fuel which is still in the early stages of development. The target material from which Actinium-227 is made is radium-226, a relatively expensive material; therefore, actinium sesquioxide (probable fuel form) will cost approximately $\$10^3$ /w. One problem associated with the use of Actinium-227 is its high power density which can cause unacceptable temperatures within the fuel core. Various matrix materials are being examined to solve this problem. While a power system utilizing Actinium-227 has not been made it appears to be an attractive radioisotope fuel.

The significance of the excess available power is dependent upon the temperature at which the energy is rejected. If it is decided to use an alkali metal coolant a high rejection temperature could be utilized which would minimize the required radiator area. However, the use of an alkali metal coolant presents a hazard in the event of a fluid line puncture. By selecting Sr^{90} as the radioisotope, at a modest increase in cost, the heat rejection problem is minimized. The longer half-life of Sr^{90} results in an initial power level of only 9.5 Kw, thereby, allowing a reduction in radiator temperature for the same area. Therefore the coolant loop can employ an innocuous fluid such as DC-200 or Dowtherm.

Table 5-13. Radioisotope Fuel and Launch Costs

Fuel	Fuel Cost \$	Total Weight of Fuel and Shield lbs	Cost of Fuel and Launch, \$
Co ⁶⁰	0	1770	1.77×10^6
Sr ⁹⁰	1.35×10^5	2070	2.21×10^6
Act ²²⁷	10^7	119	10.1×10^6
Pu ²³⁸	5.3×10^6	1110	6.41×10^6
Cm ²⁴⁴	4.4×10^5	4930	5.34×10^6

The previous analysis used a dose rate criteria of 1.0 Mr/hr at 1.0 meter to assess the comparative shielding requirements of the radioisotopes. In actuality, the allowable dose rate will depend upon the background radiation from other on-board nuclear systems and the environment as well as the location of the radioisotope heater. In order to evaluate the effect of reducing the dose rate requirements on the radioisotope cost and system weight, an analysis was performed.

Figure 5-33 illustrates the change in fuel and shield weight with changes in dose rate and power. Translating weight and power into cost in the manner formerly presented, the cost per Kw of power is calculated as shown in Figure 5-34. Obviously, increases in power level and reductions in the shielding requirements markedly change the cost of the radioisotope per Kw.

5.7.3 MISCELLANEOUS ENERGY SUPPLY APPROACHES

Other methods of supplying heat to the Space Station users were examined. These included fuel cells, batteries, chemical energy and solar cells. All of these concepts appeared relatively unattractive as compared to WHU.

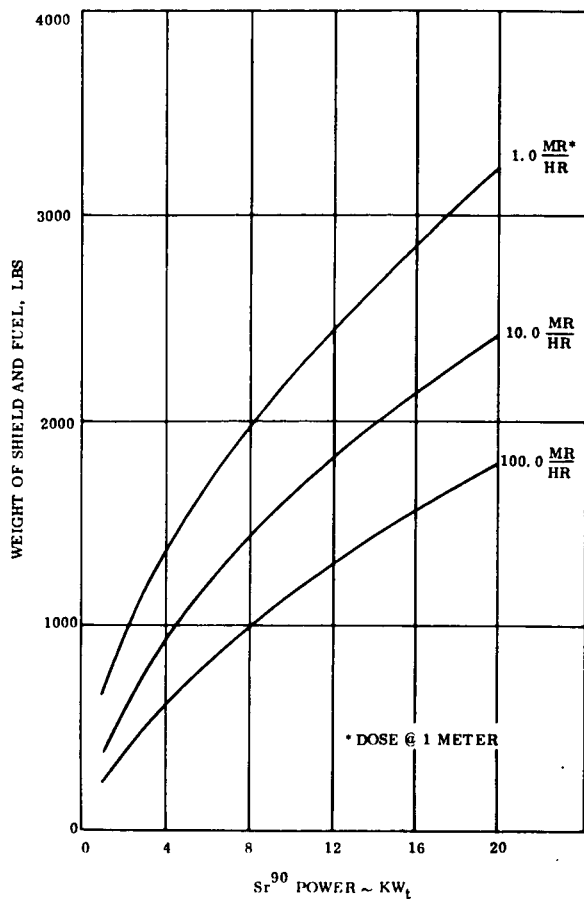


Figure 5-33. Weight of Fuel and Shield vs Dose Rate and Thermal Power

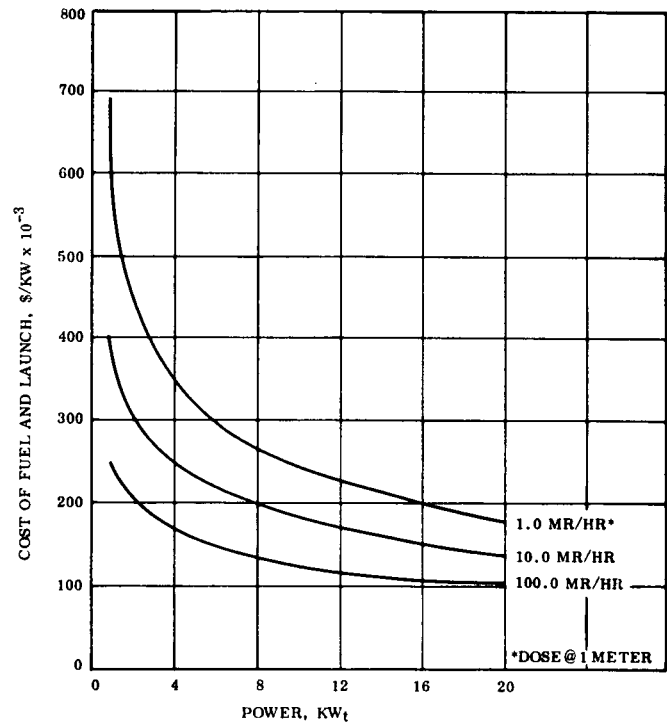


Figure 5-34. Cost of Fuel and Launch vs Dose Rate and Thermal Power

Batteries, fuel cells and chemical energy are all energy limited devices which require continuous resupply throughout the mission. Assuming an average user power requirement of 4.4 Kw for 10 years, the total weight for each of the candidates was calculated. Results are shown in Table 5-14. Solar cells provide the only reasonable concept of the four candidates, however, the effects of degradation over the extended mission lifetime will result in a higher weight than that shown in Table 5-14.

Comparison of the methods for supplying heat to the various users identified in Section 5.2 must be made on the basis of:

1. System weight
2. Reliability
3. Compatibility
4. Development, manufacturing and launch costs

Table 5-14. Miscellaneous Power Source Weights

Power Source	Energy Capacity	Total Mission Weight, lbs
Fuel Cells	$1.5 \frac{\text{lbs}}{\text{Kw-Hr}}$	5.6×10^5
Batteries	$10 \frac{\text{lbs}}{\text{Kw-Hr}}$	3.7×10^6
Hydrogen Combustion	$0.5 \frac{\text{lbs}}{\text{Kw-Hr}}$	1.9×10^5
Solar Cells	$1.0 \frac{\text{lb}}{\text{w}}$	4400

The system weight required for the alternate approaches has been presented in Section 5.7. The system weight increases for the WHU system are summarized in Table 5-15. For all four power systems the WHU concept can be incorporated into the design for an effective weight penalty of less than 350 pounds. This includes the addition of an independent heat exchanger and transmission subsystem for each of the power conversion units employed as well as reductions in radiator area. Due to its proximity to the manned areas, a transmission system for the Isotope/Brayton system is not required. The Isotope/Brayton, reactor/Brayton and reactor/organic Rankine power systems each contain 3 independent power conversion units and associated WHU subsystems within the entire system. Since the reactor/thermoelectric system does not contain entirely redundant conversion units, 2 WHU heat exchangers and transmission subsystems were coupled to the single power conversion system to obtain WHU redundancy.

Table 5-16 compares each of energy supply concepts. In general, the weight of the WHU system is less than that of the radioisotope or electric heater/powerplant approach. Use of the actinium-227 radioisotope, however, offers a isotope/shield system which is potentially lighter than any other concept considered.

C-4

Table 5-15. Weight Summary for the WHU Concept

Power System	Heat Exchanger Weight, lbs	Transmission System, lbs	Insulation, lbs	Distribution System, lbs	Radiator Weight Decrease lbs	Effective System Weight Penalty, lbs
Isotope/Brayton	30	-- 7	20	40	(86)	< 100
Reactor/Brayton	30	180	185	40	(98)	~300
Reactor/Thermoelectric	15	120	124	40	(11)	~ 300
Reactor/Organic Rankine	15	180	185	40	(82)	~ 300

Table 5-16. Comparison of Candidate Concepts

Concept	Weight lbs	Reliability	Compatibility	Development Cost	Manufact'rg & Launch Costs
Waste Heat Utilization System	1 < 350	2	2	2	1
Radioisotope System	2 120-2100	1	3	2	3
Electric Heater/Increased Power Plant	3 1900-3600	2	1	1	2

From the standpoint of reliability the radioisotope concept is rated highest due to the fact that standard flow equipment (pump, valves, etc.) are the only moving parts required in the system. Both the WHU and the electric heater/power plant system concepts depend upon the operation of sophisticated rotating machinery and/or reactor technology. However, due to the redundancy incorporated into the present designs, the attainment of adequate reliability should not constitute any major problem.

Increasing the size of the power plant to provide additional electrical heating capability may provide the simplest approach in terms of system compatibility. This concept requires a minimum of new components and does not introduce any unique technological capability. The WHU system will require redesign of the existing power conversion unit since an additional heat exchanger must be introduced into the present design. The effect of the WHU system on the control of the power plant must also be carefully investigated. Incorporation of the radioisotope concept into the Space Station presents several minor but real integration difficulties. First, the use of a radioisotope requires special handling considerations during the start-up and disposal phases of its life. Secondly, a separate heat rejection system must be employed which may aggravate an existing radiator area problem. Finally, the amount of shielding required may be a trade-off between weight and the mobility of the crew.

The development cost of each of the three approaches should not be prohibitive since the technologies involved are state-of-the-art. However, the use of the electric heater/larger power plant concept involves a minimum of development.

The cost of manufacturing and launching the candidate concepts should be least for the WHU system and highest for the radioisotope system. The lightweight and unsophisticated components associated with the WHU system are a definite advantage in this area. Increasing the size of the power plant requires higher fuel costs and substantial weight increases.

The WHU system "unit" cost is cheaper than the electrical heater/increased power plant approach. Although a detailed analysis of this comparison was not presented, this conclusion was reached using the following reasoning. The use of electrical heaters requires

an increase in the reactor thermal output which will yield a 7.26 Kw increase in the electrical output. This affects the cost of the system in two ways: first, a larger reactor system requiring more fuel, shielding material and a larger power conversion equipment is needed; secondly, the increase in the system weight will also result in a more expensive launch. The cost of designing and building a larger reactor power system cannot be easily assessed, but, may be substantial depending upon the development problems encountered. The increased launch costs (assuming $\$ 10^3$ /lb) are estimated to range between $\$2.0$ and $\$ 3.5 \times 10^6$ for the reactor/Brayton cycle. The increased costs resulting from the incorporation of the WHU system stem from a nominal redesign of the power conversion system and from including the WHU fluid loops in the design of the manned areas. In addition, the launch costs will rise $\$ 10^5$ to $\$3 \times 10^5$. Therefore, if the design and hardware costs of the WHU system can be kept in the vicinity of $\$ 3 \times 10^6$ it will definitely be less expensive than the electrical heater concept.

SECTION 6
CONCLUSIONS

Two areas of thermal energy management on board the thirty-three foot diameter NASA Space Station have been investigated during this program. First, the feasibility of employing an advanced, integrated heat transport and temperature control system to provide environmental control/life support functions was assessed. Secondly, the desirability of transporting and distributing "waste" heat from a nuclear power system to components requiring thermal energy in the cabin was evaluated.

Conclusions drawn from the first of these studies are listed below.

1. Thermal control system elements do exist that have demonstrated long life and high reliability characteristics. The Data Handbook tabulates performance and life parameters of many thermal elements.
2. Heat pipes are basically high reliability elements. Current technical understanding of the operation of these devices is sufficient to predict performance. The performance of composite wick heat pipes, however, was found to be sensitive to vapor/gas bubbles within the liquid flow passage and to fabrication techniques.
3. It is possible to design heat transport and temperature control systems, using heat pipes as primary elements, for the Space Station. Such systems can theoretically meet all thermal requirements, offer a weight advantage over the more conventional pumped liquid loop system, have inherent high reliability, and, with adequate process control and testing, would possess long functional lifetimes.
4. Of two heat pipe systems studied in detail, one utilizing variable conductance heat pipes mounted on the external radiator was judged the better.
5. This system requires the use of "high performance" heat pipes in order to be competitive, on a weight basis, to the pumped liquid loop system. Throughput capacities of up to 30 kw-ft are necessary. Development is required to attain this performance. Current state-of-the-art values are between 3 and 8 kw-ft.

6. Thermal interfacing between the heat pipes of the network is very critical to system performance. The study indicated that the application of conventional methods to this problem resulted in excessively heavy systems. An "advanced" design was suggested to yield vapor-to-vapor conductances of up to $7 \text{ w/in}^2 - ^\circ\text{F}$. Again, development is required to meet this goal. Conventional techniques produce maximum conductances of 1 to $2 \text{ w/in}^2 - ^\circ\text{F}$.
7. The modular heat pipe concept, in which a heat pipe is mechanically assembled from piece parts (interface cells and adiabatic lengths) offers significant maintenance advantages. Development of suitable mechanical couplers and wick joining processes is necessary to realize these benefits.
8. A prototype segment of the selected heat pipe system was fabricated employing "conventional" heat pipes and "advanced" interfaces. Functional thermal vacuum testing of this segment resulted in system temperature drops significantly larger than expected or desired. Specifically, thermal resistances of up to six times the design value were observed. Post-test analyses and subsequent small-scale testing indicated that the most likely cause of the large temperature drops was the presence of non-condensable gas in each heat pipe condenser (interface cell). It was felt that this gas entered the pipes during the fill procedure.
9. Evacuation, careful re-charge, and re-test of the heat pipes of one-half of this system did reduce the thermal resistances of the interface cells involved, but the minimum value was still three times that desired. It is concluded that: 1) the design value of resistance of the cells was somewhat low; and 2) the interface cell design employed is sensitive to even a minute quantity of non-condensable gas. The need for further interface cell development is thus indicated.
10. A second prototype segment of the selected heat pipe system was fabricated employing "conventional" heat pipes and "conventional" interfaces. Satisfactory system performance was attained with this system. Observed characteristics were:
 - a) Overall system temperature drop $\cong 0.8^\circ\text{F/W}$
 - b) Control of $118^\circ\text{F} \pm 3^\circ\text{F}$ at fin heat pipe evaporators
 - c) System weight of about 80 pounds.

The following conclusions were drawn from work performed during the waste heat utilization task:

1. The waste heat utilization scheme provides a feasible means of supplying various Space Station users with thermal energy. System characteristics compare favorably with those of alternative means of supplying this energy.

2. Pumped loop energy transport was found to be preferable to a heat pipe transmission system based on current heat pipe technology. If, however, high performance heat pipes and interfacing techniques were developed as called for in the advanced thermal control system study, this decision should be reviewed.
3. Either a series or parallel energy distribution system may be employed to deliver heat to the individual users. Quick-disconnect fittings would provide a considerable degree of component maintainability.
4. Each of the four nuclear power systems considered generates sufficient waste heat to supply Space Station user heat requirements. In general, 3 sources of waste heat were found in the various power conversion system designs. These were the radiation shield, working fluid loop and heat rejection loop. Using the shield as a source of waste heat is, however, complicated by nuclear system considerations.

SECTION 7 RECOMMENDATIONS

Because of the somewhat diverse nature of this program, recommendations resulting from the effort are divided into three categories. Any one of these groups can be undertaken independent of the other two.

The first group includes two recommendations which, if successfully undertaken, would be of significant benefit to the entire space community, without regard to a specific program.

1. NASA should act as coordinator for an on-going effort to generate and up-date a "Thermal Control Data Handbook." The handbook prepared on the current study should become the starting point for this industry-wide compilation.
2. The advantages of series emittance tapes over the more conventional paint thermal control coating systems seem apparent. Flight qualification and experience are required to remove any remaining doubts concerning the credibility of these tapes. If successful, NASA should promote the use of such tape systems.

The second group of recommendations assume that the basic concept of a high reliability thermal control system, as presented in this report, is found worthy of further study.

This group is divided into two tasks, element studies and system studies, which can and should be performed simultaneously.

Element Studies

1. Work should be continued (and possibly expanded) on high performance heat pipes. Efforts should center on increasing capacity, decreasing sensitivity to tilt, non-condensable gas, verification of analytical modeling methods, and standardization of fabrication and test techniques.
2. A fairly extensive study of high capacity heat pipe thermal interfacing techniques should be initiated to define important parameters, determine their effects, and permit design of a functional interface cell. This task would be empirical and analytical. Incentive for this task can be gained by comparing, on a weight basis, the best performance obtained during Phase III by an interface cell and a saddle. A 0.63 pound interface cell had a maximum conductance of 2.53 W/°F, or 4.02

W/°F/lb. The best performance by a 3.9 pound saddle was 4.65 W/°F, or 1.19 W/°F/lb. Therefore, a very significant weight reduction for interface hardware is possible using the advanced technique.

3. The interface cell test article built during Phase III of this program should be retained until after the completion of the interface task defined above. A simple fix may be found which would permit these cells to attain high conductances and system-level verification of the Phase II control concept could be immediately demonstrated.
4. The modular technique of "building-up" heat pipe from piece parts should be investigated. Acceptable methods for mechanically joining tubes and wicks should be generated and demonstrated.

System Studies

1. The heat pipe system selected for the thirty-three foot diameter Space Station on this program should be adapted to the fourteen foot diameter "modularized" Space Station. Resultant system performance and characteristics should again be compared to those of a pumped liquid loop system to ensure that the passive system benefits are maintained. In all fairness, this comparison study should be extended to include assessment of "hybrid" systems (heat pipes and pumped loops together).
2. Desirable sub-assemblies of the passive system should be defined and developed. These would include heat pipe cold plates (thermal energy collectors) and heat pipe radiator segments (thermal energy rejectors). The idea would be to generate units which could be employed for a wide variety of applications.
3. Following completion of (1) and (2) above, a structural integration design study should be performed to define actual required hardware configuration.
4. In parallel with (3), design, analyze, fabricate and test a full-scale prototype of the selected thermal control system, using a simulated structure. This task would qualify the concept for serious consideration on the Space Station and other large space vehicles in the future.

The third group of recommendations are based on the waste heat utilization task (Phase IV) of this program.

1. First, it is recommended that the use of nuclear power system waste heat be considered the "baseline" approach for supplying thermal energy where required on the Space Station.

2. The transient effects of the waste heat utilization system on the projected nuclear Electrical Power System should be determined to fully verify the compatibility of the two.
3. The choice of a pumped liquid loop for transport of waste heat should be reviewed if the decision is made to develop high performance heat pipes and interfaces as part of another program (the passive Space Station thermal control system, for example). It is felt that the required development cannot be justified solely on the basis of the waste heat application, but is viable as a by-product.

SECTION 8
NOMENCLATURE

A	-	area, sq. ft.
b	-	tortuosity factor, conventional wicking, dimensionless
C	-	specific heat, $\text{Btu}/\text{lb}_m - ^\circ\text{F}$
d	-	wick interlayer spacing, ft.
De	-	dimension parameter = $4 r_{hd}$, boiling in wicks, ft.
g	-	acceleration due to gravity, ft/sec^2
g_c	-	gravitational constant, $\text{lb}_m - \text{ft}/\text{lb}_f - \text{sec}^2$
h	-	boiling film coefficient, $\text{Btu}/\text{hr} - \text{sq. ft.} - ^\circ\text{F}$
k	-	conductivity, $\text{Btu}/\text{hr} - \text{ft} - ^\circ\text{F}$
Kch	-	channel shape factor (~ 1.2), dimensionless
K	-	conductance, $\text{Btu}/\text{hr} - ^\circ\text{F}$
l	-	effective length ($1/2 l_e + 1_{\text{adiab.}} + 1/2 l_c$), ft.
l'	-	fin length, ft.
N	-	number of channels
P	-	pressure, $\text{lb}_f/\text{sq. ft.}$
Q	-	heat flow rate, Btu/hr
r	-	radius, ft.
r_{hw}	-	channel half-width, ft.
R/M	-	gas constant, $\text{Btu}/\text{lb}_m - ^\circ\text{R} (= \frac{1}{778.2} \times \text{R}/\text{M in ft} - \text{lb}_f/\text{lb}_m - ^\circ\text{R})$
t	-	thickness of one layer of mesh, ft.
t'	-	fin thickness, ft.

T	-	temperature, $^{\circ}\text{R}$ or $^{\circ}\text{F}$
V	-	velocity, ft/sec.
W_e	-	Weber Number, dimensionless
W	-	Flow Rate, lb_m/hr
D	-	Diameter, ft.
S	-	Incident Solar Flux, $\text{Btu}/\text{hr ft}^2$
A'	-	Incident Albedo Flux, $\text{Btu}/\text{hr ft}^2$
E	-	Incident Earth Flux, $\text{Btu}/\text{hr ft}^2$
a	-	Albedo Factor, Dimensionless
L	-	Generalized length parameter, dimensionless

Greek Symbols

α	-	Solar Absorbptivity, dimensionless
ϵ	-	Hemispherical Emissivity, dimensionless
γ	-	ratio of specific heats of vapor, dimensionless
Δ	-	differential
ϵ'	-	porosity, dimensionless
η	-	viscosity, $\text{lb}_m/\text{ft-sec}$
θ	-	wetting angle, degrees
λ	-	latent heat of vaporization, Btu/lb_m
ρ	-	density, $\text{lb}_m/\text{cu ft}$
σ	-	surface tension, lb_f/ft
ϕ	-	angle of heat pipe from horizontal, degrees
σ	-	Stephan-Boltzmann Constant $\text{BTU}/\text{hr ft}^2 \text{ } ^{\circ}\text{R}$
η'	-	fin effectiveness, dimensionless

Subscripts

a	-	sonic
ar	-	artery
c	-	capillary
cn	-	condenser
e	-	evaporator
h	-	heated surface
hd	-	hydraulic
l	-	liquid phase
max	-	maximum
p	-	pipe
s	-	solid
v	-	vapor phase
w	-	wick
sK	-	effective sink
r	-	radiator
o	-	fin root

SECTION 9
REFERENCES

- 9-1 Levy, E. K., "Theoretical Investigation of Heat Pipes Operating at Low Vapor Pressures," Aviation and Space: Progress and Prospects - Annual Aviation and Space Conference, June 1968.
- 9-2 Kemme, J. E., "Heat Pipe Capability Experiments," IEEE Thermionic Conversion Specialist Conference, Nov. 1966.
- 9-3 Costello, C. P., and Frea, W. J., "The Roles of Capillary Wicking and Surface Deposits in the Attainment of High Pool Boiling Burnout Heat Fluxes," A. I. Ch. E. Journal, Vol. 10, No. 3, May 1964.
- 9-4 Allingham, W. D., and McEntire, J. A., "Determination of Boiling Film Coefficient for a Heated Horizontal Tube in Water-Saturated Wick Material," J. of Heat Transfer, Feb. 1961.
- 9-5 Moss, R. A., "Neutron Radiographic Examination of Vapor Bubble Formation as a Limitation on Planar Heat Pipe Performance," Ph.D. Thesis at Princeton University, 1968.
- 9-6 Kunz, H. R., et al, "Vapor-Chamber Fin Studies - Transport Properties and Boiling Characteristics of Wicks," NASA CR-812, Report prepared under Contract No. NAS 3-7622, Nov. 1966.
- 9-7 Conway, E. C., personal communication, 9/15/70.
- 9-8 Conway, E. C., and Kelley, M. J., "Cooling of a High Power Electronic Device," GE TIS 68SD232, April 1968.
- 9-9 Rohsenow, W., and Griffith, P., "Correlation of Maximum Heat Transfer Data for Boiling of Saturated Liquids," Chem. Eng. Prog. Symp., Ser. 52, Nov 18, 1956
- 9-10 Cotter, T. P., "Theory of Heat Pipes," Los Alamos Scientific Lab., LA-3246-MS, Feb. 1965.
- 9-11 Waters, E. D., and Hinderman, J. D., "Summary Report - Design, Fabrication and Testing of ATS-E Solar Panel/Heat Pipe Substrates," Prime Contract No. NAS5-3823, June 1969
- 9-12 MDC G0634, McDonnell Douglas Astronautics Company, July 1970, Contract NAS8-25140, MSFC-DRL-160 Line Item 13, Preliminary Systems Design Data, Volume I, Space Station Preliminary Design: Book 1, Electrical Power; Book 2, Crew Systems; Book 5, Structural/Mechanical.

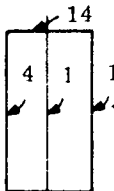
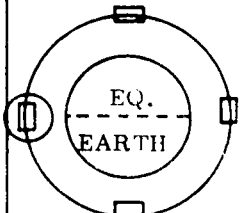

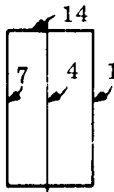
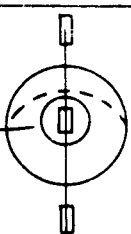

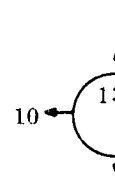


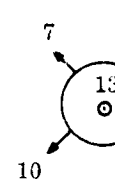
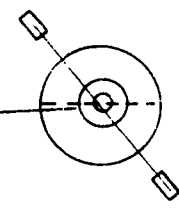

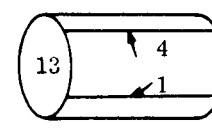
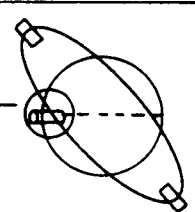


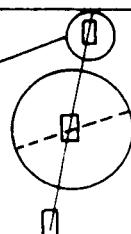
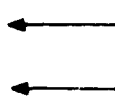
- 9-13 MDC G0605, McDonnell Douglas Astronautics Company, July 1970, Contract NAS8-25140, MSFC-DRL-160 Line Item 8, Space Station Definition: Volume V, Subsystems, Book 2, Crew Systems; Volume V, Subsystems, Book 2, Crew Systems, Appendices A through L; Volume VII, Experiment Modules, Appendix A; Volume VII, Experiment Modules, Appendices B and C.
- 9-14 MDC G0640, McDonnell Douglas Astronautics Company, August 1970, MSFC-DRL-160 Line Item 17, Mass Properties Data.
- 9-15 MDC G0592, McDonnell Douglas Astronautics Company, June 1970, Space Station Program Phase B Definition Study, 7th Technical Review.
- 9-16 MDC G0783, McDonnell Douglas Astronautics Company, February 1971, MSFC-DRL-231 Line Item 8, Report on Selected Update Tasks for Baseline Space Station, Volume II, Thermal Control.
- 9-17 NASA Technical Note, TN D-196, "Analysis of Temperature Distribution and Radiant Heat Transfer Along a Rectangular Fin of Constant Thickness," Seymour Lieblein Lewis Research Center, National Aeronautics and Space Administration.
- 9-18 Kirkpatrick, J. P., and Marcus, B. D., "A Variable Conductance Heat Pipe Flight Experiment," AIAA Paper 71-411, AIAA 6th Thermophysics Conference, Tullahoma, Tennessee, April, 1971.
- 9-19 Edelstein, F., and Hembach, R. M., "Design, Fabrication, and Testing of a Variable Conductance Heat Pipe for Equipment Thermal Control," AIAA Paper 71-422, AIAA 6th Thermophysics Conference, Tullahoma, Tennessee, April 1971.
- 9-20 Hinderman, J. D., and Waters, E. D., "Design and Performance of Non-Condensable Gas Controlled Heat Pipes," AIAA Paper 71-420, AIAA 6th Thermophysics Conference, Tullahoma, Tennessee, April 1971.
- 9-21 Skirvin, S. C., "User's Manual for the THTD Computer Program (Transient Heat Transfer -- Version D)," GE-NMPO Report P. O. No. 036-926052-TO602, June 23, 1966.

APPENDIX A
SINK TEMPERATURE PLOTS

The plots in this appendix show sink temperature as a function of time for a variety of Space Station orbits, orientations, and radiator surface properties. Definition and justification of the parameters used in forming these curves appear in the text of this report. The text also describes the method of analysis. The following is offered as explanation of the graphs.

1. The vehicle was modeled as a 12-sided polyhedron, two end surfaces, and one "cylinder-average" grouping. Thus, the sink temperatures for 15 body points were calculated and plotted. Nodes 1 through 12 are located on the cylindrical surface with node 1 being oriented as shown in Tables A-1 and 2 through 12 following sequentially around the circumference, nodes 13 and 14 are end nodes, and node 15 is the σT^4 average of nodes 1 to 12.
2. Time zero on all curves at the perigee point of each orbit (perigee conditions are described in Table A-1).
3. In some of the orbits shown, pairs of nodes around the cylinder circumference have identical sinks and only one plot appears for each pair (Figure A-4 is an example).
4. The computer code used for sink temperature calculation did not permit beta angle input. Instead, "launch time" was required which implicitly defined the orbit beta angle. Because beta angle is very sensitive to launch time, some of the desired beta angles were not obtained exactly as shown in Table A-2. This slight distortion is the explanation of the odd appearance of some of the plots that follow (Figures A-1 and A-6, for example). The effect of these perturbations on the vehicle thermal balance is negligible since the σT^4 value is significant for temperatures on the order of 100°R .

Table A-1. Orbit Orientation Definition

NO.	DAY/STA-BILIZATION	BETA/INC. ANGLE	NODAL ORIENTATION AT PERIGEE	PERIGEE DEFINITION	SOLAR VECTOR
1	80/EARTH	90/90	 NODE CENTERS SHOWN		
2	356/SUN	0/90	 NODE CENTERS SHOWN		
3	173/SUN	0/90	 NODE NORMALS SHOWN		
4	80/EARTH	0/55	 NODE NORMALS SHOWN		
5	80/EARTH	45/55	 NODE CENTER SHOWN		
6	356/SUN	78.5/55	 NODE CENTERS SHOWN		

5. The data is presented in the order given below. Three graphs are used per case.

Case	α / ϵ	Orbit	Figures
1	0.13/0.67 ↑ ↓	1	A-1 - A-3
2		2	A-4 - A-6
3		3	A-7 - A-9
4		4	A-10 - A-12
5		5	A-13 - A-15
6		6	A-16 - A-18
7	0.20/0.67 ↑ ↓	1	A-19 - A-21
8		2	A-22 - A-24
9		3	A-25 - A-27
10		4	A-28 - A-30
11		5	A-31 - A-33
12		6	A-34 - A-36
13	0.36/0.90 ↑ ↓	1	A-37 - A-39
14		2	A-40 - A-42
15		3	A-43 - A-45
16		4	A-46 - A-48
17		5	A-49 - A-51
18		6	A-52 - A-54

Table A-2. Beta Angle Comparison

Orbit	Desired Beta Angle	Actual Beta Angle
1	90°	89.05°
2	0°	0.02°
3	0°	0.04°
4	0°	-0.53°
5	45°	44.42°
6	-78.5°	-78.43°

SPACE STATION HOTTEST AVERAGE ORBIT(1) -- MAX FLUX --1/E=137.57

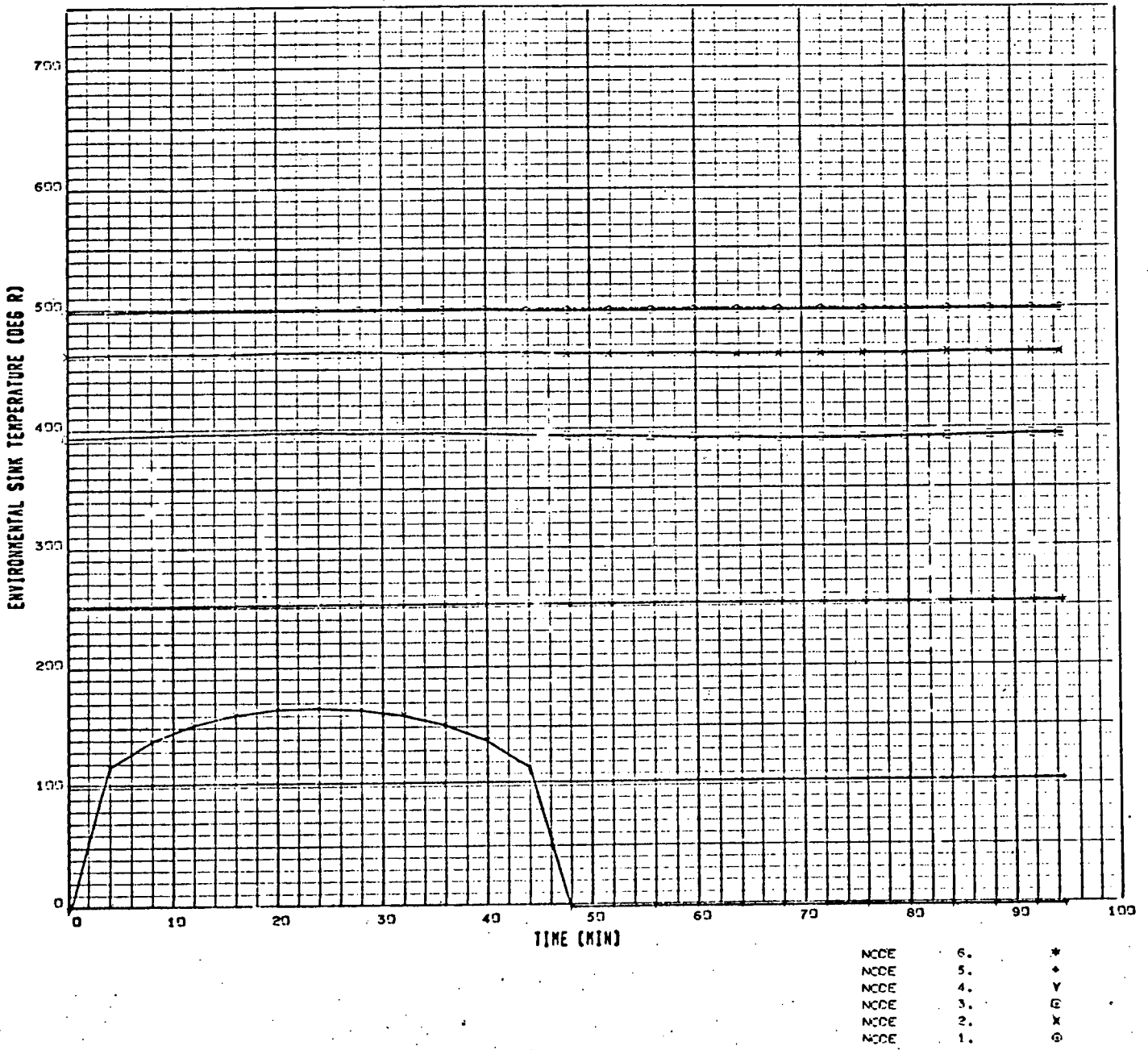


Figure A-1. Case 1

SPACE STATION HOTTEST AVERAGE ORBIT (1) -- MAX FLUX --A/E=.13/.57

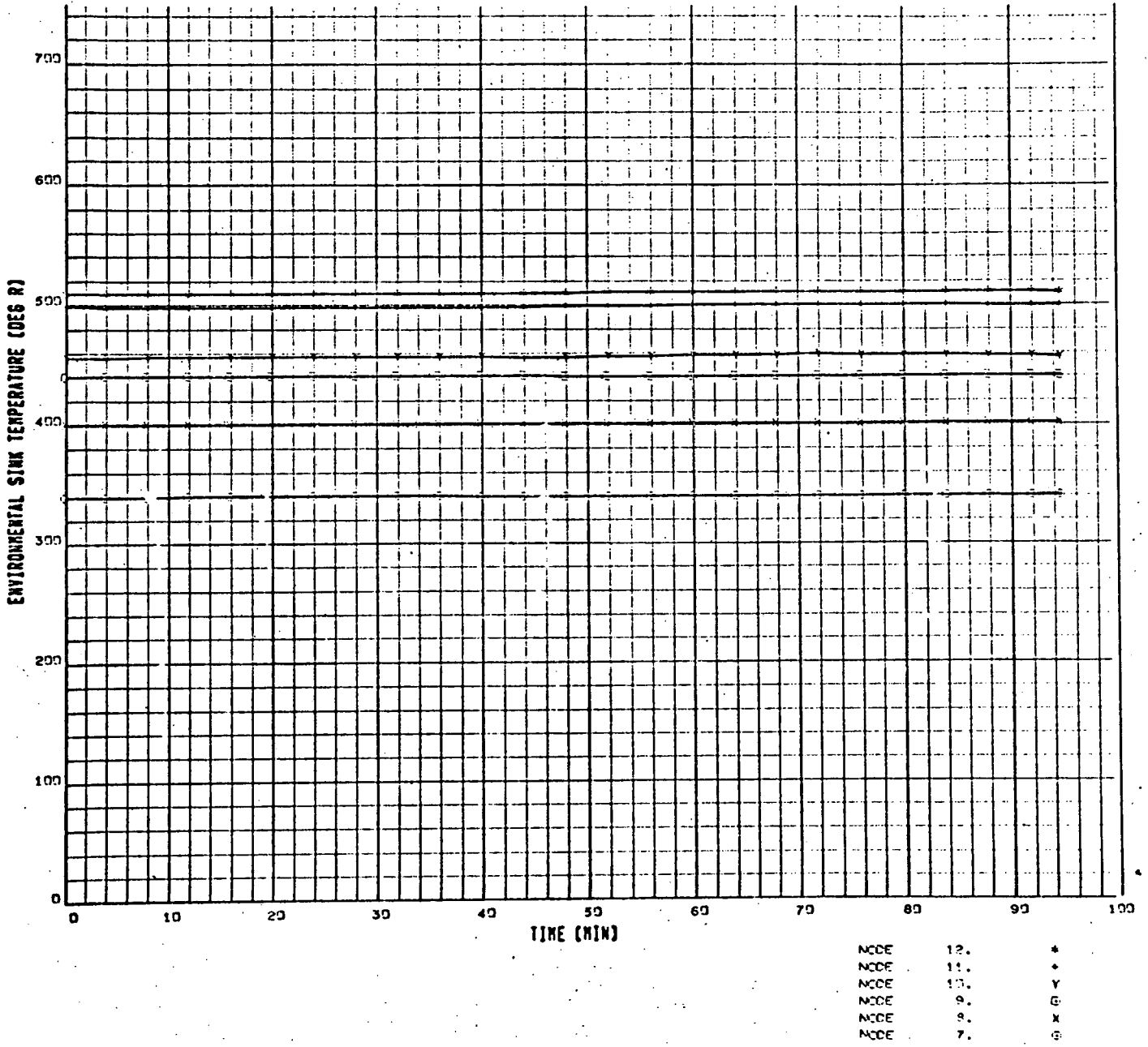


Figure A-2. Case 1

SPACE STATION HOTTEST AVERAGE ORBIT (1) -- MAX FLUX -- 1/12/67

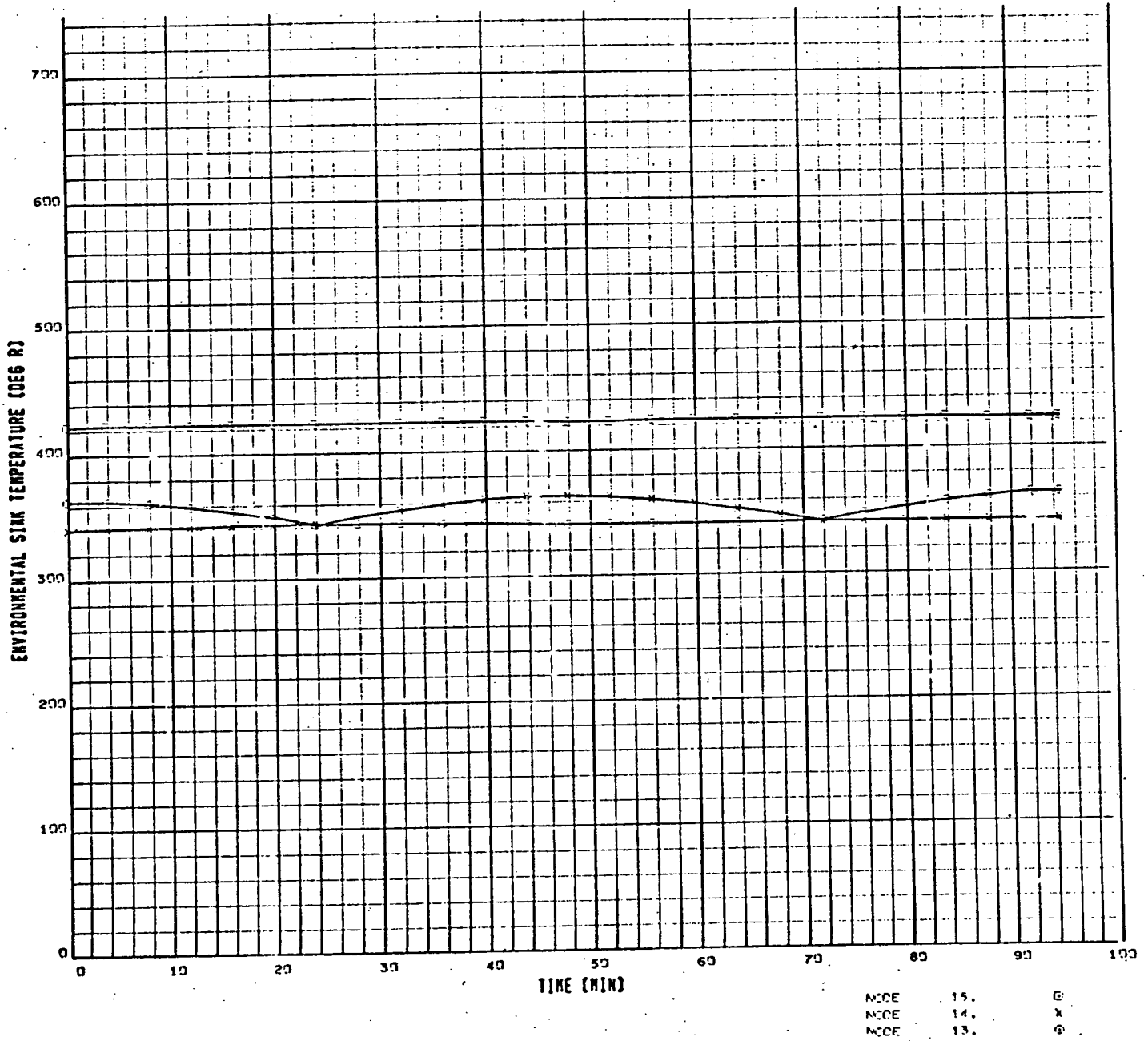


Figure A-3. Case 1

SPACE STATION HOTTEST INSTANT. CRBIT(2) -- MAX FLUX -- A/E=137.57

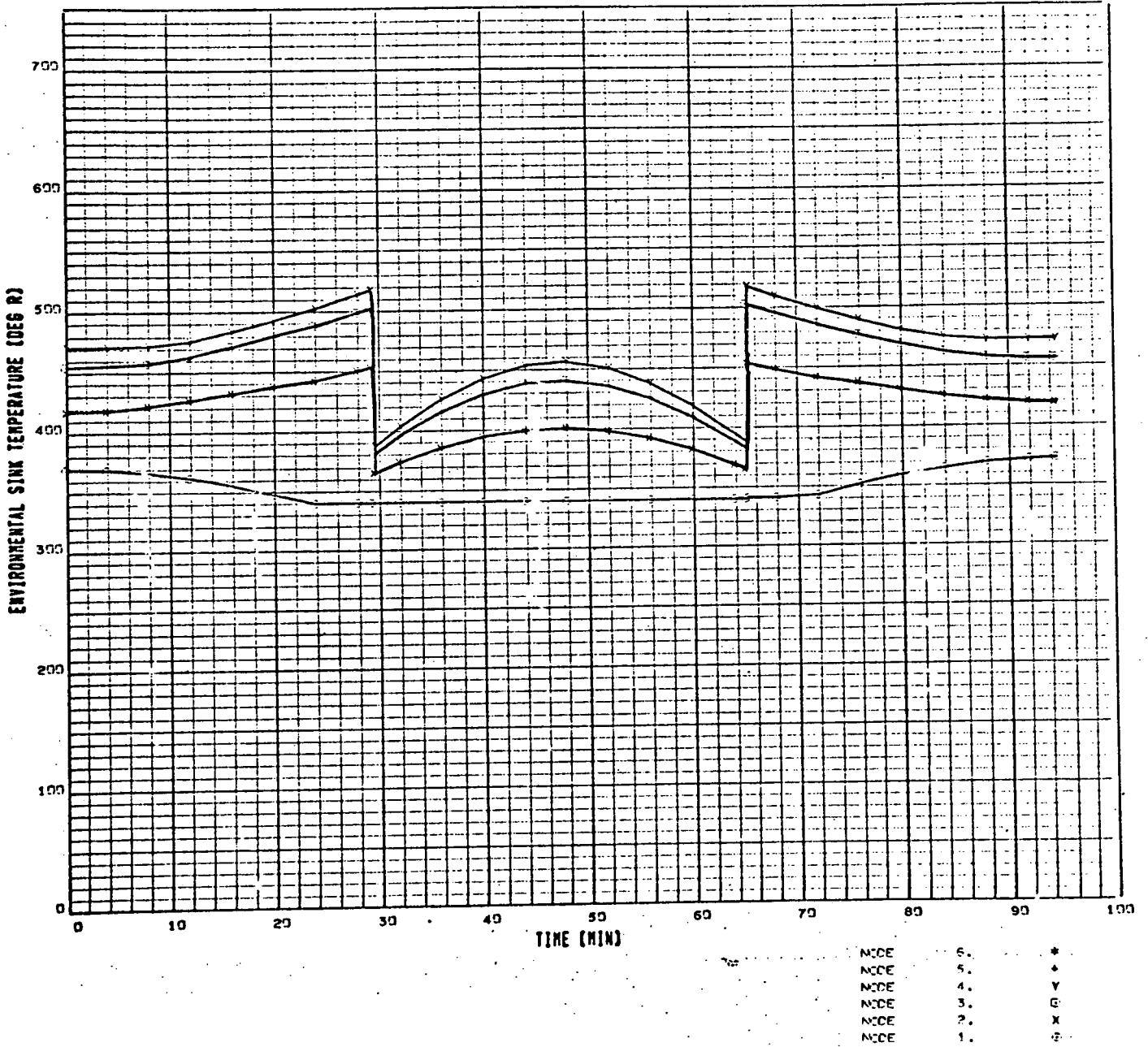


Figure A-4. Case 2

SPACE STATION HOTTEST INSTANT, ORBIT (?) -- MAX FLUX -- A/E=137.57

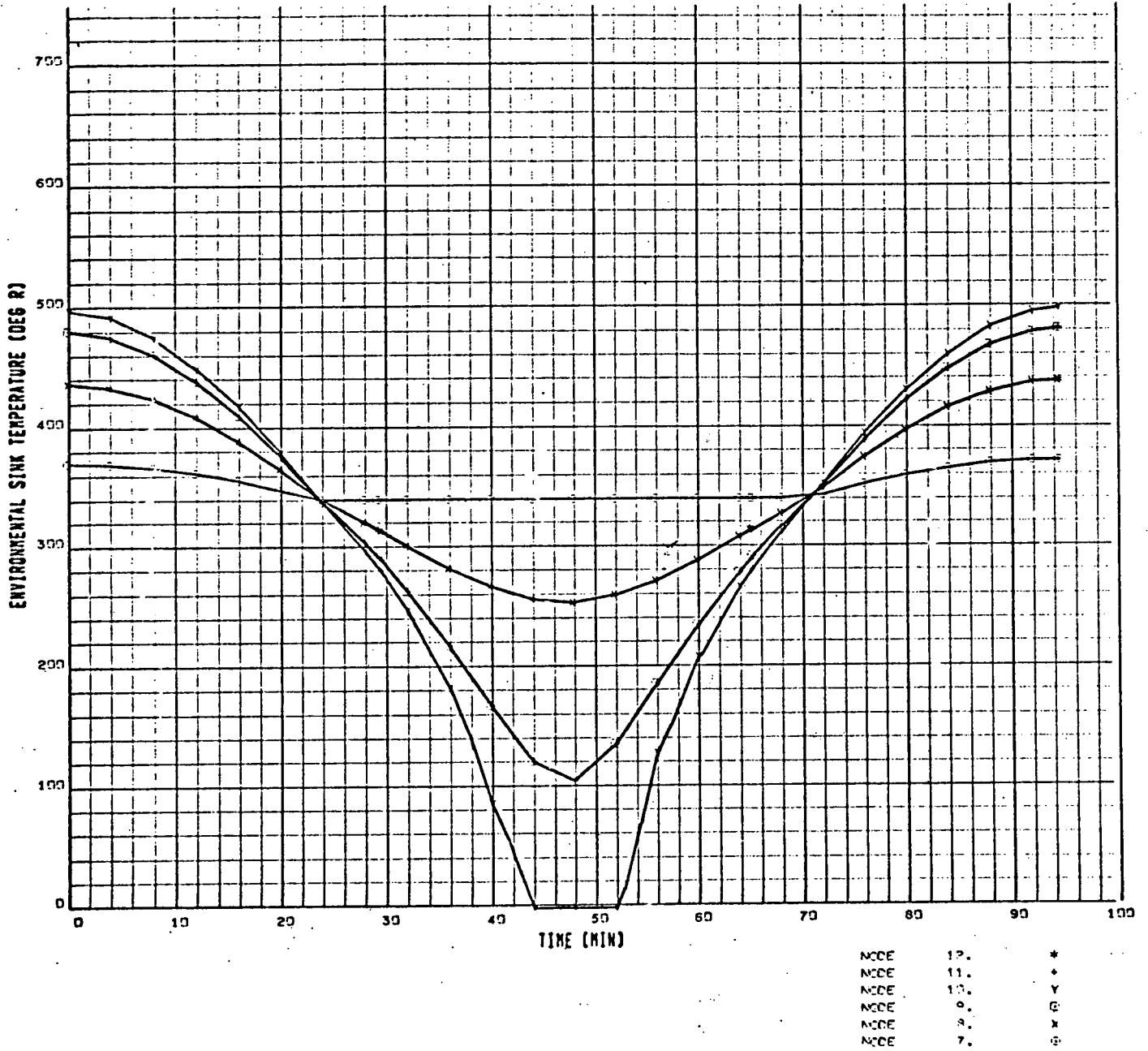


Figure A-5. Case 2

• SPACE STATION HOTTEST INSTANT. CRBIT(2) -- MAX FLUX -- A/E=13/57

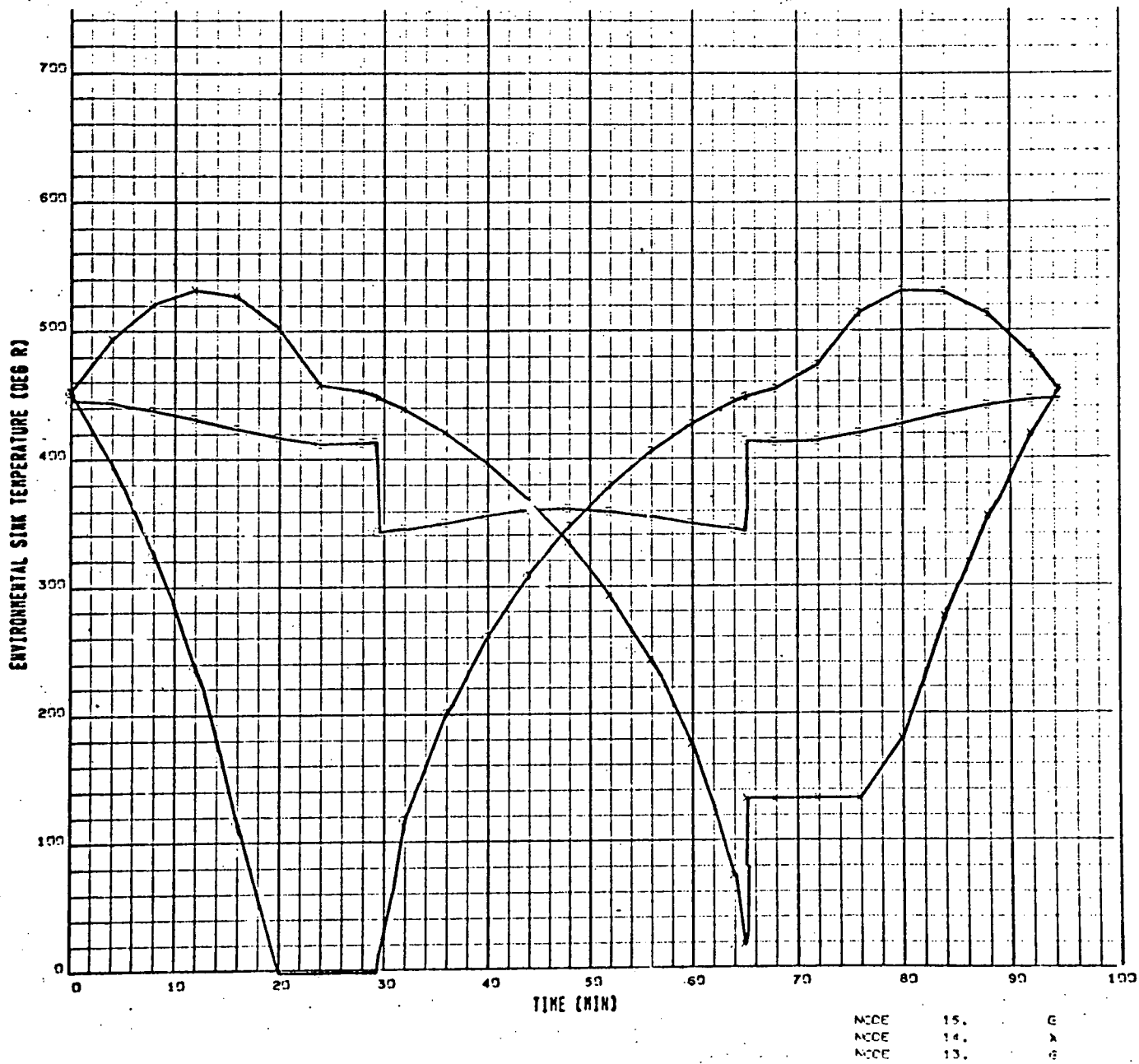


Figure A-6. Case 2

SPACE STATION COLDEST AVERAGE ORBIT(3) -- MIN FLUX --A/E=137.67

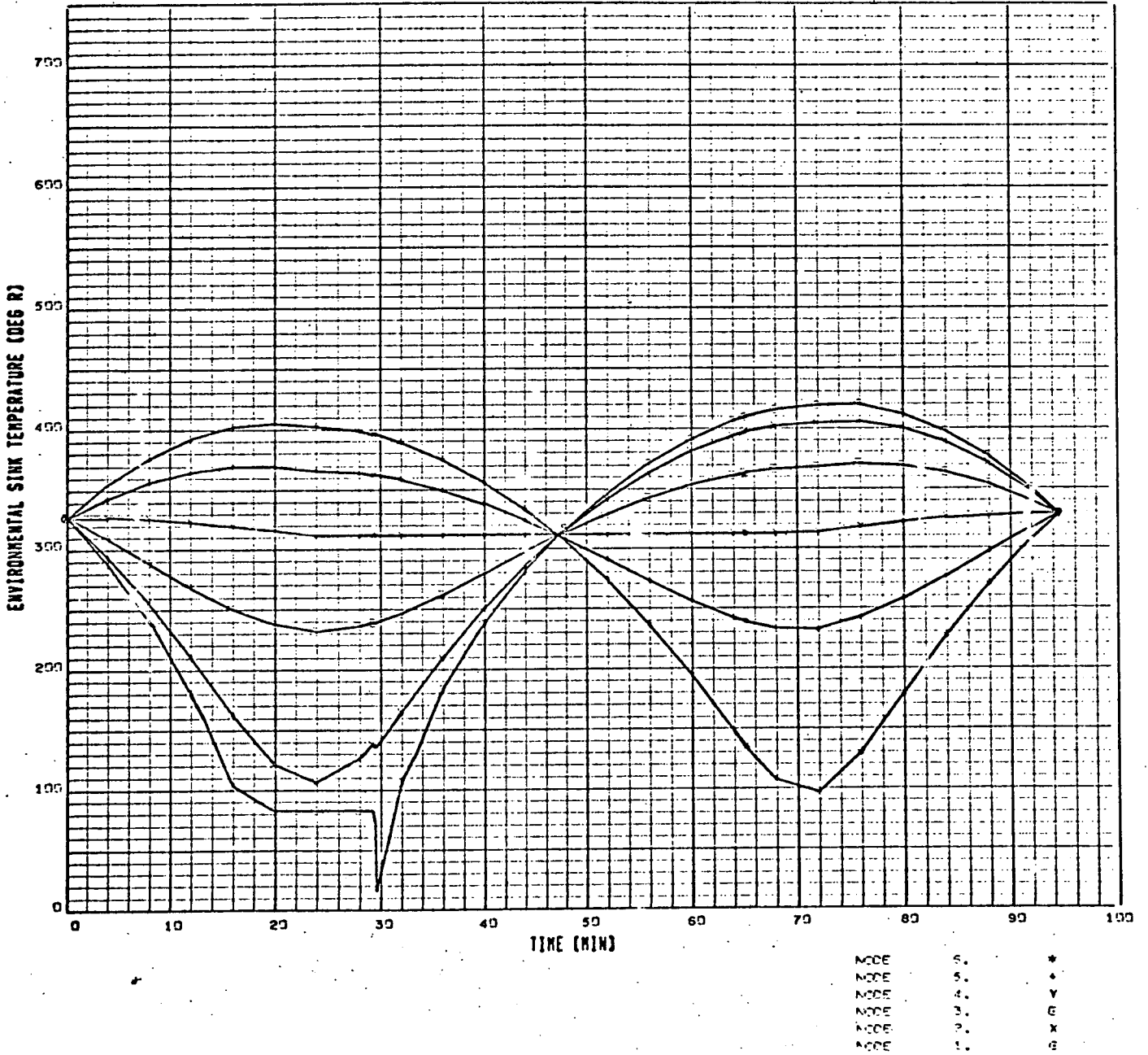


Figure A-7. Case 3

SPACE STATION COLDEST AVERAGE ORBIT (3) -- MIN FLUX -- 1/26/57

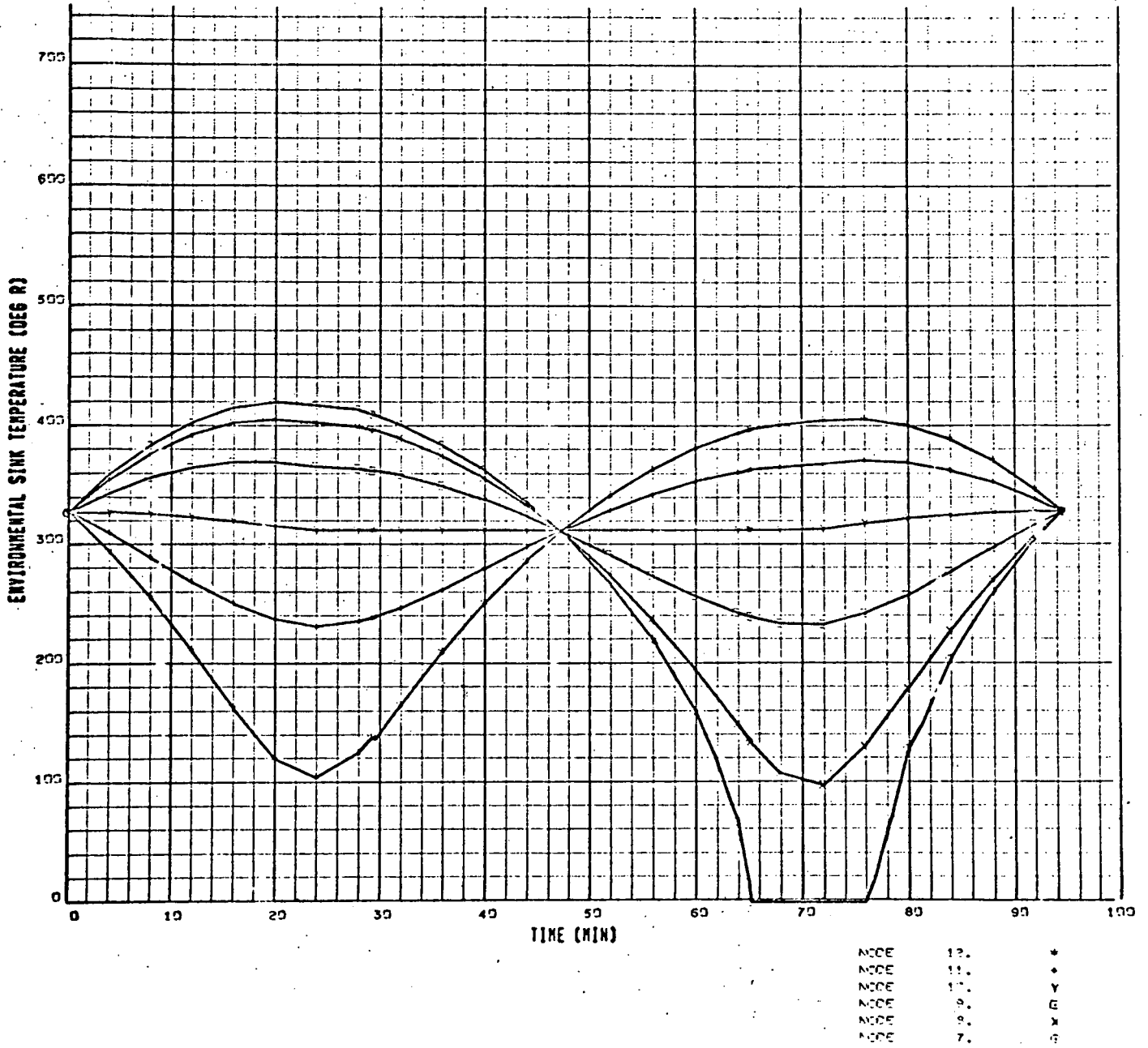


Figure A-8. Case 3

SPACE STATION COLDEST AVERAGE ORBIT(3) -- MIN FLUX -- A/EP-137.97

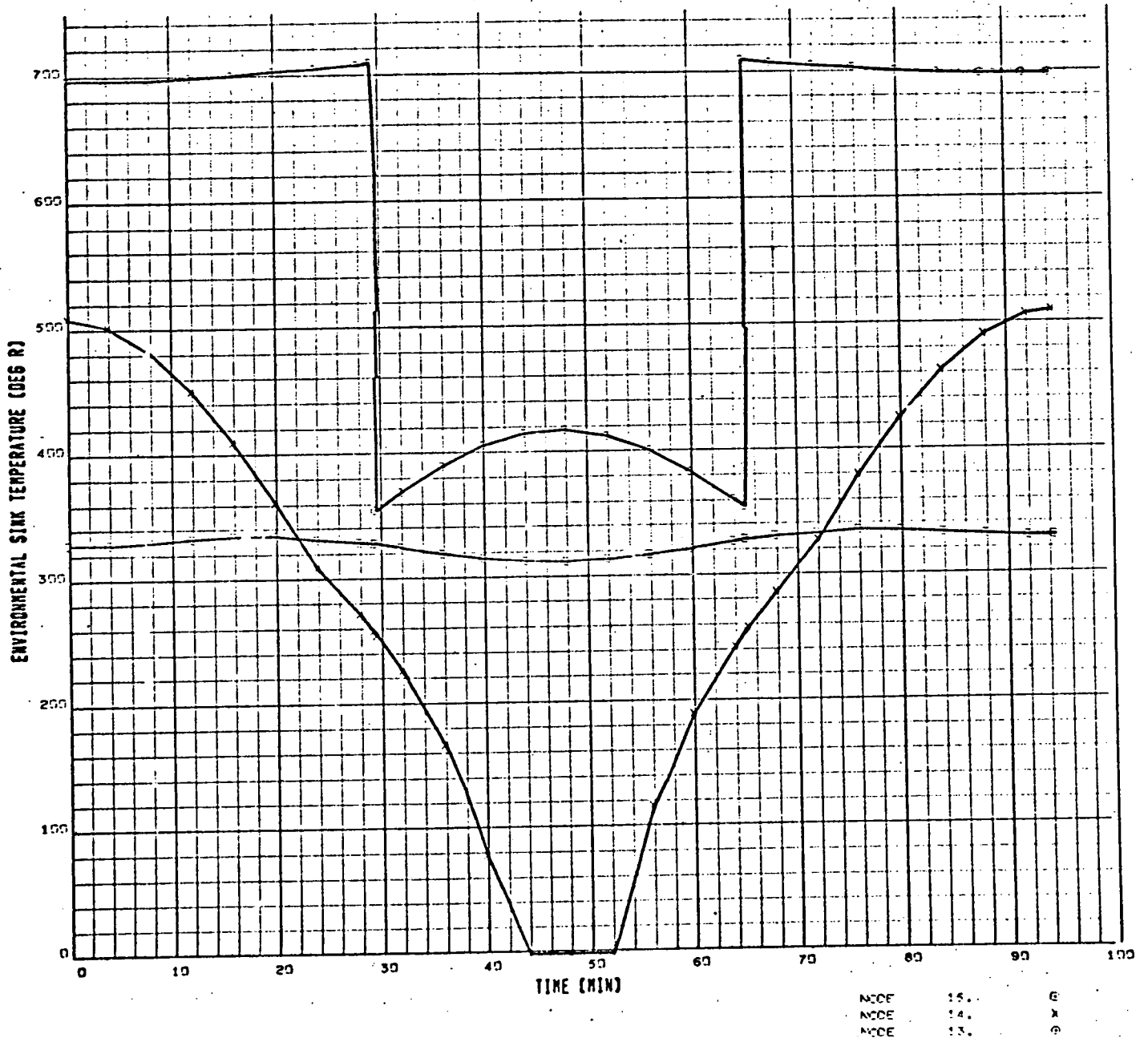


Figure A-9. Case 3

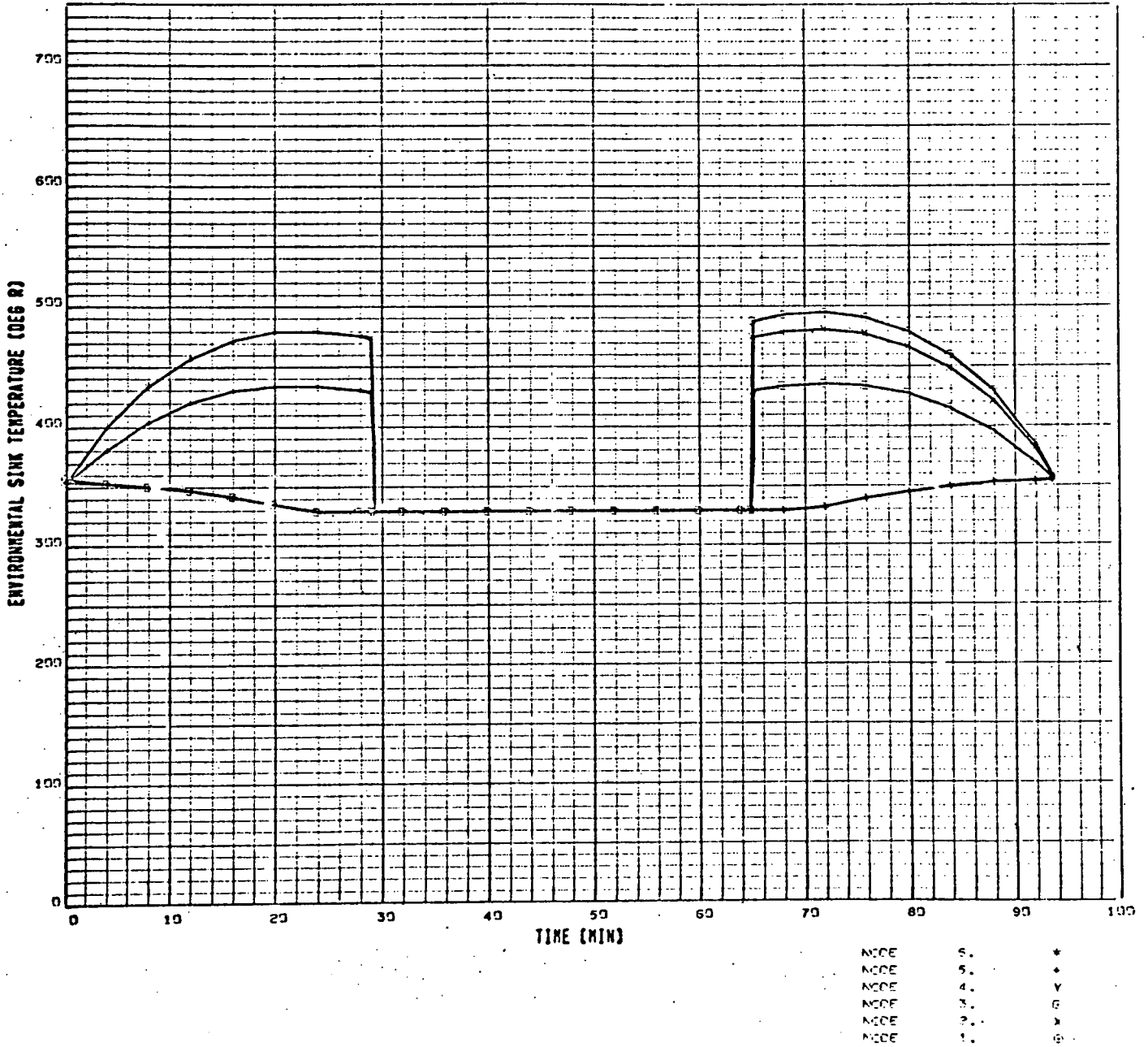


Figure A-10. Case 4

C

SPACE STATION LARGE TRANSIENT, ORBIT (1) -- NOM FLUX -- A/EP=13/57

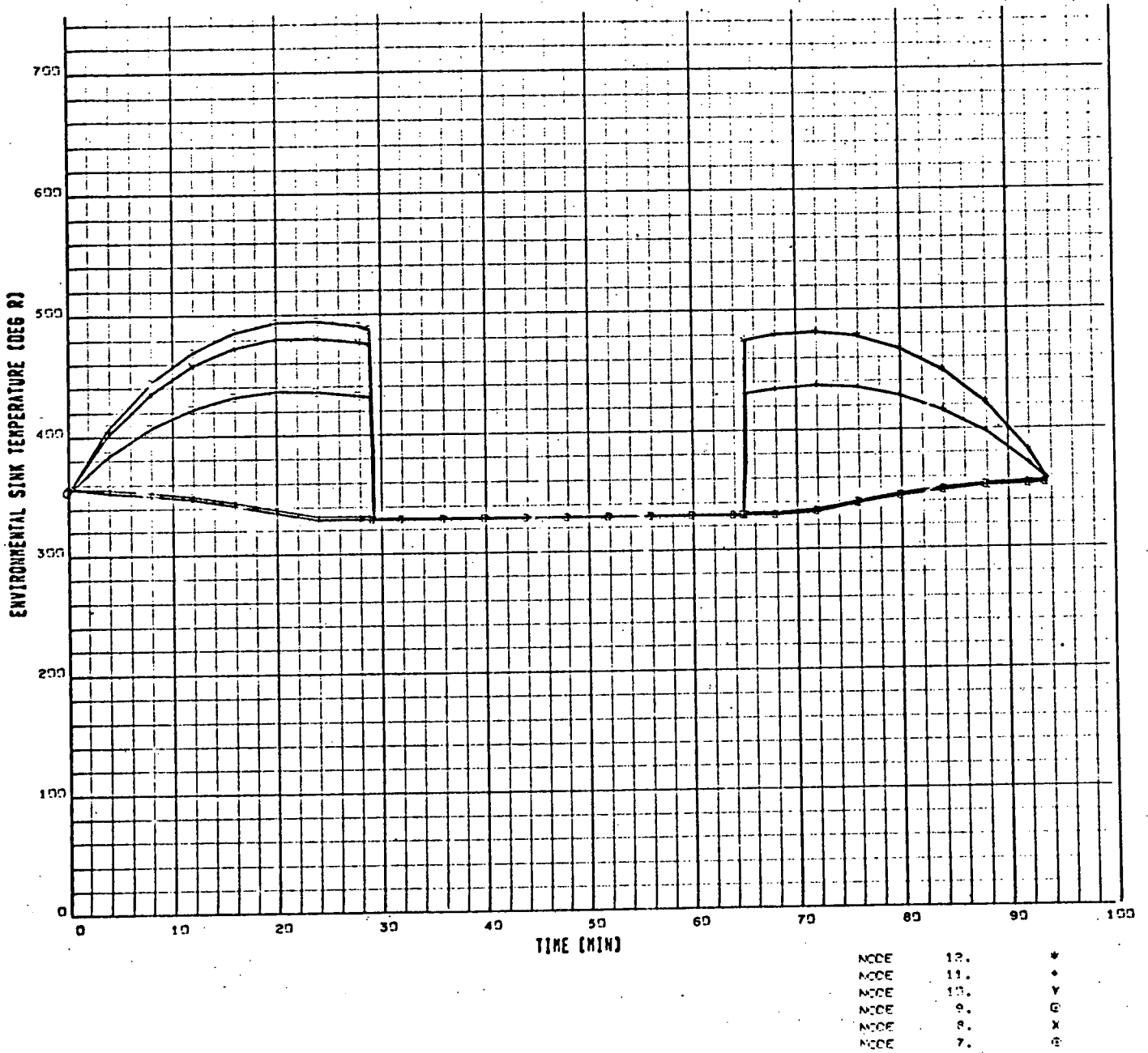


Figure A-11. Case 4

SPACE STATION LARGE TRANSIENT ORBIT (4) -- NOM FLUX -- 1/EE-137.67

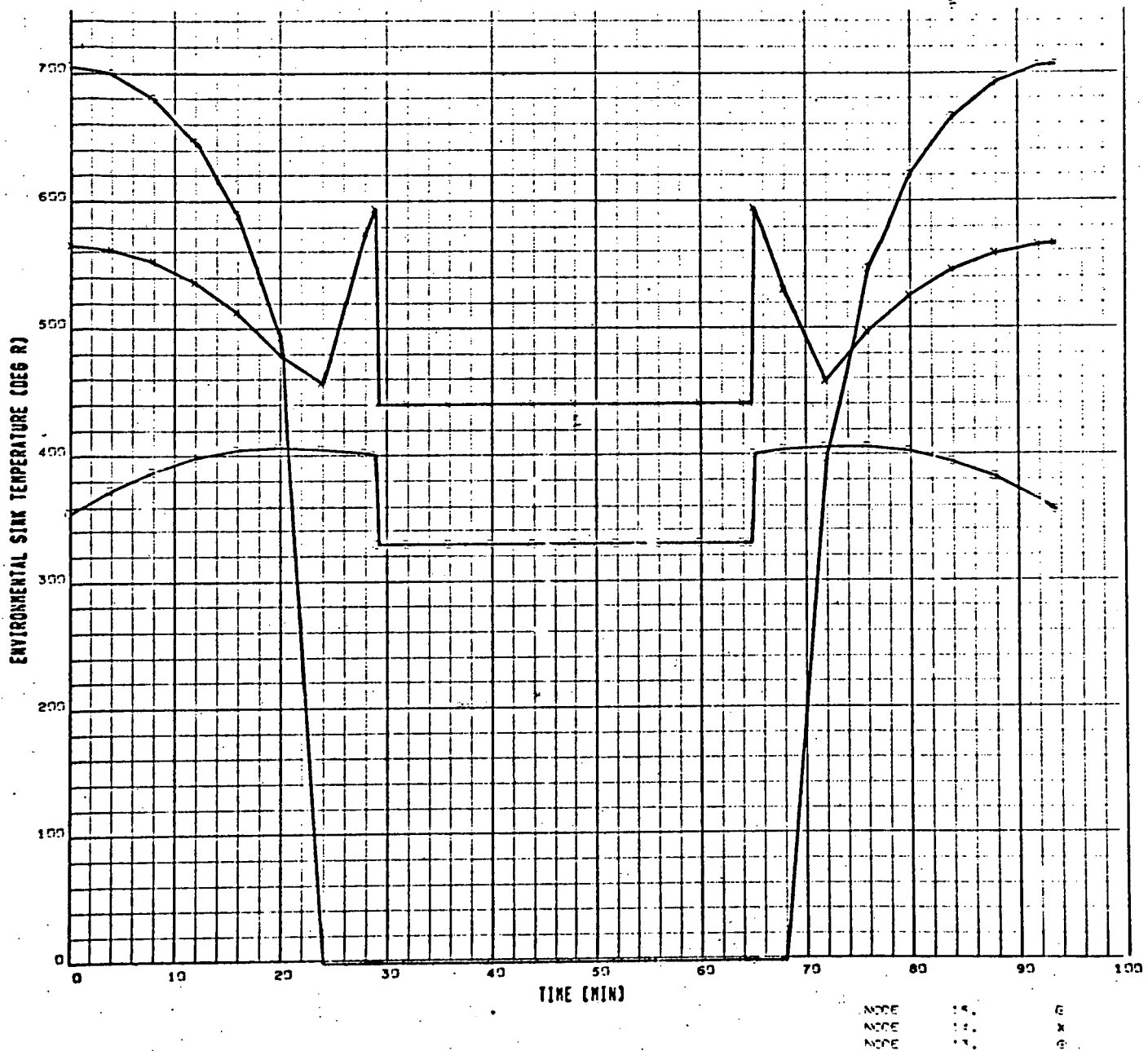


Figure A-12 . Case 4

SPACE STATION NOMINAL CREIT(5) -- NOM FLUX -- A/E=137.67

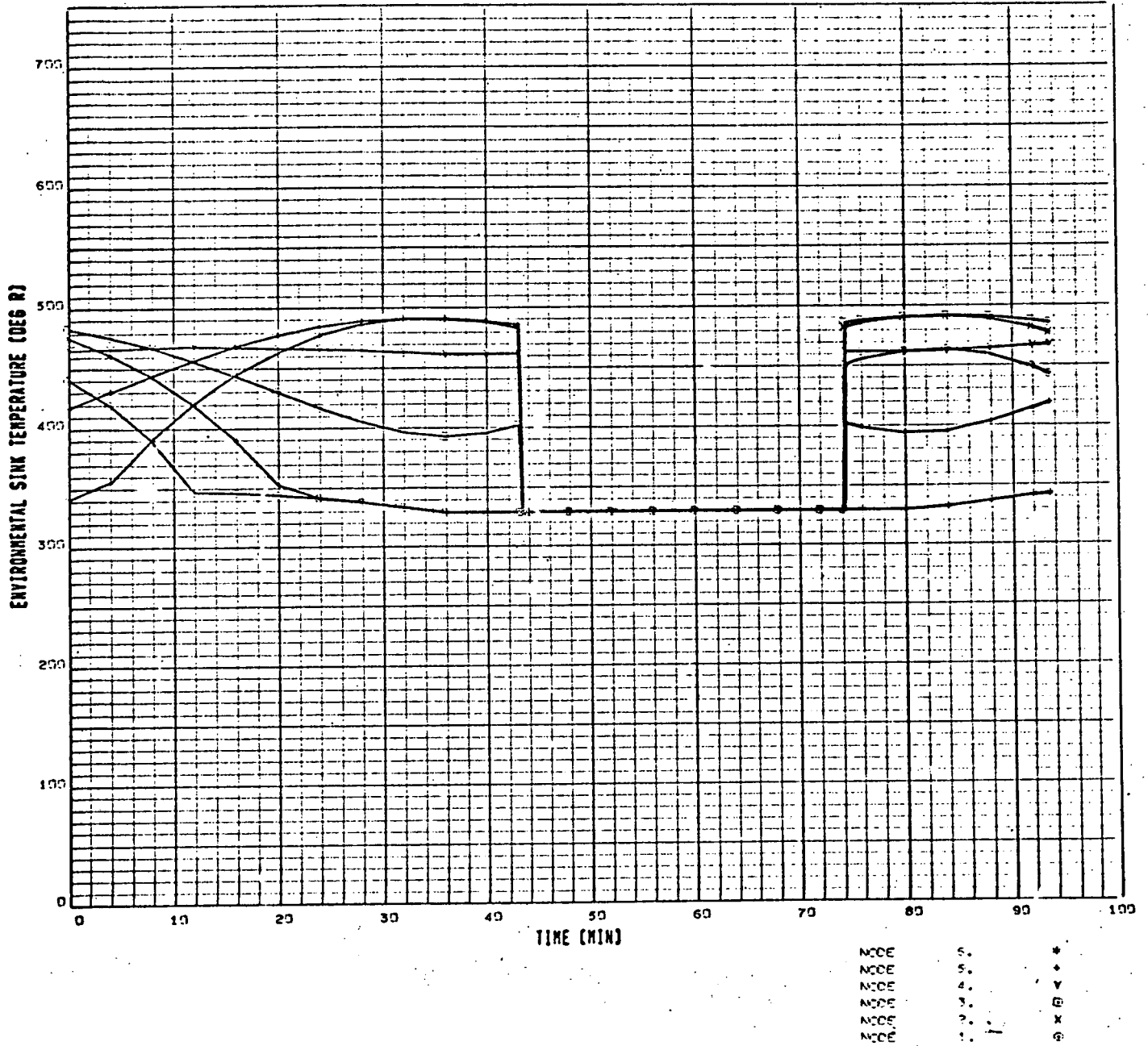


Figure A-13. Case 5

SPACE STATION NOMINAL ORBIT (5) -- NOM FLUX -- A/ER.137.97

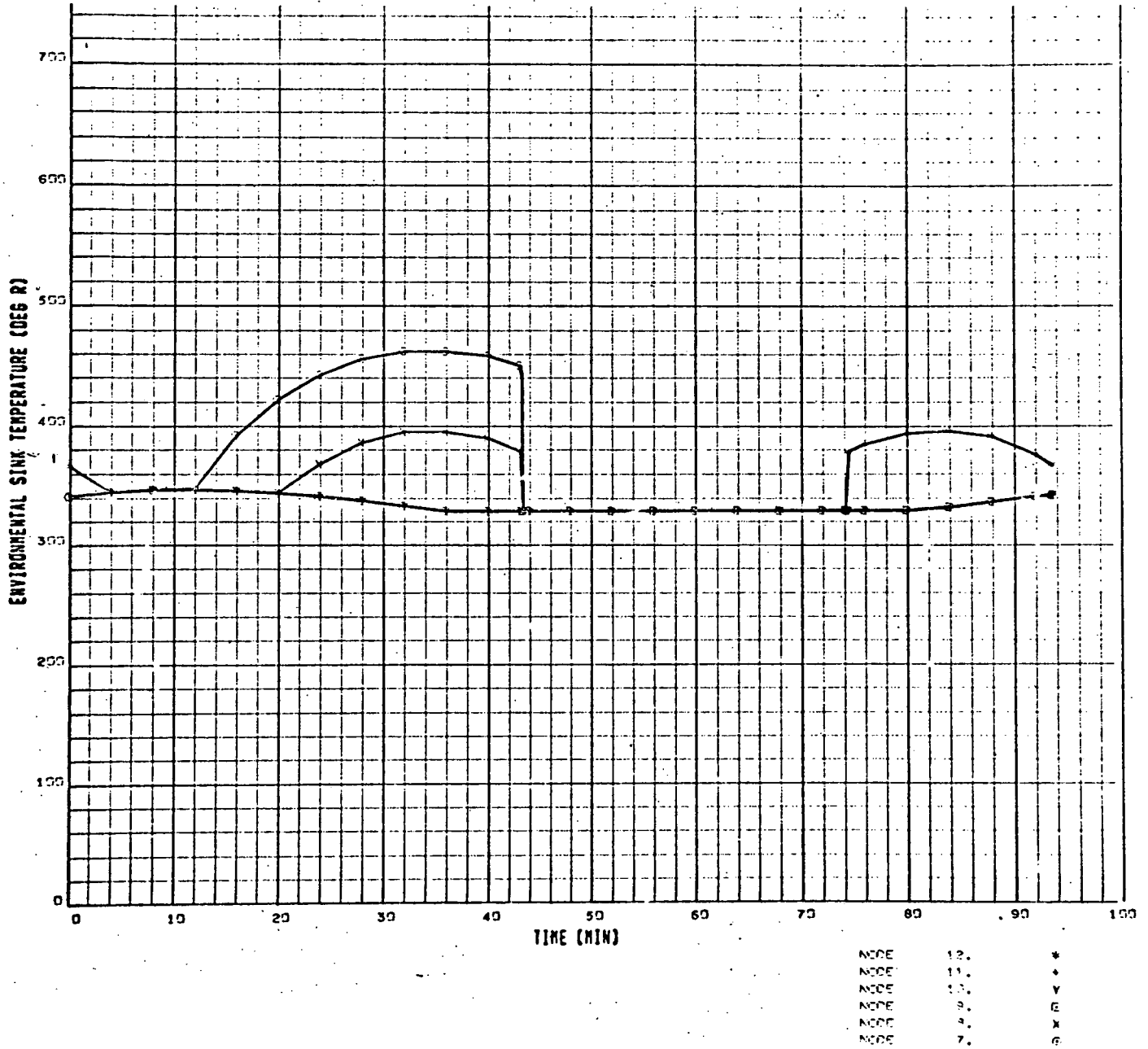


Figure A-14. Case 5

SPACE STATION NOMINAL ORBIT (5) -- NOM FLUX -- A/EE-137.67

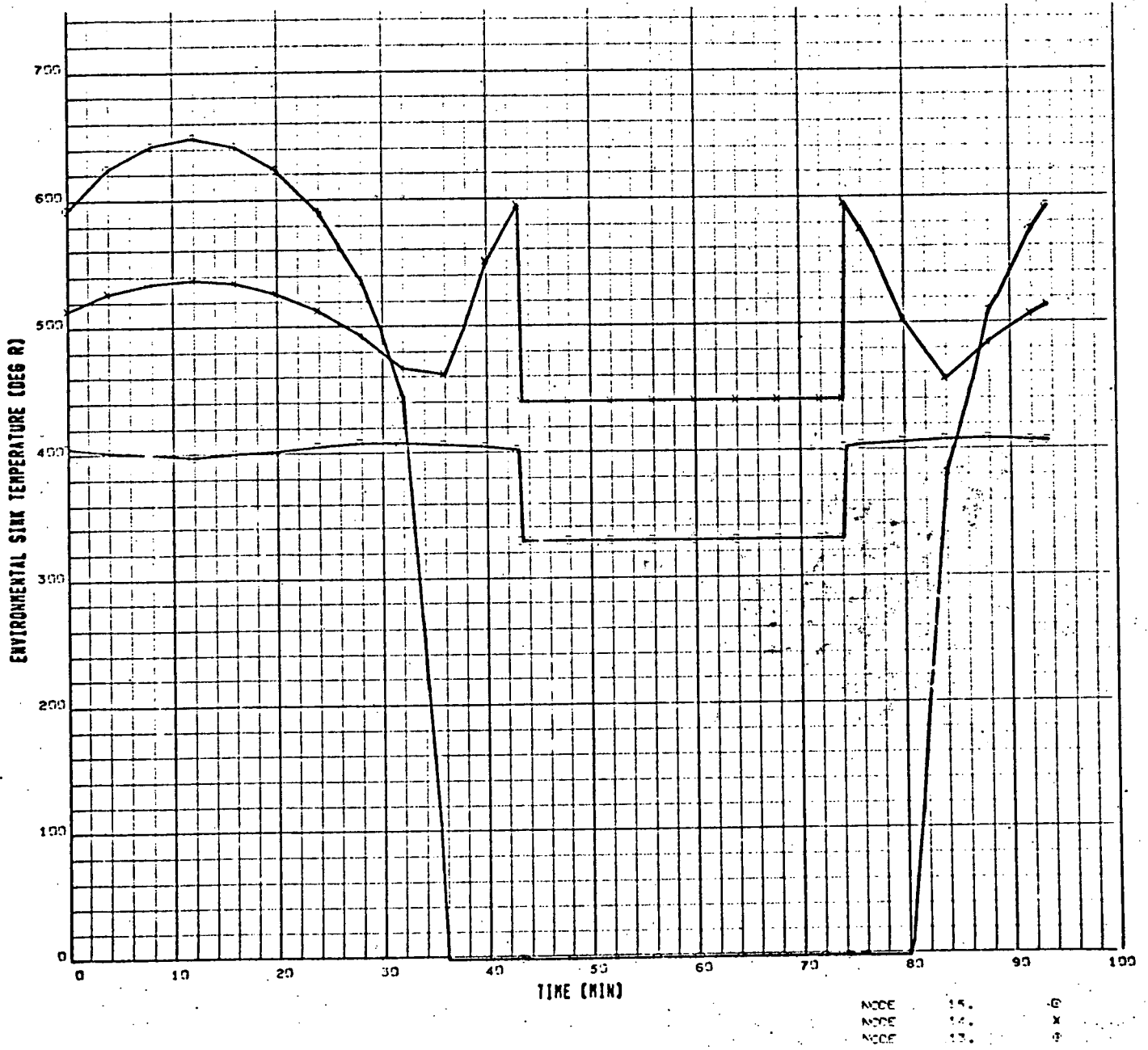


Figure A-15. Case 5

SPACE STATION NOMINAL/ACT ORBIT(S) -- MAX FLUX -- 1/28/67

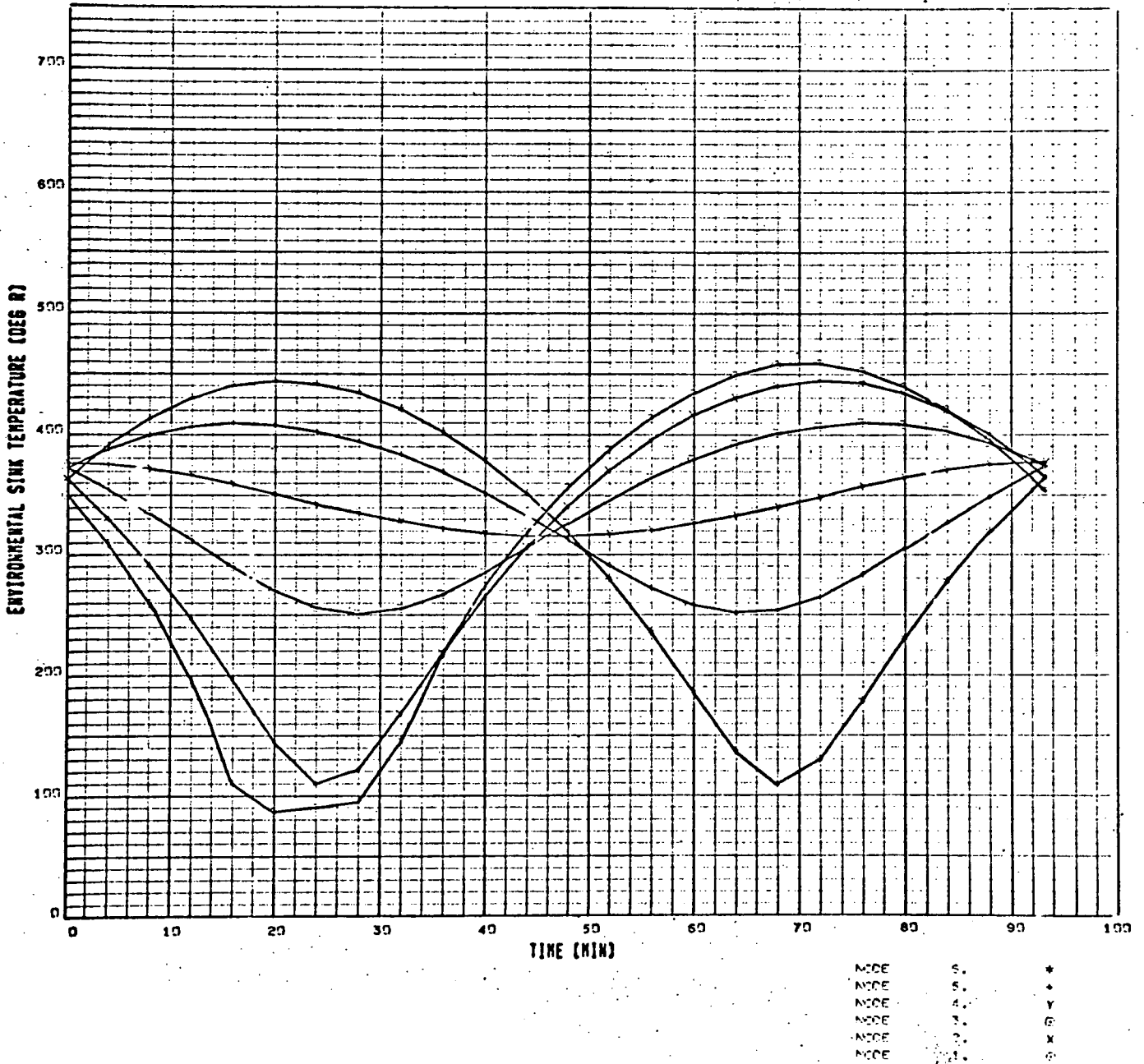


Figure A-16. Case 6

SPACE STATION NOMINAL/HOT CREDIT (S) -- MAX FLUX -- 4/EE-1237-87

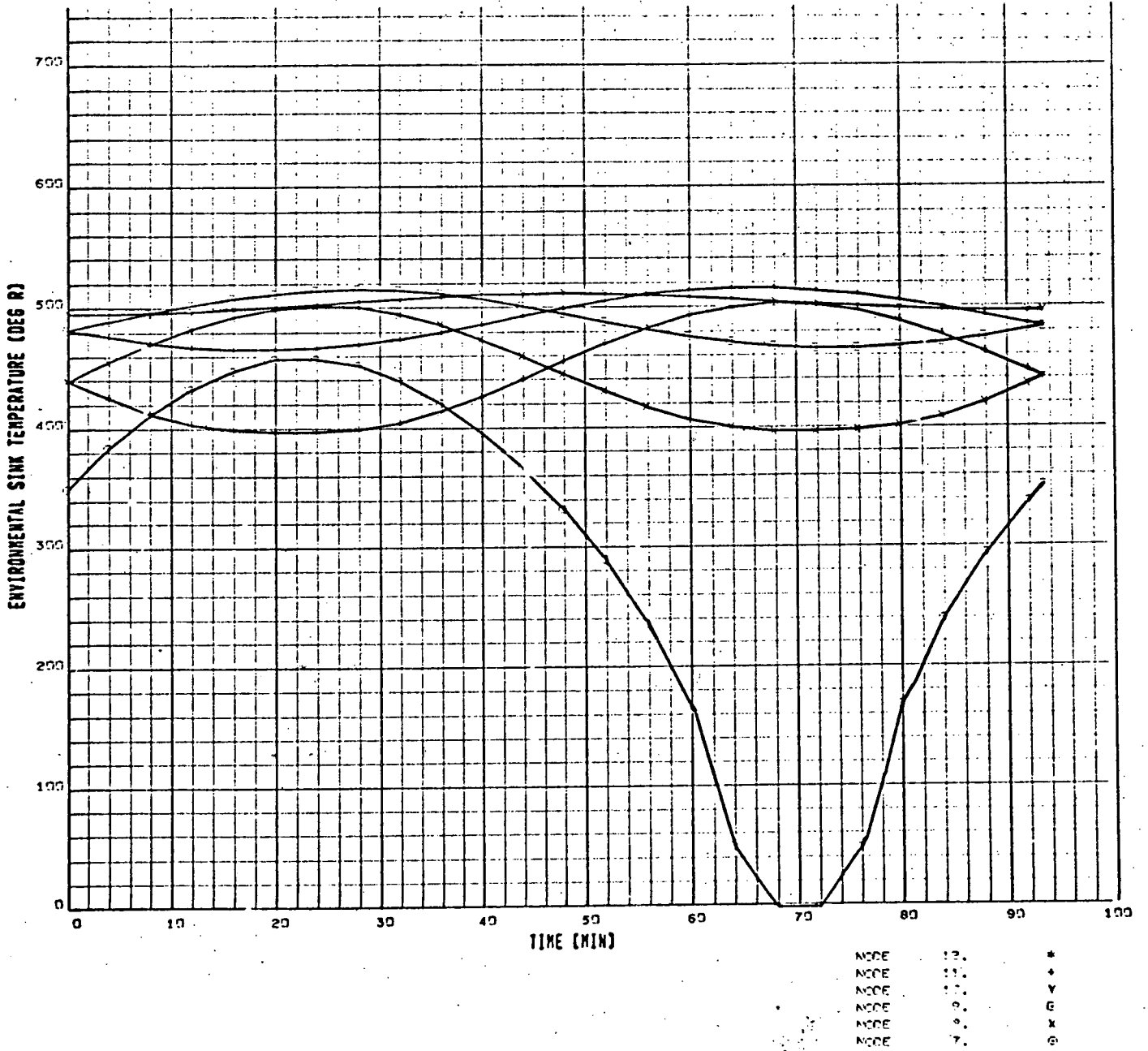


Figure A-17. Case 6

SPACE STATION NOMINAL/HOT ORBIT (E) -- MAX. FLUX -- 1/2E-13/57

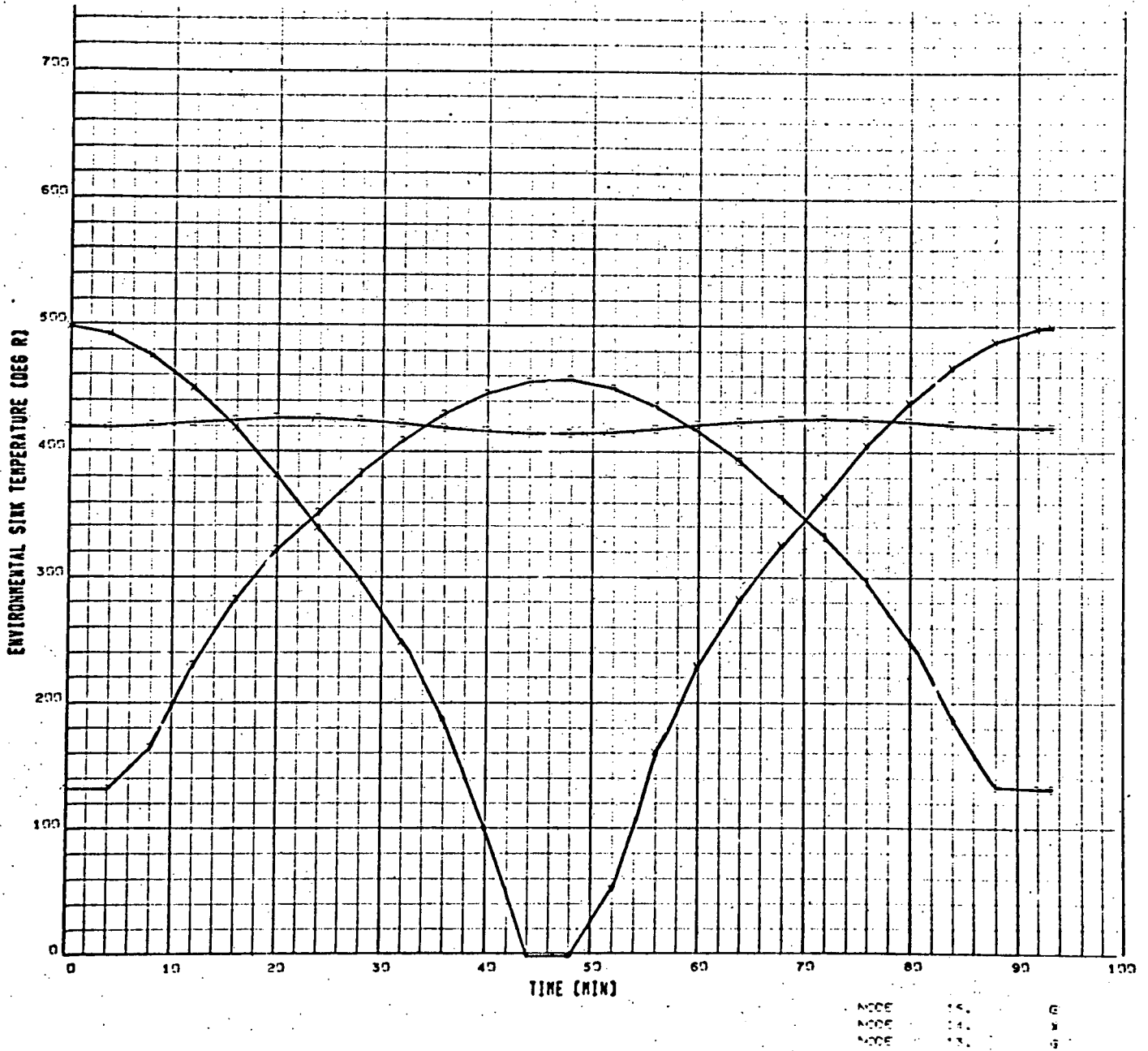


Figure A-18. Case 6

SPACE STATION HOTTEST AVERAGE ORBIT (1) -- MAX FLUX -- A/E=.20/.67

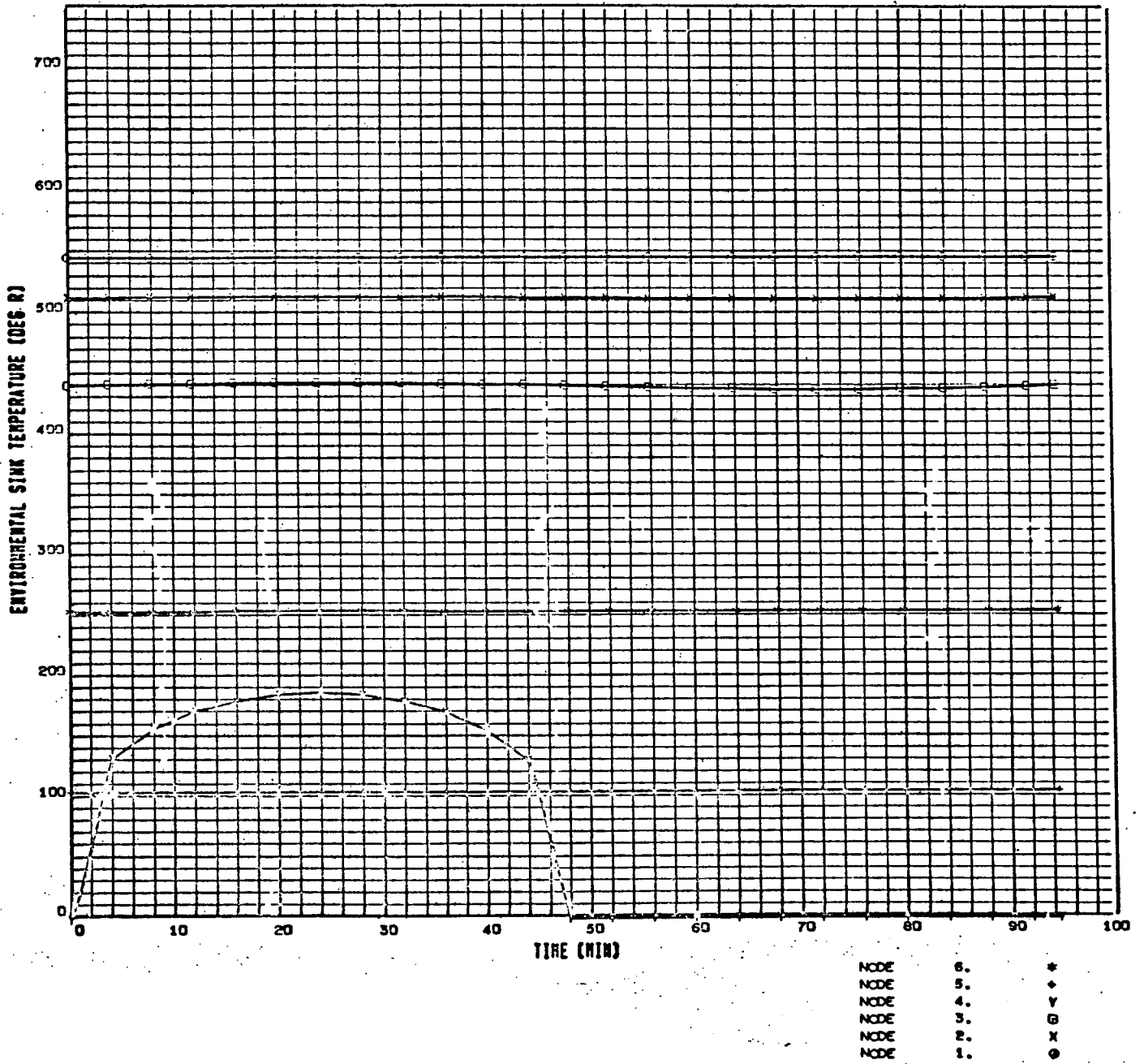


Figure A-19. Case 7

SPACE STATION HOTTEST AVERAGE ORBIT(1) -- MAX FLUX -- A/E=.20/.67

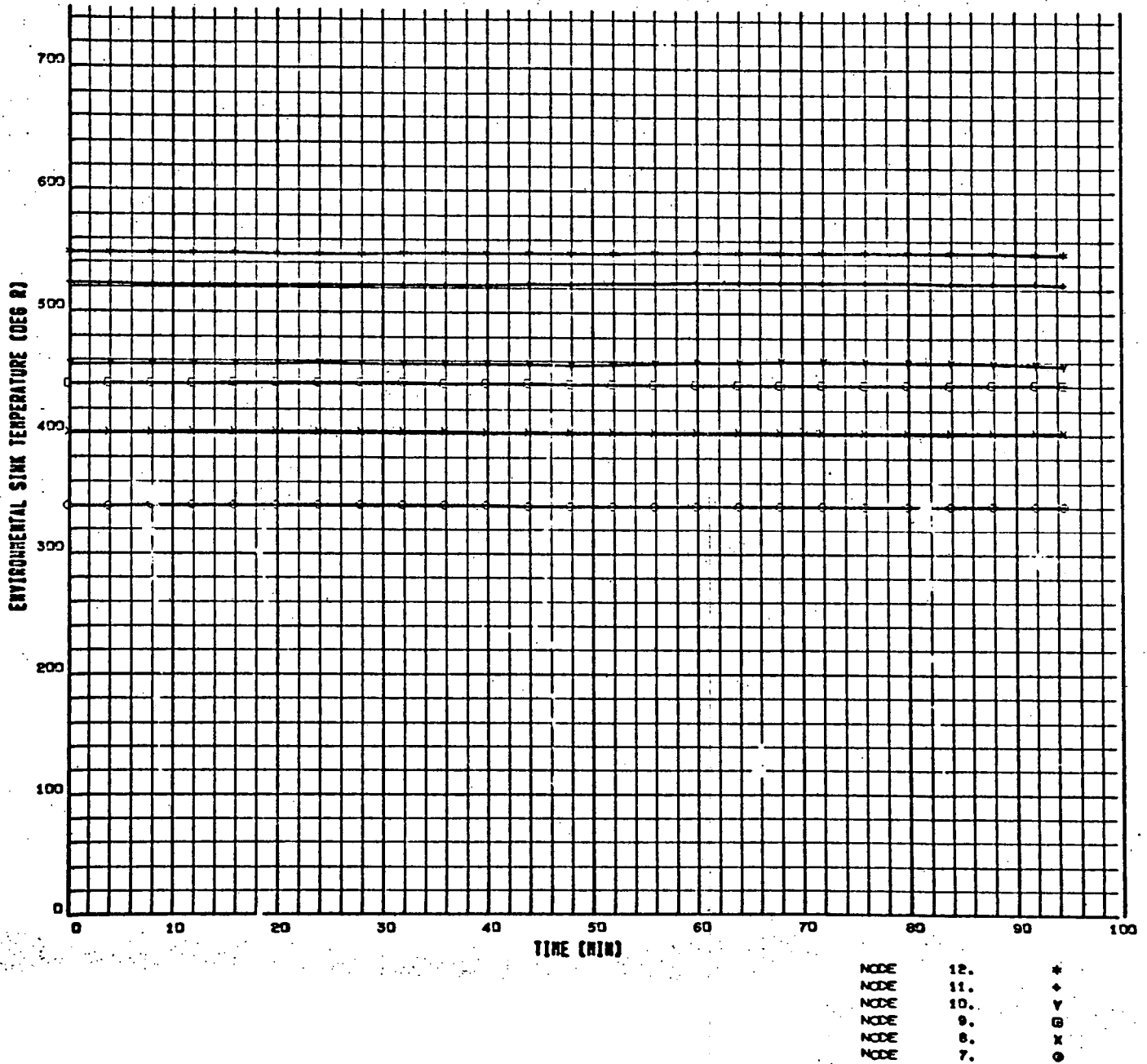


Figure A-20. Case 7

SPACE STATION HOTTEST AVERAGE CRBIT(1) -- MAX FLUX --A/E=.20/.67

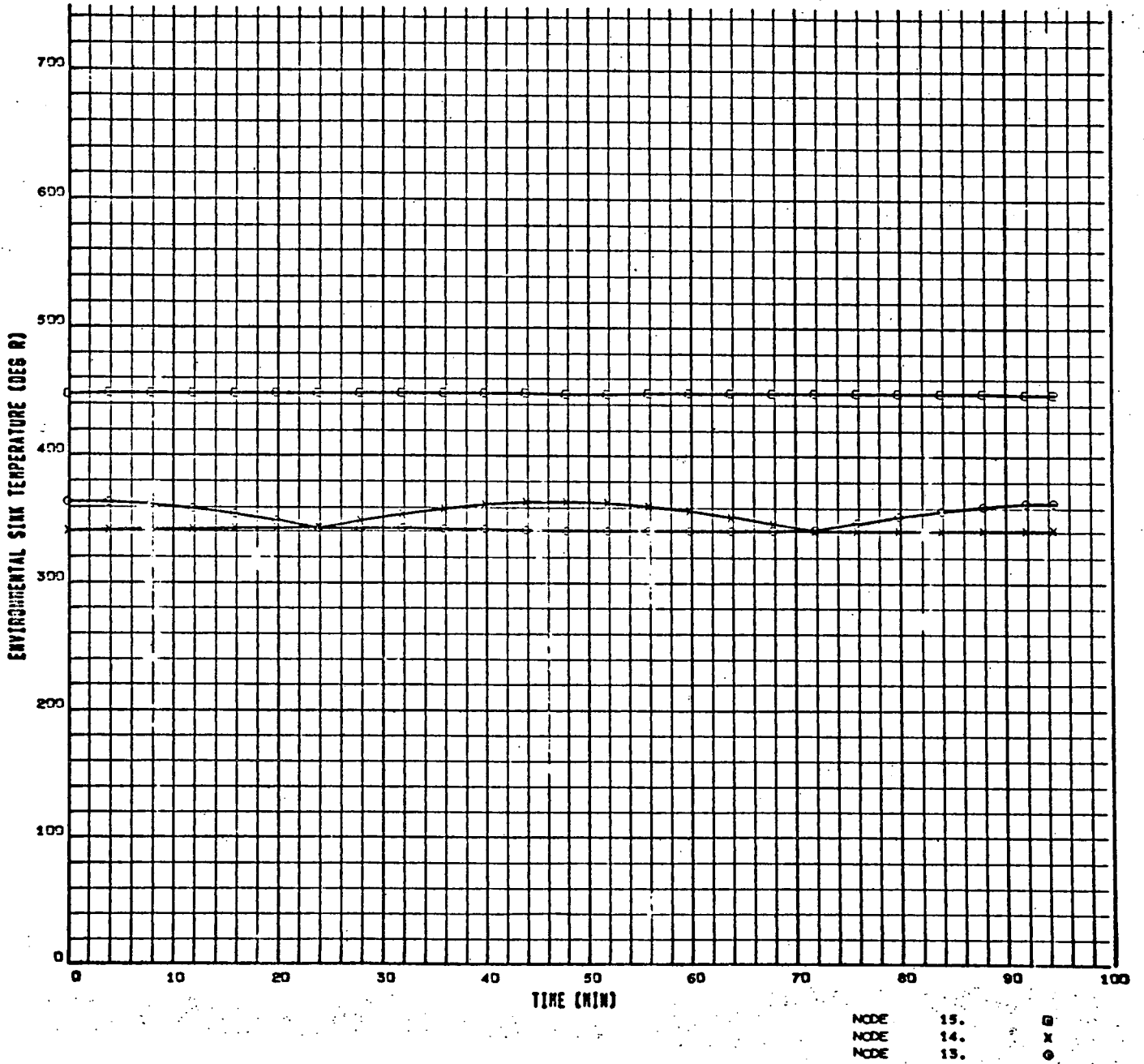


Figure A-21. Case 7

SPACE STATION HOTTEST INSTANT. CRBIT (2) -- MAX FLUX -- $A/E = .20/.67$

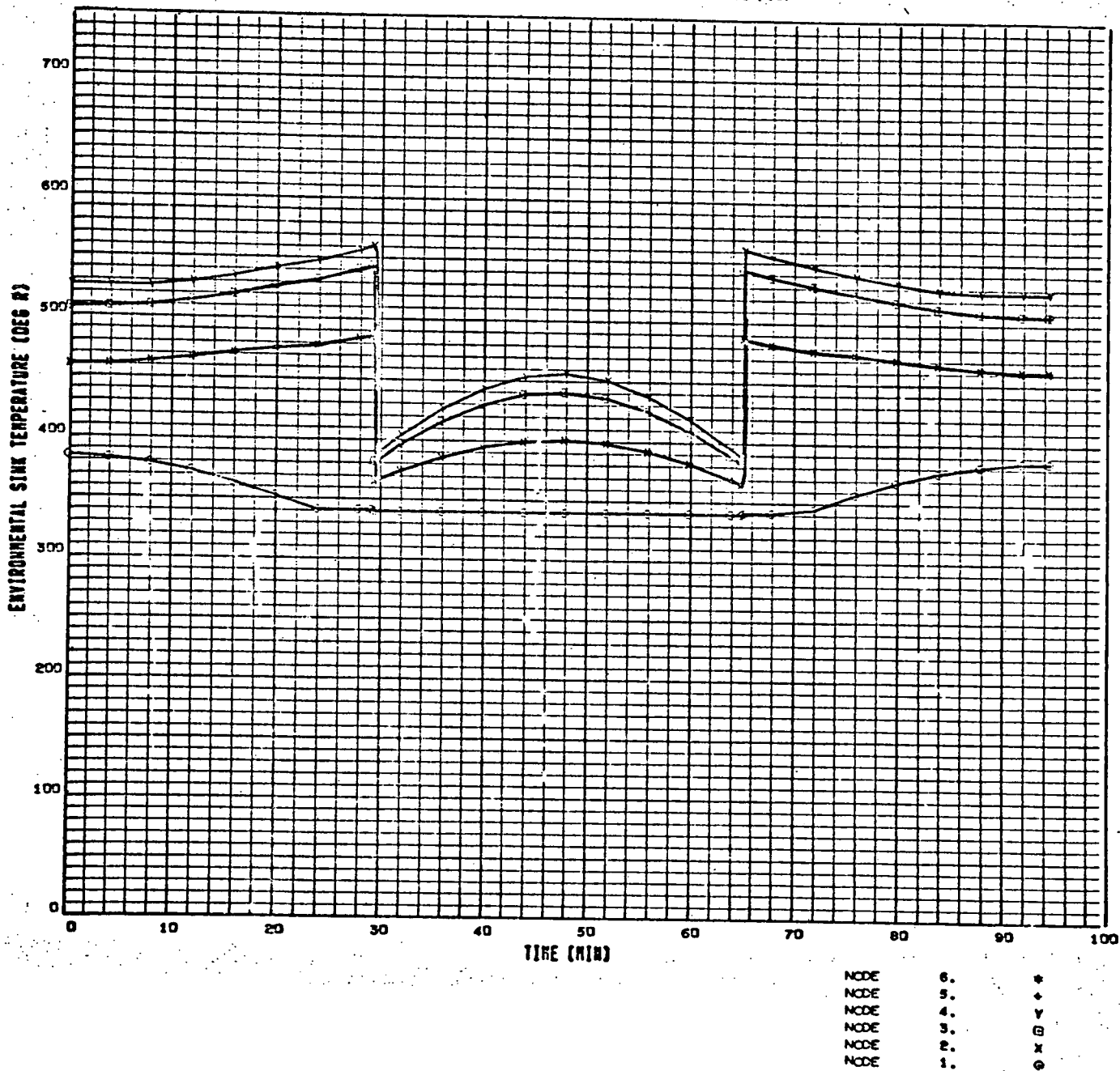


Figure A-22. Case 8

SPACE STATION HOTTEST INSTANT. CRBIT(2) -- MAX FLUX -- A/E=.25/.67

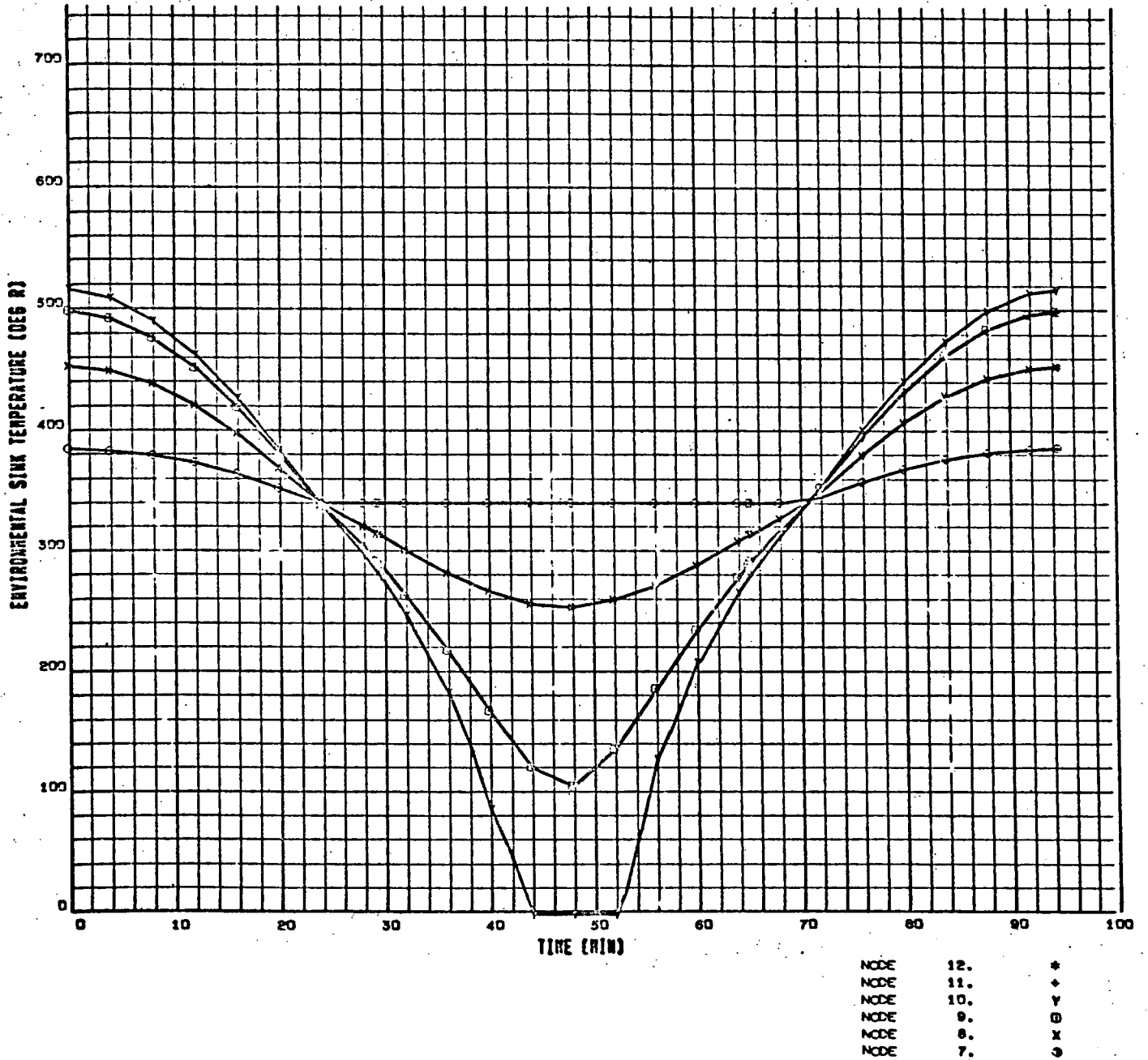


Figure A-23. Case 8

SPACE STATION HOTTEST INSTANT. CRBIT(2) -- MAX FLUX -- A/E=.20/.67

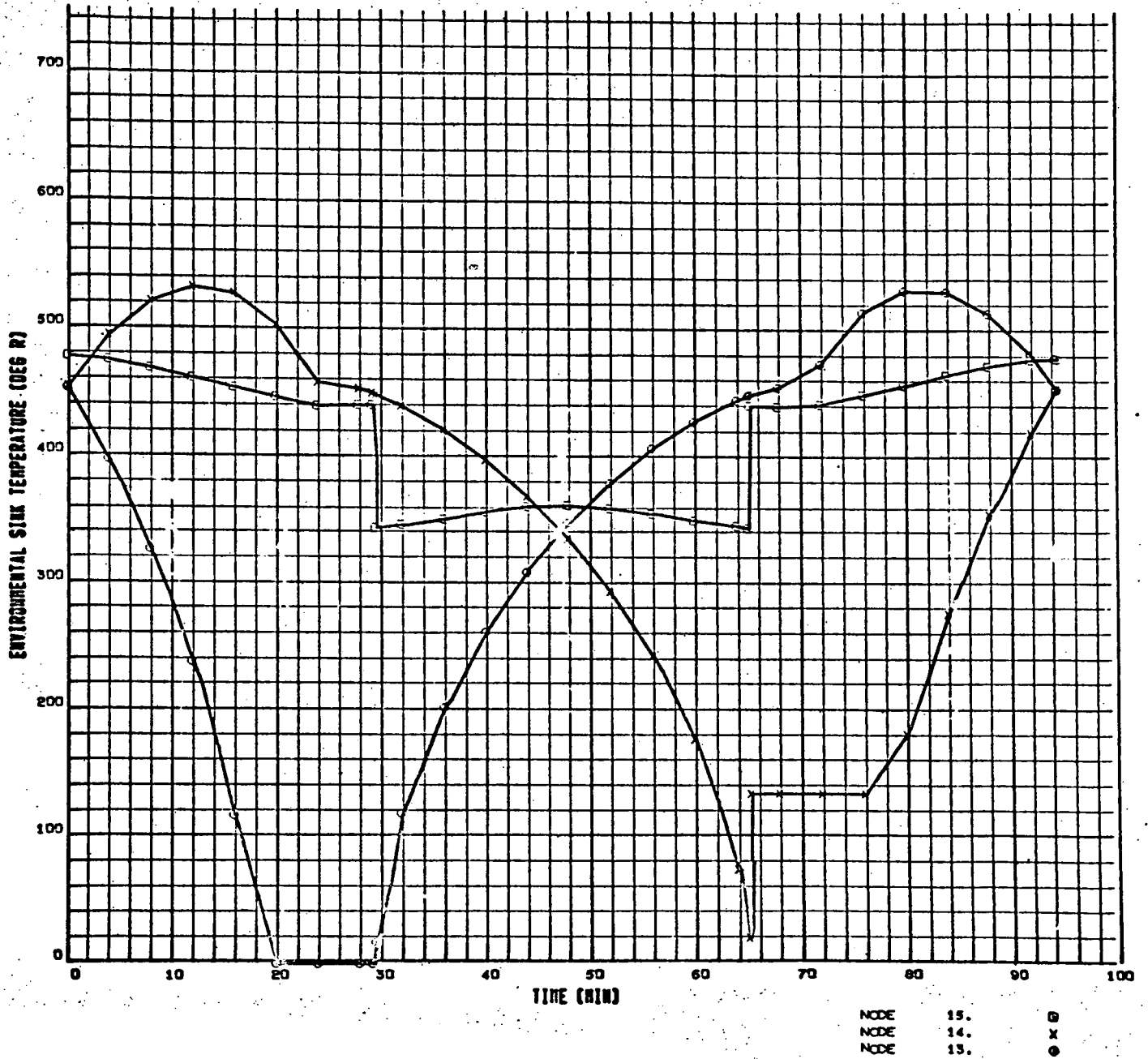


Figure A-24. Case 8

D

SPACE STATION COLDEST AVERAGE ORBIT (3) -- MIN FLUX -- A/E = .207.67

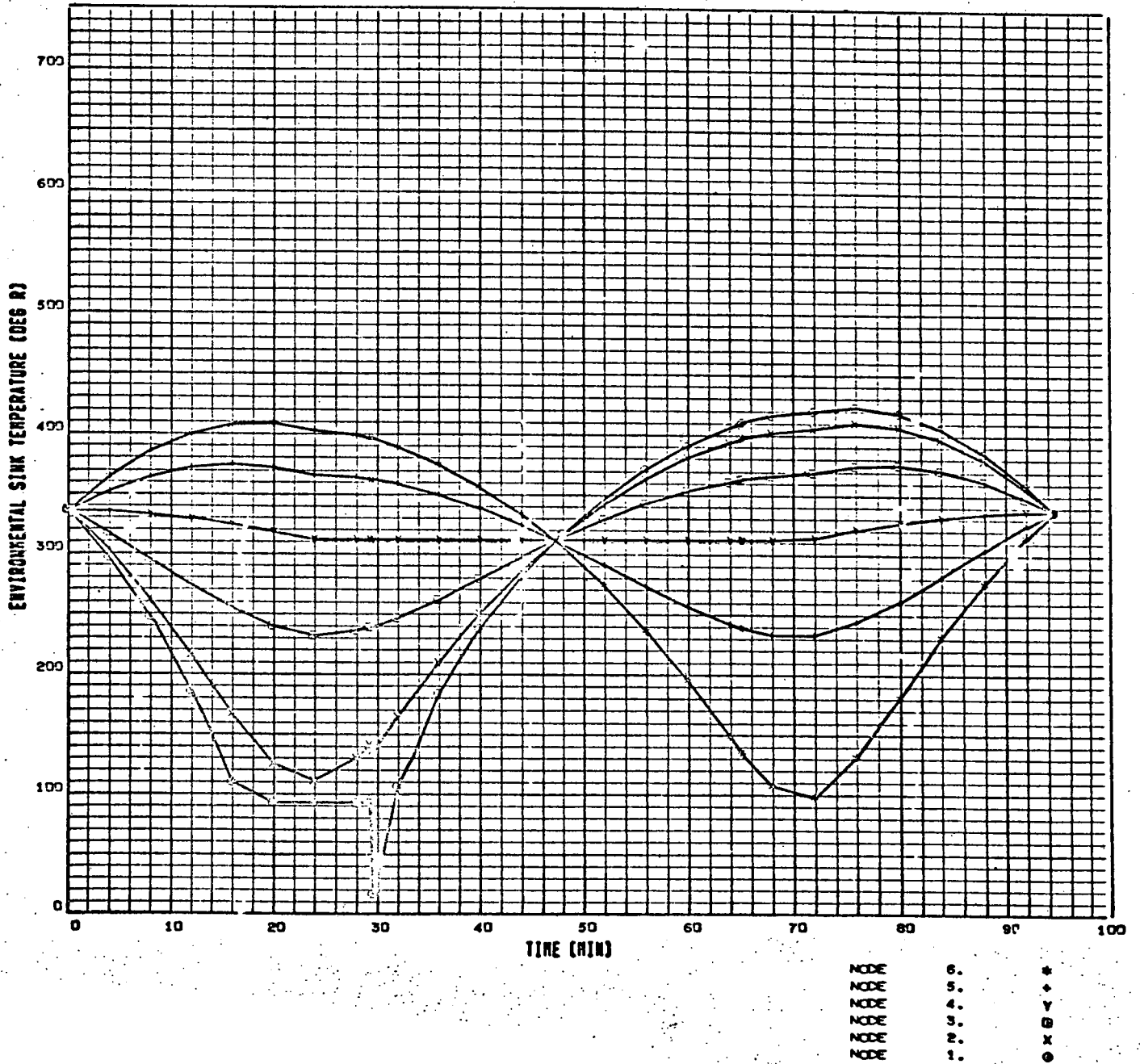


Figure A-25. Case 9

SPACE STATION COLDEST AVERAGE ORBIT (3) -- MIN FLUX -- A/E = .20/.67

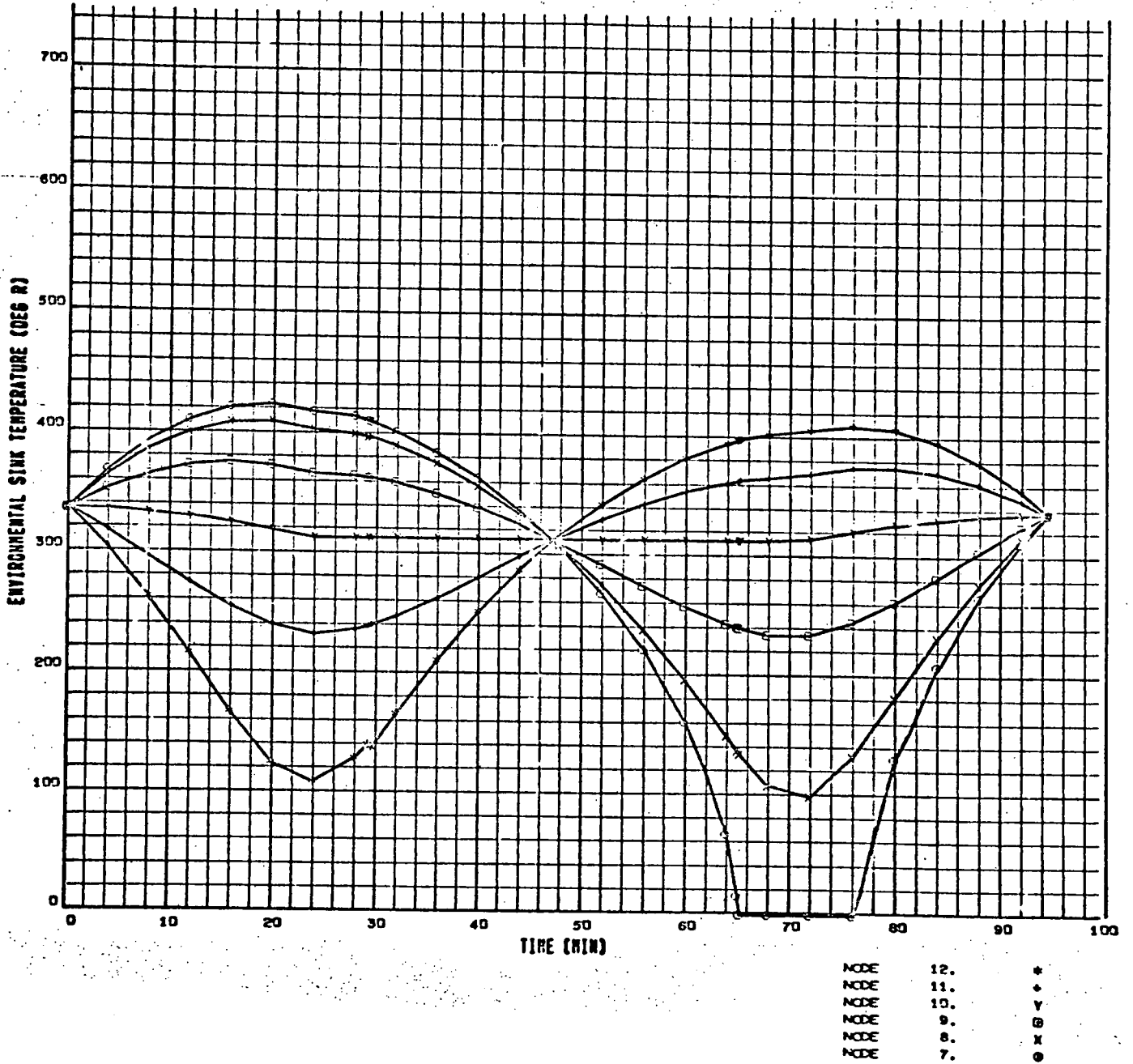


Figure A-26. Case 9

SPACE STATION COLDEST AVERAGE ORBIT (3) -- MIN FLUX --A/E=.20/.67

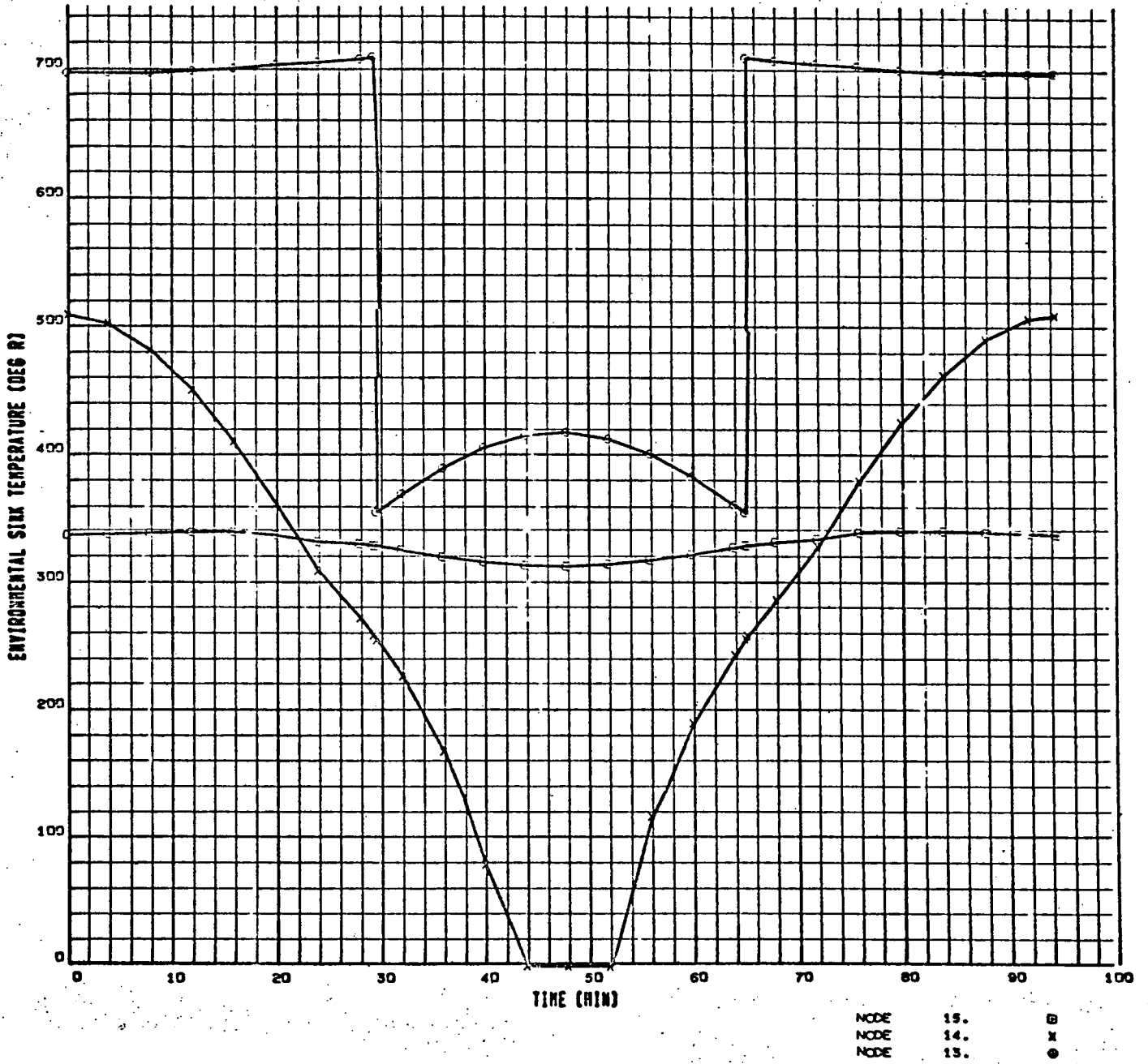


Figure A-27. Case 9

SPACE STATION LARGE TRANSIENT ORBIT (4) — NCM FLUX — A/E=.20/.67

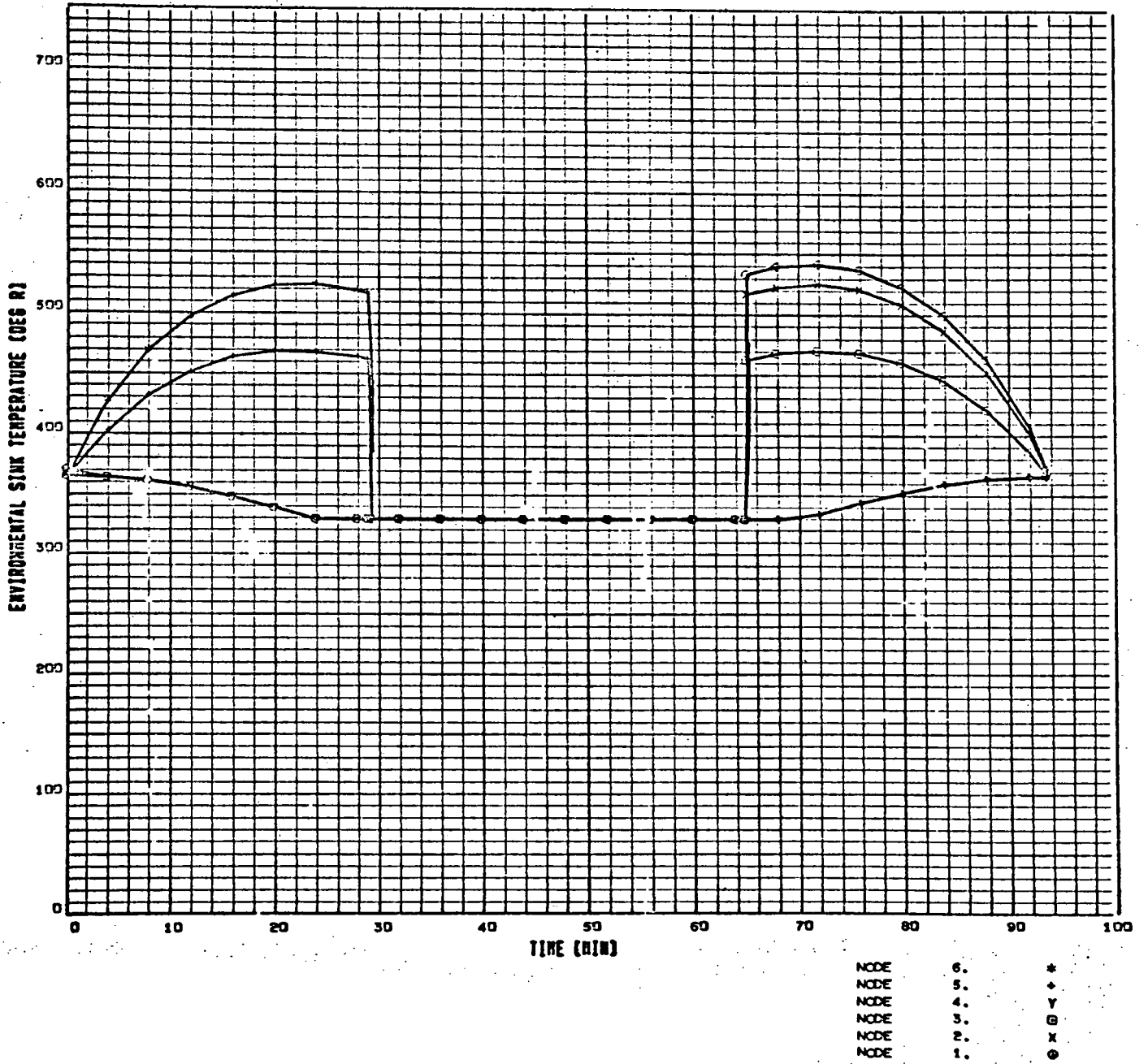


Figure A-28. Case 10

SPACE STATION LARGE TRANSIENT ORBIT (4) -- NCM FLUX -- A/E = .20/.67

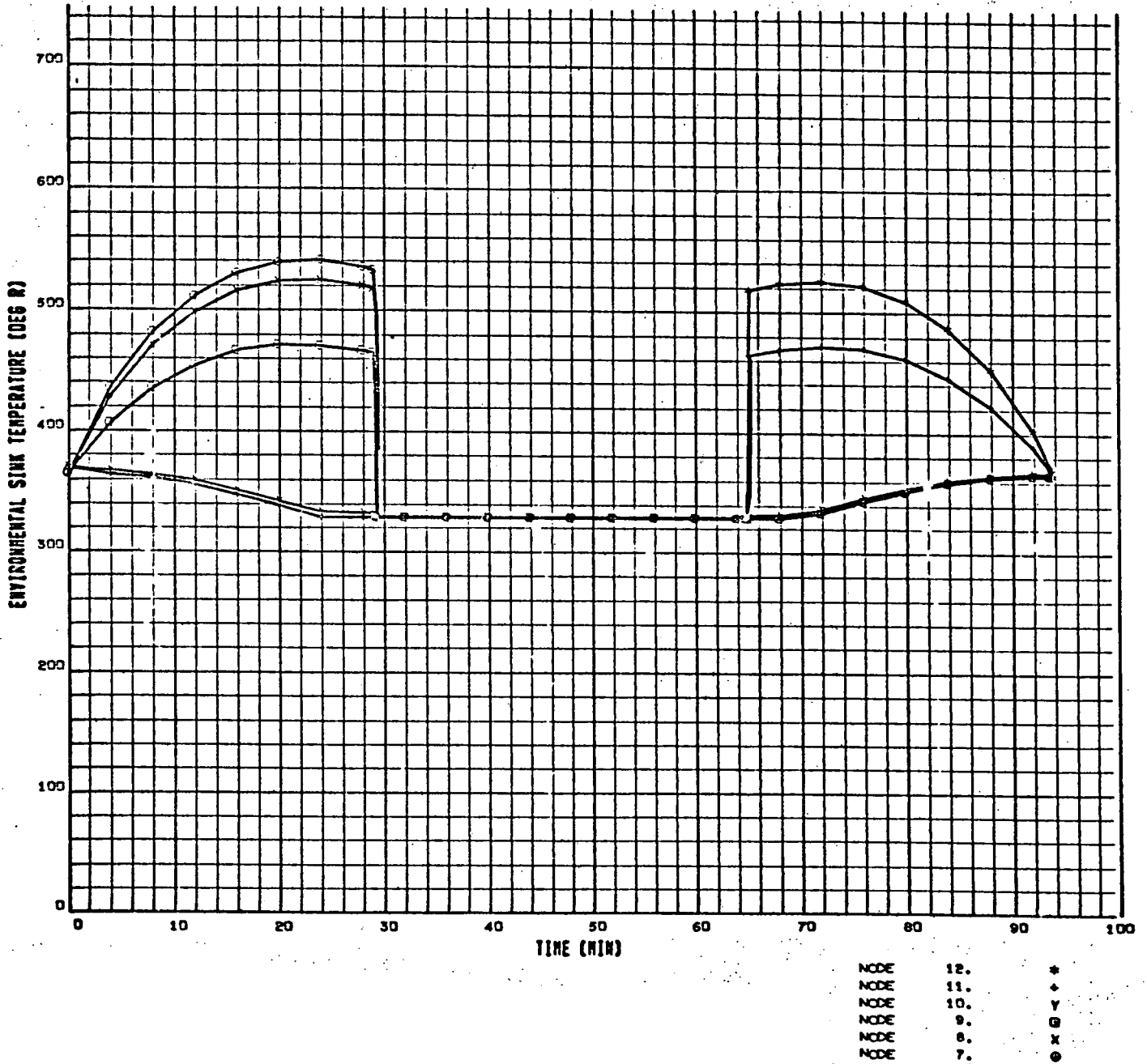


Figure A-29. Case 10

SPACE STATION LARGE TRANSIENT ORBIT (4) -- NOM FLUX --A/E=.20/.67

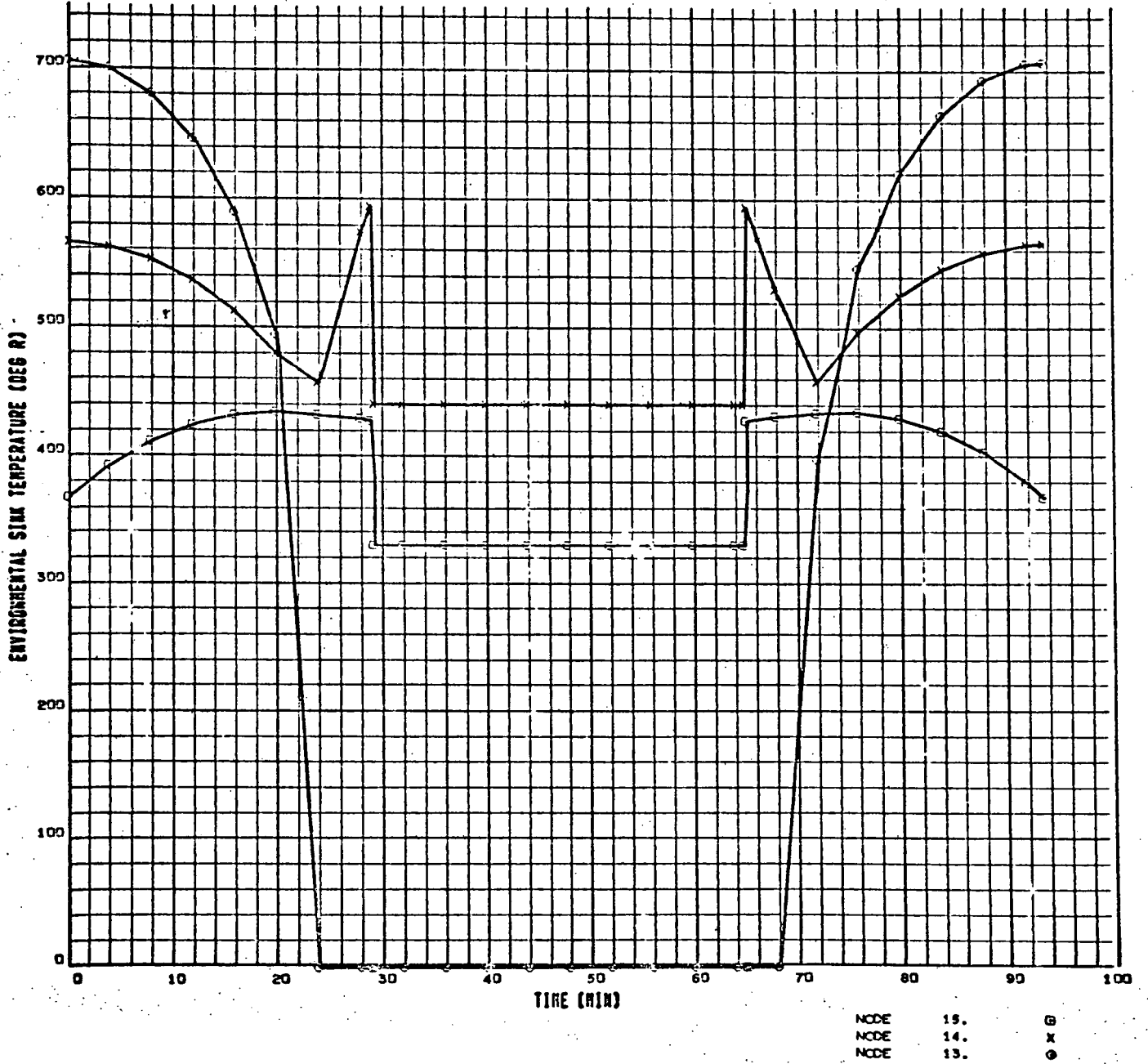


Figure A-30. Case 10

SPACE STATION NOMINAL ORBIT (5) -- NOM FLUX -- A/E=.20/.67

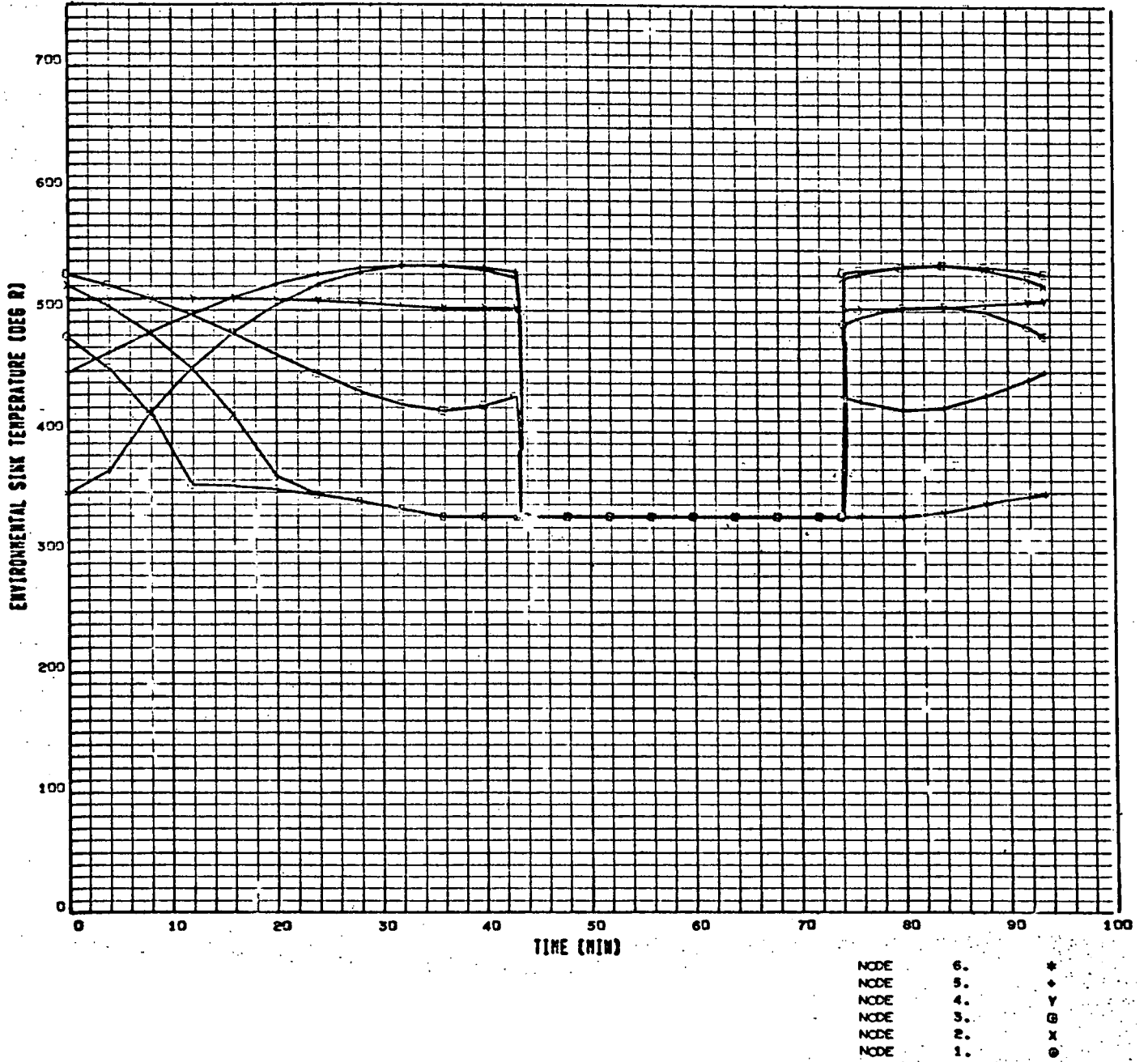


Figure A-31. Case 11

SPACE STATION NOMINAL ORBIT (5) -- NOM FLUX -- A/E=.20/.67

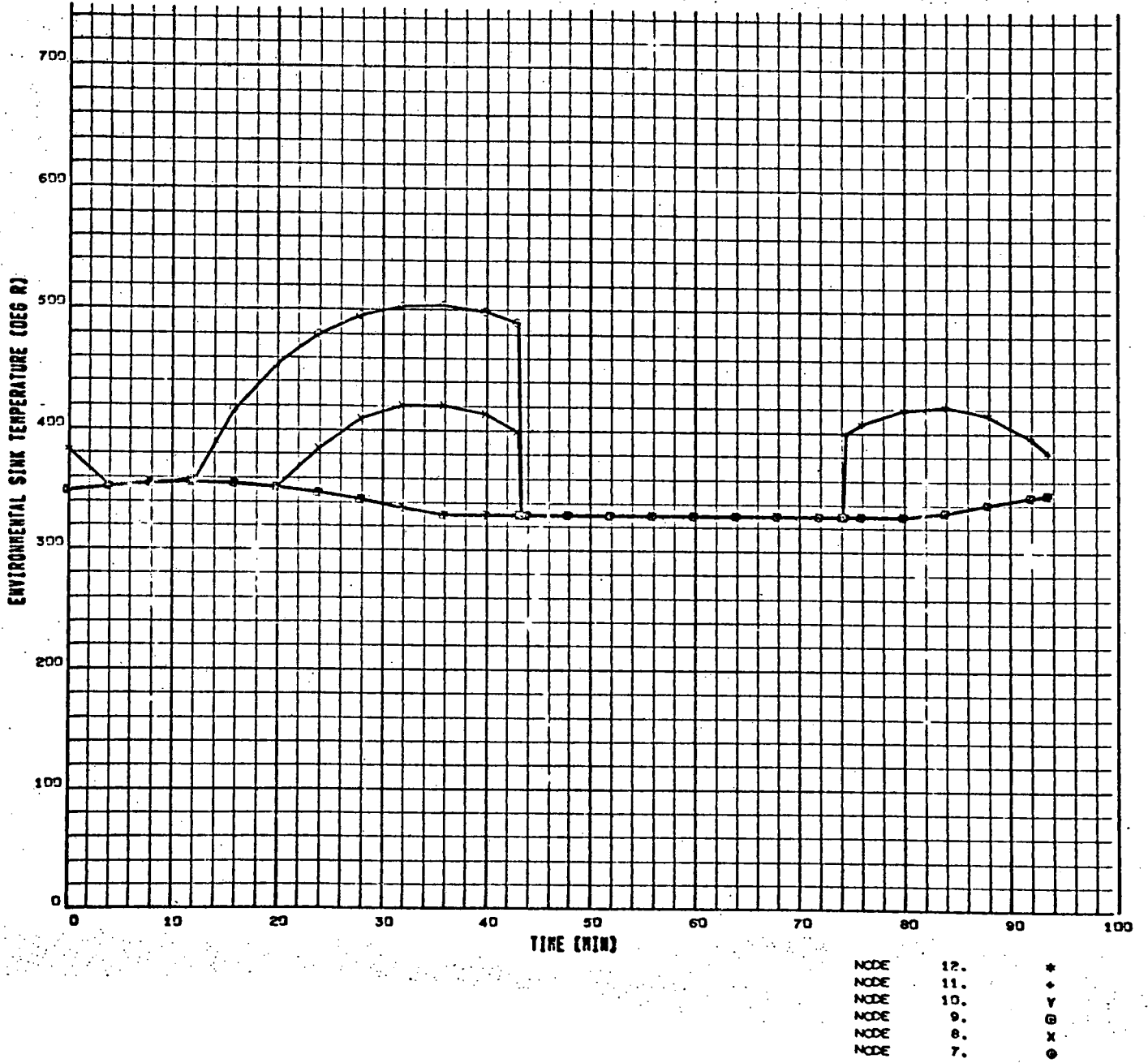


Figure A-32. Case 11

SPACE STATION NOMINAL ORBIT (5) -- NCM FLUX -- A/E=.20/.67

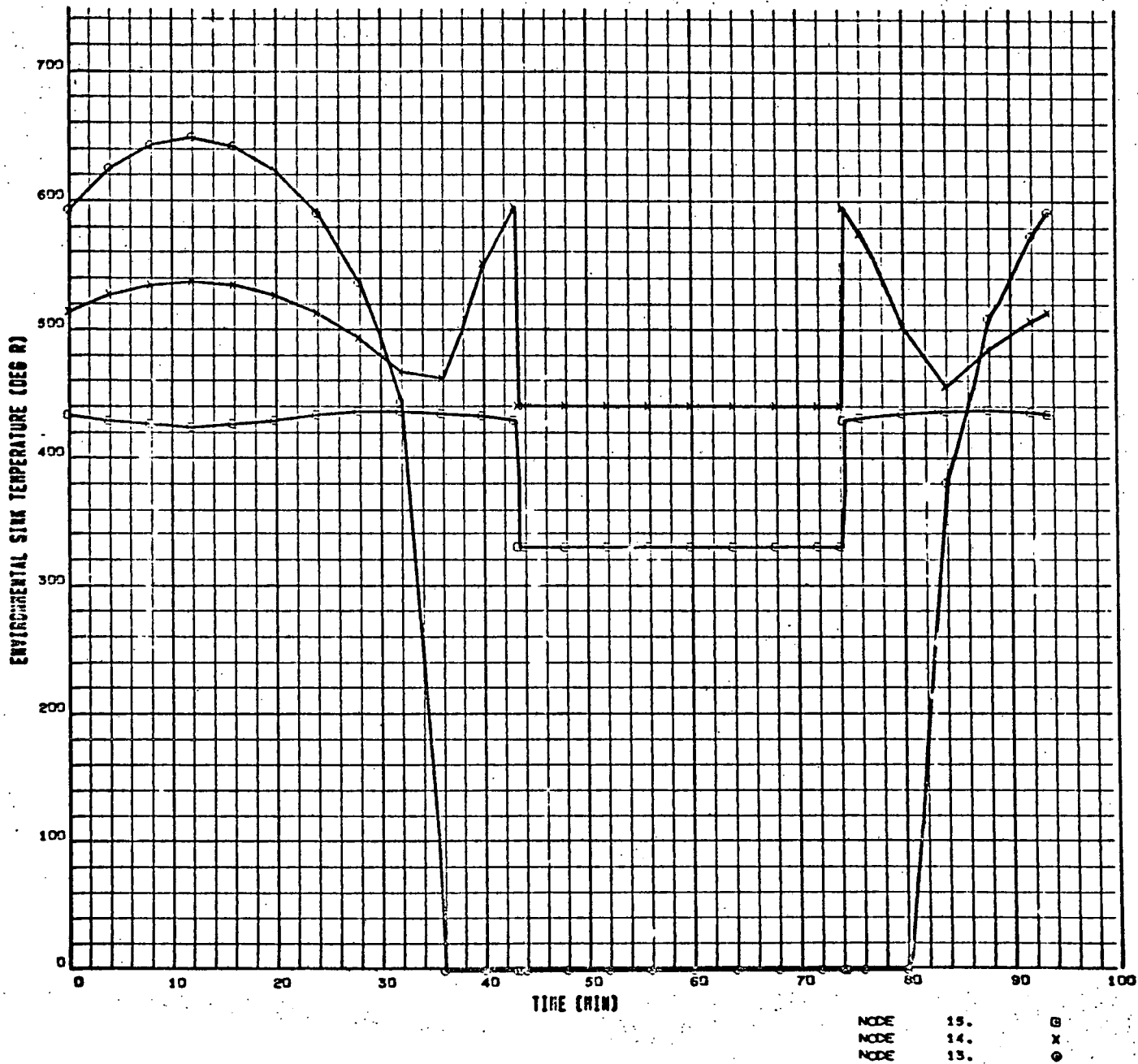


Figure A-33. Case 11

SPACE STATION NOMINAL/HOT CRBIT(5) -- MAX FLUX -- A/E=.23/.67

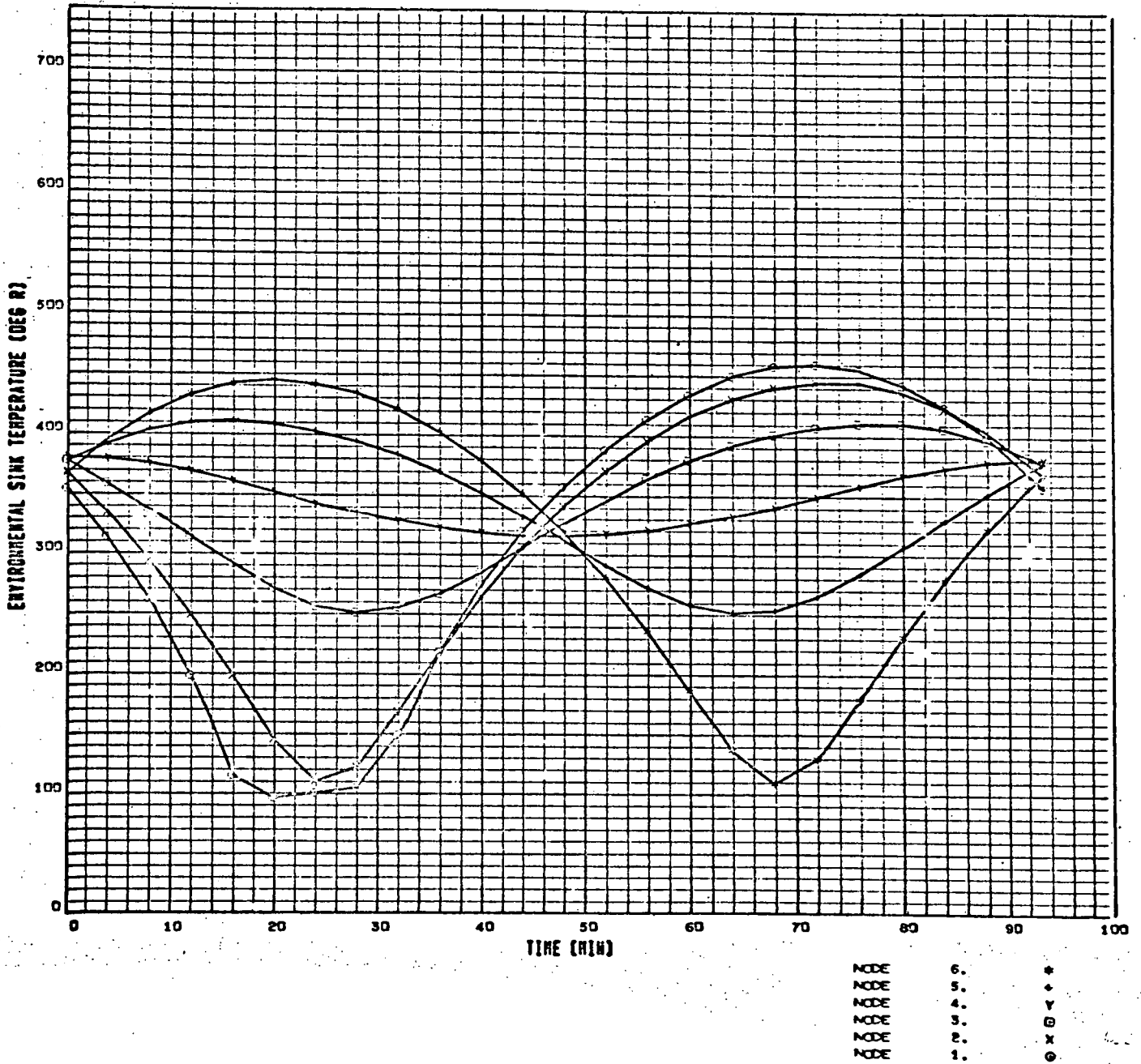


Figure A-34. Case 12

SPACE STATION NOMINAL/HCT CRBIT (S) -- MAX FLUX -- A/E=.20/.67

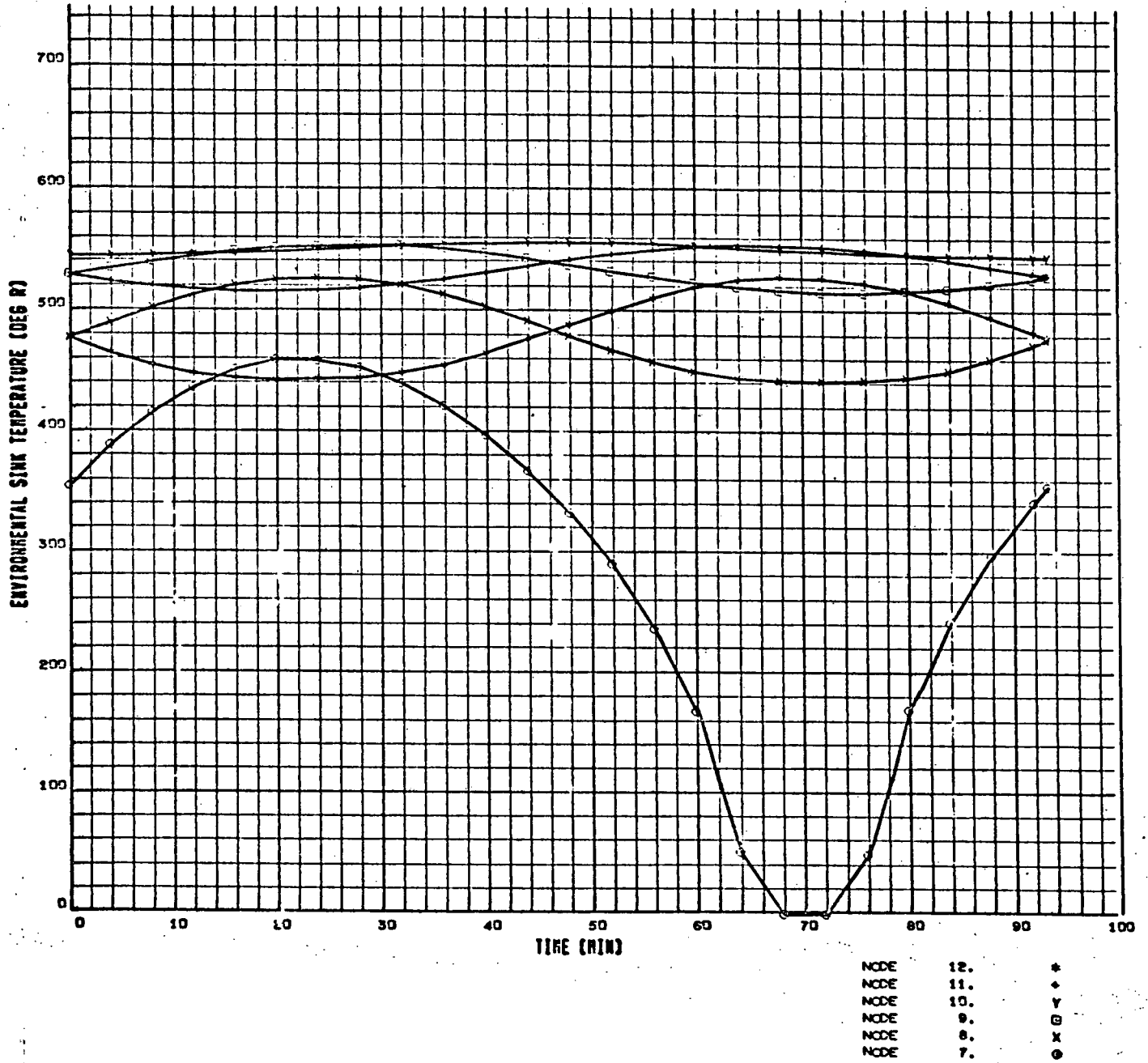


Figure A-35. Case 12

SPACE STATION NOMINAL/HOT ORBIT (6) -- MAX FLUX -- A/E=.20/.67

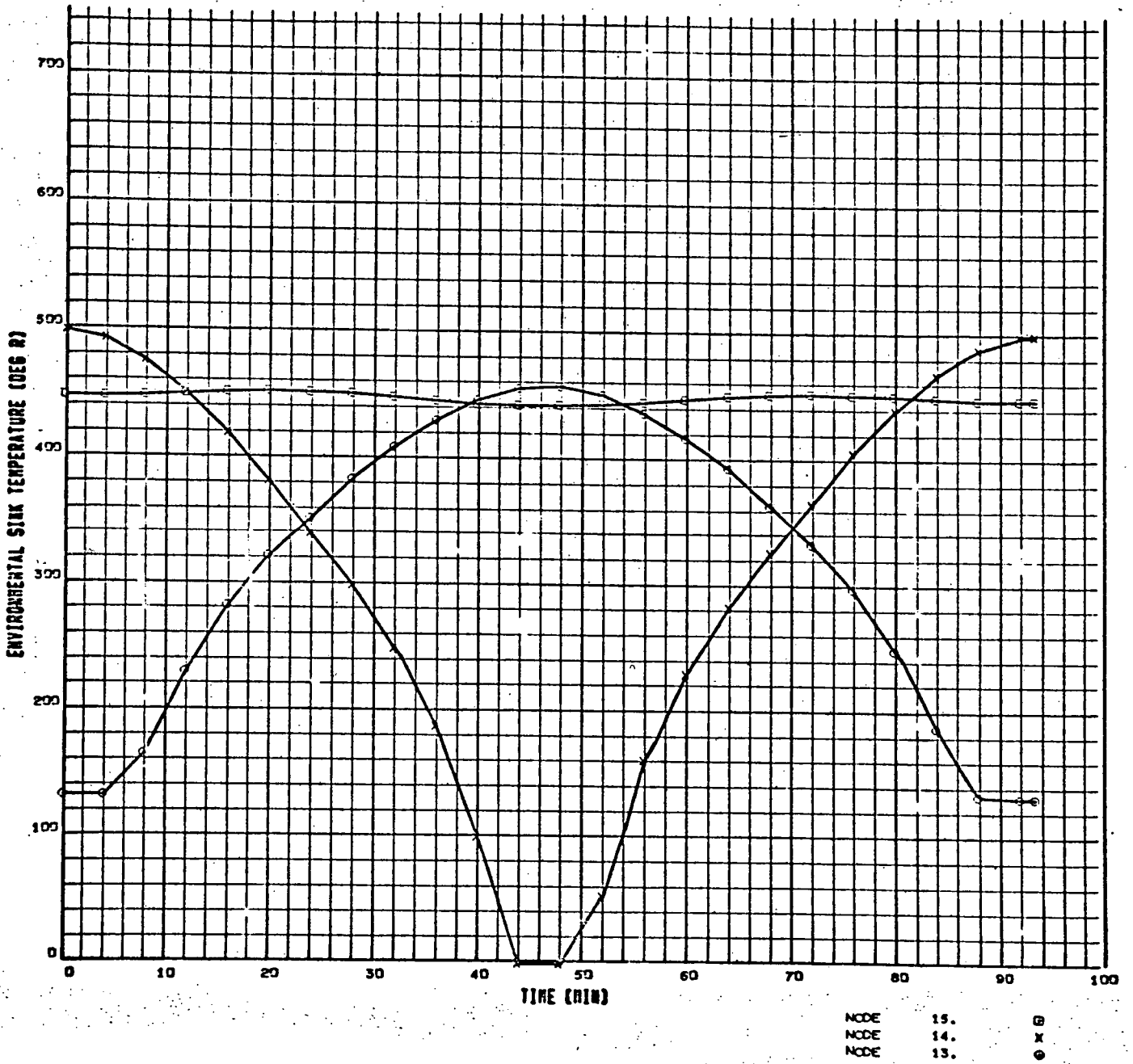
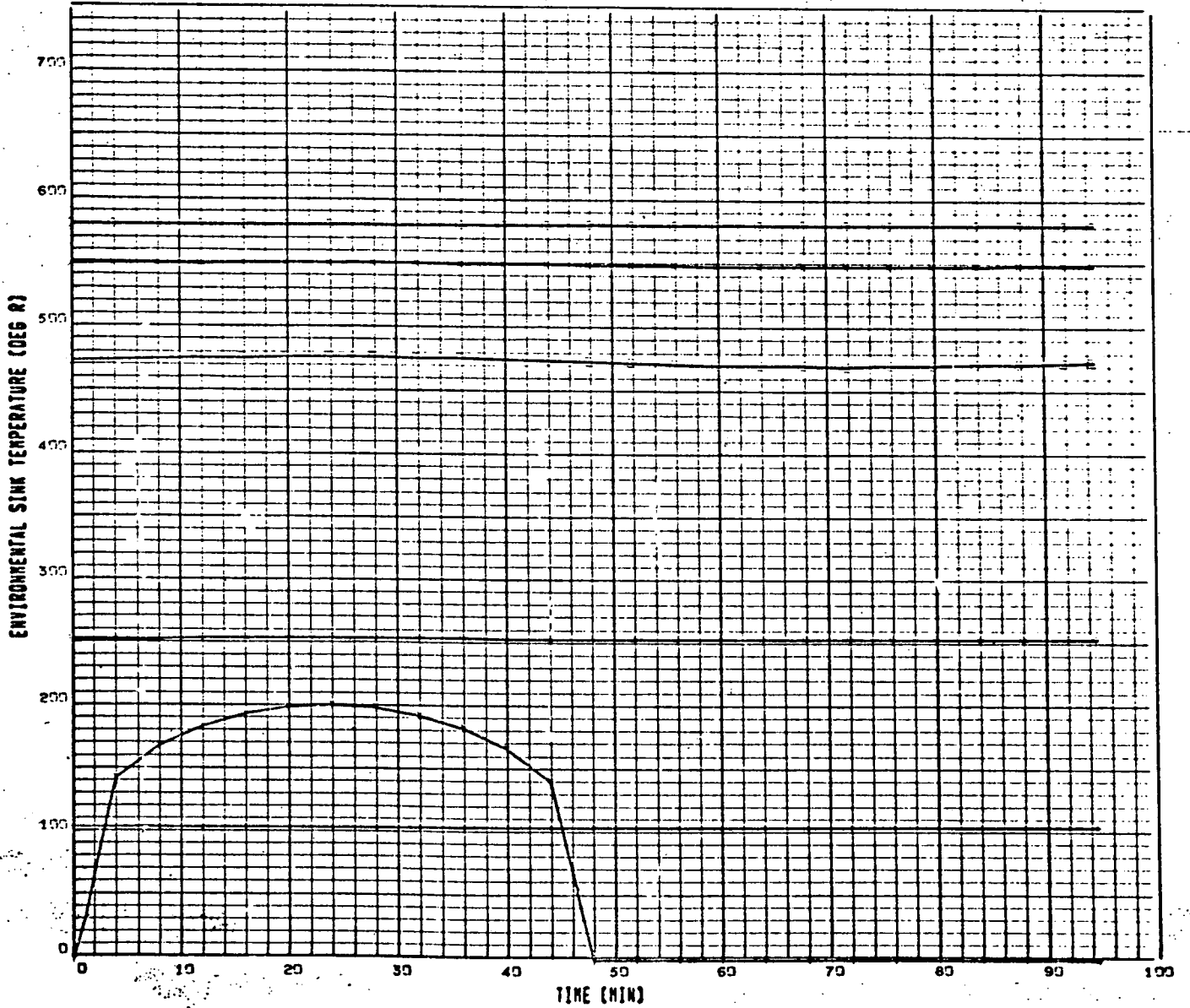


Figure A-36. Case 12

SPACE STATION HOTTEST AVERAGE ORBIT (1) -- MAX FLUX -- 1/2E=1.35/0.0



NCDE	5.	*
NCDE	5.	*
NCDE	4.	Y
NCDE	3.	G
NCDE	2.	X
NCDE	1.	G

Figure A-37. Case 13

SPACE STATION HOTTEST AVERAGE ORBIT (°) -- MAX FLUX -- 1/26/67

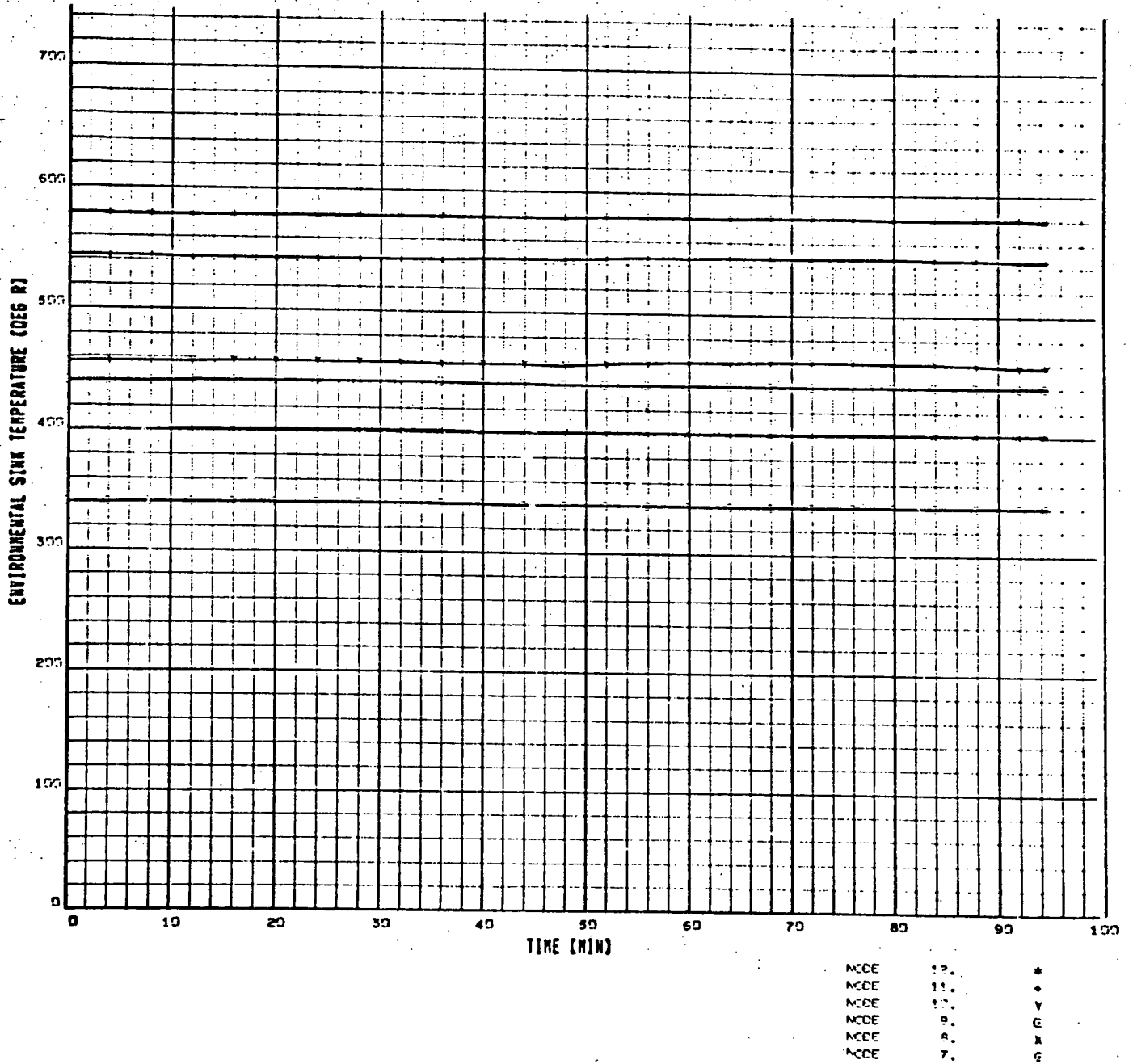


Figure A-38. Case 13

E

SPACE STATION HOTTEST AVERAGE CREDIT (°) -- MAX FLUX -- 1/26.35/80

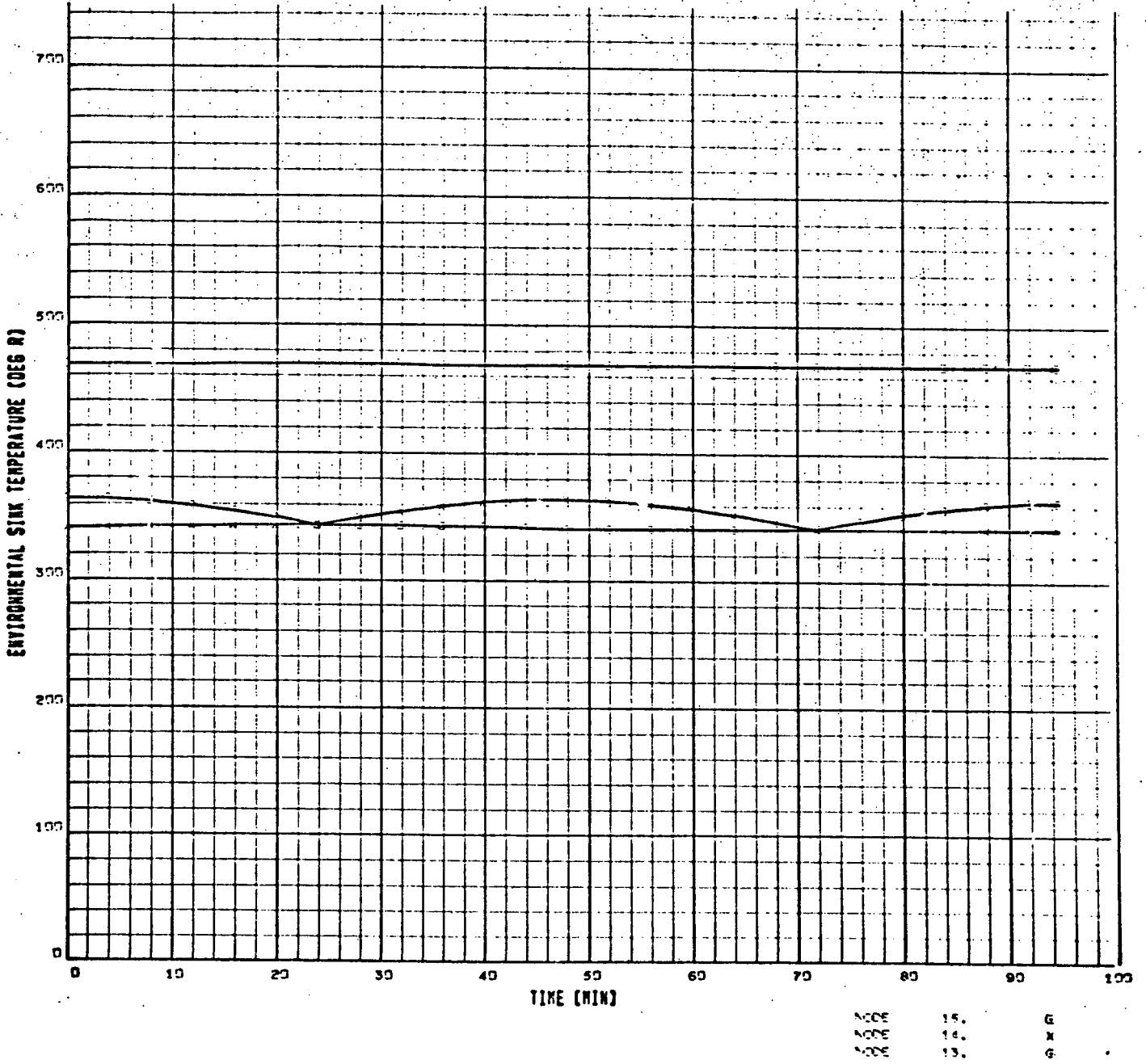


Figure A-39. Case 13

SPACE STATION HOTTEST INSTANT, CREFT(2) -- MAX FLUX -- 1/25/57, 57

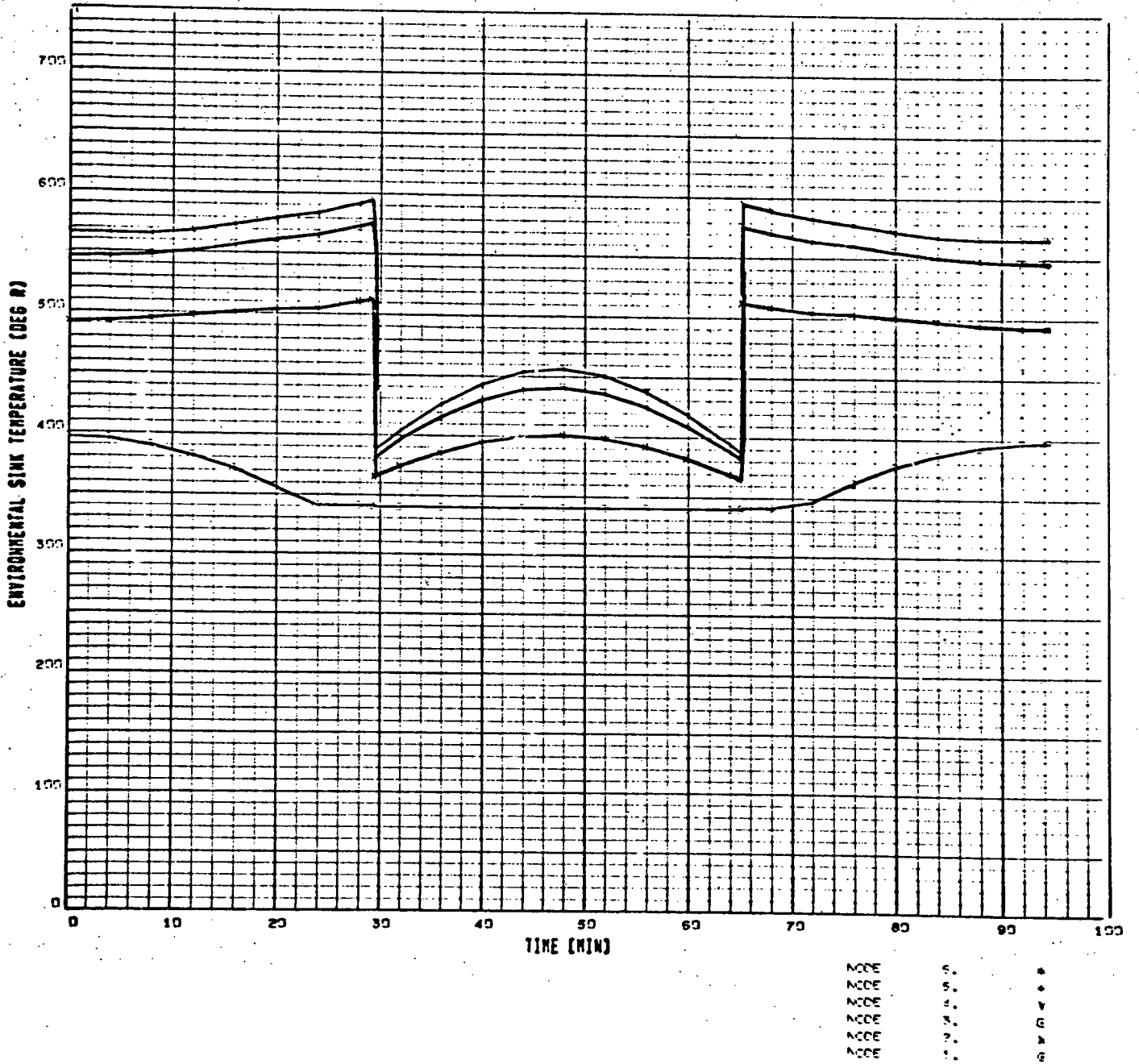


Figure A-40. Case 14

SPACE STATION HOTTEST INSTANT, CREDIT(?) -- MAX. FLUX -- AVER. 352.9°

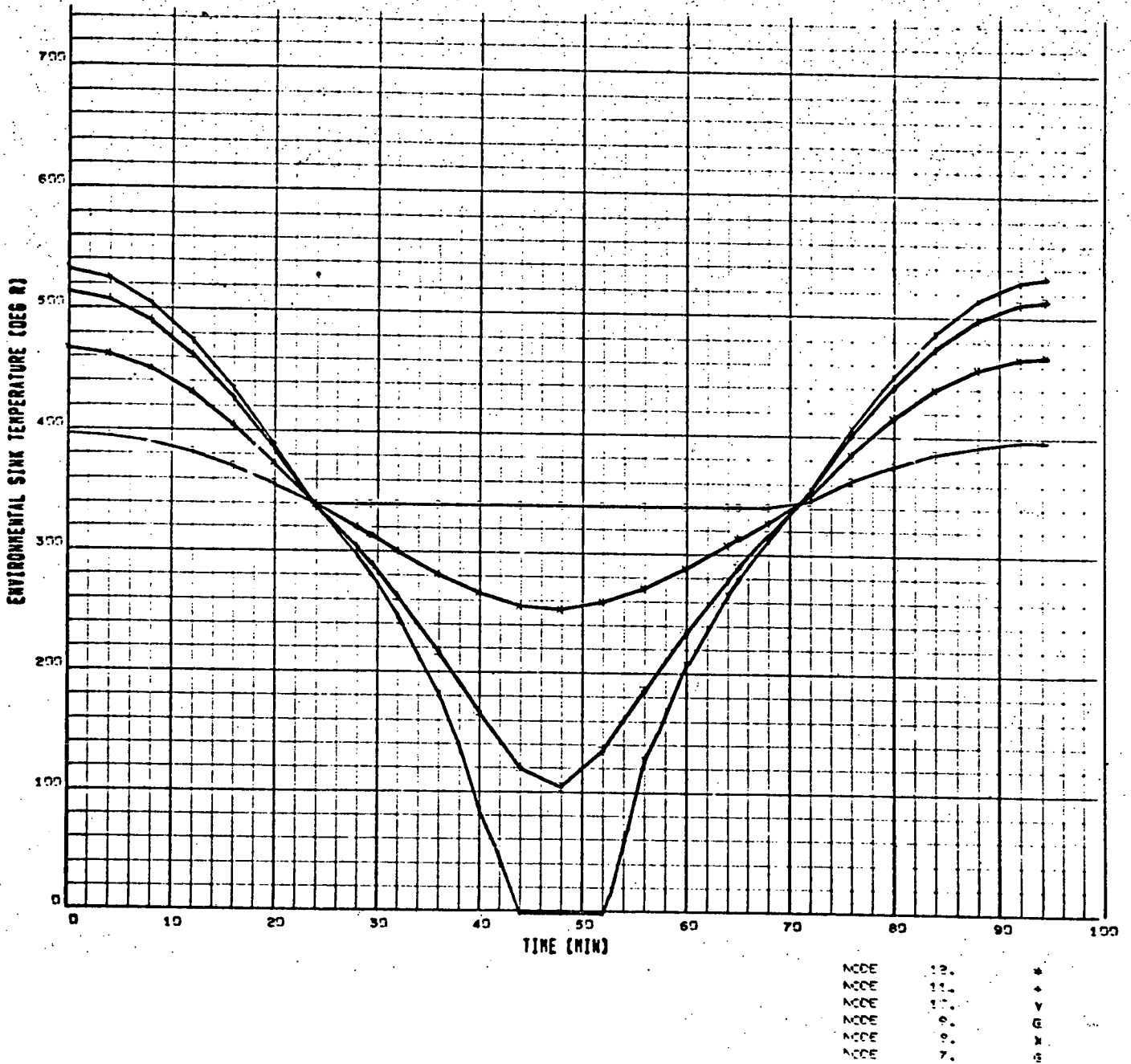


Figure A-41. Case 14

SPACE STATION HIGHEST INSTANT. ORBIT (C) -- MAX. PULL -- 1/20.00/5"

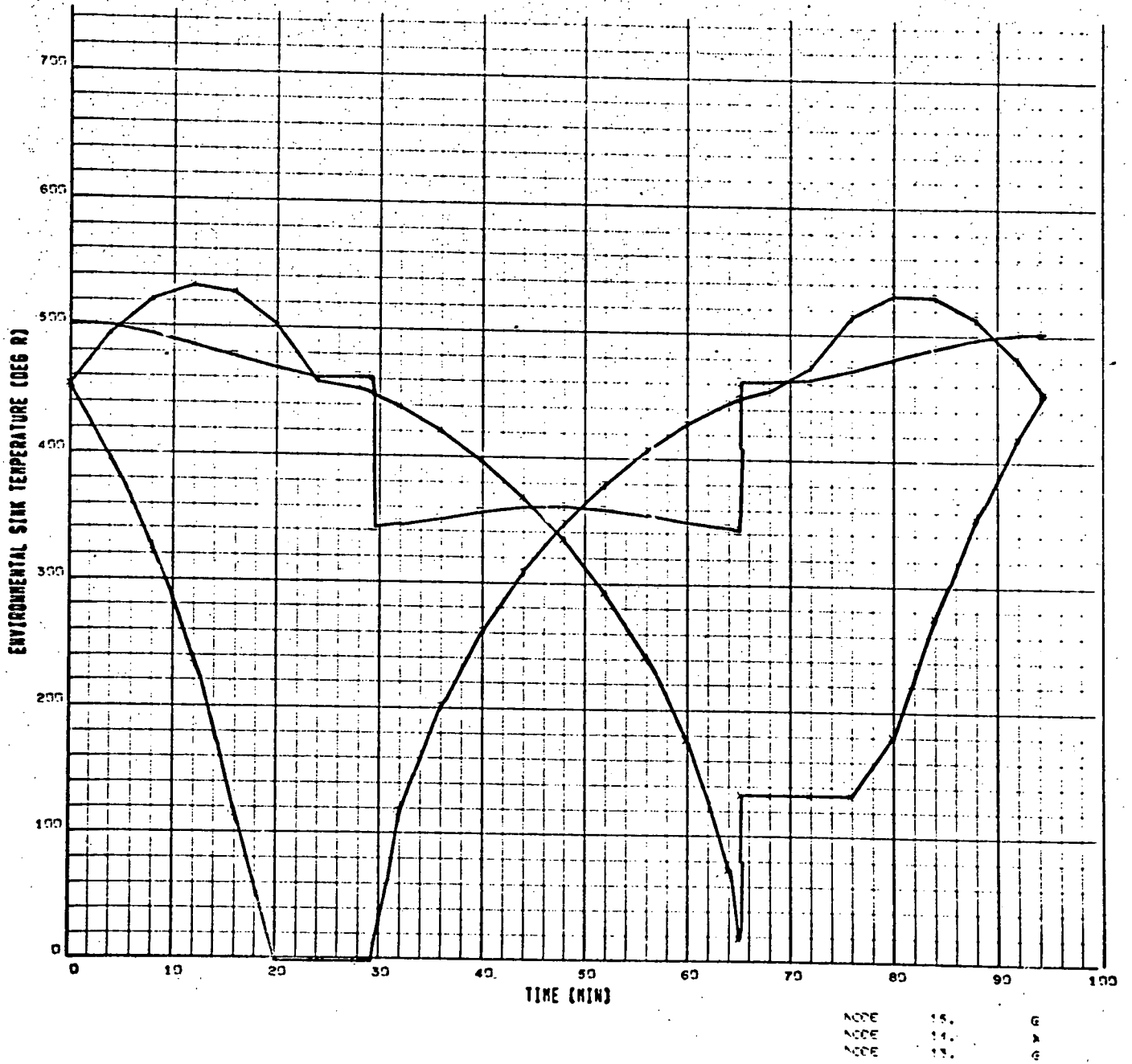


Figure A-42. Case 14

SPACE STATION COLDEST SURFACE COEFFICIENT -- MIN FLUX -- VER. 10/7/68

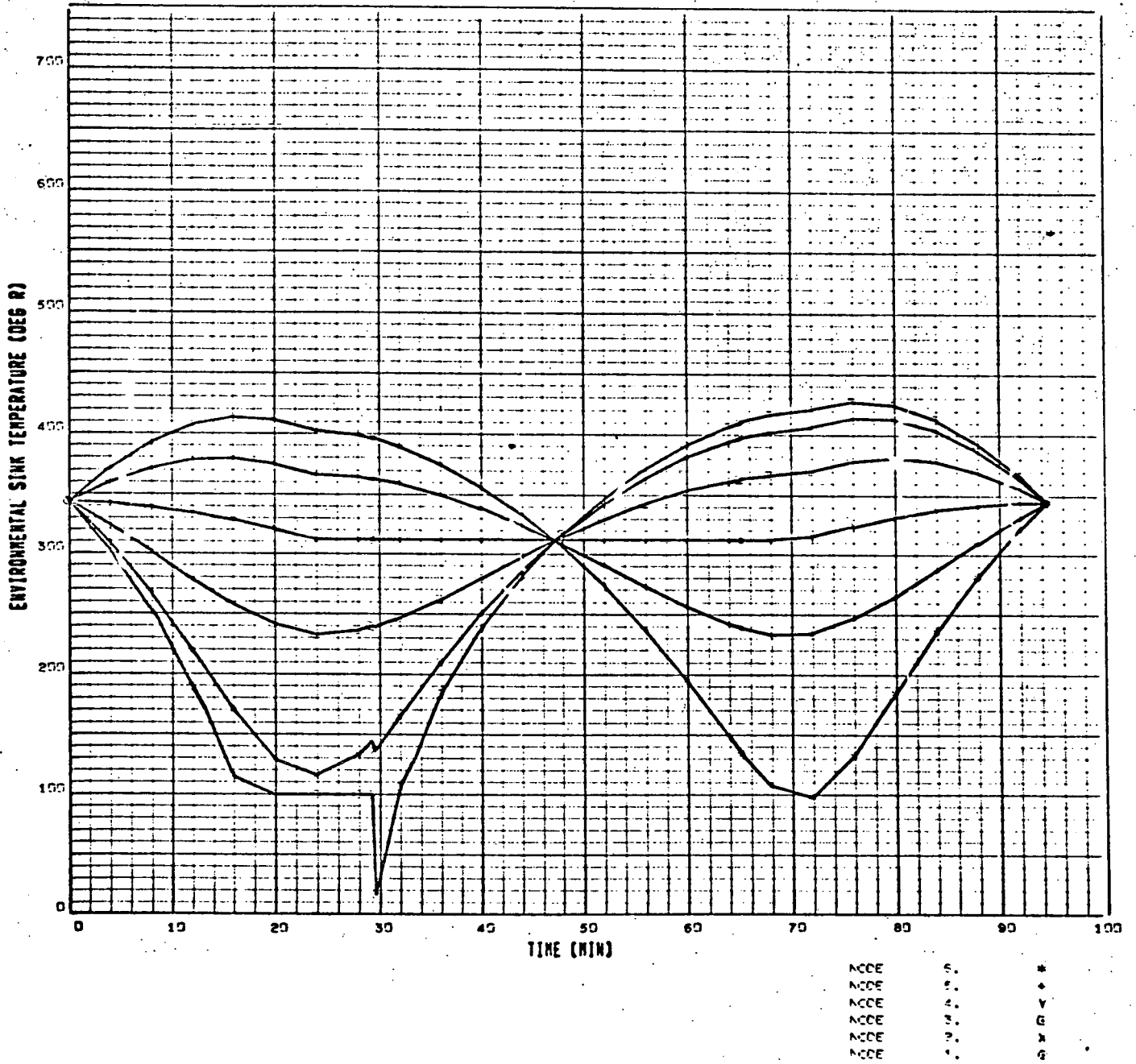
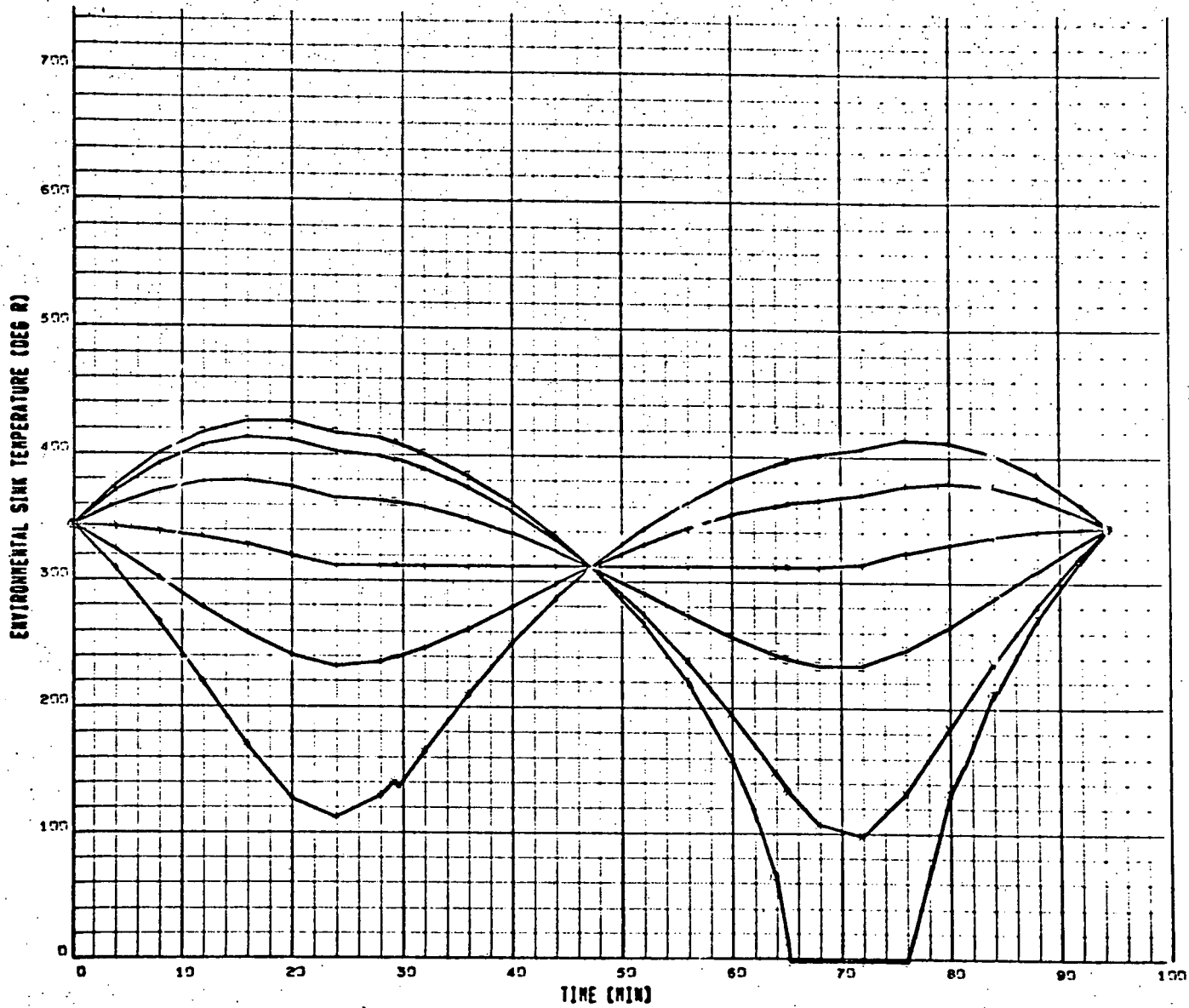


Figure A-43. Case 15

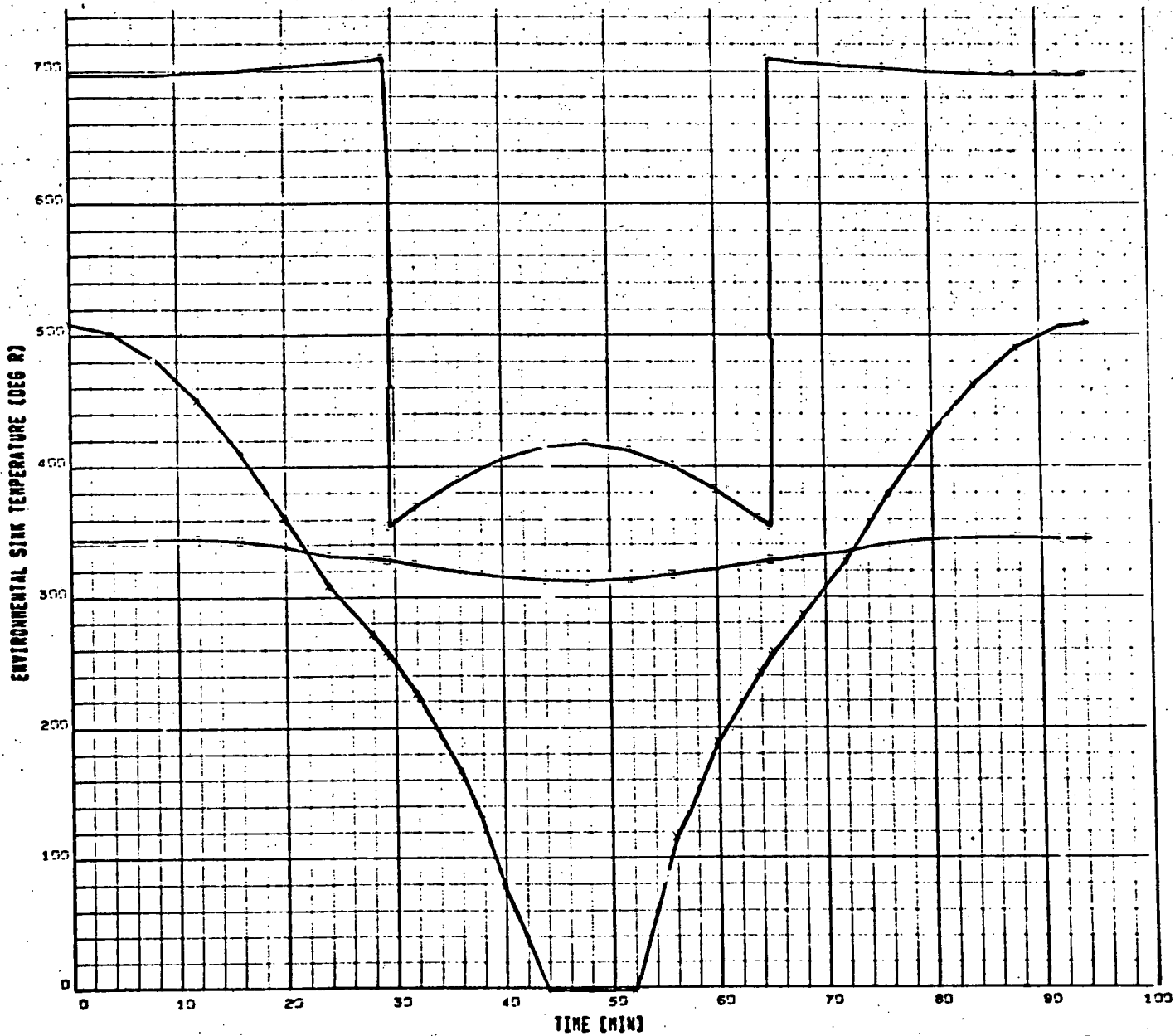
SPACE STATION COLDEST AVERAGE ORBIT (C) -- MIN FLUX -- 1/22/67



ACCE	12.	*
ACCE	11.	+
ACCE	10.	v
ACCE	9.	G
ACCE	8.	h
ACCE	7.	e

Figure A-44. Case 15

SPACE STATION COLDEST AVERAGE ORBIT (3) -- MIN FLUX -- 1/28/69



ACCE	15.	G
ACCE	14.	A
ACCE	13.	G

Figure A-45. Case 15

SPACE STATION LARGE TRANSIENT CRIT(2) -- NO FLO -- 1/28/77

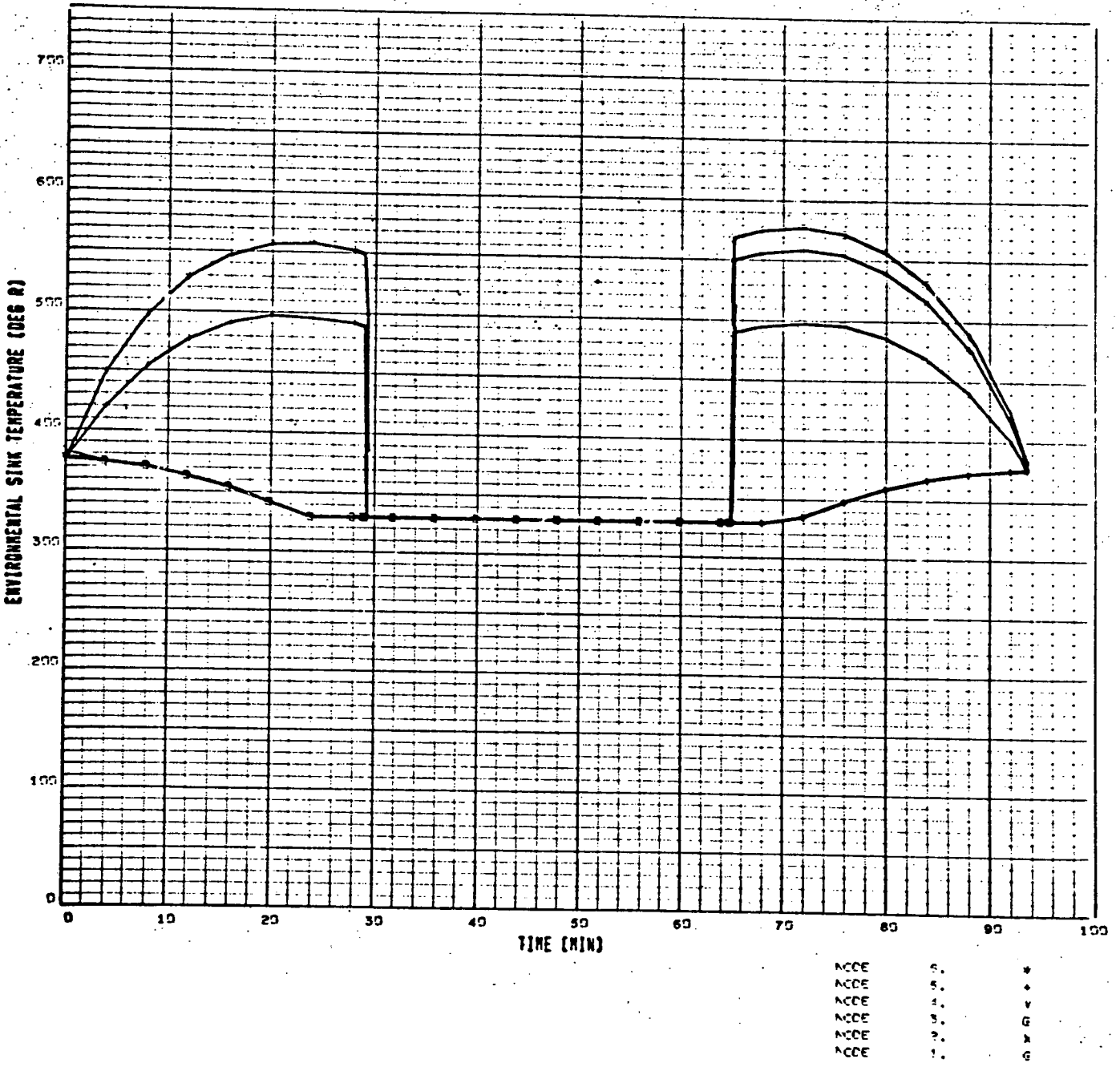


Figure A-46. Case 16

SPACE STATION LARGE TRANSIENT ORBIT (3) -- NOMELUX -- 1/25/77, 97

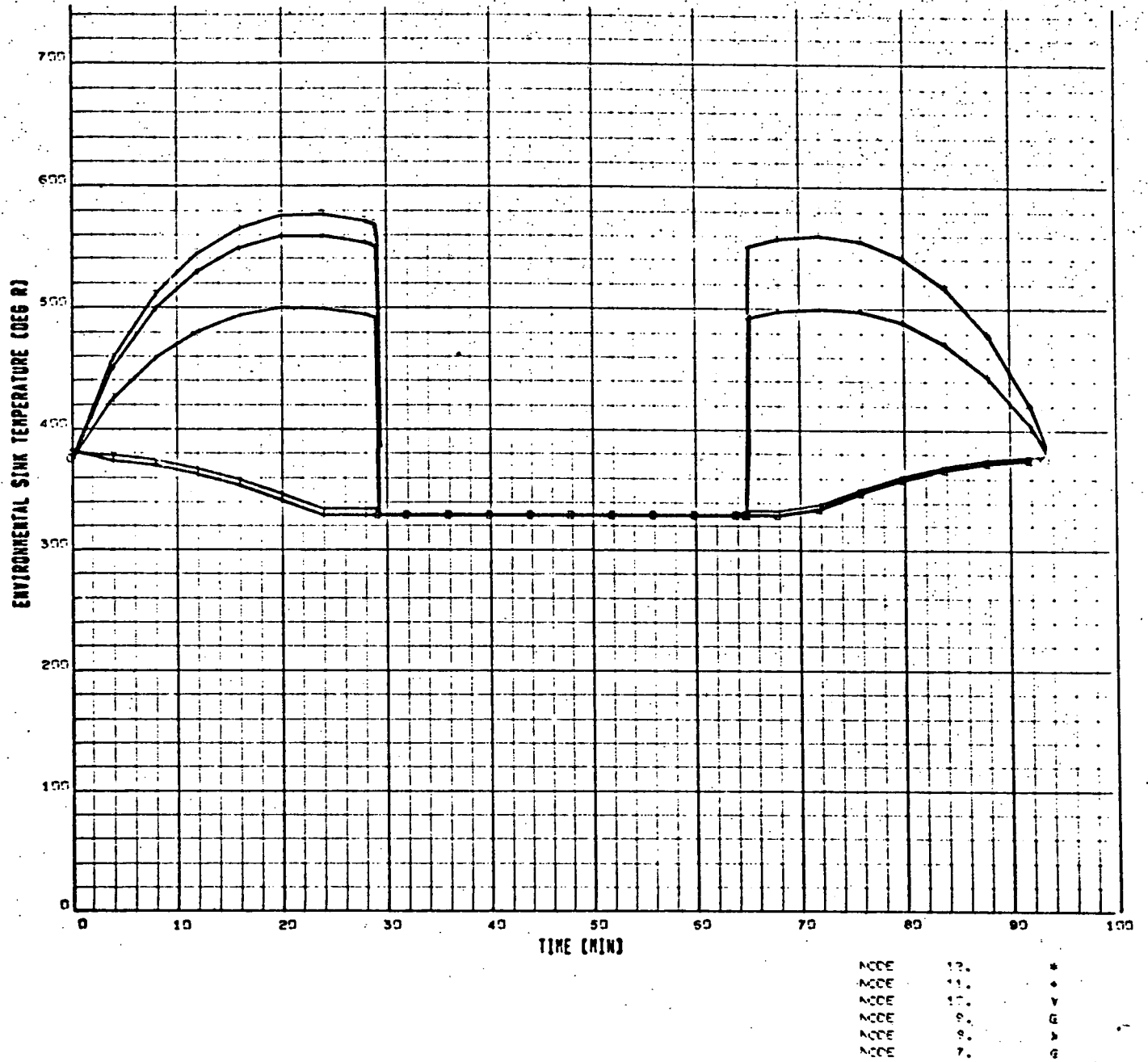


Figure A-47. Case 16

SPACE STATION LARGE TRANSIENT (REIT) -- NO. FLUX -- 1/2/72/27

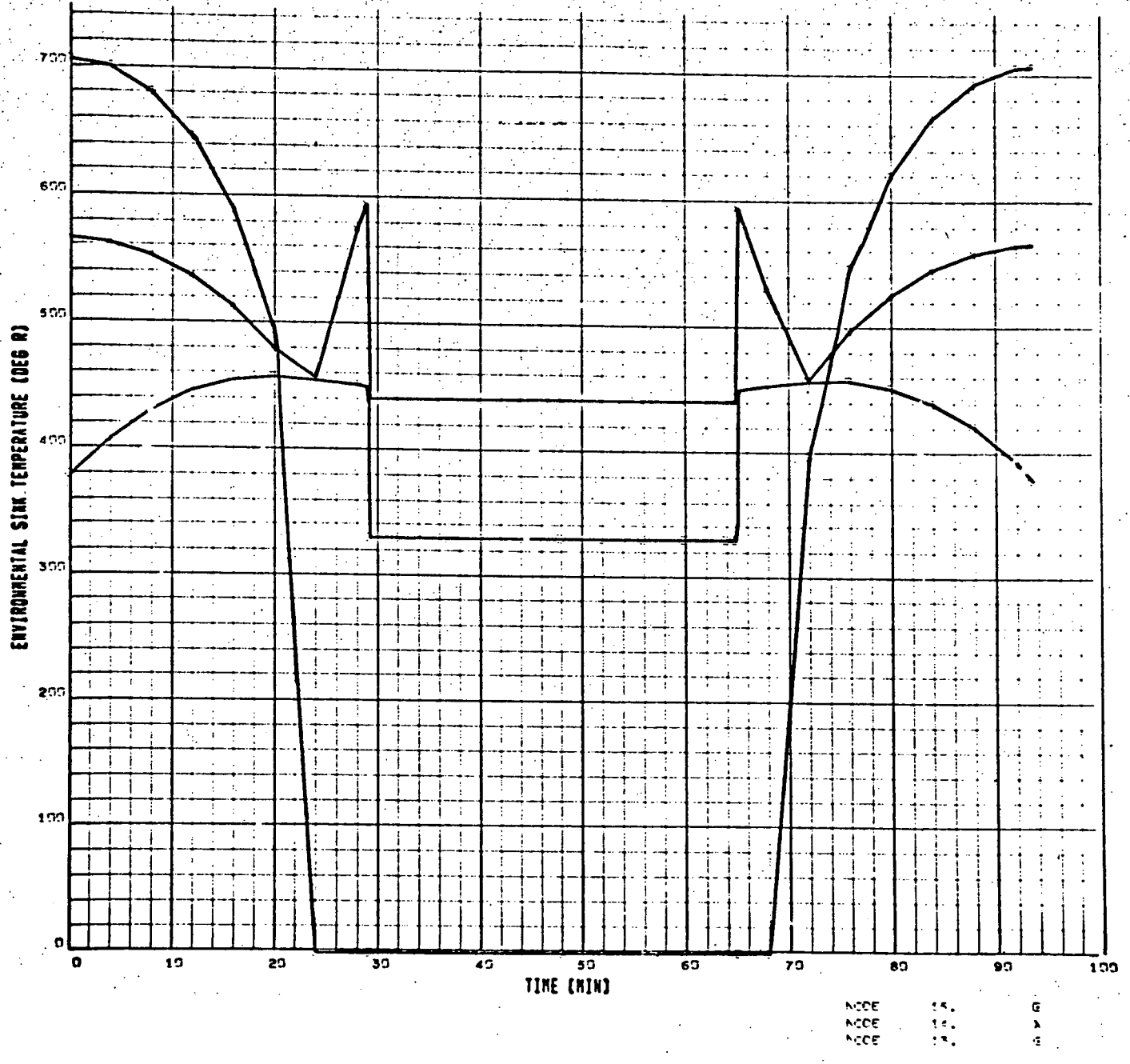


Figure A-48. Case 16

SPACE STATION NOMINAL ORBIT (5) -- NON-FLUX -- AVER. 12/2/87

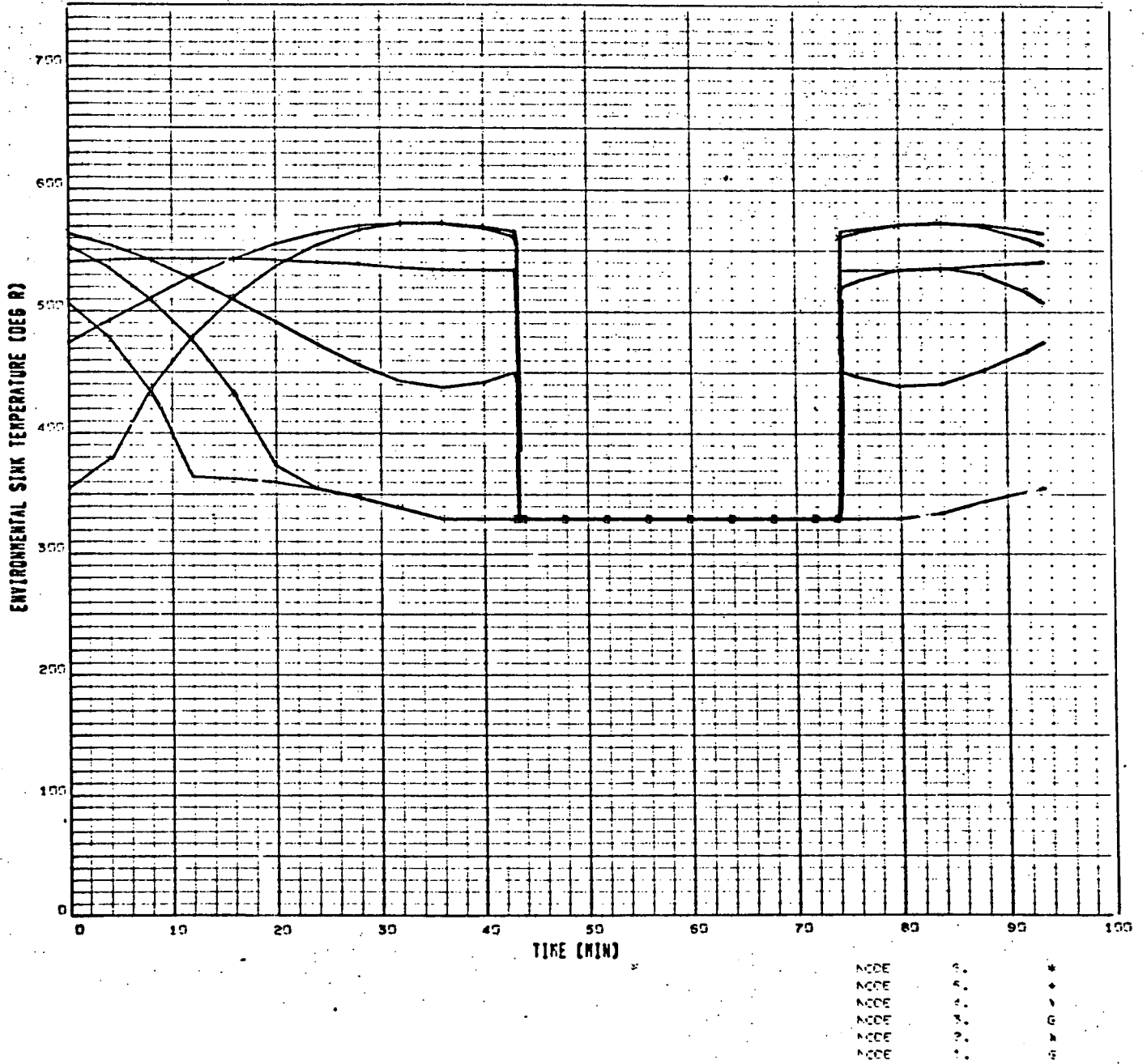
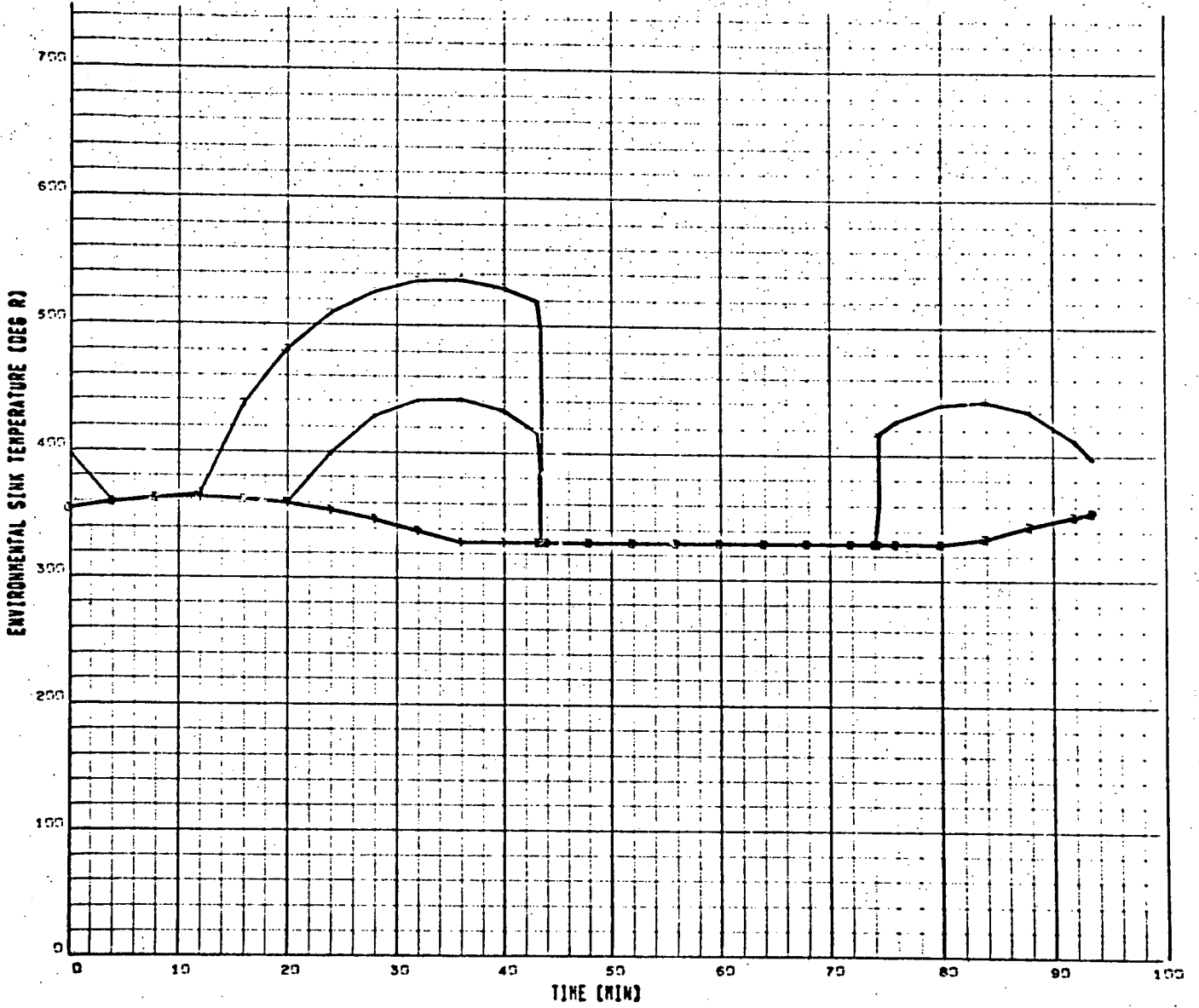


Figure A-49. Case 17

SPACE STATION THERMAL BEHAVIOR -- NON-FLUX -- 1/25, 1972



100
110
120
130
140
150
160
170
180
190
200

Figure A-50. Case 17

SPACE STATION NOMINAL OPERATING -- ACFT TRACK -- 1/28/70/9

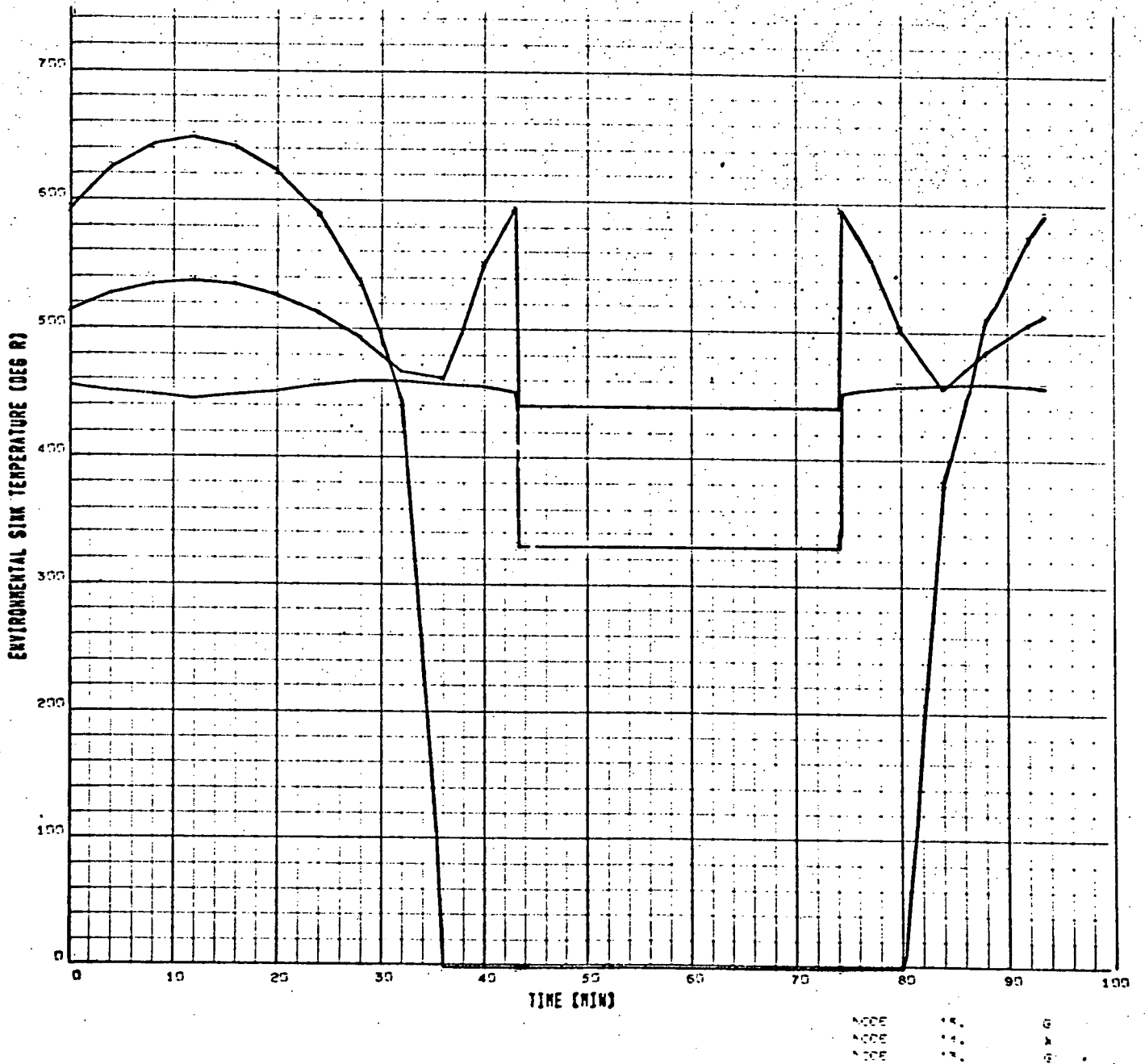


Figure A-51. Case 17

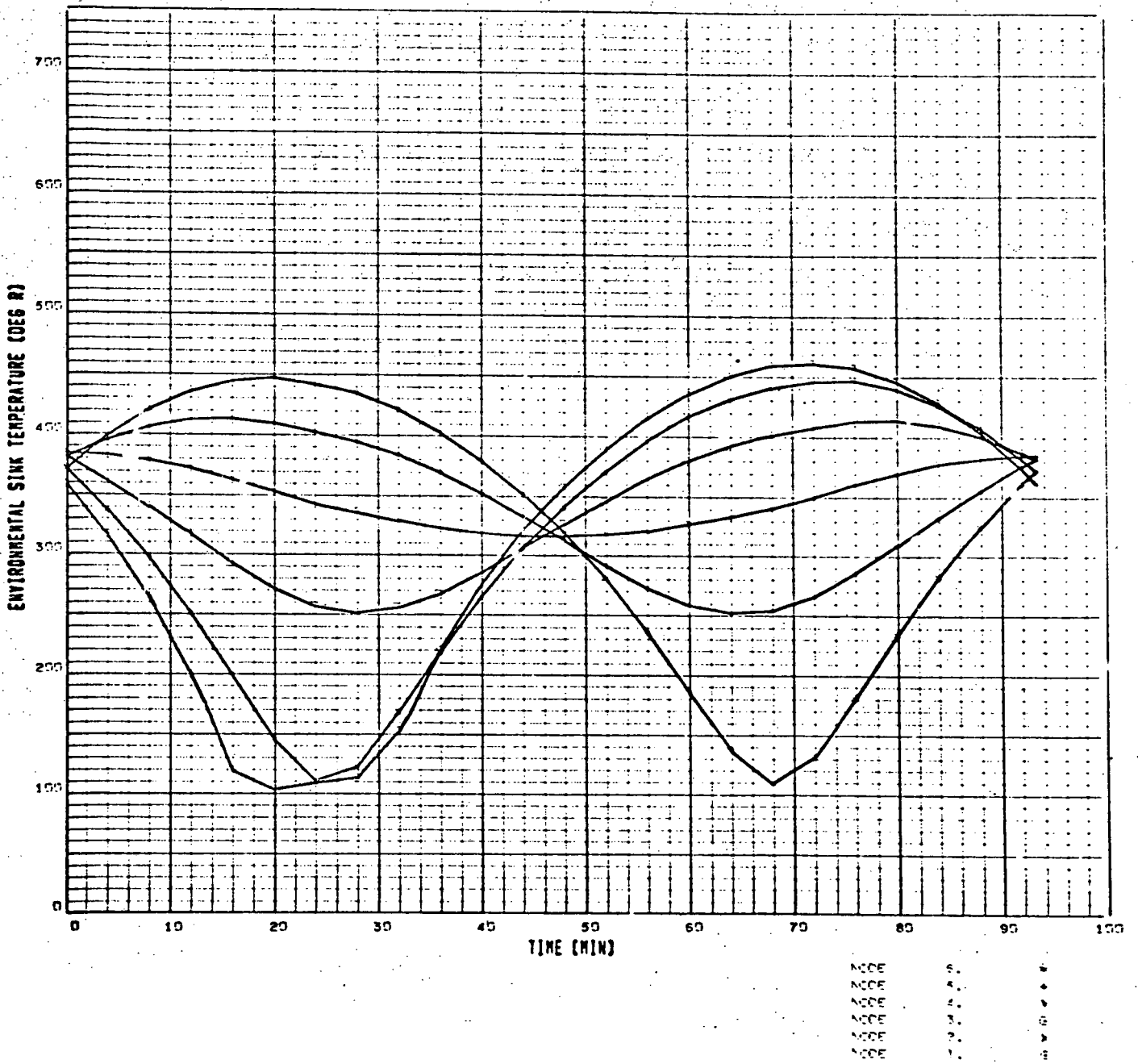


Figure A-52. Case 18

F

SPACE STATION ENVIRONMENTAL CONTROL SYSTEM -- CASE 18 -- DATE 10/2/70

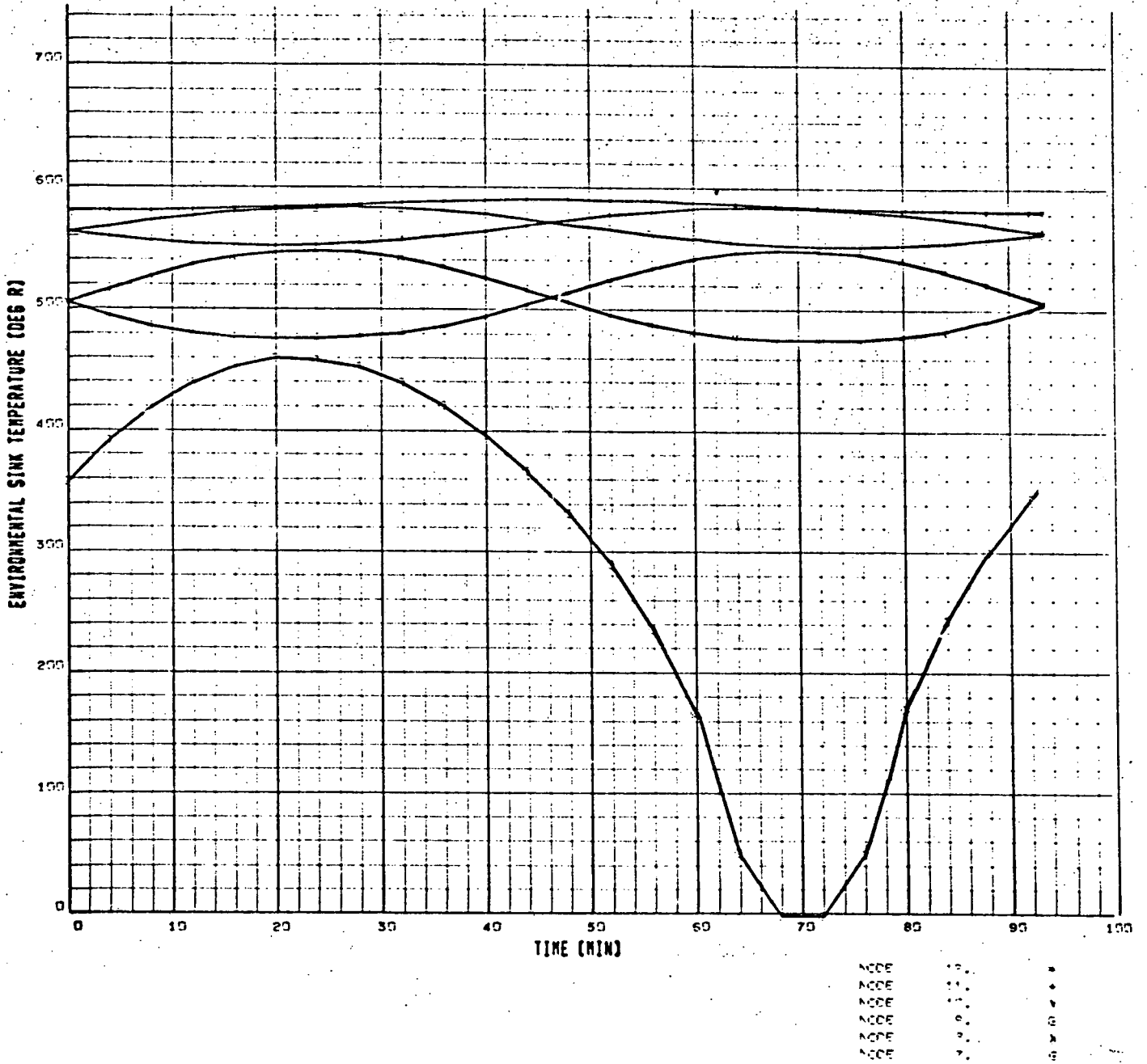


Figure A-53. Case 18

SPACE SECTOR AND IMPACT ORBIT -- CASE 18 -- 1/22.71/50

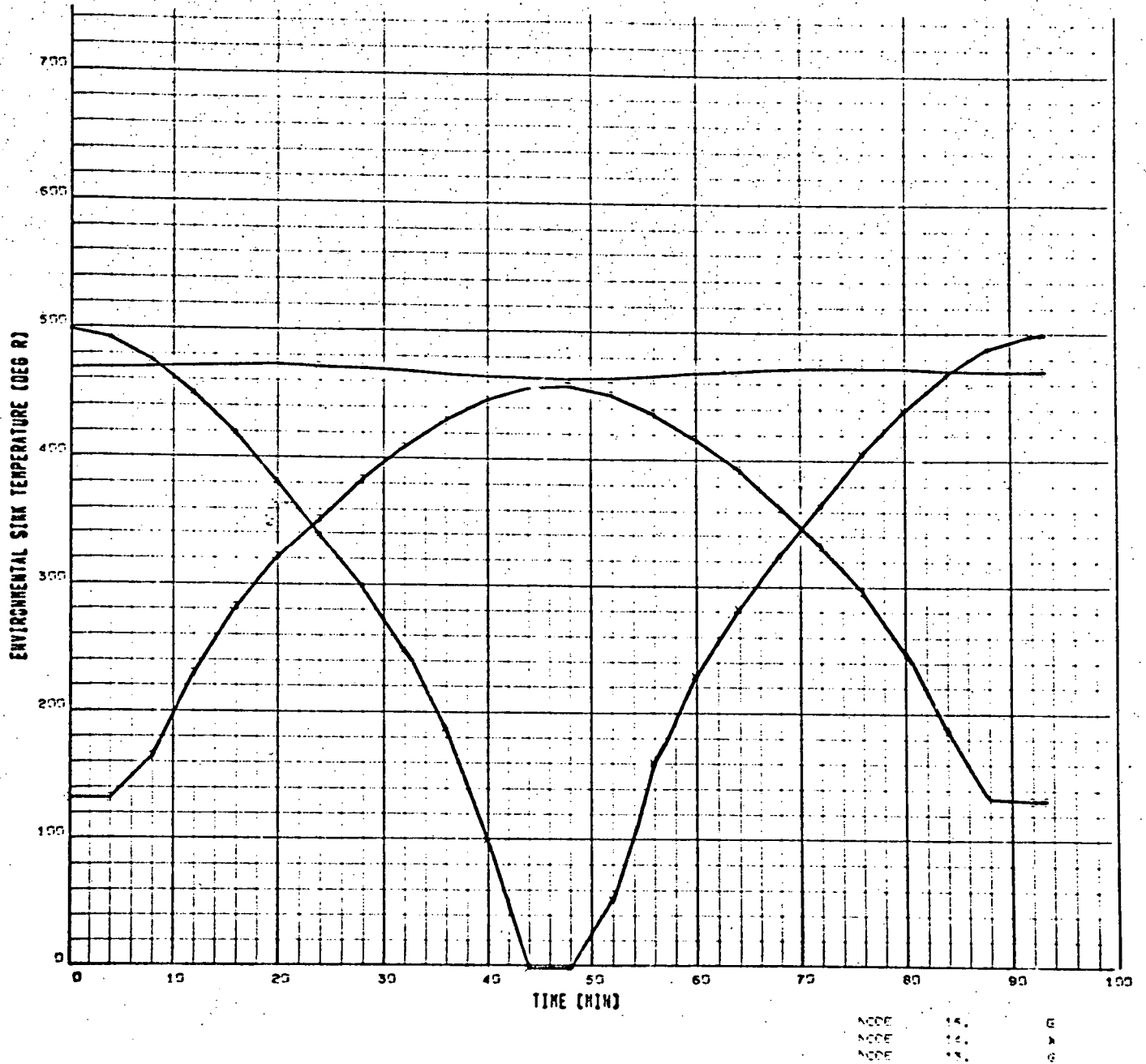


Figure A-54. Case 18

APPENDIX B
HEAT PIPE CAPACITY COMPUTER PROGRAM

- I. Function: This computer program calculates the maximum heat capacity for wick limited heat pipes. The capacity is a function of pipe geometry, working fluid, local acceleration of gravity, wick type and wick dimensions.
- II. Options: Equations have been programmed for the following wick types:
- a) Conventional - Multilayer spiral of mesh against inner tube wall.
 - b) Channel - Grooves in inner tube wall with single layer of covering mesh.
 - c) Artery - Free-standing artery with two layers of mesh around tube wall.
- III. Assumptions: The equations assume the following conditions apply:
- 1) Heat pipe fails by exceeding wick limit.
 - 2) Laminar, incompressible flow in both vapor and liquid phases.
 - 3) Meniscus radius in condenser is infinite.
 - 4) Uniform evaporation and condensation.
 - 5) Analysis basis on total heat pipe, not differential elements.
 - 6) No physical or thermal transients occur.
- IV. Input: The program was written in the Fortran language for the GE 605 timesharing computer system. Input required is:

Number of Temp Inputs = (fixed point)

This is the total number of temperatures for which fluid properties are input.

Temp, LH, DL, DV, VL, VV, ST = (all floating point)

Each input line is a temperature ($^{\circ}\text{F}$) and the associated fluid properties; latent heat (BTU/lb_m), liquid density ($\text{lb}_m/\text{cu. ft.}$), vapor density ($\text{lb}_m/\text{cu. ft.}$), liquid viscosity ($\text{lb}_m/\text{ft-sec}$), vapor viscosity ($\text{lb}_m/\text{ft-sec}$), and surface tension (lb_f/ft).

Total number of lines should agree with control above.

Local G, Total, Evap, Cond Length = (all floating point)

Input the local acceleration of gravity (ft/sec²), total length (ft), evaporator length (ft), and condenser length (ft).

Wick Control = (fixed point)

Calculations to be made for the following wicks:

- 1 = conventional only
- 2 = conventional and channel
- 3 = all three wicks
- 4 = conventional and artery
- 5 = channel only
- 6 = channel and artery
- 7 = artery only

Wick dimensional input is only required for the specified wicks.

For Screen-Recap I, Wet angle, Reflow, Por, B = (all floating point)

For metallic mesh, input minimum meniscus radius in evaporator (in.), wetting angle (degrees), capillary flow radius (in.), porosity (dimensionless), and tortuosity factor (dimensionless).

For Conventional Wick - RWI, RVI = (floating point)

Input the outer and inner radius of the wick in inches.

For Channel Wick - Nchan, Kchan, Chanaw, RVI = (one fixed point, then all floating point)

Input is number of flow channels, channel shape factor, channel half width (in.) and vapor flow radius (in.).

For Artery - RWARI, RARTI, SPI = (all floating point)

Input inner radius of wall screen (in.), artery radius (in.), and length of stem to artery (in.).

Following calculation and output, the input below is required.

Control *** (1=NF, 2=NP, 3=STOP) *** = (fixed point).

Input: 1 to change fluids
 2 to change pipe dimensions
 3 to stop

V. Output: The program output is: temperature ($^{\circ}$ F), elevation limit (in.) based on maximum supported liquid column height, the critical heat pipe angle based on the elevation limit (degrees) and the maximum heat capacity for the designated wicks (watts).

VI. Listing: A program listing follows.

LISTING OF HEAT PIPE PROGRAM

page 1 of 2

00010 DIMENSION T(12),HH(12),DL(12),DV(12),VL(12),VV(12),ST(12)
 00020 2 CONTINUE
 00030 PRINT: "NUMBER OF TEMPERATURE INPUTS"
 00040 READ:ITMAX
 00050 PRINT: "TEMP,LH,DL,DV,VL,VV,ST"
 00060 PRINT:
 00070 I=1
 00080 5 READ:T(I),HH(I),DL(I),DV(I),VL(I),VV(I),ST(I)
 00090 IF(I.EQ.ITMAX)GO TO 10
 00100 I=I+1
 00110 GO TO 5
 00120 10 QCONW=0.
 00130 QCHW=0.
 00140 QARTW=0.
 00150 PRINT: "LOCAL G,TOTAL,EVAP,COND LENGTH"
 00160 READ:G,TLG,ELG,CLG
 00170 XLF=TLG-.5*(ELG+CLG)
 00180 PRINT: "WICK CONTROL"
 00190 READ:IC
 00200 PRINT: "FOR SCREEN-RCAPI,WET ANG,RCFLOW,POR,B"
 00210 READ:RCAPI,THETA,RCFLI,EP,B
 00220 RCAP=RCAPI/12.
 00230 RCFL=RCFLI/12.
 00240 THETA=(THETA*3.1416)/180.
 00250 GO TO(30,30,30,30,35,35,40),IC
 00260 30 PRINT: "FOR CONVENTIONAL WICK-RWI,RVI"
 00270 READ:RWI,RVI
 00280 GO TO(45,35,35,40,35,35,35),IC
 00290 35 PRINT: "FOR CHANNEL WICK-NCHAN,KCHAN,CHANHW,RVI"
 00300 READ:XNO,XK,RCH,RVICH
 00310 RCHF=RCH/12.
 00320 GO TO(45,45,40,40,45,40,45),IC
 00330 40 PRINT: "FOR ARTERY WICK-RWARI,RARTI,SPI"
 00340 READ:RWARI,RARTI,SPI
 00350 45 PRINT 48
 00360 PRINT 50
 00370 J=1
 00380 15 DPAV=2.*ST(J)*COS(THETA)/RCAP
 00390 ELLIM=32.2*DPAV/(G*DL(J))
 00400 ELLIMI=ELLIM*12.
 00410 BETAC=(180./3.1416)*ARSIN(ELLIM/XLF)
 00420 GO TO(80,80,80,80,85,85,90),IC
 00430 80 RW=RWI/12.
 00440 RV=RVI/12.
 00450 XVCON=(8.*VV(J)*XLF)/(3.1416*DV(J)*(RV**4.))


```

00460      AWCON=3.1416*((RW**2.)-(RV**2.))
00470      XLCON=(B*VL(J)*XLF)/(AWCON*DL(J)*EP*(RCFL**2.))
00480      QCON=(32.2*HH(J)*(DPAV-DPGR))/(XVCON+XLCON)
00490      QCONW=(3600.*QCON)/3.413
00500
00510      GO TO(95,85,85,90,85,85,85),IC
00520 85  RVCH=RVICH/12.
00530      XVCH=(8.*VV(J)*XLF)/(3.1416*DV(J)*(RVCH**4.))
00540      DEMON=3.1416*DL(J)*XNO*((XK*RCHF)**4.)
00550      XLCH=(8.*VL(J)*XLF)/DEMON
00560      QCH=(32.2*HH(J)*(DPAV-DPGR))/(XVCH+XLCH)
00570      QCHW=(3600.*QCH)/3.413
00580      GO TO(95,95,90,90,95,90,95),IC
00590 90  RWAR=RWARI/12.
00600      RART=RARTI/12.
00610      SP=SPI/12.
00620      WP=2.*(SP+3.1416*(RWAR+RART))
00630      AV=3.1416*((RWAR**2.)-(RART**2.))
00640      XVAR=(2.*VV(J)*XLF*(WP**2.))/(DV(J)*(AV**3.))
00650      XLAR=(8.*3.1416*XLF*VL(J))/(DL(J)*(3.1416*(RART**2.))**2.)
00660      CIRLEN=SP+.5*3.1416*(RWAR+RART)
00670      ABE=CIRLEN/(ELG*EP*.001)
00680      ABC=CIRLEN/(CLG*EP*.001)
00690      XLCC=(B*VL(J)*(ABE+ABC))/(DL(J)*(RCFL**2.))
00700      QART=(32.2*HH(J)*(DPAV-DPGR))/(XVAR+XLAR+XLCC)
00710      QARTW=(3600.*QART)/3.413
00720 95  PRINT 60,T(J),ELLI, BETAC, QCONW, QCHW, QARTW
00730      IF(J.EQ.ITMAX)GO TO 20
00740      J=J+1
00750      GO TO 15
00760 20  PRINT: "*****CONTROL(1=NF,2=NP,3=STOP)"
00770      READ:III
00780      GO TO(2,10,100),III
00790 100 STOP
00800 48  FORMAT(/12X,"ELEV",4X,"CRIT",11X,"QMAX (WATTS) FOR
00810 &  FOLLOWING WICKS")
00820 50  FORMAT(4X,"TEMP",4X,"LIMIT",3X,"BETA",8X,"CONVENTIONAL"
00830 &  5X,"CHANNEL",8X,"ARTERY")
00840 60  FORMAT(3X,F6.1,3X,F6.3,3X,F4.1,3(8X,F7.1))
00850      END

```

APPENDIX C
PHASE I TEST DATA

Empirical heat pipe tests were performed as part of Phase I to compile burn-out and temperature differential information for pipes with various fluids, wicks, and shapes. Table C-1 describes the six pipes tested. Data sheets follow which present the pertinent information.

The temperature of the ice-bath sink was measured at 32^oF before testing with a calibrated thermocouple. All temperature data obtained from the electronic recorder used during actual testing was corrected to the 32^oF sink.

Table C-1. Design of Tested Heat Pipes

Pipe	Length, ft.	Tube		Type	Wick	Fill, ml
		OD, in	ID, in		Description*	
A	4	.500	.430	Conv.	4 layers of 100 mesh stainless	19.2
B	4	.500	.430	Art.	.092" artery of 200 mesh stainless + 2 layers against tube ID	11.2
C	4	.500	.430	Chan.	26 stainless spacer wires covered by 1 layer 100 mesh stainless	13.9
D	2	.500	.430	Conv.	4 layers of 100 mesh stainless	9.6
E	4	1.000	.902	Conv.	8 layers of 100 mesh stainless	108.6
F	4	Square (1 X 1)		Conv.	100 mesh stainless spot-welded to pipe wall (Aw = .174 sq.in.)	90.3

* "Stainless" infers stainless steel

Note: All tubing 304 stainless steel

TEST 1

Date 9/25/70

Pipe A

Fluid Water

Amt. of Charge (ml) 22.0

Heat Input, w	Evap. Elev, in.	Equilibrium temperatures, °F			Remarks
		Heater	Heat Pipe	Sink	
0	0	60	59 +1,-1	32	
5.5	0	63	60 +1,-1	32	
10.1	0	67	61 +2,-2	32	
20.0	0	74	62 +2,-2	32	
30.0	0	79	64 +3,-3	32	
39.6	0	85	65 +3,-3	32	
45.0	0	89	66 +3,-3	32	
51.2	0	91	69 +4,-5	32	
56.5	0				Burn-out
0	1	60	59 +1,-1	32	
4.5	1	62	60 +1,-1	32	
10.1	1	66	61 +1,-1	32	
20.0	1	72	62 +2,-2	32	
30.0	1	78	64 +2,-2	32	
39.6	1	83	64 +3,-3	32	
45.0	1				Burn-out

CONCLUSION: Burn-out at approximately 53 w with elevation= 0"

Burn-out at approximately 44 w with elevation= 1"

TEST 2

Date 10/26/70

Pipe A

Fluid Ammonia

Amt. of Charge (ml) 21.0

Heat Input, w	Evap. Elev, in.	Equilibrium temperatures, °F			Remarks
		Heater	Heat Pipe	Sink	
0	0	66	65 +0,-0	32	
20.0	0				Burn-out
10.0	0	72	67 +3,-3	32	
15.0	0	79	71 +4,-4	32	
20.0	0				Burn-out
10.0	0	73	69 +4,-4	32	
10.0	.5	73	69 +4,-4	32	
10.0	1.0	73	69 +4,-4	32	
10.0	1.5				Burn-out

CONCLUSION: Burn-out at 15 w with elevation= 0"

Burn-out at 10 w with elevation= 1.5"

TEST 3

Date 10/8/70-10/9/70

Pipe A

Fluid Methanol

Amt. of Charge (ml) 21.5

Heat Input, w	Evap. Elev, in.	Equilibrium temperatures, °F			Remarks
		Heater	Heat Pipe	Sink	
0	0	74	74 +1,-1	32	
5.0	0	88	84 +2,-2	32	
7.5	0	92	83 +3,-3	32	
10.0	0	96	84 +3,-3	32	
12.5	0	100	86 +2,-3	32	
15.0	0	97	88 +6,-6	32	Begin Burn-out
17.5	0				Burn-out
10.0	0	93	84 +3,-3	32	
10.0	1.0	94	84 +3,-3	32	
12.5	1.0	100	88 +7,-7	32	Begin Burn-out
15.0	1.0				Burn-out

CONCLUSION: Burn-out at 15 w with elevation= 0"

Burn-out at 12.5 w with elevation= 1"

TEST 4

Date 10/28/70

Pipe A

Fluid Freon- 11

Amt. of Charge (ml) 22.0

Heat Input, w	Evap. Elev, in.	Equilibrium temperatures, °F			Remarks
		Heater	Heat Pipe	Sink	
0	0	68	35 to 67	32	(below)
** Not operating in heat pipe regime . Heat leak through insulation sufficient to burn out pipe.					

CONCLUSION: Burn-out below 5 w with elevation = 0"

TEST 5

Date 9/30/70-10/1/70

Pipe B

Fluid Water

Amt. of Charge (ml) 14.0

Heat Input, w	Evap. Elev, in.	Equilibrium temperatures, °F			Remarks
		Heater	Heat Pipe	Sink	
0	0	60	53 +0,-0	32	
20.0	0	75	68 +1,-1	32	
41.4	0				Burn-out
* Added 9 ml of water (in increments of 3 ml) with heat input of 41.4 w. No recovery from burn-out conditions.					
20.0	0	76	68 +2,-2	32	Charge = 23.0 ml
25.2	0	79	69 +2,-2	32	
30.2	0	82	70 +3,-3	32	
35.5	0	86	71 +4,-3	32	
41.7	0				Burn-out

CONCLUSION: Burn-out at approximately 37 w with elevation= 0"

G _____

TEST 7

Date 10/12/70

Pipe B

Fluid Methanol

Amt. of Charge (ml) 14.0

Heat Input, w	Evap. Elev, in.	Equilibrium temperatures, °F			Remarks
		Heater	Heat Pipe	Sink	
0	0	67	67 +1,-1	32	
20.0	0				Burn-out
0	0	65	65 +1,-1	32	
10.0	0	74	68 +3,-3	32	
12.5	0				Burn-out
0	0	66	66 +1,-1	32	
10.0	0	78	71 +5,-4	32	
12.5	0				Burn-out

CONCLUSION: Burn-out at 10 w with elevation= 0"

TEST 8

Date 10/28/70

Pipe B

Fluid Freon- 11

Amt. of Charge (ml) 14.5

Heat Input, w	Evap. Elev, in.	Equilibrium temperatures, °F			Remarks
		Heater	Heat Pipe	Sink	
0	0	67	37 to 64	32	(below)
** Not operating in heat pipe regime . Heat leak through insulation sufficient to burn out pipe.					

CONCLUSION: Burn-out below 5 w with elevation= 0"

TEST 9

Date 10/7/70

Pipe C

Fluid Water

Amt. of Charge (ml) 10.5 ml

Heat Input, w	Evap. Elev, in.	Equilibrium temperatures, °F			Remarks
		Heater	Heat Pipe	Sink	
0	0	51	51 +0,-0	32	
50.0	0				Burn-out
0	0	55	52 +1,-1	32	
50.0	-1.0				Burn-out
25.0	0	75	55 +2,-2	32	
36.0	0				Burn-out
* Added 3 ml of water					
25.0	0	67	56 +2,-1	32	Charge = 13.5 ml
35.0	0				Very gradual burn-out

CONCLUSION: Burn-out at 35 w with elevation= 0"

TEST 10

Date 10/16/70

Pipe F

Fluid Water

Amt. of Charge (ml) 101.0

Heat Input, w	Evap. Elev, in.	Equilibrium temperatures, °F			Remarks
		Heater	Heat Pipe	Sink	
0	0	52	52 +1,-1	32	
100	0	94	68 +5,-5	32	
125	0	102	73 +7,-7	32	
125	1.0	103	74 +7,-7	32	
125	1.5	103	73 +8,-8	32	
125	2.0	102	73 +8,-8	32	
125	2.5	105	75 +8,-9	32	
125	3.0				Burn-out
* Set pipe elevation to 1", increased input to 250 w, incremented elevation every 30 min. by .5", and watched for burn-out. At burn-out, heater temperature was 187, heat pipe was 115 +13,-11, sink was 32, and elevation was 2.0".					

CONCLUSION: Burn-out at 125 w with elevation=2.5"

Burn-out at 250 w with elevation= 2.0"

TEST 11

Date 10/6/70

Pipe D

Fluid Water

Amt. of Charge (ml) 10.5

Heat Input, w	Evap. Elev, in.	Equilibrium temperatures, °F			Remarks
		Heater	Heat Pipe	Sink	
0	0	51	51 +0,-0	32	
20.0	0	62	55 +1,-1	32	
41.2	0	73	58 +2,-2	32	
61.2	0	84	61 +3,-3	32	
80.0	0	91	63 +4,-4	32	
100.8	0				Burn-out
80.0	0	91	64 +4,-4	32	
85.3	0	93	65 +4,-4	32	
90.4	0	95	66 +4,-4	32	
95.2	0	97	67 +4,-4	32	
100.0	0				Burn-out
60.0	0	84	61 +3,-3	32	
60.0	1.5	81	61 +3,-3	32	
65.0	1.5	81	61 +10,-3	32	
70.0	1.5				Burn-out

CONCLUSION: Burn-out at approximately 97 w with elevation= 0"

Burn-out at approximately 67 w with elevation= 1.5"

TEST 12

Date 10/21/70-10/22/70

Pipe E

Fluid Water

Amt. of Charge (ml) 117.0

Heat Input, w	Evap. Elev, in.	Equilibrium temperatures, °F			Remarks
		Heater	Heat Pipe	Sink	
0	0	68	68 +0,-0	32	
51.0	0	111	80 +5,-5	32	
73.8	0	144	83 +7,-7	32	
100.1	0	176	86 +7,-7	32	
131.0	0	215	91 +8,-8	32	
166.5	0	256	96 +10,-10	32	
100.1	0	184	87 +7,-7	32	
100.1	.5	186	89 +8,-8	32	
100.1	1.0	187	91 +8,-8	32	
100.1	1.5	186	91 +7,-7	32	
100.1	2.0	185	91 +7,-7	32	
100.1	2.5	197	94 +7,-7	32	
100.1	3.0	197	93 +7,-7	32	
100.1	3.5	197	93 +7,-7	32	
100.1	4.0	196	94 +6,-6	32	
100.1	4.5	200	95 +7,-6	32	
100.1	5.0				Burn-out
* Leveled pipe, increased input to 148.8 w, incremented elevation every 15 min. by .5 in., and watched for burn-out. At burn-out, heater temperature was 300+, heat pipe was 91 +12,-13, sink was 32, and elevation was 4.25".					

CONCLUSION: Burn-out at 100 w with elevation= 5"

Burn-out at 148.8w with elevation=4.25"